

Advances in ubiquitous sensing
applications for healthcare

Volume One

Series Editors:

Nilanjan Dey, Amira S. Ashour
Simon James Fong

U-HEALTHCARE MONITORING SYSTEMS

DESIGN AND APPLICATIONS

Volume Editors:

Nilanjan Dey, Amira S. Ashour,
Simon James Fong
and Surekha Borra



U-Healthcare Monitoring Systems

This page intentionally left blank

Advances in Ubiquitous Sensing Applications for Healthcare **U-Healthcare** **Monitoring Systems**

Volume 1: Design and Applications

Series Editors

Nilanjan Dey

Amira S. Ashour

Simon James Fong

Volume Editors

Nilanjan Dey

Techno India College of Technology, Kolkata, India

Amira S. Ashour

Faculty of Engineering, Tanta University, Egypt

Simon James Fong

University of Macau, Taipa, Macau SAR

Surekha Borra

K.S. Institute of Technology, Bangalore, India



ACADEMIC PRESS

An imprint of Elsevier

Academic Press is an imprint of Elsevier
125 London Wall, London EC2Y 5AS, United Kingdom
525 B Street, Suite 1650, San Diego, CA 92101, United States
50 Hampshire Street, 5th Floor, Cambridge, MA 02139, United States
The Boulevard, Langford Lane, Kidlington, Oxford OX5 1GB, United Kingdom

© 2019 Elsevier Inc. All rights reserved.

No part of this publication may be reproduced or transmitted in any form or by any means, electronic or mechanical, including photocopying, recording, or any information storage and retrieval system, without permission in writing from the publisher. Details on how to seek permission, further information about the Publisher's permissions policies and our arrangements with organizations such as the Copyright Clearance Center and the Copyright Licensing Agency, can be found at our website: www.elsevier.com/permissions.

This book and the individual contributions contained in it are protected under copyright by the Publisher (other than as may be noted herein).

Notices

Knowledge and best practice in this field are constantly changing. As new research and experience broaden our understanding, changes in research methods, professional practices, or medical treatment may become necessary.

Practitioners and researchers must always rely on their own experience and knowledge in evaluating and using any information, methods, compounds, or experiments described herein. In using such information or methods they should be mindful of their own safety and the safety of others, including parties for whom they have a professional responsibility.

To the fullest extent of the law, neither the Publisher nor the authors, contributors, or editors, assume any liability for any injury and/or damage to persons or property as a matter of products liability, negligence or otherwise, or from any use or operation of any methods, products, instructions, or ideas contained in the material herein.

Library of Congress Cataloging-in-Publication Data

A catalog record for this book is available from the Library of Congress

British Library Cataloguing-in-Publication Data

A catalogue record for this book is available from the British Library

ISBN: 978-0-12-815370-3

For information on all Academic Press publications
visit our website at <https://www.elsevier.com/books-and-journals>



Working together
to grow libraries in
developing countries

www.elsevier.com • www.bookaid.org

Publisher: Mara Conner

Acquisition Editor: Fiona Geraghty

Editorial Project Manager: John Leonard

Production Project Manager: Anitha Sivaraj

Designer: Matthew Limbert

Typeset by SPI Global, India

Contents

Contributors	xv
Preface	xvii
CHAPTER 1 Wearable U-HRM Device for Rural Applications	1
Mohd Imran and Mohammad Abdul Qadeer	
1 Introduction.....	1
2 U-Healthcare System in India	4
3 Application.....	4
4 Open Issues and Problems.....	5
5 Requirements of a Healthcare System	6
6 Requirement of Wearable Devices.....	7
7 Implementation	7
8 Measurement of Heart Rate and Body Temperature	8
9 Discussion	11
10 Conclusion and Future Trends	11
Glossary	12
References.....	12
CHAPTER 2 A Robust Framework for Optimum Feature Extraction and Recognition of P300 from Raw EEG.....	15
Saatvik Shah, Anirudha Kumar, Rajesh Kumar and Nilanjan Dey	
1 Introduction.....	15
2 Literature Survey	17
3 The Framework.....	19
3.1 Initialization	19
3.2 Model Setup.....	20
3.3 Postprocessor	21
3.4 Classification	25
4 Results and Discussion	26
4.1 The Dataset	27
4.2 Framework Results	27
5 Conclusion and Future Work	32
References.....	33
CHAPTER 3 Medical Image Diagnosis for Disease Detection: A Deep Learning Approach.....	37
Mrudang D. Pandya, Parth D. Shah and Sunil Jardosh	
1 Introduction.....	37

1.1 Related Work	39
2 Requirement of Deep Learning Over Machine Learning	40
2.1 Fundamental Deep Learning Architectures	41
3 Implementation Environment	52
3.1 Toolkit Selection/Evaluation Criteria	53
3.2 Tools and Technology Available for Deep Learning	53
3.3 Deep Learning Framework Popularity Levels	53
4 Applicability of Deep Learning in Field of Medical Image Processing	56
4.1 Current Research Applications in the Field of Medical Image Processing	56
5 Hybrid Architectures of Deep Learning in the Field of Medical Image Processing	57
6 Challenges of Deep Learning in the Fields of Medical Imaging	58
7 Conclusion	59
References.....	59
Further Reading	60

CHAPTER 4 Reasoning Methodologies in Clinical Decision Support Systems: A Literature Review 61

Nora Shoaip, Shaker El-Sappagh, Sherif Barakat and Mohammed Elmogy

1 Introduction.....	61
2 Methods.....	67
2.1 Research Questions.....	67
2.2 Selection Criteria	67
2.3 Search Strategy	68
3 Literature Review and Results	68
3.1 Paper Screening	69
3.2 Selecting the Most Relevant Papers.....	71
3.3 Extracting and Analyzing Concepts.....	72
3.4 Current Challenges and Future Trends	82
4 Conclusion	83
References.....	84

CHAPTER 5 Embedded Healthcare System for Day-to-Day Fitness, Chronic Kidney Disease, and Congestive Heart Failure 89

Pradeep M. Patil and Durgaprasad K. Kamat

1 Ubiquitous Healthcare and Present Chapter	90
2 Introduction.....	90

3	Frequency-Dependent Behavior of Body Composition.....	92
4	Bioimpedance Analysis for Estimation of Day-to-Day Fitness and Chronic Diseases	93
5	Measurement System for Body Composition Analysis Using Bioimpedance Principle	98
5.1	Measurement Electrodes.....	99
5.2	A FE4300 Body Composition Analyzer	99
5.3	Statistical Analysis	105
5.4	Validation of Developed Model.....	105
6	Database Generation.....	105
7	Predictive Regression Model for Day-to-Day Fitness	106
8	Predictive Regression Model for CKD	111
9	Predictive Regression Model for CHF.....	113
10	Discussion	115
11	Conclusion	115
	References.....	116

CHAPTER 6 Comparison of Multiclass and Hierarchical CAC Design for Benign and Malignant Hepatic Tumors.. 119

Nimisha Manth, Kriti and Jitendra Virmani

1	Introduction.....	120
2	Materials and Methods	123
2.1	Dataset Collection.....	123
2.2	Data Set Description.....	123
2.3	Data Collection Protocol	123
2.4	ROIs Selection	124
2.5	ROI Size Selection	125
2.6	Proposed CAC System Design.....	127
2.7	Feature Extraction Module	127
2.8	Classification Module	132
3	Results	137
3.1	Experiment 1: To Evaluate the Potential of the Three-Class SSVM Classifier Design for the Characterization of Benign and Malignant FHTs.....	139
3.2	Experiment 2: To Evaluate the Potential of SSVM-Based Hierarchical Classifier Design for Characterization Between Benign and Malignant FHTs	139
3.3	Experiment 3: Performance Comparison of SSVM-Based Three-Class Classifier Design and SSVM-Based Hierarchical Classifier Design for Characterization of Benign and Malignant FHTs.....	140

4	Discussion and Conclusion.....	141
	References.....	144
	Further Reading	146

CHAPTER 7 Ontology Enhanced Fuzzy Clinical Decision Support System 147

Nora Shoaip, Shaker El-Sappagh, Sherif Barakat and Mohammed Elmogy

1	Introduction.....	147
2	Problem Description	152
3	Related Work	153
4	The Combining of Ontology and Fuzzy Logic Frameworks.....	156
5	System Architecture and Research Methodology	160
5.1	Knowledge Acquisition	160
5.2	Semantic Modeling.....	163
5.3	The Fuzzy Modeling	164
5.4	Knowledge Reasoning.....	170
6	Conclusion	172
	References.....	174
	Further Reading	177

CHAPTER 8 Improving the Prediction Accuracy of Heart Disease with Ensemble Learning and Majority Voting Rule..... 179

Khalid Raza

1	Introduction.....	179
2	Review of Related Works	181
3	Ensemble Learning Systems	183
3.1	Diversity.....	184
3.2	Training Ensemble Members	184
3.3	Combining Ensemble Members	184
4	Materials and Methods	185
4.1	Logistic Regression	185
4.2	Multilayer Perceptron	188
4.3	Naïve Bayes.....	188
4.4	Combining Classifiers Using Majority Vote Rule.....	189
4.5	Performance Metrics.....	190
5	Result and Discussion.....	191
6	Conclusion and Future Directions.....	193
	References.....	193
	Further Reading	196

**CHAPTER 9 Machine Learning for Medical Diagnosis:
A Neural Network Classifier Optimized Via
the Directed Bee Colony Optimization Algorithm 197**

Saurabh Kumar Agrawal, Bhanu Pratap Singh,
Rajesh Kumar and Nilanjan Dey

1	Introduction.....	197
2	Neural Network Dynamics	200
3	Directed Bee Colony Optimization Algorithm	201
4	Experimental Setup.....	204
5	Result and Discussion.....	204
6	Conclusion	213
	References.....	214
	Further Reading	215

**CHAPTER 10 A Genetic Algorithm-Based Metaheuristic
Approach to Customize a Computer-Aided
Classification System for Enhanced Screen
Film Mammograms..... 217**

Heminder Kaur, Jitendra Virmani, Kriti and Shruti Thakur

1	Introduction.....	218
2	Methodology for Designing a CAD System for Diagnosis of Abnormal Mammograms	226
2.1	Image Data Set Description	228
2.2	Enhancement Methods	229
2.3	Selection of ROIs	237
2.4	Feature Extraction: Gabor Wavelet Transform Features....	241
2.5	SVM Classifier	244
3	Experimental Results.....	246
3.1	Obtaining the Accuracies of Classification of Abnormal Mammograms After Enhancement With Alpha Trimmed Mean Filter	246
3.2	Obtaining the Accuracies of Classification of Diagnosis of Abnormal Mammograms After Enhancement With Contrast Stretching	246
3.3	Obtaining the Accuracies of Classification of Diagnosis of Abnormal Mammograms After Enhancement With Histogram Equalization	247
3.4	Obtaining the Accuracies of Classification of Diagnosis of Abnormal Mammograms After Enhancement With CLAHE	247

3.5	Obtaining the Accuracies of Classification of Diagnosis of Abnormal Mammograms After Enhancement With RMSHE.....	247
3.6	Obtaining the Accuracies of Classification of Diagnosis of Abnormal Mammograms After Enhancement With Contra-Harmonic Mean.....	248
3.7	Obtaining the Accuracies of Classification of Diagnosis of Abnormal Mammograms After Enhancement With Mean Filter	248
3.8	Obtaining the Accuracies of Classification of Diagnosis of Abnormal Mammograms After Enhancement With Median Filter	248
3.9	Obtaining the Accuracies of Classification of Diagnosis of Abnormal Mammograms After Enhancement With Hybrid Median Filter.....	249
3.10	Obtaining the Accuracies of Classification of Diagnosis of Abnormal Mammograms After Morphological Enhancement.....	249
3.11	Obtaining the Accuracies of Classification of Diagnosis of Abnormal Mammograms After Morphological Enhancement, Followed by Contrast Stretching	250
3.12	Obtaining the Accuracies of Classification of Diagnosis of Abnormal Mammograms After Unsharp Masking.....	250
3.13	Obtaining the Accuracies of Classification of Diagnosis of Abnormal Mammograms After UMCA	250
3.14	Obtaining the Accuracies of Classification of Diagnosis of Abnormal Mammograms After Wavelet-Based Subband Filtering	251
4	Comparison of Classification Performance of the Enhancement Methods	251
5	Genetic Algorithm-Based Metaheuristic Approach to Customize a Computer-Aided Classification System for Enhanced Mammograms	252
6	Conclusion	254
7	Future Scope	254
	References.....	255
	Further Reading	259

CHAPTER 11 Embedded Healthcare System Based on Bioimpedance Analysis for Identification and Classification of Skin Diseases in Indian Context... 261

Pradeep M. Patil and Durgaprasad K. Kamat

1	Introduction.....	262
2	Need of Bioimpedance Measurement for Identification and Classification of Skin Diseases	263
3	System Developed for the Measurement of Human Skin Impedance	266
3.1	Skin Electrode.....	267
3.2	Impedance Converter IC AD5933	267
3.3	Microcontroller IC CY7C68013A.....	268
3.4	Personal Computer	269
4	Generation of a Database of Indian Skin Diseases.....	269
5	Impedance Indices for Identification and Classification of Skin Diseases	270
6	Identification of Skin Diseases.....	272
6.1	Wilcoxon Signed Rank Test.....	277
7	Measures of Classification of Skin Diseases	278
7.1	Box and Whisker Plot of Impedance Indices	278
7.2	Mean and Standard Deviation of Impedance Indices.....	280
8	Classification of Skin Diseases Using Modular Fuzzy Hypersphere Neural Network	281
9	Conclusion	286
	References.....	286

CHAPTER 12 A Hybrid CAD System Design for Liver Diseases Using Clinical and Radiological Data 289

Shrestha Bansal, Gaurav Chhabra, B. Sarat Chandra, Kriti and Jitendra Virmani

1	Introduction.....	289
2	Methodology Adopted	291
2.1	CAD System Design A	293
2.2	CAD System Design B.....	301
2.3	CAD System Design C: Hybrid CAD System	307
3	Discussion	310
4	Conclusion and Future Scope.....	311
	References.....	311
	Further Reading	314

CHAPTER 13 Ontology-Based Electronic Health Record Semantic Interoperability: A Survey 315

Ebtsam Adel, Shaker El-Sappagh, Sherif Barakat and
Mohammed Elmogy

1	Introduction.....	315
2	EHR and Its Interoperability	317
2.1	Introduction and Definitions	317
2.2	The Interoperability Benefits	319
2.3	The Different Interoperability Levels	320
2.4	EHR Semantic Interoperability Requirements.....	321
3	E-Health Standards and Interoperability	324
4	Ontologies and Their Role in EHR.....	332
5	Methods.....	336
5.1	Research Questions.....	336
5.2	Search Strategy	336
5.3	Search Results.....	337
5.4	Discussion.....	344
6	The Challenges of EHR Semantic Interoperability	346
7	Conclusion	347
	References.....	348

CHAPTER 14 A Unified Fuzzy Ontology for Distributed Electronic Health Record Semantic Interoperability..... 353

Ebtsam Adel, Shaker El-Sappagh, Sherif Barakat and
Mohammed Elmogy

1	Introduction.....	354
1.1	EHR Clinical and Business Benefits and Outcomes	355
1.2	EHR Semantic Interoperability Barriers and Obstacles	357
2	Related Work	360
3	Preliminaries	362
3.1	Techniques and Approaches of EHR Semantic Interoperability.....	362
3.2	EHR Standards.....	363
3.3	Ontologies.....	363
3.4	Terminologies	367
3.5	Semantic Interoperability Frameworks	369
3.6	Privacy and Security in EHR Systems.....	372
4	Methodology	373
4.1	The Proposed Framework.....	374
4.2	A Prototype Problem Example.....	381
4.3	A Comparison Study	389

5 Conclusion	389
References.....	389
Further Reading	395
Index	397

This page intentionally left blank

Contributors

Ebtsam Adel

Information Systems Department, Faculty of Computers and Information,
Mansoura University, Mansoura, Egypt

Saurabh Kumar Agrawal

Department of Electrical Engineering, Malaviya National Institute of
Technology (NIT), Jaipur, India

Shrestha Bansal

Indraprastha Institute of Information Technology, Delhi, India

Sherif Barakat

Information Systems Department, Faculty of Computers and Information,
Mansoura University, Mansoura, Egypt

Gaurav Chhabra

Jaypee University of Information Technology, Waknaghat, India

Nilanjan Dey

Department of Information Technology, Techno India College of Technology,
Kolkata, India

Mohammed Elmogy

Information Technology Department, Faculty of Computers and Information,
Mansoura University, Mansoura, Egypt

Shaker El-Sappagh

Information Systems Department, Faculty of Computers and Informatics, Benha
University, Banha, Egypt

Mohd Imran

Department of Computer Engineering, Aligarh Muslim University, Aligarh, India

Sunil Jardosh

Progress Software, Hyderabad, India

Durgaprasad K. Kamat

STES's SCOE, Pune, India

Heminder Kaur

Thapar Institute of Engineering and Technology (deemed-to-be university),
Patiala, India

Kriti

Thapar Institute of Engineering and Technology (deemed-to-be university),
Patiala, India

Anirudha Kumar

Department of Electrical Engineering, Malaviya National Institute of
Technology (NIT), Jaipur, India

Rajesh Kumar

Department of Electrical Engineering, Malaviya National Institute of Technology (NIT), Jaipur, India

Nimisha Manth

Jaypee University of Information Technology, Wakanaghhat, Himachal Pradesh, India

Mrudang D. Pandya

Information Technology Department, CHARUSAT, Anand, India

Pradeep M. Patil

JSPM's JSCOE, Pune, India

Mohammad Abdul Qadeer

Department of Computer Engineering, Aligarh Muslim University, Aligarh, India

Khalid Raza

Department of Computer Science, Jamia Millia Islamia, New Delhi, INDIA

B. Sarat Chandra

Jaypee University of Information Technology, Wakanaghhat, India

Saatvik Shah

Department of Computer Engineering, NIT Jaipur, Jaipur, India

Parth D. Shah

Information Technology Department, CHARUSAT, Anand, India

Nora Shoaip

Information Systems Department, Faculty of Computers and Information, Mansoura University, Mansoura, Egypt

BhanuPratap Singh

Department of Electrical Engineering, Malaviya National Institute of Technology (NIT), Jaipur, India

Shruti Thakur

Kamla Nehru Hospital, Shimla, India

Jitendra Virmani

CSIR-CSIO, Chandigarh, India

Preface

U-healthcare services allow the physician to monitor and manage the patient's health anywhere and anytime via the integration of medical technology, information communication technology, and wireless sensor technology. The present U-healthcare service emphasizes the common remote monitoring-based health management service and provides the biosignal measured information on a screen. The increased number of patients causes a rise in the required services that offer intelligent analysis and monitoring, irrespective of the patient's location. This motivates the necessity to develop U-healthcare monitoring systems that comprise notification in the urgent cases or at an unusual change in the patient's indicators as well as alarm services according to the patient's biosignal data and context awareness. Such a system offers more accurate measurement values compared to the traditional monitoring services due to its consideration of the patient's condition. Hence, it can reduce the patient's health risks based on the patient's measured records. This empowers the establishment of more specific and accurate—as well as more personalized—services to each patient/user.

This volume focuses on designing efficient algorithms and frameworks for U-healthcare monitoring systems that require the integration and development of the information technology service/facilities, wireless sensor technology, and clinical decision support systems (CDSS) so as to allow users to remotely check and manage their health conditions. Moreover, this volume includes recent studies that were conducted to engage the U-healthcare service in several applications. A wide variety of methods and techniques have been used to implement and design efficient monitoring systems to essentially manage patients who suffer from chronic diseases. This motivates engineers to design sensors, wireless systems, and wireless communication embedded systems to provide an integrated U-healthcare monitoring system. This volume intends to provide readers with the design and applications of the U-healthcare monitoring systems.

[Chapter 1](#) presents a standard, integrated, and implantable device for measuring heart rate that improves the estimation of the heart rate of the body and also counts the body temperature on the contextual information generated by the biosignal of the body by employing fingertip reading. The HRM module is an ergonomically standardized U-healthcare integrated device, which is helpful in rural areas.

Machine learning and Deep Learning play a vital role in analyzing medical data in U-healthcare. In [Chapter 2](#), a framework for efficient and automated creation of a variety of models geared toward the problem of classification of P300 signals is presented. We also present the classification results of intensive testing of multiple models on the data provided in the BCI Competition 3 Dataset 2, highlighting the behavior of key feature vectors and classifiers.

[Chapter 3](#) presents the state-of-the-art Deep Learning architectures such as the Convolutional Neural Network, the Deep Belief Network, the Deep Neural Network, the Recurrent Neural Network, the Stacked Auto-Encoder, and Long Short-Term

Memory. It also surveys their optimization techniques for effective medical image segmentation, classification, and analysis. The chapter also discusses the challenges in medical image analysis and open research issues.

Chapter 4 provides a comprehensive review of different reasoning techniques being used in CDSS, such as case-based reasoning (CBR), Mamdani fuzzy inference, and ontology systems. It also suggests that the hybridization of regular and mature crisp ontology reasoning with regular and mature Mamdani fuzzy reasoning is a good solution to the limitations of the current systems.

Chapter 5 explains the development of predictive regression models for day-to-day fitness, chronic kidney disease, and congestive heart failure using bioimpedance. The healthcare system for the measurement of bioimpedance and the estimation of total body water has been explained. The state-of-the-art measurement techniques for diagnosis of chronic kidney disease based on serum potassium concentration and congestive heart failure based on serum sodium concentration are further explained, along with their limitations.

Chapter 6 presents an SSVM-based multiclass system design using two binary classifiers: The SSVM classifier-1 classifies the HEM, HCC, and MET images into primary benign (HEM) and malignant (HCC or MET) cases, which are further classified by the SSVM classifier-2 into primary malignant (HCC) and secondary malignant (MET) cases.

Chapter 7 provides hybrid ontology-based fuzzy CDSS that can improve reasoning capabilities by adding a semantic reasoning mechanism to enhance the overall system intelligence. The system explicitly defines the semantics of diabetes knowledge by using OWL 2 ontology and deals with the imprecise and vague nature of its data by using fuzzy set theory. The proposed hybrid system emphasizes the significance of combining ontology and Mamdani fuzzy inference for diagnosing diabetes.

Chapter 8 presents different machine learning techniques and their ensemble effect on the prediction of heart diseases using the majority voting technique.

Chapter 9 presents a high-performance artificial neural network (ANN)-based algorithm optimized via Directed Bee Colony (DBC) to diagnose cancer, diabetes, and heart disease. A comprehensive comparison of different metanalytic studies is performed on 16 algorithms.

Chapter 10 presents a genetic algorithm-based metaheuristic approach to customize a computer-aided classification system for enhanced screen film mammograms. The effect of 14 different enhancement methods is also demonstrated.

Chapter 11 contributes toward real-time data collection, data management, system design, and analysis related to the embedded U-healthcare system's noninvasive identification and classification of skin diseases in the Indian context. The various challenges faced by dermatologists in identification and classification of skin diseases are described with reference to state-of-the-art dermatological practices. The chapter further describes a system developed for the measurement of human skin impedance.

Chapter 12 presents three different CAD systems for diagnosis of benign and malignant liver tumors based on clinical, radiological, and hybrid data. The SSVM classifier has been exhaustively used for the classification task.

Chapter 13 presents a comprehensive survey of the healthcare semantic interoperability, including its definitions, standards, schemas, models, terminologies, barriers, and future challenges using the databases ScienceDirect, IEEE Xplore, PubMed, ELSEVIER, MEDLINE, Cochanelibrary, Informit, and Springer.

Chapter 14 presents a unified semantic interoperability framework for distribution of EHR based on fuzzy ontology. This framework is expected to handle the current EHR semantic interoperability challenges, reduce the cost of the integration process, and get a higher acceptance and accuracy rate than the previous studies. While the approach of electronic remote health monitoring frameworks has been guaranteed to change regular healthcare strategies, coordinating the IoT worldview into these frameworks can additionally expand knowledge, adaptability, and interoperability. The developed framework gives a programmed alert to the closest healthcare service organization in case of a basic mischance for a regulated patient.

This book is useful to researchers, practitioners, manufacturers, professionals, and engineers in the field of biomedical systems engineering and may be referred to by students for advanced material.

We would like to express gratitude to the authors for their contributions. Our gratitude is extended to the reviewers for their diligence in reviewing the chapters. Special thanks to our publisher, Elsevier.

As editors, we hope this book will stimulate further research in developing algorithms and optimization approaches related to U-healthcare systems and machine learning for biomedical applications.

Volume Editors

Nilanjan Dey

Techno India College of Technology, Kolkata, India

Amira S. Ashour

Faculty of Engineering, Tanta University, Egypt

Simon James Fong

University of Macau, Taipa, Macau SAR

Surekha Borra

K.S. Institute of Technology, Bangalore, India

This page intentionally left blank

Wearable U-HRM device for rural applications

1

Mohd Imran, Mohammad Abdul Qadeer

Department of Computer Engineering, Aligarh Muslim University, Aligarh, India

CHAPTER OUTLINE

1	Introduction	1
2	U-Healthcare System in India	4
3	Application	4
4	Open Issues and Problems	5
5	Requirements of a Healthcare System	6
6	Requirement of Wearable Devices	7
7	Implementation	7
8	Measurement of Heart Rate and Body Temperature	8
9	Discussion	11
10	Conclusion and Future Trends	11
	References	12

1 INTRODUCTION

In the present era, IoT devices, which are a collection of multiple sensors embedded on a small single chip that is also called wearable tech, are the most common technology that continuously observes the surrounding ambient environment of a subject, then processes and analyzes that to display the desired outcome [1]. The number of wearable devices is growing at an explosive rate. According to estimates, if the rate of expansion continues, then by the year of 2020, wearable devices connected together in the world will number approximately 26 billion. This wearable technology is very reliable for measurement and early detection of diseases. These miniature sensors have a very productive application in the medicine and technology fields. The prime focus of researchers is to develop a hybridized environment where the human body is blended with these small sensors, either embedded in garments or implanted as an integrated device. They would then continuously track the biosignals generated in the body and feed the system with enormous clinical data [2]. The main

objectives of integrated wearable sensors are: (1) design and development that can accurately and obtrusively detect and record biosignals in the body, (2) deliver the biosignal data gathered through continuous monitoring to the clinical experts in a form that is entirely acceptable, and (3) design of an algorithm that can take these clinical data as an input and successfully extract the relevant data to generate possible outcomes of these physiological signals [3].

This wearable technology has tremendous applications in rehabilitation and continuous monitoring because diseases are growing at an exponential rate these days. Six out of ten people are suffering from various diseases, some of which are chronic or inherited such as diabetes, color blindness, etc. According to the data given by the World Health Organization [4], lung cancer, diabetes [5], obesity, high blood pressure, and cholesterol, are the major diseases that cause suffering all around the world. According to data provided by WHO, 4.9 million people are suffering from lung cancer due to excessive consumption of alcohol, and 7.1 million people are suffering from high blood pressure [6].

The worst habit of people is to avoid the symptoms as long as possible, which can sometimes lead to death. There are various possible reasons for such mistakes, including a lack of proper equipment as well as the unavailability of professional advisors and hospitals for special care. In underdeveloped countries, where all these problems are common, the ubiquitous healthcare monitoring system is a boon. Because these pervasive monitoring systems are small in size, less expensive, and easy to use, any person can use them anywhere, anytime.

Big data analytical tools are also an important key to the ubiquitous healthcare system [7]. By using analytical tools such as Hadoop, Sparks, etc., a huge medical database can be generated demographically [8]. Features can be extracted using any method such as component-based methods in order to classify the properties of collected data [5]. By using distributed computing, we can upload the basic symptoms that may be affected by demographic reasons. Therefore, mining the relevant data and the important and relevant keys to disease can be obtained, leading to more effective cures. When disease and its symptoms and possible solutions are available on a medical repository, this will be more reliable and effective for people around the globe.

In the near future, people will be surrounded by wearable ubiquitous wireless equipment that will assist them in all the needs of daily life. As the days pass by, people are indulging in a larger tech environment rather than sticking with traditional methods. In recent years, various studies have been conducted to develop a full body-suit that is composed of numerous sensor-monitoring circuits that can provide multiple applications, such as electrocardiogram (ECG), skin temperature measurement, etc. Researchers at the MIT media lab have developed MITHRILL [9], which is a wearable platform consisting of sensors and monitors to examine the human body. The same body suit is also used for gait analysis for understanding human behavior and cognitive computing. For the gait, MITHRILL is equipped with rate gyros, a three-axis accelerometer, and a pressure sensor. A human body is the best workplace for exploring and understanding cognitive computing as it is a source of biosignals, which are responsible for many routine processes. This ubiquitous monitoring device

focuses on the human body by continuously sensing and measuring physical phenomena. This technology has extensive applications in the medical field. By wearing these small ubiquitous healthcare devices, people can diagnose their body by themselves, thereby eliminating or reducing the need for clinical assistance. The data generated by diagnosis can also help the doctor in their treatment.

In brief, we will see that wearable technology has increased the productivity of diagnostics and biomeasurement systems. The wide range of application includes patient tracking as well as the monitoring of health and information applications for doctor-patient management systems [10,11]. Through the use of these technologies, numerous problems can be mitigated. Every physiological and psychological problem can be successfully monitored and diagnosed using the same technologies. Numerous diseases such as cardiovascular and neurological as well as noncommunicative diseases such as cancers [12] can be treated from detection to final procurement [12,13].

In comparison with rural areas, the healthcare management system is quite complex and naïve in urban areas. Remote monitoring systems have the potential to mitigate problematic patient access issues. Nearly 20% of those in the United States live in rural areas, but only 9% of physicians work in these rural areas [8]. Access may get worse over time as many organizations are predicting a shortfall in primary care providers as healthcare reform provides insurance to millions of new patients [9]. There is a large body of literature that describes the disparities in care faced by rural residents [8]. Compared to those in urban areas, those in rural areas travel two to three times farther to see a physician, see fewer specialists, and have worse outcomes for such common conditions as diabetes and heart disease [9,10]. Wearable sensors and remote monitoring systems have the potential to extend the reach of specialists in urban areas to rural areas, decreasing these disparities.

A conceptual representation of a system for remote monitoring is shown in Fig. 1. Wearable sensors are used to gather physiological and movement data, thus enabling monitoring of a patient's status. Sensors are deployed according to the clinical application of interest. Sensors to monitor vital signs (e.g., heart rate and respiratory rate)

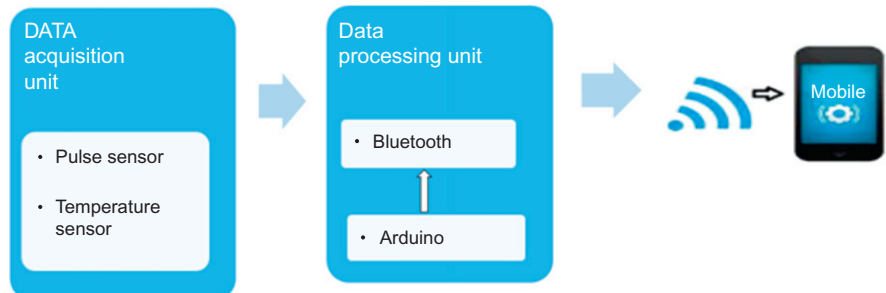


FIG. 1

System block diagram.

would be deployed, for instance, when monitoring patients with congestive heart failure or patients with chronic obstructive pulmonary disease undergoing clinical intervention. Sensors for movement data capturing would be deployed, for instance, in applications such as monitoring the effectiveness of home-based rehabilitation interventions in stroke survivors or the use of mobility assistive devices in older adults. Wireless communication is relied upon to transmit a patient's data to a mobile phone or an access point and relay the information to a remote center via the Internet. Emergency situations (e.g., falls) are detected via data processing implemented throughout the system; an alarm is sent to an emergency service center to provide immediate assistance. Family members and caregivers are alerted in case of an emergency but could also be notified in other situations when the patient requires assistance with, for instance, taking his/her medications. Clinical personnel can remotely monitor a patient's status and be alerted in case a medical decision has to be made.

2 U-HEALTHCARE SYSTEM IN INDIA

India has endeavored to make the public healthcare system more robust and reliable by blending the technological evolution with medical practices [14]. The healthcare system in rural areas across various parts of India is unique as well as complex. In these suburban areas, people are unaware of medical assurance and pervasive health-care plans. Every year, the Indian government invests numerous funds through the ministry of health and rural development in various medical plans regarding health issues of senior citizens, pregnant women, and children [13]. But due to a lack of professional healthcare advisors, inefficient medical delivery, lack of prime technology, and adherence to quality, these plans go to waste. In India, a large proportion of the population still makes their habitat in rural areas; there is a wide gap between the rural and urban population in numerous ways. These people have low accessibility to advanced medical supplies and hospitals. Therefore, they have to make their traditional way for living and healthcare or rely on government organizations. The government allies with local partners in these rural areas to provide a better alternative and reduce the living difference between rural and urban areas. But still, the people aren't capable of taking advantage of such effective schemes due to a lack of knowledge and moral support.

Hence, in such a scenario, we need to provide an approachable and effective mechanism that will cover a larger portion of the rural area. The most promising approach is the ubiquitous health monitoring systems.

3 APPLICATION

The most promising application of the health monitoring system is for the remote care of patients from a far distance. Sometimes this ubiquitous computing used in medical practices is also referred to as telemedicine [15]. By using a telemedicine

approach such as wireless monitoring of cardiac patients, it can be a boon by the constant monitoring of the heart status of patients. Remote monitoring is a most promising approach in rural areas as doctors can take care of patients from a large distance, which can be a mile or a state or a country.

Another emerging trend of ubiquitous healthcare systems is the wearable nature [16]. The practice of medicine along with the new technology of wearable suits is making a revolutionary change in the medical field. These wearable suits consist of chip combinations, also known as a motherboard or a printed circuit board (PCB) [17]. This PCB is a collection of numerous sensors as well as tracking and monitoring devices that continuously monitors the health of people and transmits the data wirelessly so that it can be mobile and truly ubiquitous in nature. People wear the monitoring device in any part of their body, and it then continuously measures various biosignals and gathers information on the ECG, temperature, heart rate, blood pressure, and blood sugar. The data gathered is then sent over the main system wirelessly. Hence such a system is easy to use as there is no need to visit the doctor more often. The concerned doctor can check the patient's status and also convey advice more promptly.

Sports is another major field for the implementation and application of ubiquitous health applications. For health issues, the fitness experts have to know the heart rate and body temperature of the athletes. They continuously measure the heart rate during a performance to ensure that their performance is unaffected. The increased heart rate from normal days may be the sign of a bad impact. So by employing the remote healthcare devices, they can monitor their performance easily.

4 OPEN ISSUES AND PROBLEMS

The medical healthcare system using the ubiquitous approach is a proven boon. Although it saves money as well as time, it also has some open issues and concerns regarding security and privacy of user data. As all the data are sent wirelessly to the main controller, there might be a chance of loss of data or a hack into the data. These are some major concerns that must be addressed in the healthcare system [18]. The introduction of ubiquitous computing is an emerging approach while at the same time it has generated many novel challenges such as reliable transmission of data, data corruption, changes in the original data, and loss in data. Sometimes, privacy regarding the patient's disease is also an important concern as patients do not want to disclose the nature of their disease [19,20]. So whenever we want to deploy a ubiquitous HRM system, we need to provide an extreme security mechanism to insure the reliability of system [21]. These are some important fields in which we have to provide extra care:

- (i) Data authentication
- (ii) Data integrity
- (iii) Data confidentiality

- (iv) Data security
- (v) Data repudiation
- (vi) Data loss
- (vii) Sender authentication
- (viii) Recipient authentication
- (ix) Communication channel security
- (x) End-to-end security
- (xi) Data encryption and decryption

Various authors have performed a survey of the literature on medical healthcare applications and their numerous challenges. Meingast et al. [22] have discussed the privacy concerns of patients such as (a) data permission of data, (b) data ownership, (c) from which resource the data has to be collected and from whom, (d) who has permission to examine the data, and (e) who is authorized to see the data without the patient's permission. In European countries, medical data is treated as sensitive material and major rules and regulations have been implemented regarding access and permission to these data so that no violation of a user's privacy can occur [5,23].

5 REQUIREMENTS OF A HEALTHCARE SYSTEM

These types of medical healthcare systems have to be technically accurate. So during the implementation of these systems, extensive parameters have to be specified. During the implementation, we need the following:

- (1) *Pulse sensor*: A pulse sensor is required to read the ups and downs of pulse through the flow of blood in the finger.
- (2) *Temperature sensor*: A temperature sensor is also fixed to read the body temperature of the subject.
- (3) *LED*: A light-emitting diode is also required. It must be able to continuously emit the light on the fingertip and read the presence and absence of blood flow in veins by measuring opacity.

These sensors can be fixed on the hand strap for the data acquisition unit. Besides these sensors, we require the data processing devices that are described below:

- (1) *Arduino kit*: The Arduino Uno board is a microcontroller based on the ATmega328. It has 14 digital input/output pins. It is easy to operate as it can be easily connected to the computer via a USB cable, AC to DC adapter, or by using battery attachment. It sends the data wirelessly to any Android smartphone via Bluetooth.
- (2) *A/D convertor*: An analog-to-digital convertor is required to convert the obtained analog data in digital form. It is then sent to the Arduino microcontroller for further processing.

After processing and measurement of the various parameters, we need a display unit for notifying the doctor/patient about their health. For this we need a U-HRM application on the Android smartphone that will accept the wireless data from the Arduino microcontroller and display it. Numerous other features can be explored such as automatic notification of health every hour as well as doctor consultation and notification regarding patient feedback. Similarly, it can suggest to the patient formal prevention methods to control variations in health.

6 REQUIREMENT OF WEARABLE DEVICES

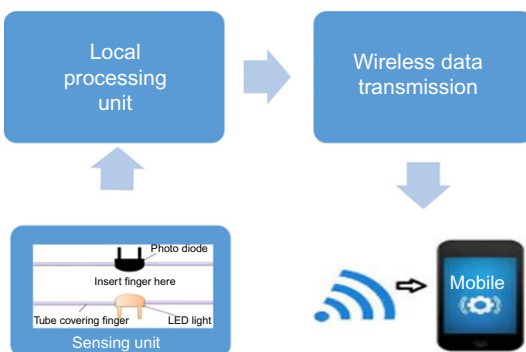
In order to be more sensitive to health measurements, the device must have certain requirements that have to be fulfilled:

- (1) *Selection of body part:* The wearable device should be planted or enclosed where the efficiency of the device should be enhanced. The selection of body part is very crucial as it affects the actual operation of the wearable device.
- (2) *Selection of material:* The material on which we are going to stick the device must be biocompatible. During the selection of the material of encapsulation, we have to be sure that the body must be nonallergic to the material of choice. The material should be potentially strong while refraining from physical changes of body temperature, humidity, and the electrical short circuit in the electronic board.
- (3) *Selection of sensors:* The designing of the circuit board of the wearable device should be such that it is compatible with multiple integrated sensors. It should be enriched with heat sensors, pulse sensors, a glucometer, GPS, a gyrometer, a pedometer, and more such sensors.
- (4) *Equipped with enhanced UI:* Because our wearable device is supported by Android OS, it provides a good visual UI, which is also an essential requirement for the wearable devices.

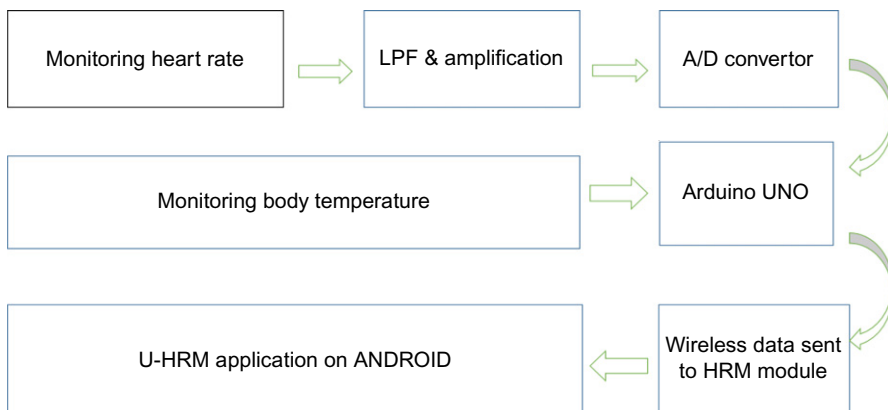
7 IMPLEMENTATION

The U-HRM device is attached on the patient's fingertip to continuously monitor the heart rate along with the temperature fluctuations in the body. The block diagram and function diagram of the proposed system is discussed later ([Fig. 2](#)).

The proposed U-HRM device in [Fig. 3](#) consists of three different modules: the data acquisition unit, the data processing unit, and the U-HRM application on the handheld device for displaying the result. Pulse sensors and temperature sensors and two sub-modules in the data acquisition unit [24]. After gathering the data, the data processing unit handles the analysis, which is performed by a low-pass filter for noise removal and, after performing, amplification, the electrical biosignal is converted into its digital equivalent by employing an analog-to-digital convertor. The digitized data is then sent

**FIG. 2**

Insight block diagram of U-HRM device.

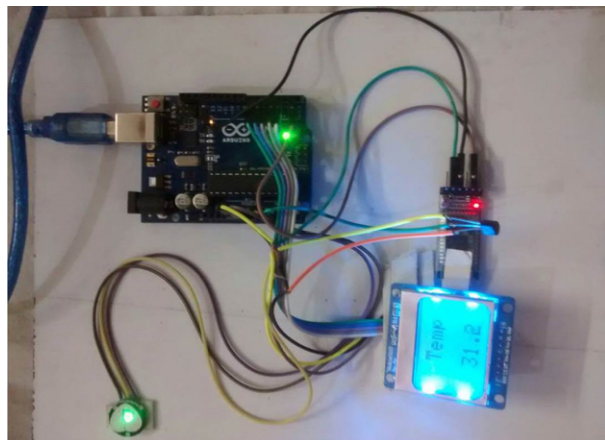
**FIG. 3**

Functional diagram of U-HRM device.

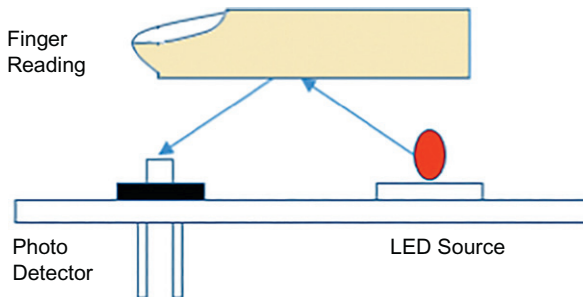
to the Arduino kit, which then transmits the wireless data to the U-HRM module. At the customer's end, there is an HRM application that receives the data and displays the result ([Figs. 4 and 5](#)).

8 MEASUREMENT OF HEART RATE AND BODY TEMPERATURE

Blood is continuously flowing throughout the entire body via the veins. There is a slight time difference between each pump of blood in the heart. The HRM device is placed on the fingertip. The LED continuously emits a bright light on the tip. Now, when there is blood in the finger's blood vessel, it has a more opaque nature

**FIG. 4**

Connection of U-HRM module with Arduino kit.

**FIG. 5**

Fingertip reading for measurement.

in comparison to when there is an absence of blood pressure in the veins; therefore, the light from the LED has less penetration on the fingertip. Now the light reflected from the fingertip is cut off and the light detector receives nothing. So with each heart pulse, the signal of the light detector varies. The presence and absence of the light is then converted into an equivalent electrical signal through the circuit.

The time duration up to which the light falling on the LDR, it goes on disturbing which yields the duration of heart pulse and inverting this time will give the count of heartbeat per minute. Because the electrical signal is analogue in nature and weak, it is fed to an amplifier that enhances and calibrates the signal. The circuit consists of the resistor, which shapes the square wave nature of the signal, and the capacitor, which acts as a feedback capacitor that stores the data and is fed further to the microcontroller device.

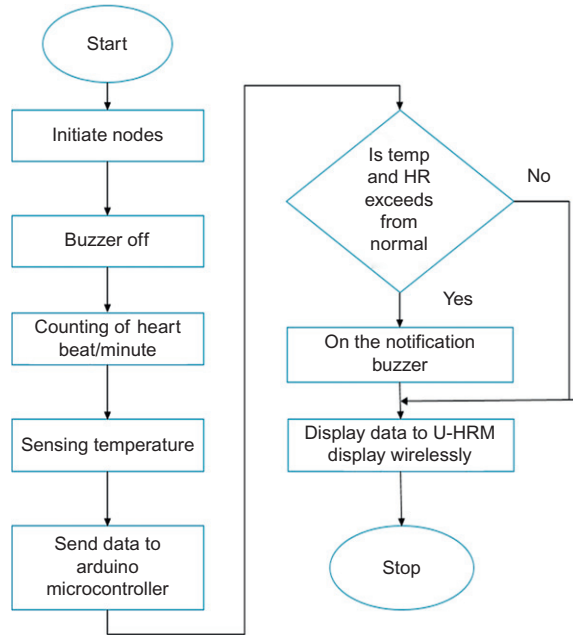


FIG. 6

Flow chart of working principal of U-HRM device.

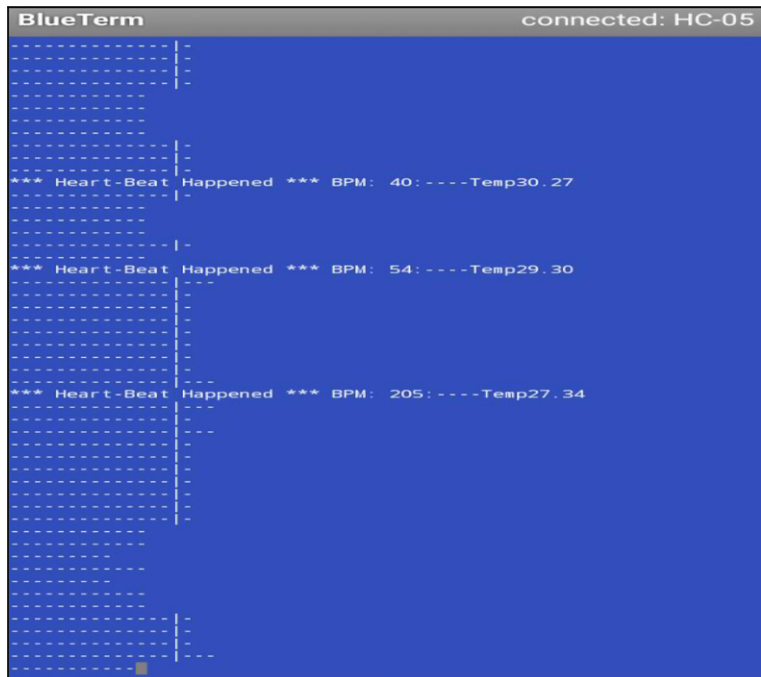


FIG. 7

U-HRM application on Android device.

For the measurement of body temperature, we employed a temperature sensor that is in contact with the skin and placed on the wrist. This sensor will give the analogue output voltage measured by the microcontroller and then converted to an equivalent digital form using an A/D convertor.

The combined reading is then sent to the Arduino controller wirelessly. The wireless communication can be of any type. In our module, we have used Bluetooth for the communication between the data analysis module and display application on the handheld device. The flowchart for the complete implementation is explained in Fig. 6 and the U-HRM application output is shown in Fig. 7.

9 DISCUSSION

The advent of wearable technology has had a deep impact on both the technical revolution and biomedical engineering. This wearable technology has given a tremendous push to the understanding and treatment of various motor, communicative, and noncommunicative diseases. For deployment of wearable sensor, the understanding of the motor physiological pattern and numerous characteristics of movement patterns used in the clinical perspective are very necessary. This development helped in the rehabilitation of various diseases such as Parkinson's [25,26], rest tremors [27], bradykinesia, rigidity, and impairment of postural balance [28,29]. By using such sensor technology, it is feasible to understand and keep track of continuous or periodical improvements in such diseases after a stroke [5,30,31].

10 CONCLUSION AND FUTURE TRENDS

This ubiquitous health monitoring system was developed to achieve a smart, accurate, and integrated device that will be economically better and more powerful. The prime objective is to deploy this monitoring device in rural areas where people have less access to affordable hospitals, doctors, and medical supplies. In rural areas, a doctor team's visit is less often and due to a lack of knowledge, people are not capable of fully utilizing their help. Sometimes it is also crowded, so very few people can get their health checkups. By keeping these things in mind, we have integrated this device that is user friendly and more accurate. The patient can easily wear this device on their wrist due to its small size. Monitoring is very easy as they have to put their fingertip on the LED and their evaluation of the heartbeat and temperature will be shown on their U-HRM application on Android devices by wirelessly transmitted data.

In the near future, as the Internet of Thing emerges in daily life, solutions and such types of healthcare monitoring devices will evolve [32].

GLOSSARY

Data decryption and encryption	It is an extra overlay on data security. By using these methodologies, one can insure only an authorized person can access and understand the data. It is an important and vital parameter when data is communicated wirelessly.
Data integrity	Data integrity infers no alteration or loss in the data after its successful reception.
HRM	Heart rate monitoring system.
Data repudiation	Data repudiation is an important threat in data security. This threat generally occurs in data communication where one party rejects or violates the agreement of some issue that has already been agreed upon.
Internet of things	It is an emerging technology that enables devices to communicate with each other. It implements the vision of ubiquitous computing [33].
Noncommunicable disease	Those diseases that have a long duration and chronic nature, for example, cardiovascular diseases such as heart attack, stroke, etc., as well as cancers (lung cancer).
Ubiquitous computing [34]	Ubiquitous computing is an emerging trend of the Internet of Things that is also sometimes called pervasive computing. The ubiquitous computing nodes are always connected to the network and can be accessed from anywhere [35].

REFERENCES

- [1] O. Arias, S. Member, J. Wurm, S. Member, Privacy and security in internet of things and wearable devices, *IEEE Trans. Multi-Scale Comput. Syst.* 1 (2015) 99–109.
- [2] P. Bonato, Advances in wearable technology and applications in physical medicine and rehabilitation, *J. Neuroeng. Rehabil.* 2 (2005) 2.
- [3] N. Dey, A. Ashour, Classification and Clustering in Biomedical Signal Processing. (Medical Information Science Reference), (2016). <https://doi.org/10.4018/978-1-5225-0140-4>.
- [4] J. Gómez, B. Oviedo, E. Zhuma, Patient monitoring system based on internet of things, *Procedia—Procedia Comput. Sci.* 83 (2016) 90–97.
- [5] L. Saba, et al., Automated stratification of liver disease in ultrasound: an online accurate feature classification paradigm, *Comput. Methods Prog. Biomed.* 130 (2016) 118–134.
- [6] World Health Organization. Global status report on noncommunicable diseases 2010. World Health 176 (2010). <https://doi.org/978-9-2415-6422-9>.

- [7] V. Yadav, M. Verma, V.D. Kaushik, Big data analytics for health systems, in: Proceedings of the 2015 International Conference on Green Computing and Internet of Things (ICGCIoT), 2015, pp. 253–258.
- [8] Yu, W. D. et al. Big data analytics in service computing—HealthCare. 170–173 (2016). <https://doi.org/10.1109/MobServ.2016.45>.
- [9] C. Otto, A. Milenković, C. Sanders, E. Jovanov, System architecture of a wireless body area sensor network for ubiquitous health monitoring, *J. Mob. Multimed.* 1 (2006) 307–326.
- [10] X. Teng, Y. Zhang, C.C. Poon, P. Bonato, Wearable medical systems for p-health, Undefined, ieeexplore.ieee.org, 2008.
- [11] Biology, P. B.-I. E. in M, Wearable sensors and systems, Undefined, ieeexplore.ieee.org, 2010.
- [12] S. Gulley, E. Rasch, L.C.-M. Care, If we build it, who will come?: Working-age adults with chronic health care needs and the medical home, Undefined, ncbi.nlm.nih.gov, 2011.
- [13] S. Lakshminarayanan, Role of government in public health: current scenario in India and future scope, *J. Family Community Med.* 18 (2011) 26–30.
- [14] Gross National Happiness Commission. Eleventh Five Year Plan. III, (2013).
- [15] H.S. Ng, M.L. Sim, C.M. Tan, C.C. Wong, Wireless technologies for telemedicine, *BT Technol. J. @ BULLET* 24 (2006).
- [16] S. Park, S. Jayaraman, Enhancing the quality of life through wearable technology, *IEEE Eng. Med. Biol. Mag.* 22 (2003) 41–48.
- [17] F. Miao, Y. Cheng, Y. He, Q. He, Y. Li, A wearable context-aware ECG monitoring system integrated with built-in kinematic sensors of the smartphone, *Sensors (Switzerland)* 15 (2015) 11465–11484.
- [18] R. Di Pietro, L.V. Mancini, Security and privacy issues of handheld and wearable wireless devices, *Commun. ACM* 46 (2003) 74–79.
- [19] M.Y. Khachane, Organ-based medical image classification using support vector machine, *Int. J. Synth. Emot.* 8 (1) (2017) 18–30.
- [20] N. Dey, A.S. Ashour, A.S. Althoupety, Thermal imaging in medical science, in: Recent Advances in Applied Thermal Imaging for Industrial Applications, IGI Global, New Delhi, 2017, pp. 87–117.
- [21] M. Al Ameen, J. Liu, K. Kwak, Security and privacy issues in wireless sensor networks for healthcare applications, *J. Med. Syst.* 36 (2012) 93–101.
- [22] M. Meingast, T. Roosta, S. Sastry, Security and privacy issues with health care information technology, 2006 International Conference of the IEEE Engineering in Medicine and Biology Society, vol. 1, IEEE, 2006, pp. 5453–5458.
- [23] EU Directive 95-46-EC—Chapter 1—Data Protection Commissioner—Ireland.
- [24] L. Zimu, et al., Wireless health monitoring system, 2010 IEEE Long Island Systems, Applications and Technology Conference, IEEE, 2010, pp. 1–4, <https://doi.org/10.1109/LISAT.2010.5478274>.
- [25] S. Katayama, Actigraph analysis of diurnal motor fluctuations during dopamine agonist therapy, *Eur. Neurol.* 46 (2001) 11–17.
- [26] J.W. Tetrud, Balancing short-term symptom control and long-term functional outcomes in patients with Parkinson's disease, *CNS Spectr.* 12 (2007) 275–286.
- [27] E.J.W. Van Someren, et al., A new actigraph for long-term registration of the duration and intensity of tremor and movement, *IEEE Trans. Biomed. Eng.* 45 (1998) 386–395.
- [28] Share, P., Vision, T., Applications, F. C. & Technology, W. Predicting the potential. 23–27 (2003).

- [29] K. Sharma, J. Virmani, A decision support system for classification of normal and medical renal disease using ultrasound images, *Int. J. Ambient Comput. Intell.* 8 (2017) 52–69.
- [30] D.A. Kozlowski, D.C. James, T. Schallert, Use-dependent exaggeration of neuronal injury after unilateral sensorimotor cortex lesions, *J. Neurosci.* 16 (1996) 4776–4786.
- [31] R.J. Nudo, B.M. Wise, F. SiFuentes, G.W. Milliken, Neural substrates for the effects of rehabilitative training on motor recovery after ischemic infarct, *Science* 272 (1996) 1791–1794.
- [32] F. Hu, D. Xie, S. Shen, in: On the application of the internet of things in the field of medical and health care, 2013 IEEE International Conference on Green Computing and Communications and IEEE Internet of Things and IEEE Cyber, Physical and Social Computing, IEEE, 2013, pp. 2053–2058, <https://doi.org/10.1109/GreenCom-iThings-CPSCom.2013.384>.
- [33] F. Wortmann, K. Flüchter, Internet of things: technology and value added, *Bus. Inf. Syst. Eng.* 57 (2015) 221–224.
- [34] G. Banavar, A. Bernstein, Software infrastructure and design challenges for ubiquitous computing applications, *Commun. ACM* 45 (2002) 92–96. ST—Software infrastructure and design cha.
- [35] M. Imran, M. Shadab, M.M. Islam, M. Haque, Skin detection based intelligent alarm clock using YCbCr model, in: S. Satapathy, A. Joshi (Eds.), *Information and Communication Technology for Intelligent Systems (ICTIS 2017) – Volume 2. ICTIS 2017. Smart Innovation, Systems and Technologies*, vol. 84, Springer, Cham, 2018.

A robust framework for optimum feature extraction and recognition of P300 from raw EEG

2

Saatvik Shah*, Anirudha Kumar†, Rajesh Kumar†, Nilanjan Dey‡

Department of Computer Engineering, NIT Jaipur, Jaipur, India* Department of Electrical Engineering, Malaviya National Institute of Technology (NIT), Jaipur, India† Department of Information Technology, Techno India College of Technology, Kolkata, India‡

CHAPTER OUTLINE

1 Introduction	15
2 Literature Survey	17
3 The Framework	19
3.1 Initialization	19
3.2 Model Setup	20
3.3 Postprocessor	21
3.4 Classification	25
4 Results and Discussion	26
4.1 The Dataset	27
4.2 Framework Results	27
5 Conclusion and Future Work	32
References	33

1 INTRODUCTION

A recent surge has been witnessed in the inflow of unique innovations for bolstering those handicapped people who have been severely disabled, such as the recent eye-tracker systems and assistive computer interfaces technologies. Direct brain computer interfaces (BCI) are one such means of interfacing that provide promising results and will have a large scope in the future [1]. They provide an augmentative communication method for patients with severe motor disabilities and those suffering from “locked-in” syndrome due to severe paralysis. Recent developments in

BCI-based systems include word spellers, cursor control, wheelchair control, neuroprostheses, and environment control [2].

Several paradigms have been introduced in BCI to stimulate generation of specific brain-oriented signals [3, 4]. Three significant and commonly generated neuro-signals are event-related desynchronization (ERD), which is triggered as sensorimotor rhythms over primary sensor/motor-cortical areas resulting from imagining movements of motor body parts; steady-state visually evoked potential (SSVEP) [5], which is spawned as an involuntary response to visual stimulation at specific frequencies, and slow cortical potential (SCP), which is triggered when slow voltage changes occur in the cortex due to cortical activation [6].

The P300 Oddball paradigm is one of the oldest and most useful applications of BCIs. P300 is an event-related potential, categorized under the set of ERD signals, induced during the process of decision making in reaction to an external stimuli. When elicited, it results in a positive deflection of voltage at a delay of around 300 ms, which can be observed in electroencephalogram (EEG) recordings. The averaging of EEG is a common method to reduce noise and time variance. P300 is especially useful in this respect as it is generated in short spells, making it possible to average multiple results obtained from the same stimulus source while also making it easier to infer its presence and obtain high P300 classification accuracy. Fig. 1 shows the presence of a P300 signal peak in the raw time series EEG data obtained from the Cz channel obtained by averaging the signals.

The chapter first proposes a robust framework, which automates the complete process of testing and detecting P300 signals by providing unique modules for pre-processing, feature extraction, and final classification by the use of linear/nonlinear classifiers. The feature vectors have been prepared by stacking different features obtained from raw EEG data. The feature extraction pipeline uses EEG-processing methods that have been studied in the available literature, popular signal-processing techniques, and finally a couple of newly proposed techniques by the authors. The classification pipeline applies a variety of classifiers in the framework on the feature set. The workflow for detecting P300 signals, as used in the proposed paper and framework, can be applied to any dataset. There has been a focus on modularity, ensuring that every block of the workflow is divided into flexible user-configurable modules. Parallel programming to make the most of a multicore architecture,

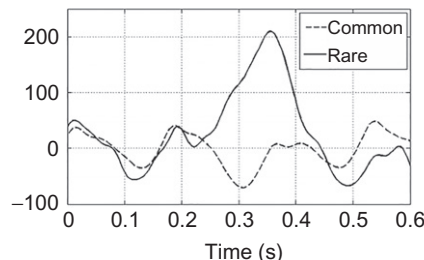


FIG. 1

P300 waveform at Cz channel.

ensuring rapid intensive module testing and caching to adhere to the principle of fast reusability of previously computed results, has also been followed.

The results have been obtained by testing the proposed framework with features extracted from raw EEG data of BCI Competition 3 Dataset 2, where subjects were made to spell a number of letters on a predefined grid. Previous research with respect to P300 has been more focused on obtaining the optimum classifier. However, the author's research work culminated in both feature extraction as well as classifier selection with a focus on deriving the most optimum features.

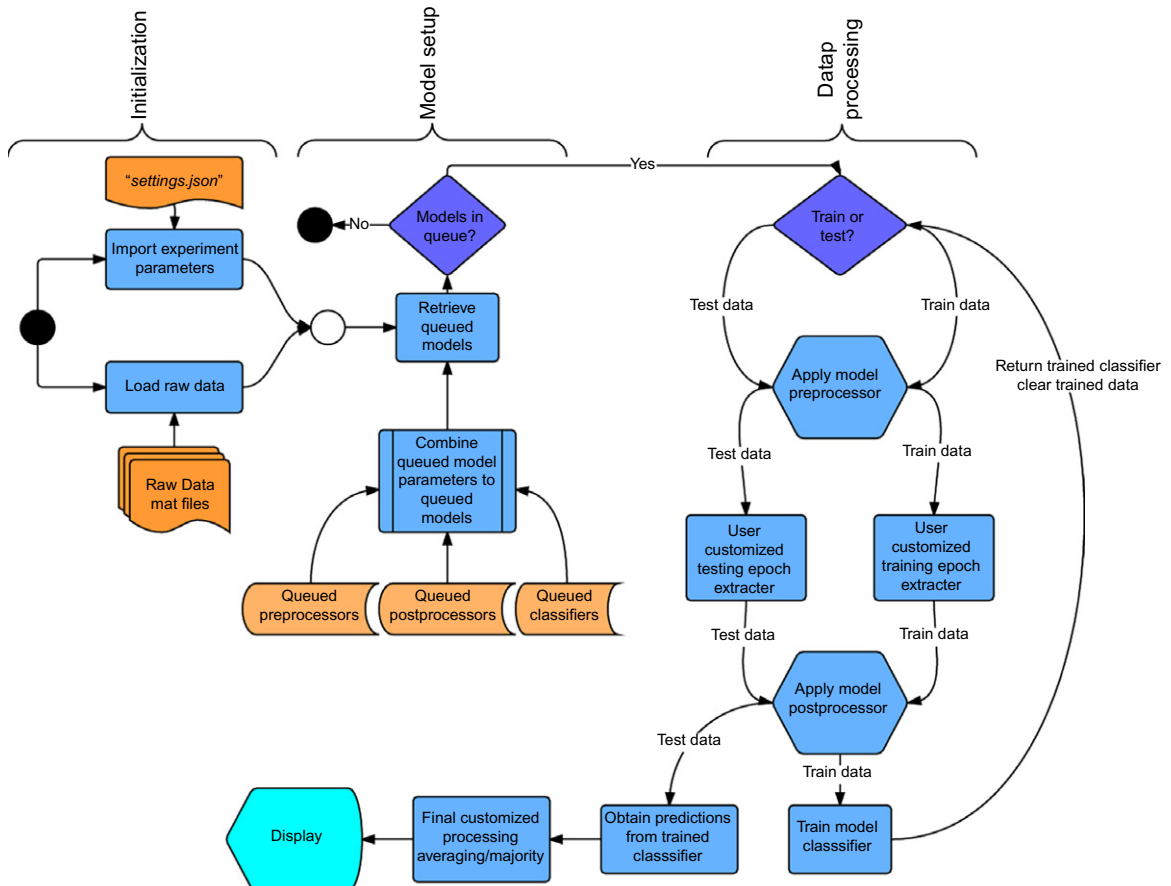
The proposed workflow was successful in providing competitive accuracies for a large as well as a small number of trials for the same training sessions as previously successful methods.

Finally, the proposed framework will be released in open source to allow use by other researchers.

This chapter is further organized as follows: [Section 2](#) provides a summary of related work, [Section 3](#) provides a comprehensive explanation of the framework used, [Section 4](#) explains the inferences and results obtained from testing the framework, and finally [Section 5](#) concludes the paper and elaborates on the future goals of this research.

2 LITERATURE SURVEY

This section provides a comprehensive study of the abundant literature available on the detection of P300 signals in EEG. The P300 speller shown in [Fig. 1](#) is the most common application of the P300 signal and most of the literature given below is applicable to the same. Many researchers have used SVMs as most of the BCI systems apply supervised learning classification. SVM creates a model based on non-probabilistic binary linear classifiers. Gu et al. [7] used a semisupervised method of a self-training sequential update of a least squares support vector machine (LS-SVM) classifier of the online detection of P300. The kernel-based learning methods such as self-training LSSVM (ST-LSSVM) for semisupervised batch processing is presented, followed by its sequential updating version, SUST-LSSVM. Sequential updating self-training-LSSVM (SUST-LSSVM) was applied in the BCI system for sequential model updating [8]. Liu et al. have included T-statistics criteria that were preceded by decorrelation by PCA decomposition [9]. The T-statistic is a ratio of the departure of an estimated parameter from its notional value and its standard value. El Dabbagh and Fakhr have focused their approach and have applied three different SVMs, namely weighted ensemble of SVM, row and column-based SVM ensemble, and channel selection with optimized SVMs [8]. In the weighted ensemble of SVM, each SVM is provided some weight to its performance to a certain pattern. In the row and column-based SVM ensemble, they have separated the row and column characters and trained them separately to form the ensemble. The best performer channels were used in the channel selection with optimized SVMs. Rakoto has used averaging of signals to improve the SNR, then applied gradient descent for optimal channel selection [10] ([Fig. 2](#) and [Table 1](#)).

**FIG. 2**

Framework block diagram.

Table 1 Literature Survey Table

Author	Method	Dataset
El Dabbagh and Fakhr [8]	Row/column-based weighed SVM ensemble with channel selection	BCI competition III dataset II
Liu et al. [9]	PCA on block averaged data followed by computation of T weights	BCI competition III dataset II
Selim et al. [11]	Bayesian linear discriminant analysis, linear support vector machine, Fisher linear discriminant analysis, generalized Anderson's task linear classifier	BCI competition III dataset II, BCI competition II dataset IIb
El Dabbagh and Fakhr [12]	Weighted ensemble of SVM, channel selection with optimized SVMs, and row/column-based SVM ensemble	BCI competition III dataset II
Li et al. [13]	Median filtering to remove noise followed by Bayesian linear discriminant analysis	BCI competition III dataset II
Zhang et al. [14]	Spatial-temporal discriminant analysis to maximize the discriminant information	BCI competition III dataset II, self-collected dataset

3 THE FRAMEWORK

The proposed framework has been used to provide an elegant workflow solution to accelerate testing of multiple classification models for P300 classification efficiently and rapidly. The core features of the framework, kept in mind while designing the framework, were modularity and exhaustive testing along with speed and parallelism:

1. *Modularity*: Individual components of the framework such as model parameters (preprocessors, postprocessors, classifiers), data loading, and certain additional utilities have been divided into separate modules according to their requirements.
2. *Comprehensive testing*: The framework allows researchers to provide as input a large combination of feature vectors, both available within the module as well as customized. It will automatically iterated through all available feature vectors with a combination of classifiers to provide results from numerous inputs.
3. *Speed and parallelism*: The framework was designed to keep speed, parallelism, and space complexity in mind. Many segments of the code have been crafted to run efficiently on a multicore architecture. Additionally, feature vectors have been cached to ensure fast reusability of previously computed results.

3.1 INITIALIZATION

In this step, the primary experiment information is imported from a file where the user stores the vital experiment parameters (referred to as “settings.json” file). Most importantly, the parameters that must be set are the sampling rate (F_s) of recorded

data, the number of characters to train (N_{tr}), the number of characters to test (N_{te}), and the number of trials to use (N_{seq}). These parameters can be manually set to experiment with different experimental conditions. Given the total number of trials denoted as T_{seq} : $N_{seq} \leq T_{seq}$, increasing the parameter N_{seq} increases the experiment time but simultaneously boosts accuracy as well.

At this point, the imported data will consist of the EEG recording, besides additional marker arrays. The EEG recording (D_{sig}) should be shaped so that there are $D_{recvals}$ number of samples, each having N_{chan} number of values for every channel.

Hence,

$$D_{sig}.shape = D_{recvals} \times N_{chan} \quad (1)$$

3.2 MODEL SETUP

The framework splits every model into four core segments.

The first three are:

1. The Queue of Preprocessors (Q_{pre})
2. The Queue of Postprocessors (Q_{popr})
3. The Queue of Classifiers (Q_{cl})

The three queues are then merged iteratively and added to the model queue (Q_m), which is a tuple of the form $(Q_{pre}, Q_{popr}, Q_{cl})$.

The fourth and final segment is fixed for every model, which is the custom epoch extractor (C_{epex}) that will be user-defined, depending on the dataset format. A C_{epex} is provided in the framework source to work with the BCI competition dataset.

Finally, after C_{epex} is added to every model, the final tuple obtained is $(Q_{pre}, C_{epex}, Q_{popr}, Q_{cl})$

3.2.1 Preprocessors

From the imported data, D_{sig} is first sent to the preprocessor, which applies a combination of the given operations on raw signals:

1. *Channel selection/rejection*: As stated earlier, every D_{sig} sample consists of N_{chan} recorded values. Passing a list of channel numbers L_{chan} to the *Channel Selection* or *Channel Rejection* block will result in the selection or rejection of L_{chan} channels from D_{sig} . This is done with the intuition of removal of highly correlated and noisy channels as well as those channels that do not provide useful features:

```
if Channel Selection :
     $N_{chan} = L_{chan}$ 
else if Channel Rejection :
     $N_{chan} = N_{chan} - L_{chan}$  (2)
```

2. *Bandpass filtering*: One of the most important steps with respect to preprocessing D_{sig} is filtering. A low-frequency band-pass filter (f) is applied to the data for

removal of noise and selecting the part of the signal contributing to the P300 component [15].

f was varied between Chebyshev, Elliptic, and Butterworth filters tested at various cutoff frequencies. The sampling rate F_s has been already provided during initialization as an experiment parameter.

Thus,

$$Q_{\text{prepr}}(D_{\text{sig}}, f) = D_{\text{sig}} \quad (3)$$

3.2.2 Custom epoch extractor (C_{epex})

The custom epoch extractor processes D_{sig} in combination with marker arrays to extract epochs from D_{sig} to obtain epoched signals E_{sig} .

$$E_{\text{sig}}.\text{shape} = N_{\text{ep}} \times E_{\text{recvals}} \times N_{\text{chan}} \quad (4)$$

where E_{sig} represents the epoched data, N_{ep} represents the number of epochs, E_{recvals} is the number of samples per epoch, and N_{chan} corresponds to the number of channels. Every epoch represents a potential P300 candidate. From available training data, the C_{epex} must also retrieve the truth value of y_{sig} , where

$$y_{\text{sig}}.\text{shape} = N_{\text{ep}} \quad (5)$$

and y_{sig} denotes whether a given epoch is a P300 event.

Another important consideration when using C_{epex} is T_{ep} , the time from the start of a potential P300 candidate up to which samples must be considered for a given epoch to test the presence of P300. This value is set to 667 ms to cover a reasonable number of values and account for latency.

```
if training:
     $C_{\text{epex}}(D_{\text{sig}}, \text{MarkerArray}, \dots) = E_{\text{sig}}, y_{\text{sig}}$ 
else if testing:
     $C_{\text{epex}}(D_{\text{sig}}, \text{MarkerArray}, \dots) = E_{\text{sig}}$ 
```

(6)

3.3 POSTPROCESSOR

Postprocessors work on E_{sig} as well as y_{sig} to produce feature vectors that can be used to train a classifier. Because this is one of the most significant steps of the classification pipeline, a large number of postprocessors have been tested. They are provided as modular inputs to a list to set up a workflow pipeline whose output is a feature vector V_f . The paper divides the set of postprocessors into those that have been newly handcrafted by the authors and those that existed previously as popular signal-processing methods or were used in the surveyed literature. The features belonging to the former category are:

1. *Converse Wavelet Transform (CWT)*: In this method, the discrete wavelet transform was modified according to the concept of the M-order filter bank. Because the P300 signal is composed of a low frequency, therefore increasing the signal resolution at a low frequency will surely intensify the features. Hence our

approach was to filter the signal into two parts and concatenate the temporal characteristics representing the lower signal frequency, downsample it, then filter it again. The process was repeated until only two samples were left. A Chebyshev filter of fourth-order and a maximum pass-band ripple of 0.5 were used for filtering. Fig. 3 depicts the procedure followed to extract the CWT.

2. *Experiment information:* Information about actual experiments such as the count of characters trained before the current epoch and the trial under consideration during the current epoch being trained. The intuition behind this feature is the addition of a time indicator, so as to provide a temporal feature as input because the quality of output P300 may vary with time due to exhaustion and other extraneous factors.

The previously used popular signal-processing methods that were tested are:

1. *Time Series EEG:* The simplest and most primitive feature, involving direct use of filtered epoched data. First, data samples from every channel in a given epoch are concatenated to form this feature vector. Following this, the time series vector is downsampled.
2. *Fourier transform:* This postprocessor converts time series data to the frequency space. The fast Fourier transform is applied to a set of samples per epoch per channel for this purpose, then converted to absolute values that are then log

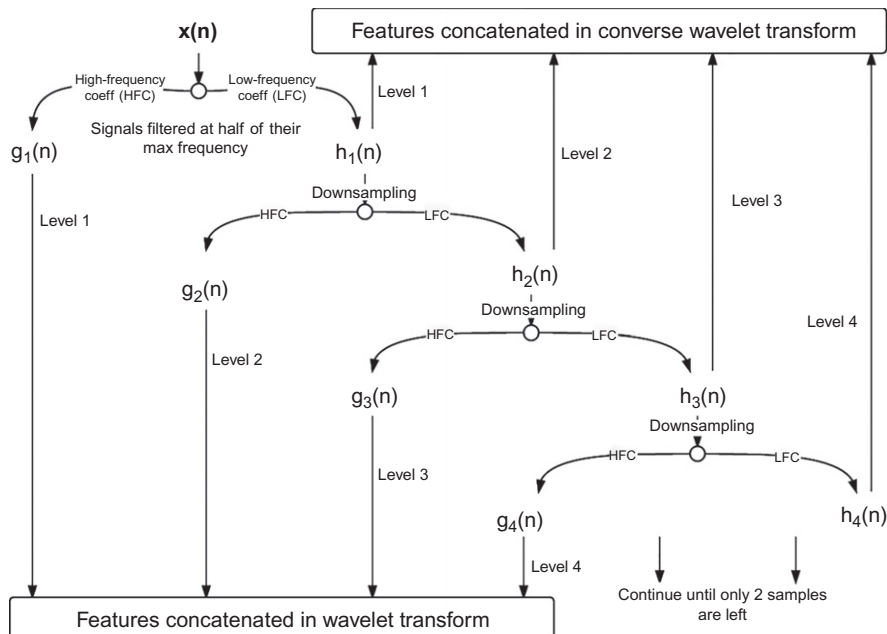


FIG. 3

Representation of wavelet and converse wavelet transform.

transformed. This transformed data is then sliced at a specific frequency and concatenated to give the required feature vector [16]:

$$X_k = \sum_{i=1}^{N-1} x_i \exp\left(-i2\pi k \frac{n}{N}\right) \quad (7)$$

- 3. *Wavelet transform:* Because the EEG signals have nonlinear frequency characteristics, that is, low-frequency components exist for long durations and high-frequency components exist for shorter durations, hence it was necessary to analyze the signal at different frequencies with different resolutions. Additionally, it is efficient in representing a combination of temporal and frequency characteristics of the signal. The discrete wavelet transform decomposes the signal into two parts. The first part represents the low frequency coefficients and the other part represents the high frequency coefficients [17–19]. The continuous wavelet transform is represented as follows:

$$\psi_s(\tau, s) = \frac{1}{\sqrt{(|s|)}} \int (x(t)^* \psi\left(t - \frac{\tau}{s}\right)^* dt) \quad (8)$$

where τ is the translation parameter, s is the scale parameter, and ψ is the transforming function, called the mother wavelet.

- 4. *xDAWN filtering:* This method was used by Alan and Rivet for enhancing the P300 evoked potentials. It is a spatial filtering technique in which the PCA of the signal is calculated, which enhances the synchronized responses occurring with the visual stimuli [20]. The visual response is mathematically modeled as

$$X = D \cdot A + N \quad (9)$$

where D is a Toeplitz matrix whose element is defined as $D_{t,k} = 1$ where (t, k) represents the stimulus onset of the k th target stimulus, A is signal collected at the respective sensor, and matrix N the ongoing activity of the user's brain as well as the artifacts. The $|X - DA|$ factor is minimized by least squares approximation and the corresponding value of matrix A is calculated.

$$A = \text{argmin} \|X - DA\|^2 \quad (10)$$

The solution of this equation is

$$A = (D_T^* D)^{-1} D_T^* X \quad (11)$$

The other method is composed of estimating the N_f spatial filters such that the synchronous response of the signals is the sum of the spatial filter projection and noise. Principle component analysis (PCA) is performed by calculating the singular value decomposition (SVD), which gives

$$A = \Sigma \Delta \Pi^T \quad (12)$$

Then this PCA decomposition is split into signal and noise subspaces. The signal subspace of Π is the spatial filter. Even if the PCA enhances the evoked

potentials, the major drawback of this solution is that the noise N is not directly taken into account to estimate the spatial filters. To overcome this, the most optimal filter is designed such that the signal to signal plus noise ratio is maximized by calculating the QR factorization of X and D by the following formula:

$$V = \arg \max_U \frac{\text{Tr}(U^T Q_X^T Q_D Q_D^T Q_X U)}{\text{Tr}(U^T U)} \quad (13)$$

where U is the matrix of spatial filters.

- 5. *Statistical features*: Basic statistical features such as mean, maximum, minimum, and standard deviation values for data samples of a given channel per epoch [21]. In addition, the skewness and kurtosis have also been calculated and used.

Skewness is the measurement of lack of symmetry, given as:

$$\text{skew}(X) = \frac{E|(X - \mu)^3|}{\sigma^3} \quad (14)$$

where μ and σ are mean and standard deviation, respectively.

Kurtosis provides the degree to which the distribution is peaked, given as:

$$\text{kurt}(X) = \frac{E|(X - \mu)^4|}{\sigma^4} \quad (15)$$

where μ and σ are the mean and standard deviation, respectively

- 6. *Peaks of Fourier transform*: First, the data has been converted to frequency domain in a manner similar to the Fourier transform postprocessor. After this, a given number of peaks (“peaks”) in the frequency series data is computed. Following this, the samples for every channel were concatenated to obtain the required feature vector.

- 7. *Hjorth parameters*: These parameters are indicators of certain statistical properties in time series data [22]. The three Hjorth parameters are:

(a) *Activity*: The activity parameter, represented by a variance of time series, can indicate the surface of the power spectrum in a frequency domain. Thus the higher this value, the greater the number of high-frequency components in the signal:

$$\text{Activity} = \text{var}(y(t)) \quad (16)$$

(b) *Mobility*: The mobility parameter is indicative of standard deviation of the power spectrum and is derived by finding the square root of the ratio of the variance of the first derivative of the signal to variance of the signal:

$$\text{Mobility} = \sqrt{\frac{\text{var}\left(y(t) \frac{dy}{dt}\right)}{\text{var}(y(t))}} \quad (17)$$

- (c) Complexity:** The complexity parameter shows the similarity of a given signal to a sine wave. It is the ratio of mobility of the first derivative of the signal to the mobility of the signal:

$$\text{Complexity} = \frac{\text{Mobility}\left(y(t)\frac{dy}{dt}\right)}{\text{Mobility}(y(t))} \quad (18)$$

These parameters are computed for samples per channel in a given epoch, after which they are concatenated over every channel to give a feature vector.

- 8. First differential of Time Series:** The first differential of time series is the first order differential of the timeseries data calculated by subtracting subsequent samples. It represents the rate of change of the signal w.r.t. the samples. The starting samples are kept as the same considering zero padding. The number of samples remains the same and the features are concatenated in the same way as the time series data:

$$\Delta = X_n - X_{n-1} \quad (19)$$

where X_n is the n th sample of the given time series data.

Finally, an additional metafeature extractor used is

1. *Downsampler*: This module accepts a previously generated feature vector and reduces the number of samples by one of two methods:
 - *Direct resampling*: In this method, every feature vector is iterated through, and during iteration, one of every k samples is selected while the rest are rejected.
 - *Averaging*: Similar to direct resampling except that instead of selecting one of every k samples, the average of every k sample is computed.

The reason it is called a metafeature extractor is because it works on previously generated features to boost results, being singularly obsolete.

3.4 CLASSIFICATION

Finally, the feature vectors obtained from the previous step are used to train a classifier. During training, the classifier is trained using N_{tr} samples of the feature vector V_f . A number of linear and nonlinear classifiers were applied to the data.

1. Linear classifiers
 - (a) Linear discriminant analysis (LDA) [23]
 - (b) Linear support vector machines [24]
2. Nonlinear/genetic classifiers
 - (a) BSA-NN [25]

- (b) Random forest ensembles [26]
- (c) RBM support vector machines [27]
- (d) Artificial neural networks (two-layer model using back-propagation to optimize weights)

Linear Discriminant Analysis looks for linear combinations of features to maximize the decision boundary between different classes of data. Linear SVM is a variant of SVM using a linear kernel, known to scale well with large datasets [25]. A backtracking search algorithm on a neural network architecture (BSA-NN) is a recent evolutionary algorithm used by the authors on the motor imagery classification, based on the evolution of a weight population, backtracking the weights to previous values on a new search path on getting stuck in local minima [28]. Random forests involve training of an ensemble of decision trees that set parameters by a greedy search based on information gain. RBM-SVM is a non-linear type of support vector machine using the RBM kernel [27]. Finally, multilayer neural networks first reduce dimensions while finding hidden relationships in the data and are then classified using a logistic regression outer layer. Those classification algorithms outperforming others or providing competitive accuracies were further ensembled to enhance results. A bagging ensemble was used for this purpose [29]. The complete workflow followed by the framework has been delineated in Fig. 2 as a step-by-step block diagram, summarizing the functionality of the framework.

4 RESULTS AND DISCUSSION

In this section, the description of the dataset used, the feature vectors providing high classification accuracy, and comparison with previous methods has been analyzed (Fig. 4).

A	B	C	D	E	F
G	H	I	J	K	L
M	N	O	P	Q	R
S	T	U	V	W	X
Y	Z	1	2	3	4
5	6	7	8	9	_

FIG. 4

P300 speller paradigm.

4.1 THE DATASET

The paper has only used recorded brain signals following the P300 speller paradigm provided in BCI competition III Dataset II. It was introduced by Farewell and Donchin in 1988 [30]. The P300 speller is a 6×6 matrix of alphanumeric characters. The user has to focus on a specific letter and the rows and columns of the matrix flash randomly. It is called the P300 speller because, after intensification of the row or column having a letter, a positive deflection is seen in the parieto-occipital region of the brain nearly after 300 ms. For spelling a desired letter, the user focuses on the letter. The visual stimuli (P300) is generated corresponding to the flashing of the row or column containing the desired character. Twelve intensifications of rows and columns, six each for rows and columns, are randomly done in one set. This set is repeated 15 times for a single character that is to be spelled.

The dataset was provided by Wadsworth Center, NYS department of Health, available on the Berlin BCI competition webpage, has been used. The data has been recorded from two different subjects, each continuing for five different spelling sessions. During each session, the subject was asked to focus on a predefined set of characters, which may be a word. All the EEG signals are recorded by a 64-channel EEG headset whose placement of electrodes is shown in Fig. 5. The signal is than band-passed between frequency 0.1–60 Hz, then digitized at a sampling frequency of 240 Hz. The intensification rate of the rows and columns has been set to 5.7 Hz. The matrix was kept blank for 75 ms after each intensification. The duration of intensification was 100 ms. After each session of 15 sets of each letter, the matrix was kept blank for 2.5 s, after which the next desired letter was shown to the subject.

The classification problem can be summarized as follows: From the given EEG data, predict whether the P300 event lies in the signal. If the signal was classified correctly, then it becomes much easier to predict the desired letter from the pattern of intensification of rows and columns.

4.2 FRAMEWORK RESULTS

As discussed earlier, the framework is being used to automatically test a large number of feature combinations by splitting the given model into preprocessor, postprocessor, and classifier steps. The results from the framework are elucidated in Table 2,

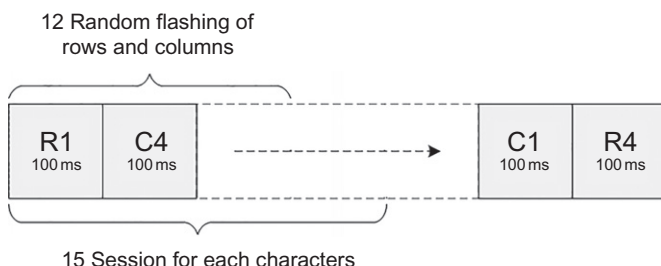


FIG. 5

Data acquisition process.

Table 2 Subject A: LDA Bagged Classifier

No.	Postprocessor	DSR	Accuracy (No. of Seq.)									
			Bagged LDA					LDA				
			8	10	12	13	15	8	10	12	13	15
1	Wavelet Transform, Converse Wavelet Transform	12	68	82	91	91	97	64	80	84	90	97
2	Converse Wavelet Transform	12	65	84	87	91	96	63	81	81	91	96
3	Time Series Wavelet Transform Converse Wavelet Transform	24	74	80	87	91	97	70	79	85	88	95
4	Hjorth Parameters, Time Series	10	65	83	90	90	96	64	81	88	91	96
5	Simple Statistical Features, Time Series, Converse Wavelet Transform	24	67	84	90	91	95	64	82	89	90	95
6	Wavelet Transform	12	70	84	85	88	95	68	83	84	87	95
7	Time Series, Converse Wavelet Transform	24	73	83	91	94	96	72	84	90	93	94
8	FFT Slice, Time Series	12/10	68	80	91	91	96	66	81	86	90	95
9	Time Series, Wavelet Transform	24	71	83	87	87	95	70	82	85	87	94
10	Time Series, Wavelet Transform, Hjorth Parameters	12	63	74	86	88	93	59	73	80	85	94
11	Time Series, Hjorth Parameters, Spectral Entropy	12	65	82	85	90	95	63	82	82	88	94
12	Time Series	12	72	82	89	91	95	70	80	87	89	94
13	Time Series, Wavelet Transform, Spectral Entropy, Hjorth Parameters	12	62	79	85	89	94	63	73	80	84	93

Note: DSR, *downsampling rate*.

which highlights those feature vectors that obtained the top 13 accuracies among all combinations of feature vectors tested using the LDA-based classifier. [Table 2](#) shows the results of classification using the metric of accuracy, both for the LDA classifier as well as an ensemble of 500 LDA classifiers. Furthermore, the paper now discusses the significant steps and methods to be followed at every stage of the framework workflow. Note that the custom epoch extraction step is dataset-dependent and thus not discussed here.

4.2.1 Preprocessing

A single Butterworth filter with a cutoff frequency between 0.1 and 15 Hz is sufficient to reduce a large component of noise from the data and serves as the best preprocessing step. These results also coincide with the suggestions of Bougrain and Saavedra [15]. During testing, it was found that channel selection gives low-quality features and results compared to using all channels.

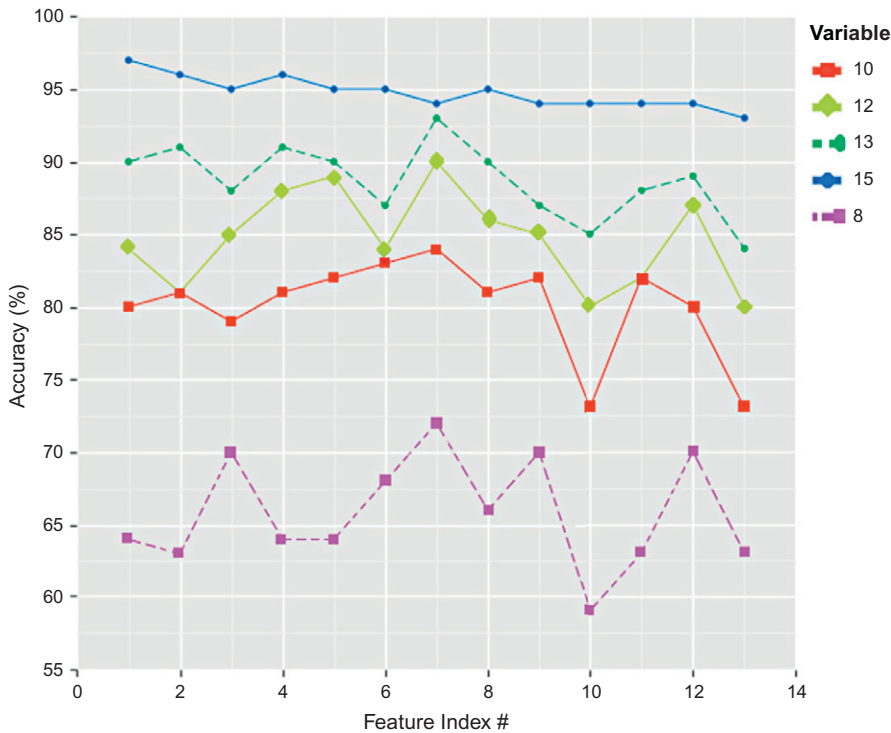
4.2.2 Postprocessing

Ten methods of postprocessing have been discussed above. Of these, the methods providing the best features are:

1. Time Series Data
2. Wavelet Transform
3. Frequency Spectrum Data
4. Converse Wavelet Transform
5. Hjorth Parameters
6. Spectral Entropy
7. Statistical Features

[Table 2](#) shows the different input feature vectors that sported accurate classification models. It can be seen that, while temporal and frequency features individually provide for a simple classification model, it is the combination of both, seen in the Wavelet Transform and the CWT, that serves the best results. Among these, the features providing the highest accuracies have been marked in bold in [Table 2](#). *Time Series data* along with *WWT* and *CWT* serve as the most significant features. Second, it is the combination of the CWT and Time Series data that is able to provide the most consistently precise results, even with lesser training sequences. The CWT is able to produce the most optimum result because the P300 signal is composed of low-frequency data, and in this method, only the low-frequency components are concatenated in this process, thus amplifying them.

While the operations discussed in the previous paragraph solely provided competitive results, using Hjorth Parameters, Spectral Entropy, and Statistical Features in combination with the former helped enhance the previous results, even maintaining stability in results obtained by using fewer sequences. The intuition behind this is that while these transformations do not provide a complete view of the data like the ones discussed earlier, they summarize certain unique inferences that can be made on the data, which a classifier might not be able to automatically identify when finding

**FIG. 6**

LDA with variable flash sequences.

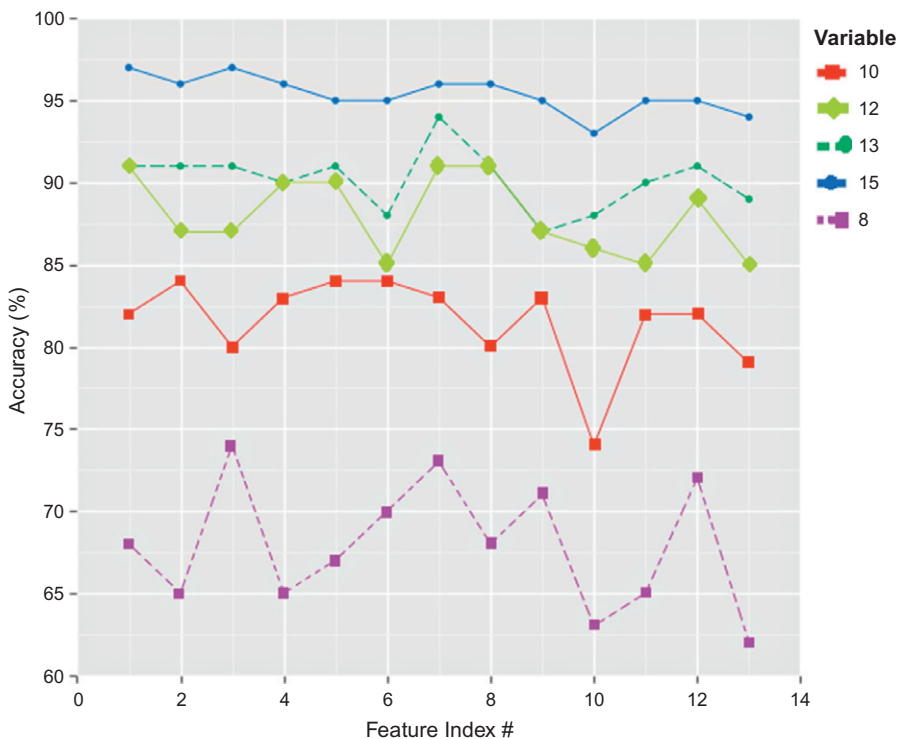
relationships in the data. This helps in providing a stable boost to the results. *Experiment Information* did not have any impact on the results, giving the same results with or without it.

The remaining features individually and in combination with other features were providing results that were not up to the mark.

4.2.3 Classification

Among the tested classifiers, the linear classifiers, namely *LDA* and *LinearSVC*, provided high classification accuracy [31]. This conforms with previous research showing that the P300 paradigm falls under the problem of linear rather than nonlinear classification. Using linear classifier ensembles provided an impetus to the results of linear classification, especially when training data was reduced by decreasing the number of sequences [32]. For ensembling, a *bagging classifier* having 500 constituent classifiers was used [33]. LDA provided the most promising results and has thus been used in Table 2. Indices in Table 2 have been used as the label on the *x*-axis of the graph.

Figs. 6 and 7 sketch the accuracies displayed in Table 2 as a graph. The most important inference that can be extrapolated from these figures is the huge boosts

**FIG. 7**

Bagged LDA with variable flash sequences.

in accuracy, which can be seen by using a bagging classifier as compared to a single one. While for a larger number of sequences, the step up is negligible, for the smaller number of sequences we see a significant escalation.

4.2.4 Performance comparison

Table 3 compares the accuracy obtained by using the discussed methodology to previously applied algorithms. The accuracy shows the number of characters that were predicted correctly out of the total given 100 characters by the corresponding methodologies mentioned on the left. The sequences of data refer to the number of times an iteration consisting of 12 random flashes of rows and columns is carried out, when trying to predict a specific letter. For complete fairness, the accuracy has not only been reported for the maximum count of 15 sequences, but over different counts of training sequences, representing how the algorithms can perform over lesser training data. It can be seen that the best results obtained by the framework are competitive with respect to previously existing algorithms, remaining consistent even with reducing input training data. Because the accuracy does not go beyond 97% it might

Table 3 Table of Comparison

Algorithm	Accuracy (No. of Seq.)				
	8	10	12	13	15
Ensembles of SVMs [20]	–	86	–	92	98
T-weighted approach [9]	–	83	–	94	90
Bayesian LDA [11]	–	–	–	–	98
Weighted ensembles [12]	–	87	–	94	96
Median filtering and Bayesian feature extraction [13]	40	50	70	75	90
Metric learning [34]	–	87	–	–	95
Li Yandong [35]	–	–	–	–	90.5
Ulrich Hoffmann [35]	–	–	–	–	89.5
Lin Zhonglin [35]	–	–	–	–	87.5
Our framework best results	74	84	91	94	97

be true that the subject participating in the session may not have focused upon some characters correctly, so whatever our algorithm is, its not able to detect it.

4.2.5 Open source implementation

The proposed framework has been implemented using entirely open source software, ensuring that it is open for use by other researchers. The complete framework has been implemented in *Python 2.7*, using the libraries *joblib/mpi4py* [36] for utilizing the multicore architecture of the device, scikit-learn's metrics, and classifiers [37]; *numpy/scipy* for using matrices; *pywavelet* [38] for applying different Wavelet transforms; and *pyeeg* for some EEG-processing operations. All these libraries have been released under open source licenses and are free to use.

5 CONCLUSION AND FUTURE WORK

This chapter proposes the dummy framework for efficient processing and accelerated classification of P300 signals. The use of multicore architecture, parallelism, modular structure, and caching significantly diminishes processing time and effort. This chapter proposes a number of feature extraction methods from raw EEG data, both newly introduced by the authors as well as previously used signal-processing methods. Finally the framework tests a large combination of such feature vectors as well as classifiers and logs the respective results. The authors have reported the feature vector and classifier combinations exhibiting high classification accuracies. The best results reported have been, for further research inference, compared with previously used methods where they demonstrate competitive accuracy in different sequences of data.

The source code for the framework is provided at <https://drrajeshkumar.wordpress.com/downloads/>. Being completely open source and using external open-source libraries, it is free for use by other researchers. The research surrounding the classification of P300 will be applied to its detection in EEG recorded in realtime using low-cost consumer EEG hardware, namely the Emotiv EPOC headset [39, 40]. This will be used to provide low-cost solutions to severely disabled individuals for effective communication.

REFERENCES

- [1] J. Wolford, Man with locked-in syndrome tweets using eye-tracking tech, (2012), <http://www.webpronews.com/man-with-locked-in-syndrome-tweets-usingeye-tracking-tech-2012-06> (accessed 25 February 2015).
- [2] M.M. Moore, Real-world applications for brain-computer interface technology, *IEEE Trans. Neural Syst. Rehabil. Eng.* 11 (2) (2003) 162–165.
- [3] C. Guger, S. Daban, E. Sellers, C. Holzner, G. Krausz, R. Carabalona, F. Gramatica, G. Edlinger, How many people are able to control a P300-based brain-computer interface (BCI)? *Neurosci. Lett.* 462 (1) (2009) 94–98.
- [4] H. Gürkök, A. Nijholt, M. Poel, Brain-computer interface games: towards a framework, in: M. Herrlich, R. Malaka, M. Masuch (Eds.), *Entertainment Computing – ICEC 2012, Lecture Notes in Computer Science*, vol. 7522, Springer, Berlin, Heidelberg, 2012.
- [5] E.C. Lalor, S.P. Kelly, C. Finucane, R. Burke, R. Smith, R.B. Reilly, G. Mcdarby, Steady-state VEP-based brain-computer interface control in an immersive 3D gaming environment, *EURASIP J. Appl. Signal Process.* 2005 (2005) 3156–3164.
- [6] J.D. Bayliss, Use of the evoked potential P3 component for control in a virtual apartment, *IEEE Trans. Neural Syst. Rehabil. Eng.* 11 (2) (2003) 113–116.
- [7] Z. Gu, Z. Yu, Z. Shen, Y. Li, An online semi-supervised brain-computer interface, *IEEE Trans. Biomed. Eng.* 60 (9) (2013) 2614–2623.
- [8] H. El Dabbagh, W. Fakhr, Multiple classification algorithms for the BCI P300 speller diagram using ensemble of SVMs, in: 2011 IEEE GCC Conference and Exhibition (GCC), IEEE, pp. 393–396.
- [9] Y. Liu, Z. Zhou, D. Hu, G. Dong, T-weighted approach for neural information processing in P300 based brain-computer interface, in: *Neural Networks and Brain, 2005. ICNN &’05*, vol. 3, IEEE, ISBN 0780394224, pp. 1535–1539.
- [10] B. Rivet, H. Cecotti, R. Phlypo, O. Bertrand, E. Maby, J. Mattout, EEG sensor selection by sparse spatial filtering in P300 speller brain-computer interface, in: 2010 Annual International Conference of the IEEE Engineering in Medicine and Biology Society (EMBC), IEEE, pp. 5379–5382.
- [11] A.E. Selim, M.A. Wahed, Y.M. Kadah, Machine learning methodologies in P300 speller brain-computer interface systems, in: *National Radio Science Conference, 2009*, pp. 1–9.
- [12] H. El Dabbagh, W. Fakhr, Enhancements of the classification algorithms for the BCI P300 speller diagram, in: 2010 5th Cairo International Biomedical Engineering Conference (CIBEC), pp. 158–162.
- [13] X.-O. Li, F. Wang, X. Chen, R.K. Ward, A P300-based BCI classification algorithm using median filtering and Bayesian feature extraction, in: 2012 IEEE 14th International Workshop on Multimedia Signal Processing (MMSP), IEEE, pp. 305–308.

- [14] Y. Zhang, G. Zhou, Q. Zhao, J. Jin, X. Wang, A. Cichocki, Spatial-temporal discriminant analysis for ERP-based brain-computer interface, *IEEE Trans. Neural Syst. Rehabil. Eng.* 21 (2) (2013) 233–243.
- [15] L. Bougrain, C. Saavedra, R. Ranta, Finally, what is the best filter for P300 detection? in: TOBI Workshop LLL-Tools for Brain-Computer Interaction, 2012.
- [16] P. Duhamel, M. Vetterli, Fast Fourier transforms: a tutorial review and a state of the art, *Signal Process.* 19 (4) (1990) 259–299.
- [17] I. Daubechies, The wavelet transform, time-frequency localization and signal analysis, *IEEE Trans. Inf. Theory* 36 (5) (1990) 961–1005.
- [18] R. Polikar, The wavelet tutorial, (1996), https://cseweb.ucsd.edu/~baden/Doc/wavelets/polikar_wavelets.pdf.
- [19] R. Polikar, The story of wavelets, in: Physics and Modern Topics in Mechanical and Electrical Engineering, 1999, pp. 192–197.
- [20] B. Rivet, A. Souloumiac, V. Attina, G. Gibert, xDAWN algorithm to enhance evoked potentials: application to brain-computer interface, *IEEE Trans. Biomed. Eng.* 56 (8) (2009) 2035–2043.
- [21] R.A. Groeneveld, G. Meeden, Measuring skewness and kurtosis, in: *The Statistician*, 1984, pp. 391–399.
- [22] B. Obermaier, C. Guger, C. Neuper, G. Pfurtscheller, Hidden Markov models for online classification of single trial EEG data, *Pattern Recogn. Lett.* 22 (12) (2001) 1299–1309.
- [23] J. Ye, R. Janardan, Q. Li, Two-dimensional linear discriminant analysis, in: *Advances in Neural Information Processing Systems*, 2004, pp. 1569–1576.
- [24] M.A. Hearst, S.T. Dumais, E. Osman, J. Platt, B. Scholkopf, Support vector machines, *IEEE Intell. Syst. Their Appl.* 13 (4) (1998) 18–28.
- [25] S.K. Agarwal, S. Shah, R. Kumar, Group based Swarm evolution algorithm (GSEA) driven mental task classifier, *Memetic Comput.* 7 (1) (2015) 19–27.
- [26] T.G. Dietterich, Ensemble learning, in: *The Handbook of Brain Theory and Neural Networks*, vol. 2, 2002, pp. 110–125.
- [27] R. Salakhutdinov, A. Mnih, G. Hinton, Restricted Boltzmann machines for collaborative filtering, in: *Proceedings of the 24th International Conference on Machine Learning*, ACM, 2007, pp. 791–798.
- [28] S.K. Agarwal, S. Shah, R. Kumar, Classification of mental tasks from EEG data using backtracking search optimization based neural classifier, *Neurocomputing* 166 (2015) 397–403.
- [29] Q. Sun, B. Pfahringer, Bagging ensemble selection, in: *AI 2011: Advances in Artificial Intelligence*, Springer, 2011, pp. 251–260.
- [30] L.A. Farwell, E. Donchin, Talking off the top of your head: toward a mental prosthesis utilizing event-related brain potentials, *Electroencephalogr. Clin. Neurophysiol.* 70 (6) (1988) 510–523.
- [31] T.G. Dietterich, Ensemble learning, in: *The Handbook of Brain Theory and Neural Networks*, vol. 2, 2002, pp. 110–125.
- [32] A. Rakotomamonjy, V. Guigue, BCI competition III: dataset II-ensemble of SVMs for BCI P300 speller, *IEEE Trans. Biomed. Eng.* 55 (3) (2008) 1147–1154.
- [33] A. Rakotomamonjy, V. Guigue, G. Mallet, V. Alvarado, Ensemble of SVMs for Improving Brain Computer Interface P300 Speller Performances, in: Springer, New York, NY, 2005, pp. 45–50.
- [34] Q. Liu, X.-G. Zhao, Z.-G. Hou, Metric learning for event-related potential component classification in EEG signals, in: *2013 Proceedings of the 22nd European Signal Processing Conference (EUSIPCO)*, IEEE, pp. 2005–2009.

- [35] D.B. Blankertz, BCI Competition III, Final Results, (2005), <http://www.bbci.de/competition/iii/results/> (Accessed 25 February 2014).
- [36] L. Dalcin, R. Paz, M. Storti, J. D'Elia, MPI for Python: performance improvements and MPI-2 extensions, *J. Parallel Distr. Comput.* 68 (5) (2008) 655–662.
- [37] F. Pedregosa, G. Varoquaux, A. Gramfort, V. Michel, B. Thirion, O. Grisel, M. Blondel, P. Prettenhofer, R. Weiss, V. Dubourg, et al., Scikit-learn: machine learning in Python, *J. Mach. Learn. Res.* 12 (2011) 2825–2830.
- [38] F. Wasilewski, Pywavelets: discrete wavelet transform in python, (2010), <https://media.readthedocs.org/pdf/pywavelets/0.2.2/pywavelets.pdf>.
- [39] M. Duvinage, T. Castermans, T. Dutoit, M. Petieau, T. Hoellinger, C. De Saedeleer, K. Seetharaman, G. Cheron, A P300-based quantitative comparison between the Emotiv Epoc headset and a medical EEG device, *Biomed. Eng.* 765 (2012) 2012.764-071.
- [40] H. Ekanayake, P300 and Emotiv EPOC: does Emotiv EPOC capture real EEG?, (2011), <http://neurofeedback.visaduma.info/P300nEmotiv.pdf>. The Solution.

This page intentionally left blank

Medical image diagnosis for disease detection: A deep learning approach

3

Mrudang D. Pandya*, Parth D. Shah*, Sunil Jardosh†*Information Technology Department, CHARUSAT, Anand, India* Progress Software,
Hyderabad, India†*

CHAPTER OUTLINE

1	Introduction	37
1.1	Related Work	39
2	Requirement of Deep Learning Over Machine Learning	40
2.1	Fundamental Deep Learning Architectures	41
3	Implementation Environment	52
3.1	Toolkit Selection/Evaluation Criteria	53
3.2	Tools and Technology Available for Deep Learning	53
3.3	Deep Learning Framework Popularity Levels	53
4	Applicability of Deep Learning in Field of Medical Image Processing	56
4.1	Current Research Applications in the Field of Medical Image Processing	56
5	Hybrid Architectures of Deep Learning in the Field of Medical Image Processing	57
6	Challenges of Deep Learning in the Fields of Medical Imagining	58
7	Conclusion	59
	References	59
	Further Reading	60

1 INTRODUCTION

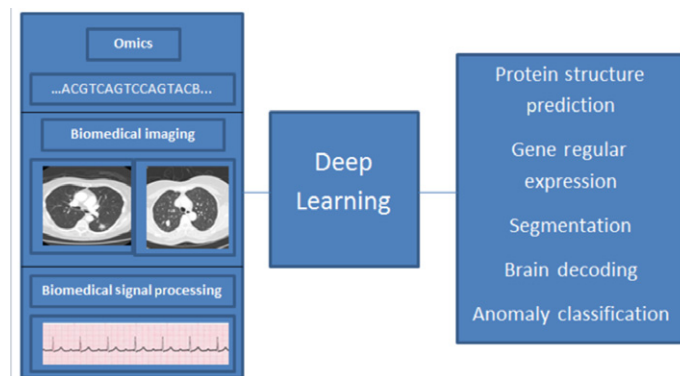
Before recent decade healthcare data availability was very hard, if it was available at that time the size of the data was very small. But in the current world, those issues are gone. Because of the incredible development in image procurement devices, the data is quite large, which makes it more applicable and effective for image analysis. This express progress in biomedical digital images and modalities involves widespread and monotonous efforts by the experts of medical domains such as radiologists, general physicians, etc. Especially for digital image analysis that includes human error,

required huge analysis and diagnosis variations depending on subject experts. To solve these kinds of issues, machine learning (ML) techniques provide automated diagnosis solutions; however, traditional ML methods are not appropriate to handle complex problems. Collaboration between high-performance computing (HPC) and ML gives us promising results in terms of complex problems. HPC and ML collaborations ultimately lead to Deep Learning (DL), and this will give ultimate results on large medical image datasets. This will give accurate analysis and diagnosis results. DL provides us automated feature selection furthermore it does not only identify the disease but also quantify prognostic goal and delivers tortuous estimate models to increase the diagnosis ability of medical experts.

Machine Learning is a most important field that is mainly helpful to make decision-making systems, recommendation systems, image analyzing systems, web searching, and so on. Several ML algorithms such as Artificial Neural Network (ANN), Random Forest (RF), the Hidden Markov Model (HMM), SVM (Support Vector Machine), Gaussian Networks (GN), etc., are applied in the fields of biomedical image processing.

Medical image processing comes under bioinformatics research. Medical digital image processing is one of the data modalities of bioinformatics. Apart from medical images, there are two more data modalities: omics (mostly sequential data) and biomedical signaling. Over the last few years, the use of such advanced DL techniques applied in the fields of medical image processing has grown rapidly. The current evidence of such systems is IBM's WATSONS [1] and GOOGLE DeepMind [2]. These projects have used DL algorithms to solve several bioinformatics problems. IBM's Watson use the ontology of patient health specification records collected by doctors for finding optimal solutions [1]. Google's DeepMind created a DeepMind health system for solving health-related problems and terminology [2]. Medical imaging domains contain raw data that may not be applied to the traditional algorithms of ML. The reason behind that is structure of medical images same times very complex (number of features are very high). So, handcrafted feature selection (ML) approaches not good for Medical Image analysis. These traditional algorithms that are mainly responsible to extract the feature Vector among such input sequences, for analysis the imaging.

Neural network architecture mainly needs feature vectors for input data. Medical image domain data needs to process the raw data images for feature vectors to give this input to such neural networks. Preprocessing of such raw data is much more expansive and quite more time consuming to do. A Deep Neural Network (DNN) helps to solve these problems through DL. Bioinformatics is broad domain to explore the DL phenomena. A beautiful definition by Merriam-Webster calls "bioinformatics as a collection of data, to do classification make prediction using feature extraction by analysis of biochemical properties and biological information using the computers." Research domains in bioinformatics are protein structure prediction, Gene expression regulation, protein classification, and anomaly classification [3–6]. Data availability in the fields of bioinformatics fall into these

**FIG. 1**

Bioinformatic modalities through Deep Learning research areas [7].

categories: omics (RNA, DNA, RNase, Protein Sequences, etc.), biomedical imaging (CTscan, MRI, PET, etc.), and biomedical signal processing (ECG, EEG, EMG, etc.). In this chapter, our main focus is on biomedical images. In Fig. 1, we show how DL can be useful in bioinformatic research areas using bioinformatic data modalities.

This chapter provides fundamental knowledge and state-of-the-art approaches about DL in the domain of medical image processing and analysis also gives the broad review of DL algorithms in biomedical image investigation problems in terms of present works and upcoming direction for future scope.

1.1 RELATED WORK

Within the scope of the u-healthcare system, Kiran Khatter and Sapana Malik [8] have contributed in malicious application detection and classification using Android mobile applications. With the use of machine learning algorithms, they have achieved malicious application detection accuracy up to 98.2% and malicious application classification accuracy up to 87.3%.

Furthermore, excellent research done by saba Lon in the field of feature classification on liver diseases using ultrasound data images. This was the automated approach using random partitioning using a back propagation algorithm [9]. They have represented their result in terms of four performance metrics: (1) sensitivity (98.08%), (2) specificity (97.22%), (3) positive predictive values (96.23%), and (4) negative predictive values (98.59%).

Komalsharma and Jitendra Virmani [10] have made a decision support system for classification of normal and medical renal disease with the use of ultrasound images. They have achieved 93.3% accuracy.

2 REQUIREMENT OF DEEP LEARNING OVER MACHINE LEARNING

Machine Learning becomes vitally important in this era that makes an individual's life easier. ML algorithms (MLA) are used for decision-making systems, recommendation systems, identifying objects from images, searching the web, etc. MLAs use training examples to uncover underlying patterns, construct models, and then make predictions on the new database that is testing an example on the model. There are several MLAs used for classification, including an Artificial Neural Network (ANN). The simple architecture of ANN consists of an input layer, an output layer, and hidden layers with processing units. These processing units take input as training examples and learn features that are used to predict class with the help of activation functions and parameters called weight. The network provides a reasonable response to noisy or incomplete input because of its property of distributed associative memory. Experience shows that these networks are very good pattern recognizers that also have the ability to learn and construct unique structures for different problems. Conventional machine-learning techniques were limited in their ability to process natural data in their raw form.

If we construct machine learning systems, then we require domain expertise and careful engineering to develop feature extractors, which convert raw data in to feature vectors that we can use as input to the neural network. Perceptron and shallow Neural Network requires handmade features as input whereas DNNs extract features by themselves with multiple hidden layers. DL is a subfield of ML. In DL feature selection is done by multiple hidden layers [11]. The invention of DL came from the study of ANNs and multilayer perceptrons because they have multiple hidden layers. DL is also called representation learning. For example, in image recognition, it can be interpreted that feature learning is done in the order of pixel, edge, texton, motif, part, and object. Similarly, in text recognition, features are learned in the order of character, word, word group, clause, sentence, and story [7]. There are three categories of DL architecture, namely DNN, Convolution Neural Network (CNN), and Recurrent Neural Network (RNN).

DNN has different architecture depending on which learning algorithm is used (supervised or unsupervised). Based on this, there are mainly three DNN architectures: Multilayer Perceptron (MLP), Deep Belief Network (DBN), and Stacked Auto-Encoder (SAE) [11].

Here is the comparison table of ML and DL; this will give excellent insight into both.

As we are concentrating on medical image analysis, there are some benefits to doing the same thing with DL instead of ML. DL has automated feature selection capability and good performance while we are dealing with large data; these features are really useful while we are dealing with medical image data ([Table 1](#)).

Table 1 Machine Learning Versus Deep Learning

Sr No.	Comparison Area	Description
1	Data dependencies	The most important difference between Deep Learning and traditional Machine Learning is its performance as the scale of data increases
2	Hardware dependencies	Deep Learning algorithms heavily depend on high-end machines, contrary to traditional Machine Learning algorithms, which can work on low-end machines
3	Feature engineering	In Machine Learning, most of the applied features need to be identified by an expert and then hand coded as per the domain and data type Deep Learning algorithms try to learn high-level features from data. This is a very distinctive part of Deep Learning and a major step ahead of traditional Machine Learning
4	Problem-solving approach	When solving a problem using a traditional Machine Learning algorithm, it is generally recommended to break the problem down into different parts, solve them individually, and combine them to get the result. Deep Learning, in contrast, advocates solving the problem end-to-end
5	Execution time	A Deep Learning algorithm takes a long time to train. This is because there are so many parameters in such an algorithm that training them takes longer than usual. The state-of-the-art Deep Learning algorithm ResNet takes about 2 weeks to train completely from scratch whereas Machine Learning comparatively takes much less time to train, ranging from a few seconds to a few hours
6	Interpretability	It is easy to interpret the reasoning behind the solution in Machine Learning but it is hard to defend the solution in terms of Deep Learning

2.1 FUNDAMENTAL DEEP LEARNING ARCHITECTURES

Before going into DL, we must know *the requirements of deep architecture over neural networks*. When we want to deal with large complex input and output processing at that time, DLA gives excellent performance instead of using neural networks. While we are dealing with neural networks, feature selection must be done externally. However, in DLA, feature selection will be done automatically. For these reasons, we have to select DLA over neural network architecture.

The fundamental construction of a DNN contains an input layer, many more hidden layers, and output layers. One of the important methodology for representation of learning is Deep Learning through which we can learn and discover several patterns available in data by increasing the level of abstraction [2]. The next question arises, Why do we need DNNs? One of the most important reasons is because it contains several layers of perceptrons (mainly containing one input, several hidden layers,

and one output layer). Other reason is single layer neural networks cannot deal with exclusive-OR like nonlinearly separable functions. For that we required multilayer networks or DNNs. DNN layers mainly compute output when the input sequence of data is given. Each layer of the input vector consists of output values of each unit of the layers that is multiplied with its weight vector of each unit that is present in each layer producing the weighted sum. Nonlinear functions such as sigmoid, hyperbolic tangent, and rectified linear unit (ReLU) are applied to the weighted sum that will compute the vision for output layers. The training of DNN architecture mainly aims to optimize the weight so that the appropriate result could be able to learn. Based on different types of layer contraction used in DNNs we have classified that networks as Multilayer Perceptron (MLP), Stacked Auto-Encoder (SAE) and Deep Belief Networks (DBN) etc.

Before we start to introduce all architecture, let us discuss the criteria used to determine the network structure.

There are basically three common criteria for all different kinds of techniques. Some techniques have different structures (CNN, RNN) but mainly all have common structures. Here, I have listed three criteria of the structures:

- (1) Input layer
- (2) Output layer
- (3) Hidden layers

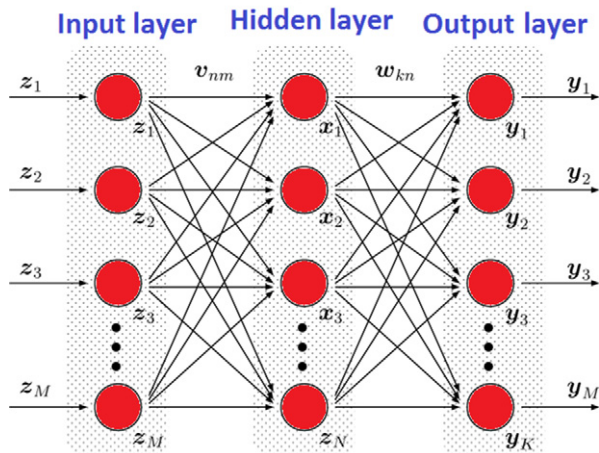
If we talk about input layer, there is only one input layer in every architecture. This layer consists of nodes or neurons. The number of nodes is dependent on the features of your data. Sometimes architecture includes one more additional layer called bias.

The output layer count in architecture is the same as the input layer. The output of this layer is in terms of class labels or values. Values you can compare with regression mode and class labels you can compare with machine mode.

Hidden layers are totally dependent on the size of the data. The bigger the data, the more hidden layers you have. When you put more hidden layers, sometimes it leads to a vanishing gradient problem. DLAs can phase this type of problem but RBM and auto encoders have solved this kind of problem. More hidden layers require more computing power. There is no such technique available that gives you the exact number of hidden layers. It always leads to trial and error.

2.1.1 *Multilayer Perceptron*

MLPs are an extension of ANNs, but these are more toward nonlinearity and layers are stacked together. These networks are trained mainly with supervised learning that requires labeled data. For training, they mainly use a back-propagation algorithm and gradient descent (by minimizing the cost of function by finding the values of parameters). Through these kinds of training techniques, we can archive optimized high-dimensional parameter space. [Fig. 2](#) indicates the basic structure of MLP with one Hidden layer.

**FIG. 2**

Basic structure of Multilayer Perceptron (MLP).

2.1.2 Deep Belief Networks

It is one kind of the generative model. It mainly joins the distribution of probability among observation and label P (label | observation). DBNs have “learning features” that means network can learn layer-by-layer with higher level features that are discovered and passes through past layer, thus more complex features that are acknowledges to get better reflected knowledge inside the input structures. The learning phase in DBN mainly contains two phases: a pretraining phase and fine-tuning. The pretraining phase is nothing but unsupervised leaning along with Stacked Restricted Boltzmann’s Machine. RBM is also used to extract the features, and after extracting the features, it mainly reconstructs the input. Several studies have been done with DBN/RBM for solving protein residue-residue contact prediction. For understanding the basic structure and flow, Fig. 3 defines the basic flow of a DBN; Fig. 4 defines how we can use RBM over DBN.

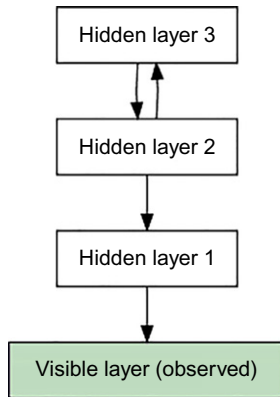
Invented by Geoff Hinton, a Restricted Boltzmann machine is an algorithm useful for dimensionality reduction, classification, regression, collaborative filtering, feature learning and topic modeling. It is using Contrastive divergences method to provide approximation for learning the weights. For training the single RBM, weights are updated with gradient descent with the following equation:

$$\Delta w_{ij}(t+1) = w_{ij}(t) + \eta \frac{\partial \log(p(v))}{\partial w_{ij}} \quad (1)$$

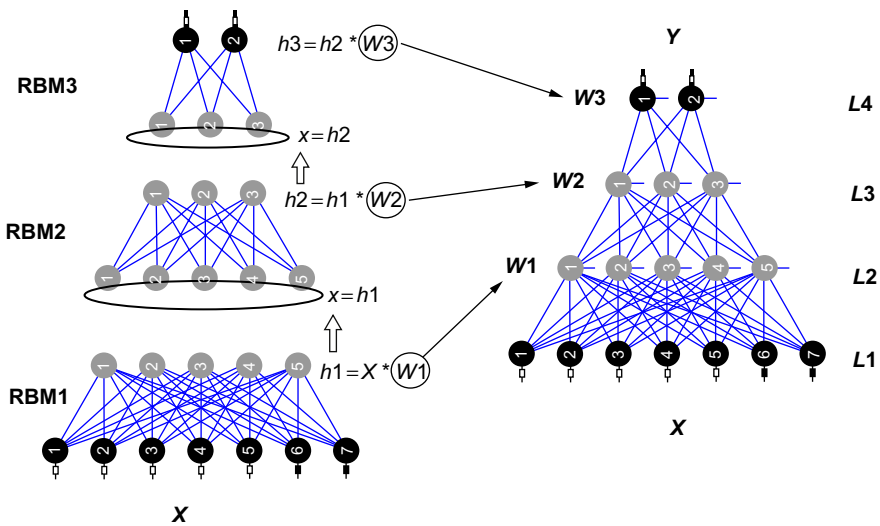
Where $p(v)$ is the probability of visible vector, Z is the partition function (used for normalizing the value), and $E(v, u)$ is the energy function assigned to the network.

These are the following steps to perform:

Visible units initialization to a training vector.

**FIG. 3**

Basic flow of a Deep Belief Network (DBN).

**FIG. 4**

DBN using RBM.

(1) With given visible units update the hidden units:

$$p(h_j = 1 | \mathbf{V}) = \sigma\left(b_j + \sum_i v_i w_{ij}\right). \quad (2)$$

(2) With given hidden units update the visible units:

$$p(v_i = 1 | \mathbf{H}) = \sigma\left(a_i + \sum_j h_i w_{ij}\right). \quad (3)$$

- (3) Reupdate the hidden units in parallel given the reconstructed visible units using the same equation as in step 2.
- (4) Do a weight update:

$$\Delta w_{ij} \propto \langle v_i h_j \rangle_{\text{data}} - \langle v_i h_j \rangle_{\text{reconstruction}} \quad (4)$$

2.1.3 Stacked Auto-Encoder

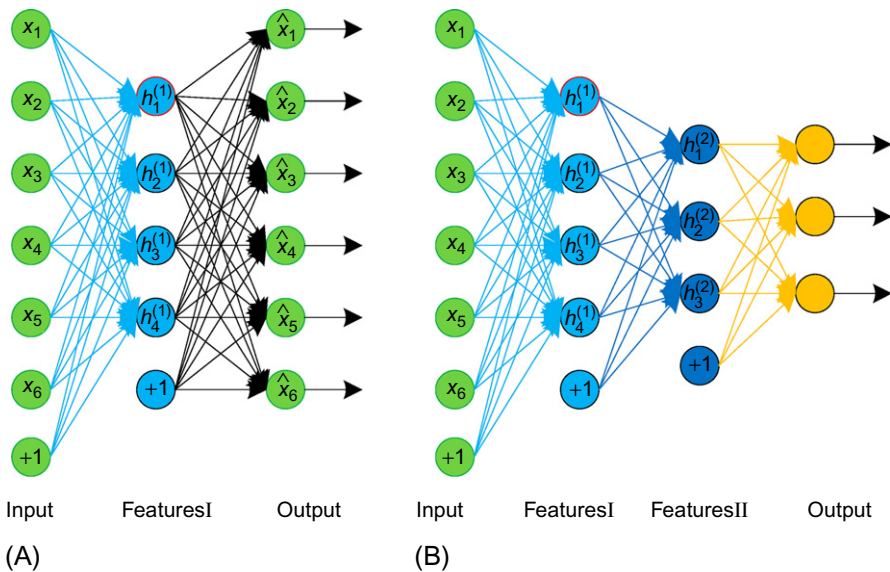
Auto-Encoder is a part of ANN, which is unsupervised pretraining procedure to train the networks. It mainly contains one input layer, one hidden layer, output layer is also similar, among these hidden layers the neurons that are used is less in number as compare to input and output layers. The working process of the network mainly compresses the original input and at output it will decompress it again to get the data back. By definition of Auto-Encoder, it mainly says that this network takes the original input, compresses it, and reconstructs the inputs that have specific meaning to extract the features for some specific application. The main goal of the network is to regenerate input by getting the target value among the input. These are again divided into three types:

- (a) *Denoising Auto-Encoder*: It is used for reconstruction of corrupted data.
- (b) *Sparse Auto-Encoder*: This type of network mainly has more numbers of several hidden units between input and output sequences that can learn from the low dimensional feature unit. It can also add some extra features to enhance the function to improve the loss for “sparsity” constraint form these several hidden units.
- (c) *Stacked Auto-Encoder*: Stacked Auto-Encoders are mainly used for pretraining the network that stacked in with a greedy layer-wise structure. It will make network to learn more deeper. These type of network mainly contains several layers. Each layer have specific function to extract the feature. As an example some layers are responsible for extracting edge form given image and other layers can find several hidden patterns. These layers are stacked together to learn the high an accurate order of features.

Auto-Encoder in biomedical images: Li et al. [12] developed the method with the use of a deeply stacked auto-encoder for denoising for solving problems of protein structure reconstruction. By using these techniques, it mainly gets the matching score to approximately 70% of the accurate result is obtained ([Fig. 5](#)).

2.1.4 Convolution Neural Networks

CNN is a specialized kind of network for processing data into grids such as topology. A CNN indicates to the network employee the mathematical operation called “convolution.” Convolution is a special kind of linear operation. The CNN approach is one kind of simple matrix multiplication ([Fig. 6](#)).

**FIG. 5**

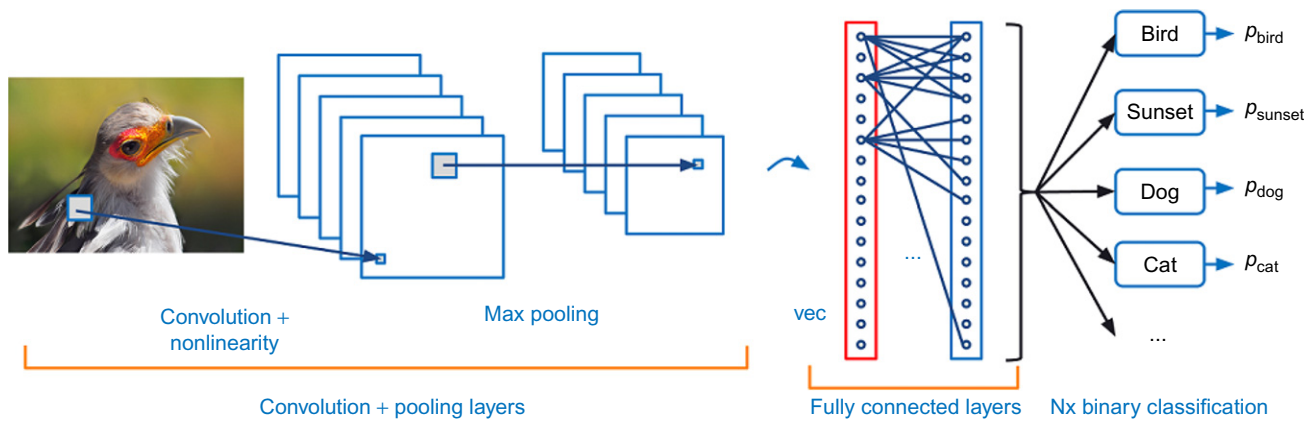
Model of Auto-Encoder.

Convolution architecture

The basic architecture contains three layers:

- (1) Conv layers (convolution).
- (2) Dimensionality reduction layers (Pooling).
- (3) Fully connected layers.

Convolution layers. The first layer in the convolutional layer is to make the input convolve. Suppose input size of an image is $32 \times 32 \times 3$. The best way to express these conv layers is to imagine a flashlight that shines over the top left of the image. The flashlight covers a 5×5 area; now these will slide across the input images. In machine learning, these flashlights are called filters (also known as kernels) and the region that it is shining over is called the receptive fields. The filter has to be the same as the depth of the input so these dimensions are $5 \times 5 \times 3$. The first position of the filter could be at the top left corner. As the filter slides over the convolving around the input images, it multiplies the values in the filter with the original input of the image (element-wise multiplications). These multiplications are all summed so now we have a single number. Repeat the process. The next step is to move these filters to 1 unit and then right again 1 unit. These processes continue. Each unique location on the input volume produces a number after sliding the filter over all the locations. Now these feature map or activation function is mapped with array size of $28 \times 28 \times 1$ (because input size is $32 \times 32 \times 3$) array of number. The reason we will

**FIG. 6**

CNN architecture.

get 28×28 accuracy is that there is a total of 784 different locations, that is, 5×5 filters on 32×32 input images. These 784 are mapped with 28×28 arrays.

Stride and pooling layers. These are the two main parameters to modify the behavior of each layer. After choosing the filter size, we also choose the stride and padding. Stride controls the filters convolving around the input volume. These filters convolve around the input volume by shifting one unit at a time. By default, these stride sizes are kept at one. Stride is normally set away to get the output in the form of an integer value (Fig. 7).

After applying a $5 \times 5 \times 3$ filter to a $32 \times 32 \times 3$ input volume, thus output volume would be $28 \times 28 \times 3$. The spatial dimensions will decrease as, applying these convolution layers, the size of the volume will decrease faster. In each layer of the network if we want to preserve the information for the original input volume. For that we want our output volume same as input volume ($32 \times 32 \times 3$). For such kind of things we required zero padding of size 2. Zero padding pads to the input volume worth zeros around the border (Fig. 8).

If a stride of and the size of zero padding is calculated by the formula given below:

$$\text{Zero padding} = \frac{(k-1)}{2} \quad (5)$$

where k = is the filter size of the input and output volume for spatial dimensions. The formula for calculating the output size given by convolution layers is:

$$O = \frac{(W - K + 2P)}{S} + 1 \quad (6)$$

where O = is the output height/length, W is the input height/length, K is the filter size, P is the padding, and S is the stride. Apply these nonlinear layers immediately after the convolution layer. The purpose of this nonlinearity to a system is to compute the linear operation during the convolution layers. Nonlinear functions such as tanh

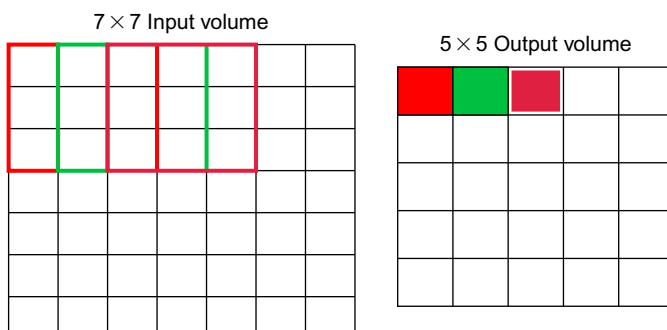
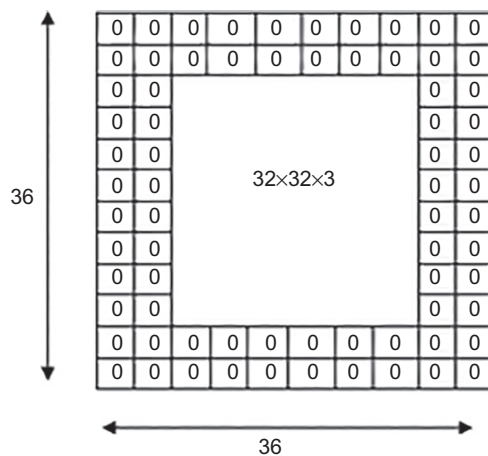
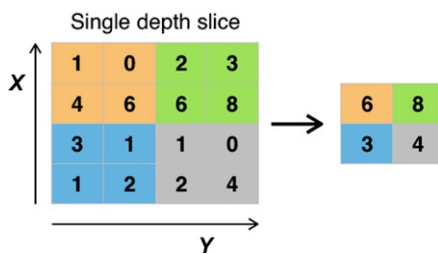


FIG. 7

Filter processing.

**FIG. 8**

The input volume is $32 \times 32 \times 3$. If we imagine two borders of zeroes around the volume, this gives us a $36 \times 36 \times 3$ volume. Then, when we apply our conv layer with our three $5 \times 5 \times 3$ filters and a stride of 1, then we will also get a $32 \times 32 \times 3$ output volume.

**FIG. 9**

Example of Maxpool with a 2×2 filter and stride of 2.

and sigmoid are used. After applying these nonlinear programs, we choose this pooling layer to downsample the layer. There are several pooling options to input the volume and output the maximum number in every subregion that filters convolve around (Fig. 9).

Fully connected. Layer is for the detection of higher level of features which is situated at the end of the network. This layer basically takes input volumes and outputs an N dimensional vector where N is the number of classes of the program. Each number of classes defines the probability of a certain class. For example, if the resulting vector for a digit classification program is [0.0.1.75.0.0.0.0.0.5], this represents that a 100% probability that the image is 2 digit. 75% probability that the image is 2 digit and so on. In this way fully connected layer extract the features to correlate the classes.

2.1.5 Recurrent Neural Network

This type of network mainly deals with sequential data. Like all other Feed Forward Networks, when all the input as well as output sequences are independent of each other (for example like predicting the next word of a sentence based on the previous knowledge of the sentence during training). In RNN architecture mainly has direct cycles for feeding back the data again to the network that mainly takes the previous information through the network and makes prediction of the next sequences. The main idea behind a RNN is to mainly have memory that mainly captures the data by performing several calculations $S_t = f(Ux_t + Ws(t - 1))$. S_t is having a hidden state over t time, U is the sum of the weight between the current and hidden, W is the weight among the previous and current hidden units of the layer in the network, V is the weight among the input and output layer, and f is the hidden layer of function (activation functions are used such as ReLu, hyperbolic tangent, etc.) RNNs mainly share these above-shown parameters (U, W, V) at every layer of the network. These mainly use back propagation while training the networks. Fig. 10 shows the RNN and bidirectional RNN networks.

T when $t = 1$ to $t = \tau$, we update the equation:

$$\begin{aligned} a^{(t)} &= b + Wh^{(t-1)} + Ux^{(t)} \\ h^{(t)} &= \tanh(a^{(t)}) \\ o^{(t)} &= c + Vh^{(t)} \\ \hat{y}^{(t)} &= \text{softmax}(o^{(t)}) \end{aligned}$$

In above questions b and c are bias vectors along with the weight matrix U , V and W form input to hidden unit, hidden to output unit, hidden to hidden connections. These above figure maps RNN to the input sequence and output sequence of the same

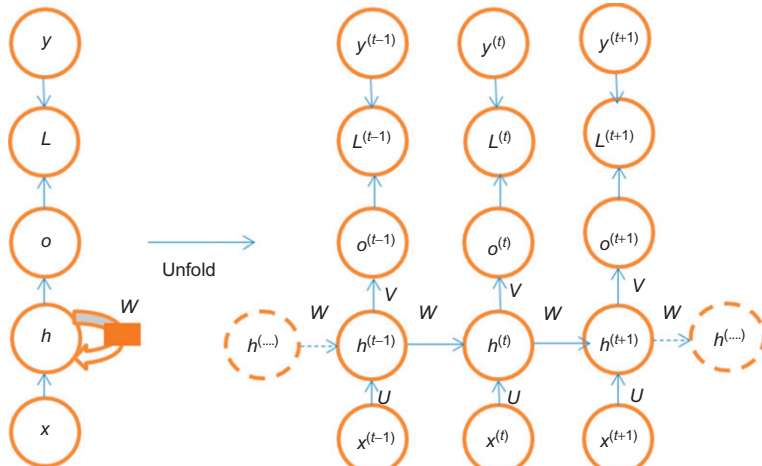


FIG. 10

RNN Deep Learning structure.

length. The total loss for a given sequence of value x is paired with sequence y value then take sum of the loss over all the time stamp.

An RNN is a network of neurons with each one directly connected to every other node. Each node is time varying by calculating the real-valued activation function. Each connection has a modifiable real value of weight node. Output nodes calculate the result and several hidden nodes mainly modify the data as per the input and output data feed to the network.

The basic difference between a feed-forward neural network and a RNN is shown in the figure. These feed-forward neurons have one connection from input to output. RNN has an extra connection from output again to input that is mainly feedback to network and along with these it also contain activation function that can flow to the loop. When many of these feed-forward and RNN are connected together, they mainly form a RNN.

RNNs mainly have two advantages:

- *Store information:* These recurrent networks are feedback to store the information over time in the form of an activation function so it mainly has to store information in a form of memory.
- *Learn from sequential data:* These may have sequential data of any length. As shown in the above figure, it is stated that using one fixed input and one fixed output may have one to many, many to one, many to many input to output sequences. So using these approaches, one can solve the problem for sequential data input to predict the next upcoming sequences.

Researchers are using the RNN along with LSTM and GRU to get more powerful results. Several researchers are using RNN along with GRU, which is the popular method for solving the problem for extracting the features for protein structure prediction. By using LSTM, it mainly has three gates: an input gate, a forget gate, and an output gate.

Why use an RNN? This type of network has advantage to make unit context to extract the information over a large set of neighborhoods specially for recognizing the images. With the help of these information these RNN can have watch over a large input space, CNN have this limitation over higher layer of abstraction. So, a recurrent network connection increases the depth when they keep the number parameter low by sharing the weight vector. Additionally, these RNNs also have the ability to handle the sequential data. These types of network also handle biologically inspired tasks, as brains can do.

How does LSTM improve the RNN?

One of the drawbacks of an RNN is that the contextual information is limited and, by using back propagation, this is quite time consuming and will not properly work. So, it is notable for vanishing or exploding the output result, mainly called the Vanishing Gradient or Exploding Gradient. These take huge time to solve the problem of vanishing gradients. These exploding gradients lead to weight oscillation that reduces the quality of the network. For storing the information over some time interval exploding

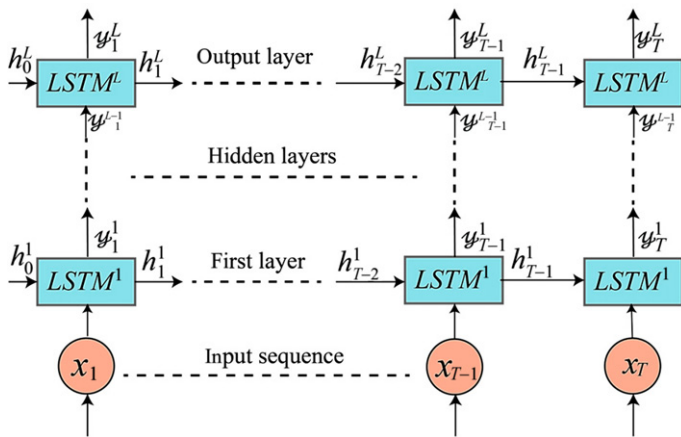


FIG. 11

LSTM basic architecture.

gradients took longer time and created the error flow. To address this problem Hocheriter uses LSTM to solve the problem of error backflow. In LSTM they are using special units that improve the RNN and create a bridge.

LSTM mainly consists of a forget gate, input gates, and an output gate. The LSTM cell is a step-wise gate, and each cell is connected in a network. The first step is the forget gate at h_{t-1} and x_t that mainly computes the output f_t over a number between 0 and 1. These cells are multiplied with the cell c_{t-1} that gets the cell to either forget everything or keep the result of the output. For example, a value of 0.5 means the cell loses/forgets 50% of the information. The next step of the input gate is updating the cell so it mainly multiplies the output of I_t and c_t and then adding these values to input $c_{t-1} \times f_t$. The final output is computed and multiplied o_t with tanh to get the previous result to $ht = o_t \times \tanh(C_t)$ and $o_t = \sigma \times W_o[ht - 1, xt] + bo$ (Fig. 11).

3 IMPLEMENTATION ENVIRONMENT

DL is a vital new domain of ML that incorporates a varied range of NN architecture intended to finish various tasks. CNN has proven to be an excellent approach for healthcare and medical image analysis. Because conventional ML needs determination and calculation of features from which the algorithm learns, DL approaches (e.g., CNN) learn the important features as well as the optimized weighting of those features to make predictions for new data. Here we will describe some of the libraries and tools that exist to aid in the proficient execution of DL as applied to healthcare and medical images.

3.1 TOOLKIT SELECTION/EVALUATION CRITERIA [13]

In this section, we have presented all criteria that are required for selection or evaluation of toolkits so you can have a clear choice of toolkit on which to work. [Table 2](#) describes all information regarding the selection or evaluation of toolkits.

3.2 TOOLS AND TECHNOLOGY AVAILABLE FOR DEEP LEARNING [13]

[Table 3](#) describes all the available tools and technology, with a short description and some sample code with the application, “How to create a deep learning model?”

3.3 DEEP LEARNING FRAMEWORK POPULARITY LEVELS [14]

Here we have shown the rankings of 23 open-source DL libraries that are valuable for data science, based on Github and Stack Overflow activity as well as Google search results. [Table 4](#) shows standardized scores where a value of 1 means one standard deviation above average (average = score of 0). See below for methods.

Table 2 Toolkit Selection Criteria [13]

Evaluation Criteria	Details
Languages	Languages are one of the important parameters for toolkit selection. Computer languages show how efficient a particular toolkit is. If we know that this particular toolkit builds using some language and we are also familiar with that language, we can work properly and if we want to modify the toolkit, then we can also give our input
Documentation	The quality of documentation and the given and explained examples in the documentation will lead you to create good solutions for your problem. Well-maintained documentation is also an indication of good stability of a toolkit
Development environment	To reduce the programming complexity for network creation, there is a clear need for a development environment. Through this we can have a connection with graphical tools and some visualization tools. So, after implementing a program, we want some graphical representation or visualization, that problem can be solved by the development environment
Execution speed	This is related to the speed of essentially organizing or segmenting the image with the trained network. This thing involved lots of calculations per pixel. For medical applications, training is less important than training speed. So execution speed is one of the important parameters for toolkit selection
Training speed	Training Speed is mainly dependent on the math libraries used in a toolkit. It is also dependent on the type of tasks and images
GPU support	In today's era of big data, medical image data size becomes very large. For this purpose, we must speed up things. GPU can give us excellent speed in comparison to CPU processing. So those

Continued

Table 2 Toolkit Selection Criteria [13]—Cont'd

Evaluation Criteria	Details
Maturity level	toolkits that have GPU integration support have more benefits than other toolkits. So GPU support we can consider as one of the selection parameters of toolkits
Model library	Maturity level is totally our subjective assessment about how mature a toolkit is? That measurement you can get by grouping a big user base, some error fixing in previous months or decent backing community
Github Commits	Toolkits have a library of code that generates networks, and the nodes have associated weights. This is like a platform where one may download various popular orientations of networks and weights
Github contributors	The older the toolkit, the more GitHub Commits are available. It is the indicator of how many times toolkits have changed after putting on the GitHub. Sometimes it is misleading because newly released toolkits have fewer commits than older ones. So at that time we cannot any decision about maturity and stability of that toolkit
	The more contributors, the more user support you have. You can explore more applications when user contributors are greater

Table 3 Deep Learning Toolkits

Toolkits	Description
Caffe	<ul style="list-style-type: none"> One of the highest rated and most mature tools created by Berkeley Vision and Learning Center Architecture is based on pure C++ or CUDA to support DL It has support of command line, Python, and MATLAB interfaces Fast Easy switching between CPU and GPU—Caffe::set mode(Caffe::GPU)
Deeplearning4j	<ul style="list-style-type: none"> It is written in Java with a Scala API It has GPU support Not very popular in medical imaging Good performance and supports multiple GPUs
Tensor flow	<ul style="list-style-type: none"> Created by Google and gathered lots of popularity It provides excellent performance and multiple CPUs and GPUs support Educational tool available as a web app (http://playground.tensorflow.org/)
Theano	<ul style="list-style-type: none"> Uses symbolic logic and written in Python Easy to build a network but challenging to create a full solution Documentation quality is fair

Table 3 Deep Learning Toolkits—Cont'd

Toolkits	Description
Keras	<ul style="list-style-type: none"> Created in Python and we can use with Theano or Tensorflow backend Easy to read and build Version 2.1.1 is the latest for keras
MXNet	<ul style="list-style-type: none"> Written in C++ with collaboration with many languages Multi-GPU support
Lasagne	<ul style="list-style-type: none"> For learning purposes, training examples are listed on GitHub Created in Python and we can say that it extension of Theano Easier to build than Theano
Cognitive Network Toolkit (CNTK)	<ul style="list-style-type: none"> Developed by Microsoft Performance is generally good Usage is currently less than many others
DIGITS	<ul style="list-style-type: none"> Developed by NVIDIA Web-based tool for developing deep networks For identification of errors in the text file, it has a network visualization tool Multiple GPU support (https://www.youtube.com/watch?v=dgxe15vCR7s)
Torch	<ul style="list-style-type: none"> Created in C Performance is very good You can get reference for Torch from the below link (http://torch.ch/docs/tutorials-demos.html)
PyTorch	<ul style="list-style-type: none"> Newcomer It is a Python front end to the Torch computational engine. It is an integration of Python with the Torch engine Performance is higher than Torch with GPU integration facility Flexible You can get reference for PyTorch from the below link (http://pytorch.org/tutorials/beginner/pytorch_with_examples.html#pytorch-nn)
Chainer	<ul style="list-style-type: none"> Difference between other toolkits and chainer is that it is building the network as a section of its computation Stores its computations rather than the programming logic

Table 4 Deep Learning Library Ranking [14]

Library	Rank	Overall	Github	Stack Overflow	Google Results
tensorflow	1	10.87	4.25	4.37	2.24
keras	2	1.93	0.61	0.83	0.48
caffe	3	1.86	1.00	0.30	0.55
theano	4	0.76	-0.16	0.36	0.55
pytorch	5	0.48	-0.20	-0.30	0.98

Continued

Table 4 Deep Learning Library Ranking [14]—Cont'd

Library	Rank	Overall	Github	Stack Overflow	Google Results
sonnet	6	0.43	-0.33	-0.36	1.12
mxnet	7	0.10	0.12	-0.31	0.28
torch	8	0.01	-0.15	-0.01	0.17
cntk	9	-0.02	0.10	-0.28	0.17
dlib	10	-0.60	-0.40	-0.22	0.02
caffe2	11	-0.67	-0.27	-0.36	-0.04
chainer	12	-0.70	-0.40	-0.23	-0.07
paddlepaddle	13	-0.83	-0.27	-0.37	-0.20
deeplearning4j	14	-0.89	-0.06	-0.32	-0.51
lasagne	15	-1.11	-0.38	-0.29	-0.44
bigdl	16	-1.13	-0.46	-0.37	-0.30
dynet	17	-1.25	-0.47	-0.37	-0.42
apache singa	18	-1.34	-0.50	-0.37	-0.47
nvidia digits	19	-1.39	-0.41	-0.35	-0.64
matconvnet	20	-1.41	-0.49	-0.35	-0.58
tflearn	21	-1.45	-0.23	-0.28	-0.94
nervana neon	22	-1.65	-0.39	-0.37	-0.89
opennn	23	-1.97	-0.53	-0.37	-1.07

4 APPLICABILITY OF DEEP LEARNING IN FIELD OF MEDICAL IMAGE PROCESSING [15]

Recognizing anomalies and quantifying dimensions and modifications over time are the initial tasks for image analysis. Machine learning based automated tools are really key features to enhance the quality of image analysis. The DL technique is a comprehensively useful technique that provides state-of-the-art accuracy. DL has opened new doors in medical image scrutiny. DL applications in medical domains cover a large range of complications, going from cancer detection and disease monitoring to custom-made behavior suggestions. Nowadays, numerous sources of data from medical digital imaging (X-ray, CT, and MRI scans) and genomic sequences have brought a huge quantity of information to the physician.

4.1 CURRENT RESEARCH APPLICATIONS IN THE FIELD OF MEDICAL IMAGE PROCESSING

Here is the list of current research applications of DL in the field of medical image processing:

- Tumor detection (skin cancer, lung cancer, breast cancer, brain cancer etc.)
- Tracking tumor development

- Blood flow quantification and visualization
- Medical interpretation
- Diabetic retinopathy [16]
- Alzheimer's and Parkinson's diseases detection
- Liver disease detection [9]
- Renal disease detection [10]

5 HYBRID ARCHITECTURES OF DEEP LEARNING IN THE FIELD OF MEDICAL IMAGE PROCESSING [17]

One of the state-of-the-art approaches is the DL hybrid architecture approach. This approach generally combines two or more individual DLAs and makes a hybrid architecture. Here is the list of some hybrid architectures, although they are not at the maturity level.

- Convolutional Auto-Encoder (CAE).
- Deep Spatiotemporal Neural Networks (DST-NNs).
- Multidimensional Recurrent Neural Network (MD-RNNs).

Below is a list of different papers that include work on hybrid approaches with their application domains ([Table 5](#)).

Table 5 Hybrid Approaches in Medical Domains [18–20]

Author	Database	Application
Tom Brosch [18]	They have used 5–250 samples for segmentation from the MS clinical dataset	Multiple sclerosis lesion segmentation <i>Model used:</i> CAE
Mohammed Shameer Iqbal [19]	Here they have taken 20 students dataset of their 0–9 handwritten digits images and audio data. In totality they have created 2000 handwritten images and 2000 audio recording data of 0–9 digits	Character classification from two different modalities: image and audio <i>Model:</i> Deep belief network with contractive stacked restricted Boltzmann machine
Sayan Ghosh [20]	1. Flickr8k and Flickr30k (Image) 2. DISFA and BP4D datasets (Psychological Distress)	1. Prediction of psychological distress 2. Detection of facial action units using multilabel CNN <i>Model:</i> Multilabel CNN

6 CHALLENGES OF DEEP LEARNING IN THE FIELDS OF MEDICAL IMAGINING [17]

Although DL has given excellent performance in almost all bioinformatic applications, it still faces some challenges, as described below:

Unavailability of large data & imbalance data: Especially in cancer domain because of some security reasons, we cannot get large amounts of data. Biomedical imagining data modalities have lots of imbalanced data for classification into sub-categories. Until now, several DLAs have achieved outstanding results over large data. To do this for biomedical imaging is quite a challenging task. To overcome these problems for such Medical Imagining through use of good preprocessing algorithms, cost-responsive learning and algorithmic change.

Changing from a higher level to a very specialized level: There is one unfair criticism against DL, and that is it's higher level representation, which we can call black box. DL gives exceptional outcomes but because of higher level representation or black box kind of approach we know extremely few things regarding how such outcomes are resulted inside. In biomedical areas, it is quite difficult to produce accurate solutions because of several studies that are mainly related to human health. So, DL methodologies have to adopt specialized level (white box) learning instead of higher level learning.

Thus selection of an appropriate architecture and hyper parameters of Deep Learning: One should know the proper function of each architecture in DL for obtaining vigorous and consistent outputs. As per the input data types and research objectives of such DLAs, performance may vary. Yet several functionalities are not understood. When DLA is selected at that time, there are lots of hyper parameters that we have to take under consideration, for example, hyper parameters such as learning rates, the number of hidden layers, initial weight values, bias values, learning iterations, etc. Proper value selection of the hyper parameter makes a valuable change in the performance of the DLA.

Hybrid and multimodality DL: Hybrid architecture we can generally know as a combination of more than one DLA. The biomedical fields offer different types of data modalities, as described in the above sections. But if we consider biomedical image modality, they offer lots of formats such as X-ray, MRI, PET, CT etc. So with the use of such modalities, we get better solutions to the problems. Some of the researchers, such as Suk et al. and Soleymani et al. [11], have proposed different multimodalities for Alzheimer's disease classification and emotion detection, respectively.

Speeding up these DLAs: In this era of big data, any application-related database becomes larger and larger. To analyze these kind of data using DL architectures require large amount of time. To get faster result and speed up the performance of the learning we can use GPUs.

7 CONCLUSION

Over the last few years, these DLAs have found a vital spot in the direction of the automation or computerization of our everyday life, delivering tremendous improvements by comparing these conventional machine learning algorithms (MLAs). By looking toward the contribution of DL in today's era, researchers are thinking that by the next 10–15 years, DL will give full automation to humans for their daily activities. Utilization of DL benefits in healthcare, especially in the medical image domain, is growing faster and faster. First, we have stated the basic requirements of the DL algorithm over machine learning architectures. After that we have detailed understanding of all architectures along with limitations and advantages. We have also stated the implementation environments for evaluating the performance. In the final section, we highlighted state-of-the-art applications of biomedical imaging analysis using DL.

Therefore, several research organizations are mainly working on DL, based on the efficient solution that mainly encourages using these techniques on biomedical imagining. By analyzing machine learning or deep learning effects on the real world, human will soon be replaced in almost all medical-related applications. However, we should not only consider the solution but also several challenges that reduce the growth of medical data. One of the greatest challenges is the unavailability of such an annotated dataset. Generally Deep Learning methods provides positive feedback but if we are considering healthcare data for analysis it is also a challenging task for DL methods because healthcare data required higher sensitive values.

REFERENCES

- [1] J.D. Miller, Learning IBM Watson Analytics, Packt Publication Ltd, Livery Place, 2016, pp. 1–25. ISBN 978-1-78588-077-3.
- [2] D.M. Health, Google DeepMind, <https://www.deepmind.com/health>, 2016.
- [3] P. Baldi, G. Pollastri, The principled design of large-scale recursive neural network architectures-dag-RNNs and the protein structure prediction problem. *J. Mach. Learn. Res.* 4 (2003) 575–602.
- [4] O. Denas, J. Taylor, Deep modeling of gene expression regulation in an Erythropoiesis model, International Conference on Machine Learning workshop on Representation Learning, Atlanta, Georgia, USA, 2013.
- [5] S. Lee, M. Choi, H-S. Choi, et al. FingerNet: deep learning-based robust finger joint detection from radiographs. In: Biomedical Circuits and Systems Conference (BioCAS), 2015 IEEE. 2015. p. 1–4. IEEE.
- [6] P. Mirowski, D. Madhavan, Y. LeCun, et al., Classification of patterns of EEG synchronization for seizure. *Int. Fed. Clin. Neurophysiol.* 120 (2009) 1927–1940, Published by Elsevier Ireland Ltd. <https://doi.org/10.1016/j.clinph.2009.09.002>.
- [7] S. Min, B. Lee, S. Yoon. “Deep learning in bioinformatics.” arxiv preprint arxiv:1603.06430 (2016).

- [8] S. Malik, K. Khatter, Malicious application detection and classification system for android mobiles, *Int. J. Ambient Comput. Intell.* 9 (1) (2018) 95–114.
- [9] L. Saba, N. Dey, A.S. Ashour, S. Samanta, S.S. Nath, S. Chakraborty, et al., Automated stratification of liver disease in ultrasound: an online accurate feature classification paradigm, *Comput. methods Prog. Biomed.* 130 (2016) 118–134.
- [10] K. Sharma, J. Virmani, A decision support system for classification of normal and medical renal disease using ultrasound images: a decision support system for medical renal diseases, *Int. J. Ambient Comput. Intell.* 8 (2) (2017) 52–69.
- [11] Y. LeCun, Y. Bengio, G. Hinton, Deep learning, *Nature* 521 (7553) (2015) 436–444.
- [12] H. Li, Q. Lyu, J. Cheng, A template-based protein structure reconstruction method using deep autoencoder learning, *J. Proteomics Bioinform.* 9 (2016) 306–313, <https://doi.org/10.4172/jpb.1000419>.
- [13] B.J. Erickson, P. Korfiatis, Z. Akkus, T. Kline, K. Philbrick, “Toolkits and libraries for deep learning”, Published online: 17 March 2017
- [14] https://github.com/thedataincubator/datascience/blogs/blob/master/output/DL_libraries_final_Rankings.csv.
- [15] A.-R. Ali, “Deep learning applications in medical imaging”, September 14, 2017.
- [16] Z. Li, N. Dey, A.S. Ashour, L. Cao, Y. Wang, D. Wang, et al., Convolutional neural network based clustering and manifold learning method for diabetic plantar pressure imaging dataset, *J. Med. Imaging Health Inform.* 7 (3) (2017) 639–652.
- [17] M. Pandya, S. Jardosh, Applications and challenges of deep learning in the field of bio-informatics, *Int. J. Comput. Sci. Inform. Secur.* 15 (7) (2017).
- [18] T. Brosch, Y. Yoo, L.Y.W. Tang, D.K.B. Li, A. Traboulsee, R. Tam, Deep convolutional encoder networks for multiple sclerosis lesion segmentation, in: N. Navab et al., (Ed.), *MICCAI 2015*, Part III, 2015, pp. 3–11. LNCS 9351.
- [19] M.S. Iqbal, D.L. Silver, A scalable unsupervised deep multimodal learning system, *Proceedings of the Twenty-Ninth International Florida Artificial Intelligence Research Society Conference*, 2016.
- [20] S. Ghosh “Challenges in deep learning for multimodal applications”, *Proceedings of the 2015 ACM on International Conference on Multimodal Interaction*, Pages 611–615, University of Southern California, Los Angeles, CA.

FURTHER READING

- [21] S.S. Ahmed, N. Dey, A.S. Ashour, D. Sifaki-Pistolla, D. Bălas-Timar, V.E. Balas, J.M.R. Tavares, Effect of fuzzy partitioning in Crohn’s disease classification: a neuro-fuzzy-based approach, *Med. Biol. Eng. Comput.* 55 (1) (2017) 101–115.
- [22] N. Dey, A.S. Ashour, A.S. Althoupety, Thermal imaging in medical science, in: *Recent Advances in Applied Thermal Imaging for Industrial Applications*, IGI Global—United States of America, 2017, pp. 87–117.
- [23] N. Dey, A.S. Ashour (Eds.), *Classification and Clustering in Biomedical Signal Processing*, first ed., IGI Global—United States of America, 2016 (April 7, 2016).
- [24] O. Azzabi, C.B. Njima, H. Messaoud, New approach of diagnosis by timed automata, *Int. J. Ambient Comput. Intell.* 8 (3) (2017) 76–93.
- [25] M.Y. Khachane, Organ-based medical image classification using support vector machine, *Int. J. Synth. Emot.* 8 (1) (2017) 18–30.

Reasoning methodologies in clinical decision support systems: A literature review

4

Nora Shoaip*, Shaker El-Sappagh[†], Sherif Barakat*, Mohammed Elmogy[‡]

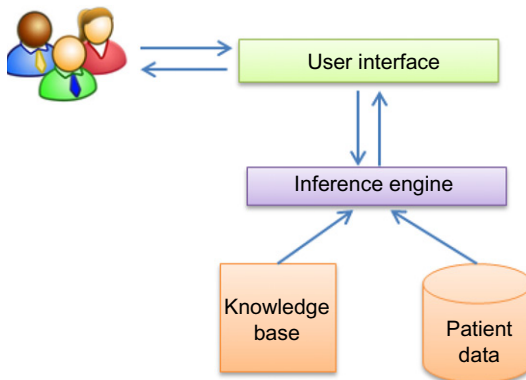
*Information Systems Department, Faculty of Computers and Information, Mansoura University,
Mansoura, Egypt* Information Systems Department, Faculty of Computers and Informatics, Benha
University, Benha, Egypt[†] Information Technology Department, Faculty of Computers and
Information, Mansoura University, Mansoura, Egypt[‡]*

CHAPTER OUTLINE

1	Introduction	61
2	Methods	67
2.1	Research Questions	67
2.2	Selection Criteria	67
2.3	Search Strategy	68
3	Literature Review and Results	68
3.1	Paper Screening	69
3.2	Selecting the Most Relevant Papers	71
3.3	Extracting and Analyzing Concepts	72
3.4	Current Challenges and Future Trends	82
4	Conclusion	83
References	84	

1 INTRODUCTION

In the last decade, great work in the expert system was performed in medical diagnosis. It attempted to use CDSS for reasoning large and complex medical domains [1]. CDSS helps physicians in selecting appropriate treatments and making proper decisions to improve the quality of the medical diagnosis. As shown in Fig. 1, most CDSSs consist of three parts: the first part is the knowledge base that contains the rules, the second part is an **inference engine** that applies logical rules to the knowledge base to deduce new knowledge, and the third part is a communication mechanism show the results to the user. The reasoning is true power and an important task performed by the inference engine of the CDSSs, which combine medical

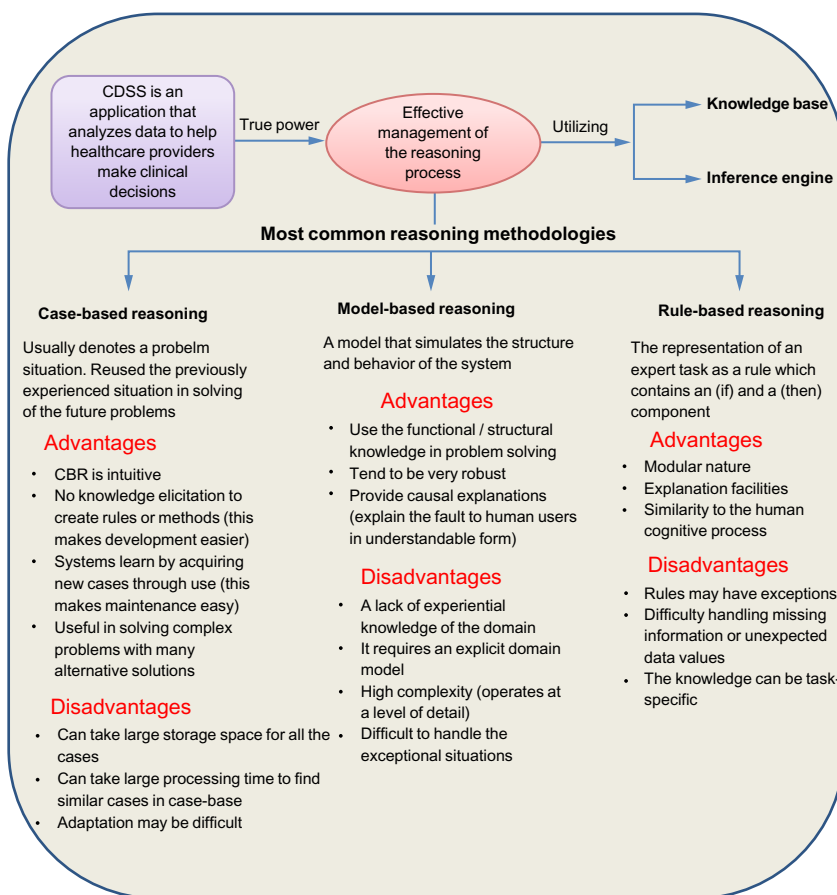
**FIG. 1**

The CDSS component.

knowledge with patient-specific data to generate relevant decisions. The reasoning methodologies provide powerful tools and techniques for manipulating knowledge to make an inference and a decision as well as solve the problem. The reasoning process in a medical diagnostic is a complex process as it has to consider many different facts, including the patient's history, current symptoms, test results, received therapies, and possible allergies as well as map those conditions to a list of possible matching diagnoses. There are different reasoning methods suitable for different knowledge representations and application areas [2,3]. The most common reasoning methodologies are MBR, rule-based reasoning (RBR), and case-based reasoning (CBR). In addition, Fig. 2 shows the advantage and disadvantages of the CDSS description and reasoning methodologies.

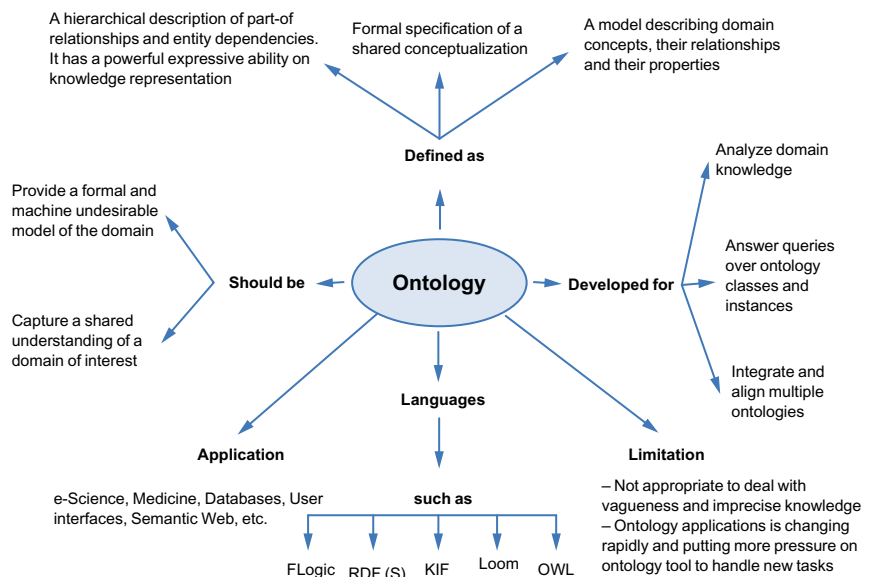
To provide successful suggestions, an ontology system is proposed [4]. Using ontology in building CDSS systems is widely adopted because it has many advantages, such as being a proper technique for knowledge representation, supporting modularity and enhancing scalability by giving the capabilities of describing, reusing, and sharing patient data [5]. Fig. 3 shows a general definition of ontology as well as the limitations, applications, and languages.

Many recent studies noted that ontologies and its languages are not suitable to handle the vagueness of knowledge [6]. To overcome this problem, a fuzzy ontology system has been developed that combine's fuzzy logic with ontology reasoning. Fuzzy ontology has vagueness-handling capabilities and modeling capabilities [7]. It can help in understanding semantic relationships by applying fuzzy logic to deal with the vagueness of data. Recently, type-2 fuzzy ontology (T2FO) [8–10] was developed whereas fuzzy type-2 deals with the fuzziness of fuzzy membership. Type-2 fuzzy sets provide additional degrees of freedom that can make it possible to handle uncertainties that involve the varying opinions and preferences of experts. Table 1 shows a comparison between Type-1 fuzzy logic and Type-2 fuzzy logic. Li et al. [11] showed that T2FO achieved more accurate results than T1FO in dealing with imprecise knowledge.

**FIG. 2**

The CDSS description.

Rule-based systems (RBS) [12–14] use a classical way to represent human knowledge, which is the use of “IF-THEN” rules. For real modeling systems, classical tools are unsuccessful in handling the complexity, imprecision, uncertainty, and vagueness. Fuzzy systems are an important tool for modeling complex systems. This leads to Fuzzy rule-based systems (FRBSs) [15] where fuzzy logic may be used as a tool for successfully handling uncertainty and vagueness while increasing the flexibility of inference methods with approximate reasoning methods of fuzzy logic. The FRBS systems have been widely used, and they achieved good results in many different studies. These FRBSs [16] are appropriate to receive the information as input facts, provide semantic conclusions, and finally return knowledge that can be readable by humans and easily maintained. Fig. 4 shows general notes of fuzzy rule-based systems. A fuzzy inference system (FIS) is based on three stages, as shown in Fig. 5.

**FIG. 3**

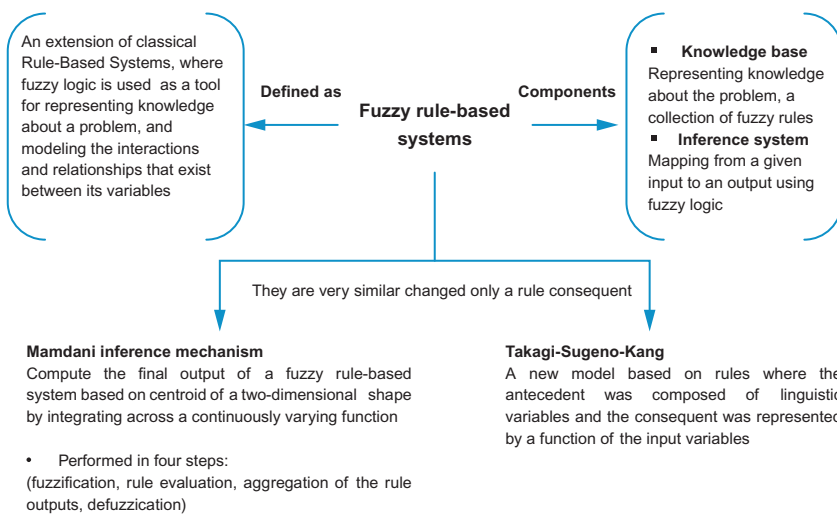
An overview of ontology definition.

Table 1 A Comparison Between Type-1 and Type-2 Fuzzy Logic

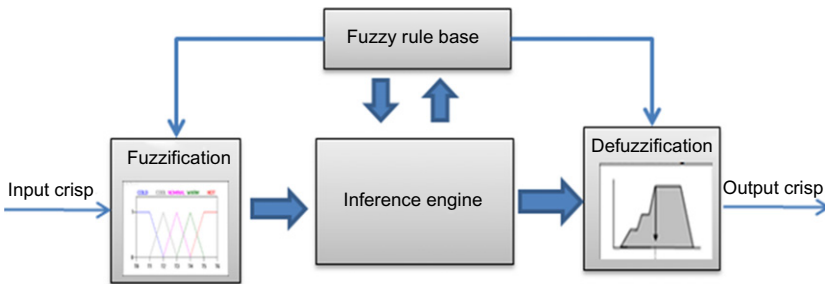
Type-1 Fuzzy Logic	Type-2 Fuzzy Logic
Deals with crisp membership A generalization of a crisp set and its membership grade is a crisp number in $[0, 1]$ The membership functions (MFs) of Type 1 fuzzy sets are one-dimensional The T1FLS consists of a Fuzzifier, inference engine, rule base, and Defuzzifier	Deals with the fuzziness of fuzzy membership Characterized by a fuzzy membership, and its membership grade for each element of this set is a fuzzy set in $[0, 1]$ The MFs of type 2 fuzzy sets are three-dimensional The T2FLS consists of a Fuzzifier, inference engine, rule base, type-reducer, and Defuzzifier

The fuzzification stage transforms numerical values into membership degrees. The inference engine applies logical rules to the knowledge base and deduces new knowledge. The defuzzification stage yields a crisp value from the rule aggregation result.

The most commonly used techniques are the Mamdani and Takagi-Sugeno-Kang (TSK) approaches [17,18]. Many researchers noted that the Mamdani approach is better than the TSK model in real problems to detect understandable human knowledge [17]. On the other hand, other researchers showed that the Mamdani fuzzy structure requires a higher computational effort because it is needed to calculate a

**FIG. 4**

A general review of fuzzy rule-based systems.

**FIG. 5**

A fuzzy inference system.

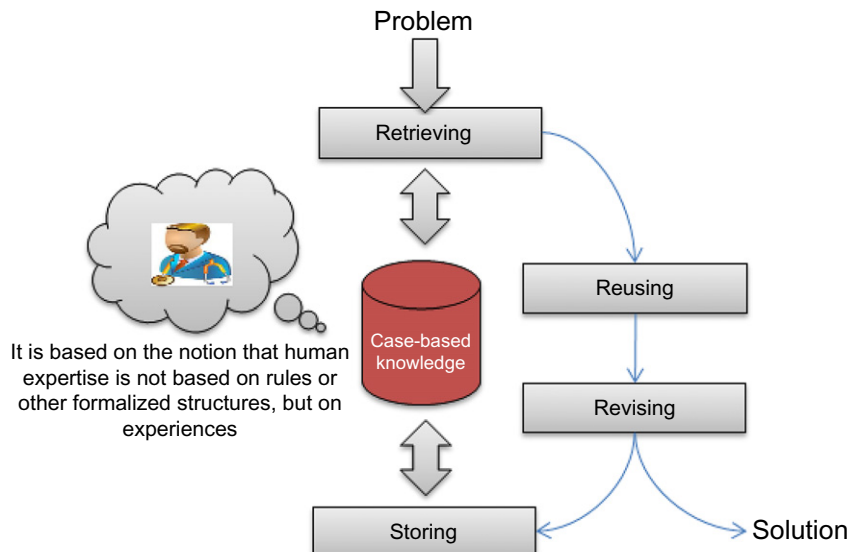
whole membership function, which is then defuzzified [17]. This advantage to the TSK approach makes it highly useful despite the success of Mamdani fuzzy reasoning regarding dealing with uncertainty. As shown in [Table 2](#), the most fundamental difference between the Mamdani-type FIS and the Sugeno-type FIS is the way the crisp output is generated from the fuzzy inputs.

CBR has been used in many CDSS applications because it has a high user acceptance, can propose solutions to the incomplete problem, and improves over time as the case base grows. [Fig. 6](#) shows the general notes of problem solving by CBR.

The ultimate goal of this survey is to give an overview of scientific literature directions in CDSS with a focus on reasoning methodologies and their practical

Table 2 Comparison Between Mamdani and Takagi-Sugeno-Kang

Mamdani	Sugeno
Mamdani FIS uses the technique of defuzzification of a fuzzy output	Sugeno-type FIS uses a weighted average to compute the crisp output
Mamdani FIS has output membership functions	Has no output membership functions
The expressive power and interpretability	No expressive power because the consequents of the rules are not fuzzy
FIS entails a substantial computational burden	Computationally efficient and works well with optimization and adaptive techniques
Less flexible in system design	More flexible in system design. It can be integrated with the ANFIS tool to optimize outputs
Widely accepted for capturing expert knowledge. It allows us to describe the expertise in a more intuitive, more human-like manner	Better processing time because the weighted average replaces the time-consuming defuzzification process

**FIG. 6**

The general description of problem-solving by CBR.

applications in the medical field. We discuss some of their main challenges. The study focuses on studying the roles of fuzzy ontology and fuzzy logic in the CDSS implementation given in the literature. We try to identify future trends in this domain, and we suggest the combination of ontology and Mamdani fuzzy inference in a hybrid CDSS system.

This survey is formed as follows. [Section 2](#) shows the methodology conducted in our review. In [Section 3](#), we draw the current status and highlight important issues depending on the results of the reviewed papers. Finally, [Section 4](#) highlights our conclusion and future works.

2 METHODS

We adopted a search methodology involving the definition of research questions, the determination of selection criteria, and the description of the search strategy.

2.1 RESEARCH QUESTIONS

The primary questions of this review are as follows:

Which reasoning techniques have been used in CDSS? What is the accuracy of using different reasoning techniques in real applications? What are the limitations of existing reasoning techniques that have been used? How do we enhance the reasoning process in DSS?

2.2 SELECTION CRITERIA

The articles were selected from all English language studies from 2009 through November 2017. We used several libraries and database search engines such as the Institute of Electrical and Electronics Engineers (IEEE), Springer Link, PubMed, CiteSeerX, ScienceDirect, and ELSEVIER. The articles were included in this study if they met the following criteria:

Specified	Fuzzy reasoning OR ontology reasoning OR rule-based reasoning OR case-based reasoning applied to medical side
Language	English
Period	Published between 2009 and November 2017
Content	Journal articles
Search topics	Computer science, artificial intelligence, medicine and health, and biomedical informatics
Disease restrictions	There were no disease restrictions but brief cancer
Database	Included data about medical side
Vocabulary term searches	(Fuzzy reasoning OR ontology reasoning OR rule-based reasoning OR case-based reasoning) moreover, (medical, health, or clinical decision support system, cancer)
Results	Searched in (title and abstract) Produced results based on using reasoning techniques in clinical decision support systems

2.3 SEARCH STRATEGY

As illustrated in Fig. 7, the search strategy contains four processes: paper screening, paper selecting, extracting and analyzing concepts, and identifying a future trend. In paper screening, the initial papers associated with the application of reasoning methodologies were extracted on the medical side. We selected papers according to the search criteria, aiming at knowledge extraction from medicine with a “reasoning” term appearing in their title, abstract, and keywords in the following electronic databases: IEEE Xplore, Springer Link, PubMed, Citeseer, and Science Direct. To ensure that the most relevant papers were obtained, the screening and examination were done many times. Initial papers extracted from the paper screening process passed to the paper selection. It was an exhaustive and very precise examination stage for all initial papers. The abstract and introduction of each paper were read. The papers that tended completely to the objective of this review were selected, and the other papers were deleted. Finally, 134 papers published between 2009 and 2017 were retained. The relevant papers were studied carefully to extract concepts, analysis, applications, and drawbacks of reasoning techniques that have been used in CDSS. Finally, the current issue is discussed, and future trends are drawn.

3 LITERATURE REVIEW AND RESULTS

Our search identified 1886 papers across different electronic databases. These papers are used as an initial database. After reviewing these papers carefully, we selected 134 relevant articles that are more interesting and suitable for the goals of this paper. These goals are to become fully aware of the reasoning methodologies commonly

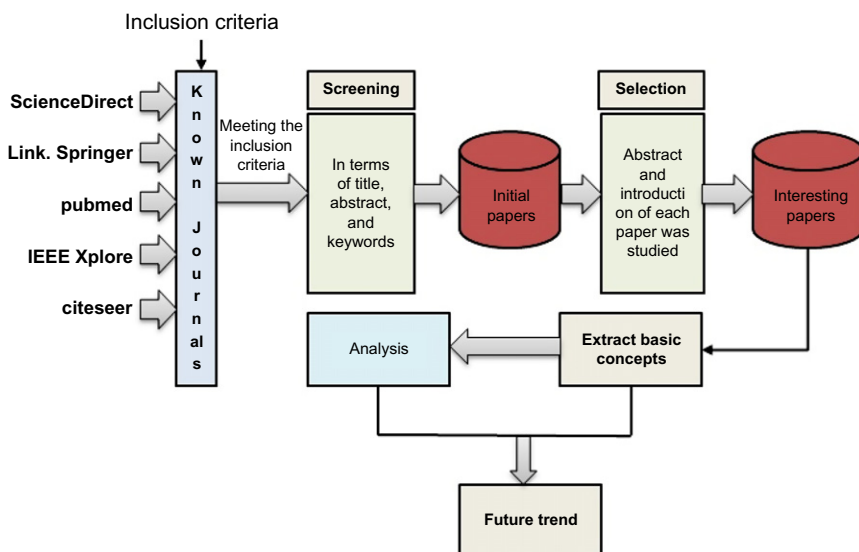


FIG. 7

The mentioned framework for the search strategy.

used to improve CDSS, discuss some of the main problems, and survey some of the relevant articles that used reasoning methodologies on the medical side. Finally, we are trying to find the future trends to solve that problem and the expected challenges facing us while achieving it.

3.1 PAPER SCREENING

The initial search step was done according to the search criteria in the following electronic databases: IEEE Xplore, Springer Link, PubMed, Citeseer, and Science Direct. In this section, the search refinements are processed in four iteration phases. The search query was ((clinical decision support system OR cancer OR medical diagnosis) AND (ontology reasoning OR fuzzy reasoning OR rule-based reasoning OR fuzzy logic OR case-based reasoning)). We utilized a mix of keywords and term searches (particularly in titles, abstracts, and keywords of the papers) in addition to search topics (computer science, artificial intelligence, medicine and health, and biomedical informatics). In each iteration, the exclusion criteria were done in the selected electronic databases to reflect the importance and accuracy of the selected papers. It involved papers that were not in English, industrial, duplicates, or theoretical. After four rounds of screening and examination as shown in Fig. 8, we, at last, chose 134 as the beginning papers significant to the survey. Fig. 9 shows the initial selected paper numbers from different electronic databases. Fig. 10 shows the initial paper numbers obtained from the period between 2009 and 2017.

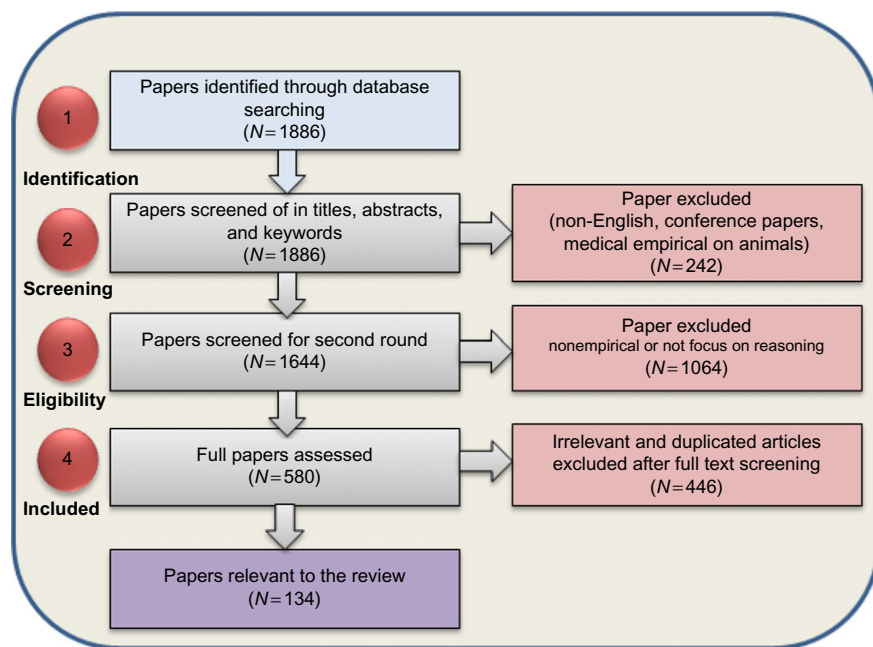
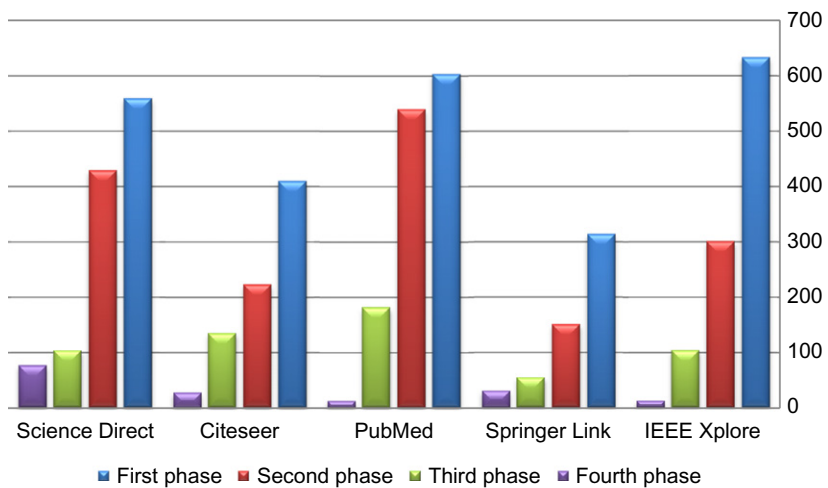
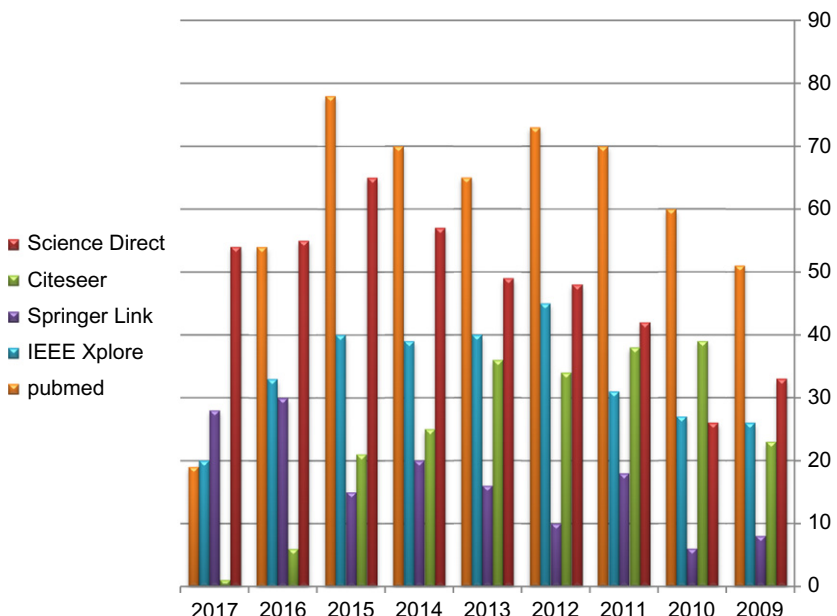


FIG. 8

An overview of the paper retrieval process.

**FIG. 9**

The number of selected papers from different electronic databases during four iteration phases.

**FIG. 10**

The number of initial papers obtained from the period of 2009 to 2017.

3.2 SELECTING THE MOST RELEVANT PAPERS

After a few rounds of exhaustive examination of the 1886 starting papers, we chose 134 papers significant to the objective of this review. Fig. 11 shows the number of selected papers obtained from the period between 2009 and 2017. It shows the increasing number of published papers related to the reasoning methodologies, especially in the last 4 years. Fig. 12 shows the grouping of selected papers according to the reasoning methodologies. It shows that CBR is the most used reasoning technique within the scope of our selected papers. Fig. 13 shows the grouping of selected papers according to medical diagnosis. About 38% focused on cancer, 29% focused on diabetes, and 55% manipulated another medical diagnosis. Fig. 14 shows the grouping of selected papers according to cancer type. It shows that breast cancer drew attention from researchers.

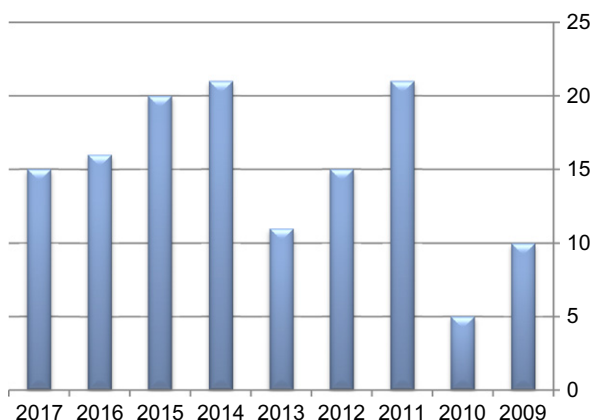


FIG. 11

The number of selected papers obtained from the period of 2009 to 2017.

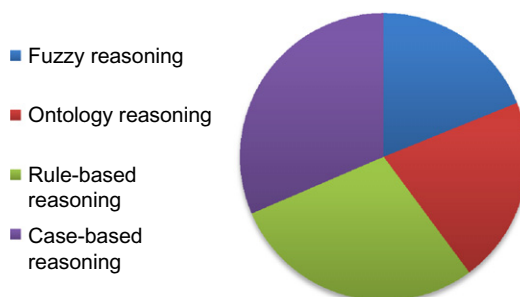
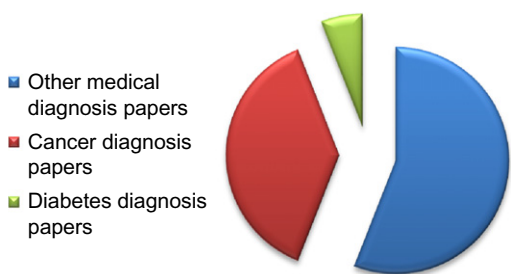
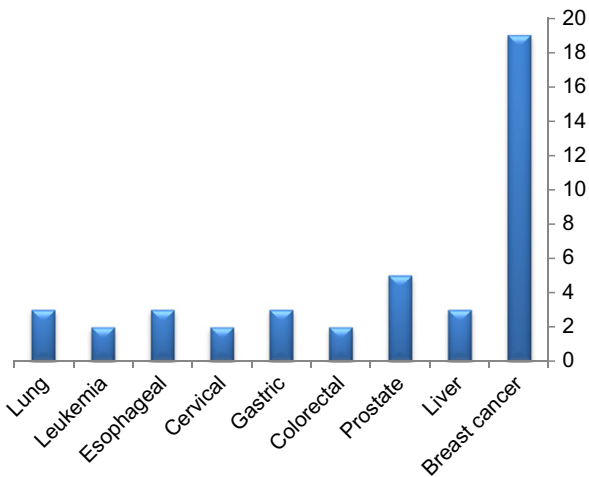


FIG. 12

The grouping of selected papers according to reasoning methodologies.

**FIG. 13**

The grouping of chosen papers according to medical diagnosis.

**FIG. 14**

The grouping of chosen papers according to cancer type.

3.3 EXTRACTING AND ANALYZING CONCEPTS

In the following subsections, the relevant papers are studied carefully to extract concepts and analysis about reasoning techniques that have been used in CDSS. Developing a CDSS model is an emergent task for many researchers who care about finding the most accurate and timely medical diagnoses, improving the semantic effectiveness, utilizing vague knowledge, enhancing the reasoning methodologies, and increasing the interoperability with the healthcare applications. As far as we know, few researchers focused on providing a useful survey of different reasoning methodologies used in building CDSSs. Pandey and Mishra [19] presented a useful study of the area of the medical expert system (MES). It uses different and combined methods of knowledge-based systems such as RBR, MBR, and CBR and intelligent

computing methods such as ANN and GA. Ahmed et al. [2] focused on the reasoning methodologies commonly used in evolving expert systems for diabetes diagnosis. The result of using these methodologies shows that CBR is the best one that provides dominant knowledge representations.

3.3.1 Rule-based reasoning

In medical diagnosis research, there are many models that have used Mamdani fuzzy inference systems. Basçiftçi and Hatay [12] established a rule base to facilitate diabetes treatment. They examined all diabetes probabilities by taking (10) indications (1024 cases). A reduced 15 main rules were obtained to establish the rule base and implement a program by the Delphi programming language 7. The accuracy of using 768 Indian patients was 97.13% in diabetes patients. Lukmanto and Irwansyah [15] proposed a fuzzy hierarchical model to perform early detection of diabetes. The accuracy result by using a real dataset collected from hospital laboratories in Indonesia was 87.46%. This method needed further development to improve functioning.

Pal et al. [13] developed an MES based on Mamdani inference for early detection of coronary artery disease (CAD). According to the result, there is a large gap between the specificity and sensitivity. It means there are more healthy people detected as unhealthy. Kim et al. [20] tried to provide a useful recommendation to coronary heart disease patients by proposing an adaptive prediction support model based on Mamdani. By using a real dataset, they built a fuzzy rule-based system by using a decision tree rule induction algorithm, which was validated by medical experts. Their model achieved a 69.22% accuracy rate.

Ling and Nguyen [21] detected the presence of hypoglycemic episodes. It depends on using GA with a fuzzy inference system. By using a dataset of 16 children with type 1 diabetes mellitus (DM), this model achieved a suitable specificity and high sensitivity. Ling and Nguyen [22] tried to identify the presence of hypoglycemic episodes. They proposed a fuzzy reasoning model with wavelet mutation. For a type 1 DM real dataset, the model achieved a good result. Mago et al. [1] designed an MES based on using a Mamdani inference algorithm to enhance the confidence level for the treatment of a broken tooth of the dentists. This system is easy to use by making a simple and interactive graphical user interface (GUI). d'Acierno et al. [23] designed and implemented fuzzy-based DSS for diagnosing breast masses. It integrated ontology and fuzzy rule-based models. The evaluation test is done using the Wisconsin Breast Cancer Dataset. Canavese and Ortega [24] evaluated urban environment sanitation and human health by using a real case study collected from Brazil. They designed a fuzzy rule-based system based on a Mamdani algorithm. Samuel et al. [25] implemented a web-based DSS, which used a fuzzy inference system for detecting typhoid fever. The evaluation test is done using a real dataset from Nigeria; the system accuracy was 94%. The model can be enhanced by doing the integration between fuzzy logic and ANN. Kunhimangalam et al. [26] developed a CDSS based on fuzzy logic for defining the type of neuropathy. The used dataset is integrated with medical records database. The accuracy of that system was 93.27%. Sharma and Choudhary [27] tried to improve accuracy for an Epistaxis

diagnosis. They implemented a web-based CDSS named “Disease Diagnosis.” Minutolo et al. [28] proposed guideline-based DSSs to handle the imprecise knowledge. The evaluation of this study achieved good satisfaction for medical users. Saez et al. [29] tried to build a rule-based CDSS for detection of DM that supported semantic interoperability. The model used a binding method based on an XML for mapping knowledge and rules to and from the CDSS.

3.3.2 Ontology reasoning

A number of proposed approaches have used an ontology system for knowledge representation. For example, Jaya [4] defined an ontology system for improving the accuracy of a DM diagnosis in an earlier stage. The Protégé tool environment was used for owl file construction for classes, objects, and attributes. The approach lacked an efficient retrieval methodology. The semantic retrieval should be forced to be an efficient retrieval. Chen et al. [5] developed an ontology-based medication system of the real dataset at Kaohsiung. It was responsible for giving an alert when it found any medication that can affect bone scans. They need to extend the proposed system to cover all imaging examinations for nuclear medicine. Reyes-Ortiz et al. [30] presented an ontology model for structuring medical knowledge to be computer-understandable information and support clinical diagnoses. For developing a semantic intelligent knowledge base, El-Sappagh and Farman [31] designed a diabetes diagnosis ontology (DDO) within a framework. The ontology was used to represent diabetes entities. For future lines, we must focus on improving and upgrading the DDO and developing a CDSS system to cover diabetes treatment.

Medical ontology systems may sometimes fail due to a fuzzy problem, which is related to the medical symptom. Some proposals have considered using fuzzy ontology. Lee and Wang [32] tried to provide a semantic description for detecting DM by developing a new fuzzy expert. It created the use of fuzzy ontology and a semantic fuzzy decision-making agent. Díaz et al. [6] tried to provide the representation of human activity by using fuzzy ontology. Fuzzy concepts and relations were used to help in reasoning about uncertain and incomplete knowledge. Also, they produced benefits through the recognition process. For future lines, we must implement interfaces for end users and model human behavior changes. Vyas and Pal [7] developed a fuzzy ontology model for the detection of malaria. The evaluation of this study was done using a dataset, which includes symptoms of malaria. The system’s accuracy achieved 95%, but it becomes low when adding more diseases. El-Sappagh et al. [3] proposed an OWL2 ontology for detecting DM. The system achieved an accuracy of 97.67%.

A recent development is the appearance of T2FO in several studies. Lee et al. [8] created a novel T2FO for food ontology and diet assessment. The experiments were done using a dataset collected from Tainan, and it achieved feasibility for diet assessment. For future lines, this proposed method needs to include the genetic learning mechanism. Lee et al. [9] proposed knowledge representation applications based on T2FO for diabetic diet recommendations. The evaluation of this study showed that using T2FO could better deal with the uncertainties than T1FO. For future lines,

we must provide automatic learning of the ontology learning and apply the proposed agent to other areas of diet, such as losing weight. Lee et al. [10] presented a mechanism for diet linguistic recommendation for Taiwanese meals. It was built by using T2FLS and FML. This proposed mechanism achieved a greater accuracy than the classical fuzzy logic system. Future works involve dealing with the complexity of encoding the chromosomes and developing the proposed mechanism as a smartphone app.

3.3.3 Ontology-based fuzzy decision support system

The combination of ontology and FRBS was discussed in a few studies. Esposito and Pietro [33] proposed an ontology-based fuzzy decision support system (OBFDSS). They applied medical knowledge regarding ontology and fuzzy rules to a zero-order Sugeno-type fuzzy inference engine to classify a cerebral white matter lesion (WML). Ontology is responsible for representing the expert's knowledge and providing simple and intuitive DSS results. Fuzzy logic is responsible for handling fuzziness knowledge and performing the decision-making process. The evaluation of this system showed that this DSS offered a good way to classify WML in real clinical settings. Yagquinuma et al. [18] tried to provide meaningful inferences called an HyFOM reasoner that was able to combine MFIS and fuzzy ontology. It used three different reasoners: crisp ontology, fuzzy ontology, and MFIS. If the application needs knowledge related to a numerical property, first get the required inputs from the fuzzy ontology, then use MFIS to have a numerical property output, and finally, the output comes back to the ontology to be added with other fuzzy ontology reasoning tasks. Torshizi et al. [34] represented a hybrid fuzzy intelligent system, which combines Mamdani inference and ontologies in two modules. It was used for the diagnosis of benign prostatic hyperplasia (BPH). The first module used Mamdani inference to define the BPH riskiness level. The second module used ontologies to represent the expert's knowledge and provided simple and intuitive outcomes.

Focusing on the integration of the fuzzy rule and fuzzy ontology reasoning, some important limitations need to be addressed. The hybrid inference engine architecture, including the ontology reasoner, performs reasoning using the ontology assertions and definitions. Fuzzy rule reasoning is used to infer the resulting value using fuzzy rules and fuzzy operations. So, ontology has been used as a second or separate layer in reasoning. It has not enhanced the inference of the fuzzy component.

3.3.4 Case-based reasoning

CBR drew attention from some researchers because it did not require an explicit domain model. Gu et al. [35] used CBR to generate records of dental cases. It produced a good model for diagnosing and managing medical records and applications. Cancer [36] is a critical disease that is considered a leading cause of death worldwide. In 2015, about 8.8 million deaths occurred from cancer. Due to the complexities of the cancer domain, several CDSS have been built. Selecting the reasoning methodologies used in these CDSSs is often a challenging issue as it supports reasoning processes as performed by health professionals. Table 3 presents the selected

Table 3 Some of the Selected Papers Concerned With Cancer

Author Reference	Year	Context	Project Aims	Methods	Results
Min et al. [37]	2009	Prostate cancer	Deal effectively with the heterogeneity of biomedical data to enhance the integration of two medical databases	They developed an ontology-based approach that can solve the semantic heterogeneity problem	Achieved the efficient and effective search and retrieval of the information across two databases
Hassan et al. [38]	2010	Wisconsin breast cancer	Present a model for classifying breast lesions benign or malignant with high accuracy	They build a model using a feature selection based on the area under the ROC, then utilized the hidden Markov model (HMM)-fuzzy approach to get minimized fuzzy rules	Achieved more classification accuracy than most other classification models
Van den Branden et al. [39]	2011	Lung cancer	Integrate CBR to support clinical decision making for clinical experience reuse	They developed a CBR and a generic retrieval mechanism system to complement Excelicare	Show that CBR is a key to successful sharing and reusing of electronic patient records that captured cases
Fan et al. [40]	2011	Liver disorders and breast cancer	Produce accurate and comprehensible decision rules to help doctors in medical diagnoses	They presented an integration of a CBR and a fuzzy decision tree	Achieved high accuracy equal to 98.4% for breast cancer and 81.6% for liver disorders
Keles et al. [41]	2011	Breast cancer	Enhance physician's abilities for making their decisions	They built an expert system for diagnosis of breast cancer (Ex-DBC). It used the neurofuzzy method to found the fuzzy rules	Achieved 97% specificity, 81% negative, and 96% positive predictive values

Lopez et al. [42]	2011	Breast cancer	Build appropriate medical application interface and easily show the result to help medical users Help the oncologist in new treatments	They used CBR and ROC plots as visualization tools They developed a nonlinear CBR model that enabled the reusing of knowledge collected from the oncologist to use in treating new patients	Based on results, they produced a user-friendly tool Achieved accuracy equal to 94.36%
Mishra et al. [43]	2011	Prostate cancer	Assist oncologists in defining potion plans for patients	They proposed a CBR model that specifies a potion related to radiotherapy planning for prostate cancer patients	Achieved a high rate of treatment for most of the patients
Petrovic et al. [44]	2011	Prostate cancer	Determine the gene mechanisms; manage a substantial number of genes and a deficient sample size for breast cancer	They used learning of Bayesian networks to infer breast cancer using a gene regulatory network	Achieved 0.79203 (under the ROC curve)
Ahmad et al. [45]	2012	Breast cancer	Build a hybrid model to bring more precise outcomes for medical experts	They integrated CBR and a particle swarm optimization	Result accuracy is 97.4% and 76.8% for breast cancer and liver cancer, respectively
Chang et al. [46]	2012	Liver and breast cancer	Provide automated support for medical decisions in the Nottingham University Hospitals	They implemented a fuzzy rules system that contains 12 if-then fuzzy rules to utilize a treatment recommendation protocol for medical specialists	Increase the performance to 88.1%
Garibaldi et al. [16]	2012	Breast cancer			

Continued

Table 3 Some of the Selected Papers Concerned With Cancer—*Cont'd*

Author Reference	Year	Context	Project Aims	Methods	Results
Ranwez et al. [47]	2012	Breast cancer	Support user interactions and client cooperation such as document observation or ontology adjustment	They proposed a graph based on relevant concepts; identified an optimized algorithm to define these concepts, and highlighted the relationships between them	Suggest novel prospects for real-time user interactions
Wang et al. [48]	2012	Esophageal cancer	Enhanced prognostic scoring frameworks for esophageal disease	They used a fuzzy logic system	Performed consistently better ($AUC = 0.745$) in a cohort of 271 patients
Eccher et al. [48a]	2013	Cancer therapies	Overcome any issues with the guideline-based decision support system	They used ontology and collected rules to classify cancer therapies	Ontology can be utilized to find problems related to data consistency in the therapies recorded
Gay et al. [49]	2013	Breast cancer	Present another method for registering family risk given pointers that consider the structure of the family	They identified new indicators, rules, and strategies to register them from family trees	The outcomes demonstrate the practicality of our technique
Maramis et al. [50]	2013	Cervical cancer	Facilitate medical association studies by introducing an exploration framework based on a semantic approach	They built up a semantic modeling named ASSIST	The model can guess medical hypotheses automatically by performing case-control association studies

Salvi et al. [51]	2013	Breast cancer	Deal with heterogeneous data problems efficiently to be stored, processed, and communicated	They designed an ontology that can integrate and handle all heterogeneous data	Achieved and approved in a pilot and can be used as an open source for additional research
Teodorovic et al. [52]	2013	Thyroid cancer	Build a predictive model with improved performance for thyroid cancer treatment	They presented an integration model of CBR and Bee Colony Optimization (BCO). The weights of the parameters are detected with BCO. Used CBR to identify the doctor's expertise	Achieved a good reflection of reality
Sharaf-El-Deen et al. [53]	2014	Thyroid diseases and Breast cancer	Increase CBR system accuracy	Integrated CBR and rule-based reasoning	Achieved accuracy of 99.53% and 99.33% for thyroid disease and breast cancer, respectively
Hamed [54]	2015	Esophageal cancer	Automatically assess the degree of esophageal cancer risk to be perfectly adjusted	They proposed an adaptive fuzzy reasoning algorithm, where fuzzy Petri nets represent the fuzzy production rules	The result shows the effectiveness of this algorithm
Mahmoodian et al. [11]	2015	Cancer drug	Deal with the uncertainties that affect chemotherapy scheduling of cancer patients	They used T1FL and T2FL optimized by a genetic algorithm	Proposed method superior to type1 and type2 fuzzy logic in dealing with drug regimens
Miranda and Felipe [55]	2015	Breast cancer	Provide a method to be a powerful connection between the computer system and specialist, which can achieve more effective results	They implemented a computer-aided diagnosis tool to classify breast lesions automatically	Achieved accuracy 76.67% for nodules and 83.34% for calcifications

Continued

Table 3 Some of the Selected Papers Concerned With Cancer—*Cont'd*

Author Reference	Year	Context	Project Aims	Methods	Results
Nguyen et al. [56]	2015	Breast cancer and Cleveland heart disease	Deal with computational costs and uncertainty challenges that face a classification model	They implemented an approach called GSAM that integrates a fuzzy standard additive model and a genetic algorithm	An approach that is a useful tool that supports decisions for medical practitioners
Ping et al. [57]	2015	Liver cancer	Produce a model that can help in treating liver disease with enhanced execution	They proposed multiple measurement case-based reasoning (MMCBR)	MMCBR achieves a performance better than classical CBR
Shen et al. [58]	2015	Gastric cancer	Explore the ontological practices in CDSS	They proposed a model that integrates CBR and a multiagent system	A model has been created for explaining the implementation of knowledge acquisition
Wang et al. [59]	2015	Esophageal cancer	Provide an easy and powerful system helping in esophageal cancer treatment	For modeling and survival prediction, they presented an adaptive neurofuzzy inference system (ANFIS)	Achieves an accurate system for treating esophageal cancer patients
Hoogendoorn et al. [60]	2016	Colorectal cancer	Improve predictive performance	They developed a technique with the medical ontology to match the encoded notes	Accurate predictive models (AUC of 0.896)
Nguyen and Nahavandi [61]	2016	Lymphoma, leukemia cancer, and prostate	Select appropriate genes that are used as inputs to interval T2FL	They proposed a combination between interval T2FL and modification to the analytic hierarchy process	Achieves a powerful tool used for cancer classification
Saraiva et al. [62]	2016	Gastrointestinal	Improved CBR approach to increase diagnostic accuracy	They applied rule-based reasoning to improve the case-based reasoning retrieval process	As compared to a CBR approach, the diagnosis accuracy increased by 22.92%

Yılmaz et al. [63]	2016	Lung cancer	Provided instructions for lung cancer patients to exterminate the risk	They presented a neurofuzzy logic model	Provides a great study to people aiming to reduce the risk of cancer
Dongxiao et al. [64]	2017	Breast cancer	Produce an application and implementation of a CBR that can overcome the difficulty of extracting important attributes from human experts	They used a weighted heterogeneous value distance metric and a genetic algorithm	For two case studies, accuracy for the first case is 0.938 and 0.927 for the second case
Nilashi et al. [65]	2017	Breast cancer	Present a new system for classification of breast cancer	They developed a fuzzy rule-based reasoning system. It used expectation maximization (EM) to cluster the data in similar groups and classification and regression trees (CART) to bring the fuzzy rules to classify breast cancer	The system can be used to assist medical practitioners in the healthcare practice in a good way
Ramos-González et al. [66]	2017	Lung cancer	Provide accurate diagnosis with a reduced set of genes	They proposed a novel case-based reasoning framework with gradient boosting-based feature selection	The model achieved accuracy rates greater than those of traditional microarray analysis techniques

set of papers introducing frameworks to build a model that can produce more accurate results in cancer diagnosis. CBR is the most-used reasoning technique for cancer diagnosis in the following selected papers.

3.4 CURRENT CHALLENGES AND FUTURE TRENDS

This paper surveys the literature on reasoning techniques for CDSS, with a focus on future trends. The study of selected papers in the previous section can answer our research questions. As shown in many experimental studies, CBR is an effective technique and has high user acceptance. It can propose solutions to an incomplete problem. So, it has been used in a great number of medical research studies. Mamdani fuzzy inference has widespread acceptance and is well suited to human input. Ontology systems improve reusability and interoperability.

However, there are some limitations of existing reasoning techniques. First, the case adaptation process in CBR is a significant challenge. In many cases, the adaptation process is done manually by domain experts. Second, the Mamdani fuzzy structure requires a higher computational effort. Third, in ontology it is difficult to find ready-made ontologies to match a user's need. Finally, fuzzy ontology has been criticized by many researchers [67–69]. It has many critical and fundamental limitations including:

- The constraints of existing fuzzy description logic reasoners, such as FuzzyDL, Fire, and DeLorean.
- The limitations of existing underlying fuzzy description logics, such as fuzzy *SHOIN*(\mathcal{D}) and fuzzy *ALC*.
- The unclear and not unified methods for the fuzzy ontology construction process and tools.

Currently, many ontology reasoners and rule engines have become available, but few of them support DL reasoning and rules at the same time, even though OBFDSS still has some important limitations to be discussed. Ontology has been used as a second and separate layer in reasoning. It has not enhanced the inference of the fuzzy component. Esposito and Pietro [33] presented the best model, but they relied on gathering knowledge from experts only. They didn't concentrate on the possibility of collecting patient medical data from distributed electronic health record (EHR) systems and using machine learning techniques as a source of rules. This step can enhance the level of automation and interoperability of the CDSS. Yagquinuma et al. [18] attempts to use the Mamdani fuzzy inference system when the applications need knowledge associated with a numerical value. It uses a fuzzy ontology to get input to Mamdani FIS, then is inferred out and returned back to the ontology to be used by other fuzzy ontology reasoning tasks. Torshizi et al. [34] used ontology and fuzzy logic as two separate models. Each model has a specific and nonoverlapping job.

Our future trend is looking to combine ontology and Mamdani fuzzy inference in a hybrid CDSS system. The hybrid model is the most logical step to improve the

fuzzy expert system by adding a semantic reasoning process to its capabilities. There are many reasons for this decision. First, the fuzzy expert systems are stable and have been mathematically proved, and there are many fuzzy reasoners such as Mamdani. In addition, crisp ontology and its special case of (standard) medical ontologies have stable, crisp description logic, such as $\mathcal{SR\!OIC}(\mathcal{D})$; well-known languages, such as OWL 2; and well-established reasoners.

In such a sense, we expect to face some challenges including:

- Proposing a semantically intelligent hierarchical fuzzy expert system. It focuses on a Mamdani-based fuzzy rule-based approach and enhances its intelligence by hybridizing it with ontology semantics and reasoning.
- Collecting all the information usually analyzed by experts and CPGs, grouping this information, fuzzifying it according to suitable membership functions, and building a complete linguistic rule base based on the integration of expert and CPG knowledge with knowledge extracted from training data.
- Concentrating on the possibility of collecting patient medical data from distributed EHR systems in an automated way. This step enhances the level of automation and interoperability of CDSS. Moreover, the resulting rules will have a dynamic nature where the number of diseases, medications, and drugs is not explicitly defined.
- Emphasizing the possibility of building a transparent CDSS. It concentrates on the possibility of collecting patient medical data from distributed EHR systems in an automated way. The patient's medical concepts are compared with the ontology concepts using a proposed semantic similarity algorithm. Then, this level of similarity is used in evaluating fuzzy rules. This step enhances the level of automation and interoperability of CDSS. Moreover, the resulting rules will have a dynamic nature where the number of diseases, medications, and drugs is not explicitly defined.
- It uses a real case for implementation and testing, which is a challenge because medical data are often secure inside hospitals.

4 CONCLUSION

In this paper, the different reasoning methodologies applied to CDSS are analyzed. The manuscript described the current published literature in Science Direct, Springer Link, PubMed, IEEE Xplore, Elsevier, and Citeseer between 2009 and 2017. In this analysis, it has been concluded that almost all existing applications focus on using CBR, Mamdani fuzzy inference, ontology-based fuzzy decision support systems, ontology systems, and rule-based systems in CDSS. CBR and Mamdani fuzzy inference have a widespread acceptance and are well suited to human input. From this review, the ontology-based fuzzy CDSS could be a good choice. Most of these models used the ontology and fuzzy logic as two separate models, and no real overlapping occurs. There are some serious points to be discussed to enhance the

inference of the fuzzy component. Ontology can be used to enhance the inference capabilities of the regular fuzzy inference application. In the future, we will deeply study this possibility and apply it to a real-world problem, such as medical or industrial ones.

REFERENCES

- [1] V.K. Mago, N. Bhatia, A. Bhatia, A. Mago, Clinical decision support system for dental treatment, *J. Comput. Sci.* 3 (2012) 254–261.
- [2] I.M. Ahmed, M. Alfonse, M. Aref, A.-B.M. Salem, Reasoning techniques for diabetics expert systems, *Procedia Comput. Sci.* 65 (2015) 813–820.
- [3] S. El-Sappagh, M. Elmogy, A. Riad, A fuzzy-ontology-oriented case-based reasoning framework for semantic diabetes diagnosis, *Artif. Intell. Med.* 65 (2015) 179–208.
- [4] A. Jaya, A standard methodology for the construction of symptoms ontology for diabetes diagnosis, *Int. J. Comput. Appl.* 14 (2011) 47–51. Citeseer.
- [5] J.-J. Chen, P.-W. Wang, Y.-C. Huang, H.-C. Yen, Applying ontology techniques to develop a medication history search and alert system in Department of Nuclear Medicine, *J. Med. Syst.* 36 (2012) 737–746.
- [6] N. Díaz Rodríguez, M.P. Cuéllar, J. Lilius, M. Delgado Calvo-Flores, A fuzzy ontology for semantic modelling and recognition of human behavior, *Knowl.-Based Syst.* 66 (2014) 46–60.
- [7] N. Vyas, P.R. Pal, Performance evaluation of fuzzy based ontology system for identification of malaria disease, *Int. J. Comput. Appl.* 107 (2014) 10–14.
- [8] C.-S. Lee, M.-H. Wang, G. Acampora, C. Hsu, H. Hagras, A novel type-2 fuzzy markup language based ontology and its application to diet assessment, *Int. J. Intell. Syst.* 25 (2010) 1187–1216.
- [9] C.S. Lee, M.H. Wang, H. Hagras, A type-2 fuzzy ontology and its application to personal diabetic-diet recommendation, *IEEE Trans. Fuzzy Syst.* 18 (2010) 374–395.
- [10] C.S. Lee, M.H. Wang, S.T. Lan, Adaptive personalized diet linguistic recommendation mechanism based on type-2 fuzzy sets and genetic fuzzy markup language, *IEEE Trans. Fuzzy Syst.* 23 (2015) 1777–1802.
- [11] H. Mahmoodian, S. Salem, K. Shojaei, Adaptively adjusted footprint of uncertainty in interval type 2 fuzzy controller for cancer drug delivery, *Procedia Comput. Sci.* 76 (2015) 360–367.
- [12] F. Basçiftçi, Ö.F. Hatay, Reduced-rule based expert system by the simplification of logic functions for the diagnosis of diabetes, *Comput. Biol. Med.* 41 (2011) 350–356.
- [13] D. Pal, K.M. Mandana, S. Pal, D. Sarkar, C. Chakraborty, Fuzzy expert system approach for coronary artery disease screening using clinical parameters, *Knowl.-Based Syst.* 36 (2012) 162–174. Elsevier Science Publishers B. V.
- [14] B. Malmir, M. Amini, S.I. Chang, A medical decision support system for disease diagnosis under uncertainty, *Expert Syst. Appl.* 88 (2017) 95–108.
- [15] R.B. Lukmanto, E. Irwansyah, The early detection of diabetes mellitus (DM) using fuzzy hierarchical model, *Procedia Comput. Sci.* 59 (2015) 312–319.
- [16] J.M. Garibaldi, S.-M. Zhou, X.-Y. Wang, R.I. John, I.O. Ellis, Incorporation of expert variability into breast cancer treatment recommendation in designing clinical protocol guided fuzzy rule system models, *J. Biomed. Inform.* 45 (2012) 447–459.

- [17] B. Bede, I.J. Rudas, Takagi-Sugeno approximation of a Mamdani fuzzy system, *Advance Trends in Soft Computing: Proceedings of WCSC 2013*, December 16–18, San Antonio, Texas, USA, Springer International Publishing, 2014, pp. 293–300.
- [18] C.A. Yaginuma, M.T.P. Santos, H.A. Camargo, M. Reformat, in: *A FML-based hybrid reasoner combining fuzzy ontology and Mamdani inference*, *Fuzzy Systems (FUZZ), 2013 IEEE International Conference on*, 2013, pp. 1–8.
- [19] B. Pandey, R. Mishra, Knowledge and intelligent computing system in medicine, *Comput. Biol. Med.* 39 (2009) 215–230.
- [20] J.-K. Kim, J.-S. Lee, D.-K. Park, Adaptive mining prediction model for content recommendation to coronary heart disease patients, *Cluster Comput.* 17 (2014) 881–891.
- [21] S.S.H. Ling, H.T. Nguyen, Genetic-algorithm-based multiple regression with fuzzy inference system for detection of nocturnal hypoglycemic episodes, *IEEE Trans. Inf. Technol. Biomed.* 15 (2011) 308–315.
- [22] S.H. Ling, H.T. Nguyen, Natural occurrence of nocturnal hypoglycemia detection using hybrid particle swarm optimized fuzzy reasoning model, *Artif. Intell. Med.* 55 (2012) 177–184.
- [23] A. d'Acierno null, M. Esposito, G. De Pietro, An extensible six-step methodology to automatically generate fuzzy DSSs for diagnostic applications, *BMC Bioinformatics* 14 (2013) 1–19.
- [24] D. Canavese, N.R.S. Ortega, A proposal of a fuzzy rule-based system for the analysis of health and health environments in Brazil, *Ecol. Indic.* 34 (2013) 7–14. Elsevier Science.
- [25] O.W. Samuel, M.O. Omisore, B.A.A. Ojokoh, Web-based decision support system driven by fuzzy logic for the diagnosis of typhoid fever, *Expert Syst. Appl.* 40 (2013) 4164–4171. Pergamon Press, Inc.
- [26] R. Kunhimangalam, S. Ovallath, P.K. Joseph, A clinical decision support system with an integrated EMR for diagnosis of peripheral neuropathy, *J. Med. Syst.* 38 (2014) 1–14.
- [27] M.C. Sharma, M.T. Choudhary, A web based fuzzy expert system for epistaxis diagnosis, *Int. J. Comput. Sci. Inform. Technol.* 6 (2015) 4062–4068. Citeseer.
- [28] A. Minutolo, M. Esposito, G.D. Pietro, A fuzzy framework for encoding uncertainty in clinical decision-making, *Knowl.-Based Syst.* 98 (2016) 95–116.
- [29] C. Saez, A. Breso, J. Vicente, M. Robles, J.M. Garcia-Gomez, An HL7-CDA wrapper for facilitating semantic interoperability to rule-based Clinical Decision Support Systems, *Comput. Methods Prog. Biomed.* 109 (2013) 239–249.
- [30] J.A. Reyes-Ortiz, A.L. Jiménez, J. Cater, C.A. Meléndez, P.B. Márquez, M. García, Ontology-based knowledge representation for supporting medical decisions, *Res. Comput. Sci.* 68 (2013) 127–136. Citeseer.
- [31] S. El-Sappagh, F. Ali, DDO: a diabetes mellitus diagnosis ontology, *Appl. Inform.* 3 (2016) 1–28.
- [32] C.S. Lee, M.H. Wang, A fuzzy expert system for diabetes decision support application, *IEEE Trans. Syst. Man Cybern. B Cybern.* 41 (2011) 139–153.
- [33] M. Esposito, G.D. Pietro, An ontology-based fuzzy decision support system for multiple sclerosis, *Eng. Appl. Artif. Intell.* 24 (2011) 1340–1354.
- [34] A.D. Torshizi, M.H.F. Zarandi, G.D. Torshizi, K. Eghbali, A hybrid fuzzy-ontology based intelligent system to determine level of severity and treatment recommendation for Benign Prostatic Hyperplasia, *Comput. Methods Prog. Biomed.* 113 (2014) 301–313.

- [35] D.-X. Gu, C.-Y. Liang, X.-G. Li, S.-L. Yang, P. Zhang, Intelligent technique for knowledge reuse of dental medical records based on case-based reasoning, *J. Med. Syst.* 34 (2010) 213–222.
- [36] WHO, Available from: <http://www.who.int/mediacentre/factsheets/fs297/en/>, 2017. Accessed 8 November 2017.
- [37] H. Min, F.J. Manion, E. Goralczyk, Y.-N. Wong, E. Ross, J.R. Beck, Integration of prostate cancer clinical data using an ontology, *J. Biomed. Inform.* 42 (2009) 1035–1045.
- [38] M.R. Hassan, M.M. Hossain, R.K. Begg, K. Ramamohanarao, Y. Morsi, Breast-cancer identification using HMM-fuzzy approach, *Comput. Biol. Med.* 40 (2010) 240–251.
- [39] M. Van den Branden, N. Wiratunga, D. Burton, S. Craw, Integrating case-based reasoning with an electronic patient record system, *Artif. Intell. Med.* 51 (2011) 117–123.
- [40] C.-Y. Fan, P.-C. Chang, J.-J. Lin, J. Hsieh, A hybrid model combining case-based reasoning and fuzzy decision tree for medical data classification, *Appl. Soft Comput.* 11 (2011) 632–644.
- [41] A. Keles, S.A. Kele, U. Yavuz, Expert system based on neuro-fuzzy rules for diagnosis breast cancer, *Expert Syst. Appl.* 38 (2011) 5719–5726.
- [42] B. Lopez, C. Pous, P. Gay, A. Pla, J. Sanz, J. Brunet, eXiT*CBR: a framework for case-based medical diagnosis development and experimentation, *Artif. Intell. Med.* 51 (2011) 81–91.
- [43] N. Mishra, S. Petrovic, S. Sundar, A self-adaptive case-based reasoning system for dose planning in prostate cancer radiotherapy, *Medical Physics* 38 (2011) 6528–6538. American Association of Physicists in Medicine.
- [44] S. Petrovic, N. Mishra, S. Sundar, A novel case based reasoning approach to radiotherapy planning, *Expert Syst. Appl.* 38 (2011) 10759–10769.
- [45] F. Ahmad, S. Deris, N. Othman, The inference of breast cancer metastasis through gene regulatory networks, *J. Biomed. Inform.* 45 (2012) 350–362.
- [46] P.-C. Chang, J.-J. Lin, C.-H. Liu, An attribute weight assignment and particle swarm optimization algorithm for medical database classifications, *Comput. Methods Prog. Biomed.* 107 (2012) 382–392.
- [47] V. Ranwez, S. Ranwez, S. Janaqi, Subontology extraction using hyponym and hypernym closure on is-a-directed acyclic graphs, *IEEE Trans. Knowl. Data Eng.* 24 (2012) 2288–2300.
- [48] C.Y. Wang, T.F. Lee, C.H. Fang, J.H. Chou, Fuzzy logic-based prognostic score for outcome prediction in esophageal cancer, *IEEE Trans. Inf. Technol. Biomed.* 16 (2012) 1224–1230.
- [48a] C. Eccher, A. Scipioni, A.A. Miller, A. Ferro, D.M. Pisanelli, An ontology of cancer therapies supporting interoperability and data consistency in EPRs, *Comput. Biol. Med.* 43 (2013) 822–832.
- [49] P. Gay, B. Lopez, A. Pla, J. Saperas, C. Pous, Enabling the use of hereditary information from pedigree tools in medical knowledge-based systems, *J. Biomed. Inform.* 46 (2013) 710–720.
- [50] C. Maramis, M. Falekakis, I. Lekka, C. Diou, P. Mitkas, A. Delopoulos, Applying semantic technologies in cervical cancer research, *Data Knowl. Eng.* 86 (2013) 160–178.
- [51] D. Salvi, M. Picone, M.T. Arredondo, M.F. Cabrera-Umpierrez, A. Esteban, S. Steger, T. Poli, Merging person-specific bio-markers for predicting oral cancer recurrence through an ontology, *IEEE Trans. Biomed. Eng.* 60 (2013) 216–220.
- [52] D. Teodorovic, M. Šelmić, L. Mijatovi, Combining case-based reasoning with Bee Colony Optimization for dose planning in well differentiated thyroid cancer treatment, *Expert Syst. Appl.* 40 (2013) 2147–2155.

- [53] D.A. Sharaf-El-Deen, I.F. Moawad, M.E. Khalifa, A new hybrid case-based reasoning approach for medical diagnosis system, *J. Med. Syst.* 38 (2014) 1–9.
- [54] R.I. Hamed, Esophageal cancer prediction based on qualitative features using adaptive fuzzy reasoning method, *J. King Saud Univ. Comput. Inform. Sci.* 27 (2015) 129–139.
- [55] G.H.B. Miranda, J.C. Felipe, Computer-aided diagnosis system based on fuzzy logic for breast cancer categorization, *Comput. Biol. Med.* 64 (2015) 334–346.
- [56] T. Nguyen, A. Khosravi, D. Creighton, S. Nahavandi, Classification of healthcare data using genetic fuzzy logic system and wavelets, *Expert Syst. Appl.* 42 (2015) 2184–2197.
- [57] X.-O. Ping, Y.-J. Tseng, Y.-P. Lin, H.-J. Chiu, F. Lai, J.-D. Liang, G.-T. Huang, P.-M. Yang, A multiple measurements case-based reasoning method for predicting recurrent status of liver cancer patients, *Comput. Ind.* 69 (2015) 12–21.
- [58] Y. Shen, J. Colloc, A. Jacquet-Andrieu, K. Lei, Emerging medical informatics with case-based reasoning for aiding clinical decision in multi-agent system, *J. Biomed. Inform.* 56 (2015) 307–317.
- [59] C.-Y. Wang, J.-T. Tsai, C.-H. Fang, T.-F. Lee, J.-H. Chou, Predicting survival of individual patients with esophageal cancer by adaptive neuro-fuzzy inference system approach, *Appl. Soft Comput.* 35 (2015) 583–590.
- [60] M. Hoogendoorn, P. Szolovits, L.M. Moons, M.E. Numans, Utilizing uncoded consultation notes from electronic medical records for predictive modeling of colorectal cancer, *Artif. Intell. Med.* 69 (2016) 53–61.
- [61] T. Nguyen, S. Nahavandi, Modified AHP for gene selection and cancer classification using type-2 fuzzy logic, *IEEE Trans. Fuzzy Syst.* 24 (2016) 273–287.
- [62] R. Saraiva, M. Perkusich, L. Silva, H. Almeida, C. Siebra, A. Perkusich, Early diagnosis of gastrointestinal cancer by using case-based and rule-based reasoning, *Expert Syst. Appl.* 61 (2016) 192–202.
- [63] A. Yilmaz, S. Ari, Ü. Kocabıçak, Risk analysis of lung cancer and effects of stress level on cancer risk through neuro-fuzzy model, *Comput. Methods Prog. Biomed.* 137 (2016) 35–46.
- [64] D. Gu, C. Liang, H. Zhao, A case-based reasoning system based on weighted heterogeneous value distance metric for breast cancer diagnosis, *Artif. Intell. Med.* 77 (2017) 31–47.
- [65] M. Nilashi, O. Ibrahim, H. Ahmadi, L. Shahmoradi, A knowledge-based system for breast cancer classification using fuzzy logic method, *Telematics Inform.* 34 (2017) 133–144.
- [66] J. Ramos-González, D. López-Sánchez, J.A. Castellanos-Garzón, J.F. de Paz, J. M. Corchado, A CBR framework with gradient boosting based feature selection for lung cancer subtype classification, *Comput. Biol. Med.* 86 (2017) 98–106.
- [67] F. Bobillo, U. Straccia, The fuzzy ontology reasoner fuzzy DL, *Knowl.-Based Syst.* 95 (2016) 12–34.
- [68] F. Bobillo, M. Delgado, J. Gómez-Romero, in: A crisp representation for fuzzy backslashcal SHOIN with fuzzy nominals and general concept inclusions, *Uncertainty Reasoning for the Semantic Web I: ISWC International Workshops, URSW 2005–2007*, Springer, Berlin, Heidelberg, 2008, pp. 174–188 Revised Selected and Invited Papers.
- [69] G. Stoislos, G. Stamou, J. Pan, Handling imprecise knowledge with fuzzy description logic, *International Workshop on Description Logics (DL 06)*, 2006, Lake District, UK, 2006.

This page intentionally left blank

Embedded healthcare system for day-to-day fitness, chronic kidney disease, and congestive heart failure

5

Pradeep M. Patil*, Durgaprasad K. Kamat[†]

JSPM's JS COE, Pune, India* STES's SCOE, Pune, India[†]

CHAPTER OUTLINE

1 Ubiquitous Healthcare and Present Chapter	90
2 Introduction	90
3 Frequency-Dependent Behavior of Body Composition	92
4 Bioimpedance Analysis for Estimation of Day-to-Day Fitness and Chronic Diseases	93
5 Measurement System for Body Composition Analysis Using Bioimpedance Principle	98
5.1 Measurement Electrodes	99
5.2 AFE4300 Body Composition Analyzer	99
5.3 Statistical Analysis	105
5.4 Validation of Developed Model	105
6 Database Generation	105
7 Predictive Regression Model for Day-to-Day Fitness	106
8 Predictive Regression Model for CKD	111
9 Predictive Regression Model for CHF	113
10 Discussion	115
11 Conclusion	115
References	116

1 UBIQUITOUS HEALTHCARE AND PRESENT CHAPTER

The hectic lifestyle of people leads to a loss of fitness, and can further lead to some chronic disease conditions. The maintenance of fitness is a primary requirement today and has costs associated with it. This is applicable to healthy individuals as well as people suffering from some chronic diseases such as kidney disease and congestive heart failure. The body composition is an indicator of an individual's fitness status. The proportion of lean mass to fat mass, which is an indicator of fitness, can be judged by bioimpedance analysis. The bioimpedance measurements find widespread acceptability in body composition analysis because they are noninvasive, low cost, and simple. The present chapter explains an embedded healthcare system for the non-invasive assessment of human body composition. The system is able to measure weight scale as well as body composition. The system consists of an analog front-end AFE4300 measurement board that is used in bioimpedance measurement. A four-electrode configuration is used to measure whole body impedance. The silver/silver-chloride (Ag/Ag-Cl) electrodes normally used in ECG measurements are attached to the human body for bioimpedance measurements. The database of a healthy population, chronic kidney disease, and congestive heart failure is generated on a personal computer. The user interface installed on the personal computer is simple. The database files are simple Excel (.csv format) files having low storage requirements. Statistical analysis is used for the development of predictive regression models for estimating total body water. Predictive regression models are developed for day-to-day fitness, chronic kidney disease, and congestive heart failure. Predictive models are based on measured bioimpedance and recorded anthropometric parameters of the human body. The described system is a good candidate for U-healthcare systems because of the simplicity of the user interface and methodology. The prediction of total body water and its further use in predicting fat-free mass and fat mass are based on statistical analysis and simple mathematical formulae. The time required for the estimation of total body water, fat-free mass, and fat mass is small, which calls for widespread use of the system. The system is useful for checking day-to-day fitness for a healthy population. The estimation of total body water using state-of-the-art medical practices requires checking serum electrolyte concentrations of blood samples. This is a painful to the patients having chronic diseases. With the use of noninvasive and real-time measurements, the embedded system described in this chapter is a boon to patients having chronic kidney disease and congestive heart failure.

2 INTRODUCTION

The human body consists of many chemical compounds that, in turn, are made up of elements that are found throughout nature. Inorganic compounds include water and minerals whereas organic compounds are found in fat, protein, carbohydrates, and nucleic acids. Water is a major constituent of the human body, forming 65%–90%

of the composition of living cells while also being present in intercellular body fluids. The body composition of individuals differs in terms of fat percentages. Obesity also does not mean excess fat; it has been observed that persons with obesity have more body water in comparison with body fat. Proteins are about 16% and are found in hair, fingernails, and human skin in large amounts. Minerals in the form of salts and metals account for about 6% of the body. Sodium, potassium, calcium, chlorine, and iron are some of the minerals commonly observed in the human body. About 1% of human body mass is occupied by other carbohydrates and sugar. Glucose is a source of energy, although it is not freely available in the bloodstream at any given time. Four elements—oxygen, carbon, hydrogen, and nitrogen—form approximately 96% of human body weight with a lot of that in the form of water; although significantly, the human body needs calcium, phosphorus, magnesium, sodium, potassium, chlorine, and sulfur. The functions performed by these nutrients regulate the pH of the body, building bones and cell structures, carrying charges, and driving chemical reactions.

The models of human body composition use anthropometric data and are useful in predicting body composition of all age groups. The study of human body composition was initially based on chemical analysis of the whole body or body segments. It has been observed that excess body fat may lead to cardiovascular disease. The two-compartment model of human body composition, although 50 years old, finds its place in these situations. In the two-compartment model, human body weight is divided into two parts: fat-free mass and fat mass [1–3]. Essential and storage fat are the two components of total body fat. Fat present in the heart, lipid-rich tissues throughout the central nervous system, muscles, bone marrow, liver, lungs, spleen, intestines and kidneys forms the essential fat. It is higher in women than in men, and is required for the normal activities of the human body. The storage fat, present beneath the human skin and surrounding internal body organs, helps in maintaining body temperature in addition to protecting the internal body parts. The small amounts of essential fats are also found in lean body mass. The day-to-day activities and lifestyle of people affect the percentage of body fat. The body composition methods such as hydrostatic weighing, skinfolds, and bioelectrical impedance analysis (BIA) are based on the assumption of the two-compartment model of the human body. These methods assume the total body weight to be composed of fat mass and fat-free-mass [4,5]. The three-compartment model divided the fat-free mass into two parts: water content and other solids such as minerals and proteins. Normally, the isotopic dilution method has been used to measure the total body in the three-compartment model. The four-compartment model divides the fat-free mass into visceral protein, total body water, and body cell mass. The mass of body protein is measured with neutron activation analysis while the bone mineral content is measured by dual-energy X-ray absorptiometry. This is additional overhead for the four-compartment model. Thus, an increase in the number of body composition compartments is associated with a proportionate increase in measurement methods; these methods are independent of one another [1].

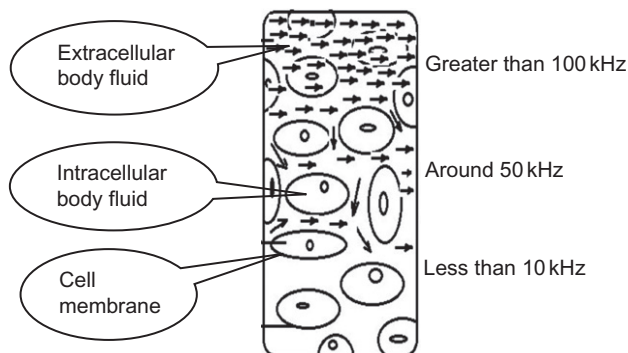
Bioimpedance measurement is useful in body composition analysis. In bioimpedance measurement, an alternating electric current is passed through the human body

via electrodes attached at specific locations on the body. The electric current flowing through the human body passes through a low-resistance path. The tissues that have more body water provide this low-resistance path to the passage of alternating current. The physiological parameters of interest are computed with arithmetic transformations based on measured bioimpedance. The impedance vector is expressed as either magnitude and phase or reactance and resistance. The magnitude-phase representation is useful in measurements involving tissue differentiation. The reactance-resistance relationship provides a convenient graphical representation of tissue characteristics and is more convenient in characterizing individual tissues. Being conductive, body fluids offer resistance to current flow. The capacitive reactance is offered by components such as tissue interfaces and cell membranes [6]. The dimensions along with specific resistance decide the impedance of a conductor.

The passive electrical properties of the human body can be studied by dividing the composition of the body into three main parts: intracellular, extracellular, and the cell membrane. The intracellular and extracellular fluids are ionic and hence work as electrolytes having mobile charge carriers. The cell membranes are very thin, having nanometer dimensions, and are made up of phospholipid bilayers. Therefore, cell membranes act as insulators. Thus, any application of alternating current causes polarization of ionic charges around the cell membranes. Hence, cell membranes acting as capacitors offer reactance to the flow of alternating current while electrolytes around the cell membranes offer resistance to current flow. The extracellular electrolyte can be simulated as a pure resistor that shunts the series combination of intracellular resistance and capacitance of a cell membrane. With cell membranes being capacitive, the behavior of cells is frequency dependent. At low frequencies, the current does not penetrate the cell membranes and flows through extracellular spaces. As the frequency of the applied alternating current increases, the cell membranes offer lower capacitive reactance and hence the current penetrates the cell membranes and finds paths both through the extracellular as well as intracellular media. The current mostly flows through intracellular media, being lower in resistance path than the extracellular composition. The frequency dependence of body composition is useful in studying the properties of specific tissues. A low frequency such as 5 kHz is useful in the measurement of extracellular body fluid volumes while high frequencies above 500 kHz are useful in the measurement of both extracellular as well as intracellular fluid volumes [7]. The application of only these two extreme frequencies limits the study of body composition. Bioelectrical impedance spectroscopy provides a better solution to this by providing multifrequency measurements.

3 FREQUENCY-DEPENDENT BEHAVIOR OF BODY COMPOSITION

The human body allows the passage of alternating current through it. The primary reason behind this conductive behavior is the abundance of body fluids in the form of electrolytes. The frequency of applied alternating currents provides a mechanism

**FIG. 1**

Path of alternating current through the human body at various frequencies.

of differential measurements. The choice of frequency for a particular measurement decides the amplitude of the signals being applied to the body. At low frequencies, even a small amplitude of applied current can be painful to the body. The low frequency measurements (less than about 10 kHz) are useful in extracellular fluid volume analysis. As the applied frequency increases, the threshold of pain of the body also increases. Hence, the choice of the frequency range for measurement in bioimpedance analysis (BIA) is based on the compromise between these factors. The path of alternating current through the body at various frequencies is shown in [Fig. 1](#).

The higher the applied frequency, the more the conductance of the body due to a decrease in capacitance reactance at higher frequencies. Thus, currents at higher frequencies (more than 100 kHz) very easily penetrate the human body. The measurements at higher frequencies are useful in the estimation of total body water while measurements at low frequencies provide an estimate of extracellular fluids [\[8\]](#).

4 BIOIMPEDANCE ANALYSIS FOR ESTIMATION OF DAY-TO-DAY FITNESS AND CHRONIC DISEASES

BIA is useful in studying the electrical properties of biological material and changes over time. Real-time BIA instruments are used for quantifying human blood circulation and breathing [\[9\]](#). BIA helps researchers and medical professionals in estimating body composition and knowing body fluid status. BIA involves the application of a small alternating current to the body and the impedance is calculated by measuring the voltage drop across the current path. This method can be used to measure blood flow, monitor heart status, and perform similar functions for medical research and diagnostic purposes. Medical professionals can use BIA for analysis and classification of diseases in various domains. With BIA being simple, inexpensive, and non-invasive, it can be used in wearable medical appliances and therefore can be useful in the long-term treatment of certain diseases. It also forms the basis of objective,

long-term approaches to treatment. BIA can be used objectively for day-to-day health analysis and hence in certain cases, it can be useful in domestic treatment. The diagnosis is noninvasive, low cost, painless, precise, and safe because of the availability of a vast variety of instruments and software in various application domains. The research in the field of bioimpedance measurements has led to the development of empirical equations that are useful in computing total body water, which can be further used in the calculation of fat-free mass. The variations in machines and methodologies used in BIA may result in around 10% differences in the computed results of body fat. As there are a large variety of different equations, variables, and reference methods in BIA, some common standards must be established by researchers and experts in the field.

It is valuable to measure the body composition of malnourished patients to monitor their response for refeeding and further avoiding chronic diseases. The use of direct measurement techniques for clinical monitoring is expensive. So, indirect measurement techniques such as bioelectrical impedance can be used. Malnutrition significantly alters body composition. Energy malnutrition results in the wasting of body fat and lean mass. Protein malnutrition results in proportionately greater wasting of lean mass than fat mass. In lean mass, the intracellular or body cell mass is less in comparison with extracellular mass. The plasma volume is less within the extracellular mass. The process is clinically significant because of the occurrence of edema. The protein and intracellular potassium are reduced within the body cell mass. All these body composition changes cannot be determined with simple height and weight measurements. The bioelectrical impedance provides a convenient clinical technique in these situations for the estimation of body composition [10]. The clinical applications of bioelectrical impedance include chronic diseases such as chronic kidney disease (CKD) and congestive heart failure (CHF), where the distribution of fluids in the body is unbalanced. The assumptions of impedance and total body water are invalid in these cases. BIA finds its presence in the literature of biomedical engineering over the years. Normal applications involve the estimation of body composition. Although simple and low cost, BIA technology needs a lot of support from different medical standards to reach maturity [9].

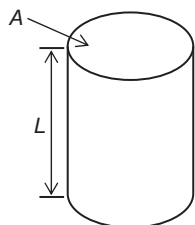
Some image processing and allied techniques are available for disease diagnosis in the field of biomedical engineering. Saba et al. [11] proposed an accurate and reliable detection system for fatty liver disease using the Levenberg-Marquardt Back Propagation Network (BPN) classifier that was used to classify the liver disease into normal and abnormal categories. Ahmed et al. [12] combine a back-propagation neural network fuzzy classifier and a neurofuzzy model for diagnosing Crohn's disease. Sharma et al. [13] proposed an efficient decision support system for the detection of medical renal disease using a small feature space consisting of only second order gray-level cooccurrence matrix (GLCM) statistical features computed from raw renal ultrasound images. They explored the potential of five texture feature vectors computed using GLCM statistics exhaustively for a differential diagnosis between normal and MRD images using an SVM classifier. Dey et al. [14] reviewed various concepts of thermal imaging and application areas with special reference to the

prediction of breast cancer. A connected component technique has been proposed by Sambyal et al. [15] for text extraction and character segmentation using maximally stable extremal regions (MSERs) for text line formation, followed by connected components to determine separate characters. A Sobel edge detector is used as it reduces the execution time but at the same time maintains the quality of the results. Li et al. [16] proposed an effective method for analyzing plantar pressure images in order to obtain the key areas of foot plantar pressure characteristics of diabetic patients. Dey et al. [17] explained the significance of biomedical imaging processing in the diagnosis of pathological conditions. The techniques of pattern recognition are divided into clustering and classification. Using operating time, Azzabi et al. [18] studied the diagnosis of failures with timed automata. A diagnoser that employs observable events for the detection and location of faults has been constructed. Using brain MRI and knee MRI images, Khachane et al. [19] analyzed the performance of different feature extraction techniques for the purpose of classification of medical images.

Bioimpedance analysis has been used for the estimation of body composition of healthy people as well as in chronic diseases. Healthy people need to maintain day-to-day fitness for efficient working. The estimation of day-to-day fitness can be evaluated using a predictive regression model developed on the basis of BIA.

Over the years, there has been a paradigm shift in the healthcare scenario from hospital-centric to personal (domestic) healthcare. This change has brought down healthcare costs, especially in chronic disease conditions. Chronic diseases account for 75% of the total healthcare cost in developed countries. Bioimpedance measurements are useful in CKD for the assessment of overhydration state, which is useful in the estimation of the amount of fluid to be removed by ultrafiltration. Ferreira et al. [20] developed a handheld device for domestic treatment of CKD. It is based on tetrapolar bioimpedance measurements and textile electrodes. The performance has been evaluated using similar commercial bioimpedance spectrometers. The health status of CKD patients is based on their nutritional status. Dumler et al. [21] applied single-frequency (50 kHz) bioimpedance analysis for determining the nutritional status in dialysis patients. It has been observed that the losses in fat-free mass and body cell mass can be detected by bioimpedance analysis, which is not apparent in body weight measurement. Hence, the body composition parameters can be monitored in CKD using BIA.

CHF causes local fluid accumulation in parts of the human body and is a major cause of hospitalization and mortality. Patients are advised of the use of drugs post hospitalization based on the case history of the patient during hospitalization. The body hydration status of CHF patients can be monitored domestically by BIA. The decision of rehospitalization is based on the level of local fluid accumulation [22]. Diseases such as CKD, CHF, and diabetes are closely associated with reduced heart rate variability. Abtahi et al. [23] developed a biofeedback device that enables the measurement of an electrocardiogram and thoracic electrical bioimpedance. The device is based on the Android operating system and uses a Bluetooth interface for recording the electrocardiogram. The respiratory bioimpedance signal has been

**FIG. 2**

Cylinder with uniform resistivity.

recorded using thoracic electrodes. The developed system has been useful in increasing heart rate variability and reducing heart rate.

In bioimpedance analysis, the body is assumed to be a cylindrical conductor with a cross-sectional area A and length L having uniform resistivity, as shown in Fig. 2. The impedance of the cylinder can be calculated using Eq. (1).

$$Z = \frac{\rho L}{A} \quad (1)$$

where

Z is the impedance of biological and geometrical system in ohm,

ρ is the volume resistivity in ohm-cm,

A is the conductor cross-sectional area in cm^2 and

L is the conductor length in cm.

Multiplying by L to numerator and denominator on the right side of Eq. (1), we get

$$Z = \rho \frac{L^2}{V} \quad (2)$$

where

V is the volume of cylinder $= A \times L$.

Rearranging Eq. (2), we get

$$V = \rho \frac{L^2}{Z} \quad (3)$$

Eq. (3) shows that for a uniform cylindrical conductor, there is a direct proportion of volume to the square of the length of the conductor and impedance relates volume in inverse proportion [24]. Thus, if the human body is assumed to be cylindrical, then electrically determined biological volume is inversely related to the impedance of human body [25]. The segmental body composition analysis of the body assumes five body segments—two arms, two legs and a trunk—and each individual body segment is assumed to be cylindrical. Hence, Eq. (3) applies equally to human body segments. Further, the complex impedance of the body is capacitive and hence the impedance of the body is represented mathematically as,

$$Z = R + jX_c \quad (4)$$

where

R is the resistance of the body or body segment and

X_c is the reactance of the body or body segment.

In BIA, the body is assumed to be a uniform cylinder, so in Eq. (3), we can replace the impedance of cylinder (Z) by the impedance of the body (Z_{body}); the length of cylinder (L) by the height of body (H); and the volume of the cylinder (V) by the volume of the conducting components in the body. This volume, for BIA, is the total body water as it forms the main portion of body composition and the major conducting component of the body. Thus, by analogy, at a high frequency (above 100 kHz) of alternating current, Eq. (3) can be written as,

$$\text{Volume of TBW} = \rho \frac{H^2}{Z_{\text{body}}} \quad (5)$$

where

TBW is total body water in liters,

ρ is the resistivity of the body in $\Omega\text{-cm}$,

H is the stature (height) of the body in cm and

Z_{body} is the body impedance in Ohms.

It is difficult to accurately determine the specific resistance of the live human body. Measurements on cadavers lead to erroneous results as the specific resistance may change after death and do not reflect the effects of live bodily processes [26].

Hence, the estimation of total body water (TBW) is performed indirectly using the parameter H^2/Z , along with other anthropometric parameters of the body such as weight, age, and sex.

The general form of the equation is given by Eq. (6).

$$TBW = \left(A \times \frac{H^2}{Z} \right) + (B \times Wt) + (C \times \text{Age}) + (D \times \text{Sex}) + E \quad (6)$$

where

TBW is the total body water in liters,

H is the height in cm,

Z is the impedance magnitude in Ohms,

Wt is the weight in kg,

Age in years,

Sex male = 1, female = 0,

A, B, C, D, E are regression coefficients.

In this chapter, linear regression prediction models have been developed with the use of the Statistical Package for the Social Sciences (SPSS). Models have been developed for day-to-day fitness, CHF, and CKD. These equations are used for the calculation of TBW. H^2/Z is also called the impedance quotient (or impedance index) and many studies have confirmed that the impedance quotient is highly correlated with TBW. Assuming a constant hydration factor (73%) for the FFM, FFM can be calculated by Eq. (7).

$$FFM = \frac{TBW}{0.73} \quad (7)$$

where

FFM is the fat-free mass in kg,

TBW is the total body water in liters.

Fat-free mass when subtracted from the total body weight provides fat mass (FM). Fat mass is given by Eq. (8).

$$FM = \text{Weight} - FFM \quad (8)$$

where

FM is the fat mass in kg,

Weight in kg,

FFM is the fat-free mass in kg.

Eqs. (7) and (8) give the body composition in a two-compartment model. When these equations are applied to the human body, many assumptions are made including homogeneity, uniform current distribution, and a uniform cross-sectional area. When applying these equations, a constant specific resistivity is assumed for the whole body, even though there can be different individual specific resistivity for various tissues [27].

5 MEASUREMENT SYSTEM FOR BODY COMPOSITION ANALYSIS USING BIOIMPEDANCE PRINCIPLE

Body composition measurements can be performed noninvasively using the bioimpedance technique. This section explains the system developed for body composition measurement using bioimpedance. A four-electrode configuration is used to measure the body's bioimpedance. The AFE4300 low-cost analog front-end is used to measure the impedance of the body at 50 kHz. Four electrodes connected to the body provide the input signal to the AFE4300. The measured bioimpedance forms one of the input parameters to the development of the predictive regression model. Fig. 3 shows a block diagram of the system used in the development of predictive regression models.

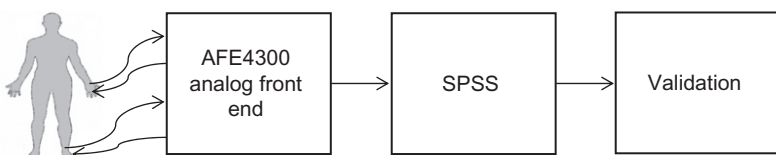


FIG. 3

Block diagram of system developed for predictive regression model.

5.1 MEASUREMENT ELECTRODES

The bioimpedance measurement system is physically connected to the body with the help of electrodes. Body fluids are ionic in nature while the measurement system works on the basis of electronic charge transfer. This ionic-to-electronic transfer is achieved with the help of electrodes attached to the skin surface. The skin is capacitive due to a multilayer structure. The contact resistance between skin and the measurement electrode is reduced by cleaning the skin below the electrode with alcohol. Silver/silver-chloride (Ag/Ag-Cl) electrodes that are normally used in ECG applications can be used for bioimpedance measurements as they have an electrolyte gel coating that reduces electrode polarization. Ag/Ag-Cl electrodes are also helpful in improving the skin's conductive properties as the electrolyte gel coating penetrates through the outer layers of the skin. The applied pressure of the electrodes, the thickness of the skin below the electrodes, and the biological properties of the skin such as secretions are also responsible for determining the contact resistance.

Bioimpedance measurements typically employ two- or four-electrode configurations. In the two-electrode configuration, the current application and voltage measurement is performed by the same set of electrodes. The internal resistance of the electrodes affects the measurement of impedance in the two-electrode configuration. Hence, four-electrode or tetra-polar set up is used in bioimpedance measurement. The tetra-polar electrode setup has been used in many bioimpedance measurements because of its inherent advantages over the two-electrode configurations. The application of current in the tetra-polar setup is through a pair of electrodes that are physically in the outer position. The voltage is measured with a pair of electrodes located along the path of current flow in the body and hence typically occupies a position between the voltage electrodes. This measurement configuration offers high input impedance and avoids a loading effect for effective voltage measurement. This helps in reducing skin electrode contact impedance and helps in deep-tissue impedance measurement. Even movement artifacts, skin temperature, and hydration do not affect the measurements in this configuration. The distance between current injecting and voltage measurement electrodes should be large to detect the voltage signal from a region having uniform current distribution [28]. The system developed uses four dry gel-type ECG electrodes to reduce contact resistance between the skin and electrodes. The current-injecting electrodes are connected to the dorsal part of the palm and toe while voltage is measured by two electrodes connected to the wrist and ipsilateral part of the ankle. The measurements are performed at a single frequency of 50 kHz.

5.2 AFE4300 BODY COMPOSITION ANALYZER

The analog front end AFE4300 can be used in weighing scales and in the measurement of body composition. AFE4300 has an on-chip analog-to-digital converter with 16-bit resolution and a conversion speed of 860 SPS. This ADC can be used in both weight scale and body composition measurement. An on-chip instrumentation

amplifier has been used in weight scale measurement. The gain of this amplifier is set by a resistor connected externally to the board. The offset correction in the weighing scale is performed by a digital-to-analog converter with a 6-bit resolution. A driver circuit for the load cells of the weighing scale has been provided that offers measurements of ratios.

The body composition measurements are performed by the AFE4300. The measurement of body composition involves the application of alternating current to the body. A pattern generator along with a DAC generate a sinusoidal signal to be injected into the human body. A voltage-to-current converter applies this sinusoidal current into the body between two terminals. The impedance of the body causes a voltage drop across these two terminals and is measured with a differential amplifier, rectified, and its amplitude measured by the on-chip ADC. The supply voltage range for AFE4300 IC is between 0.2 and 0.6 V. The operating temperature for AFE4300 is between 0°C and 70°C. [Fig. 4](#) shows the hardware system used for body composition measurement.

The AFE4300 EVM-PDK demonstration board evaluates the AFE4300 device. The board can be used in the weighing scale as well as the measurement of body composition. The board can be used for a single application at a time. The AFE4300 EVM-PDK demonstration board contains the following items:

- AFE4300 EVM printed circuit board (PCB).
- MMB3 modular motherboard.
- USB cable.

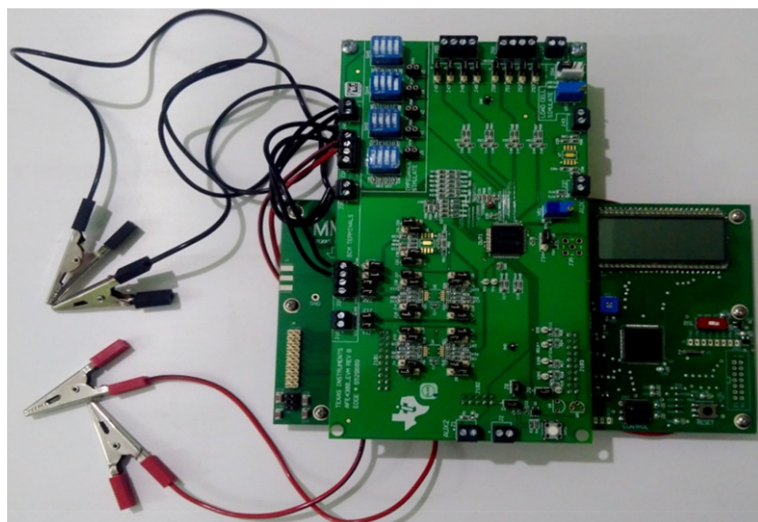
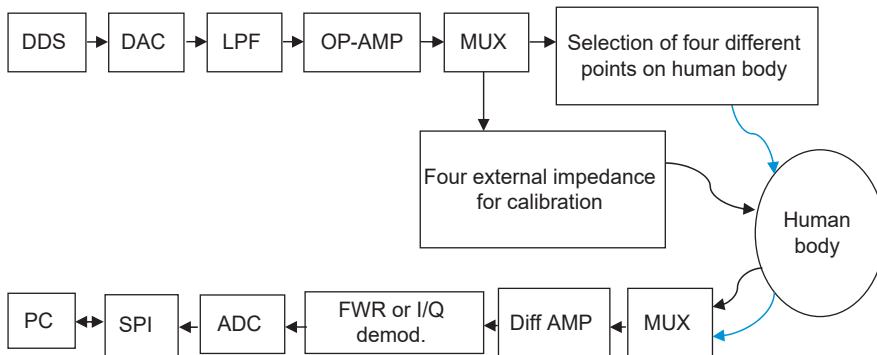


FIG. 4

AFE4300 board used for body composition analysis.

**FIG. 5**

AFE4300 operated in FWR or I/Q demodulation.

The demonstration board has an MMB3 motherboard that is useful in making a connection to the evaluation board. The MMB3 board comes bundled with a USB port and a USB cable, which are useful in recording measurements on a personal computer. This helps in the generation of a database for further analysis. The FE4300 provides a graphical user interface (GUI) that is installed on the personal computer for setting the body composition parameters and recording the body composition results.

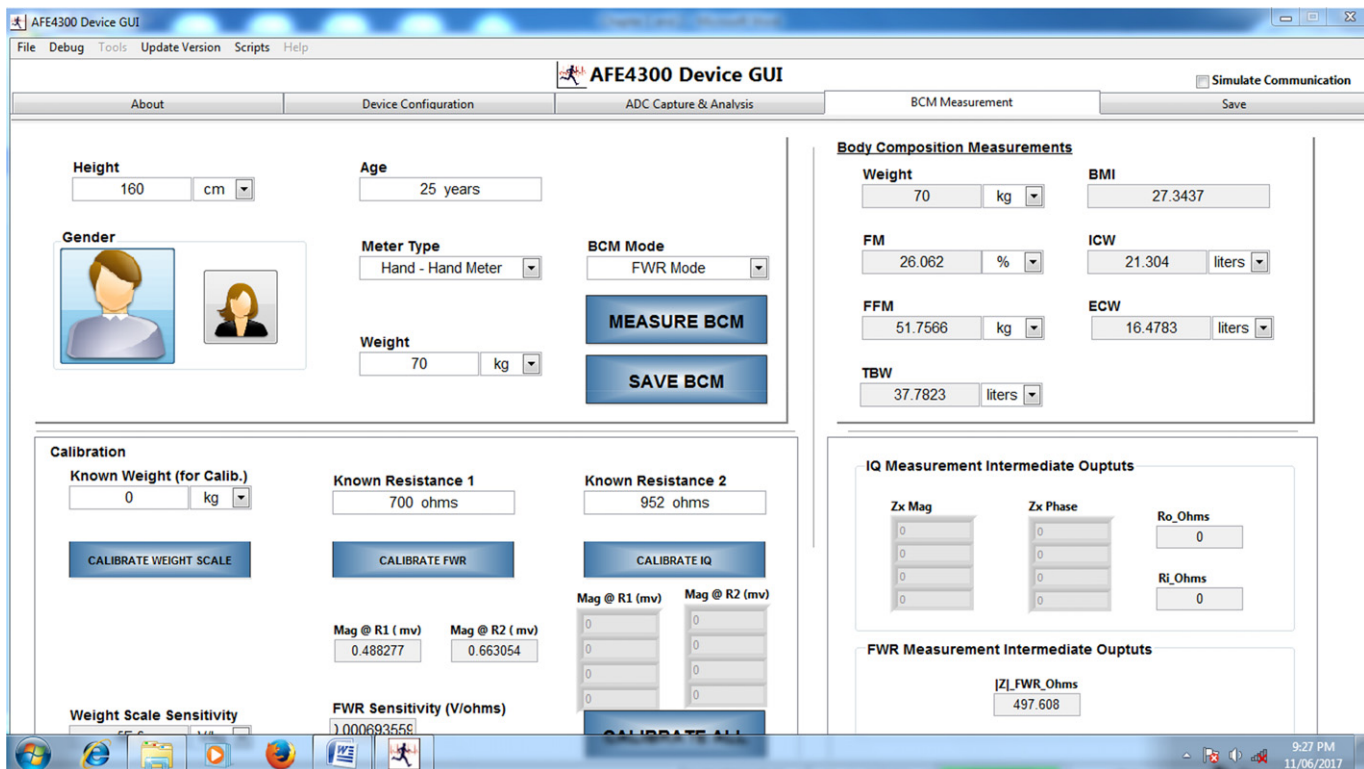
The AFE4300 can be operated in full-wave rectifier (FWR) or I/Q demodulator modes. Fig. 5 shows the block diagram of the AFE4300 impedance spectrometer operated in full wave rectification and I/Q demodulation mode. A direct digital synthesizer generates the sinusoidal signal. The output of the digital-to-analog converter is filtered and the images are removed by the second-order filter. The DC currents are blocked by a capacitor. Thus, DC currents are not applied to the body. The current to be applied to the body is controlled by a resistor. An analog multiplexer provides the end point for injecting the current into the body.

The application of current to the body with the help of the AFE4300 can be performed by choosing four contact points on the body. The return path of the current is through another multiplexer. This completes the current loop for the measurement of the unknown impedance of the body. If we select FWR demodulator mode, we get only the impedance magnitude. If we want to measure both the magnitude and the phase of impedance, then the I/Q demodulator mode is selected [29,30].

In FWR mode, the body composition measurement is performed at a single frequency and we get only the magnitude of impedance. Single-frequency measurement is performed at 50 kHz frequency. Fig. 6 show impedance measurements in FWR mode with AFE4300 GUI.

The procedure to measure the impedance of the body using the FWR mode is as follows:

- Turn on BCM control tab and select AFE4300 DAC frequency as 50 kHz.
- Connect current injection electrodes to IOUT0 and IOUT1, potential measurement electrodes to the VSENS0 and VSENS1.

**FIG. 6**

Impedance measurements in FWR mode with AFE4300 GUI.

- Make I/Q OFF from I/Q demodulator block.
- Enter height and select gender, enter age of person, select meter type as hand-to-hand meter, then enter weight.
- Calibrate FWR mode, select BCM mode as FWR mode, and then measure BCM.

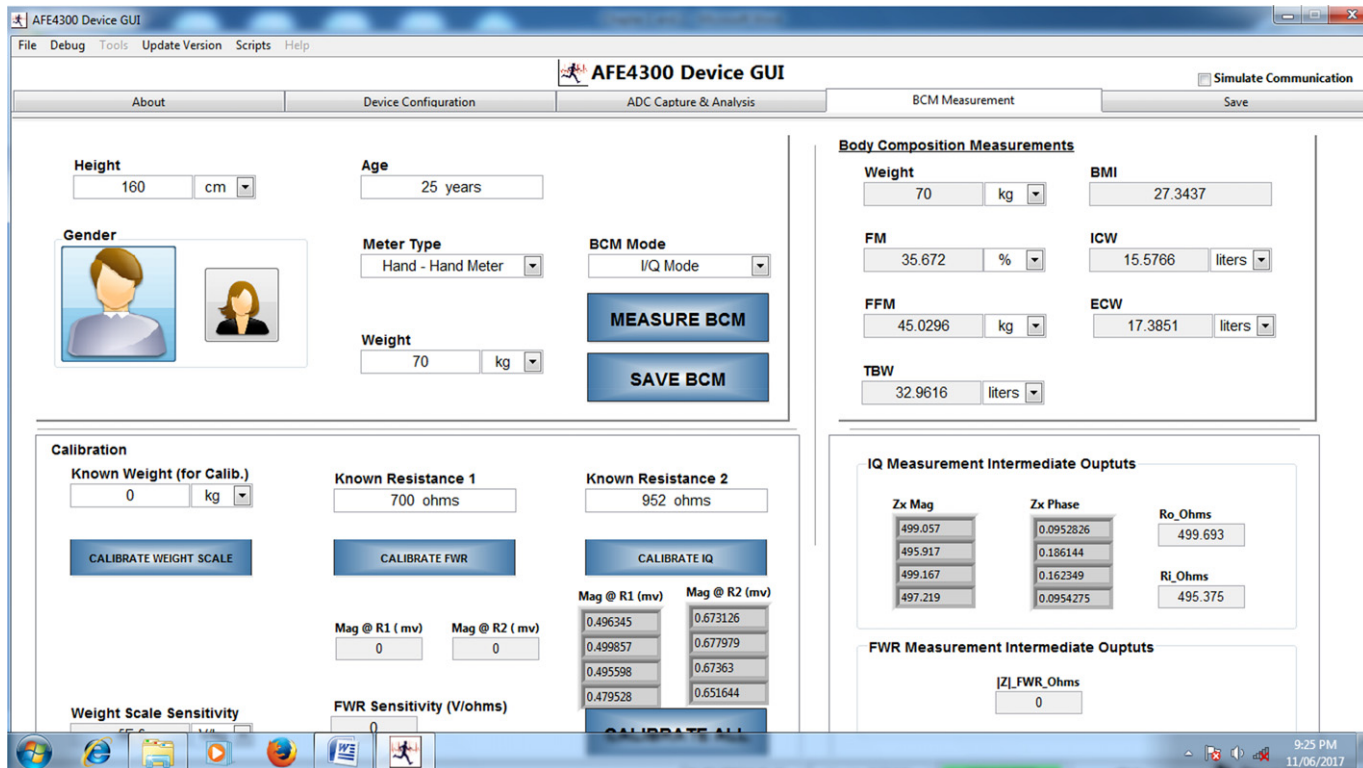
In I/Q demodulation mode, multifrequency measurement is performed that provides impedance in the form of magnitude and phase. Multifrequency measurement is performed at five logarithmic frequencies from 8 to 128 kHz. Fig. 7 shows impedance measurements in I/Q demodulation mode with AFE4300 GUI.

The procedure to measure body impedance using I/Q demodulation mode is as follows:

- Turn on BCM control tab and select AFE4300 DAC frequency as 8 KHz.
- Connect current injection electrodes to IOUT0 and IOUT1, potential measurement electrodes to the VSENS0 and VSENS1.
- Make I/Q ON from I/Q demodulator block.
- Enter height and select gender, enter age of person, select meter type as hand-to-hand meter, then enter weight.
- Calibrate I/Q mode, select BCM mode as I/Q mode, and then measure BCM.

The same procedure is repeated for measurements at other frequencies.

The I/Q demodulation mode provides readings useful in complex impedance plots (Cole plots) of the body for a selected frequency of measurement. The complex impedance plot shows the relationship between capacitive reactance and resistance of the body as a function of frequency. In the complex impedance plots, R_0 indicates resistance at zero frequency. It represents the resistance of only extracellular body fluids. R_∞ indicates resistance offered by total body fluids. When the frequency is very low, the cellular membrane offers high impedance. This leads to a high impedance path for the current through the cells and hence current cannot pass through the intracellular matter. The impedance measured at very low frequencies is resistive, represented by R_0 . With an increase in frequency, the current penetrates the cell membranes and the capacitive reactance of the human body also increases. The frequency increases and reaches a certain threshold, called the characteristic frequency (f_c), where capacitive reactance is at the maximum. After this frequency, capacitive reactance decreases with an increase in applied frequency, as the cell membranes lose their capacitive characteristics. At very high frequencies, the impedance of the body is resistive, represented by R_∞ . The impedance of the body decreases at high frequencies with an increase in conducting body fluids. This typically happens because of an increase in the amount of conductive intracellular fluid that offers a low resistance path to the applied alternating current. The AFE4300 board for body composition analysis provides values of R_0 , R_∞ , and the intermediate impedance values (in terms of magnitude and phase angle) when a particular frequency is applied in I/Q demodulation mode. The real (resistive) and imaginary (capacitive) values of the complex impedance can be obtained as cosine and sine components

**FIG. 7**

Impedance measurements in I/Q demodulation mode with AFE4300 GUI.

of the measured complex impedance, respectively. These values can be used in a complex impedance plot. This plot can be further used to study the frequency selective behavior of body components.

5.3 STATISTICAL ANALYSIS

The predictive regression models are developed in the SPSS. SPSS is a tool for statistical analysis of data. There are various features available with SPSS. SPSS facilitates advanced statistical analysis. There are a large number of machine learning algorithms bundled with SPSS. SPSS can be deployed across different applications. Facilities such as open source extensibility make SPSS useful for the latest statistical applications. Laymen as well as statistical experts can use SPSS. The size as well as complexity of the project do not limit the applicability of SPSS. This is because of the easy-to-use, flexible, and scalable features of SPSS [31].

5.4 VALIDATION OF DEVELOPED MODEL

The total body water is measured by the developed model using the recorded anthropometric parameters of a subject. The serum electrolyte concentration of the same subject is measured and total body water is computed empirically. The total body water values of these two methods are compared for validation purposes.

6 DATABASE GENERATION

The development of predictive regression models requires a direct method. This direct method measures the total body water invasively using serum electrolyte concentration, measured from blood samples taken from the body. The measurements have been carried out for serum sodium and serum potassium. Serum electrolyte parameters are measured and analyzed in the laboratory. The EM-360 biochemical analyzer is used to measure serum electrolyte concentration. The AFE4300 EVM-PDK board has been used to measure the impedance of the body. The measured values of total body water from this direct method are used as the output of the developed predictive regression model during the development phase of the model. The coefficients of the predictive model (see Eq. 6) are computed statistically. Various anthropometric parameters of the body recorded during the measurement are height, weight, impedance, age, and sex of the subjects. The values of these parameters are used in the development of predictive regression models for day-to-day fitness, CKD, and CHF. Once developed, the predictive model can be used in the estimation of total body water using measured bioimpedance and recorded anthropometric parameters of human body. The estimated total body water is used to compute the fat-free mass and fat mass using Eqs. (7) and (8), respectively.

The concentration of sodium and potassium varies in body fluids. The electrolyte concentration of serum sodium in the blood sample of a healthy subject ranges from 135 to 145 mmol/L. Similarly, for a healthy subject, the range of serum potassium is from 3.5 to 5.5 mmol/L. Sodium maintains a normal blood pressure. It supports the working nerves and muscles and regulates the fluid balance of the body. The body maintains a sodium balance to avoid hyponatremia and hypernatrmia. Hyponatremia is caused because of a low level of sodium in blood while hypernatrmia is due to an increase in sodium level in the blood.

In this chapter, the predictive regression models are based on the measured concentration of serum sodium and serum potassium. Burtis et al. [32] state that total body water is 42 L for a serum sodium concentration of 145 mmol/L and for serum potassium concentration of 4 mmol/L. This relation has been used to calculate proportionate values of total body water on the basis of serum sodium concentration and serum potassium concentration to compute total body water required in the model development. Total body water is a dependent variable while height, weight, impedance, age, and sex of subject are independent variables. The predictive regression models have been developed for day-to-day fitness, CKD, and CHF.

7 PREDICTIVE REGRESSION MODEL FOR DAY-TO-DAY FITNESS

The predictive regression models described in this chapter are developed using the SPSS popularly used in the health sciences. The predictive regression models are developed using multiple regression analysis. In multiple regression, the value of a single variable is predicted using the values of multiple other variables. The variable that we want to predict becomes a dependent, outcome, target, or criterion variable. The variables used in the prediction of dependent variables are independent, predictor, explanatory, or regressor variables. Multiple regression analysis is useful when we want to judge the overall fit of a model and the contribution of individual predictors in the model.

In developed predictive regression models, TBW is criterion variable while the anthropometric parameters of the body—height, weight, age, sex, and bioimpedance—are predictor variables. The predictive regression models have been developed for day-to-day fitness, CKD, and CHF.

The sample database used for the development of a predictive regression model for day-to-day fitness includes 16 healthy male and 16 healthy female subjects, all randomly selected from the Maharashtra state. **Table 1** shows the sample values in the generated database for healthy female subjects. **Table 2** shows the sample values in the generated database for healthy male subjects.

Using SPSS, multiple regression analysis has been carried out on the generated database. The initial step in multiple regression analysis involves checking whether the given data can be analyzed using multiple regression. There are some assumptions that need to be satisfied by the data to give a valid result. However, real-time data may not fit into all these assumptions. But even if the data fails certain

Table 1 Database for Healthy Female Subjects

Subjects	Impedance (Ohms)	Height (cm)	H^2/Z (cm²/ Ohm)	Weight (kg)	Age (Years)	Sex	Serum Sodium (mmol/L)	TBW by Serum Sodium (L)
1	497.59	160	51.45	50	24	0	136	39.39
2	477.92	168	59.06	52	28	0	142	41.13
3	476.92	158	52.34	45	20	0	135	39.10
4	499.01	162	52.59	58	34	0	140	40.55
5	478.31	164	56.23	48	26	0	141	40.84
6	491.49	159	51.44	52	38	0	138	39.97
7	492.11	152	46.95	43	30	0	136	39.39
8	497.21	157	49.57	48	35	0	144	41.71
9	478.21	168	59.02	64	47	0	142	41.13
10	498.61	153	46.95	60	45	0	136	39.39
11	484.29	166	56.90	46	52	0	139	40.26
12	499.02	158	50.03	66	43	0	137	39.68
13	482.39	162	54.40	68	31	0	145	42.00
14	486.91	152	47.45	42	18	0	143	41.42
15	479.24	168	58.89	49	29	0	139	40.26
16	492.18	153	47.56	53	46	0	141	40.84

Table 2 Database for Healthy Male Subjects

Subjects	Impedance (Ohms)	Height (cm)	H ² /Z (cm ² / Ohm)	Weight (kg)	Age (Years)	Sex	Serum Sodium (mmol/L)	TBW by Serum Sodium (L)
1	503.51	165	54.07	60	25	1	137	39.68
2	502.01	172	58.93	76	28	1	142	41.13
3	498.02	168	56.67	64	29	1	135	39.10
4	497.66	164	54.04	72	32	1	143	41.42
5	510.11	178	62.11	76	39	1	144	41.71
6	505.18	166	54.55	73	25	1	136	39.39
7	499.62	170	57.84	64	22	1	140	40.55
8	506.36	174	59.79	70	28	1	145	42.00
9	511.23	178	61.98	69	41	1	137	39.68
10	498.62	166	55.26	72	45	1	139	40.26
11	507.47	167	54.96	66	42	1	145	42.00
12	497.58	178	63.68	70	52	1	138	39.97
13	519.38	162	50.53	48	19	1	143	41.42
14	505.07	174	59.94	68	52	1	136	39.39
15	497.81	178	63.65	72	56	1	144	41.71
16	502.49	166	54.84	65	46	1	141	40.84

Table 3 Model Summary Table for Day-to-Day Fitness

Model Summary				
Model	R	R Square	Adjusted R Square	Std. Error of the Estimate
1	0.217 ^a	0.047	-0.094	0.99406

^aPredictors: (constant), sex, age, H²/Z, Wt.

assumptions, some obvious solutions are always available. The different assumptions are explained here. The first assumption is that a continuous scale has been used for the dependent variable. If the dependent variable is measured on an ordinal scale, then ordinal regression is carried out rather than multiple regression. The second assumption is that there are two or more categorical or continuous independent variables. Dichotomous moderator analysis is required for dichotomous independent variables. The next assumption is that there should be an independence of observations that can be checked using the Durbin-Watson statistic test. The dependent variable and each of the independent variables need to linearly related. Also, the collection of independent variables should be linearly related to the dependent variables. These relationships can be checked visually with the help of scatterplots and partial regression plots. If the relationship is not linear, then a nonlinear regression analysis or transform needs to be run on the given data. The next assumption is that the data need to show homoscedasticity and do not show multicollinearity. When the variances remain similar along the line of best fit, it is homoscedasticity. The high correlation among the independent variables indicates multicollinearity. In the case of multicollinearity, it is difficult to understand the contribution of individual independent variables to the variance explained in the dependent variables and also leads to technical issues in calculating a multiple regression model. The next assumption is that significant outliers, high leverage points, or highly influential points should not be there. These terms represent unusual observations in the data set. The next assumption states that there should be a normal distribution of residuals, which can be checked using a histogram and other techniques.

There are seven steps that are followed in multiple regression analysis in SPSS statistics when all the assumptions are satisfied. Multiple regression analysis is run on the given database of healthy male and female subjects and generates few tables. **Table 3** shows the model summary table for day-to-day fitness. The table depicts R , R square, adjusted R square, and the standard error of the estimate. This table explains how far a regression model fits given data. The multiple correlation coefficient R is a measure of prediction quality of the dependent variable; in our case TBW. The coefficient of determination R^2 determines the variance proportion of independent variables in dependent.

Table 4 shows ANOVA table for day-to-day fitness. The good fit of the regression model for the given data is depicted by the F -ratio.

Table 4 ANOVA Table for Day-to-Day Fitness

ANOVA ^a							
Model		Sum of Squares		df	Mean Square	F	Sig.
1	Regression	1.322		4	0.331	0.335	0.852 ^b
	Residual	26.680		27	0.988		
	Total	28.003		31			

^aDependent variable: TBW.^bPredictors: (constant), sex, age, H²/Z, Wt.**Table 5** Coefficients Table for Day-to-Day Fitness

Coefficients ^a						
Model		Unstandardized Coefficients		Standardized Coefficients		Sig.
		B	Std. Error	Beta	t	
1	(Constant)	38.294	2.389		16.027	0.000
	H ² /Z	0.029	0.047	0.151	0.626	0.537
	Wt	0.017	0.027	0.191	0.621	0.540
	Age	-0.009	0.019	-0.100	-0.470	0.642
	Sex	-0.188	0.539	-0.101	-0.350	0.729

^aDependent variable: TBW.

Table 5 shows the coefficients table for day-to-day fitness that is generated by SPSS analysis. **Table 5** is useful in developing the predictive regression model for day-to-day fitness. The coefficients of the predictive regression model and constant are given in the B column. All the coefficients are the estimates having a range or confidence interval decided by standard error. The standard error tells how good the model fits based on the range or confidence intervals of B column coefficients.

In this statistical analysis, 95% confidence intervals are used. The critical value (α) is 0.05 for a 95% confidence interval. The degrees of freedom is the difference between sample size and the number of coefficients, including the constant. So, the degrees of freedom are $32 - 5 = 27$. Referring to a standard two-tailed test table (The t -table), for degrees of freedom (df) 27 and critical value (α) 0.05, the critical value for this model is 2.052. Now, the multiplication of critical value (2.052) and standard error of a coefficient gives 95% confidence intervals of that coefficient or constant. For example, 95% confidence intervals for constant (38.294) are (33.39, 43.20). Thus, we are 95% confident that constant will take up any value in the interval (33.39, 43.20). Confidence intervals of all other coefficients can be calculated on similar lines. The “ t ” score is the ratio of value of a particular coefficient or constant

to its standard error. The “*t*” and “sig” values indicate the acceptance or rejection of the null hypothesis. If the “*t*” value is greater than the critical value (± 2.052), then we reject the null hypothesis. In [Table 5](#), all the “*t*” values of coefficients are less than the critical value. So, our hypothesis of the relationship between the criterion and predictor variable is accepted. This can be proved otherwise using the “sig” or “*p*” value. If the “*p*” value is less than 0.05, then we reject the null hypothesis. In this work, all “*p*” values are greater than 0.05, so we accept that there is a significant relationship between criterion and predictor variables. Standardized coefficients are the “B” coefficients obtained when we run standardized multiple regression. The standardized multiple regression takes up new sample values of the coefficients that are computed by dividing the individual sample value of a coefficient by the standard deviation of all the sample values of that coefficient.

Using [Table 5](#), we get the predictive regression model for day-to-day fitness (using Eq. 6).

$$TBW = 0.029 \times \frac{H^2}{Z} + 0.017 \times Wt - 0.009 \times Age - 0.188 \times Sex + 38.294 \quad (9)$$

The “Model” column in the coefficients table ([Table 5](#)) indicates that one model is represented by the table. There are four variables used in the predictive regression model for day-to-day fitness: H^2/Z , Wt, Age, and Sex and a constant. The column “B” indicates the coefficients of the variables in the predictive regression model for day-to-day fitness and also a constant term (see Eq. 9). The statistical significance of these coefficients is indicated by the “Sig” column. All the values of that column (excepting the value corresponding constant) are far greater than 0.05, indicating that the coefficients have a significant impact on the prediction of the dependent variable (TBW).

8 PREDICTIVE REGRESSION MODEL FOR CKD

The kidney acts as a regulator of the acid base, potassium, and the sodium balance. This regulatory mechanism of the kidney is hampered in CKD. CKD causes disorders in extracellular fluid (ECF) volume. The extracellular fluid in CKD patients shows some common patterns. One of the most common ECF imbalances involves mild ECF volume expansion. The most common signs of this type of ECF disturbance involve salt-sensitive hypertension and left ventricular hypertrophy. In more severe cases, the ECF volume expands with the nephrotic syndrome. In some CKD cases, the ECF volume reduces, typically named salt-wasting syndrome. In general, CKD causes an expansion of the extracellular fluid volume that typically contributes to hypertension [33]. The kidney performs the regulatory function of potassium balance to prevent both hyperkalemia and hypokalemia. In CKD patients, salt and water retention is extremely common. This results in the beginning of hypertension and the development of CHF in these patients. The cardiac disease often accompanies the evolution of CKD and hence the treatment of the sodium balance in these patients

Table 6 Model Summary Table for Chronic Kidney Disease

Model Summary				
Model	R	R Square	Adjusted R Square	Std. Error of the Estimate
1	0.347 ^a	0.120	-0.010	3.65027

^aPredictors: (constant), sex, age, Wt, H²/R.

Table 7 ANOVA Table for Chronic Kidney Disease

ANOVA ^a						
Model		Sum of Squares	df	Mean Square	F	Sig.
1	Regression	49.233	4	12.308	0.924	0.465 ^b
	Residual	359.760	27	13.324		
	Total	408.993	31			

^aDependent variable: TBW.

^bPredictors: (constant), sex, age, Wt, H²/R.

to control hypertension and also improve cardiac function without adversely affecting CKD is a real challenge. The high prevalence of type II diabetes and hypertension, which are increasingly common in the world's population, further results in progressive damage to the kidney, resulting in CKD. The prevalence of CKD increases as the population ages. CKD causes disturbances in the acid base, potassium, and the sodium balance, which in severe cases can result in death. Recognizing and managing disturbances in the acid base and the electrolyte balance are challenging tasks for medical professionals. Recognizing these abnormalities in the early stages of CKD is important to clinicians. This requires frequent checking of these parameters. A noninvasive, cost-effective, and painless method such as bioimpedance measurement in such diseases is a boon to both patients and clinicians [34].

Using the methodology explained in [Section 6](#), a predictive regression model has been developed for CKD. [Table 6](#) shows the model summary table for CKD. [Table 7](#) shows the ANOVA table for CKD. [Table 8](#) shows the coefficients table of the predictive regression model for CKD that is generated by SPSS analysis. [Table 8](#) is useful in developing the predictive regression model for CKD.

Using [Table 8](#), we get the predictive regression model for CKD (using Eq. 6).

$$TBW = 0.236 \times \frac{H^2}{Z} - 0.229 \times Wt - 0.225 \times Age - 1.278 \times Sex + 79.618 \quad (10)$$

The “Model” column in the coefficients table ([Table 8](#)) indicates that one model is represented by the table. There are four variables used in the predictive regression model for CKD: H²/Z, Wt, Age, and Sex and a constant. The column “B” indicates the coefficients of the variables in the predictive regression model of CKD and also a

Table 8 Coefficients Table for Chronic Kidney Disease

Coefficients ^a					
Model	Unstandardized Coefficients		Standardized Coefficients	<i>t</i>	Sig.
	<i>B</i>	Std. Error	Beta		
1	(Constant)	79.618	13.632	5.841	0.000
	<i>H</i> ² / <i>R</i>	0.236	0.174	1.359	0.185
	Wt	-0.229	0.176	-1.301	0.204
	Age	-0.225	0.156	-1.446	0.160
	Sex	-1.278	1.623	-0.787	0.438

^aDependent variable: TBW.

constant term (see Eq. 10). The statistical significance of these coefficients is indicated by the “Sig” column. All the values of the “Sig” column (excepting the value corresponding constant) are far greater than 0.05, indicating that the coefficients have a significant impact on the prediction of the dependent variable (TBW).

9 PREDICTIVE REGRESSION MODEL FOR CHF

In CHF, the heart has an inadequate pumping capacity for blood, resulting in lung congestion or veins experiencing a backup pressure of blood. A number of years are required to develop CHF being a chronic condition and manifest as shortness of breath and edema. The physical symptoms of CHF include an increased respiratory rate with accessory muscle use, liver enlargement, ascites, and altered heart sounds. CHF can be associated with obesity, hypertension, type II diabetes, infections, and heart valve disorders. The cardiovascular conditions such as atherosclerosis and hypertension along with lifestyle and environmental factors are responsible for CHF development. The causal factors that lead to CHF include high sodium content in diet, emotional excesses, air pollution, and specific pharmaceutical medications [35].

Using the methodology explained in Section 6, a predictive regression model has been developed for CHF. Table 9 shows the model summary table for CHF. Table 10 shows the ANOVA table for CHF. Table 11 shows the coefficients table for the predictive regression model of CHF that is generated by SPSS analysis. Table 11 is useful in developing the predictive regression model for CHF.

Using Table 11, we get the predictive regression model for CHF (using Eq. 6).

$$TBW = 0.017 \times \frac{H^2}{Z} - 0.151 \times Wt - 0.052 \times Age - 1.024 \times Sex + 45.443 \quad (11)$$

The “Model” column in the coefficients table (Table 11) indicates that one model is represented by the table. There are four variables used in the predictive regression

Table 9 Model Summary Table for Congestive Heart Failure

Model Summary				
Model	R	R Square	Adjusted R Square	Std. Error of the Estimate
1	0.601 ^a	0.361	0.267	2.06371

^aPredictors: (constant), sex, H²/R, Wt, age.

Table 10 ANOVA Table for Congestive Heart Failure

ANOVA ^a						
Model		Sum of Squares	df	Mean Square	F	Sig.
1	Regression	65.059	4	16.265	3.819	.014 ^b
	Residual	114.990	27	4.259		
	Total	180.049	31			

^aDependent variable: TBW.

^bPredictors: (constant), sex, H²/R, Wt, age.

Table 11 Coefficients Table for Congestive Heart Failure

Coefficients ^a						
		Unstandardized Coefficients		Standardized Coefficients		
Model		B	Std. Error	Beta	t	Sig.
1	(Constant)	45.443	9.763		4.655	0.000
	H ² /R	0.017	0.072	0.042	0.230	0.820
	Wt	-0.151	0.054	-0.485	-2.792	0.009
	Age	-0.052	0.094	-0.101	-0.557	0.582
	Sex	-1.024	0.792	-0.216	-1.293	0.207

^aDependent variable: TBW.

model of CHF: H^2/Z , Wt, Age, and Sex and a constant. The column “B” indicates the coefficients of the variables in the predictive regression model of CHF and also a constant term (see Eq. 11). The statistical significance of these coefficients is indicated by the “Sig” column. All the values of that column (excepting the values corresponding constant and variable weight) are far greater than 0.05, indicating that the coefficients H^2/Z , Age, and Sex have significant impact on the prediction of the dependent variable (TBW). The weight does not seem to have a significant impact on the prediction of total body water in the case of CHF.

10 DISCUSSION

The predictive regression models have been developed for day-to-day fitness, CKD, and CHF. The predictive regression model developed for day-to-day fitness (see Eq. 9) is useful for healthy people to know the proportion of fat in their body weight. The knowledge of fat content helps healthy people to plan regular exercise and gym activities.

The hemodialysis patients have constant changes in body fluids. This is roughly estimated using weight measurements. The predictive regression model developed for CKD (see Eq. 10) is useful for hemodialysis patients. The developed model is based on a single-frequency (50 kHz) bioimpedance measurement. Hence, single-frequency bioimpedance analysis is useful in the estimation of total body water in pre- and posthemodialysis.

CHF is characterized by local fluid accumulation in the body. The predictive regression model developed for CHF (see Eq. 11) is useful in making decisions about rehospitalization of patient.

The AFE4300 board has been used in the development of predictive regression models. The actual application of the developed models requires their implementation in the embedded programs (firmware), which can be downloaded onto the AFE4300 development board. This implies that the development board can be used for estimation of the day-to-day fitness of healthy people by implementing the predictive regression model for day-to-day fitness in the firmware of the AFE4300 board. The AFE4300 board can be used for CKD and CHF by implementing respective predictive regression models in the firmware of the AFE4300 board.

11 CONCLUSION

This chapter presents the application of an embedded healthcare system for the development of predictive regression models for day-to-day fitness, CHF, and CKD. The human body contains various chemical compounds such as water, minerals, protein, carbohydrates, nucleic acids, etc., with water being a major and electrically conductive constituent of the body. A small alternating current is applied to the body using AFE4300 and bioimpedance is measured. The anthropometric parameters of the body such as height, weight, age, and sex are simultaneously recorded. The serum electrolyte concentration from the blood samples are measured using an EM-360 biochemical analyzer. A database is generated for statistical analysis. Multiple regression analysis is used to develop the predictive regression models for day-to-day fitness, CKD, and CHF. The predictive regression models are validated by comparing the computed value of the total body water using the developed model, with that obtained by analyzing the blood samples using serum electrolyte concentrations.

REFERENCES

- [1] K. Ellis, Human body composition: *in vivo* methods, *Physiol. Rev.* 80 (2) (2000) 649–680.
- [2] ThoughtCo. [Online]. <https://www.thoughtco.com/chemical-composition-of-the-human-body-603995>.
- [3] LiveScience. [Online]. <https://www.livescience.com/3505-chemistry-life-human-body.html>.
- [4] L. Kravitz, V. Heyward, Getting a grip on body composition, *IDEA Today* 10 (4) (1992) 34–39.
- [5] B. Zemel, Body composition during growth and development, in: N. Cameron, B. Bogin (Eds.), *Human Growth and Development*, second ed., Academic Press, Elsevier, Boston, 2012, pp. 461–486. Chapter 18.
- [6] V. Heyward, ASEP methods recommendation: body composition assessment, *J. Exerc. Physiol.* 4 (4) (2001) 497–504.
- [7] A. Ward, A. Jackson, M. Pollock, Generalized equations for predicting body density of women, *Med. Sci. Sports Exerc.* 12 (3) (1980) 175–181.
- [8] M. Carter, F. Zhu, P. Kotanko, M. Kuhlmann, L. Ramirez, S. Heymsfield, G. Handelman, N. Levina, Assessment of body composition in dialysis patients by arm bioimpedance compared to MRI and ^{40}K measurements, *Blood Purif.* 27 (4) (2009) 330–337.
- [9] S. Dhar and Q. Hossain, “Non-invasive bio-impedance measurement using voltage-current pulse technique,” in *International Conference on Electrical, Electronics and Biomedical Engineering (ICEEBE)*, Penang, Malaysia, 2012, pp. 70–74.
- [10] G. Golub, C. Van Loan, An analysis of the total least squares problem, *SIAM J. Numer. Anal.* 17 (6) (1980) 883–893.
- [11] L. Saba, N. Dey, A. Ashour, S. Samanta, S. Nath, S. Chakraborty, J. Sanches, D. Kumar, R. Marinho, J. Suri, Automated stratification of liver disease in ultrasound: an online accurate feature classification paradigm, *Comput. Methods Prog. Biomed.* 130 (2016) 118–134.
- [12] S. Ahmed, N. Dey, A. Ashour, D. Sifaki-Pistolla, D. Balas-Timar, V. Balas, J. Manuel, R. Tavares, Effect of fuzzy partitioning in Crohn’s disease classification: a neuro-fuzzy-based approach, *Med. Biol. Eng. Comput.* 55 (1) (2017) 101–115.
- [13] K. Sharma, J. Virmani, A decision support system for classification of normal and medical renal disease using ultrasound images: a decision support system for medical renal diseases, *Int. J. Ambient Comput. Intell.* 8 (2) (2017) 52–69.
- [14] N. Dey, A. Ashour, A. Althoupety, Thermal imaging in medical science, in: *Recent Advances in Applied Thermal Imaging for Industrial Applications*, IGI Global, India, 2017, pp. 87–117. Chapter 4.
- [15] N. Sambyal, P. Abrol, Feature based text extraction system using connected component method, *Int. J. Synth. Emot.* 7 (1) (2016) 41–57.
- [16] Z. Li, N. Dey, A. Ashour, L. Cao, Y. Wang, D. Wang, P. McCauley, V. Balas, K. Shi, S. Fuqian, Convolutional neural network based clustering and manifold learning method for diabetic plantar pressure imaging dataset, *J. Med. Imaging Health Inform.* 7 (3) (2017) 639–652.
- [17] N. Dey, A. Ashour (Eds.), *Classification and Clustering in Biomedical Signal Processing*, IGI Global, Hershey, 2016.
- [18] O. Azzabi, C. Njima, H. Messaoud, New approach of diagnosis by timed automata, *Int. J. Ambient Comput. Intell.* 8 (3) (2017) 76–93.

- [19] M. Khachane, Organ-based medical image classification using support vector machine, *Int. J. Synth. Emot.* 8 (1) (2017) 18–30.
- [20] J. Ferreira, I. Pau, K. Lindecrantz, F. Seoane, A handheld and textile-enabled bioimpedance system for ubiquitous body composition analysis. An initial functional validation, *IEEE J. Biomed. Health Inform.* 21 (5) (2017) 1224–1232.
- [21] F. Dumler, M. Kilates, Body composition analysis in chronic dialysis patients: a longitudinal study, *Hong Kong J. Nephrol.* 5 (1) (2003) 24–28.
- [22] G. Parrinello, D. Torres, S. Paterna, P. Pasquale, C. Trapanese, M. Cardillo, M. Bellanca, S. Fasullo, G. Licata, Early and personalized ambulatory follow-up to tailor furosemide and fluid intake according to congestion in post-discharge heart failure, *Intern. Emerg. Med.* 8 (3) (2013) 221–228.
- [23] F. Abtahi, A. Berndtsson, S. Abtahi, F. Seoane, K. Lindecrantz, in: Development and preliminary evaluation of an Android based heart rate variability biofeedback system, 36th Annual International Conference of the IEEE Engineering in Medicine and Biology Society, Chicago, IL, 2014, pp. 3382–3385.
- [24] W. Bolonchuk, H. Lukaski, P. Johnson, G. Lykken, Assessment of fat free mass using bioelectrical impedance measurements of the human body, *Am. J. Clin. Nutr.* 41 (1985) 810–817.
- [25] K. Cole, R. Cole, Dispersion and absorption in dielectrics I. Alternating current characteristics, *J. Chem. Phys.* 9 (4) (2004).
- [26] H. Burger, J. Van Milaan, Measurements of the specific resistance of the human body to direct current, *Acta Med. Scand.* CXIV (VI) (1943) 584–607.
- [27] M. Khaled, M. Khatun, M. Haque, I. Kabir, D. Mahalanabis, in: Single, dual and multi-frequency bioimpedance to measure human body composition, Annual International conference of the IEEE Engineering in Medicine and Biology Society, Birmingham, USA, 1995, pp. 1.87–1.88.
- [28] A. Stahn, E. Terblanche, H. Gunga, Use of bioelectrical impedance: general principles and overview, in: V.R. Preedy (Ed.), *Handbook of Anthropometry: Physical Measures of Human Form in Health and Disease*, Springer, New York, 2012, pp. 49–90. Chapter 3.
- [29] B. Sanchez, A. Praveen, E. Bartolome, K. Soundarapandian, R. Brago, Minimal implementation of an AFE4300-based spectrometer for electrical impedance spectroscopy measurements, *J. Phys.* 434 (1) (2013) 1742–6596.
- [30] V. Yang, P. Aroul and K. Wen. (2013) Texas Instruments [Online]. www.ti.com/lit/an/sbaa202/sbaa202.pdf.
- [31] IBM Analytics. [Online]. <https://www.ibm.com/analytics/data-science/predictive-analytics/spss-statistical-software>.
- [32] C. Burtis, E. Ashwood, D. Bruns, *Fundamental of Clinical Chemistry*, sixth ed., Saunders, Philadelphia, PA, 2008. an Imprint of Elsevier.
- [33] D. Ellison, Treatment of disorders of sodium balance in chronic kidney disease, *Adv. Chronic Kidney Dis.* 24 (5) (2017) 332–341.
- [34] J. Kraut, Disturbances in acid-base, potassium, and sodium balance in patients with CKD: new insights and novel therapies, *Adv. Chronic Kidney Dis.* 24 (5) (2017) 272–273.
- [35] I. Lloyd. (2013) NDhealthFACTS. [Online]. http://www.ndhealthfacts.org/wiki/Congestive_Heart_Failure.

This page intentionally left blank

Comparison of multiclass and hierarchical CAC design for benign and malignant hepatic tumors

6

Nimisha Manth*, Kriti†, Jitendra Virmani‡

Jaypee University of Information Technology, Waknaghat, Himachal Pradesh, India*

Thapar Institute of Engineering and Technology (deemed-to-be university), Patiala, India†

CSIR-CSIO, Chandigarh, India‡

CHAPTER OUTLINE

1 Introduction	120
2 Materials and Methods	123
2.1 Dataset Collection	123
2.2 Data Set Description	123
2.3 Data Collection Protocol	123
2.4 ROIs Selection	124
2.5 ROI Size Selection	125
2.6 Proposed CAC System Design	127
2.7 Feature Extraction Module	127
2.8 Classification Module	132
3 Results	137
3.1 Experiment 1: To Evaluate the Potential of the Three-Class SSVM Classifier Design for the Characterization of Benign and Malignant FHTs	139
3.2 Experiment 2: To Evaluate the Potential of SSVM-Based Hierarchical Classifier Design for Characterization Between Benign and Malignant FHTs	139
3.3 Experiment 3: Performance Comparison of SSVM-Based Three-Class Classifier Design and SSVM-Based Hierarchical Classifier Design for Characterization of Benign and Malignant FHTs	140
4 Discussion and Conclusion	141
References	144
Further Reading	146

1 INTRODUCTION

The classic sonographic appearance of a typical focal hepatic tumor (FHTs) makes the diagnosis easier. However, the differentiation between atypical FHTs from ultrasound (US) is a quite challenging task faced by radiologists in day-to-day practice. It is mainly due to the existence of overlapping sonographic appearances of benign and malignant FHTs [1–6]. The B-mode US is nonradioactive, inexpensive in nature, noninvasive, and possesses real-time imaging capabilities, therefore it is considered the preferred choice for the characterization of FHTs [2,3]. Therefore, a computer-aided characterization (CAC) system for primary benign and malignant FHTs, based on liver US images, is highly desired. In the current study, an efficient smooth support vector machine (SSVM)-based hierarchical CAC system was designed using a comprehensive and diversified image database with (a) typical and atypical cases of hemangioma (HEM) and metastatic carcinoma (MET), and (b) small as well as large hepatocellular carcinoma (HCC) tumors.

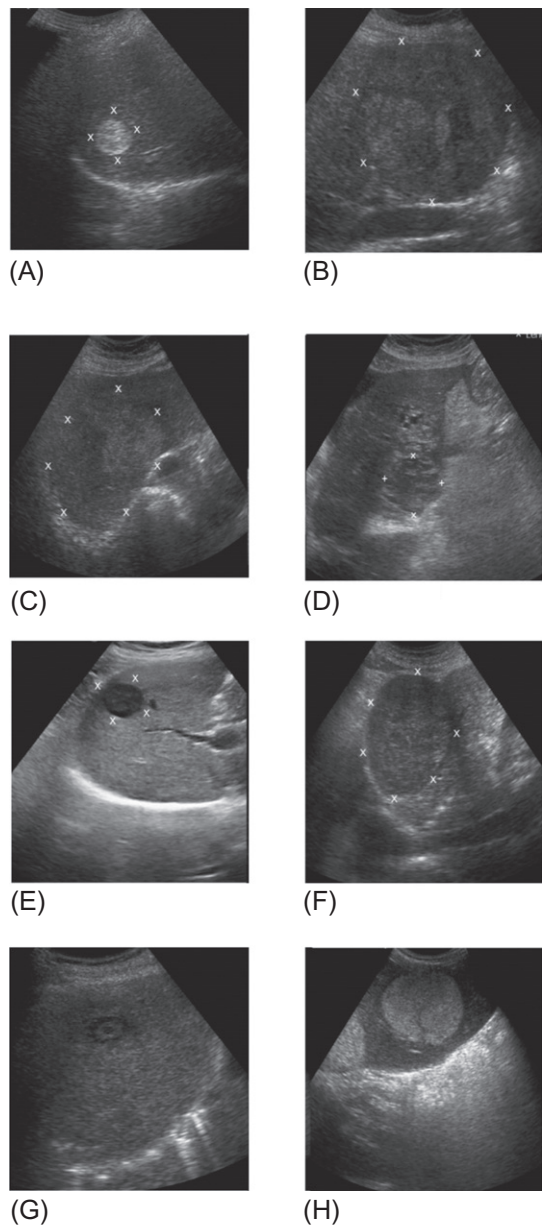
The present study was carried out to design a hierarchical CAC system for the differential diagnosis between primary benign (HEM), primary malignant (HCC), and secondary malignant (MET) FHTs. In the current study, benign FLL that is, HEM is considered, as it is the most common benign FHT [1,4]. Among malignant FHTs, HCC [7–9] (the most commonly occurring primary malignant FHT) and MET [1,2,10] (the most commonly occurring secondary malignant FHT) have been considered for analysis.

In all, 70% of the HEM cases discovered during routine clinical practice are cases of typical HEMs. These typical hemangiomas appear as homogeneously hyperechoic FHTs with well-defined boundaries [1,2,11–15]. The sonographic appearance of a typical case of MET FHT is a “bull’s-eye.”[11,16]

The atypical HEMs can exhibit either a hypoechoic or isoechoic appearance, overlapping with the appearance of certain HCC and atypical MET FHTs [1,11,17]. The sonographic appearances exhibited by atypical MET FHTs vary over a wide range from being anechoic to hypoechoic, hyperechoic, and isoechoic; in some cases, they can even exhibit mixed echogenicity [1,2,11,16,18,19].

The HCC frequently develops on top of cirrhosis (a condition where the liver parenchyma becomes coarse textured and nodular) [1,2,10–13,18–21]. As the sonographic appearance of HCC FHTs varies considerably over a wide range, even in small and large HCCs, no single appearance can be considered typical for these FHTs. The HCC images used in the current study contain both small hepatocellular carcinomas (SHCCs) of a size less than 2 cm as well as large hepatocellular carcinomas (LHCCs) with a size larger than 2 cm. The SHCCs appearance varies from hypoechoic to hyperechoic; however, the LHCCs have a mixed echogenic appearance [1,18]. The sample images of these FHTs, that is, the HEM, HCC, and MET, are shown in Fig. 1.

The diagnosis of FHTs using US images is quite challenging due to factors such as (a) the sensitivity of the US imaging modality for the diagnosis of small FHTs

**FIG. 1**

Sample liver ultrasound images. (A) Typical hemangioma (homogeneously hyperechoic appearance). (B) Atypical hemangioma (showing mixed echogenicity). (C) Atypical hemangioma (showing mixed echogenicity). (D) Small HCC (showing mixed echogenicity). (E) Small HCC (hypoechoic appearance). (F) Large HCC (showing mixed echogenicity). (G) Typical MET ("bull's eye" appearance). (H) Atypical MET (showing hyperechoic appearance).

(size less than 2 cm) developed on a coarse-textured liver with cirrhosis is severely limited [1,2,5,11,18], (b) the appearances of atypical HEMs, HCCs, and atypical MET FHTs on US are highly overlapping [1,2,5,11,22], and (c) limited sensitivity for detection of FHTs that are isoechoic, that is, exhibiting the same echogenicity as that of the surrounding liver [1,21]. It is expected that the extraction of discriminatory texture features that are difficult to visualize, followed by an efficient classifier design with comprehensive data from each image subclass can reduce some of these limitations.

A brief review of the literature in which CAC systems for FHTs have been proposed is presented in Table 1.

To compute reliable estimates of texture features, a minimum of 800 pixels is required [25–27]. However, different regions of interest (ROI) sizes have been used in different studies, for example in [23,24] the ROI size is only 10×10 , in studies [6,10,12,13], the ROI size is 32×32 , and in [14] the ROI size is 64×64 . Necrotic areas inside FHTs are not considered for extracting the inside ROIs (IROIs). For extracting the surrounding ROIs (SROIs), inhomogeneous areas including blood vessels and ducts are not considered. Therefore, in the current study, taking a larger size ROI was not possible. In studies [14,21,24], the features extracted from IROIs only are considered for analysis. Also, the classification of images in the dataset in different subclasses such as typical and atypical hemangioma or metastatic carcinoma and SHCC/LHCC FHTs is not described.

The current study investigates the contribution of SROIs for characterization between benign and malignant FHTs using (a) single multiclass classifier design and (b) hierarchical classifier design. The SSVM classifier has been used for the classification task [5,28,29].

Table 1 Related Studies Carried Out for the Classification of Liver Diseases

Related Study	No. of Classes	Features	Classifier
Virmani et al. [6]	5	Statistical, GLCM, GLRLM, FPS, Laws, Gabor	NN ensemble
Virmani et al. [10]	2	GLCM, GLRLM, FPS and Laws'	SVM
Virmani et al. [12]	5	Statistical, GLCM, GLRLM, FPS, Laws, Gabor	KNN, PNN, NN
Virmani et al. [13]	5	Statistical, GLCM, GLRLM, FPS, Laws, Gabor	SVM
Yoshida et al. [14]	2	Wavelet packet based	NN
Manth et al. [15]	2	Statistical, GLCM, GLRLM, FPS, Laws, Gabor	SVM, SSVM
Sujana et al. [23]	3	GLRLM	LDA, NN
Poonguzhalil et al. [24]	4	Autocorrelation, edge frequency GLCM and Laws' features	NN

2 MATERIALS AND METHODS

With the development of computer technology, different artificial intelligence, and data mining and machine learning techniques, a lot of opportunities have been provided to various researchers for developing CAD systems for analysis and monitoring of different diseases using medical images captured using various modalities such as X-ray, ultrasound, CT scan, PET scan, MRI, and thermal imaging [30–34]. For the characterization of liver disorders, CAC systems prove to be useful in efficiently assisting the radiologists in validating their diagnosis as well as monitor the textural changes that can be exhibited if a benign FHT becomes a malignant FHT over time. There is a need for CAC systems for the differentiation of liver diseases because it has been noted that different FHTs have variable sonographic appearances, making it difficult for the radiologists to clearly differentiate between them. This is where CAC systems prove helpful and assist the radiologists in interpreting the US of an FHT by providing a second opinion on the diagnosis.

2.1 DATASET COLLECTION

The dataset for the current study consists of liver US images. The details of the dataset collection are shown in [Fig. 2](#).

2.2 DATA SET DESCRIPTION

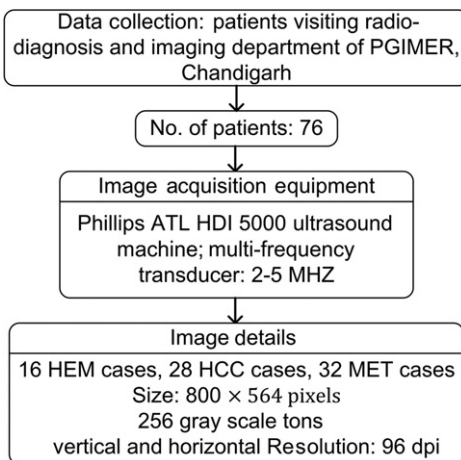
The image dataset description is given in [Table 2](#).

Finally, the final dataset consists of a total of 331 ROIs with 255 IROIs and 76 SROIs.

To design the efficient CAC system, it is ensured that the training data should include FHTs from all image subclasses. A description of the training and testing dataset is given in [Table 3](#).

2.3 DATA COLLECTION PROTOCOL

The presence of hemangioma, hepatocellular carcinoma, and metastasis FHTs was confirmed by experienced radiologists based on their experience by visualizing the appearances of these FHTs on US as well as through a patient's clinical history and appearances on other imaging modalities such as CT or MRI, pathological examinations, and biopsies. Only the HCC FHTs developed on a cirrhotic liver were considered. The size of the FHTs was observed in both longitudinal as well as transverse views. The HCC FHTs whose size was less than 2 cm were labeled as SHCC and the ones with a size greater than 2 cm were labeled as LHCC.

**FIG. 2**

Details of data collection.

Table 2 Dataset Description

Total Images (76)			
No. of IROIs: 255, No. of SROIs: 76			
	HEM	HCC	MET
Total no. of images	16 Typical cases: 10 Atypical cases: 6	28 Small HCC: 13 Large HCC: 15	32 Typical cases: 12 Atypical cases: 20
Total FHTs	16	28	32
Total no. of IROIs	70 Typical IROIs: 27 Atypical IROIs: 43	90 Small HCC IROIs: 19 Large HCC IROIs: 71	95 Typical IROIs: 14 Atypical IROIs: 81
Total no. of SROIs	16	28	32

2.4 ROIs SELECTION

The ROIs in the current work have been extracted manually using the MATLAB software. The location of IROIs and SROI for each tumor was freezed with input from the experienced radiologists, as shown in [Fig. 3](#).

- (a) In order to crop IROIs, necrotic areas within the lesions were ignored.
- (b) For cropping SROIs, inhomogeneous regions such as liver ducts and blood vessels were not considered.
- (c) The SROIs were cropped at the depth of the lesion center.

Table 3 Description of Training and Testing Dataset

Training Data Set Description			
	HEM	HCC	MET
Total no. of images (44)	10	16	18
Total no. of FHTs	10 Typical cases: 7 Atypical cases: 3	16 Small HCC: 7 Large HCC: 9	18 Typical cases: 7 Atypical cases: 11
Total no. of IROIs (140)	40 Typical IROIs: 22 Atypical IROIs: 18	50 Small HCC IROIs: 10 Large HCC IROIs: 40	50 Typical MET IROIs: 9 Atypical MET IROIs: 41
Total no. of SROIs (44)	10	16	18

Testing Data Set Description			
	HEM	HCC	MET
Total no. of images (32)	6	12	14
Total no. of FHTs	6 Typical cases: 3 Atypical cases: 3	12 Small HCC: 7 Large HCC: 9	14 Typical cases: 5 Atypical cases: 9
Total no. of IROIs (135)	40 Typical IROIs: 22 Atypical IROIs: 18	50 Small HCC IROIs: 10 Large HCC IROIs: 40	45 Typical IROIs: 5 Atypical IROIs: 40
Total no. of SROIs (40)	10	16	14

2.5 ROI SIZE SELECTION

The size of the ROI is selected such that it contains at least 800 pixels for computation of reliable texture properties. For the classification of FHTs, different ROI sizes have been considered in the literature, such as 10×10 pixels [23,24], 32×32 pixels [6,10,12,13], and 64×64 pixels [14]. For the current study, multiple ROIs of size 32×32 pixels have been extracted from each lesion, keeping in view the facts mentioned below:

- (a) The 1024 pixels in an ROI size of 32×32 give a sampling distribution that is adequate for computing reliable statistics.
- (b) Due to the presence of necrotic areas within certain FHTs, extracting ROIs of a size greater than 32×32 pixels was considerably difficult.

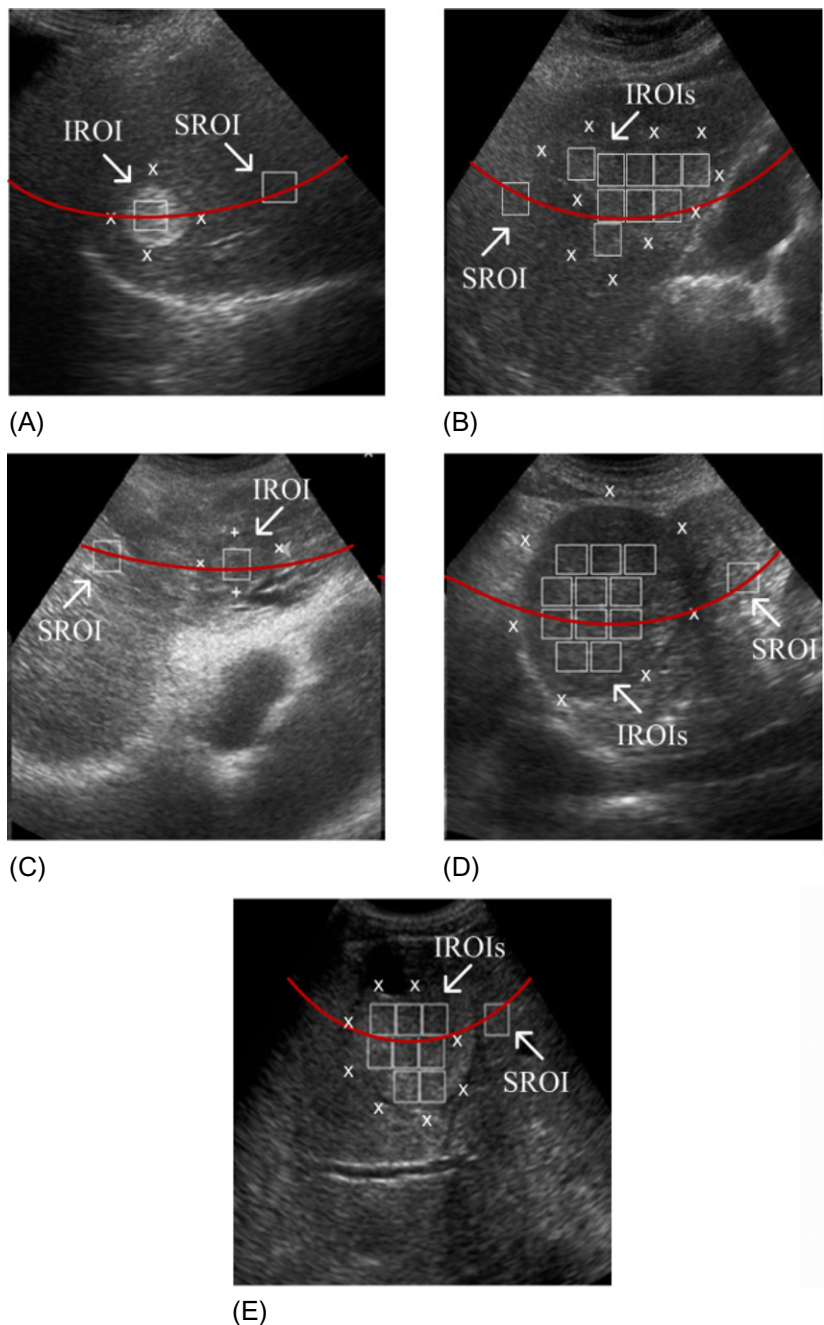


FIG. 3

Sample liver ultrasound images with marked IROIs and SROIs (A) typical HEM; (B) atypical HEM; (C) SHCC; (D) LHCC; and (E) atypical MET.

- (c) As inhomogeneous regions in the surrounding liver parenchyma should be avoided for extracting the SROI for each lesion, considering an ROI size of greater than 32×32 pixels was practically impossible.
- (d) With smaller ROIs, the time taken for feature computation is less and also more ROIs are available for training the classifier with an adequate number of samples.

2.6 PROPOSED CAC SYSTEM DESIGN

The CAC system for the characterization between primary benign (HEM), primary malignant (HCC), and secondary malignant (MET) FHTs has been proposed in the current study.

For the present classification task, the database of 255 IROIs and 76 SROIs extracted from 76 US liver images has been considered for analysis. The CAC system includes feature extraction and classification modules.

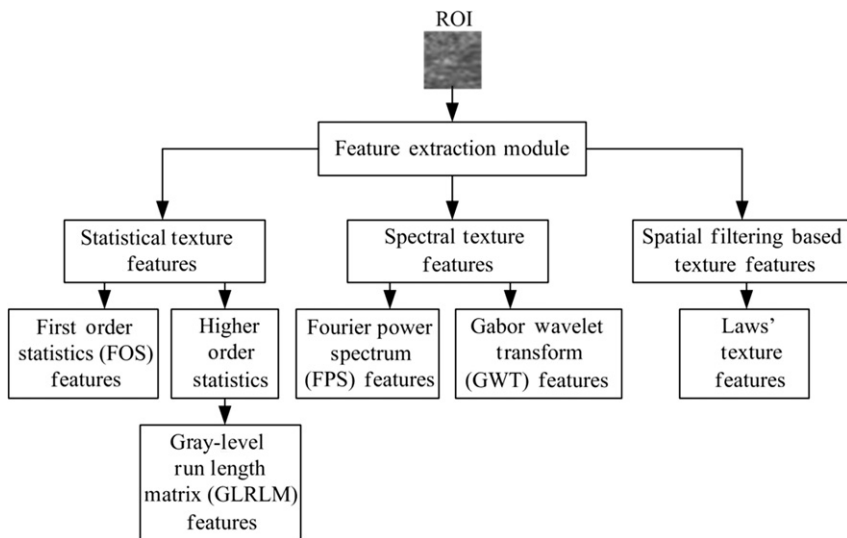
In the process of feature extraction, texture features have been calculated using (a) statistical features including first-order statistical and higher-order statistical features, (b) spectral features including FPS-based features and GWT-based features, and (c) signal processing-based Laws' features. The texture feature set of a length of 146 features (73 features computed only from IROIs and 73 ratio features computed from IROIs and corresponding SROIs) is considered for analysis. The distribution of ROIs in each image class among training testing data is depicted in [Table 2](#). The SSVM classifier has been implemented in the classification module.

2.7 FEATURE EXTRACTION MODULE

Two types of texture feature vectors have been computed in this module, that is, (a) a texture feature vector computed from regions inside the lesion (IROIs) only, and (b) a texture ratio feature vector computed using IROI and the corresponding SROI.

Both these texture feature vectors are computed using statistical, spectral, and signal processing-based filtering-based methods. The methods for feature extraction can be broadly categorized into statistical methods, spectral methods, and spatial filtering-based methods. It was decided to consider all the types of feature description methods for a comprehensive representation of texture. These features are depicted in [Fig. 4](#). The description of these features is given in [Fig. 5](#).

The texture feature extraction methods are of three types: statistical, spectral, and spatial filtering-based. Under statistical methods, the features are computed from raw images. FOS features are computed from the histograms of the images. The GLRLM features are computed using the gray level run length matrix formed for the images based on the runs of the gray levels in the image. Under spatial methods, the images are transformed into a frequency domain and then different features are computed. FPS features are computed after transforming the image using the Fourier transform

**FIG. 4**

Texture features calculated in the present study.

and the Gabor features are computed after transforming the image using the Gabor wavelet transform (GWT). Under signal processing methods, the images are first filtered using some predefined masks to enhance some properties and then the texture features are computed.

The real parts of the Gabor wavelet filters used in the current study are shown in Fig. 6 and sample images showing the resultant liver images after passing through these filters are shown in Figs. 7–9.

The Gabor filters can be represented as a product of sine/cosine waves with a Gaussian function. The one-dimensional Gabor functions are described in Eqs. (1) and (2).

$$f_{even}(x) = G(x) \cos(2\pi\omega_o x) \quad (1)$$

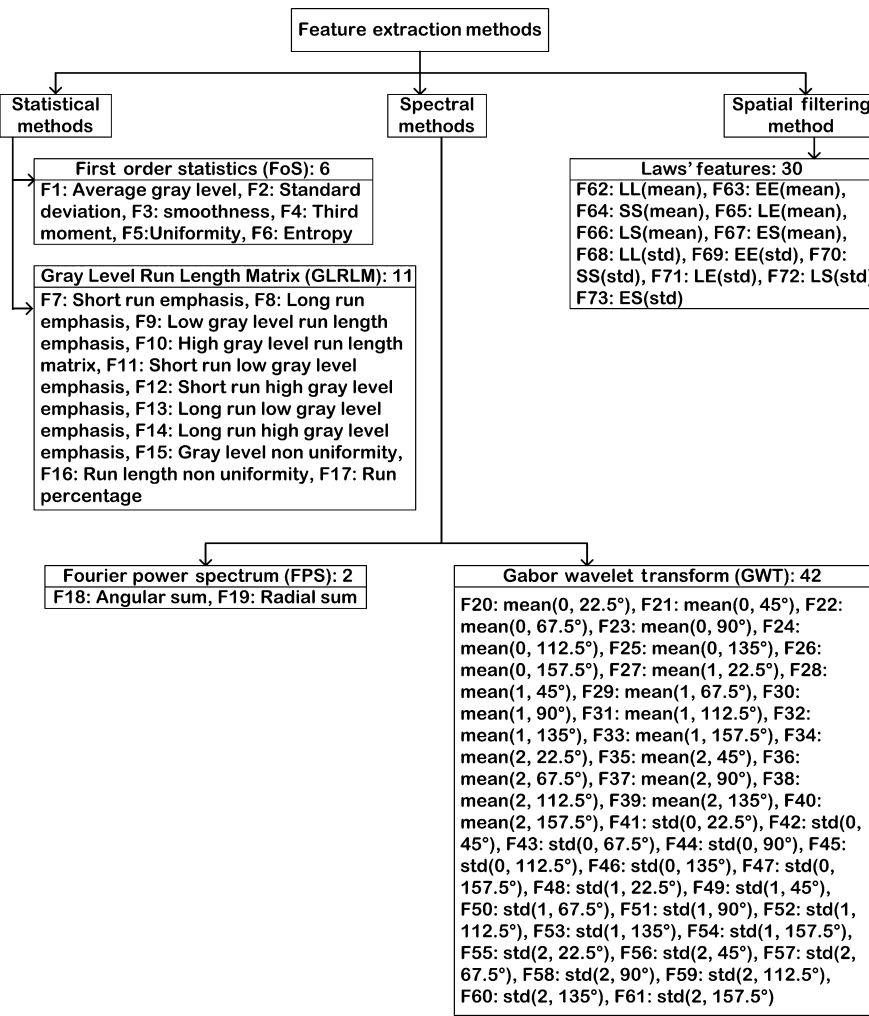
$$f_{odd}(x) = G(x) \sin(2\pi\omega_o x) \quad (2)$$

where $G(x)$ represents a Gaussian function given as:

$$G(x) = \frac{1}{\sqrt{2\pi}\sigma} e^{-(x^2/2\sigma^2)} \quad (3)$$

For applying the Gabor transform to images, two-dimensional filters are required. The one-dimensional Gabor functions can be extended to two-dimensional Gabor functions as follows:

$$f_{even}(x, y) = G(x, y) \cos(2\pi\omega_{xo}x + 2\pi\omega_{yo}y) \quad (4)$$



F74-F146: 73 texture ratio features corresponding to above features (F1-F73). The features F1-F73 are calculated for both IROIs and SROIs so as to compute 73 texture ratio features

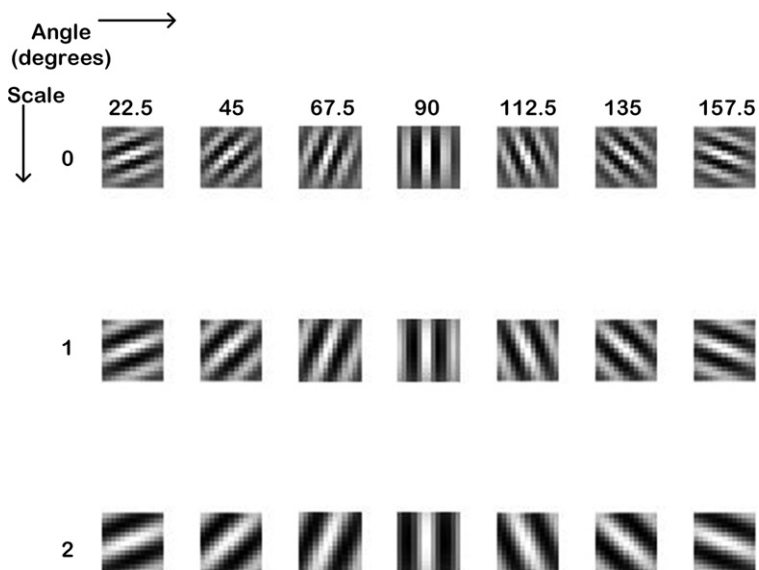
FIG. 5

Description of extracted features.

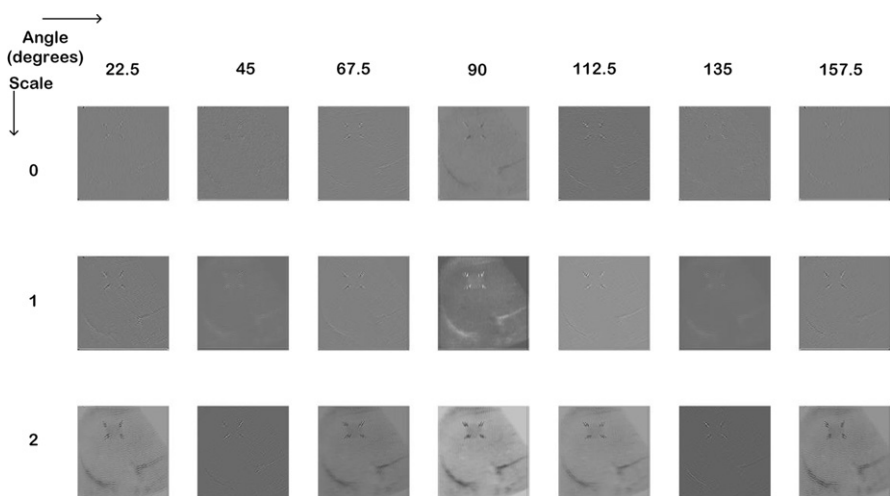
$$f_{odd}(x, y) = G(x, y) \sin(2\pi\omega_{xo}x + 2\pi\omega_{yo}y) \quad (5)$$

where $G(x, y)$ represents a two-dimensional Gaussian function given as:

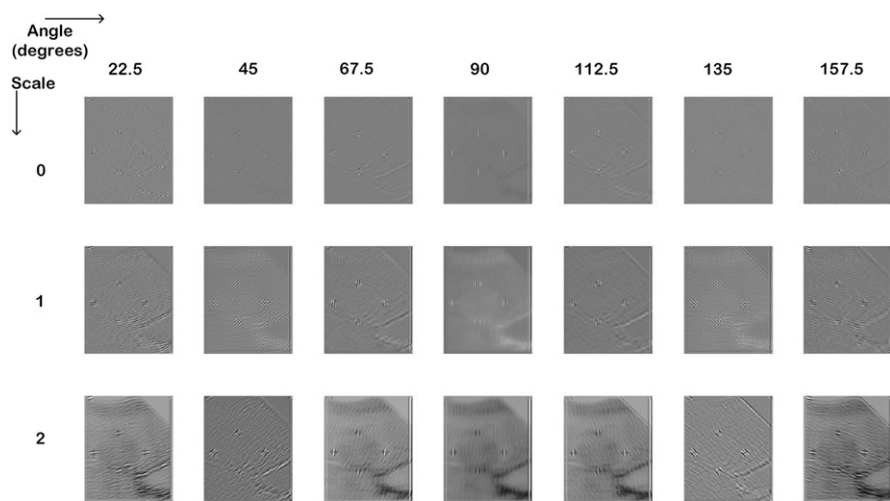
$$G(x, y) = \frac{1}{2\pi\sigma_x\sigma_y} e^{\left(-\frac{x^2}{2\sigma_x^2} - \frac{y^2}{2\sigma_y^2}\right)} \quad (6)$$

**FIG. 6**

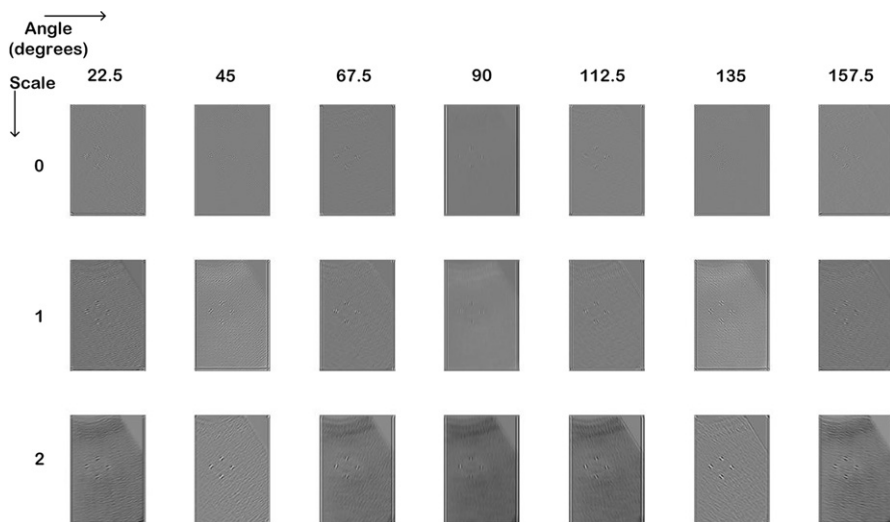
Real parts of Gabor wavelet filters.

**FIG. 7**

Real parts of a benign liver ultrasound image after passing through Gabor filters.

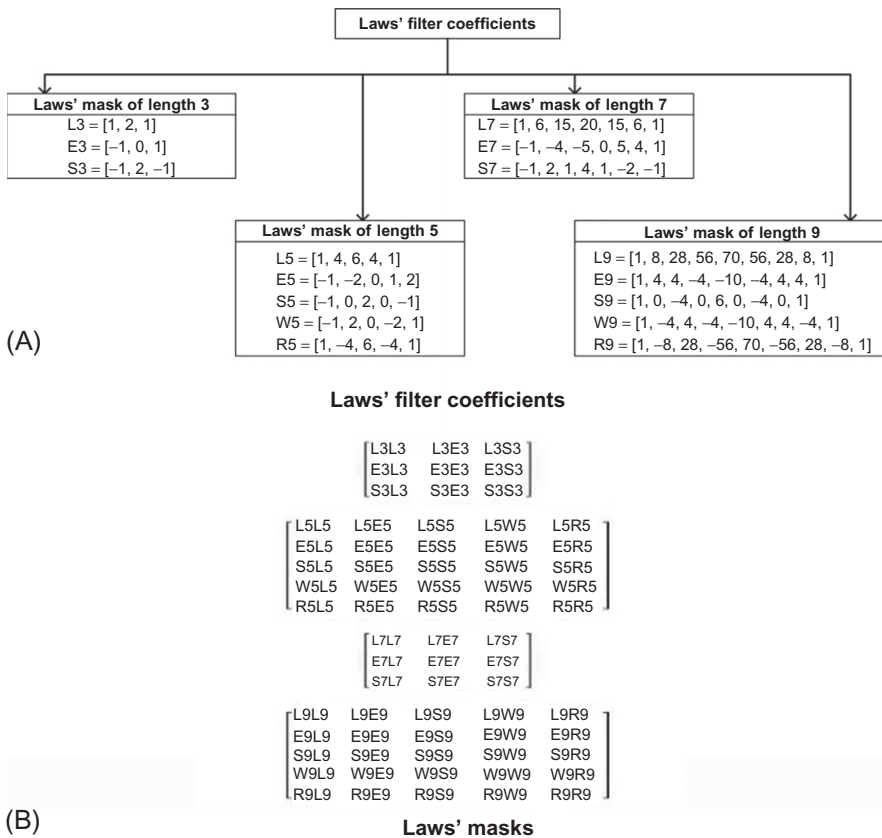
**FIG. 8**

Real parts of a primary malignant liver ultrasound image after passing through Gabor filters.

**FIG. 9**

Real parts of a secondary malignant liver ultrasound image after passing through Gabor filters.

The different Laws' masks used in the current study are described in Fig. 10 and the results of the application of these Laws' masks (e.g. Laws mask of length 5) have been observed on a standard test image: Barbara.png and a few liver US images. These results are shown in Figs. 11–14. The Laws' masks have been applied on both standard test images as well as liver images. Fig. 11 is shown for understanding purposes as the benchmark images have all the types of texture information, that is,

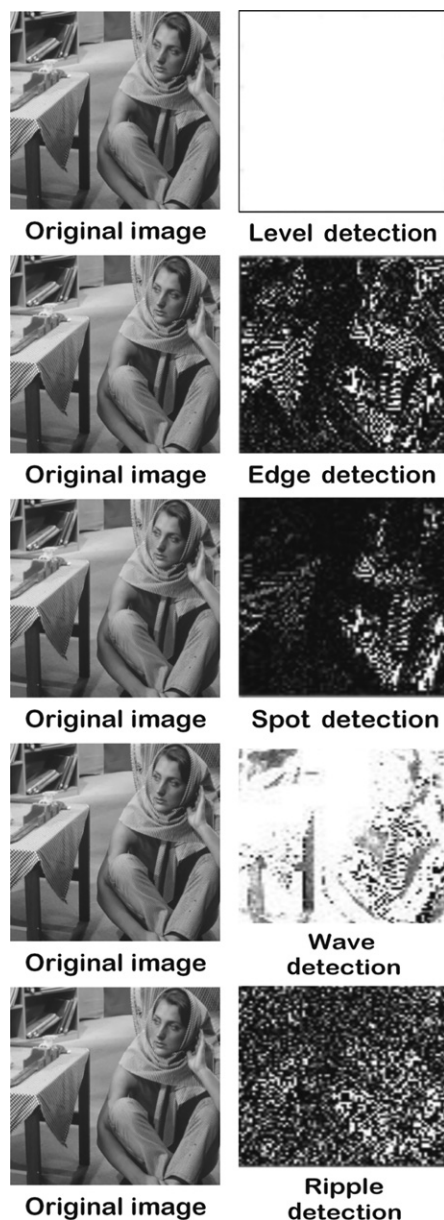
**FIG. 10**

Different Laws' one-dimensional filter coefficients and their corresponding masks.

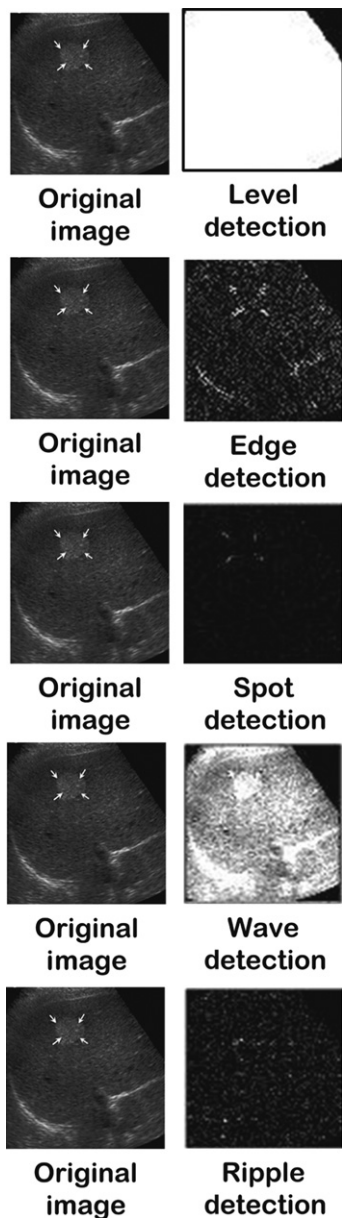
oriented texture, homogeneous texture, heterogeneous texture, and random texture. Therefore, the performance of various Laws' filters to capture the underlying textural properties of the region can be better understood using benchmark images. The corresponding application of Laws' mask to liver images is also shown in Figs. 12–14.

2.8 CLASSIFICATION MODULE

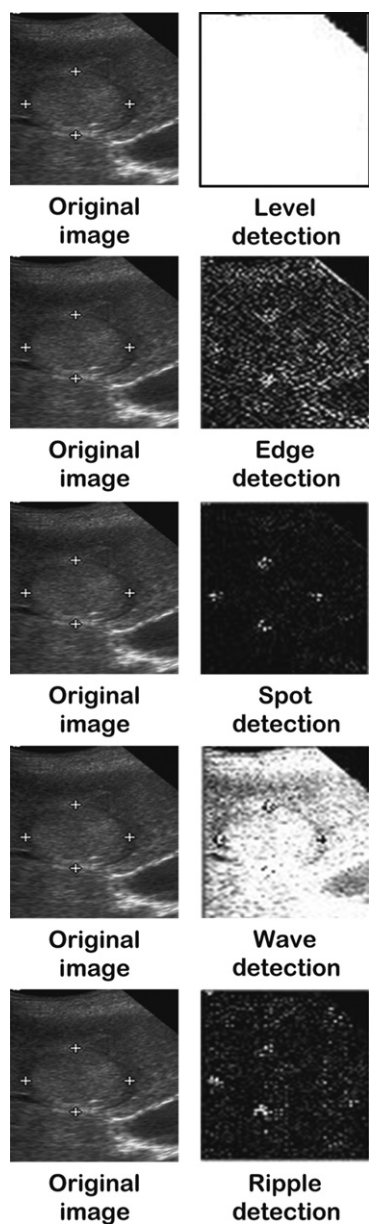
In the current study, the classification task has been performed in two ways: (a) three-class classification task carried out by using a single SSVM classifier, and (b) three-class classification task carried out by using two SSVM binary classifiers arranged in a hierarchical framework. These two SSVM classifiers provide stepwise classification for the generalized three-class classification problem in two stages. In the first stage, the SSVM binary classifier-1 was used to classify test cases from all three classes into primary benign (i.e., HEM) or malignant (i.e., HCC or MET) cases. The predicted

**FIG. 11**

Results of applying Laws' mask of length 5 on Barbara image.

**FIG. 12**

Results of applying Laws' mask of length 5 on primary benign liver image.

**FIG. 13**

Results of applying Laws' mask of length 5 on primary malignant liver image.

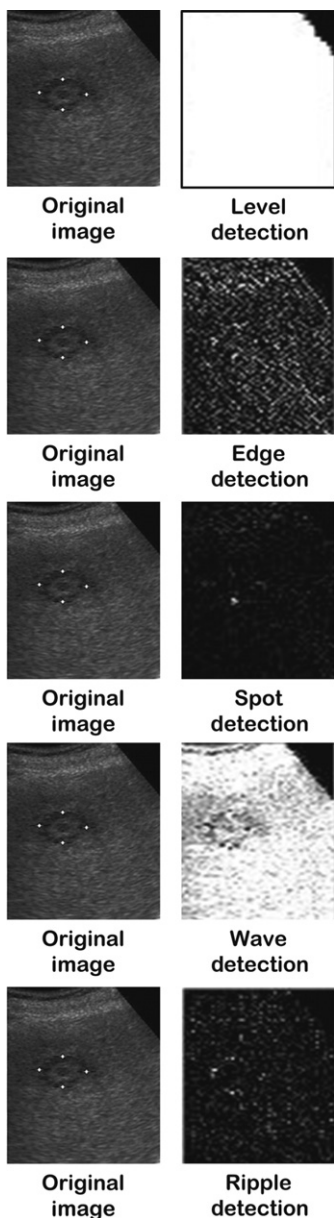
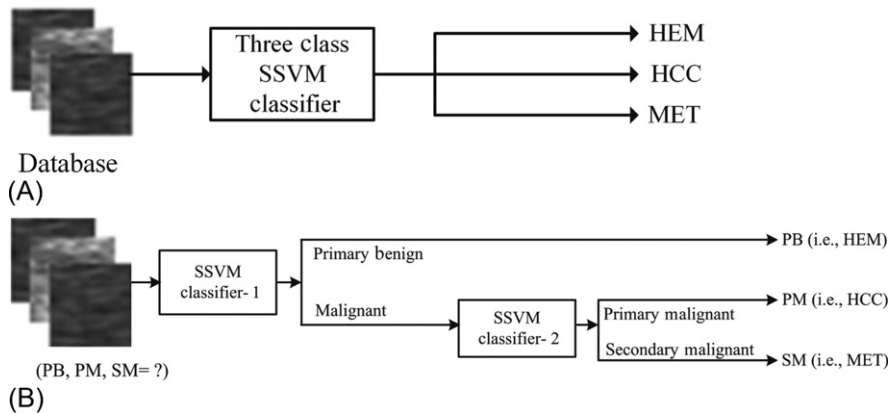


FIG. 14

Results of applying Laws' mask of length 5 on secondary malignant liver image.

**FIG. 15**

Architecture of classification module (A) SSVM-based three-class classifier, (B) SSVM-based hierarchical classifier.

malignant cases were then provided as the input to SSVM binary classifier-2. The second classifier further classified the malignant cases into primary malignant (i.e., HCC) or secondary malignant (i.e., MET) cases. The decision is made at SSVM classifier-1 whether the ROI selected by radiologists is benign or malignant. If further investigation of malignant instances such as HCC or MET is required, then the instance will be passed to SSVM classifier-2. The classification module is shown in Fig. 15.

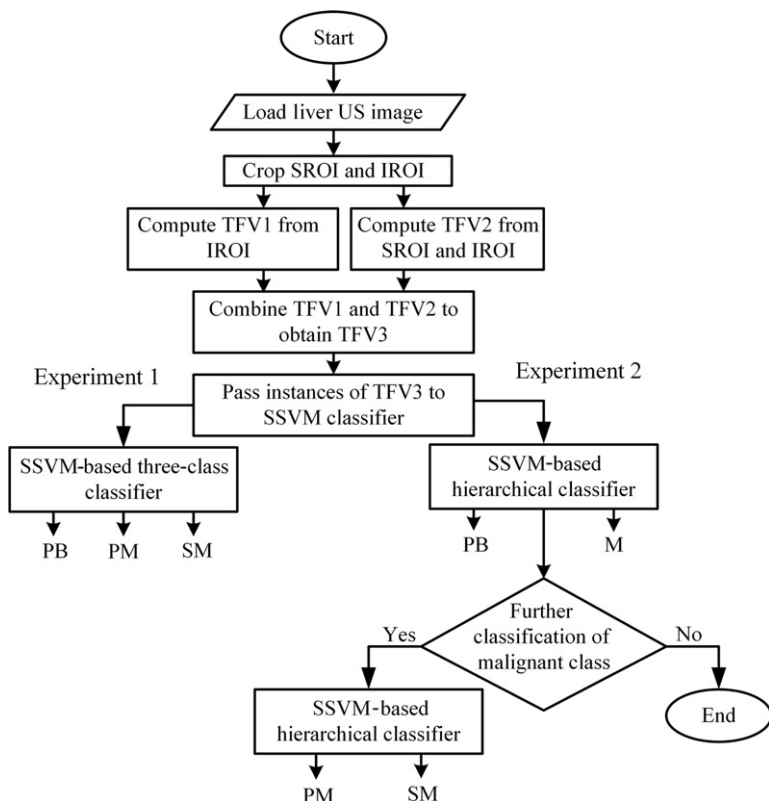
2.8.1 SSVM classifier

This classifier was implemented using the SSVM toolbox [35]. It uses a smoothing method for the unconstrained optimization reformulation, depending on the conventional quadratic program associated with the SVM [35,36]. For further details on the working of the SSVM classifier refer to [37]. Some of the advantages of the SSVM classifier are its speed, strong convexity, and infinite differentiability.

3 RESULTS

The experimental workflow for designing the CAC system to characterize the primary benign, primary malignant, and secondary malignant FHTs is shown in Fig. 16.

A two-stage hierarchical framework was designed using SSVM binary classifiers. Each binary classifier was trained independently. The dataset description and the bifurcation of the dataset into disjoint training and testing datasets for each binary classifier is shown in Table 3. For the implementation of the above CAC system, various experiments were conducted, as given in Table 4.

**FIG. 16**

Experimental workflow for designing a hierarchical CAC system for characterizing the FHTs.

Table 4 Experiment Description

Experiment No.	Description
Expt 1	To evaluate the potential of a three-class SSVM classifier design for the characterization of benign and malignant FHTs
Expt 2	To evaluate the potential of an SSVM-based hierarchical classifier design for the characterization of benign and malignant FHTs
Expt 3	Performance comparison of SSVM-based three-class classifier design and SSVM-based hierarchical classifier design for the characterization of benign and malignant FHTs

Table 5 Classification Results of Three-Class SSVM Classifier

TFV (<i>l</i>)	Confusion Matrix				OCA (%)	ICA _{PB} (%)	ICA _{PM} (%)	ICA _{SM} (%)
		PB	PM	SM				
TFV1 (73)	PB	26	3	1	63.5	86.7	42.5	66.7
	PM	11	17	12				
	SM	5	10	30				
TFV2 (73)	PB	29	1	0	75.7	96.7	82.5	55.6
	PM	2	33	5				
	SM	1	19	25				
TFV3 (146)	PB	25	0	5	82.6	83.3	72.5	91.1
	PM	1	29	10				
	SM	4	0	41				

TFV, texture feature vector; l, length of TFV; TFV1, TFV 1 containing IROI features only; TFV2, TFV 2 containing ratio features only; TFV3, combined TFV containing IROI features and ratio features; OCA, overall classification accuracy; ICA, individual class accuracy; ICA_{PB}, ICA of primary benign class; ICA_{PM}, ICA of primary malignant class; ICA_{SM}, ICA of secondary malignant class.

3.1 EXPERIMENT 1: TO EVALUATE THE POTENTIAL OF THE THREE-CLASS SSVM CLASSIFIER DESIGN FOR THE CHARACTERIZATION OF BENIGN AND MALIGNANT FHTs

The classification potential of TFV1, TFV2, and TFV3 was tested using a single three-class SSVM classifier. The obtained results are shown in [Table 5](#).

It can be observed that OCA values of 63.5%, 75.7%, and 82.6% have been achieved with TFV1, TFV2, and TFV3, respectively. The highest OCA is achieved using TFV3. The ICA values obtained with respect to TFV3 are 83.3%, 72.5%, and 91.1% for primary benign, primary malignant, and secondary malignant cases, respectively, and the number of misclassified cases is 20/115.

3.2 EXPERIMENT 2: TO EVALUATE THE POTENTIAL OF SSVM-BASED HIERARCHICAL CLASSIFIER DESIGN FOR CHARACTERIZATION BETWEEN BENIGN AND MALIGNANT FHTs

In this experiment, the classification potential of TFVs was tested using an SSVM-based hierarchical classifier for binary classification between primary benign and malignant FHTs. The CAC system consists of two SSVM binary classifiers arranged in a hierarchical framework. The results of the SSVM classifier-1 are reported in [Table 6](#) and the SSVM classifier-2 are reported in [Table 7](#). In [Table 6](#), the OCA values yielded by the SSVM classifier 1 for TFV1, TFV2, and TFV3 are 85.2%, 96.5%, and 97.4%, respectively; it is seen that TFV3 yields the highest classification accuracy. The ICA values obtained w.r.t TFV3 are 90% and 100% for primary benign and malignant cases. The number of misclassified cases in SSVM-1 are 3/115. In [Table 7](#), the OCA values yielded by SSVM classifier 2 for TFV1,

Table 6 Classification Performance of SSVM Classifier-1

TFV (<i>l</i>)	Confusion Matrix			OCA (%)	ICA _{PB} (%)	ICA _M (%)
		PB	M			
TFV1 (73)	PB	14	16	85.2	46.7	98.9
	M	1	84			
TFV2 (73)	PB	26	4	96.5	86.7	100
	M	0	85			
TFV3 (146)	PB	27	3	97.4	90.0	100
	M	0	85			

TFV, texture feature vector; *l*, length of TFV; TFV1, TFV 1 containing IROI features only; TFV2, TFV 2 containing ratio features only; TFV3, combined TFV containing IROI features and ratio features; OCA, overall classification accuracy; ICA, individual class accuracy; ICA_{PB}, ICA of primary benign class; ICA_M, ICA of malignant class.

Table 7 Classification Performance of SSVM Classifier-2

TFV (<i>l</i>)	Confusion Matrix			OCA (%)	ICA _{PM} (%)	ICA _{SM} (%)
		PM	SM			
TFV1 (73)	PM	34	6	69.4	85.0	55.6
	SM	20	25			
TFV2 (73)	PM	36	4	80.0	90.0	71.1
	SM	13	32			
TFV3 (146)	PM	31	9	89.4	77.5	100
	SM	0	45			

TFV, texture feature vector; *l*, length of TFV; TFV1, TFV 1 containing IROI features only; TFV2, TFV 2 containing ratio features only; TFV3, combined TFV containing IROI features and ratio features; OCA, overall classification accuracy; ICA, individual class accuracy; ICA_{PM}, ICA of primary malignant class; ICA_{SM}, ICA of secondary malignant class.

TFV2, and TFV3 are 69.4%, 80%, and 89.4%, respectively; the highest OCA is yielded by TFV3. The ICA values obtained w.r.t TFV3 are 77.5% and 100% for primary malignant and secondary malignant cases, respectively. The number of misclassified cases in SSVM-2 are 9/85.

3.3 EXPERIMENT 3: PERFORMANCE COMPARISON OF SSVM-BASED THREE-CLASS CLASSIFIER DESIGN AND SSVM-BASED HIERARCHICAL CLASSIFIER DESIGN FOR CHARACTERIZATION OF BENIGN AND MALIGNANT FHTs

In this experiment, the performance comparison of SSVM-based three-class classifier design and SSVM-based hierarchical classifier design for characterization between benign and malignant FHTs was carried out. The results are reported in Table 8.

Table 8 Classification Performance of Three-Class SSVM Classifier and SSVM-Based Hierarchical Classifier

Classifier Used	Confusion Matrix			OCA (%)	No. of Misclassified Cases
	PB	PM	SM		
SSVM multiclass classifier	PB	25	0	5	82.6 20/115
	PM	1	29	10	
	SM	4	0	41	
Classifier Used	Confusion Matrix			CA (%)	No. of Misclassified Cases
		PB	M	97.4 (3/115)	
SSVM hierarchical classifier-1	PB	27	3	89.6 12/115	
	M	0	85		
SSVM hierarchical classifier-2	PM	31	9	89.4 (9/85)	
	SM	0	45		

OCA, overall classification accuracy; CA, classification accuracy; PB, primary benign class; PM, primary malignant class; SM, secondary malignant class.

The OCA value achieved with the three-class classifier and the hierarchical classifier are 82.6% and 89.6%, respectively. The OCA for the hierarchical classifier is obtained by adding the total misclassified cases obtained at each stage of the hierarchical framework.

The misclassification analysis for the SSVM-based three-class classifier design and the SSVM-based hierarchical classifier design for the characterization of benign and malignant FHTs is reported in Table 9.

The SSVM-based three-class classifier yielded 20 (20 out of 115 cases) misclassifications, that is, five, 11, and four for primary benign, primary malignant, and secondary malignant classes, respectively. A total of 12 (12 out of 115 cases) misclassifications were yielded by the SSVM-based hierarchical classifier, including three (three out of 115 cases) and nine (nine out of 85 cases) misclassification cases for individual classifiers in the hierarchical framework. It is worth mentioning that in both stages, all the cases of the secondary malignant class were classified correctly.

4 DISCUSSION AND CONCLUSION

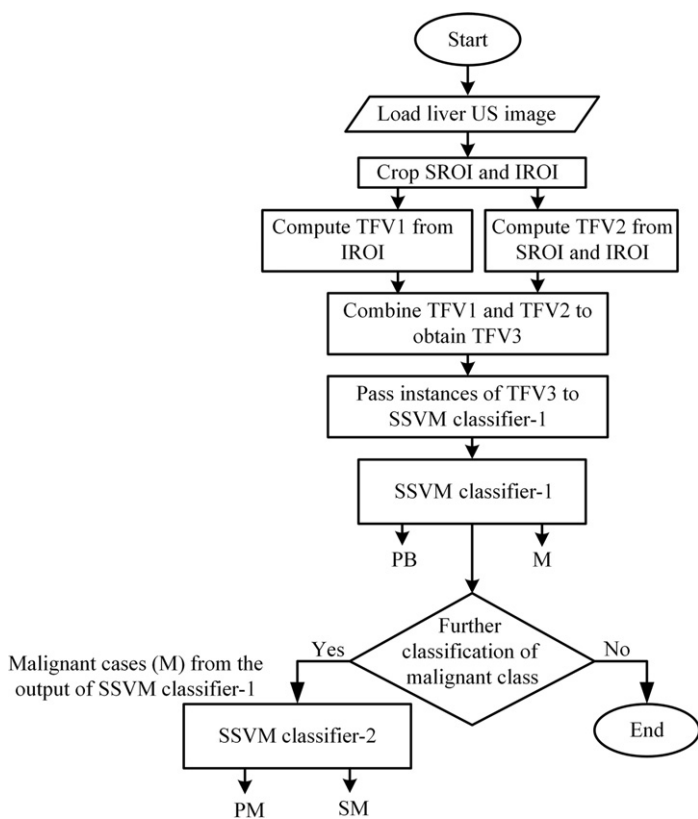
In the present study, an efficient SSVM-based hierarchical CAC system for classifying benign and malignant FHTs of gray scale liver US images was proposed. By visualizing the performance of SSVM-based hierarchical classifier design, it has been observed that:

Table 9 Misclassification Analysis of the Testing Dataset With Three-Class SSVM Classifier and SSVM-Based Hierarchical Classifier

	PB	PM	SM
<i>Misclassification analysis of SSVM based multiclass classifier</i>			
Total cases	30 Typical HEM: 5 Atypical HEM: 25	40 Small HCC: 9 Large HCC: 31	45 Typical MET: 5 Atypical MET: 40
ICA	ICA _{PB} = 83.3% ICA _{TypicalHEM} = 100% ICA _{AtypicalHEM} = 80.0%	ICA _{PM} = 72.5% ICA _{SHCC} = 77.8% ICA _{LHCC} = 70.9%	ICA _{SM} = 91.1% ICA _{TypicalMET} = 100% ICA _{AtypicalMET} = 90.0%
Correctly classified cases	25	29	41
Misclassified cases	5	11	4
Misclassified cases	5 out of 25 atypical HEM cases	2 out of 9 SHCC cases 9 out of 31 LHCC cases	4 out of 40 atypical MET cases
Description			
<i>Misclassification analysis of SSVM based hierarchical classifier</i>			
Total cases	30 Typical HEM: 5 Atypical HEM: 25	40 Small HCC: 9 Large HCC: 31	45 Typical MET: 5 Atypical MET: 40
ICA	ICA _{PB} = 90% ICA _{TypicalHEM} = 100% ICA _{AtypicalHEM} = 88.0%	ICA _{PM} = 77.5% ICA _{SHCC} = 77.8% ICA _{LHCC} = 77.4%	ICA _{SM} = 100% ICA _{TypicalMET} = 100% ICA _{AtypicalMET} = 100%
Correctly classified cases	27	31	45
Misclassified cases	3	9	0
Misclassified cases	3 out of 25 atypical HEM cases	2 out of 9 SHCC cases 7 out of 31 LHCC cases	–
Description			

ICA, individual class accuracy; ICA_{PB}, ICA of primary benign class; ICA_{TypicalHEM}, ICA of typical HEM class; ICA_{AtypicalHEM}, ICA of atypical HEM class; ICA_{PM}, ICA of primary malignant class; ICA_{SHCC}, ICA of small HCC class; ICA_{LHCC}, ICA of large HCC class; ICA_{SM}, ICA of secondary malignant class; ICA_{TypicalMET}, ICA of typical MET class; ICA_{AtypicalMET}, ICA of atypical MET class.

- (a) The TFV3, the texture feature vector formed by combining the ratio features (IROI features/SROI features), and the features computed from the IROIs obtain highest classification accuracy in all cases.
- (b) The typical cases of primary benign and secondary malignant class have been classified correctly with ICA 100%.

**FIG. 17**

Proposed design of a hierarchical CAC system for classifying benign and malignant FHTs.

- (c) The atypical cases of secondary malignant class have been correctly classified with ICA 100% while the atypical cases of primary benign class show better performance with an SSVM-based hierarchical classifier (with ICA 88%).
- (d) The performance of LHCC cases of primary malignant class improved with an SSVM-based hierarchical classifier (with ICA 77.4%) in comparison to an SSVM-based multiclass classifier (with ICA 70.9%).

From the obtained results, it can be concluded that the SSVM-based hierarchical CAC system design finds usefulness in clinical settings for assisting radiologists in differential diagnosis among benign and malignant FHTs.

The workflow of the proposed CAC system design is shown in Fig. 17.

REFERENCES

- [1] Harding J., Callaway M., “Ultrasound of focal liver lesions”, *Rad Magazine*, vol. 36, no. 424, pp. 33–34.
- [2] R.B. Jeffery, P.W. Ralls, *Sonography of Abdomen*, Raven, New York, 1995.
- [3] J. Virmani, V. Kumar, N. Kalra, N. Khandelwal, A rapid approach for prediction of liver cirrhosis based on first order statistics, *Proceedings of IEEE International Conference on Multimedia, Signal Processing and Communication Technologies, IMPACT-2011*, 2011, pp. 212–221.
- [4] J. Virmani, V. Kumar, N. Kalra, N. Khandelwal, in: Prediction of liver cirrhosis based on multi-resolution texture descriptors from B-mode ultrasound, *Int. J. Converg. Comput.* 1 (1) (2013) 19–37.
- [5] J. Virmani, V. Kumar, N. Kalra, N. Khandelwal, SVM-based characterization of liver cirrhosis by singular value decomposition of GLCM matrix, *Int. J. Artif. Intell. Softw. Comput.* 4 (1) (2013) 276–296.
- [6] J. Virmani, V. Kumar, N. Kalra, N. Khandelwal, Neural network ensemble based CAD system for focal liver lesions using B-mode ultrasound, *J. Digit. Imaging* 27 (4) (2014) 520–537.
- [7] Mitrea D., Nedevschi S., Lupșor M., Socaciu M., Badea R., “Exploring texture-based parameters for noninvasive detection of diffuse liver diseases and liver cancer from ultrasound images”, In: Proceedings of 8th WSEAS International Conference on Mathematical Methods and Computational Techniques in Electrical Engineering, pp. 259–265, 2006.
- [8] D. Mitrea, S. Nedevschi, M. Lupșor, M. Socaciu, R. Badea, in: Improving the textural model of the hepatocellular carcinoma using dimensionality reduction methods, *Proceedings of 2nd International Conference on Image and Signal Processing, CISP '09*, vol. 1, no. 5, 2009, pp. 17–19.
- [9] Mitrea D., Nedevschi S., Lupșor M., Socaciu M., Badea R., “Advanced classification methods for improving the automatic diagnosis of the hepatocellular carcinoma, based on ultrasound images”, In: Proceedings of 2010 IEEE International Conference on Automation Quality and Testing Robotics (AQTR), vol. 2, no. 1, pp. 1–6, 2010.
- [10] J. Virmani, V. Kumar, N. Kalra, N. Khandelwal, Characterization of primary and secondary malignant liver lesions from B-mode ultrasound, *J. Digit. Imaging* 26 (6) (2013) 1058–1070.
- [11] J. Bates, *Abdominal Ultrasound How Why and When*, second ed., Churchill Livingstone, Oxford, 2004, pp. 80–107.
- [12] J. Virmani, V. Kumar, N. Kalra, N. Khandelwal, A comparative study of computer-aided classification systems for focal hepatic lesions from B-mode ultrasound, *J. Med. Eng. Technol.* 37 (4) (2013) 292–306.
- [13] J. Virmani, V. Kumar, N. Kalra, N. Khandelwal, PCA-SVM based CAD system for focal liver lesions using B-mode ultrasound images, *Def. Sci. J.* 63 (5) (2013) 478–486.
- [14] H. Yoshida, D.D. Casalino, B. Keserci, A. Coskun, O. Ozturk, A. Savranlar, Wavelet packet based texture analysis for differentiation between benign and malignant liver tumors in ultrasound images, *Phys. Med. Biol.* 48 (2003) 3735–3753.
- [15] N. Manth, J. Virmani, V. Kumar, N. Kalra, N. Khandelwal, Application of texture features for classification of primary benign and primary malignant focal liver lesions, in: A. I. Awad, M. Hassaballah (Eds.), *Image Feature Detectors and Descriptors*, vol. 630, Springer International Publishing, Cham, 2016, pp. 385–409.

- [16] N. Manth, J. Virmani, V. Kumar, N. Kalra, N. Khandelwal, in: Despeckle filtering: performance evaluation for malignant focal hepatic lesions, Proceedings of 2nd IEEE International Conference on Computing for Sustainable Global Development (INDIACoM-2015), 2015, pp. 1897–1902.
- [17] J.H. Pen, P.A. Pelekmans, Y.M. Van Maercke, H.R. Degryse, A.M. De Schepper, Clinical significance of focal echogenic liver lesions, *Gastrointest. Radiol.* 11 (1) (1986) 61–66.
- [18] M. Colombo, G. Ronchi, *Focal Liver Lesions-Detection, Characterization, Ablation*, Springer, Berlin, 2005, pp. 167–177.
- [19] J.A. Soye, C.P. Mullan, S. Porter, H. Beattie, A.H. Barltrop, W.M. Nelson, The use of contrast-enhanced ultrasound in the characterization of focal liver lesions, *Ulster Med. J.* 76 (1) (2007) 22–25.
- [20] M. Di Martino, G. De Filippis, A. De Santis, D. Geiger, M. Del Monte, C.V. Lombardo, M. Rossi, S.G. Corradini, G. Mennini, C. Catalano, Hepatocellular carcinoma in cirrhotic patients: prospective comparison of US, CT and MR imaging, *Eur. Radiol.* 23 (4) (2013) 887–896.
- [21] Tiferes D.A., D’Ippolito G., “Liver neoplasms: imaging characterization”, *Radiol. Bras.*, vol. 41, no. 2, pp. 119–127.
- [22] Y. Kimura, R. Fukada, S. Katagiri, Y. Matsuda, Evaluation of hyperechoic liver tumors in MHTS, *J. Med. Syst.* 17 (3/4) (1993) 127–132.
- [23] S. Sujana, S. Swarnamani, S. Suresh, Application of artificial neural networks for the classification of liver lesions by image texture parameters, *Ultrasound Med. Biol.* 22 (9) (1996) 1177–1181.
- [24] S. Poonguzhal, B. Deepalakshmi, G. Ravindran, in: Optimal feature selection and automatic classification of abnormal masses in ultrasound liver images, Proceedings of IEEE International Conference on Signal Processing, Communications and Networking, ICSCN’07, 2007, pp. 503–506.
- [25] A.M. Badawi, A.S. Derbala, A.B.M. Youssef, Fuzzy logic algorithm for quantitative tissue characterization of diffuse liver diseases from ultrasound images, *Int. J. Med. Inform.* 55 (1999) 135–147.
- [26] K. Fukunaga, *Introduction to Statistical Pattern Recognition*, Academic, New York, 1990.
- [27] Y.M. Kadah, A.A. Farag, J.M. Zurada, A.M. Badawi, A.M. Youssef, Classification algorithms for quantitative tissue characterization of diffuse liver disease from ultrasound images, *IEEE Trans. Med. Imaging* 15 (4) (1996) 466–478.
- [28] C.J.C. Burges, A tutorial on support vector machines for pattern recognition, *Data Min. Knowl. Disc.* 2 (2) (1998) 1–43.
- [29] I. Guyon, J. Weston, S. Barnhill, V. Vapnik, Gene selection for cancer classification using support vector machines, *J. Mach. Learn.* 46 (1–3) (2002) 1–39.
- [30] S.S. Ahmed, N. Dey, A.S. Ashour, D. Sifaki-Pistolla, D. Bălas-Timăr, V.E. Balas, J.M. R. Tavares, Effect of fuzzy partitioning in crohn’s disease classification: a neuro-fuzzy-based approach, *Med. Biol. Eng. Comput.* 55 (1) (2017) 101–115.
- [31] K. Sharma, J. Virmani, A decision support system for classification of normal and medical renal disease using ultrasound images: a decision support system for medical renal diseases, *Int. J. Ambient Comput. Intell.* 8 (2) (2017) 52–69.
- [32] N. Dey, A.S. Ashour, A.S. Althoupety, Thermal imaging in medical science, in: *Recent Advances in Applied Thermal Imaging for Industrial Applications*, IGI Global, USA, 2017, pp. 87–117.

- [33] N. Dey, A.S. Ashour (Eds.), Classification and Clustering in Biomedical Signal Processing, IGI Global, USA, 2016.
- [34] M.Y. Khachane, Organ-based medical image classification using support vector machine, *Int. J. Synth. Emot.* 8 (1) (2017) 18–30.
- [35] S.W. Purnami, A. Embong, J.M. Zain, S.P. Rahayu, A new smooth support vector machine and its applications in diabetes disease diagnosis, *J. Comput. Sci.* 1 (2009) 1003–1008.
- [36] Y.J. Lee, O.L. Mangasarian, SSVM: A smooth support vector machine for classification, *Comput. Optim. Appl.* 20 (1) (2001) 5–22.
- [37] K.J. Virmani, S. Thakur, Application of statistical texture features for breast tissue density classification, in: A.I. Awad, M. Hassaballah (Eds.), *Image Feature Detectors and Descriptors*, vol. 630, Springer International Publishing, Cham, 2016, pp. 411–435.

FURTHER READING

- [38] O. Azzabi, C.B. Njima, H. Messaoud, New approach of diagnosis by timed automata, *Int. J. Ambient Comput. Intell.* 8 (3) (2017) 76–93.
- [39] A.M. AlShahrani, M.A. Al-Abadi, A.S. Al-Malki, A.S. Ashour, N. Dey, Automated system for crops recognition and classification, in: *Applied Video Processing in Surveillance and Monitoring Systems*, IGI Global, USA, 2017, pp. 54–69.

Ontology enhanced fuzzy clinical decision support system

7

Nora Shoaip*, Shaker El-Sappagh[†], Sherif Barakat*, Mohammed Elmogy[‡]

Information Systems Department, Faculty of Computers and Information, Mansoura University, Mansoura, Egypt Information Systems Department, Faculty of Computers and Informatics, Benha University, Benha, Egypt[†] Information Technology Department, Faculty of Computers and Information, Mansoura University, Mansoura, Egypt[‡]*

CHAPTER OUTLINE

1	Introduction	147
2	Problem Description	152
3	Related Work	153
4	The Combining of Ontology and Fuzzy Logic Frameworks	156
5	System Architecture and Research Methodology	160
5.1	Knowledge Acquisition	160
5.2	Semantic Modeling	163
5.3	The Fuzzy Modeling	164
5.4	Knowledge Reasoning	170
6	Conclusion	172
References	174	
Further Reading	177	

1 INTRODUCTION

Diabetes mellitus (DM) is an influential factor in increasing morbidity and mortality. As stated in 2014 by the International Diabetes Federation (IDF), 8.3% of the worldwide population suffers from diabetes. By 2030, this percentage is expected to be ~10% [1]. The undiscovered instances of DM reach up to 179 million [2]. According to the World Health Organization (WHO), 4.6 million deaths in 2011 were caused by diabetes, and it will occupy the seventh place among diseases causing death in 2030. According to the IDF, the financial burden of diabetes was \$612 billion in 2014. The American Diabetes Association (ADA) [3] classifies diabetes into T1DM (10% of diabetics) and T2DM (90% of diabetics). DM is asymptomatic, as the levels

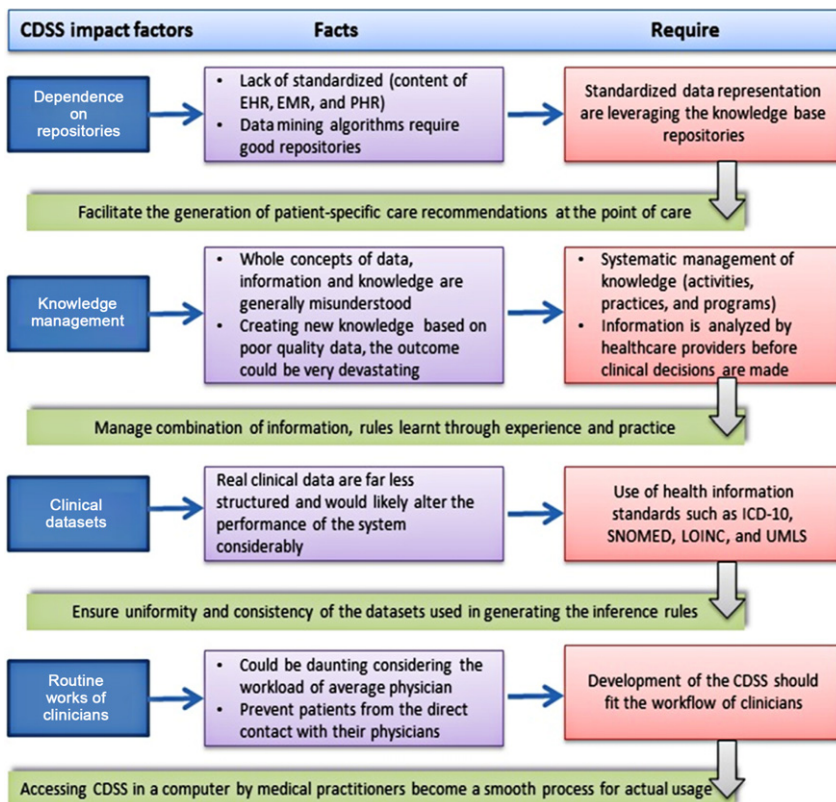
of glucose increase only gradually after some time. DM may lead to severe complications because it may remain undiscovered for a long time. An estimated 25% of T2DM cases in the United States remain undiagnosed [4]. Therefore, the early diagnosis of DM is critical. However, DM has a multifaceted nature that has complex associations with different illnesses and is joined with a wide assortment of treatments.

The morbidity and mortality cases of DM are unsatisfactory all over the world. It is additionally affected by the uncertainty of its features. The effectiveness of a disease therapy is mainly dependent on the timing and the accuracy level. The conventional DM diagnosis system is inadequate and requires new techniques. In Egypt, as a developing country, the system of manual examination of patients under the problem of population explosion is not an easy task; of course, there is an incompatibility between the number of patients and the number of medical experts. This leads to an increase in the percentage of errors in diagnosis because it includes a very large number of cases every day [5].

A diabetes diagnosis is a reasoning process. For diabetes, the diagnosis d is a function $d = f(t_1, t_2, \dots, t_n)$, for n features, and t_1, \dots, t_a are symptoms, t_{a+1}, \dots, t_b are physical examinations, t_{b+1}, \dots, t_c are lab tests, t_{c+1}, \dots, t_d are complications, t_{d+1}, \dots, t_e are drugs, and t_{e+1}, \dots, t_n are demographics, $a + b + c + d + e = n$. Fuzzy mathematics is the best method for the implementation of this function where attributes $t_i, n = 1 \dots n$ can be represented by fuzzy numbers [6]. As a result, the system can detect DM early and warn infected people in order to reduce the severity of this disease. This has led to the development and implementation of CDSS to gain success in the diabetes domain [7].

CDSS is software intended to help health professionals make a decision by providing knowledge at an appropriate manner and time [1,8,9]. More generally, CDSS can facilitate efficient and effective personalized decisions, reduce errors, and enhance the nature of medicinal services given to patients. There are many impact factors affecting CDSS, such as knowledge management and routine works of clinicians. Fig. 1 shows these impact factors, their facts, and required modifications. A DM diagnosis requires the complete history of the patient, which includes many features to be evaluated such as kidney-related features, liver-related features, urination analysis features, related diseases, medications, symptoms, lab tests, etc.

Physicians must enter the patient data, which interrupts the clinical workflow of physicians. So, the integration of a CDSS system is a good solution to this issue [1,10,11]. In 2015, Anderson et al. [4] studied the efficiency of a DM diagnosis CDSS based on the full EHR data (e.g., medications, diseases, lab tests, symptoms, etc.) and asserted the improvements of the resulting classification. CDSS can get patient's features from a distributed environment automatically and identify the disease's risk level [7]. Moreover, the diabetes diagnostic task is complex. Due to the difficult nature of medical diagnosis, it often has uncertainty, vagueness, and inconsistencies as well as other difficulties in the determination of accurate measurement standards because of the natural diversity of expert opinion in the disease diagnosis.

**FIG. 1**

The CDSS impact factors.

Surprisingly, few studies appropriately discussed diabetes diagnosis CDSS implementation [12]. This fact magnified the significance of our study.

Patient data are often distributed over EHR systems, and they use different formats with different levels of granularities (i.e., different semantics) [9]. The automation of data collection to generate the patient profile requires standardization of the terminology to overcome the problems of interoperability [10], and enhance semantic interpretability of the resulting system. Several studies have been published to allow CDSS to collect the data of each patient from EHR [13]. In the diabetes domain, two main types of data are found: numerical data and textual or unstructured data. Concerning numerical features such as lab tests, they are always vague and imprecise so that they can be treated directly as linguistic variables using fuzzy logic [11]. Fuzzy CDSS uses fuzzy logic in representing knowledge and the reasoning process. It could support: (1) the reduction of human errors, (2) the transformation of vague knowledge related to experts to linguistic rules, (3) the processing of

uncertain diagnostic symptoms, and (4) the ease of communication between doctors and patients [7].

On the other hand, for other textual features such as diseases, symptoms, and a patient's current medications, if we treat these as regular categorical features, their semantics will be lost. Let us give an example. Hypertension is a disease related to diabetes, and it is an effective and influential factor in its diagnosis. Hypertension is stored in EHR with various names and has numerous different related diseases. According to SNOMED CT (SCT), hypertension is associated with 178 other diseases.

Another example, in 2016, the Canadian Diabetes Association (CDA) guidelines asserted that diabetes diagnosis rules must check the existence of cardiovascular disease. However, according to an SCT 2016 release, there are more than 6320 medical concepts and diseases related to this concept. CDSS gets patient's attributes from EHR. Then, it finds the semantic relationships between retrieved concepts and the modeled concepts modeled in the CDSS knowledge base to imitative the doctor's reasoning.

Chen et al. [14] proposed an antidiabetes drug recommendation established by fuzzy logic and ontology. They tested the conditions of hypoglycemia, liver, kidneys, and the heart to make a condition. However, there are no semantics in their tests. For example, they tested whether the heart, liver, and kidneys are normal or abnormal. Tsipouras et al. [15] proposed a fuzzy CDSS for coronary artery disease (CAD) diagnosis, and their dataset has features for the patient's history of diabetes mellitus, hypertension, and hyperlipidemia. However, the authors treated this data as binary (true/false) without any semantics. All these diseases have hierarchies of related diseases. For example, hyperlipidemia has a subtree of 56 subdiseases in SCT. The resulting system will not be smart enough to detect that hyperalphalipoproteinemia must be treated as hyperlipidemia. Debabrata et al. [16] proposed a fuzzy CDSS for CAD and checked whether the patient has specific diseases such as hypertension. However, they check for a disease by checking some of its medical tests. For example, to determine if the patient has diabetes, they tested the fasting blood sugar. This solution is not practical from many points. First, some tests are very large. Second, no semantic reasoning can be achieved. The same issue appeared in [17], which checked the existence of specific diseases and symptoms by yes/no flags. Collecting all these concepts in an ontology and using this ontology to determine the level of similarity improved the semantic accuracy [18–20].

The automation and integration with EHR of the resulting system will be totally affected. The best solution to handle this challenge is by binging fuzzy CDSS with standard ontologies based on standard terminologies such as SCT. Ontology can enhance CDSS by preserving semantic relationships between its concepts. This idea has been used by several CPG languages such as EON, GLIF, Asbru, and GEM to solve the Arden syntax language problems such as curly braces [10]. Using existing standard medical ontologies can enhance the interoperability between the EHR environment and CDSS such as RxNorm, GO, and SCT. However, diabetes diagnosis problems have no studies in this regard.

Current diabetes diagnosis must deal with two principal issues. First, variables have associated vagueness, so using a linguistic label to refer to their values instead of a numerical value is much more natural. Second, some patient data, including related complications, do not have an explicit representation of their semantics. For the first problem, fuzzy set theory proves successful in handling vague knowledge [21] by providing nonlinear mapping between inputs and outputs. For the second problem, ontology has been used to implement diabetes CDSS systems [14]. However, without appropriate handling of these challenges in a single solution, the CDSSs cannot effectively assist the clinical practice. To the very best of our knowledge, there has not been any effort in this direction. Based on the achieved results of the roles of ontology and fuzzy logic in CDSS implementation, it seems to be effective and up to date to combine ontology and fuzzy logic in a hybrid CDSS system. Our goal is to show how ontology can enhance the semantic reasoning and accuracy of fuzzy medical rule-based systems. We have represented DM knowledge regarding nonnumerical features in the form of ontology, which allows adding semantics to it and makes the knowledge base maintenance easier as well as reuses components among different systems. The paper utilizes Mamdani, knowledge, and experts in diabetes management. The Mamdani approach is widely used in fuzzy expert system models [22]. Mamdani can detect human knowledge from real-world more effectively than TSK (Takagi-Sugeno-Kang) [23].

In view of this, the lack of an applicable and efficient knowledge base system for estimating the diabetic risk factors requires the implementation of an intelligent CDSS system. In our study, a hybrid system for helping physicians in diabetes diagnosis is presented, and it has the following main contributions.

- It proposes a semantically intelligent hierarchical fuzzy expert system for diabetes diagnosis. It focuses on a Mamdani-based, fuzzy rule-based AI approach and enhances its intelligence by hybridizing it with ontology semantics and reasoning.
- It collects all the information usually analyzed by experts and CPGs, groups this information, fuzzifies it according to suitable membership functions, and builds a complete linguistic rule base based on the knowledge integration from an expert and CPG with knowledge gained from training data.
- Two main techniques are utilized, including the building of a hierarchical fuzzy system and the use of a hybrid method for a sophisticated derivation of fuzzy linguistic rules.
- Textual features in fuzzy rules including patient complications, symptoms, and medications are treated as semantic concepts of the ontology. The used ontology is diabetes diagnosis ontology (DDO). It is an OWL2 ontology, which is available in BioPortal. It is based on the most recent version of Basic Formal Ontology (BFO 2) [24], and it contains 6444 concepts related to diabetes.
- The paper emphasizes the possibility of building a transparent CDSS. It concentrates on the possibility of collecting patient medical data from distributed EHR systems in an automated way. The patient's medical concepts are compared

with the ontology concepts using a proposed semantic similarity algorithm; then, this level of similarity is used in evaluating fuzzy rules. This step enhances the level of automation and interoperability of CDSS. Moreover, the resulting rules will have a dynamic nature where the number of diseases, medications, and drugs is not explicitly defined.

- The study implements and tests the proposed framework using real cases.

This paper is formed as follows. The problem description will be defined in [Section 2](#). [Section 3](#) presents the related works. [Section 4](#) shows the combining ontology and fuzzy logic frameworks. In [Section 5](#), we discuss the proposed framework and highlight its modules. At last, our conclusion and future works will be found in [Section 6](#).

2 PROBLEM DESCRIPTION

Diabetes diagnosis identifies the risk level of a patient to be diabetic or prediabetic [\[25\]](#). Early diagnosis is critical for normal and prediabetes patients to prevent them from developing diabetes by changing their lifestyle (e.g., diet, physical practices, etc.), and for people with diabetes to avoid complications of diabetes by medication. Diabetes remains a health trouble regardless of the availability of several medicines and research studies [\[1\]](#). The first and most effective step in diagnosis is to identify the patient's symptoms [\[2,7,26\]](#). Bickley and Szilagyi [\[26\]](#) confirmed the right steps for diagnosis. Physicians began collecting the signs of a disease such as symptoms, medical history, family history, and complications, then collected laboratory tests. Concerning diabetes, there are some lab tests such as HbA1c, OGTT, or FPG that are appropriate for direct screening of prediabetes or diabetes.

However, diabetes may not be discovered for years [\[2\]](#). Heydari et al. [\[27\]](#) asserted that diabetics are undiagnosed for at least 4–7 years. As much as 30% of the total diabetic population has unrecognized diabetes. This delay causes complications and complicates the care process [\[3\]](#). It has been estimated that nearly a third of all deaths from diabetic ketoacidosis occur in individuals with no known history of diabetes. In 2015, ADA asserted that in the United States, one-quarter of those with diabetes are undiagnosed; therefore, when they are diagnosed, they have complications [\[3\]](#). As a result, there are other factors affecting diabetes diagnoses, which can detect diabetes even if the lab tests are in abnormal or normal ranges [\[28\]](#).

Many studies investigated the contributing factors for DM diagnosis, such as [\[4\]](#) (1) the current patient diseases related to diabetes, macrovascular diseases, and others. (2) Drug-, hormone-, or chemical-induced diabetes: these medications could affect glucose levels (e.g., glucocorticoids, chemotherapy agents, antipsychotics, mood stabilizers, etc.), destroy pancreatic β -cells such as pentamidine, or impair insulin action [\[29\]](#), affect insulin secretion (e.g., calcineurin inhibitors, steroid agents, etc.), and cause weight gain (e.g., antidepressants and antipsychotics). (3)

Environmental factors, for example, gender, age, smoker, and race, etc., and (4) Symptoms, for example, polydipsia, polyphagia, vision, polyuria, etc. [25].

For example, the ADA [3] confirmed that a type 2 diabetes (T2DM) diagnosis requires the signs related to insulin resistance. Anderson et al. [4] asserted the combination of complications, medications, and symptoms in addition to lab tests to diagnose diabetes. This combination enhances the automation and accuracy of CDSS results and supports the creation of treatment and medication plans [4]. They used 298 features from EHR data. There are many lab tests required from patients, but these tests are not suitable with some complications. For example, HbA1c is not appropriate for medical examination for patients with anemia, hemoglobinopathies, EPO therapy, and severe hyperlipidemia [3,29]. Luzi et al. [30] asserted that the HbA1c diagnosis limits must be decreased in patients with CVD. Diabetes and many other diseases have similar symptoms such as obesity, which is considered a common risk factor for cardiovascular disease (CVD) and T2DM.

Moreover, there are roughly 100 complications related to diabetes. They can be used in addition to physical activity, diet programs, and education to introduce a plan for diabetes. Liu et al. [31] defined the complications (roughly the top 10 complications) related to diabetes. Heydari et al. [27] studied 200 newly diagnosed diabetics and asserted the existence of retinopathy, neuropathy, nephropathy, hypertension, and hyperlipidemia at the time of diagnosis. In addition, medications may prompt hyperglycemia through an assortment of systems, incorporating changes in insulin discharge and affectability and coordinating cytotoxic impacts on pancreatic cells. These medications incorporate atorvastatin, statins, rosuvastatin, antibiotics, and simvastatin [32]. On the other hand, the most popular drug for cardiovascular use is statins. As a result, a diabetes diagnosis is affected not only by a set of lab tests but also with the patient's current complications, symptoms, and drugs being taken. For example, Ramezankhani et al. [33] built a decision tree for diabetes diagnosis with 60 features. To be helpful and to consider all these features, diabetes diagnosis systems must be integrated with the hospital's EHR systems to automatically collect all possible data related to diabetes.

3 RELATED WORK

This section discusses the current studies on our problem and points to the limitations that motivated this research. DM diagnosis has been studied with different techniques [1,2]. One of the most popular diagnosis tools is by using the risk score calculators. However, these calculators used a small number of factors and were not gathered in a semantic way. So, they are not efficient for diabetes diagnosis. To provide a clinically meaningful output, the different modeling approaches are acquired from heterogeneous sources [2]. But, the full integration of CDSS is not achieved yet [9]. Zarkogianni et al. [2] produced a survey on the latest studies and developments in the diabetes field.

There are many methodologies and advances have been proposed since 1960, but diabetes still needs more and more. Shankaracharya et al. [18] identified the most critical list of features needed to diagnose diabetes. Subsets of this list have been used as input spaces for various techniques (e.g., support vector machine, artificial neural network) and other nonknowledge-based machine-learning algorithms. Many researchers have tried to assist in diagnosing diabetes by building several models using these algorithms. However, these techniques only generate an unrealistic oversimplification of reality. Moreover, these algorithms work in a black box way with very sophisticated computations, which is hard for physicians to understand. As a result, they cannot justify their results, and physicians cannot trust them [34]. In addition, there is a big correlation between the complex clinical database and high costs because they need a long learning time and are complex.

The other choice is knowledge-based (KB) [35] systems, which are AI programs with the knowledge base and inference engines such as rule-based techniques and case-based techniques. Rule-based systems are best suited for problem solving when the system being analyzed is a single purpose and the rules for solving the problems are clear and do not change with high frequency. Case-based systems are common and extremely important in human cognition; solving new problems depends on the other cases stored in a library and the ability to learn new cases [19]. These systems have been widely used for diabetes detection [1,7,9]. Ahmed et al. [35] surveyed the artificial intelligence techniques for building KB systems including rule-based and case-based reasoning. In early 1970, MYCIN was proposed as a first rule-based system for antimicrobial infections. Karegowda et al. [36] developed a diabetes rule-based classification model. It integrated the k-means and decision tree (DT). These systems deal with crisp data only, but the medical diagnosis is more complex because of a web of information uncertainty, vagueness, and incompleteness [11].

Sherimon and Krishnan [1] identified the main reasons of inapplicability for knowledge-based CDSS. In the medical world, nothing is black and white. Expert knowledge is often represented with vague terms, and patients often describe their states using imprecise concepts [11]. CDSS knowledge must be represented in a suitable format [13]. Fuzzy logic has a mathematical model to treat uncertainty in disease diagnosis and supports the verbal representation of medical concepts [14,37]. Fuzzy systems provide transparent and interpretable models with enhanced semantics that are easy to understand and trust by experts. Fuzzy logic is easily related to the way of expert thinking and can handle the imprecision of symptoms and uncertainty of diagnoses [7,9,35]. In addition, fuzzy classifications are less vulnerable to noise data. In recent years, there has been a great expansion in medical applications based on fuzzy sets. Lai et al. [38] detected hypoglycemia by using the fuzzy system. D'Acierno et al. [7] tried to detect breast cancer by developing a fuzzy system. Seki and Mizumoto [39] proposed a new way to deal with fuzzy systems called single input rule modules, and used this for diabetes diagnosis.

On the other hand, some parts of knowledge are often represented using medical concepts, and the semantic relationships among these concepts must be detected by the inference system to be more intelligent [1,18,19,22]. As a result, ontology can be

used to build the system semantics and rules can be built by a semantic rule language such as SWRL [22]. The ontology querying is achieved by some languages such as SQWRL, SPARQL, etc. Ontology is based on a formal description logic (DL), and it has the capability of (i) modeling the concepts and their relationships in a domain, and (ii) reasoning and checking consistency. There are many ontology representation languages (e.g., RDF(s), OWL1, and OWL2), which are based on many DLs (e.g., $\mathcal{SHIF}(\mathcal{D})$, $\mathcal{SHOIN}(\mathcal{D})$, and $\mathcal{SROIQ}(\mathcal{D})$) and many reasoners (e.g., Pellet, HermiT, Fact++, etc.). Ontology is used in many medical types of research, such as diabetes [1]. Sherimon and Krishnan [1] proposed OntoDiabetic. This is an ontology-based CDSS for diabetes. They introduced a set of ontologies and implemented the NICE CPG's rules.

Classical ontology cannot handle vague knowledge. Fuzzy ontologies can be used to overcome the fuzzy nature of medical knowledge. The fuzzy ontology combines fuzzy logic with ontology reasoning. Fuzzy ontology has been used in many studies. Lee and Wang [12] have proposed a fuzzy ontology expert system based on five layers called fuzzy diabetes ontology (FDO). It is entirely concerned with the creation of the fuzzy ontology, and fuzzy reasoning was very abstract; moreover, the used dataset was of the Pima Indian dataset, which is not diabetes descriptive.

The integration of crisp ontology and fuzzy logic has multiple paths. First, some methodologies concentrate on implementing particular OWL ontologies [40]. However, it is still not enough to model a real application, and the fuzzy OWL under development won't turn into a W3C proposed standard soon [41]. Second, crisp ontologies are extended with some fuzzy rule representation languages such as f-SWRL [24] and using FuzzyJess APIs to reason over it. Again, there are no suitable reasoners for this extension because FuzzyJess has no plugin in protégé and the capabilities of fuzzy logic reasoning are limited. Third, Bobillo and Straccia [42] have proposed FuzzyOWL2Ontology. The authors started to base the fuzzy ontology on formal fuzzy DL.

There are many existing fuzzy DLs, for example, fuzzy SHOIN (D) and fuzzy SROIQ (D). Moreover, fuzzy ontology reasoners such as Fire and fuzzyDL have been implemented. Ontology can be written in a regular crisp ontology editor because the fuzzification elements are added as annotations. Specific parsers are used to translate FuzzyOWL2Ontology into a language that can be used by a fuzzy DL reasoner. However, all existing fuzzy DLs have decidability limitations, as recently stated by Borgwardt et al. [41], and existing fuzzy ontology tools, parsers, and reasoners have not reached a mature state yet [42]. Those works such as Delorean are translating fuzzy ontologies into its crisp DLs, and use DL reasoners such as Pellet.

The previous limitations could explain the reduced use of knowledge-based CDSS in daily practice [9]. One possible solution to these limitations is to integrate the reasoning capabilities of the fuzzy rule-based systems and crisp medical ontology. The resulting system could exhibit highly sophisticated reasoning capabilities, and thus, advance more efficient care performance. Chen and Huang [43] used fuzzy and ontology reasoning to automatically generate the weather news by using two features calculated from ontology and a third statistical one.

In the proposed approach, some features of the inference system's rules are modeled as ontology concepts and linked to medical ontologies. The other features are modeled as fuzzy linguistic variables. There are many advantages to this approach. First, it enhances the semantics of the resulting system. For example, if the rule contains the condition <current complication = Hypertension>, then we need to test whether the patient has hypertension or any of its subdiseases by referring to the mentioned ontology. The semantic will be handled for symptoms and drugs as well. Second, the resulting system supports the integration and interoperability with the EHR system because ontology can detect the relationship between collected terms. Third, the system models the domain's vague knowledge using the mature FES methodology. La-Ongsri and Roddick [44] tried to use this approach in data modeling by designing some fields as ontology concepts while the other fields are of regular type. Torshizi et al. [22] tried to combine ontology and fuzzy rule-based reasoning to diagnose and treat benign prostatic hyperplasia. However, the proposed system has independent modules for these techniques. Sherimon and Krishnan [1] checked for some complications when diagnosing diabetes, but the ontology was crisp and the checked difficulties had no semantics. Chen et al. [14] used ontology and fuzzy logic in antidiabetic drug recommendations. However, ontology is used as a second and separate layer in reasoning; it has not enhanced the inference of the fuzzy component.

An OBFDSS hybrid model has been developed to support physicians in diabetes diagnosis problems. This work combines fuzzy logic and ontology with the aim of having the representing semantic capabilities and reasoning with vagueness capabilities. Such a CDSS encodes the medical knowledge of the diabetes experts' background or common reasoning knowledge regarding ontology. The ontology concepts, relationships, properties, and axioms are based on the most recent diabetes CPGs, literature studies, and domain expert experience. Ontology is used to represent the semantic structure as well as calculate the clinical similarity between the compared diseases, medications, and symptoms related to diabetes. Then, the level of similarity is passed to a fuzzy inference engine. The contribution of our work is the development of a semantically intelligent fuzzy expert system. We will enhance the inference capabilities of the regular fuzzy system with the OWL2 ontology reasoning capabilities.

4 THE COMBINING OF ONTOLOGY AND FUZZY LOGIC FRAMEWORKS

As mentioned, fuzzy ontology [45] can represent and reason over imprecise or vague information in an effective way. Some real-world applications, especially in the medical domain, require more effective representation and reasoning. Fuzzy ontology is heavily limited to its domains or its purposes. It is required for unique identifiers and the conceptual structure representing each concept in a terminology system to allow an unambiguous interpretation of the concept meaning across

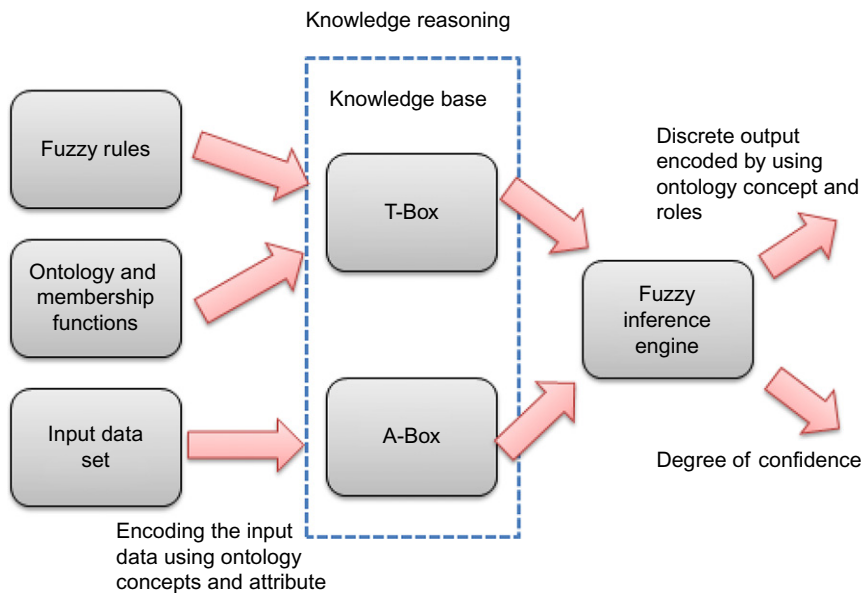
systems. In addition, there are limitations of existing fuzzy description logic reasoners such as FuzzyDL, Fire, and DeLorean, and other limitations of existing underlying fuzzy description logics such as fuzzy ALC and fuzzy SHOIN (D). The fuzzy ontology [46,47] construction process and tools are unclear and not unified methods. For rule-based systems, the rule extraction from experts is intensive, and many rules are inherently dependent on other rules. The addition of new knowledge to the system is a complex task. So rule-based systems are very time consuming to build and maintain. This leads to the propose hybrid systems that can:

- Overcome these limitations and have the approximate human reasoning capabilities of concluding from existing vague data.
- Enhance the semantics of the resulting system. For example, if the rule contains the condition <current complication = Hypertension>, then we need to test whether the patient has hypertension or any of its subdiseases by referring to the mention ontology. The semantic will be handled for symptoms and drugs as well.

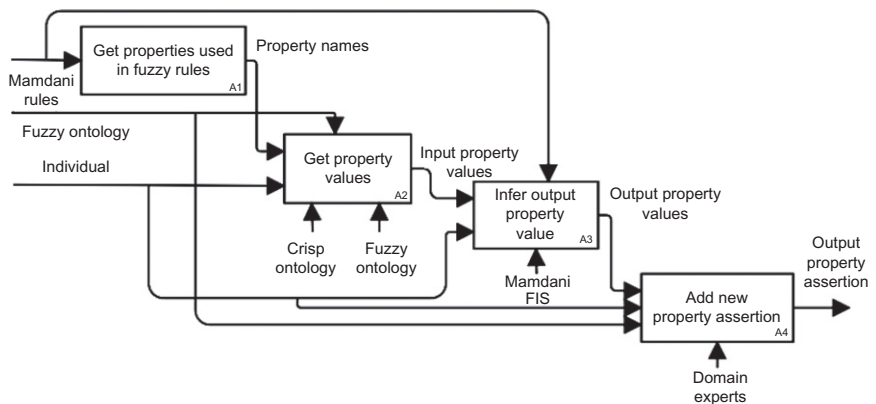
There are a few proposal frameworks that tried to support the idea of combining ontology and fuzzy logic formalisms. For example, Esposito and Pietro [48] proposed an OBFDSS. They applied medical knowledge regarding ontology and fuzzy rules to a zero-order Sugeno-type fuzzy inference engine to classify a cerebral white matter lesion (WML). Ontology is responsible for representing the expert's knowledge and providing simple and intuitive DSS results. Fuzzy logic is responsible for handling fuzziness knowledge and performing the decision-making process. The evaluation of this system showed that this DSS offered a good way to classify WML in real clinical settings. The block diagram architecture of knowledge reasoning is shown in Fig. 2.

Yagquinuma et al. [49] tried to provide meaningful inferences, called an HyFOM reasoner, that is able to combine Mamdani inference and fuzzy ontology. They provided the outputs of Mamdani FIS to the fuzzy ontology reasoning tasks. Based on fuzzy rules, Mamdani inference can be utilized to deduce crisp output. To further clarify, if the application needs knowledge related with a numerical property, first get the required inputs from the fuzzy ontology, then use Mamdani inference to have a numerical property output, and finally, the output comes back to the ontology to be added with other fuzzy ontology reasoning tasks. The architecture of knowledge reasoning is shown in Fig. 3. As shown in the HyFOM architecture, it uses three different reasoners. The first one is a crisp ontology that is responsible for performing reasoning and query answering concerned with crisp definitions. The second one is fuzzy ontology to perform reasoning tasks that contain a fuzzy concept. The third one is Mamdani that utilizes fuzzy rules and fuzzy operations to infer the crisp output value.

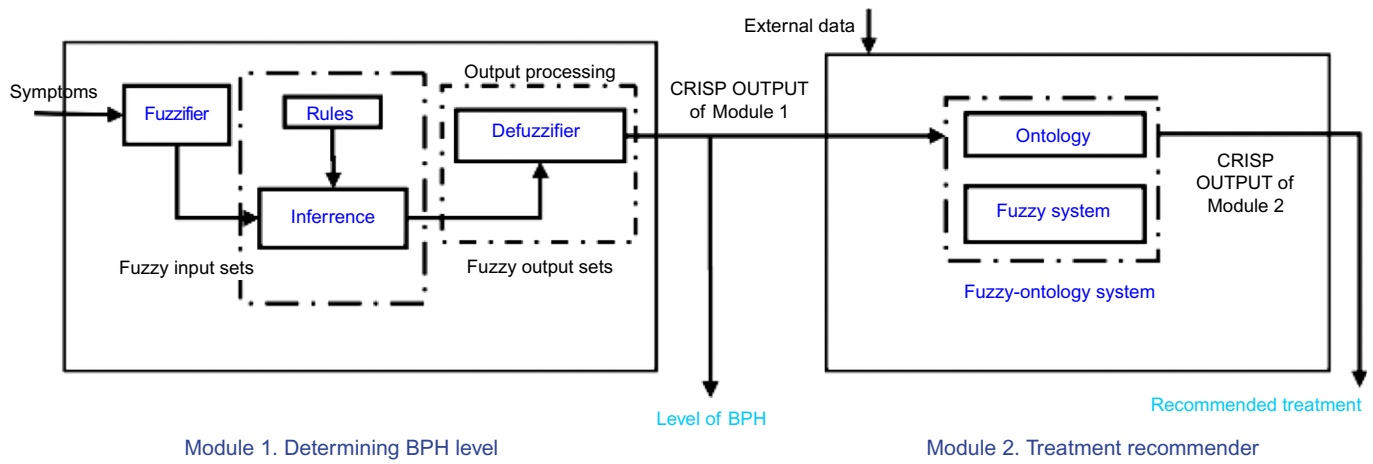
Torshizi et al. [50] represented a hybrid fuzzy intelligent system that combines Mamdani inference and ontologies in two modules. It is used for diagnosis of benign prostatic hyperplasia (BPH). The first module used Mamdani inference to define the BPH riskiness level and the second module used ontologies to represent the expert's

**FIG. 2**

The knowledge reasoning block diagram [48].

**FIG. 3**

The HyFOM reasoner architecture [49].

**FIG. 4**

The hybrid fuzzy intelligent system architecture [50].

knowledge and provide simple and intuitive outcomes. The architecture of this molding is shown in Fig. 4.

Focusing on the integration of the fuzzy rule and fuzzy ontology reasoning, some important limitations must be addressed. A hybrid inference engine architecture, including an ontology reasoner, performs reasoning using the ontology assertions and definitions. Fuzzy rule reasoning is used to infer the result value using fuzzy rules and fuzzy operations. So, ontology has been used as a second or separate layer in reasoning. It has not enhanced the inference of the fuzzy component.

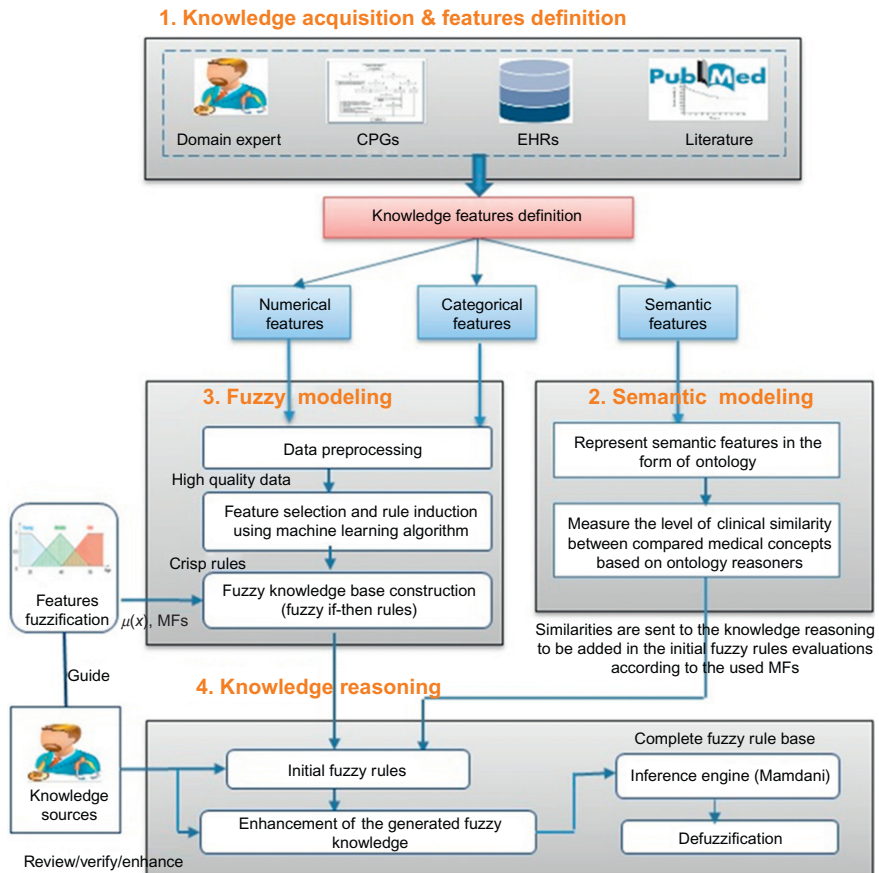
5 SYSTEM ARCHITECTURE AND RESEARCH METHODOLOGY

We propose this semantically intelligent fuzzy CDSS system. It is a powerful tool in the diagnosis of diabetes. It involves building a complete linguistic fuzzy rule base based on the integration of expert and CPG with other knowledge extracted from training data and knowledge extracted from a semantic model. This step enhances the level of automation and interoperability of CDSS. Essentially, our model is described in four stages: knowledge acquisition and features definition, semantic modeling, fuzzy modeling, and knowledge reasoning. Fig. 5 shows the proposed system structure. Each of these individual blocks has many phases, and they will be explained. The proposed relies on the construction of a semantically intelligent fuzzy CDSS system responsible for:

- (i) Collecting all the knowledge usually analyzed by experts, CPGs, distributed EHR, and literature.
- (ii) Having the ability to represent semantic features in the form of ontology and to measure the clinical similarity between medical concepts. These similarities are then sent to the reasoning module to be added in the final fuzzy rules evaluations, according to the used MFs.
- (iii) Generating fuzzy knowledge using machine learning algorithms from the processing of medical data, and enhancing this knowledge by a domain expert and CPG knowledge.
- (iv) Building a complete linguistic fuzzy rule base based on the integration of knowledge extracted from experts and CPGs with knowledge extracted from training data and other knowledge extracted from semantic models. This step enhances the level of automation and interoperability of CDSS.
- (v) Making inferences according to the Mamdani inference process.
- (vi) Drawing conclusions for supporting the clinicians' in their everyday practice.

5.1 KNOWLEDGE ACQUISITION

Knowledge acquisition (KA) is a step to efficiently acquire the knowledge for diabetes diagnosis. This study collects diabetes knowledge from medical experts, recent literature, EHR databases, and recent CPGs. The knowledge engineers have had

**FIG. 5**

The proposed system blocks diagram structure.

several meetings with the medical experts from Mansura University Hospitals, Mansura, Egypt. Diabetes diagnosis literature [1,14,33,35,36,51,52], CPGs [25], and databases [19] are analyzed as well. A dataset is gathered from a symptomatic biochemical lab (AutoLab, Mansura, Egypt) from 2010 to 2013. There are 67 eligible patients. The data set is distributed as 13.7% normal patients, 53% diabetic patients, and 33.3% prediabetic patients.

These knowledge sources participate in determining the risk factors, fuzzification, diagnosis CPGs, decision criteria, and validation steps. All the risk factor categories and their associated metrics that are needed to diagnose diabetes are identified in Table 1. The system inputs have three main categories: numerical, categorical, and semantic. The numerical category is the set of features that will be modeled as fuzzy linguistic variables. These features are a set of lab tests. The second

Table 1 List of System Variables (Diabetes Risk Factors)

Category	Subcategory (#)	Features
Numerical category	Sugar level tests (4) Kidney function test (5) Hematological profile (13) Lipid profile (4) Tumor marker (3) Urine analysis (9) Liver function test (8)	2hPG, FPG, HbA1C, OGTT Serum potassium, serum uric acid, serum urea, etc. Prothrombin, eosinophils, white cell count, platelet count, MCHC, hematocrit, Hbg, red cell count HDL cholesterol, LDL cholesterol, total cholesterol, triglycerides Ferritin, carcinoma antigen (CA)-125, alpha-fetoprotein (AFP) serum Glucose, bilirubin, pus, blood, RBcs, crystals protein SGOT(AST), alkaline phosphatase, SGPT (ALT), direct bilirubin, total bilirubin, albumin, total protein
Categorical	Demographics (4) Physical examination (24)	Gender, residence, race, education, ethnicity Age, family history of diabetes, smoking, BMI, physical activity, alcohol drinking, blood pressure, waist circumference, etc.
Semantic (ontology-based)	Symptoms (153) Complications (~3000) Drugs (~1000)	Fatigue, vision, urination frequency (polyuria), thirst (polydipsia), hunger (polyphagia), etc. Acute disease as bacterial infection diseases, coma, digestive system diseases, metabolic diseases, etc. and chronic diseases as nonvascular diseases (nervous system diseases, skin disease, etc.) and vascular diseases (nephropathy, neuropathy, retinopathy, etc.) Antiinfective, antiallergenic, CNS drug, immunotherapeutic, retinoid, analgesic, anesthetic, etc.

category is the categorical features, including patient demographic and physical examination features. There are 24 physical examinations related to a diabetes diagnosis. The third category is the semantic features, which contain the patient's current complications, drugs taken, and symptoms.

5.2 SEMANTIC MODELING

DDO [20] is a standard ontology based on BFO ontology and OGMS as two popular top-level ontologies. It is implemented using the protégé tool, and its consistency and coverage are checked. Also, it is based on the SNOMED CT standard terminology. DDO has more than 3000 diseases related to diabetes organized into two main hierarchies (i.e., Acute and Chronic), 153 symptoms, 24 physical examinations, and more than 1000 drugs related to diabetes by either affecting the insulin level, pancreas function, sugar level, or others. In this version of the project, we will not treat symptoms as semantic DDO concepts because the available dataset does not support this processing. Moreover, to facilitate the implementation of the proposed model, we only concentrate on the lab tests and physical examinations that appear in the used dataset. For the semantic testing of the study, the *diseases* and *drugs* concepts in DDO are utilized.

Semantic modeling is related to the ability to represent semantic features in the form of ontology and to measure the clinical similarity among medical concepts.

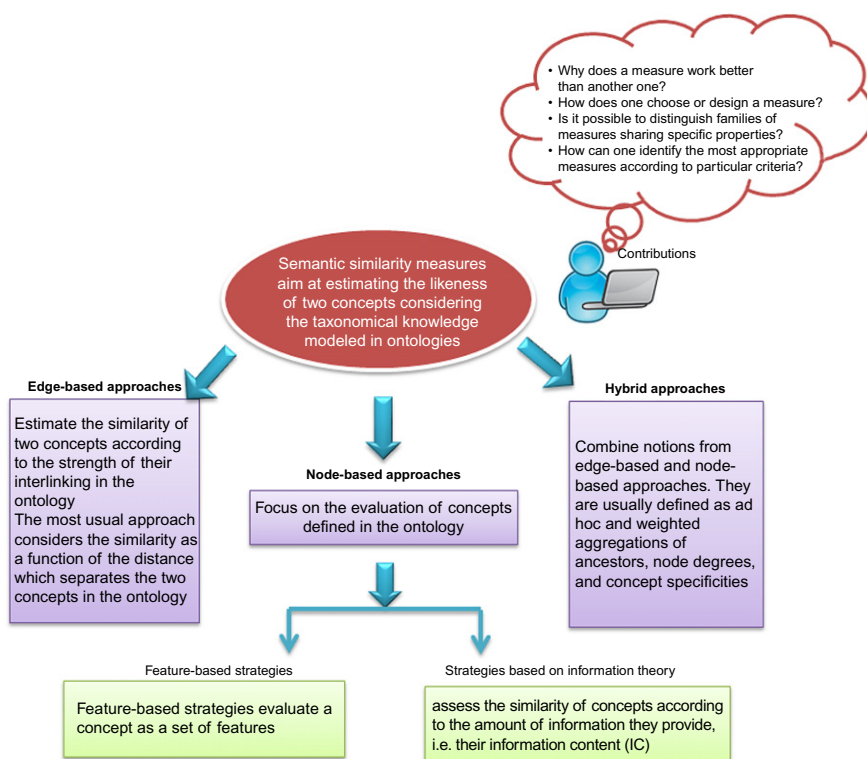
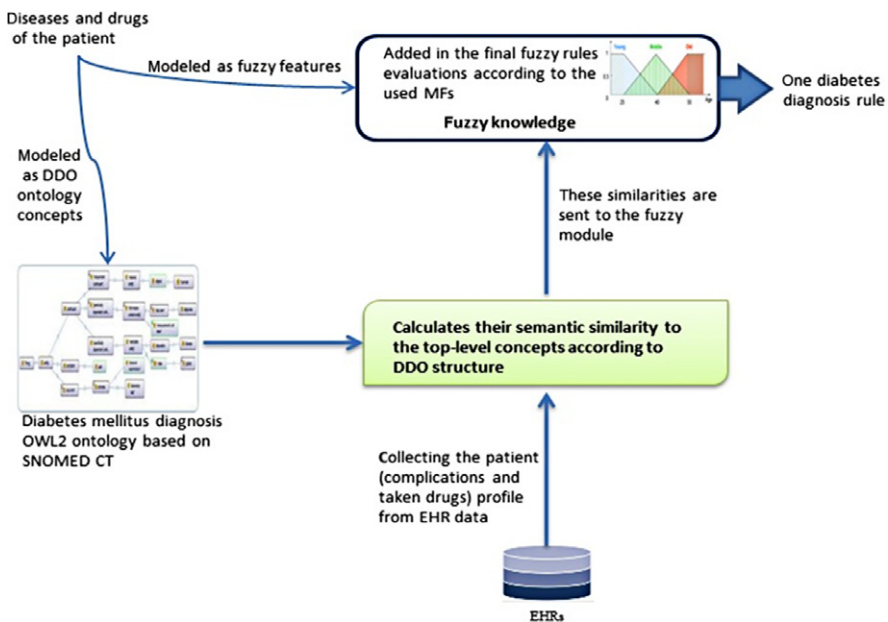


FIG. 6

The semantic similarity description diagram.

**FIG. 7**

The semantic block diagram.

Fig. 6 shows the major definition of semantic similarity. For the first requirement, we propose OWL2 ontology based on the SNOMED CT standard medical terminology for diabetes. The ontology is freely available in the BioPortal at <http://bioportal.bioontology.org/ontologies/DDO>. DDO organizes the diabetes diagnosis with all needed knowledge and risk factors. It has 6444 concepts, 48 properties, and 6356 annotations. We concentrate on the diabetes-related complications, symptoms, drugs, and chemical substances. Semantic similarity between the patient's complications, drugs, and symptoms and the fuzzy knowledge base concepts are calculated based on DDO ontology using an ontology reasoner such as Pellet or Fact++. **Fig. 7** shows the major steps of the semantic similarity block diagram.

5.3 THE FUZZY MODELING

This step produces the fuzzy aspects of the proposed system. Several issues must be considered to generate the fuzzy model, including the definition of the fuzzy features and the associated fuzzy terms, fuzzy rules, and the utilized fuzzy inference engine. The fuzzy model could be defined by three types of knowledge including CPGs, the experience of domain physicians, and the processing of EHR data. Domain expert knowledge is often expressed as some linguistic IF-THEN rules; there are so many studies that only utilize expert knowledge [14]. By utilizing

EHR data, there are several methods to create fuzzy knowledge, including (i) the induction of a crisp DT and converting it to fuzzy rules, and (ii) the induction of a fuzzy DT. However, each of these methods alone is incomplete. The combination of these methods can generate a complete fuzzy system. First, we generate fuzzy knowledge from the processing of medical data, and next, we enhance this knowledge by a domain expert and CPG knowledge. The details of each step are discussed below.

5.3.1 Raw EHR data preprocessing

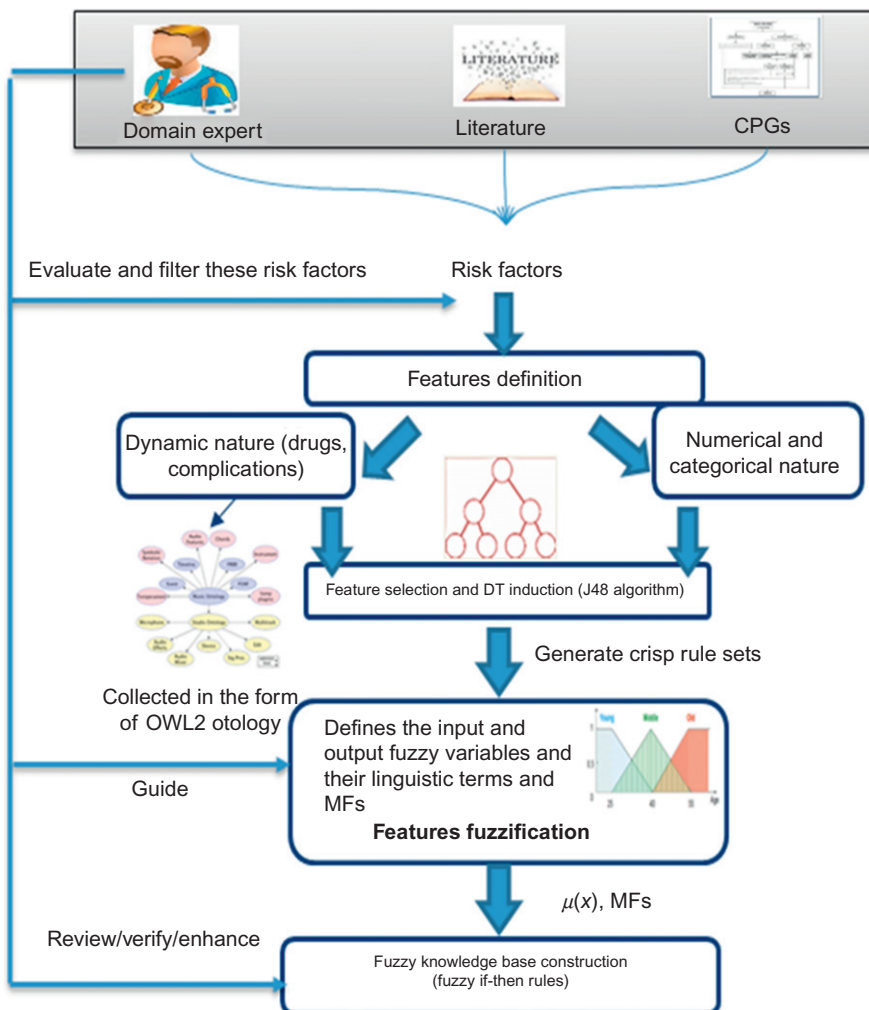
The first step to deal with medical data is to verify that the data are correct and accurate. This step removes noises, outliers, and missing values from the data. The study applies the following steps: data cleaning, outlier removal, encoding, discretization, normalization, and unification of units of measurement (UoMs). Data cleaning fixes any errors in the data. Outlier removal filters abnormal values. The encoding step facilitates the formatting of unstructured data.

For each feature with missing values, the class of the missing value is determined, the mean value of the tested feature is computed for this specific class, and the resulting value replaces the missing value. Handling the problem of a small dataset is done by data normalization and discretization. Normalization is in the range [0, 1]. Discretization is done by defining bins according to features while normal ranges are defined by CPGs and domain experts.

5.3.2 Features definition and fuzzification

As shown in Fig. 8, this step is mainly based on domain expert knowledge, a deep literature survey, and the most recent CPGs such as CDA, ADA, NICE, and a national guideline clearinghouse [25]. By deeply studying the CPGs and the literature, the diabetes diagnosis' initial list of risk factors is determined. Medical experts evaluate and filter these factors. Some of them are listed in Table 1 where most features are of a numerical and categorical nature. In addition, some other features with a dynamic nature such as diabetes-related complications and drugs are collected in the form of OWL2 ontology. In the next step, decision trees using a C4.5 algorithm are used to filter these features, select the best list, and generate crisp rule sets.

The next step is the features fuzzification. This step defines fuzzy variables, their linguistic terms, and MFs. The shapes, numbers, and sizes of used fuzzy sets are determined according to the experts' intuition. These decisions determine the resulting system's accuracy and interpretability. Table 2 shows a sample of fuzzy membership functions and their equations. For each variable, its universe of discourse is defined. For each fuzzy term, the MF shape, equation, scale, parameters, and level of overlap are defined. The modeled MFs and used fuzzy terms semantics are outlined through long arrangements with the area specialists and experts and the analysis of the dataset and most recent CPGs. Then, the fuzzy intervals and their MFs are tuned by the experts. The most three popular types are the triangular MF, the trapezoidal MF, and the Gaussian MF [53,54]. The triangular and trapezoidal MFs are linear functions that are used in real-time implementations. They require small

**FIG. 8**

The features definition and fuzzification block diagram.

computations as compared with nonlinear function, such as Gaussian, that is used for the complex system. Gaussian MFs [55] are simpler in design because they are easier to represent and optimize, always continuous, and faster for small rule bases, whereas trapezoidal are simpler in the analysis. Among these MFs, we consider trapezoidal MF and its special triangular form to be adequate to capture the vagueness in our system because of its ability to contain more fuzzy information; moreover, these linear functions are simple and contain less computation.

Table 2 A Sample of Fuzzy Membership Functions and Their Equations

Linguistic Variables	Membership Functions	Membership Functions Equations
	<p style="text-align: center;"><i>Fuzzy feature: Age</i></p>	$\mu_{\text{Young}}(x) = \begin{cases} 0 & x > 40 \\ \frac{40-x}{10} & 30 \leq x \leq 40 \\ 1 & x < 30 \end{cases}$ $\mu_{\text{MiddleAged}}(x) = \begin{cases} 0 & x \leq 30 \\ \frac{x-30}{10} & 30 < x \leq 40 \\ \frac{50-x}{10} & 40 < x < 50 \\ 0 & x \geq 50 \end{cases}$ $\mu_{\text{Old}}(x) = \begin{cases} 0 & x < 40 \\ \frac{x-40}{10} & 40 \leq x \leq 50 \\ 1 & x > 50 \end{cases}$
	<p style="text-align: center;"><i>Fuzzy feature: Serum creatinine</i></p>	$\mu_{\text{Low}}(x) = \begin{cases} 0 & x > 0.95 \\ \frac{0.95-x}{0.45} & 0.5 \leq x \leq 0.95 \\ 1 & x < 0.5 \end{cases}$ $\mu_{\text{Normal}}(x) = \begin{cases} 0 & x \leq 0.5 \\ \frac{x-0.5}{0.45} & 0.5 < x \leq 0.95 \\ \frac{1.4-x}{0.45} & 0.95 < x < 1.4 \\ 0 & x \geq 1.4 \end{cases}$ $\mu_{\text{High}}(x) = \begin{cases} 0 & x < 0.95 \\ \frac{x-0.95}{0.45} & 0.95 \leq x \leq 1.4 \\ 1 & x > 1.4 \end{cases}$

Continued

Table 2 A Sample of Fuzzy Membership Functions and Their Equations *Continued*

Linguistic Variables	Membership Functions	Membership Functions Equations
	<p style="text-align: center;"><i>Fuzzy feature: BMI</i></p> <p style="text-align: center;">Input variable "BMI"</p>	$\mu_{\text{Underweight}}(x) = \begin{cases} 0 & x > 24.25 \\ \frac{24.25 - x}{5.75} & 18.5 \leq x \leq 24.25 \\ 1 & x < 18.5 \end{cases}$ $\mu_{\text{Normal}}(x) = \begin{cases} 0 & x \leq 18.5 \\ \frac{x - 18.5}{5.75} & 18.5 < x \leq 24.25 \\ \frac{30 - x}{5.75} & 24.25 < x < 30 \\ 0 & x \geq 30 \end{cases}$ $\mu_{\text{Overweight}}(x) = \begin{cases} 0 & x \leq 24.25 \\ \frac{x - 24.25}{5.75} & 24.25 < x \leq 30 \\ \frac{35.75 - x}{5.75} & 30 < x < 35.75 \\ 0 & x \geq 35.75 \end{cases}$ $\mu_{\text{Obese}}(x) = \begin{cases} 0 & x < 30 \\ \frac{x - 30}{5.75} & 30 \leq x \leq 35.75 \\ 1 & x > 35.75 \end{cases}$

Table 3 Rules Extracted From the Decision Tree

Rule	Conjunctive Antecedent (IF Part)			Consequent (THEN Part)
	HbA1c	2hPG	FPG	
R1	HbA1c \geq 6.55	–	–	Diabetic
R2	HbA1c < 6.55	2hPG \leq 187.5	–	Prediabetes
R5	6.25 \leq HbA1c < 6.55	2hPG > 187.5	FPG \geq 137.5	Diabetic
R3	HbA1c < 6.55	2hPG > 187.5	–	Normal
R4	6.25 \leq HbA1c < 6.55	2hPG \leq 187.5	–	Prediabetes
R6	6.25 \leq HbA1c < 6.55	2hPG > 187.5	FPG < 137.5	Prediabetes

5.3.3 Features selection and DT induction

Building the system knowledge base is a difficult problem. There are many methods for creating this knowledge, including extracting rules from experts [33], formulating CPGs into rules [9], or extracting rules and learning MFs from learning data using data-mining techniques including DT, fuzzy DT, neural networks, genetic algorithms, etc. In this module, we use a DT algorithm, a domain expert, and CPGs to extract a set of crisp rules that have high coverage and high accuracy. The DT algorithm has an embedded feature selection capability. Using a reduced feature set, the resulting system requires fewer training patterns; the training process takes less time; the generated rules require less storage; and the classifier generates higher comprehensibility, interpretability, and generalization capabilities. To enhance the accuracy and performance of DT, the study uses DT for dimensionality reduction by removing redundant and irrelevant features from the previously selected feature list. This is perfectly in line with the current literature and CPGs. The produced trees are tested using the test dataset, then transformed into sets of rules. Each DT is converted into a series of IF-THEN rules. To enhance the accuracy and performance of DT, the study uses DT for dimensionality reduction by removing redundant and irrelevant features from the previously selected feature list. As asserted by Kim et al. [34], the rule base has to be cross-checked, validated, and enhanced with the domain expert knowledge and the recent CPGs. Using our dataset, the study utilizes a powerful classification technique, that is, DT, to create the required inference rules [33]. Recently, Meng et al. [52] have compared DT with artificial neural network and logistic regression for diabetes diagnosis, and it had the better accuracy of 77.87%. CART, ID3, C4.5, CHAID, MSDT, and C5.0 are some common algorithms of DTs. This study constructs the DT using a C4.5 algorithm [51], which automatically selects the appropriate feature at each node using a specific algorithm such as information gain or Gini's index. Table 3 is an example of a DT created for the sugar level lab tests. HbA1c is the most important lab test to diagnose diabetes. This is perfectly in line with the current literature and CPGs.

5.4 KNOWLEDGE REASONING

5.4.1 Initial fuzzy knowledge base construction

In this step, we fuzzify the crisp rules by fuzzifying the rule hard decision boundaries using MFs [19]. The OR and AND are converted to t-conorm and t-norm respectively. According to the modeled membership functions, the study makes fuzzification of all crisp rule conditions. Rules are grouped into distinct sets; each belongs to a specific reasoning and decision-making task.

The usual way for modeling fuzzy knowledge is writing fuzzy <IF (condition) THEN (conclusion)> rules by an expert [7]. An alternative way is represented by fuzzy modeling to gain a rule base from data automatically; however, interoperability is not guaranteed, and redundancy often occurs. In Mamdani fuzzy models, the expert domain is responsible for the fuzzification and rule-base construction [14]. In the study model, the knowledge base consisted of diagnostic rules based on the knowledge collected from diabetes CPGs, diabetes EHR data, and domain expert knowledge.

5.4.2 Enhancement of the generated fuzzy knowledge

The knowledge base of CDSS is one of the most critical components, and developing it is the most cumbersome process. As a result, this step takes steps to assure the completeness of the fuzzy knowledge base (see Fig. 9). A complete and accurate fuzzy rule base improves the system interpretability and accuracy. The two utilized

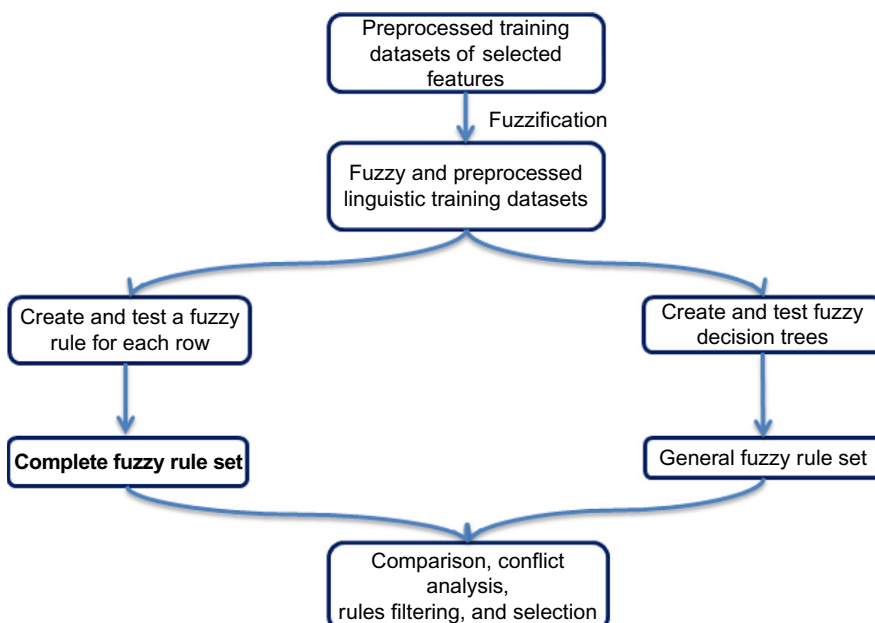


FIG. 9

Knowledge base enhancement.

techniques are based on fuzzy rules induction from training data. The training sets only contain the previously selected features. The first region-based technique is based on fuzzy decision trees (FDTs) for each group of features. Fuzzy-DT integration enhances robustness, noise immunity, and the applicability of the resulting rules [51]. The study uses the fuzzy C4.5 algorithm, which improves the performance of C4.5. First, we fuzzified the previously preprocessed training sets with the preexisting linguistic labels of fuzzy sets. Second, we performed some preprocessing for the generated discretized data by removing the redundant vectors. Finally, we created the FDTs by applying the C4.5 algorithm. A set of compact rules will be extracted from the decision trees by traversing all paths from the root to leaves using the AND operator.

5.4.3 The inference engine

This section uses fuzzy logic to map a given input to an output [21]. There are many inference mechanisms such as Mamdani, Takagi-Sugeno, or Tsukamoto. We use the Mamdani fuzzy inference technique, which is the most commonly used technique [38]. The Takagi-Sugeno model is intuitive, adaptive, and the consequents of fuzzy rules are propositions. It is more suitable for medical classification. In addition, the Mamdani technique enhances the interpretability of the resulting model [39]. As shown in Fig. 10, after the inputs are fuzzified according to their MFs, they are applied to all rules antecedents using a fuzzy version of modus ponens.

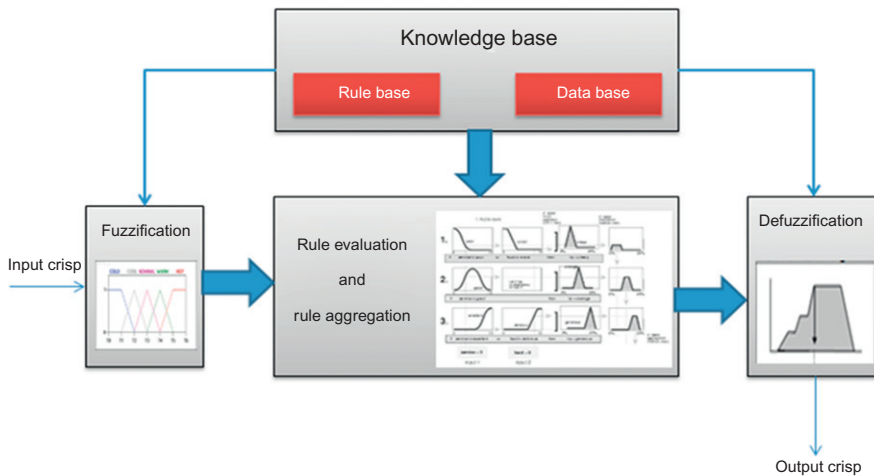
There are two inference or implication mechanisms used in FISs: the clipping method and the scaling method [16]. If input data fired a rule, the output is then applied to the consequent's MF, and this implication operator produces the rule-level fuzzy value (RLFV). Practically, the FIS knowledge base is a collection of disjunctive rules, and it gets multiple fired fuzzy rules from the input. The system-level fuzzy value (SLFV) is calculated using the t-conorm or s-norm operator to the resulting RLFVs. The s-norm is a relation of the form $s : [0, 1] \times [0, 1] \rightarrow [0, 1]$. The most used t-conorm operator is aggregation (i.e., union, max, or, sum) on all the RLFVs. Finally, the defuzzification function is based on A-FATI (the first aggregate, then infer) mode.

5.4.4 The defuzzification process

Defuzzification is optional. There are many methods for defuzzification: center of gravity (CG), maximum center average (MCA), largest of maximum (LOM), mean of maximum (MOM), centroid average (CA), and smallest of maximum (SOM) [49]. This study uses the center of gravity technique (centroid) on the defuzzified values, which is the most widely used technique [37].

5.4.5 Framework evaluation

In Section 4, we defined some related frameworks for combining ontology and fuzzy logic. We try to produce a comparative study of these hybrid models and our proposed model. As observed in Table 4, our proposal framework overcomes other models in:

**FIG. 10**

Mamdani fuzzy inference engine steps.

- Improving the fuzzy expert system by adding a semantic reasoning process to Mamdani capabilities and not using ontology as a second and separate layer in reasoning.
- Supporting learning by a complete linguistic fuzzy rule base based on the integration of experts and CPGs with other knowledge extracted from training data and knowledge derived from a semantic model.
- Supporting interoperability. It concentrates on the possibility of collecting patient medical data from distributed EHR systems in an automated way.

6 CONCLUSION

Diabetes is a severe and complex medical problem. We tried to discuss the existing problem and the technical aspects of current diabetes diagnosis. A CDSS can give a strong boost to the medical field. It can improve medical diagnosis by providing suitable decisions for helping physicians in selecting appropriate treatments. To build CDSS, many different techniques are used, including ontology and Mamdani fuzzy inference for knowledge representation and reasoning. These studies did not achieve the suitable accuracy and compatibility with the electronic health record environment. Implementing a distributed CDSS system that can semantically and automatically understand the meaning of patient's data and automatically utilize these data in its decision is a complex challenge. We propose a hybrid ontology and fuzzy-based CDSS to support physicians in diabetes risk level diagnosis problems. This a novel idea to improve the capabilities of existing fuzzy systems by integrating them with

Table 4 Comparison Between a Hybrid Model and Our Proposed Model

Models	Esposito and Pietro [48]	Yaginuma et al. [49]	Torshizi et al. [50]	Our Proposed Model
Purpose	Classify cerebral white matter lesion (WML) and obtain a measure of their volumes	Provide a case study involving the domain of food safety demonstrated	Diagnosing severity level and recommending appropriate therapies for patients having benign prostatic hyperplasia	Support physicians in diabetes diagnosis problem
Hybrid model	An ontology-based fuzzy decision support system (DSS) combining ontology and fuzzy rules to a zero-order Sugeno	Proposed HyFOM reasoner that combines Mamdani inference and fuzzy ontology	A hybrid fuzzy intelligent system combining Mamdani inference and ontologies	A hybrid ontology-based fuzzy decision support system (OBFDSS) combining ontology and Mamdani fuzzy inference
Formal integration	The fuzzy inference responsible for linking the rules in the T-Box (terminological box) with the data in the A-Box (assertional box) and performing the decision-making process	Used three reasoners (crisp ontology, fuzzy ontology, and Mamdani) separately	Used ontologies and Mamdani as two separate main modules	Improve the fuzzy expert system by adding a semantic reasoning process to its capabilities
Collecting knowledge	From human experts and range from informal or semistructured interviews	With supervision of PNCRC (National Plan for Control of Residues and Contaminants)	Experts, physicians, and written sources	Knowledge usually analyzed by experts, physicians, CPGs, distributed EHR
Support learning	No	No	No	Yes
Support interoperability	No	No	No	Yes

the semantic reasoning of ontologies. It explicitly defines the semantics of diabetes knowledge by using ontology and deals with the imprecise and vague nature of its data by using fuzzy set theory. In other words, some patient attributes are first designed as semantic features such as patient symptoms, drugs, and complications, and then these features and other features such as lab tests are modeled as fuzzy features. The importance of our work comes from the current lack of studies related to the integration of the formal integration between the ontology semantics and FES reasoning, especially in the medical domain. The ontology acts as an integral and complementary component of the FES. In the future, we hope to stratify and apply our hybrid model to develop and implement automated diabetes diagnosis in real distributed clinical settings.

REFERENCES

- [1] P. Sherimon, R. Krishnan, Onto diabetic. An ontology-based clinical decision support system for diabetic patients, *Arab. J. Sci. Eng.* 41 (3) (2016) 1145–1160.
- [2] K. Zarkogianni, E. Litsa, K. Mitsis, P. Wu, C. Kaddi, C. Cheng, M. Wang, K. Nikita, A review of emerging technologies for the management of diabetes mellitus, *IEEE Trans. Biomed. Eng.* 62 (12) (2015) 2735–2749.
- [3] American Diabetes Association, Diabetes care, <http://www.diabetes.org/>, 2016.
- [4] A. Anderson, et al., Electronic health record phenotyping improves detection and screening of type 2 diabetes in the general United States population: a cross-sectional, unselected, retrospective study, *J. Biomed. Inform.* 60 (2016) 162–168.
- [5] W. Yao, A. Kumar, CONFlexFlow: integrating flexible clinical pathways into clinical decision support systems using context and rules, *Decis. Support Syst.* 55 (2013) 499–515.
- [6] R. Seising, From vagueness in medical thought to the foundations of fuzzy reasoning in medical diagnosis, *Artif. Intell. Med.* 38 (2006) 237–256.
- [7] A. d'Acierno, M. Esposito, G. De Pietro, An extensible six-step methodology to automatically generate fuzzy DSSs for diagnostic applications, *BMC Bioinformatics* 14 (2013) S4.
- [8] A. Miller, B. Moon, S. Anders, R. Walden, S. Brown, D. Montella, Integrating computerized clinical decision support systems into clinical work: a meta-synthesis of qualitative research, *Int. J. Med. Inform.* 84 (12) (2015) 1009–1018.
- [9] A. Minutolo, M. Esposito, G. De Pietro, A fuzzy framework for encoding uncertainty in clinical decision-making, *Knowl.-Based Syst.* 98 (2016) 95–116.
- [10] L. Ahmadian, R. Cornet, N. de Keizer, Facilitating pre-operative assessment guidelines representation using SNOMED CT, *J. Biomed. Inform.* 43 (2010) 883–890.
- [11] M. de Britoa, et al., Support system for decision making in the identification of risk for body dysmorphic disorder: a fuzzy model, *Int. J. Med. Inform.* 82 (2013) 844–853.
- [12] C. Lee, M. Wang, A fuzzy expert system for diabetes decision support application, *IEEE Trans. Syst. Man Cybern. B Cybern.* 41 (2011) 139–153.
- [13] T. Chang, H. Kao, J. Wu, Y. Su, Improving physicians' performance with a stroke CDSS: a cognitive fit design approach, *Comput. Hum. Behav.* 54 (2016) 577–586.
- [14] S. Chen, Y. Huang, R. Chen, S. Yang, T. Sheu, Using fuzzy reasoning techniques and the domain ontology for anti-diabetic drugs recommendation, *ACIIDS 2012, Part I, LNAI*, vol. 7196, Springer-Verlag, Berlin, Heidelberg, 2012, pp. 125–135.

- [15] M. Tsipouras, T. Exarchos, D. Fotiadis, A. Kotsia, K. Vakalis, K. Naka, L. Michalis, Automated diagnosis of coronary artery disease based on data mining and fuzzy modeling, *IEEE Trans. Inf. Technol. Biomed.* 12 (2008) 447–458.
- [16] P. Debabrata, et al., Fuzzy expert system approach for coronary artery disease screening using clinical parameters, *Knowl.-Based Syst.* 36 (2012) 162–174.
- [17] S. Alayon, R. Robertson, S. Warfield, J. Ruiz-Alzola, A fuzzy system for helping medical diagnosis of malformations of cortical development, *J. Biomed. Inform.* 40 (2007) 221–235.
- [18] S. Harispe, D. Sanchez, S. Ranwez, S. Janaqi, J. Montmain, A framework for unifying ontology-based semantic similarity measures a study in the biomedical domain, *J. Biomed. Inform.* 48((2014) 38–53.
- [19] S. El-Sappagh, M. Elmogy, A. Riad, A fuzzy-ontology-oriented case-based reasoning framework for semantic diabetes diagnosis, *Artif. Intell. Med.* 65 (2015) 179–208.
- [20] S. El-Sappagh, F. Ali, DDO: a diabetes mellitus diagnosis ontology, *Appl. Inform.* 3 (2016) 1–28.
- [21] N.H. Phuong, V. Kreinovich, Fuzzy logic and its application in medicine, *Int. J. Med. Inform.* 62 (2001) 165–173.
- [22] A. Torshizi, M. Zarandi, G. Torshizi, K. Eghbali. A hybrid fuzzy-ontology based intelligent system to determine level of severity and treatment recommendations for Benign Prostatic Hyperplasia. *Comput. Methods Programs Biomed.*, 113(1) 301–313.
- [23] T.W. Liao, Classification of welding flaw types with fuzzy expert systems, *Expert Syst. Appl.* 25 (2003) 101–111.
- [24] J.Z. Pan, G. Stoilos, G. Stamou, V. Tzouvaras, I. Horrocks, f-SWRL. A fuzzy extension of SWRL, *J. Data Semant Emergent Semant* 4090 (2006) 28–46.
- [25] National Institute for Health and Care Excellence (NICE), <https://www.nice.org.uk/>, 2015.
- [26] L.S. Bickley, P.G. Szilagyi, Bates' Guide to Physical Examination and History Taking, eighth ed., Lippincott Williams and Wilkins, Philadelphia, 2003.
- [27] I. Heydari, V. Radi, S. Razmjou, A. Amiri, Chronic complications of diabetes mellitus in newly diagnosed patients, *Int. J. Diabetes Mellit.* 2 (2010) 61–63.
- [28] R. Chen, Y. Huang, C. Bau, S. Chen, A recommendation system based on domain ontology and SWRL for anti-diabetic drugs selection, *Expert Syst. Appl.* 39 (2012) 3995–4006.
- [29] Canadian Diabetes Association, <https://www.diabetes.ca>, 2015.
- [30] A. Luzi, et al., A1c value for diabetes diagnosis in subjects with established cardiovascular disease, *Acta Diabetol.* 52 (2015) 999–1001.
- [31] L. Liu, J. Tang, Y. Cheng, A. Agrawal, W. Liao, A. Choudhary, Mining diabetes complication and treatment patterns for clinical decision support, *Proceedings of the 22nd ACM International Conference on Information and Knowledge Management*, 2013, pp. 279–288.
- [32] U. Anyanwagu, I. Idris, R. Donnelly, Drug-induced diabetes mellitus. Evidence for statins and other drugs affecting glucose metabolism, *Clin. Pharmacol. Ther.* 99 (4) (2015) 390–400.
- [33] A. Ramezankhani, et al., Applying decision tree for identification of a low risk population for type 2 diabetes. *Tehran Lipid and Glucose Study, Diabetes Res. Clin. Pract.* 105 (2014) 391–398.
- [34] J. Kim, J. Lee, D. Park, Y. Lim, Y. Lee, E. Jung, Adaptive mining prediction model for content recommendation to coronary heart disease patients, *Cluster Comput.* 17 (2014) 881–891.

- [35] I.M. Ahmed, M. Alfonse, M. Aref, A.-B.M. Salem, Reasoning techniques for diabetics expert systems, *Procedia Comput. Sci.* 65 (2015) 813–820.
- [36] A. Karegowda, V. Punya, M. Jayaram, A. Manjunath, Rule based classification for diabetic patients using cascaded K-means and decision tree C4.5, *Int. J. Comput. Appl.*, 45(12) 0975-8887.
- [37] A. Papadopoulos, D. Kalivas, T. Hatzichristos, Decision support system for nitrogen fertilization using fuzzy theory, *Comput. Electron. Agric.* 78 (2011) 130–139.
- [38] J. Lai, F. Leung, S. Ling, H. Nguyen, Hypoglycaemia. Detection using fuzzy inference system with multi-objective double wavelet mutation differential evolution, *Appl. Soft Comput.* 13 (2013) 2803–2811.
- [39] H. Seki, M. Mizumoto, SIRMs. Connected fuzzy inference method adopting emphasis and suppression, *Fuzzy Sets Syst.* 215 (2013) 112–126.
- [40] J. Zhai, M. Li, K. Zhou, Linguistic variable ontology and its application to fuzzy semantic retrieval, *Commun. Comput. Inform. Sci.* 106 (2010) 188–195.
- [41] S. Borgwardt, F. Distel, R. Peñaloza, The limits of decidability in fuzzy description logics with general concept inclusions, *Artif. Intell.* 218 (2015) 23–55.
- [42] F. Bobillo, U. Straccia, An OWL ontology for fuzzy OWL 2, Proc. of 18th Int. Symp. on Foundations of Int. Systems, ser. ISMIS 09, 2009, pp. 151–160.
- [43] S. Chen, M. Huang, Automatically generating the weather news summary based on fuzzy reasoning and ontology techniques, *Inf. Sci.* 279((2014) 746–763.
- [44] S. La-Ongsri, J. Roddick, Incorporating ontology-based semantics into conceptual modeling, *Inf. Syst.* 52 (2015) 1–20.
- [45] F. Bobillo, U. Straccia, The fuzzy ontology reasoner fuzzy DL, *Know.-Based Syst.* 95 (2016) 12–34.
- [46] F. Bobillo, M. Delgado, J. Gómez-Romero, A crisp representation for fuzzy backslashcal SHOIN with fuzzy nominals and general concept inclusions, *Uncertainty Reasoning for the Semantic Web I: ISWC International Workshops, URSW 2005–2007*, Springer, Berlin, Heidelberg, 2008, pp. 174–188 Revised Selected and Invited Papers.
- [47] G. Stoislos, G. Stamou, J. Pan, Handling imprecise knowledge with fuzzy description logic, *International Workshop on Description Logics (DL 06)*, Lake District, UK, 2006.
- [48] M. Esposito, G.D. Pietro, An ontology-based fuzzy decision support system for multiple sclerosis, *Eng. Appl. Artif. Intell.* 24 (2011) 1340–1354.
- [49] C.A. Yagquinuma, M.T.P. Santos, H.A. Camargo, M. Reformat, A FML-based hybrid reasoner combining fuzzy ontology and Mamdani inference, *2013 IEEE International Conference on Fuzzy Systems (FUZZ)*, 2013, pp. 1–8.
- [50] A.D. Torshizi, M.H.F. Zarandi, G.D. Torshizi, K. Eghbali, A hybrid fuzzy-ontology based intelligent system to determine level of severity and treatment recommendation for Benign Prostatic Hyperplasia, *Comput. Methods Programs Biomed.* 113 (2014) 301–313.
- [51] W. Pedrycz, Z.A. Sosnowski, Genetically optimized fuzzy decision trees, *IEEE Trans. Syst. Man Cybern. B Cybern.* 35 (2005) 633–641.
- [52] X. Meng, Y. Huang, D. Rao, Q. Zhang, Q. Liu, Comparison of three data mining models for predicting diabetes or prediabetes by risk factors, *Kaohsiung J. Med. Sci.* 29 (2013) 93–99.
- [53] R.B. Lukmanto, E. Irwansyah, The early detection of diabetes mellitus (DM) using fuzzy hierarchical model, *Procedia Comput. Sci.* 59 (2015) 312–319.

- [54] D. Pal, K.M. Mandana, S. Pal, D. Sarkar, C. Chakraborty, Fuzzy Expert System Approach for Coronary Artery Disease Screening Using Clinical Parameters, *Know.-Based Syst.* 36 (2012) 162–174 Elsevier Science Publishers B. V.
- [55] T.J. Ross, Membership functions, fuzzification and defuzzification, in: P.S. Szczepaniak, P.J.G. Lisboa, J. Kacprzyk (Eds.), *Fuzzy Systems in Medicine*, in: *Studies in Fuzziness and Soft Computing*, vol. 41, Physica, Heidelberg, 2000.

FURTHER READING

- [56] A. Ciaramella, M.G.C.A. Cimino, F. Marcelloni, U. Straccia, Combining fuzzy logic and semantic web to enable situation-awareness in service recommendation, *Database and Expert Systems Applications: 21st International Conference, DEXA 2010, Bilbao, Spain, August 30–September 3, 2010, Proceedings, Part I*, Springer, Berlin, Heidelberg, 2010, pp. 31–45.

This page intentionally left blank

Improving the prediction accuracy of heart disease with ensemble learning and majority voting rule

8

Khalid Raza*Department of Computer Science, Jamia Millia Islamia, New Delhi, INDIA*

CHAPTER OUTLINE

1	Introduction	179
2	Review of Related Works	181
3	Ensemble Learning Systems	183
3.1	Diversity	184
3.2	Training Ensemble Members	184
3.3	Combining Ensemble Members	184
4	Materials and Methods	185
4.1	Logistic Regression	185
4.2	Multilayer Perceptron	188
4.3	Naïve Bayes	188
4.4	Combining Classifiers Using Majority Vote Rule	189
4.5	Performance Metrics	190
5	Result and Discussion	191
6	Conclusion and Future Directions	193
	References	193
	Further Reading	196

1 INTRODUCTION

Heart diseases, medically known as cardiovascular diseases (CVD) or strokes, are the number one cause of death worldwide. As per the World Heart Federation Report of 2016, one out of three deaths are a result of CVD, despite the fact that the majority of premature heart diseases are preventable. The financial burden of CVD was \$863 billion, which is estimated to increase by 22% by 2030, costing \$1.044 billion [1]. CVDs are caused due to narrowed, blocked, or stiffened blood vessels that prevent

the required supply of blood to the heart, brain and other parts of the body. There are various types of CVDs, but narrowing or blockage of the coronary arteries is the most common form of heart disease; it occurs slowly over time. The coronary arteries are blood vessels whose job is to supply blood to the heart. Other forms of heart disease may be related to valves in the heart that may not pump well and cause heart failure. Some of the most common symptoms of heart disease are chest pains, shortness of breath, numbness, weakness, and pain in the neck, jaw, throat, upper abdomen, or back. However, there are some controlling factors that help us reduce the risk of heart disease, such as controlled blood pressure, lower cholesterol, avoiding smoking, and regular exercise. Mostly, a CVD might not be diagnosed until a heart attack, angina, stroke, or heart failure occurs. Therefore, it is important to monitor the cardiovascular parameters and consult doctors.

The advancement in computing and information technologies has allowed the health industry to collect and store routine medical data that helps in critical medical decisions. The stored patients' data can be analyzed to make the necessary medical decisions, which may involve prediction, diagnosis, image analysis, and line of treatments. The healthcare system has a wealth of available data, and thus it is information rich but unfortunately knowledge poor. Over the last few decades, machine learning algorithms have been playing a pivotal role in solving complex, highly non-linear classification and prediction problems. Hence, it is possible to develop a prediction model that would predict the presence or absence of heart disease based on various heart-related symptoms (features). In any disease prediction task, it is a paramount requirement that a prediction algorithm classify a healthy patient as accurately as possible. Otherwise, misclassification may result in a healthy patient undergoing unnecessary treatment. Hence, the accurate prediction of any disease, including heart disease, is of paramount importance.

Different machine learning algorithms, including decision tree, random forest, naïve Bayes, support vector machine (SVM), and artificial neural networks (ANNs), have been widely used in many of the disease classification and prediction problems. Some of these applications include heart disease [2–10], diabetes [3,11,12], Parkinson's [3], hypertension [11], the Ebola virus (EV) prognosis and prediction [13], RNA-seq data classification [14], and biomedical image classification [15–18]. However, the development of a machine learning-based disease prediction model and medical decision-making is a nontrivial task [4]. Some of the important issues are data acquisition, collection, and organization, which are used for training the machine learning system. In many real-life problems, including biomedical, large datasets over a long duration are needed, which are mostly unavailable.

Owing to an increase in the aging population, new chronic diseases, and rapid advancement in information and communication technology (ICT) as well as the Internet of Things (IoT), people have become more health conscious and patients have become health consumers. The healthcare system has evolved from traditional, classical e-Health to m-Health, telemedicine, and now ubiquitous healthcare (u-Health) [19]. One of the purposes of the U-Healthcare system is to monitor patients' everyday activities and warn the patients or health workers in case of

problems. In addition, a U-Healthcare monitoring system also collects patient's everyday data for trend analysis and medical research. In the context of the theme of the book *U-Healthcare Monitoring Systems: Design and Applications*, in this chapter we present an ensemble method to improve the prediction accuracy of heart disease based on a patient's clinical reports. The proposed method may be integrated into the U-Healthcare monitoring system for heart disease diagnosis, which may warn patients and healthcare workers while helping cardiologists in the necessary decision-making. The chapter is organized as follows. [Section 2](#) reviews the previous related works while [Section 3](#) describes a basic overview of ensemble systems and their features. [Section 4](#) covers materials and methods describing the architecture of the proposed ensemble model, descriptions of considered classifiers, and majority voting rules. [Section 5](#) presents results and discussion. Finally, [Section 6](#) concludes the chapter by citing some future work directions.

2 REVIEW OF RELATED WORKS

In the literature, most of the heart disease prediction models have been trained and tested on University of California at Irvine Machine Learning (UCI-ML) repository datasets consisting of risk factors (features) such as age, sex, chest pain, blood pressure, cholesterol, blood sugar, electrocardiographic results, maximum heartbeat rate, etc. In this section, we have reviewed the machine learning models based on these risk factors, especially UCI-ML datasets, because our proposed ensemble model presented in this paper is also based on these datasets. But other types of risk factors for heart disease such as heart rate variability (HRV) [20], blood pressure, plasma lipid, Glu, and UA have also been used in the literature to design prediction models.

Kononenko [21] applied various machine learning techniques and compared the performance on eight medical datasets using five different parameters: performance, transparency, explanation, reduction, and missing data handling. Out of different evaluation parameters, the performance of the naive Bayes, seminaive Bayes, back propagation, and kNN methods have been rated as "very good." In terms of transparency, decision tree has been rated as "very good." For missing data handling parameters, naive Bayes and seminaive Bayes have been labeled as "very good." The result of [21] does not provide any quantitative accuracy of prediction models. Palaniappan and Awang [2] developed a prototype for Intelligent Heart Disease Prediction Systems having a web-based interface for a "what-if" query, which utilizes three classifiers: decision tree, naïve Bayes and ANN. The survey on machine learning applications in healthcare systems, particularly in heart disease prediction, can be found in [22,23]. The survey in [22] states that decision tree and Bayesian classification outperform the other techniques while kNN, ANN, and clustering-based classification do not perform well. According to the recent survey by Kadi et al. [23], who have done an empirical study on 149 papers published during 2000–2015 for the prediction of cardiology, ANN, decision tree, and SVM were

found to be the most frequently used machine learning techniques. In terms of prediction accuracy, ANN and SVM were found to be more efficient than other techniques. The empirical study in the two papers [22,23] contradicted in making a general statement about highly accurate machine learning techniques for heart disease prediction. This contradiction may be because of differences in the datasets and risk factors under consideration.

Researchers have proved that the performance of a base classifier can be improved by the ensemble system. Ozciit and Gulten [3] proposed a rotation forest ensemble classifier consisting of 30 different machine learning algorithms and evaluated their performance on three different datasets: Parkinson's, diabetes, and heart disease. Before the training ensemble classifier, the feature reduction was done using correlation-based feature selection (CFS). Their results state that base classifiers achieve an average accuracy of 72.15%, 77.52%, and 84.43% for diabetes, heart disease, and Parkinson's, respectively. For RF ensemble classifiers, the average accuracy goes to 74.47%, 80.49%, and 87.13% for the respective diseases. Austin et al. [5] found that the tree-based method performed better over conventional classification methods for heart failure predication. They took datasets from the EFFECT study (Enhanced Feedback for Effective Cardiac Treatment) consisting of 9943 and 8339 patients diagnosed for the first (EFFECT-1) and second (EFFECT-2) phase of study [24,25], respectively. They considered all 34 predictor variables (features). The result by Austin and collaborators [5] showed that the random forest technique achieved the highest sensitivity and PPV (positive predicted value) of 0.89 and 0.61, respectively; however, the sensitivity remains 0.37 for the EFFECT-2 dataset. Pandey et al. [6] performed a similar kind of study and applied a pruned J48 decision tree with a reduced error pruning method for the prediction of heart disease, which receives an accuracy of 73.79% (out of 103 testing samples, 76 have been classified accurately). They also found that out of 16 different features, fasting blood sugar has been the most important attribute, giving better classification over other attributes.

An extreme learning machine (EML) has also been applied for heart disease prediction on UCI-ML repository datasets and the results show an accuracy of 80% [7]. Santhanam and Ephzibah [26] have designed a hybrid genetic-fuzzy (genetic algorithm and fuzzy logic) model and tested on UCI-ML datasets, which shows an accuracy of 86%. Another hybrid classifier, the orthogonal local preserving projection (OLPP) technique for feature dimension reduction and gravitational search algorithm (GSA) with Levenberg-Marquardt training in ANN has also been developed and tested by Poornima and Gladis [27] on similar UCI-ML datasets. In a recent study [28], the comparative evaluation of six machine learning algorithms for heart disease prediction was performed. Among the six techniques, the highest prediction accuracy of 85% was reported for logistic regression. In order to improve the prediction accuracy, in this paper, we have developed an ensemble model comprised of three machine learning techniques with majority voting rule. The result of our developed ensemble method outperforms the previously developed single classification models.

3 ENSEMBLE LEARNING SYSTEMS

Over the past few decades, multiple classifier systems, often known as ensemble learning systems, have been playing an effective role and are extremely versatile applications in a wide spectrum of problems. Ensemble is the art of combining various learners together in order to improve the prediction power and stability of the classification model. It is a powerful way to increase the prediction accuracy of a classification model. The way various prediction models are combined is termed ensemble learning. In fact, ensemble systems were originally germinated to ameliorate prediction accuracy by reducing variance. They have been successfully applied to solve a large variety of machine learning problems, including feature selection, confidence estimation, incremental learning, and various classification and prediction problems [29]. Ensemble-based learning and decision-making is not new to us. As human beings, we use such a technique in our daily routine to make important decisions, such as seeking advice from different experts, taking consultations from more than one doctor before getting a major medical treatment, asking for referees before hiring an applicant, and reading user reviews before buying a product, to name a few. Also, ensemble learning is used to improve the confidence of a classification model by weighting various individual classifiers, and combining them to reach to a final decision [30]. The schematic diagram of a typical ensemble learning system is shown in Fig. 1.

In ensemble systems, the models are different from each other, including differences in population, hypothesis, modeling technique, and initial seed. As reported in [29], there are three pillars of ensemble systems: diversity (training dataset selection for each classifier), training ensemble members (process to generate classifier members, where members are chosen through classifier selection or classifier fusion), and combining ensemble members (combining rule for getting ensemble decision).

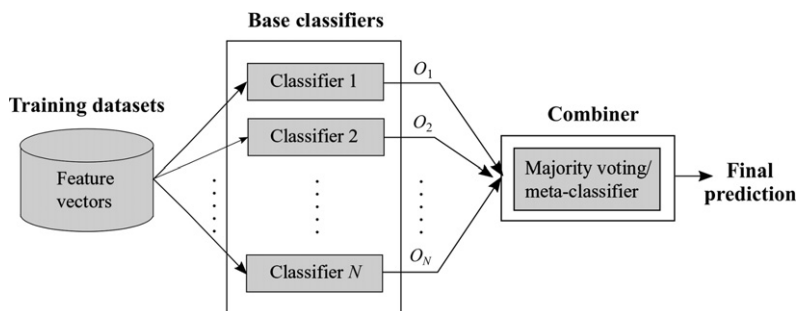


FIG. 1

A schematic diagram of a typical ensemble learning system.

3.1 DIVERSITY

The diversity refers to the diversity in the results (or errors) of ensemble members, which is very important in ensemble systems. The lack of diversity leads to poor performance. There are several ways to achieve diversity in ensemble systems, but taking different subsets of a training dataset is the most commonly applied approach. Different data sampling and selection methods lead to a different kind of ensemble algorithm. For instance, bootstrapped replicas of datasets have given birth to bagging algorithms. Bagging algorithms, also known as “bootstrap aggregating,” was originally introduced by Breiman [31]. Given a set of n data points, bagging chooses a set of data points of size n by sampling uniformly with replacement from original data points. It generates a resampled dataset in which some data points appear multiple times and others do not appear at all. If by doing so, the learning algorithm is unstable, the bagging algorithm would produce a diverse ensemble of training sets. Similarly, sampling using a distribution favoring previously misclassified samples is the basic principle of the boosting algorithm [32]. It is an iterative method that adjusts the weight of an observation of last classification, and weights of misclassified observations are increased. The main idea of boosting is that it converts the weak classifier into a strong one over several iterations. There are many boosting algorithms such as adaptive boosting (AdaBoost), gradient tree boosting, and XGBoost. When different subsets of the input feature are used to train each classifier of the ensemble system, it is known as random subspace methods (RSM) [29,33]. In general, bagging, boosting, and RSM are generally applied to decision tree to produce ensemble classifiers and are found superior to a single classifier. However, these techniques have also been applied with classifiers other than decision tree [32]. Besides bagging, boosting, and RSMs, diversity can be achieved by injecting randomness into the training algorithm. For instance, decision tree algorithms can be randomized by introducing randomness in the process of selecting which feature and threshold to split on [30]. The diversity has also been achieved by manipulating the output labels of the given training dataset.

3.2 TRAINING ENSEMBLE MEMBERS

This step is the core of any ensemble learning system. Several methods have been proposed and applied for training ensemble members; however, bagging, boosting and its variants, and stacking (stack generalization) are the most commonly used approaches. These techniques have been extensively reviewed in the literature [29,30,32].

3.3 COMBINING ENSEMBLE MEMBERS

The third pillar of the ensemble system is the method to combine individual classifiers to make consolidated results. The mechanism used for combining classifiers depends on the type of classifier used. For classifiers producing discrete-valued label output,

a simple majority voting technique can be applied. However, there are several classifiers that produce continuous valued class output, and those output values are interpreted as the support assigned to each class by the classifier. For such classifiers, in addition to majority, we have a wide range of choices such as arithmetic means, products or sum, or most sophisticated techniques such as decision templates. Most of these combiners are used just after training is over. However, some complex combining algorithms may need an additional training step. In this paper, the three best performing classifiers—logistic regression, naïve Bayes, and ANN—have been ensembled, and the majority voting technique has been applied for combining these classifiers. The detailed methodology is discussed in the next section.

4 MATERIALS AND METHODS

The StatLog heart disease dataset available in the University of California at Irvine Machine Learning (UCI-ML) repository datasets consisting of several risk factors (features) has been used in this study. In fact, the dataset belongs to R. Detrano and his group from the VA Medical Center, compiled at the Cleveland Clinic Foundation under the StatLog project [34]. The dataset comprises 270 samples, out of which 120 samples have heart disease (presence) and 150 samples do not have heart disease (absence) without any missing values. Although the dataset consists of 75 heart disease risk factors (features), only 13 distinct features have been used in the literature, including this paper, for the prediction of heart disease, which is described in Table 1. All the 13 distinct features with their corresponding values have been visualized in Fig. 2 in the form of an area plot. For the exploratory analysis of multivariate data having discrete and continuous valued attributes, we have constructed a decision tree-like structure using the Chi Squared Automated Interaction Detector (CHAID) method available in the SPSS software tool [35], as shown in Fig. 3.

The CHAID method performs multilevel splits of data into decision tree, which is suitable for even larger datasets. The probabilities for splitting and merging both were set to 0.01. The CHAID decision tree deciphers the patient's health condition and gives cardiologists a better understanding and discriminatory ability about the disease.

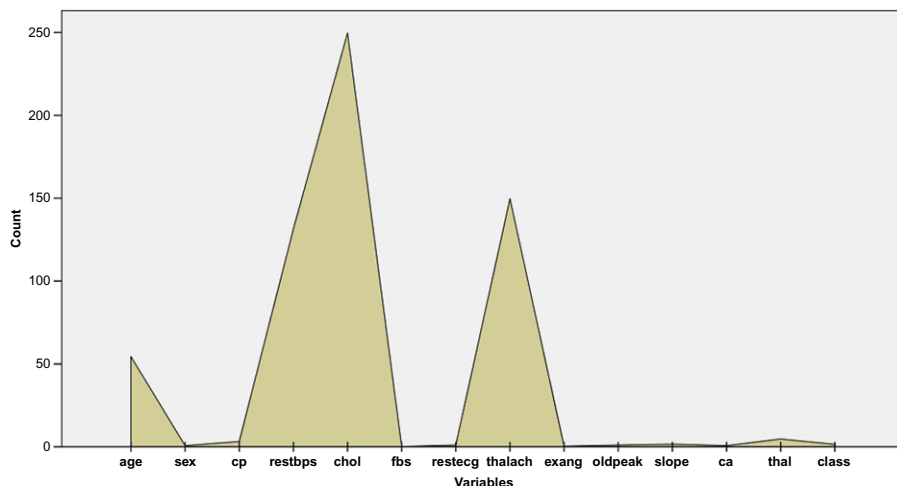
In this paper, the three best performing classifiers for predicting heart disease—logistic regression (accuracy = 85%), ANN (accuracy = 84%), and naïve Bayes (accuracy = 83%), as reported in [28]—have been ensembled, trained, and combined with the majority voting rule to improve the prediction accuracy. The architecture of the proposed ensemble classification model is depicted in Fig. 4.

4.1 LOGISTIC REGRESSION

It is a discriminative and appropriate classification method when the dependent variable has a binary outcome. Like all regression analysis, the LR is also applied to find the relationship between one dependent binary variable and one or more independent

Table 1 Attribute Description of StatLog Heart Disease Dataset

Attribute	Data Type	Attribute description
age	Real	Age (in years)
sex	Binary	0—female, 1—male
cp	Nominal	Chest pain type (1—typical angina, 2—atypical angina, 3—nonangina, 4—asymptomatic)
restbps	Real	Resting blood pressure (mm of Hg)
chol	Real	Serum cholesterol (mg/dL)
fbs	Binary	Fasting blood sugar >120 mg/dL (1—true, 0—false)
resteeg	Nominal	Resting electrocardiographic results (0—normal, 1—having ST-T wave normality, 2—probable/defined left ventricular hypertrophy)
thalach	Real	Maximum recorded heart rate
exang	Binary	Angina induced by exercise (1—yes, 0—false)
oldpeak	Real	ST depression tempted by workout comparative to rest
slope	Nominal	Slant of the peak exercise ST segment (1—upsloping, 2—flat, 3—downsloping)
ca	Real	Major vessels colored by fluoroscopy
thal	Nominal	3—normal, 6—fixed defect, 7—reversible defect
class	Binary	Represent present or absence of heart disease (1—absence, 2—presence)

**FIG. 2**

Area plot of dataset (x-axis represents attributes and y-axis presents its mean value of the entire dataset).

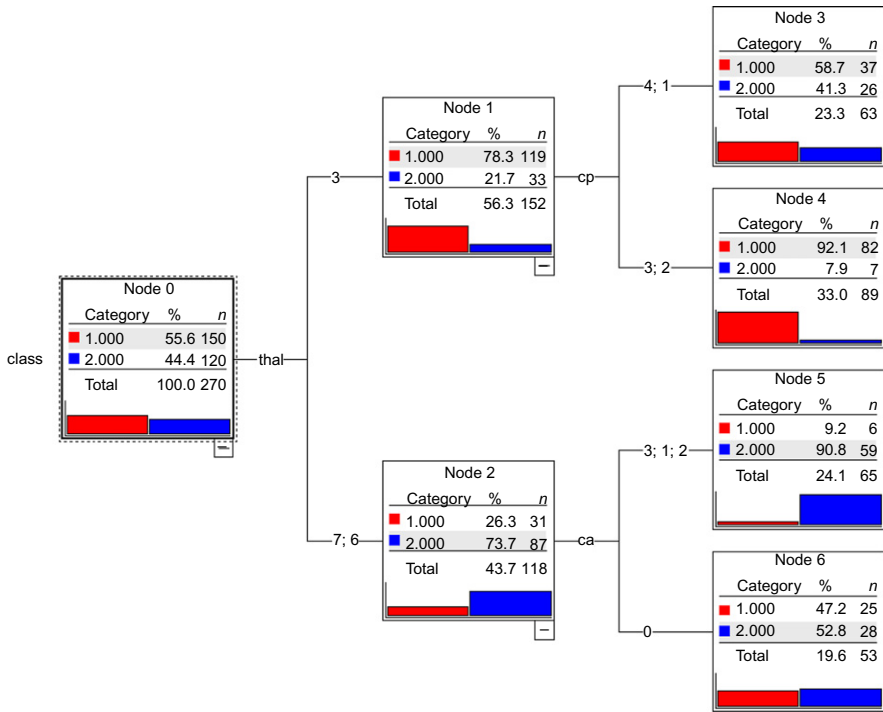


FIG. 3

CHIAD analysis of StatLog heart disease dataset.

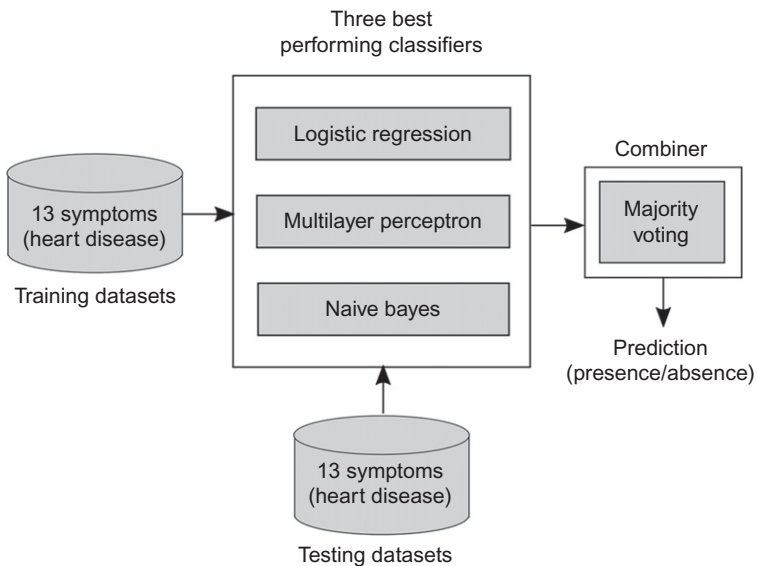


FIG. 4

Architecture of the proposed ensemble model.

variable(s) [36]. It is basically a generalized linear model that computes the probability of the occurrence of an event x by fitting data onto a logistic curve [11]:

$$f(\vec{x}) = \frac{1}{1 + e^{-\vec{a}\vec{x}}} \quad (1)$$

Where \vec{a} is the vector that contains the regression coefficient. There is one coefficient per independent variable. The LR has been found to perform well in the health informatics domain [11].

4.2 MULTILAYER PERCEPTRON

Multilayer perceptron (MLP), a kind of ANN, is a computational model inspired by the biological nervous system. It is used for classification and regression problems where there are nonlinear relationships between dependent and independent variables. A standard neural network has an input layer, one or more hidden layer(s), and one output layer. Each layer contains artificial nodes, known as neurons (processing elements). Neurons are interconnected, which computes values depending upon the given inputs by feeding it forward through the network. Like ANN, MLP is defined by three different parameters: (i) a connection pattern between neurons of different layers, (ii) a training algorithm to adjust synaptic weights, and (iii) an activation function that transforms a neuron's total weighted input to output [37,38]. Connection patterns are broadly classified as feed-forward neural networks and recurrent neural networks (RNNs). The back-propagation algorithm is the most popular and widely used for training ANN. During the process of ANN training, computed errors are propagated back and weights are adjusted. The most important features of ANN are its robustness to noisy data and its capability to learn to estimate multivariate nonlinear function. Here, we have considered a feed-forward neural network with a back-propagation training algorithm. Detailed discussions on ANN can be found in [37,39,40].

4.3 NAÏVE BAYES

The naïve Bayes classification algorithm belongs to the family of probabilistic classifiers that applies the Bayes theorem. It has been extensively studied since the 1950s and is widely used for various classification problems, including text and document categorization, spam filtering, disease classification, and automatic medical diagnosis. The naïve Bayes algorithm relies on the assumption that there is a strong independence between a given set of features to predict a class. This method is easy to build, highly scalable, applicable to very large datasets, requires a number of parameters (features), and is known to outperform even highly sophisticated methods in several real-life problems [28].

The posterior probability $P(c | x)$ for class c , given feature x , can be computed from $P(c)$, $P(x)$, and $P(x | c)$ using the Bayes theorem:

$$P(c | x) = \frac{P(x | c) P(c)}{P(x)} \quad (2)$$

where $P(c)$ and $P(x)$ are the prior probability of class c and feature x , respectively. $P(x | c)$ is the probability of feature x , given class c , which is called likelihood. The posterior probability of class c for a given set of independent features $X = \{x_1, x_2, \dots, x_n\}$ can be computed as:

$$P(c | X) = P(x_1 | c) \times P(x_2 | c) \times \dots \times P(x_n | c) \times P(c) \quad (3)$$

Naïve Bayes also performs well for multiclass problems. As far as the categorical input variables are concerned, naïve Bayes performs well compared to numerical variables. With several advantages, the naïve Bayes classifier suffers from zero frequency problems and its strong assumption of independent features. However, zero frequency problems can be solved by smoothing techniques such as the Laplace estimation [41–43].

4.4 COMBINING CLASSIFIERS USING MAJORITY VOTE RULE

The output of an ensemble system is highly dependent on how the output of the classifiers in an ensemble system is combined. Hence, combining classifiers in an ensemble system is an interesting research problem. For the label outputs, majority vote rule is the most widely used method [44]. In case of continuous outputs, such as posteriori probabilities, a max, min, average, or some other linear combination can be used. Even a classifier can be used as a metaclassifier for combining outputs of ensemble members. In this study, majority vote has been applied due to its better performance over other linear and metaclassifier combiners.

The root of majority vote (consensus in context to electoral theory) is traced back to the ancient Greek and Roman senates, but it became established in 1356 for the election of German kings [45]. The majority voting rule exists in three forms: (i) *unanimous voting*, where all the classifiers must agree with a prediction, (ii) *simple majority*, where prediction need to be at least one more than 50% of the classifiers, and (iii) *plurality* or *majority voting*, where the highest number of votes is considered for the ensemble decision whether the sum of those exceeds 50%. In case classifier outputs are independent, the majority voting rule combiner always improve the prediction performance [44]. Suppose that class label outputs of classifier D_i are given as c -dimensional binary vectors:

$$[d_{i,1}, \dots, d_{i,c}] \in \{0, 1\}^c, \quad i = 1, \dots, N \quad (4)$$

where $d_{i,j} = 1$, if classifier D_i label x in w_j , and 0 otherwise. The majority voting rule would give an ensemble decision for class w_k , if the following Eq. (5) is satisfied:

$$\sum_{i=1}^N d_{i,k} = \max_{j=1}^c \sum_{i=1}^N d_{i,j} \quad (5)$$

In case of two classes ($c = 2$), the majority vote coincides with simple majority rule (50% of vote +1). As per Eq. (4), a majority voting rule would predict an accurate class label if at least $\lfloor N/2 + 1 \rfloor$ classifiers correctly predict the class label [45]. In our proposed model, $N = 3$ means that the model will correctly predict if at least two classifiers correctly predict the class label.

4.5 PERFORMANCE METRICS

The performance metrics used in this paper are based on the count of true positives (TPs), true negative (TNs), false positive (FPs), and false negatives (FNs), as described below:

Sensitivity: It describes the probability of a classifier to predict the result as positive when disease is present. It is also known as true positive rate (TPR) and can be computed as:

$$\text{Sensitivity} = \frac{TP}{TP + FN} \quad (6)$$

Specificity: It is a probability of a classifier to predict the result as negative when disease is not present. It is also known as true negative rate (TNR), and can be computed as:

$$\text{Specificity} = \frac{TN}{TN + FP} \quad (7)$$

Positive predicted value (PPV): The probability of a classifier that the disease is present when the test is positive. It is also known as precision, and can be computed as:

$$PPV = \frac{TP}{TP + FP} \quad (8)$$

Negative predictive value (NPV): The probability of a classifier that the disease is not present when the test is negative. It can be computed as:

$$NPV = \frac{TN}{TN + FN} \quad (9)$$

Accuracy: It is one of the primary metrics applied to assess the performance of a classifier. It is computed as the percent of the samples classified correctly, and can be computed as:

$$\text{Accuracy} = \frac{TP + TN}{TP + TN + FP + FN} \quad (10)$$

Matthews correlation coefficient (MCC): The MCC metric is based on the correlation coefficient between the observed and predicted class, returning value in the range $[-1, +1]$. $MCC = +1$ shows a perfect prediction, $MCC = 0$ represents no better than random prediction, and $MCC = -1$ shows full disagreement between the observed and predicted. In general, this metric is accepted as a balanced measure, even if the class size is very distinct. MCC is defined as:

$$MCC = \frac{TP \cdot TN - FP \cdot FN}{\sqrt{(TP + FP) \cdot (TP + FN) \cdot (TN + FP) \cdot (TN + FN)}} \quad (11)$$

False discovery rate (FDR): It assesses the proportion of TPs that is incorrectly classified. It may be used for testing multiple hypotheses. It is defined as:

$$FDR = \frac{FP}{FP + TP} \quad (12)$$

AU-ROC: It is also a valuable and mostly used performance measure for classification problems. AU-ROC is computed using area under the receiver operating characteristic (ROC) curve—plotted using TPR versus FPR at different threshold values. AU-ROC is a good measure for performance comparison because it compares the performance across an entire range of class distributions and error values. It is defined as:

$$AU-ROC = \frac{1}{2} \left(\frac{TP}{TP+FN} + \frac{TN}{TN+FP} \right) \quad (13)$$

F1 score: It is interpreted as the weighted average (or harmonic mean) of the precision and recall. An *F1* score of 1 is considered as best while 0 is worst. *F*-measures do not take the TNs into account. The *F1* score can be computed as:

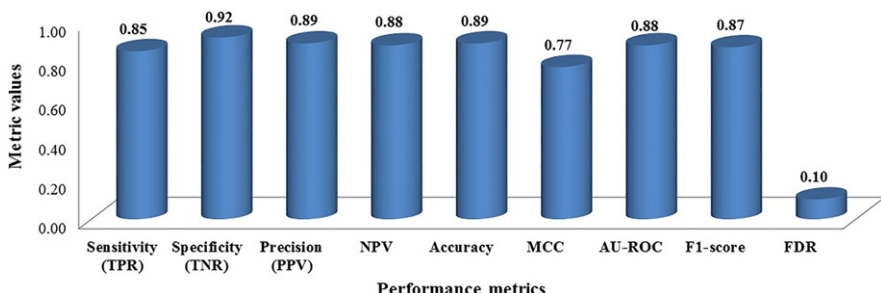
$$F1 \text{ score} = 2 \times \frac{\text{Precision} \times \text{Recall}}{\text{Precision} + \text{Recall}} \quad (14)$$

5 RESULT AND DISCUSSION

The proposed ensemble model was developed and simulated on Weka 3.8 [46] and RapidMinerStudio 7.0 [47] software tools. The model was applied on the StatLog heart disease dataset having a total of 270 patient samples. Out of 270 samples, 120 belonged to the presence of heart disease and 150 belonged to the absence of heart disease. The proposed model was trained and tested with data samples, partitioned 10-fold cross validation. The results of the predictions are shown in the confusion matrix (Table 2), showing TPs, TNs, FPs) and FNs. Out of 120 positive cases, the model was able to accurately predict 102 cases (true positives). Out of 150 negative cases, it was able to accurately prediction 138 (true negatives). The prediction accuracy of the proposed model in terms of various performance metrics has been shown in Fig. 5. It achieves sensitivity (TPR), specificity (TNR), and precision (PPV) of 0.85, 0.92, and 0.89, respectively. Accuracy, MCC, AU-ROC, and *F1* score have been computed to be 0.89, 0.77, 0.88, and 0.87, respectively. The FDR has been 0.10. The prediction accuracy of the proposed ensemble model has been compared

Table 2 Confusion Matrix (Presence/Absence of Heart Disease)

Actual	Predicted		
	Present	Absent	Actual total
Present	102 (TPs)	18 (FNs)	120
Absent	12 (FPs)	138 (TNs)	150
Predicted total	114	156	

**FIG. 5**

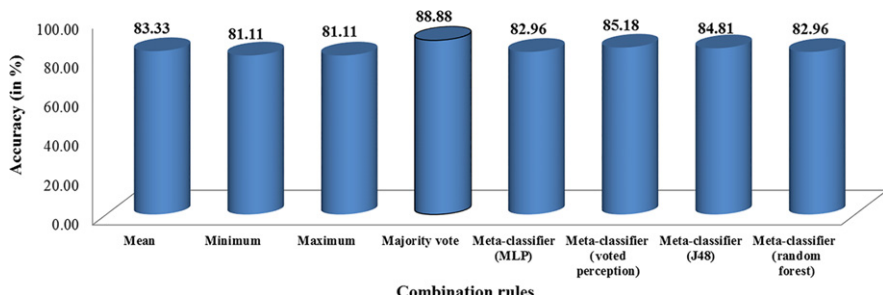
Performance of the proposed ensemble prediction model on the StatLog heart disease dataset.

Table 3 Comparison of Proposed Ensemble Model With Other State-of-the-Art Models in Terms of Accuracy

Methods	Accuracy (%)
Rotation forest ensemble classifiers [3]	80.49
Pruned J48 decision tree with reduced error pruning [6]	73.79
Extreme learning machine (ELM) [7]	80
Hybrid genetic-fuzzy model [26]	86
Logistic regression [28]	85
<i>Proposed ensemble model</i>	88.88

with other previously proposed models tested on the same dataset, as shown in Table 3. It can be seen in Table 3 that the proposed ensemble model achieves an accuracy of 88.88%, which is better than other models, and 3.88% higher than Logistic regression [28] and 2.88% higher than the hybrid genetic-fuzzy model [26].

The proposed ensemble model consisting of three classifiers—logistic regression, multilayer perceptron, and naïve Bayes—has been finalized using a trial-and-error process and due to its better classification accuracy. Similarly, to combine the output of ensemble members, different available rules such as mean, minimum maximum, majority vote, and various metaclassifiers (MLP, voted perception, J48, and random forest) have been exercised but majority vote rule outperforms the other combining methods, as shown in Fig. 6. Therefore, majority vote has been finalized as the combiner in the proposed ensemble model. Hence, our study concludes that using the best performing individual classifiers (such as logistic regression, multilayer perceptron, and naïve Bayes) can be combined using the majority voting rule to improve the prediction accuracy of heart disease.

**FIG. 6**

Performance of the proposed ensemble prediction model with different combination rules on the StatLog heart disease dataset.

6 CONCLUSION AND FUTURE DIRECTIONS

This work focuses on the development of an accurate and reliable prediction model for heart disease in a patient using ensemble learning. In this work, the three best performing classification algorithms, namely logistic regression, multilayer perceptron, and naïve Bayes, and majority voting rule are applied to combine the output of the classifiers. The proposed ensemble method was finalized using a trial-and-error process, which achieved a classification accuracy of 88.88%, which is better than any other single classifier model. The model is robust and reliable in the sense that a group of classification algorithms is used for making the classification decision and safeguarding it from incorrect classification. For a multivariate analysis of data, having both discrete and continuous valued attributes, the CHAID decision tree is constructed for exploratory data analysis.

The main purpose of the proposed ensemble model is to improve the prediction accuracy, robustness, and reliability of the model for heart disease and avoid any misdiagnosis of patients. However, there is still scope for improvement. To diagnose and treat the patient correctly, it is necessary to test the proposed method over a larger dataset with more clinical features. Also, with the advancement in capturing a patient's data electronically, an expert diagnosis system can be integrated with the data collection software tool, which would support the cardiologists in making critical decisions.

REFERENCES

- [1] World Heart Federation Report, <http://www.world-heart-federation.org/>, 2016. Accessed 1 December 2016.
- [2] S. Palaniappan, R. Awang, in: Intelligent heart disease prediction system using data mining techniques, 2008 IEEE/ACS International Conference on Computer Systems and Applications, 2008, pp. 108–115.

- [3] A. Ozcift, A. Gulten, Classifier ensemble construction with rotation forest to improve medical diagnosis performance of machine learning algorithms, *Comput. Methods Prog. Biomed.* 104 (3) (2001) 443–451.
- [4] S.U. Ghumbre, A.A. Ghatol, in: *Heart disease diagnosis using machine learning algorithm*, Proceedings of the International Conference on Information Systems Design and Intelligent Applications, 2012, pp. 217–225.
- [5] P.C. Austin, J.V. Tu, J.E. Ho, D. Levy, D.S. Lee, Using methods from the data-mining and machine-learning literature for disease classification and prediction: a case study examining classification of heart failure subtypes, *J. Clin. Epidemiol.* 66 (4) (2013) 398–407.
- [6] A.K. Pandey, P. Pandey, K.L. Jaiswal, A heart disease prediction model using Decision Tree, *IUP J. Comput. Sci.* 7 (3) (2013) 43.
- [7] S. Ismaeel, A. Miri, D. Chourishi, in: *Using the Extreme Learning Machine (ELM) technique for heart disease diagnosis*, IEEE Canada International Humanitarian Technology Conference, 2015, pp. 1–3.
- [8] L. Verma, S. Srivastava, P.C. Negi, A hybrid data mining model to predict coronary artery disease cases using noninvasive clinical data, *J. Med. Syst.* 40 (7) (2016) 1–7.
- [9] R. Rajkumar, K. Anandakumar, A. Bharathi, Coronary artery disease (CAD) prediction and classification—a survey, *ARPN J. Eng. Appl. Sci.* 11 (9) (2006) 5749–5754.
- [10] Y.T. Lo, H. Fujita, T.W. Pai, Prediction of coronary artery disease based on ensemble learning approaches and co-expressed observations, *J. Mech. Med. Biol.* 16 (01) (2016) 1640010.
- [11] B. Farran, A.M. Channanath, K. Behbehani, T.A. Thanaraj, Predictive models to assess risk of type 2 diabetes, hypertension and comorbidity: machine-learning algorithms and validation using national health data from Kuwait—a cohort study, *BMJ Open* 3 (5) (2013):e002457.
- [12] M. Heydari, M. Teimouri, Z. Heshmati, S.M. Alavinia, Comparison of various classification algorithms in the diagnosis of type 2 diabetes in Iran, *Int. J. Diabetes Dev. Countries* 36 (2) (2015) 167–173.
- [13] A. Colubri, T. Silver, T. Fradet, K. Retzepi, B. Fry, P. Sabeti, Transforming clinical data into actionable prognosis models: machine-learning framework and field-deployable app to predict outcome of Ebola patients, *PLoS Negl. Trop. Dis.* 10 (3) (2016) e0004549.
- [14] A. Jabeen, N. Ahmad, K. Raza, Machine learning-based state-of-the-art methods for the classification of RNA-Seq data, in: N. Dey, A. Ashour, S. Borra (Eds.), *Classification in BioApps*. Lecture Notes in Computational Vision and Biomechanics, vol. 26, Springer, Cham, 2018.
- [15] S.S. Ahmed, N. Dey, A.S. Ashour, D. Sifaki-Pistolla, D. Bălas-Timar, V.E. Balas, J. M. Tavares, Effect of fuzzy partitioning in Crohn’s disease classification: a neuro-fuzzy-based approach, *Medical Biol. Eng. Comput.* 55 (1) (2017) 101–115.
- [16] O. Azzabi, C.B. Njima, H. Messaoud, New approach of diagnosis by timed automata, *Int. J. Ambient Comput. Intell.* 8 (3) (2017) 76–93.
- [17] M.Y. Khachane, Organ-based medical image classification using support vector machine, *Int. J. Synth. Emot.* 8 (1) (2017) 18–30.
- [18] N. Dey, A.S. Ashour (Eds.), *Classification and Clustering in Biomedical Signal Processing*, IGI Global, USA, 2016.
- [19] F. Touati, R. Tabish, U-healthcare system: state-of-the-art review and challenges, *J. Med. Syst.* 37 (3) (2013) 9949.

- [20] M.K. Moridani, S.K. Setarehdan, A.M. Nasrabadi, E. Hajinasrollah, Analysis of heart rate variability as a predictor of mortality in cardiovascular patients of intensive care unit, *Biocybern. Biomed. Eng.* 35 (4) (2015) 217–226.
- [21] Y. Zhu, J. Wu, Y. Fang, Study on application of SVM in prediction of coronary heart disease, *J. Biomed. Eng.* 30 (6) (2013) 1180–1185.
- [22] J. Soni, U. Ansari, D. Sharma, S. Soni, Predictive data mining for medical diagnosis: an overview of heart disease prediction, *Int. J. Comput. Appl.* 17 (8) (2011) 43–48.
- [23] I. Kadi, A. Idri, J.L. Fernandez-Aleman, Knowledge discovery in cardiology: a systematic literature review, *Int. J. Med. Inform.* 97 (2017) 12–32.
- [24] J.V. Tu, L. Donovan and D. Lee, Quality of cardiac Care in Ontario: EFFECT (enhanced feedback for effective cardiac treatment), Institute for Clinical Evaluative Sciences (2004).
- [25] J.V. Tu, L.R. Donovan, D.S. Lee, J.T. Wang, P.C. Austin, D.A. Alter, D.T. Ko, Effectiveness of public report cards for improving the quality of cardiac care: the EFFECT study: a randomized trial, *JAMA* 302 (21) (2009) 2330–2337.
- [26] T. Santhanam, E.P. Ephzibah, Heart disease prediction using hybrid genetic fuzzy model, *Indian J. Sci. Technol.* 8 (9) (2015) 797.
- [27] V. Poornima, D. Gladis, Hybrid classifier and orthogonal local preserving projection for heart disease prediction, *Int. J. Appl. Eng. Res.* 10 (15) (2015) 35470–35480.
- [28] A.K. Dwivedi, Performance evaluation of different machine learning techniques for prediction of heart disease, *Neural Comput. Appl.* (2016) 1–9.
- [29] R. Polikar, Ensemble Learning, in: C. Zhang, Y. Ma (Eds.), *Ensemble Machine Learning: Methods and Applications*, Springer, New York, 2012, pp. 1–34.
- [30] T.G. Dietterich, Ensemble learning, in: *The Handbook of Brain Theory and Neural Networks*, second ed., The MIT Press, Cambridge, 2002, pp. 110–125.
- [31] L. Breiman, Bagging predictors, *Machine Learning* 24 (2) (1996) 123–140.
- [32] M. Skurichina, R.P. Duin, Bagging, boosting and the random subspace method for linear classifiers, *Pattern Anal. Appl.* 5 (2) (2002) 121–135.
- [33] T.K. Ho, The random subspace method for constructing decision forests, *IEEE Trans. Pattern Anal. Mach. Intell.* 20 (8) (1998) 832–844.
- [34] R. Detrano, A. Janosi, W. Steinbrunn, M. Pfisterer, J.J. Schmid, S. Sandhu, et al., International application of a new probability algorithm for the diagnosis of coronary artery disease, *Am. J. Cardiol.* 64 (5) (1989) 304–310.
- [35] SPSS, IBM SPSS Statistics for Windows, Version 20.0, Armonk, NY: IBM Corp.
- [36] D.W. Hosmer Jr., S. Lemeshow, R.X. Sturdivant, *Applied Logistic Regression*, vol. 398, John Wiley & Sons, New York, 2013.
- [37] S. Haykin, *Neural Networks and Learning Machines*, third ed. Pearson, New Jersey.
- [38] K. Raza, A.N. Hasan, A comprehensive evaluation of machine learning techniques for cancer class prediction based on microarray data, *Int. J. Bioinforma. Res. Appl.* 11 (5) (2015) 397–416.
- [39] I.A. Basheer, M. Hajmeer, Artificial neural networks: fundamentals, computing, design, and application, *J. Microbiol. Methods* 43 (1) (2000) 3–31.
- [40] B. Yegnanarayana, *Artificial Neural Networks*, PHI Learning Pvt Ltd, India, 2009.
- [41] I. Rish, in: An empirical study of the naive Bayes classifier, *IJCAI 2001 Workshop on Empirical Methods in Artificial Intelligence*, 3 (22) 2001, pp. 41–46.
- [42] L. Jiang, D. Wang, Z. Cai, X. Yan, Survey of improving naive Bayes for classification, *International Conference on Advanced Data Mining and Applications*, Springer, Berlin, Heidelberg, 2007, pp. 134–145.

- [43] M. Kirk, *Thoughtful Machine Learning*, first ed., O'Reilly, USA, 2017, Chapter 4.
- [44] J. Kittler, M. Hatef, R.P. Duin, J. Matas, On combining classifiers, *IEEE Trans. Pattern Anal. Mach. Intell.* 20 (3) (1998) 226–239.
- [45] L.I. Kuncheva, *Combining Pattern Classifiers: Methods and Algorithms*, John Wiley & Sons, New York, 2004.
- [46] M. Hall, E. Frank, G. Holmes, B. Pfahringer, P. Reutemann, I.H. Witten, The WEKA data mining software: an update, *ACM SIGKDD Explor. Newslett.* 11 (1) (2009) 10–18.
- [47] M. Hofmann, R. Klinkenberg, *RapidMiner: Data Mining Use Cases and Business Analytics Applications*, CRC Press, Boca Raton, 2013.

FURTHER READING

- [48] I. Kononenko, Machine learning for medical diagnosis: history, state of the art and perspective, *Artif. Intell. Med.* 23 (1) (2001) 89–109.
- [49] A. Jabeen, N. Ahmad, K. Raza, Machine learning-based state-of-the-art methods for the classification of RNA-Seq data, in: N. Dey, A. Ashour, S. Borra (Eds.), *Classification in BioApps*, Lecture Notes in Computational Vision and Biomechanics, vol. 26, Springer, 2018, pp. 133–172.

Machine learning for medical diagnosis: A neural network classifier optimized via the directed bee colony optimization algorithm

9

Saurabh Kumar Agrawal*, Bhanu Pratap Singh*, Rajesh Kumar*, Nilanjan Dey[†]

Department of Electrical Engineering, Malaviya National Institute of Technology (NIT), Jaipur, India* Department of Information Technology, Techno India College of Technology, Kolkata, India[†]

CHAPTER OUTLINE

1 Introduction	197
2 Neural Network Dynamics	200
3 Directed Bee Colony Optimization Algorithm	201
4 Experimental Setup	204
5 Result and Discussion	204
6 Conclusion	213
References	214
Further Reading	215

1 INTRODUCTION

In this chapter, the diagnosis of breast cancer, diabetes, and heart disease is being considered. In 2008, around 7.6 million people died of cancer, from out of which 458,000 deaths were due to breast cancer (<http://www.who.int/mediacentre/factsheets/fs297/en/>). In the United States, there is a death every 33 seconds as a consequence of heart disease (<http://www.theheartfoundation.org/heart-disease-facts/heart-disease-statistics/>). According to the National Diabetes Fact Sheet 2011, 25.8 million people in the United States suffer from diabetes and approximately 7.0 million remain undiagnosed (<http://www.diabetes.org/diabetes-basics/diabetes-statistics/>). Reliable and fast methods are essential in the diagnosis of such diseases.

197

Data-mining techniques, such as classification, clustering, prediction, etc., have found wide applications for medical diagnosis in epidemiological areas, primarily due to their speed. A majority of the applications of data-mining techniques in medicine have used classification techniques [1]. Many ongoing research works use different techniques for cataloging the different classes of medical problems.

The speed factor is incorporated in any computer-aided system. Different approaches have been proposed for reliability consideration. A few of the research works have utilized unsupervised learning-based algorithms and statistical classification, such as radial bias function (RBF) and the Bayesnet algorithm, respectively. Supervised learning algorithms are generally more frequently used in such applications. In supervised learning, the weights of the artificial neural network (ANN) are optimized by gradient decent, such as back propagation (BP). However, it is difficult to generalize BP due to its tendency to converge to local minima. Heuristic-based techniques such as genetic algorithm (GA), particle swarm optimization (PSO), and artificial bee colony (ABC) exhibit a greater probability of attaining global optima as compared with the gradient decent. However, heuristic techniques lack speed when compared with the gradient method. A hybridized gradient and heuristic approach such as GALM provides improved results. A few other methods that have been used in medical diagnosis are bagging, multiboost, NBTree, Ridor, Voting Feature Intervals (VFI), and K-star.

Of the mentioned methods, the practicality and convenience of ANNs has been realized due to their successful application in numerous problems in a variety of fields with varying degrees of complexity [2–6]. ANN is highly useful for solving nonlinear systems, or systems where the input-output relation is either unknown or greatly complex. The choice of algorithm in the ANN is based on the complexity of the problem. The main component of the neural network consists of adaptability, capability, learning, and generalization [7]. In the medical domain, ANN may be used to map a disease-related attribute to the output of the diagnosis process to provide computation aid to the medical diagnosis. The application of ANN to any application presents several challenges, which include optimal selection of parameters such as learning rate, initial weights, and the number of neurons along with the selection of the weight-updating rule and the respective algorithm.

Lately, several approaches have been purposed to design ANN's with the help of many nature-based algorithms. GA is a probabilistic approach that mimics the process of natural evolution. This algorithm considers the enormous set of possibilities as a genetic sequence and the emphasis on reproduction of the fittest gene sequence. GA comprises three operations—selection, crossover, and mutation—to reproduce a new population [8]. Some authors have used hybrid techniques to combine GA with a derivative approach. This hybrid approach initially tries to find the optimum result with the help of GA. After that the generated population is used for optimization in the help of differential-based techniques [7]. PSO [9] has its roots in swarm intelligence and depends on both the local and global performance of the swarm. This algorithm mimics the social behavior of a group. This algorithm represents each solution as a particle that searches for the best position by adjusting its velocity according to a concept derived from the behavior of bird flocking and fish schooling.

This technique does not use the gradient and has a smaller degree of randomness, so it can be applied on a wider classification domain [9, 10]. The robustness of PSO has permitted its use in the classification of the medical domain with higher accuracy. The comparison of PSO with many other conventional techniques has also been done by the authors of the reference paper [11].

Some advanced mechanisms [12] have also been suggested. This paper uses a random population-based evolution strategy. It utilizes its own adaptive parameters to control the step size for a generation of the new mutated population. A new selection operator was proposed, which helps in creating the mating pool and then provides the other survivors for the next generation, which helps in maintaining the diversity of individuals so that the best result among all could be selected for receiving the most optimized result.

The other method to overcome the inadequacy of all the algorithms includes the hybridization of evolutionary search (ES), GA, PSO, and ANN, and is named EAP-SONN [8], where ES and GA have the advantage of maintaining the global search while PSO helps in fine tuning the local individual values for better or optimal solutions. For performing the exploitation task in a better way, BP and the Levenberg Marquardt training networks are used to attain faster and more accurate results.

In this paper, we have done an extensive comparison with the algorithms that have been implemented by various authors [7, 11, 13, 14]. Though gradient descent approaches, are generally faster than heuristic approaches, the important upshot of the bioinspired algorithms over the gradient algorithms is their adaptive property that enables them to work on the principal of making the whole population toward a better fitness for the search of the most optimized result. Another shortcoming of gradient-based approaches is their dependency on initial population for generation of the final optimal solution. Gradient-based approaches try to reach a nearby minima, which might be a local minima. The recent advancements for classification by the use of nature-inspired algorithms involve the use of bee algorithms for the classification. Other bee algorithms are bee colony optimization (BSO), bee system (BS) [15], and artificial bee colony (ABC) [16]. Bee algorithms mimic the waggle dance performed by bees to share site information. We have proposed DBC [17], which is based on the group decision-making strategy of bees for site selection and forming the new colony. DBC uses both consensus and quorum processes for decision-making. The ability of the DBC to create a profound parallelism by increasing the number of dimensionalities of the search makes DBC a faster algorithm than other algorithms. The computation time of DBC has been compared to GA and PSO. Also, the flavor of the heuristic search increases the search space and hence increases the probability of finding an optimal solution. A disadvantage associated with random direct search or heuristic-based algorithms is a different solution at every iteration. This drawback is outperformed with the DBC algorithm as it always gives a unique solution and hence increases the reliability of the algorithm while containing the important components of classification, that are its accuracy and speed.

This paper is further organized as follows: Section 2 formulates the neural network dynamics that are to be optimized. Section 3 describes the DBC algorithm, the

bee search methodology, and the design of algorithms. Section 4 details the medical diagnosis dataset used in the experiment. Section 5 compares and tabulates the results of our algorithm. Section 6 concludes that the DBC algorithm is faster, more accurate, and gives a unique solution.

2 NEURAL NETWORK DYNAMICS

Artificial intelligence algorithms are used predominately to assist medical diagnosis [18]. The ability of a neural network to solve nonlinear problems has made these systems a popular choice in epidemiological areas.

A three-layer architecture design (input-hidden-output) is used for diagnosis. Let N_i be the number of neurons in the input layer, N_h be the number of neurons in the hidden layer, and N_o be the number of neurons in the output layer. Let $x^{(i)} = \{x_1, x_2, \dots, x_{N_i}\}$ be the input pattern and $y^{(i)} = \{y_1, y_2, \dots, y_{N_o}\}$ be the corresponding output. The fitness function (Ψ) for optimization can be as follows:

$$\Psi_{\max}(\theta) = \text{Max} \left(\frac{1}{m} \sum_{i=1}^m \text{cost}(h_\theta x^{(i)}, y^{(i)}) \right) \quad (1)$$

where $m \in \{N_i, N_h\}$ and θ is weights vector $\theta = \{w_1, w_2, \dots, w_{N_h(N_i+N_o)+2}\}$ that is to be optimized and the cost function is chosen as:

$$\text{cost}(h_\theta x^{(i)}, y^{(i)}) = \frac{1}{(h_\theta x^{(i)} - y^{(i)})^2} \quad (2)$$

where $h_\theta x^{(i)}$ is a sigmoid function that is used to map one layer to its preceding layer, which is given as follows:

$$h_\theta x^{(i)} = \frac{1}{1 + e^{-\sum_{j=1}^m \theta_j^{(i)} x^i}} \quad (3)$$

The fitness function as given in Eq. (1) is a function of weights (θ) so the algorithm has to search for optimum set weights such that errors in the system can be reduced. We are using the mean square error (MSE) function as given in Eq. (2) to calculate the error. The reciprocal rule is used to convert a minima problem into a maxima problem such that the fitness function (Ψ) as given in Eq. (1) is formulated using the summing up reciprocal of MSE. MSE is a nonconvex function, hence it can have more than one minima. Out of them, only one would be a global minima and the rest would be local minima. So, DBC makes efforts to find this optimal or near optimal solution. Fig. 1 delineates the neural network architecture used in this paper. b_1 and b_2 denote the bias unit. θ_{ih} and θ_{ho} denote the weights between the input-hidden layer and the hidden-output layer, respectively.

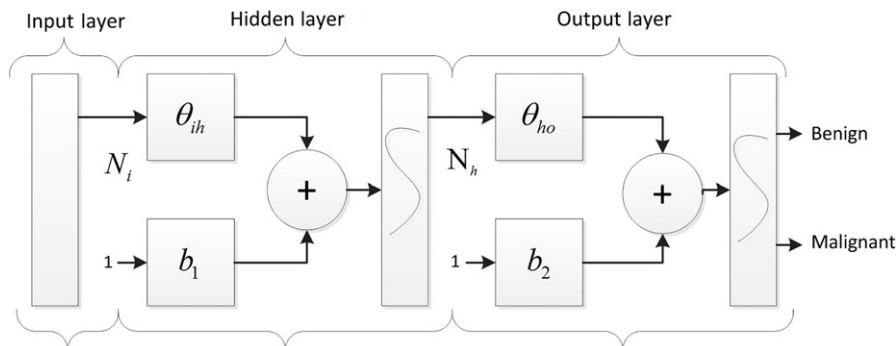


FIG. 1

NN architecture.

3 DIRECTED BEE COLONY OPTIMIZATION ALGORITHM

Real-world optimization problems are challenging to solve and many applications also have to deal with NP-hard problems. To solve such problems, optimization algorithms are required, which promises not the optimal but a good solution to the problem. There is no guaranteed tool to provide the optimal solution for NP problems. New optimization algorithms are evolving that may provide a better solution to the generated problems. Nature-inspired algorithms such as PSO and the cuckoo algorithm have gained popularity due to their high efficiency and efficacy. In this problem as well, we have optimized the ANN structure with three different nature-inspired algorithms. The comparison has been done between most the commonly used bioinspired algorithms, that is, GA, swarm intelligence-based PSO, and the newly proposed directed bee colony (DBC) optimization algorithm from our earlier literature [17]. The researchers are familiar with the former two algorithms, hence a brief overview and the description of only DBC is illustrated below. Researchers have largely focused on swarm-inspired algorithms as the decisions made by the swarms are robust. Apart from providing the best result, they tend to save a lot of energy of the swarm because of the mutual guidance between swarm members. DBC has also been inspired from the food searching analogy in bee swarms.

The bees tend to achieve a common goal in the society, which helps them to achieve higher accuracy and speed. The bees are sent to different fragments of the whole search space. The quiescent bees then tend to find the optimized result in their subregion. The bee remembers the last two best sites and passes the information regarding the optimal position. The best food site is chosen by one of the deciding methods either consensus or quorum. There are certain assumptions in the algorithm such as the bees live and act in a specified environment and not beyond it, bees tend to achieve a common particular task, the waggle dance passes whole

information without any loss, and bees will not die. Hence the energy may change w.r.t. bee quantity but total bees remain constant during the process are considered.

An exploration region $FSR \in R^d$, $d = 1, \dots, n$ is a bounded region representing a feasible solution to a problem, a grid on FSR , $G = \{E_i\}_{i=1}^N$ to be a set of elements, E_i , such that $E_i \in R^d$, $\bar{E}_i = R^d$, $\bar{E}_i \cap E_j = \emptyset, i \neq j$ and $\cup E_i = FSR$, where \bar{E}_j denotes the interior of E_i and \emptyset is an empty set. A subexploration region $E_i = FIV^m$ is a vector of m integers that represents feasible solutions to the problem and a food index variable $FIV \in c$ is an integer that is allowed in a food search region. $c \subset Z^q$ is a set of all integers that are allowed in FSR . The requirement that $FIV \in c$ is called constraint.

In DBC, all the bees are allotted an environment (i.e., FSR). FSR corresponds to search space. Each quiescent bee is allotted a lattice point. The position of the bee suggests the position of the bee in the environment and the evaluated function value for the bee. The range of the j th parameter is denoted by $[W_{ji}, W_{jf}]$, where the former represents the lower bound for the parameter and the latter denotes the upper bound. The variables decide the total dimension of the lattice. Thus the lattice of the objective function, which is governed by d number of parameters, can be viewed as a d -dimensional lattice unit. There is a different axis representing each of the parameters and this will also denote the range of the parameter. The lattice illustration is shown in Fig. 2. The search methodology is explained in detail in the next section. The starting point of the bee is taken to be the midpoint of each step or bounds for that parameter. The midpoint of the total group of the bees is given by Eq. (4).

$$\left[\frac{W_{1i} + W_{1f}}{2}, \frac{W_{2i} + W_{2f}}{2}, \dots, \frac{W_{ni} + W_{nf}}{2} \right] \quad (4)$$

The analogy of the algorithm has been adopted by bees and only four locations at a time are memorized for future exploration of the search space. The Nelder-Mead (NM) algorithm is adopted for optimization. The most adopted process of NM based on geometric operations—reflection, expansion, contraction, and shrinking—is applied. The NM algorithm is depicted as the DBC food search algorithm. It generates a sample of $n + 1$ points in the search space (i.e., FSR). The points are arranged according to their objective function value depicted as the fitness value of the point. The fitness values are arranged from $S[0]$ to $S[n]$, where the former depicts the best value and the latter the worst value. The algorithm then evaluates the center m of the n best points and then reflects it to obtain a new point r . If r is better than the best solution of the present iteration, further expansion in the direction is done; otherwise, r replaces the worst point (i.e., $S[n]$). Then the contraction point is created somewhere between r and m . Contraction is processed when the value of e is not better than r . The exchange of $S[n]$ along with c will be made if c is better than r ; otherwise not. When no search direction is found, the exploration shrinks by moving all the points except the best one onto the best solutions direction. The parameters have been taken as $\alpha = 1$, $\beta = 1/2$, $\gamma = 1$, and $\sigma = 1/2$.

After returning from their exploration, bees pass on the individual optimal solution to the centralized system that chooses a preferable solution from the food search space. A food quality index $FQI : FSR \rightarrow R$ is a measure of the quality of solution

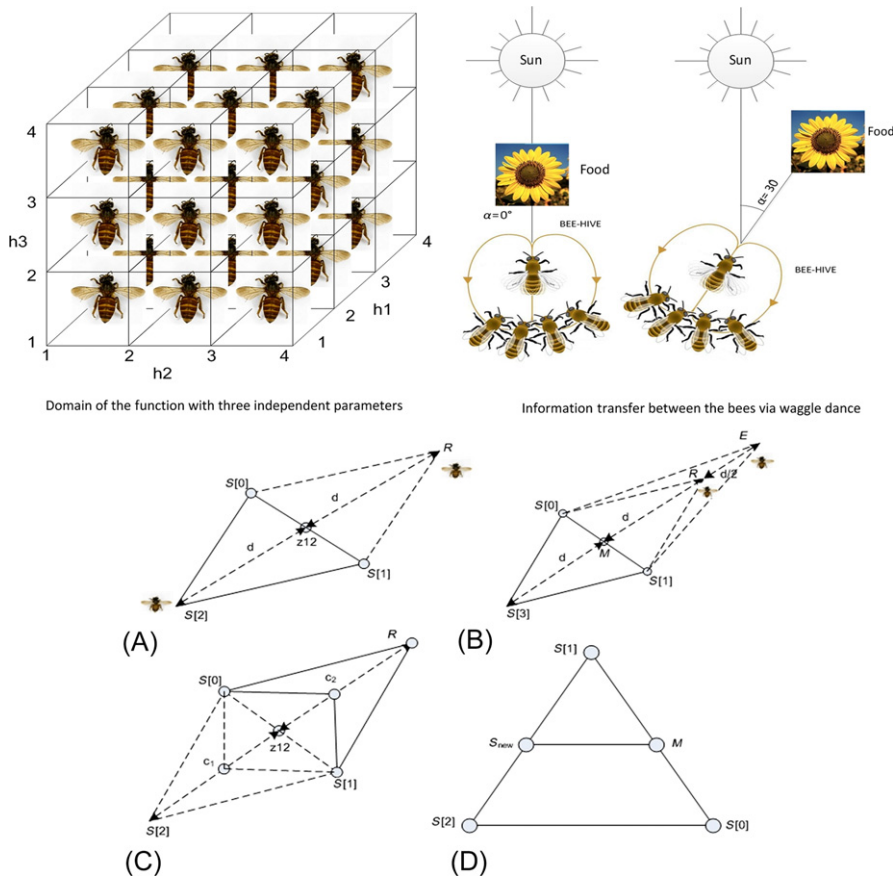


FIG. 2

DBC search methodology and analogy. Bees search movements with the proposed algorithm (A) starting of the motion in search of solution, (B) extension in the direction of optimal point, (C) contraction of the movement in case optimal point quality is not good, and (D) shrinking of the space toward optimistic solution.

that is represented by the bee food search procedure. There is an FQI, that is obtained by the optimal solution for each bee in the FSR. The FQI is mathematically equivalent to the food value (FV) obtained by each bee.

$$FQI(i) = \min(FV(i)) \quad (5)$$

The problem that occurs in most of the algorithms is, when more than one point has the equal optimal value, it fails to decide which one to choose. In DBC, when a bee encounters such a situation, it chooses the nearest optimal point from its starting point and reports the same to the hive. As also discussed, the two methods employed by the bee swarm decision for finding the best nest site are consensus and quorum.

In consensus, the whole group decides on selecting the global best solution, which is replicated as the best solution among all the optimal solutions of the bees.

$$f(X_G) = \min(FQI(i)) \quad (6)$$

In quorum, the best optimal food site is decided as soon as the best site reaches the quorum (threshold) value (*QuoThresh*). The value of the threshold also plays a vital role. If the *QuoThresh* is too high, then the computational time would decrease but the results may be inaccurate, and if its too low, the computational time would increase substantially.

The algorithm has been summarized in [Algorithms 1](#) and [2](#) along with a flowchart ([Fig. 3](#)).

4 EXPERIMENTAL SETUP

This section deals with the information of the data taken for the examination. The problems of the medical domain taken for the evaluation are breast cancer, heart disease, and diabetes. The datasets are collected from the University of California at Irvine (UCI) repository of the machine learning database [\[19\]](#) and PROBEN1 [\[20\]](#).

The three problems deemed for the evaluation have been divided into training sets and the testing examples. The problems taken up have been illustrated as:

- 1. Breast cancer:** This problem has 699 example sets. The first 500 sets have been taken for the training of the NN and the last 199 for the evaluation of the classification error percentage (CEP). An NN of 9-6-2 (nine inputs, six hidden units, and two output units) is taken.
- 2. Diabetes:** This problem has 768 examples. The first 500 example sets have been taken for training and the last 268 sets have been taken for the evaluation of the CEP. An NN of 8-5-2 is taken for this problem.
- 3. Heart disease:** This problem has 920 example sets. The first 600 were taken for training of the NN and the last 320 were taken for the evaluation for CEP. An NN of 35-23-2 has been taken for heart disease.

The maximum number of iterations taken for each of the problems was 100 though with DBC; the CEP for each problem remained the same for every iteration. The architecture of the ANN has been illustrated in [Table 1](#). The lower (W_{ji}) and upper bound (W_{jj}) for weights is set as -10 and 10 , respectively.

5 RESULT AND DISCUSSION

Comparing and contrasting with the other nature-inspired algorithms is discussed in this section. The threefold tasks that have been accomplished for classification of diseases by the use of DBC are unique solution, least time consumption, and comparable accuracy. The bioinspired algorithm leads to better and global solutions but the randomness of the approach ensures a different solution after every run. The

Algorithm 1 DBC ALGORITHM

Input: $f(x)$: Objective function to minimize
Input: BEES: Number of bees, Swarm: swarm of the BEES,
 $BestSol$: best food site
Input: Var: Number of dimensions, W_i : Lower bound for each dimension sequentially
Input: W_j : Upper bounds for each dimension
Input: QuoThresh: Quorum threshold, Iter = 1, Flag = False
Output: OptimalFood_Site → the global best solution found

```

1 // Generate swarm in the FSR ;
2 Swarm ← GeneratePopulation (BEES, Var,  $W_i$ ,  $W_j$ );
3  $a \in rand(0, 1)$ ;  $b \in rand(0, 1)$ ;
4 // Selection of the Swarm Decision Technique to ascertain best nest site. ;
5 if  $a < b$  then
6   GoTo Line 9;
7 else
8   GoTo Line 23;
9 // Quorum Technique;
10  $BestSol = MAX\_VALUE$ ;
11 while Iter < BEES do
12   // Call Nelder-Mead Algorithm for best food site of bee sequentially. ;
13   Sol = Call Algorithm 2 ←  $Swarm_{Iter}$ ;
14   if Sol < BestSol then
15     BestSol = Sol;
16   if BestSol < QuoThresh then
17     Flag = True;
18     break;
19   Iter = Iter + 1;
20 if Flag == True then
21   GoTo Line 30;
22 else
23   // Move To Consensus Approach ;
24   Continue;
25 // Consensus Technique
26 while Iter < BEES do
27   Sol = Call Algorithm 2 ←  $Swarm_{Iter}$ ;
28   if Sol < BestSol then
29     BestSol = Sol;
30   Iter = Iter + 1;
31 OptimalFood_Site = BestSol;
32 return OptimalFood_Site;
```

Algorithm 2 NELDER-MEAD ALGORITHM AS DBC FOOD SEARCH ALGORITHM

Input: $f(x)$: Objective function to minimize
Input: $n + 1$: number of points in simplex
Input: $\alpha, \beta, \gamma, \sigma$: reflection, expansion, contraction, and shrink coefficients
Output: $x^* \rightarrow$ the best solution candidate found

```

1   $S \leftarrow createPop(n + 1);$ 
2  while stop criterion not met do
3       $S \leftarrow sortPop(S, f);$ 
4      // Center of mass: determine the center of mass of the  $n$  best
         points;
5       $m \leftarrow \frac{1}{n} \sum_{i=0}^{n-1} S[i];$ 
6      // Reflection: reflect the worst point over  $m$ ;
7       $r \leftarrow m + \alpha(m - S[n]);$ 
8      if  $f(S[0]) < f(r) < f(S[n])$  then
9           $S[n] \leftarrow r$ 
10     else
11         if  $f(r) \leq f(S[0])$  then
12             // Expansion: try to search further in this direction;
13              $e \leftarrow r + \gamma(r - m);$ 
14             if  $f(e) < f(r)$  then
15                  $S[n] \leftarrow e;$ 
16             else
17                  $S[n] \leftarrow r;$ 
18     else
19          $b \leftarrow true;$ 
20         if  $f(r) \geq f(S[n - 1])$  then
21             // Contraction: a test point between  $r$  and  $m$ ;
22              $c \leftarrow \beta r + (1 - \beta)m;$ 
23             if  $f(c) < f(r)$  then
24                  $S[n] \leftarrow c;$ 
25                  $b \leftarrow false;$ 
26         if  $b=true$  then
27             // Shrink toward the best solution candidate  $S[0]$ ;
28             for  $i$  from  $n$  down to 1 do
29                  $S[i] \leftarrow S[0] + \sigma(S[i] - S[0]);$ 
30 return  $S[0];$ 
```

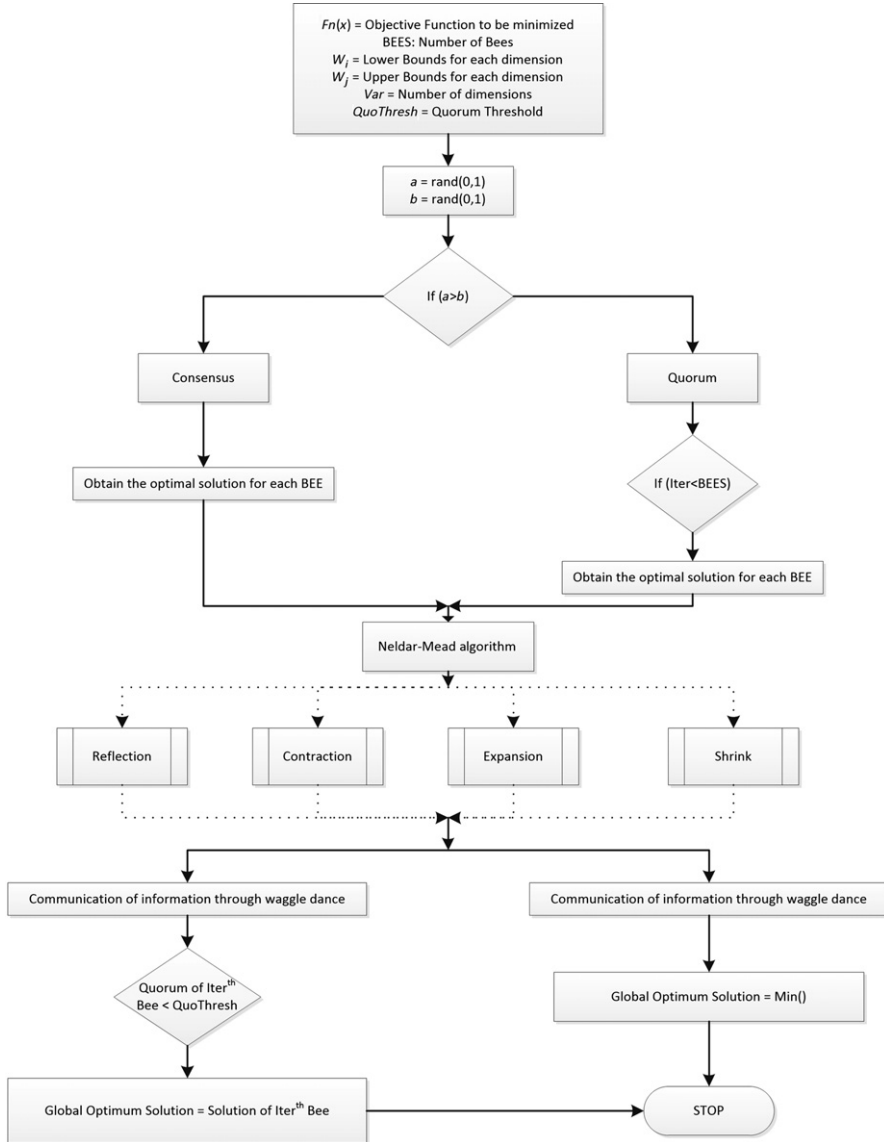


FIG. 3

Flowchart of DBC algorithm.

Table 1 Architecture of ANN

Problem	Cancer	Diabetes	Heart
Training pattern	500	500	600
Testing pattern	199	268	320
Max iteration	100	100	100
Input nodes	9	8	35
Hidden nodes	6	5	23
Output nodes	2	2	2

peculiarity of DBC is the uniqueness of its solution. After every run, the solution rendered by DBC remains the same, thus making it more reliable for online applications. In the medical domain, where the assortment of the affected role is done into the benign or malignant category, the uniqueness of the classification is of great significance. Moreover, the accuracy of classification by the algorithm is also very crucial in the medical field as the problem of the patient needs to be diagnosed as soon as possible. Hence the accuracy of the bioinspired algorithms has also been compared with DBC [7, 11, 13, 14]. On average, the accuracy of DBC came out to be second best among all available algorithms used on these datasets. Previous implementations have also used three quadrants of the data for training and the rest for testing. The problem with most of the other algorithms is that they may have the tendency to converge at local minima, thus the optimum solution rendered by the algorithm is different after every run. The third characteristic of DBC is its least optimization time as compared to the other bioinspired algorithms. DBC divides the search space in small regions, just as a bee is assigned to a particular region for a food search. So once a search space is covered by a bee, other members would not have to go through that area. This strategy reduces the effort made for a particular point in the region. Whereas in other bioinspired algorithms, one point can be covered more than once due to the nature of randomness in the algorithm. Hence the time taken by the DBC is least among other nature-inspired algorithms. Thus we observed and verified that the required features for cataloging of the affected role in the medical domain are justified by DBC. For better justification of results, five cross-validation methods have been used. The comparison of the CEP is given below. The results have been taken from some recent findings [11, 14]. Other than accuracy, the standard deviation of the result rendered by the algorithm is also of great significance. The value of standard deviation has also been compared here in [Tables 2–5](#). The value of standard deviation advertises that with what rate the algorithm is providing the same result. The method of comparison is the same as that adopted by the authors of [14]. The ranking method is also applied in two criteria by finding the average values of the CEP and standard deviation and also the sum of the ranking of the algorithm of each problem.

The first criterion for the comparison includes taking the average of all the CEP [14]. According to the average CEP value attained by the algorithm rank is assigned to them. This has been done for both the CEP as well as the standard deviation to check both the qualities of classification as well as accuracy.

In criterion 2, again the ranking method has been adopted but the ranks were given individually for all three domains. The algorithm has been assigned a rank according to its CEP for each domain. Later, the sum of all the individual ranks has been taken for allotting the final rank to each of the algorithms. The same criterion has also been applied for the standard deviation of the CEPs attained by each of the algorithms. The criteria have been applied on both CEPs as well as the standard deviation in order to check both classification accuracy as well as the recurrence of the same accuracy for more promising results in run-time applications.

Table 2 Average Classification Error Percentages and Ranking of the Techniques on Basis of Criterion 1

Algorithms	Cancer	Diabetes	Heart	Average of CEP	Rank
RBF	20.27	39.16	45.25	34.89	17
GA	16.76	36.46	41.5	31.57	16
GABP	1.43	36.46	54.3	30.73	15
LM	3.17	25.77	34.73	21.22	14
K star	2.44	34.05	26.7	21.06	13
VFI	7.34	34.37	18.42	20.04	12
Ridor	6.36	29.31	22.89	19.52	11
NBTree	7.69	25.52	22.36	18.52	10
Bagging	4.47	26.87	20.25	17.19	9
MlpAnn	2.93	29.16	19.46	17.18	8
multiboost	5.59	27.08	18.42	17.03	7
GALM	0.02	28.29	22.66	16.99	6
BP	0.91	21.76	27.41	16.69	5
PSO	3.68	24.97	21.41	16.69	4
Bayesnet	4.19	25.52	18.42	16.04	3
DBC	2.75	21.25	18	14	2
ABC	2.81	22.39	14.47	13.22	1

The computational time taken by the algorithm to reach the optimal solution has also been tabularized in [Table 6](#). The computation time of DBC has been compared with the same dataset and the same machine with PSO and GA. The computational time is also of utmost importance because, during run-time operations, the result needs to be computed with negligible standard deviation along with unparalleled accuracy.

To check correction of the implemented binary classification test, some statistical measures such as sensitivity and specificity are evaluated. Sensitivity is a measure of the fraction of actual positives that is correctly recognized as such (e.g., the percentage of sick people who are correctly recognized as having the disease). It is also referenced as the true positive rate or the recall rate. Specificity measures the negative fraction of the dataset that is correctly recognized (e.g., the percentage of healthy people who are correctly identified as not having the disease), which is also known as the true negative rate. A perfect predictor would be defined as 100% sensitive (i.e., predicting all people from the sick group as sick) and 100% specific (i.e., not predicting anyone from the healthy group as sick). The resultant output of classification can be cataloged in four categories: true positive (TP), false positive (FP), true negative (TN), and false negative (FN). These terms are defined as:

- True positive: Malign subject correctly diagnosed as sick.
- False positive: Benign subject incorrectly identified as sick.

Table 3 Average Standard Deviation and Ranking of the Techniques on Basis of Criterion 1

Algorithms	BP	LM	GA	GABP	GALM	DBC	PSO	GMR GA	IPSO Net
Cancer	0.28	1.29	6.15	4.87	0.11	0.00	1.58	0.19	0.0057
Diabetes	0.38	3.26	0	0	1.15	0.00	3.17	0.63	0.0123
Heart	1.48	3.68	14.68	20.03	0.82	0.00	2.72	1.14	0.0342
Average	0.71	2.74	6.94	8.3	0.69	0.00	2.49	0.66	0.0174
Rank	5	7	8	9	4	1	6	3	2

Table 4 Average Classification Error Percentages and Ranking of the Techniques on the Basis of Criterion 2

Algorithms	Cancer	Rank of Cancer	Diabetes	Rank of Diabetes	Heart	Rank of Heart	Total Sum of the Ranks	Final Rank
RBF	20.27	17	39.16	15	45.25	14	46	13
GA	16.76	16	36.46	14	41.5	13	43	12
GABP	1.43	3	36.46	14	54.3	15	32	11
Ridor	6.36	13	29.31	10	22.89	9	32	11
VFI	7.34	14	34.37	13	18.42	3	30	10
K star	2.44	4	34.05	12	26.7	10	27	9
NBTree	7.69	15	25.52	5	22.36	7	27	9
LM	3.17	8	25.77	6	34.73	12	26	8
Bagging	4.47	11	26.87	7	20.25	5	23	7
multiboost	5.59	12	27.08	8	18.42	3	23	7
MlpAnn	2.93	7	29.16	11	19.46	4	22	6
PSO	3.68	9	24.97	4	21.41	6	19	5
GALM	0.02	1	28.29	9	22.66	8	18	4
Bayesnet	4.19	10	25.52	5	18.42	3	18	4
BP	0.91	2	21.76	3	27.41	11	14	3
ABC	2.81	6	22.39	2	14.47	1	9	2
DBC	2.75	5	21.25	1	18	2	8	1

Table 5 Average Standard Deviation and Ranking of the Techniques on the Basis of Criterion 2

Algorithms	BP	LM	GA	GABP	GALM	DBC	PSO	GMR GA	IPSO Net
Cancer	0.28	1.29	6.15	4.87	0.11	0.00	1.58	0.19	0.0057
Rank for cancer	5	6	9	8	3	1	7	4	2
Diabetes	0.38	3.26	0	0	1.15	0.00	3.17	0.63	0.0123
Rank for diabetes	3	7	1	1	5	1	6	4	2
Heart	1.48	3.68	14.68	20.03	0.82	0.00	2.72	1.14	0.0342
Rank for heart	5	7	8	9	3	1	6	4	2
Sum of rank	13	20	18	18	11	3	19	12	6
Rank	5	8	6	6	3	1	7	4	2

Table 6 Table for Comparison of Computational Time (in Seconds)

Medical Problem	PSO	GA	DBC
Cancer	209.6	342.23	197.06
Diabetes	178	300	153.66
Heart	763.84	1280	601.356
Total	1151.44	1922.23	952.08

Table 7 Statistical Analysis of DBC

Medical Problem	Sensitivity	Specificity	Precision
Cancer	0.9932	0.9331	0.9663
Diabetes	0.7399	0.8144	0.6498
Heart	0.7906	0.8419	0.7885

- True negative: Benign subject correctly identified as healthy.
- False negative: Malign subject incorrectly identified as healthy.

Based on these terms, sensitivity is defined as

$$\text{Sensitivity} = \frac{TP}{TP + FN} \quad (7)$$

Specificity is defined as

$$\text{Specificity} = \frac{TN}{TN + FP} \quad (8)$$

Precision is defined as

$$\text{Precision} = \frac{TP}{TP + FP} \quad (9)$$

The statistical analysis of DBC has been given in **Table 7**. The range of all three parameters is between 0 and 1.

6 CONCLUSION

The chapter discusses the methods that have been applied for the classification problems. Directed Bee Colony (DBC) algorithm has been described and implemented for the classification of three problems of the medical domain: diabetes, cancer, and heart disease. The algorithm mimics bee behavior and uses both consensus and quorum methods to make decisions about nectar site selection. The properties of bees such as the waggle dance and the exploration of food have been exploited where a parallel group search is being executed, thus reducing computational time for reaching the optimal solution. The main upshot of DBC is that it removes the

randomness that is being faced by many nature-based algorithms. The bees are directed in a particular area for the search of the best food. This analogy is used for finding the optimal solution as the search is directed in a restricted expanse and hence results in a unique solution after every run. The classification results of DBC have been compared with other algorithms such as RBF, GA, GABP, Ridor, VFI, K star, NB tree, LM, bagging, multiboost, MlpANN, PSO, GALM, and ABC. No signal algorithm gives optimum accuracy for all three problems, but the overall accuracy of DBC is good and the best for diabetes. The results shown earlier demonstrate the reliability and robustness of the algorithm. It can also be manifested from the results that the algorithm is most suitable for the online classification appraising the property of generating a unique solution every time. In the medical domain, a faster and reliable (in terms of zero unique solution) classification can augment a better significance in the diagnosis process.

REFERENCES

- [1] R. Dybowski, G. Vanya, *Clinical Applications of Artificial Neural Networks*, Cambridge University Press, Cambridge, MA, 2001.
- [2] C.M. Bishop, *Neural Networks for Pattern Recognition*, vol. 5, Oxford University Press, UK, 1995.
- [3] H.A. Bourlard, N. Morgan, *Connectionist Speech Recognition: A Hybrid Approach*, vol. 247, Springer, New York, NY, 1994.
- [4] P. Cortez, M. Rocha, J. Neves, Evolving time series forecasting ARMA models, *J. Heuristics* 10 (4) (2004) 415–429.
- [5] A.S. Weigend, *Time Series Prediction: Forecasting the Future and Understanding the Past*, Avalon Publishing, California, 1994.
- [6] T. Masters, *Signal and Image Processing With Neural Networks: A C++ Sourcebook*, John Wiley & Sons, Inc., New York, NY, 1994.
- [7] E. Alba, J. Francisco Chicano, Training neural networks with GA hybrid algorithms, *Geneticand Evolutionary Computation GECCO 2004*, Springer, Berlin, Heidelberg, 2004, pp. 852–863.
- [8] D.E. Goldberg, *Genetic Algorithms in Search, Optimization, and Machine Learning*, ninth, Pearson Education, India, 2005.
- [9] J. Kennedy, Particle swarm optimization, *Encyclopediaof Machine Learning*, Springer, USA, 2010, pp. 760–766.
- [10] M. Dorigo, M. Birattari, T. Stutzle, Ant colony optimization, *IEEE Comput. Intell. Mag.* 1 (4) (2006) 28–39.
- [11] I. De Falco, A.D. Cioppa, E. Tarantino, Facing classification problems with particle swarm optimization, *Appl. Soft Comput.* 7 (3) (2007) 652–658.
- [12] L.M. Almeida, T.B. Ludermir, A multi-objective memetic and hybrid methodology for optimizing the parameters and performance of artificial neural networks, *Neurocomputing* 73 (7) (2010) 1438–1450.
- [13] M. Carvalho, T.B. Ludermir, Hybrid training of feed-forward neural networks with particle swarm optimization, *Neural Information Processing*, Springer, Berlin, Heidelberg, 2006, pp. 1061–1070.

- [14] D. Karaboga, C. Ozturk, A novel clustering approach: artificial bee colony (ABC) algorithm, *Appl. Soft Comput.* 11 (1) (2011) 652–657.
- [15] D. Teodorovic, P. Lucic, G. Markovic, M.D. Orco, Bee colony optimization: principles and applications, in: Proceedings of the 8th Seminar on Neural Network Applications in Electrical Engineering, NEUREL 2006, 2006, pp. 151–156.
- [16] D. Karaboga, B. Basturk, A powerful and efficient algorithm for numerical function optimization: artificial bee colony (ABC) algorithm, *J. Glob. Optim.* 39 (3) (2007) 459–471.
- [17] R. Kumar, Directed bee colony optimization algorithm, *Swarm Evol. Comput.* (17) (2014) 60–73.
- [18] P.J. Lisboa, A.F. Taktak, The use of artificial neural networks in decision support in cancer: a systematic review, *Neural Netw.* 19 (4) (2006) 408–415.
- [19] A. Asuncion, D. Newman, UCI Machine Learning Repository, Schl. Inf. Comput. Sci., Univ. of California, Irvine, CA, 2007.
- [20] L.L. Prechelt, PROBEN1-A set of neural network benchmark problems and benchmarking rules, Faculty of Informatics, University of Karlsruhe, 1994. Technical Report 21/94.

FURTHER READING

- [21] K.M. Passino, T.D. Seeley, P.K. Visscher, Swarm cognition in honey bees, *Behav. Ecol. Sociobiol.* 62 (3) (2008) 401–414.
- [22] K. Passino, T.D. Seeley, Modeling and analysis of nest-site selection by honey bee swarms: the speed and accuracy trade-off, *Behav. Ecol. Sociobiol.* 59 (2006) 427–442.
- [23] T. Seeley, S. Camazine, J. Sneyd, Collective decision-making in honey bees: how colonies choose among nectar sources, *Behav. Ecol. Sociobiol.* 28 (4) (1991) 277–290.
- [24] T. Seeley, P.K. Visscher, K.M. Passino, Group decision making in honey bee swarms, *Am. Sci.* 94 (2006) 3.
- [25] T.D. Seeley, *The Wisdom of the Hive*, Harvard University Press, Cambridge, 1995.
- [26] R. Eberhart, J. Kennedy, A new optimizer using particle swarm theory, in: Proceedings of the Sixth International Symposium on Micro Machine and Human Science, MHS '95, Nagoya, 1995, pp. 39–43.
- [27] R. Eberhart, Y. Shi, J. Kennedy, *Swarm Intelligence*, Morgan Kaufmann, Massachusetts, 2001.

This page intentionally left blank

A genetic algorithm-based metaheuristic approach to customize a computer-aided classification system for enhanced screen film mammograms

10

Heminder Kaur*, Jitendra Virmani†, Kriti*, Shruti Thakur‡

*Thapar Institute of Engineering and Technology (deemed-to-be university), Patiala, India**

CSIR-CSIO, Chandigarh, India† Kamla Nehru Hospital, Shimla, India‡

CHAPTER OUTLINE

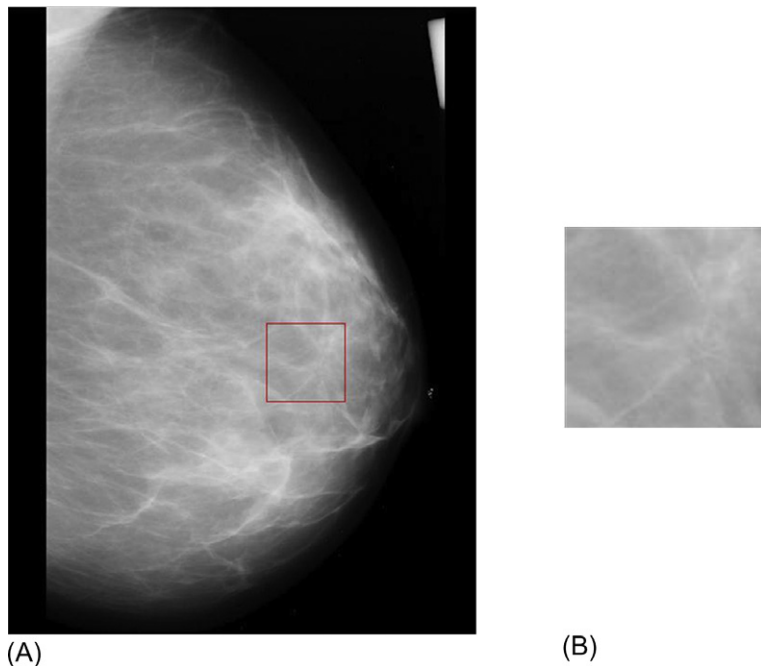
1 Introduction	218
2 Methodology for Designing a CAD System for Diagnosis of Abnormal Mammograms	226
2.1 Image Data Set Description	228
2.2 Enhancement Methods	229
2.3 Selection of ROIs	237
2.4 Feature Extraction: Gabor Wavelet Transform Features	241
2.5 SVM Classifier	244
3 Experimental Results	246
3.1 Obtaining the Accuracies of Classification of Abnormal Mammograms After Enhancement With Alpha Trimmed Mean Filter	246
3.2 Obtaining the Accuracies of Classification of Diagnosis of Abnormal Mammograms After Enhancement With Contrast Stretching	246
3.3 Obtaining the Accuracies of Classification of Diagnosis of Abnormal Mammograms After Enhancement With Histogram Equalization	247
3.4 Obtaining the Accuracies of Classification of Diagnosis of Abnormal Mammograms After Enhancement With CLAHE	247
3.5 Obtaining the Accuracies of Classification of Diagnosis of Abnormal Mammograms After Enhancement With RMSHE	247
3.6 Obtaining the Accuracies of Classification of Diagnosis of Abnormal Mammograms After Enhancement With Contra-Harmonic Mean	248

3.7 Obtaining the Accuracies of Classification of Diagnosis of Abnormal Mammograms After Enhancement With Mean Filter	248
3.8 Obtaining the Accuracies of Classification of Diagnosis of Abnormal Mammograms After Enhancement With Median Filter	248
3.9 Obtaining the Accuracies of Classification of Diagnosis of Abnormal Mammograms After Enhancement With Hybrid Median Filter	249
3.10 Obtaining the Accuracies of Classification of Diagnosis of Abnormal Mammograms After Morphological Enhancement	249
3.11 Obtaining the Accuracies of Classification of Diagnosis of Abnormal Mammograms After Morphological Enhancement, Followed by Contrast Stretching	250
3.12 Obtaining the Accuracies of Classification of Diagnosis of Abnormal Mammograms After Unsharp Masking	250
3.13 Obtaining the Accuracies of Classification of Diagnosis of Abnormal Mammograms After UMCA	250
3.14 Obtaining the Accuracies of Classification of Diagnosis of Abnormal Mammograms After Wavelet-Based Subband Filtering	251
4 Comparison of Classification Performance of the Enhancement Methods	251
5 Genetic Algorithm-Based Metaheuristic Approach to Customize a Computer-Aided Classification System for Enhanced Mammograms	252
6 Conclusion	254
7 Future Scope	254
References	255
Further Reading	259

1 INTRODUCTION

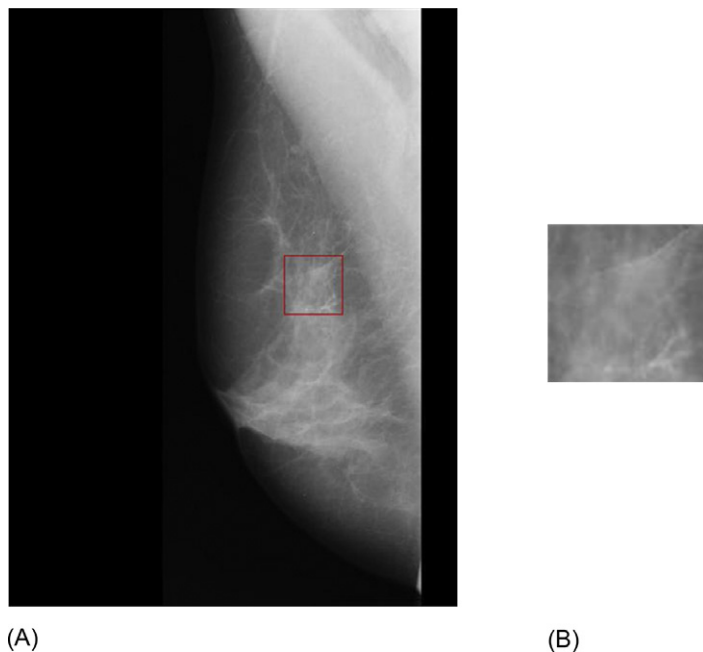
In 2012, approximately 1.67 million new cases of breast cancer were diagnosed and 522,000 people died from the disease, according to IARC Globocan, 2012. The causes of breast cancer are still unknown and hence, diagnosis of the disease at earlier stages is the foundation of breast cancer control [1]. If breast cancer is detected early and ample treatment is available, there is a high chance that it may be cured. According to the Mammographic Image Analysis Society (MIAS) database, breast images are divided into seven classes, namely, normal, calcifications, circumscribed masses, spiculated masses, ill-defined masses (miscellaneous), architectural distortion, and asymmetry. The appearances of these abnormalities and a marked region of interest (ROI) are described in Figs. 1–6.

- (a) Normal: A sample normal mammogram exhibiting no abnormality is presented in Fig. 1.
- (b) Calcifications: Breast calcifications appear as white dots on a mammogram. Microcalcifications are calcium deposits that are either scattered in the mammary glands or usually found in clusters. A sample image of a mammogram with calcification is depicted in Fig. 2.

**FIG. 1**

Normal mammogram from MIAS [2] dataset: (A) “mdb050” with ROI marked; (B) cropped ROI of normal mammogram.

- (c) Circumscribed masses: These are closely packed and lobular or round/oval shaped. A sample image of a mammogram with a circumscribed mass is depicted in [Fig. 3](#).
- (d) Spiculated masses: Spiculated lesions consist of a central mass with spicules radiating in one or many directions. A sample image of a mammogram with a circumscribed mass is presented in [Fig. 4](#).
- (e) Miscellaneous: These are the masses that don't have a definite shape. A sample image of a mammogram with a circumscribed mass is shown in [Fig. 5](#).
- (f) Architectural distortion: In architectural distortion, the normal oriented texture pattern of a mammogram, which is characterized as converging toward the nipple, is distorted. Any definite mass is also not visible [3]. A sample image of a mammogram with a circumscribed mass is shown in [Fig. 6](#).
- (g) Asymmetry: The classification of asymmetry is usually done by aligning left and right mammograms according to the pectoral muscle line orientation [4]. Hence, this abnormality is not taken for classification in this study. A sample image of a mammogram with a circumscribed mass is shown in [Fig. 7](#).

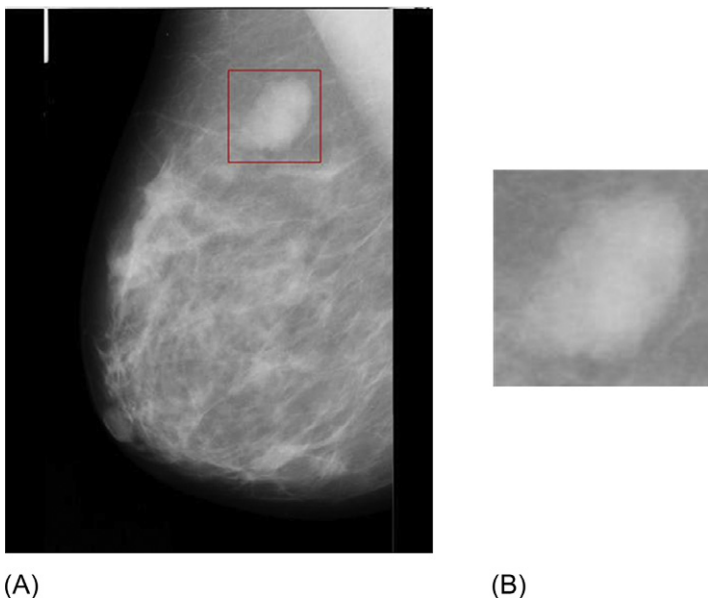
**FIG. 2**

Sample mammogram from MIAS [2] dataset showing calcification: (A) “mdb213” with abnormality marked; (B) cropped ROI of abnormality.

The various imaging techniques in the diagnosis of breast cancer are mammography, ultrasonography (US), computerized tomography (CT), and magnetic resonance imaging (MRI). Mammography is the most widely used imaging modality for breast cancer screening [5]. Mammography is the process in which low energy x-rays are used for examining the human breast for screening and diagnosis.

An issue with mammographic images is that they lack contrast, so the radiologists find it difficult to detect the indistinct signs of cancer such as calcifications and masses, which may thus be overlooked. Thus, there is a significant need for computer-aided diagnostic (CAD) systems that will help radiologists in detecting suspicious regions that otherwise may be missed. Such systems may serve as a second opinion to the radiologists [5]. Many researchers have done remarkable work and have attempted to enhance and classify the images by proposing various methodologies of preprocessing, feature extraction, and classification. A survey on the research work on classification of abnormal regions in mammograms done on the MIAS database [2] during the last few years is shown in Table 1.

The feature selection/optimization techniques have been used by various researchers in their studies, carried out on different medical images for reducing the number of extracted features, that is, removing redundant features that give no

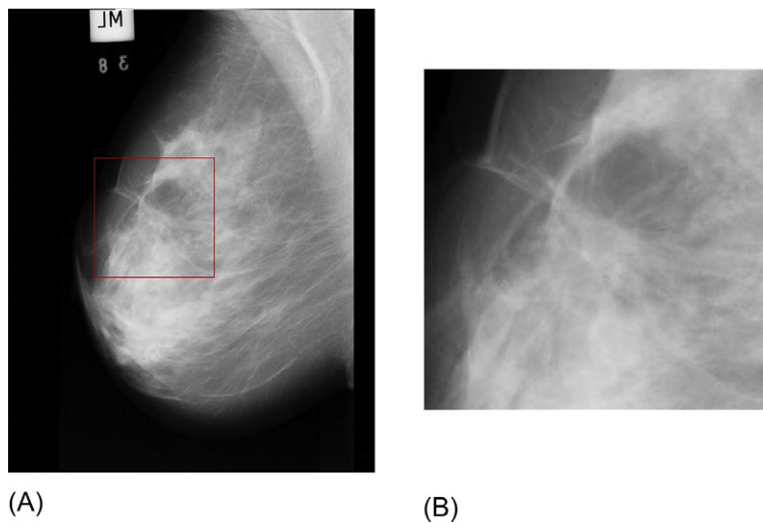


(A)

(B)

FIG. 3

Sample mammogram from MIAS [2] dataset showing circumscribed mass: (A) “mdb015” with abnormality marked; (B) cropped ROI of abnormality.

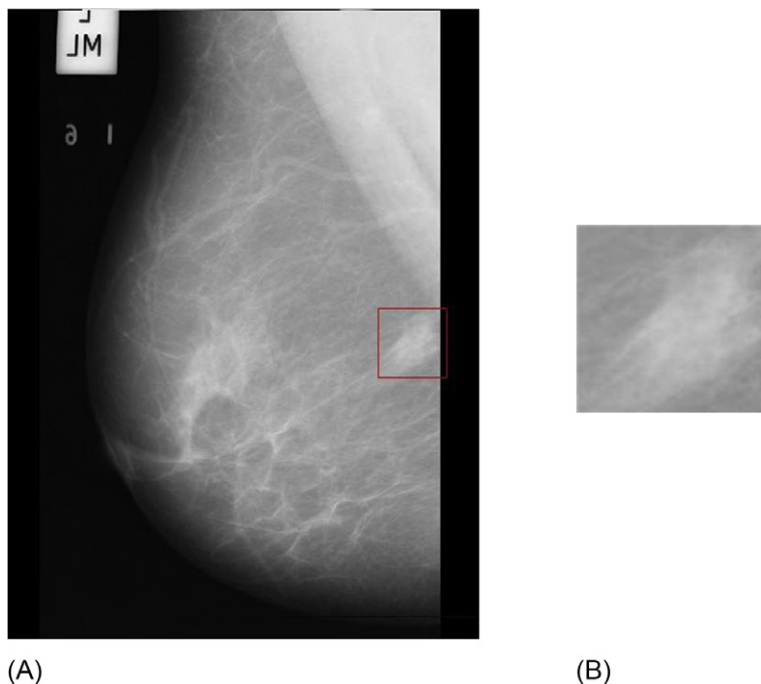


(A)

(B)

FIG. 4

Sample mammogram from MIAS [2] dataset showing spiculated mass: (A) “mdb204” with abnormality marked; (B) cropped ROI of abnormality.

**FIG. 5**

Sample mammogram from MIAS [2] dataset showing ill-defined mass: (A) “mdb267” with abnormality marked; (B) cropped ROI of abnormality.

information for tissue characterization [33–39]. This reduction in the feature set results in improved classification accuracy and reduced computation time.

From Table 1, it has been observed that very few studies employ preprocessing techniques for image enhancement [6,17,22,27,32] before subjecting them to classification. Also, only three studies [8,26,28] report the use of optimization for selecting features from the set of extracted texture features. The study in [8] reports the use of an optimization algorithm on the spatial features whereas the studies [26,28] do not specify the method of feature extraction. Based on the above observations, the present work has been carried out with a view to test the potential of feature extraction techniques in the transform domain and feature selection algorithms for classifying the normal and abnormal breast tissue using enhanced mammographic images. For feature extraction in the transform domain, the images are transformed to the frequency domain and the features are extracted on various scales, as scale is considered to be a dominant characteristic because the human visual system is said to process the images in a multiscale way [40,41]. The genetic algorithm-based metaheuristic search approach for feature selection has been applied to the extracted texture feature

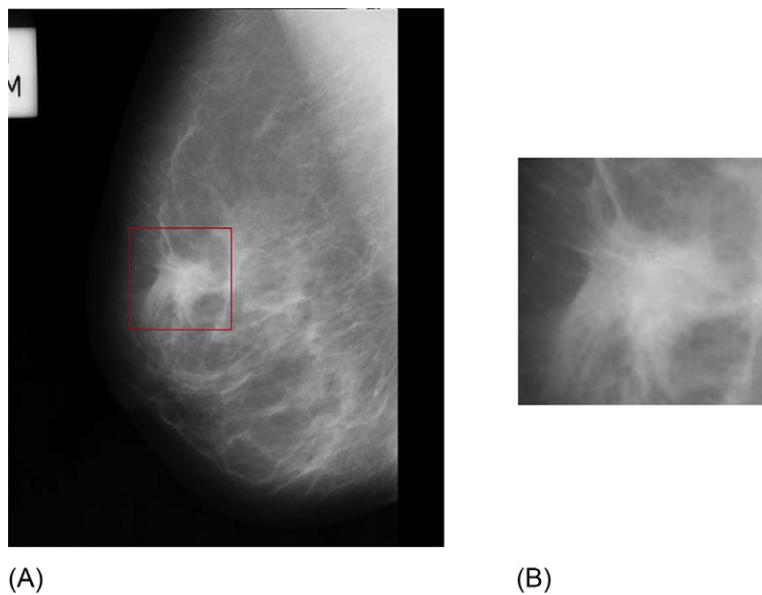


FIG. 6

Sample mammogram from MIAS [2] dataset showing architectural distortion: (A) “mdb117” with abnormality marked; (B) cropped ROI of abnormality.

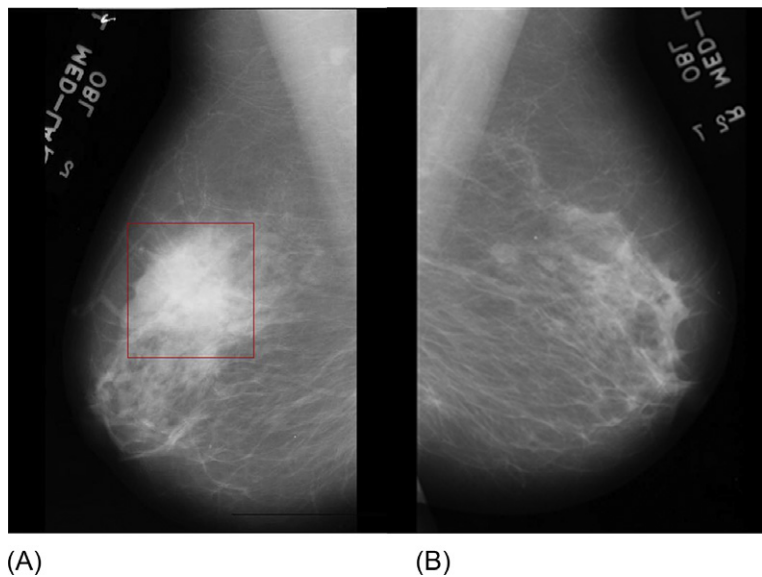


FIG. 7

Sample mammograms from MIAS [2] dataset showing asymmetry: (A) “mdb081” with abnormality marked on right mammogram; (B) “mdb082” depicting left mammogram of the same patient.

Table 1 Brief Details of Works on Classification of Mammograms in the MIAS [2] Dataset

Related Study	Class of Abnormality	Techniques	Classifier	Acc. (%)
Anna Rejani et al. [6]	Tumors	Gaussian soothing filter, CS, Top-hat operation and DWT	SVM	Sens. of 88.75
Beura et al. [7]	All	Comb. of DWT and GLCM	BPNN	98
Jona et al. [8]	Microcalcification, spiculation, circumscribed	GLCM and GSO for feature selection	SVM	94
Ibrahima et al. [9]	All	Wavelet transform	kNN and LDA	58.59 (LDA) 76.59 (kNN)
Amal et al. [10]	All	Gabor and local binary patterns	ANN	98.75
Eltoukhy et al. [11]	All	Curvelet transform	SVM	85.48
Shanthi et al. [12]	Microcalcification, masses and AD	Fractal analysis, Gabor filter, multiscale surrounding region dependence method	SRAN	98.44
Leena Jasmine et al. [13]	Microcalcification	Nonsubsampled contourlet transform (NSCT)	SVM	98.5
Eltoukhy et al. [14]	All	Wavelet transform	SVM	94.79
Eltoukhy et al. [15]	All	Wavelet and curvelet transform	SVM	91.19
Qayyum et al. [16]	All	Otsu's segmentation, removal of pectoral muscle and GLCM	SVM	96.55
Shah [17]	All	Median filter, morphological, wavelet transform, and triangular mask Intensity histogram-based texture features	Neural network	95.37

Table 1 Brief Details of Works on Classification of Mammograms in the MIAS [2] Dataset—cont'd

Related Study	Class of Abnormality	Techniques	Classifier	Acc. (%)
Mousa et al. [18]	Mass and microcalcification	Wavelet decomposition	ANFIS	Sens. of 79.2
Buciu et al. [19]	Microcalcification, circumscribed masses, spiculated masses	Gabor wavelets	Proximal-SVM	84.37
Karmilasari et al. [20]	All	Morphology and GLCM	SVM	60; 85 (if testing data taken from inside training data)
Jehlol et al. [21]	All	Second-order statistical features	Random forest	98.8
Lothe Savita et al. [22]	Masses	CLAHE, DFT Shape features and GLCM	SVM	86.84
Phadke et al. [23]	All	Fusion of local and global features	SVM	93.17
Setiawan et al. [24]	All	Laws' texture energy measures	ANN	93.9
Pratiwi et al. [25]	All	GLCM features	RBFNN	93.98
Qader et al. [26]	All	PCA + ICA	Fuzzy classifier	84.03
Talha [27]	All	GP filter-based noise removal Fusion of DCT and DWT	SVM	96.97
Christoyianni et al. [28]	All	Independent component analysis	Neural networks	88.23
Sondele et al. [29]	Mass and calcification	Bidimensional empirical mode decomposition	ANN	82.4
Herwanto et al. [30]	Mass and microcalcification	Statistical features and GLCM	Association technique	83

Continued

Table 1 Brief Details of Works on Classification of Mammograms in the MIAS [2] Dataset—cont'd

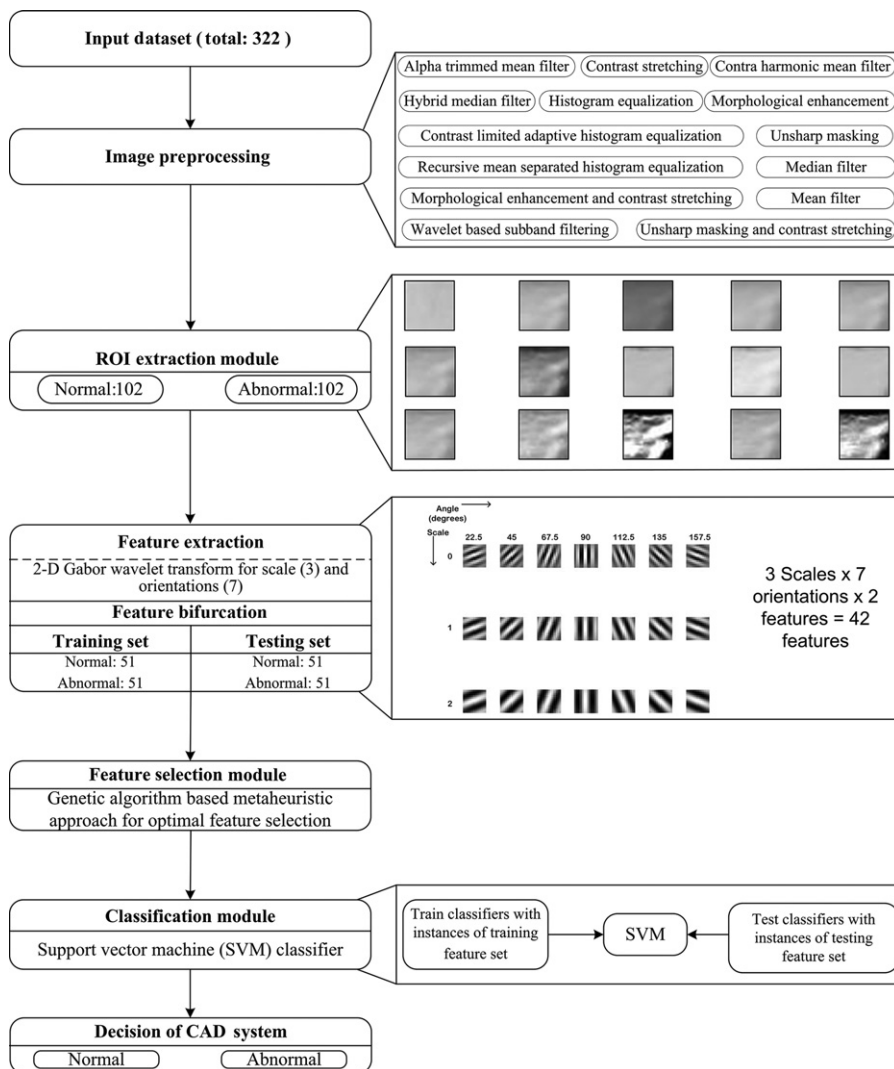
Related Study	Class of Abnormality	Techniques	Classifier	Acc. (%)
Anitha et al. [31]	Mass	Wavelet features	SVM	95
Nguyen et al. [32]	Mass	Local contrast thresholding	Rule-based	Sens. of 84.62
Nguyen et al. [32]	Microcalcification	Local contrast thresholding	Rule-based	Sens. of 84

Acc., accuracy; Sens., sensitivity; CS, contrast stretching; SVM, support vector machine; DWT, discrete wavelet transform; GLCM, gray level cooccurrence matrix; BPNN, back-propagation multilayer neural network; GSO, genetical swarm optimization; kNN, k nearest neighbors; LDA, linear discriminant analysis; CLAHE, contrast limited adaptive histogram equalization; DFT, discrete Fourier transform; ANN, artificial neural network; AD, architectural distortion; SRAN, self-adaptive resource allocation network; ANFIS, adaptive neuro-fuzzy inference system; RBFNN, radial basis function neural network; DCT, discrete cosine transform; GP, genetic programming; All, calcification, circumscribed masses, spiculated masses, ill-defined masses, architectural distortion and normal.

set for obtaining the optimal number of features as it has been asserted by various researchers that an optimal texture feature set results in improved classification accuracy as well as reduced computation time [33–39].

2 METHODOLOGY FOR DESIGNING A CAD SYSTEM FOR DIAGNOSIS OF ABNORMAL MAMMOGRAMS

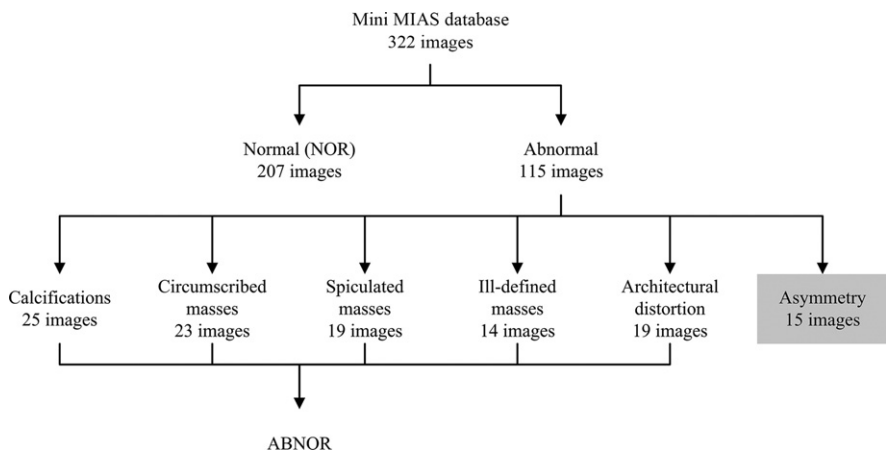
With the evolution of computer technology, image processing algorithms, and different machine learning techniques, ample opportunities have been presented to various researchers for investigating the potential of different computer algorithms for diagnosis, analysis, and monitoring of different diseases using medical images captured using various modalities such as x-ray, ultrasound, CT scan, PET scan, MRI, thermal imaging etc. [40–47]. The analysis here refers to a quantitative analysis of textural patterns exhibited by various tissues using computer-based algorithms resulting in an accurate distinction between normal and abnormal tissues. With the help of different artificial intelligence and machine learning-based computer programs, the changes exhibited by the tissues from normal to abnormal can also be monitored quantitatively and further characterization can be done. For the characterization of normal and abnormal breast tissues, CAD systems prove to be useful in efficiently assisting the radiologists to validate their diagnosis [6–32]. There is a need of CAD systems for the differentiation of normal and abnormal breast tissues using mammograms because it has been noted that normal and abnormal breast tissues

**FIG. 8**

Methodology followed for designing a CAD system for the diagnosis of abnormal mammograms.

exhibit different textural patterns on a mammogram. These may sometimes overlap, making it difficult for radiologists to clearly differentiate between the breast tissues.

The methodology followed in this study for the design of a CAD system for diagnosing abnormal mammograms is depicted in Fig. 8.

**FIG. 9**

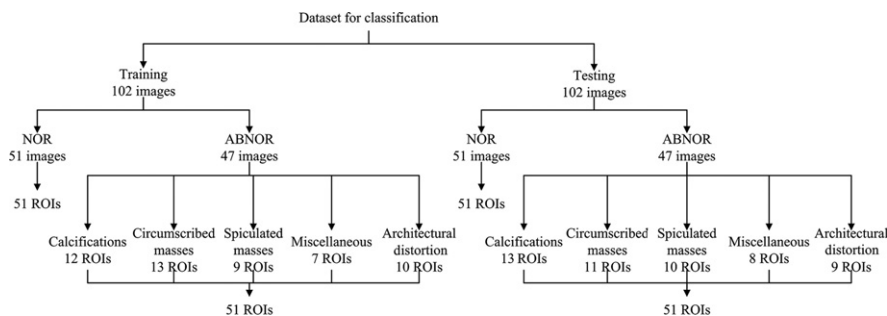
Mini MIAS [2] dataset description.

2.1 IMAGE DATA SET DESCRIPTION

The mammograms used in the current study are obtained from the mini-MIAS mammographic database, which contains 322 images that are each 1024 pixels \times 1024 pixels in size. The database provides the information about the center of abnormality, if any, and the approximate radius (in pixels) of a circle enclosing the abnormality. There are a total of 207 normal cases, 64 benign, and 51 malignant images. The abnormalities are categorized into six classes, namely, calcifications, well-defined/circumscribed masses, spiculated masses, ill-defined masses, architectural distortion, and asymmetry [2].

A total of 102 abnormal images were selected from the database. They were then divided into two sets for training and testing, with each set containing 51 images. The images were divided such that all classes of abnormalities, except asymmetry, were present in both sets. Also, the training and testing sets contain both the benign and malignant images. A total of 102 normal images were randomly selected from the dataset. Thus, the training and testing sets contain 102 images each: 51 normal and 51 abnormal.

The shaded region in Fig. 9, that is, the asymmetry, is not considered in this work. This is due to the fact that for classifying asymmetry, the observation needs to be done with respect to the same area on the other breast [4]. The classification of asymmetry is usually done by aligning the left and right mammograms according to the pectoral muscle line orientation. The distribution of images for training and testing sets is presented in Fig. 10. Some images contain multiple abnormal regions, so the number of ROIs is greater than the number of images taken.

**FIG. 10**

Description of dataset used in the SVM classifier.

2.2 ENHANCEMENT METHODS

In the present work, 14 different enhancement methods have been applied on the original mammogram images, before ROI extraction. Some of these methods show significant improvement in the image contrast while the abnormalities are also visually enhanced. The enhancement methods used are depicted below:

2.2.1 Alpha trimmed mean filter

It is a windowed nonlinear filter and varies between a median and mean filter. The concept behind this filter is to discard the most atypical elements around the neighborhood of a given element and calculate mean value using the rest of them.

The algorithm followed by this method is:

- (1) Place a window over an element.
- (2) Order the elements in ascending order.
- (3) Discard the elements at the end and at the beginning of the ordered set.
- (4) Take an average of the remaining elements.

The sample images enhanced with the alpha trimmed mean filter are depicted in [Fig. 11](#).

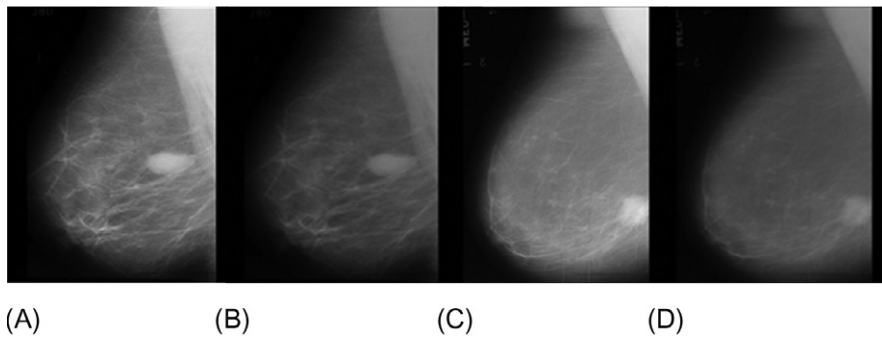
2.2.2 Contrast adjustment

The contrast in a mammogram is increased, resulting in a greater separation between foreground and background [\[48\]](#). The transformation used for contrast stretching is depicted in [Fig. 12](#).

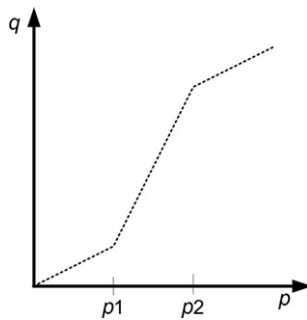
The resulting images after applying the contrast stretching operation on mammogram images are depicted in [Fig. 13](#).

2.2.3 Histogram equalization

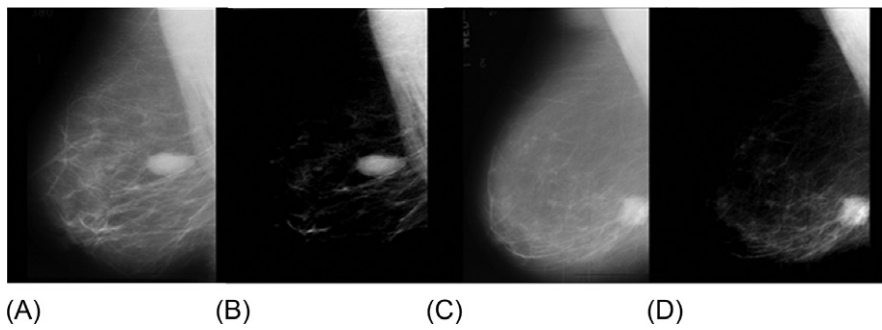
In this enhancement method, an input image is mapped to the output image to uniformly distribute the gray values over the complete grayscale range in the output image. Thus, the contrast range in an image is increased [\[49,50\]](#). The resulting images after applying histogram equalization on mammogram images are depicted in [Fig. 14](#).

**FIG. 11**

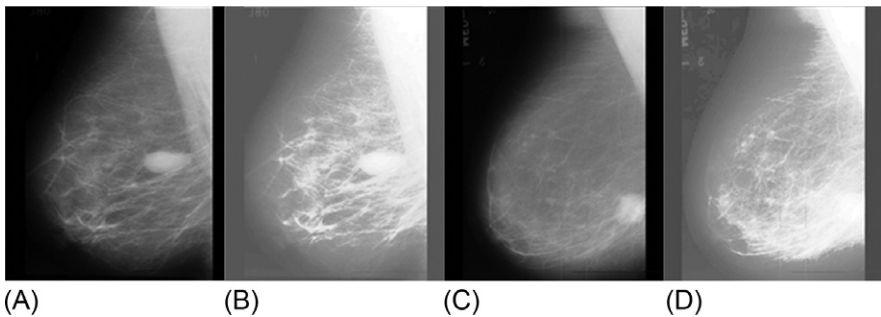
Sample images before and after enhancement with alpha trimmed mean filter: (A) “mdb025” from MIAS; (B) “mdb025” after enhancement; (C) “mdb271” from MIAS [2]; (D) “mdb271” after enhancement.

**FIG. 12**

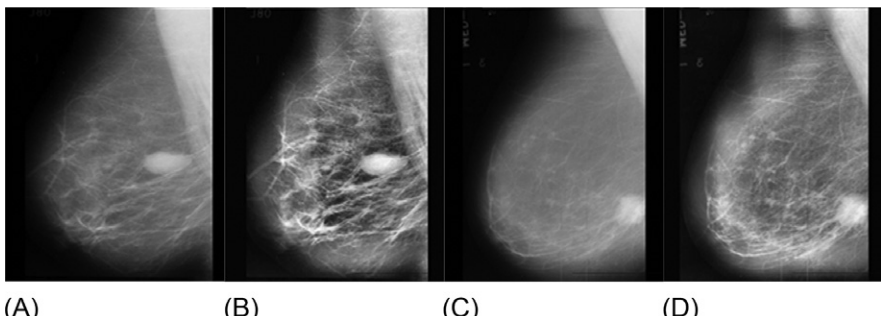
Contrast stretching between p_1 and p_2 .

**FIG. 13**

Sample images before and after contrast stretching: (A) “mdb025” from MIAS [2]; (B) “mdb025” after enhancement; (C) “mdb271” from MIAS [2]; (D) “mdb271” after enhancement.

**FIG. 14**

Sample images before and after histogram equalization: (A) “mdb025” from MIAS; (B) “mdb025” after enhancement; (C) “mdb271” from MIAS [2]; (D) “mdb271” after enhancement.

**FIG. 15**

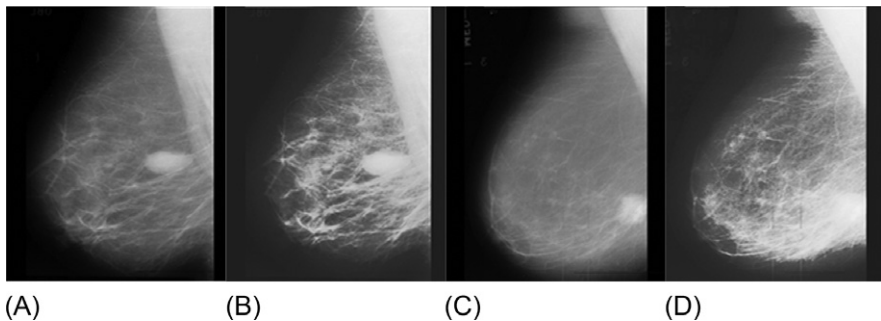
Sample images before and after enhancement with CLAHE: (A) “mdb025” from MIAS; (B) “mdb025” after enhancement; (C) “mdb271” from MIAS [2]; (D) “mdb271” after enhancement.

2.2.4 Contrast limited adaptive histogram equalization

Contrast limited adaptive histogram equalization (CLAHE) is performed on small data regions rather than the entire image. The image is partitioned into small contextual areas and the technique of histogram equalization is applied on each of these regions. The hidden features of an image are enhanced using this method [29,51,52]. The sample images enhanced with the CLAHE method are depicted in Fig. 15.

2.2.5 Recursive mean separated histogram equalization

The brightness of an image often changes during the process of contrast enhancement during histogram equalization. Bihistogram equalization (BBHE) is another technique in which the input image’s histogram is separated into two parts, based on

**FIG. 16**

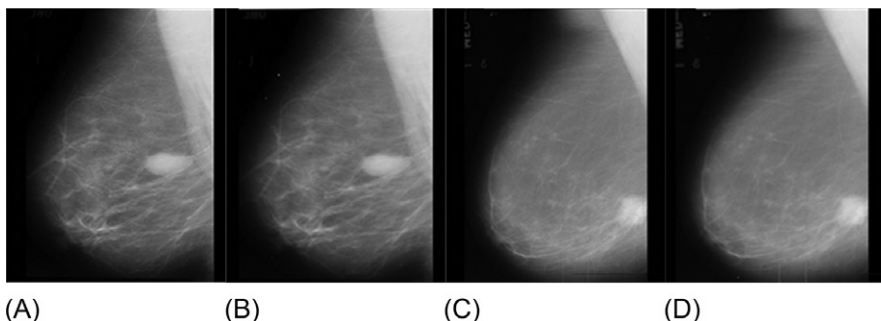
Sample images before and after enhancement with RMSHE: (A) “mdb025” from MIAS; (B) “mdb025” after enhancement; (C) “mdb271” from MIAS [2]; (D) “mdb271” after enhancement.

its mean before equalizing. The original brightness of an image is preserved to a certain extent by this method [53].

In recursive mean separated histogram equalization (RMSHE), the separation is performed iteratively, where each new histogram is further separated based on the respective mean. The output image’s mean brightness converges to that of the input image with the increase in number of mean separations. The sample images enhanced with the RMHSE method are depicted in Fig. 16.

2.2.6 Contra harmonic mean filter

This filter is used to remove Gaussian noise and preserve edges. The results of applying a contra-harmonic mean filter on mammograms are depicted in Fig. 17.

**FIG. 17**

Sample images before and after applying contra-harmonic mean filter: (A) “mdb025” from MIAS; (B) “mdb025” after enhancement; (C) “mdb271” from MIAS [2]; (D) “mdb271” after enhancement.

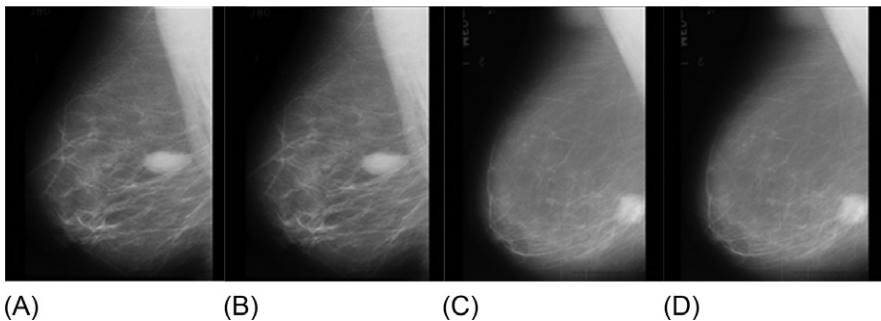


FIG. 18

Sample images before and after applying mean filter: (A) “mdb025” from MIAS; (B) “mdb025” after enhancement; (C) “mdb271” from MIAS [2]; (D) “mdb271” after enhancement.

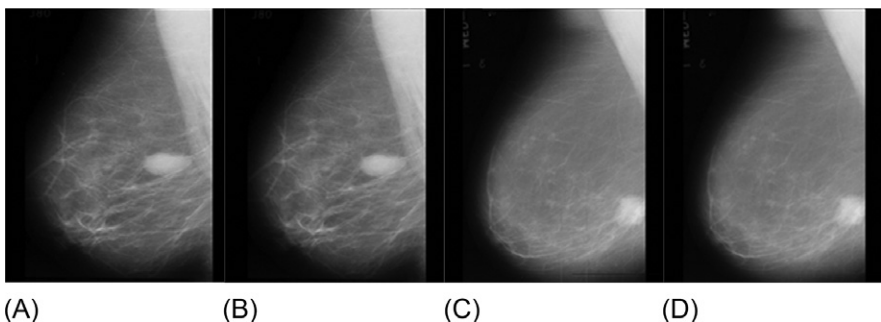


FIG. 19

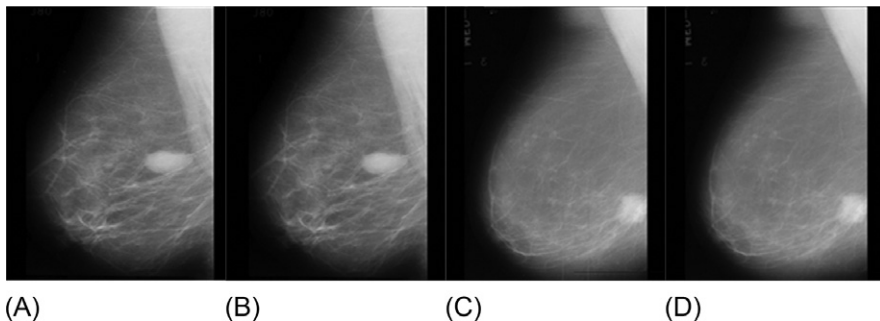
Sample images before and after applying median filter: (A) “mdb025” from MIAS; (B) “mdb025” after enhancement; (C) “mdb271” from MIAS [2]; (D) “mdb271” after enhancement.

2.2.7 Mean filter

The mean filter is a windowed spatial filter in which the center element of the window is replaced by the mean of all the pixel values in that window. The sample images enhanced with a mean filter are depicted in Fig. 18.

2.2.8 Median filter

The median filter is also a windowed spatial filter. Here, the center element of the window is replaced by the median of all the pixels in that window. The sample images enhanced with a median filter are depicted in Fig. 19.

**FIG. 20**

Sample images before and after applying hybrid median filter: (A) “mdb025” from MIAS; (B) “mdb025” after enhancement; (C) “mdb271” from MIAS [2]; (D) “mdb271” after enhancement.

2.2.9 Hybrid median filter

ThisIt is a windowed filter that can remove impulse noise and preserve edges. In comparison to the median filter, it can preserve corners more effectively [54]. Two median values are calculated in a window: the median of pixels in the horizontal and vertical directions, and the median of pixels in a diagonal direction. The filtered value is the median of these two median values and the central pixel. Some sample images enhanced by applying a hybrid median filter are presented in Fig. 20.

2.2.10 Morphological enhancement

Morphology is an image processing method that deals with the form and shape of an image. Morphological filters are used to sharpen images [55–57]. Dilation and erosion are the two basic morphological operators, where dilation selects the brightest value in the neighborhood of the structuring element and erosion selects the darkest value in a neighborhood. Many operations are derived from these operators, such as opening and closing. Opening an image refers to erosion followed by dilation whereas closing refers to dilation followed by erosion. Top hat transforms are used for locally extracting structures from an image. The top hat transform is evaluated by subtracting the opening of the original image from the original image (Eq. 1), and the bottom hat transform is evaluated by subtracting the original image from its closing (Eq. 2) [58].

$$\text{Top} - \text{Hat}(TH) = OI - (OI \circ SE) \quad (1)$$

$$\text{Bottom} - \text{Hat}(BH) = (OI \bullet SE) - OI \quad (2)$$

where OI = original image; SE = structuring element; \circ = morphological opening operation; \bullet = morphological closing operation.

The bright areas are added and the dark areas subtracted from the original image, resulting in the contrast enhancement [59] (Eq. 3).

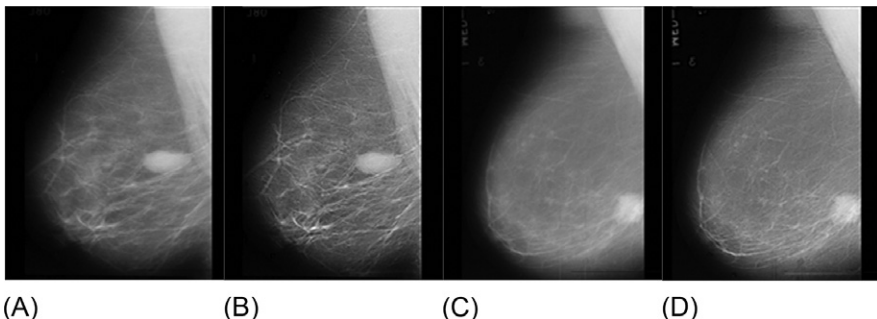


FIG. 21

Sample images before and after applying morphological enhancement: (A) “mdb025” from MIAS; (B) “mdb025” after enhancement; (C) “mdb271” from MIAS [2]; (D) “mdb271” after enhancement.

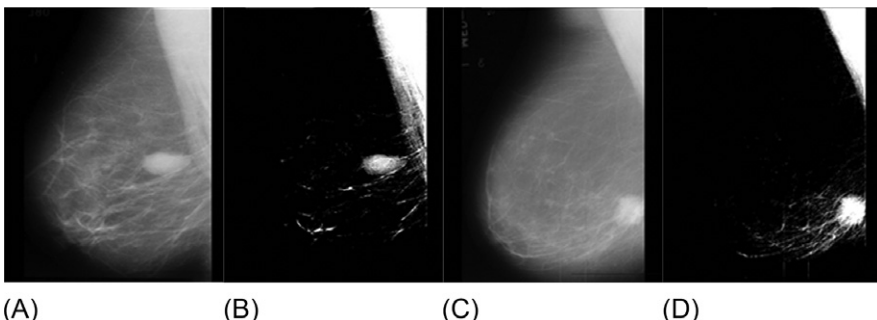


FIG. 22

Sample images before and after applying combination of morphological enhancement and contrast stretching: (A) “mdb025” from MIAS; (B) “mdb025” after enhancement; (C) “mdb271” from MIAS [2]; (D) “mdb271” after enhancement.

$$\text{Enhanced image (EI)} = OI + TH - BH \quad (3)$$

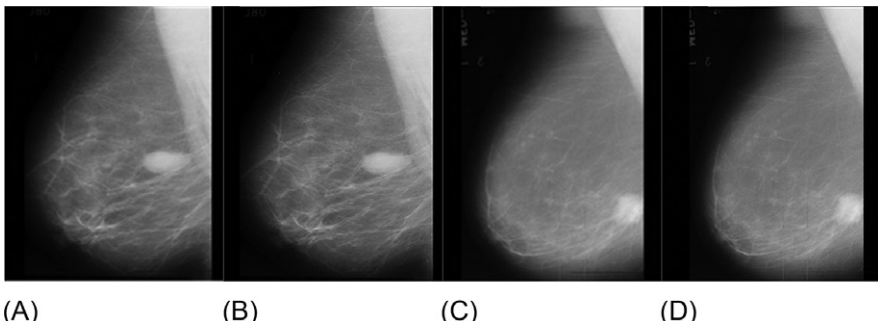
Some sample morphologically enhanced mammographic images are presented in Fig. 21.

2.2.11 Morphological enhancement and contrast stretching

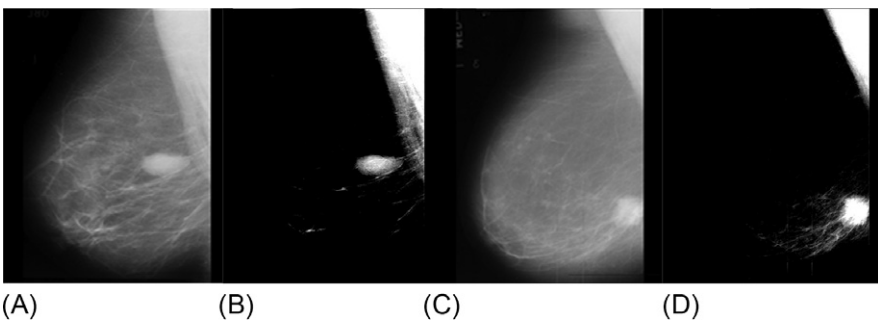
To enhance the visibility of mammographic features, a combination of two enhancement methods is proposed. The results of the application of morphological enhancement followed by contrast stretching are depicted in Fig. 22 [60–62].

2.2.12 Unsharp masking

An “unsharp mask” is used for sharpening a mammogram and edge detection. The process works by obtaining an unsharp mask by subtracting a slightly blurred version of the original image from the original. This mask is then used to selectively increase

**FIG. 23**

Sample images before and after applying unsharp masking: (A) “mdb025” from MIAS; (B) “mdb025” after enhancement; (C) “mdb271” from MIAS [2]; (D) “mdb271” after enhancement.

**FIG. 24**

Sample images before and after applying combination of unsharp masking and contrast stretching: (A) “mdb025” from MIAS; (B) “mdb025” after enhancement; (C) “mdb271” from MIAS [2]; (D) “mdb271” after enhancement.

the contrast along the edges, which yields a sharper final image. Thus, an unsharp filter reduces low frequency details and amplifies high frequency details [61,63].

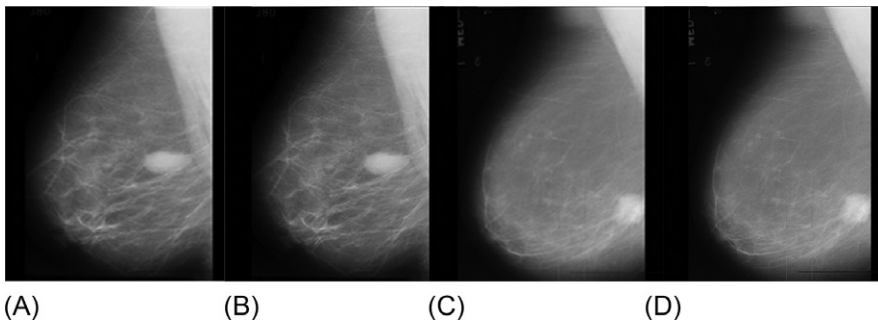
The results after applying unsharp masking to mammograms are presented in Fig. 23.

2.2.13 Unsharp masking and contrast stretching

The results of enhancements with unsharp masking followed by contrast stretching are depicted in Fig. 24 [62].

2.2.14 Wavelet based subband filtering

Wavelet transform, also called multiresolution analysis, analyzes the signal at different frequencies with different resolutions. It is applied to a mammogram, which results in the decomposition of a mammographic image into band-pass subband

**FIG. 25**

Sample images before and after applying wavelet subband filter: (A) “mdb025” from MIAS; (B) “mdb025” after enhancement; (C) “mdb271” from MIAS [2]; (D) “mdb271” after enhancement.

images. Two statistical features, mean and standard deviation, are evaluated for all the subband images. In high frequency subbands, the mean value is used for a threshold to inhibit noise amplification [62]. Some sample enhanced images by wavelet filter are presented in Fig. 25. The sample images of mammogram depicting the results of all enhancement methods and their respective histograms and intensity profiles are represented in Figs. 26–28.

The enhanced mammographic images were also shown to a participating radiologist for clinical validation. On the basis of visual perception, the radiologist graded the enhanced images in comparison to the original images (without enhancement) with grade values ranging from 1 to 10 where 1 signifies poor visual quality of the image and 10 signifies high visual quality. The average grades obtained for each enhancement method are shown in Table 2.

From the grading obtained by the radiologist, it is observed that three enhancement methods—contrast stretching, morphological enhancement and contrast stretching, and unsharp masking and contrast stretching (UMCA)—provide clinically acceptable images in which the abnormalities are better highlighted.

2.3 SELECTION OF ROIs

The size of an ROI needs to be selected with forethought so that it contains minimal noise and a maximum region of abnormality.

Before selecting the ROI size, a survey is done on some previous related works; this is described in Table 3.

2.3.1 Selection of ROI size

Initially, the ROIs of sizes 32×32 pixels, 64×64 pixels, and 128×128 pixels are cropped, which are depicted in Fig. 29 and studied based on their accuracies of classifying abnormalities on raw images, that is, without any enhancements.

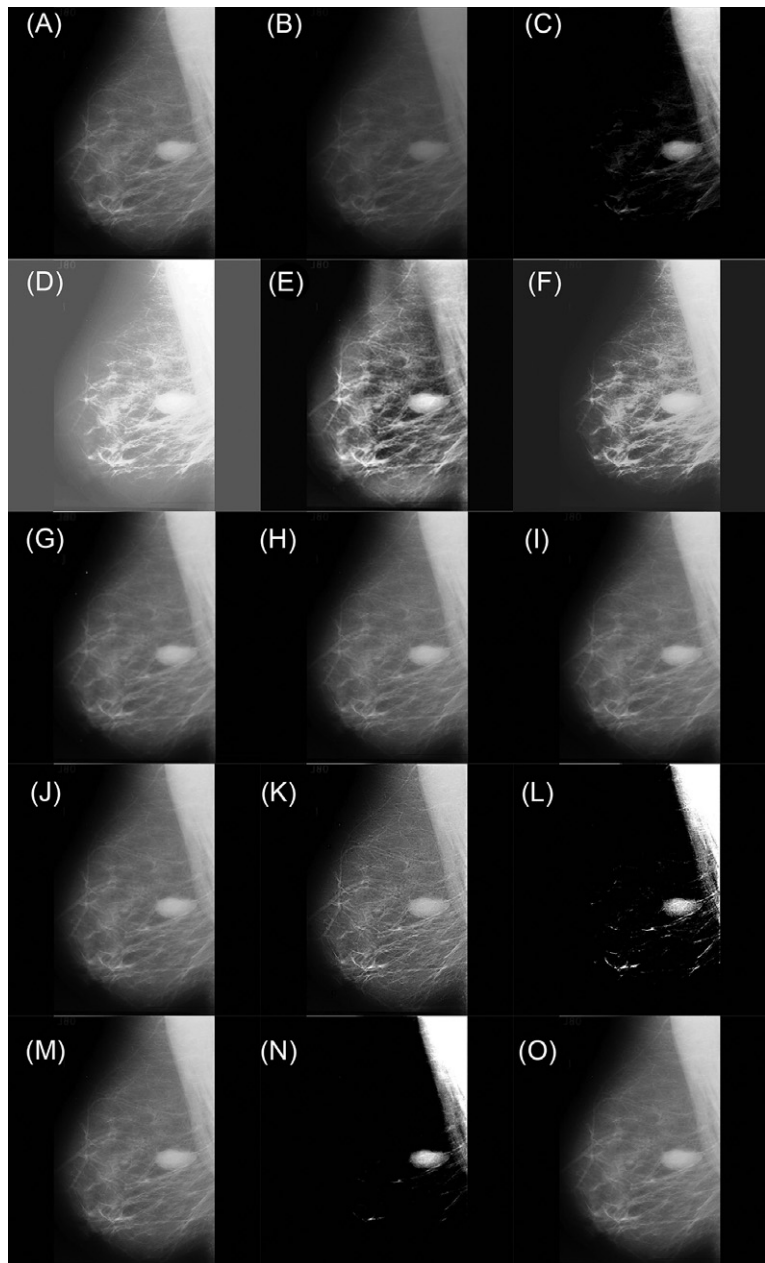
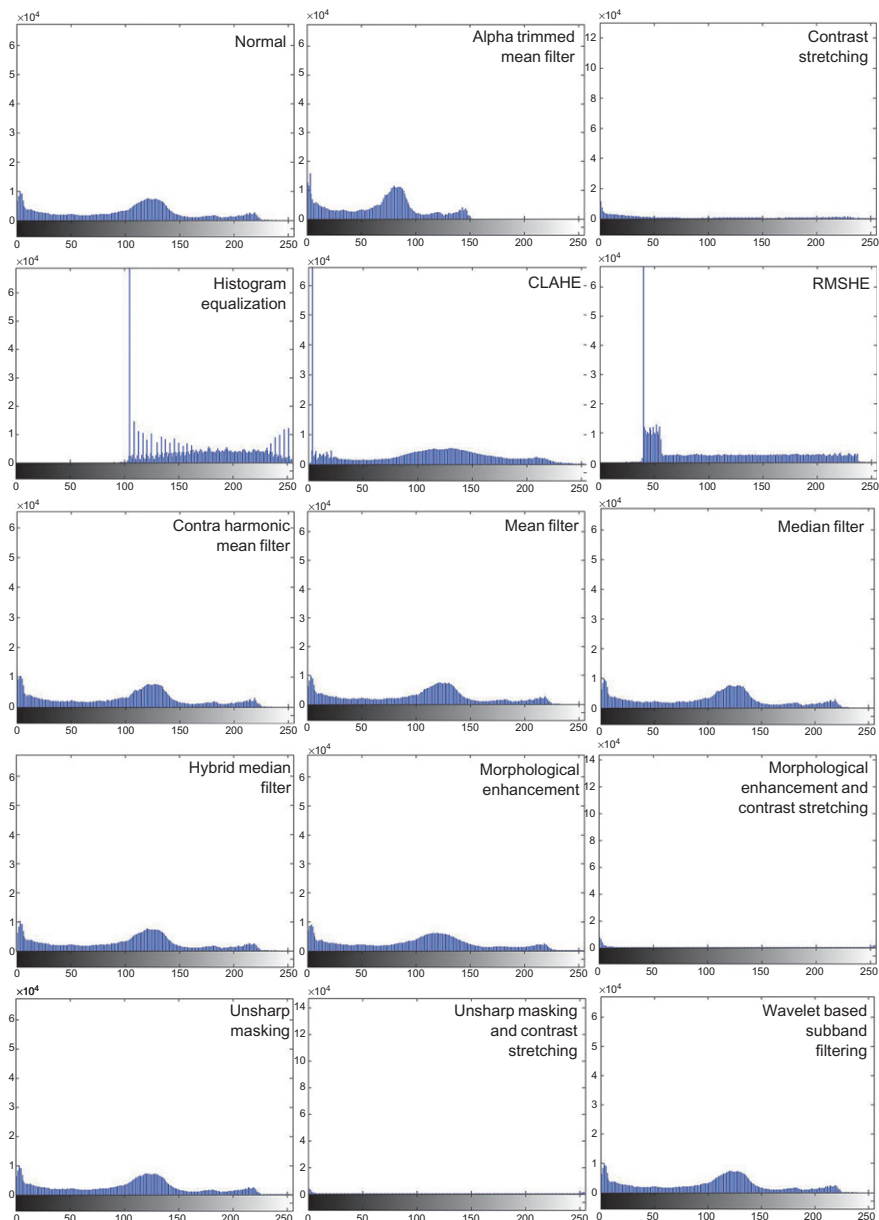


FIG. 26

Comparison of all enhancement methods used on a sample mammogram “mdb025” from MIAS [2] dataset: (A) original mammogram (without enhancement); (B) alpha-trimmed mean filter; (C) contrast stretching; (D) histogram equalization; (E) CLAHE; (F) RMSHE; (G) contra harmonic mean filter; (H) mean filter; (I) median filter; (J) hybrid median filter; (K) morphological enhancement; (L) morphological enhancement and contrast stretching; (M) unsharp masking; (N) unsharp masking and contrast stretching; (O) wavelet based subband filtering.

**FIG. 27**

Resulting histograms of a sample mammogram “mdb025” from MIAS [2] dataset with and without enhancements.

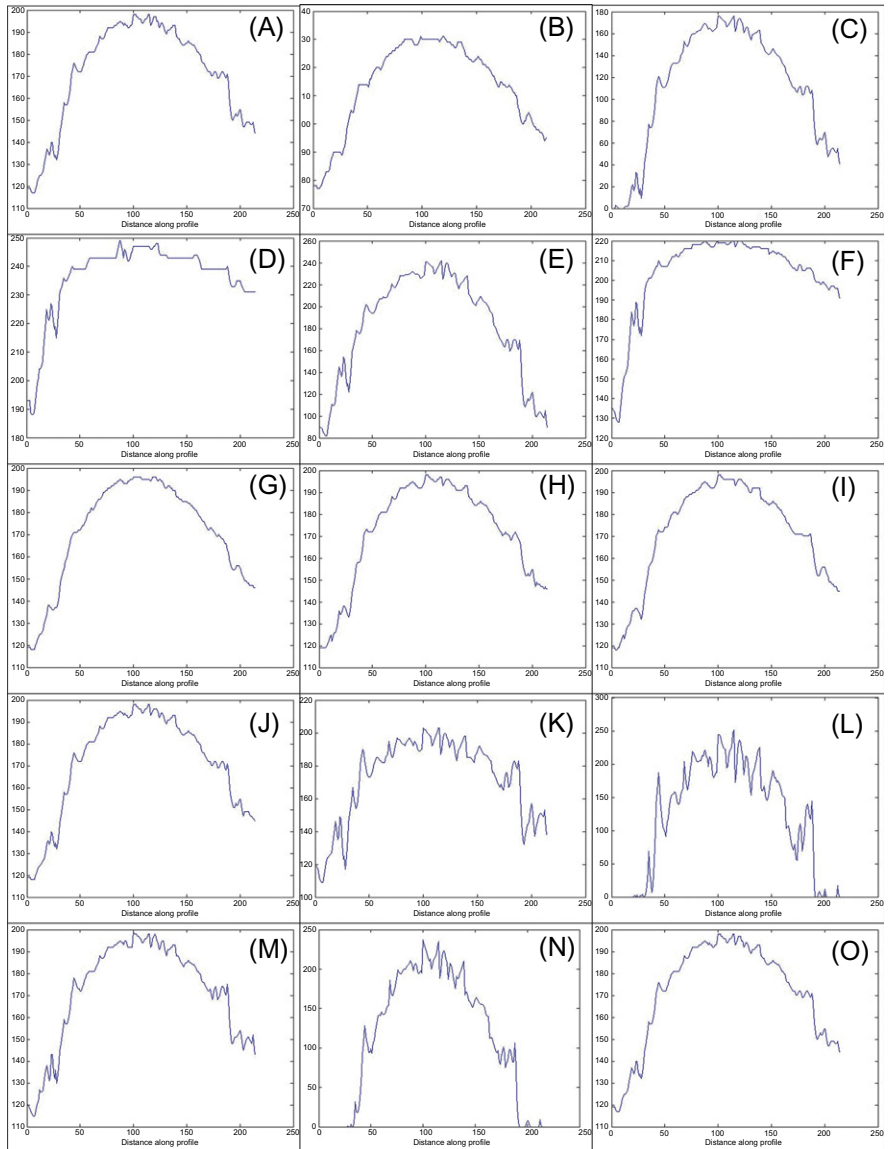


FIG. 28

Intensity profiles of the regions of abnormality of all enhancement methods used on a sample mammogram “mdb025” from MIAS [2] dataset: (A) original mammogram (without enhancement); (B) alpha trimmed mean filter; (C) contrast stretching; (D) histogram equalization; (E) CLAHE; (F) RMSHE; (G) contra harmonic mean filter; (H) mean filter; (I) median filter; (J) hybrid median filter; (K) morphological enhancement; (L) morphological enhancement and contrast stretching; (M) unsharp masking; (N) unsharp masking and contrast stretching; (O) wavelet based subband filtering.

Table 2 Radiologist's Grading of Enhanced Images

Enhancement Method	Grade
Alpha trimmed mean filter	3
Contrast stretching	8
Histogram equalization	1
CLAHE	6
RMSHE	4
Contra-harmonic mean filter	5
Mean filter	5
Median filter	5
Hybrid median filter	5
Morphological enhancement	6
Morphological enhancement and contrast stretching	9
Unsharp masking	6
Unsharp masking and contrast stretching	9
Wavelet-based subband filtering	5

(a) [Table 4](#) shows the confusion matrices and accuracies observed with different ROI sizes. It is examined from the table that the accuracy for ROIs of size 128×128 pixels has decreased, (b) it is shown pictorially in [Fig. 29](#) that ROIs of size 128×128 pixels also contain regions surrounding the abnormality, which affect the texture analysis. This justifies the decrease in accuracy of this ROI size in [Table 3](#). The ROIs of size 64×64 pixels also contain extra regions. It is observed that 32×32 pixel ROI size contains minimal or no surrounding area at all and most of the ROI region is composed of abnormality only, and (c) furthermore, according to the studies in [\[66–69\]](#), ROI size must not be less than 800 pixels to provide an adequate sample size condition for estimating reliable statistics. Thus, sizes lower than 32×32 pixels are not extracted for analysis.

Thus, 32×32 pixel ROIs are considered for further studies as they cover a very small surrounding area and contain more pixels than the minimum requirement of 800. Similarly, ROIs of size 32×32 pixels are extracted from the normal mammograms. A sample ROI of a mammogram image from the MIAS [\[2\]](#) database is presented in [Fig. 30](#).

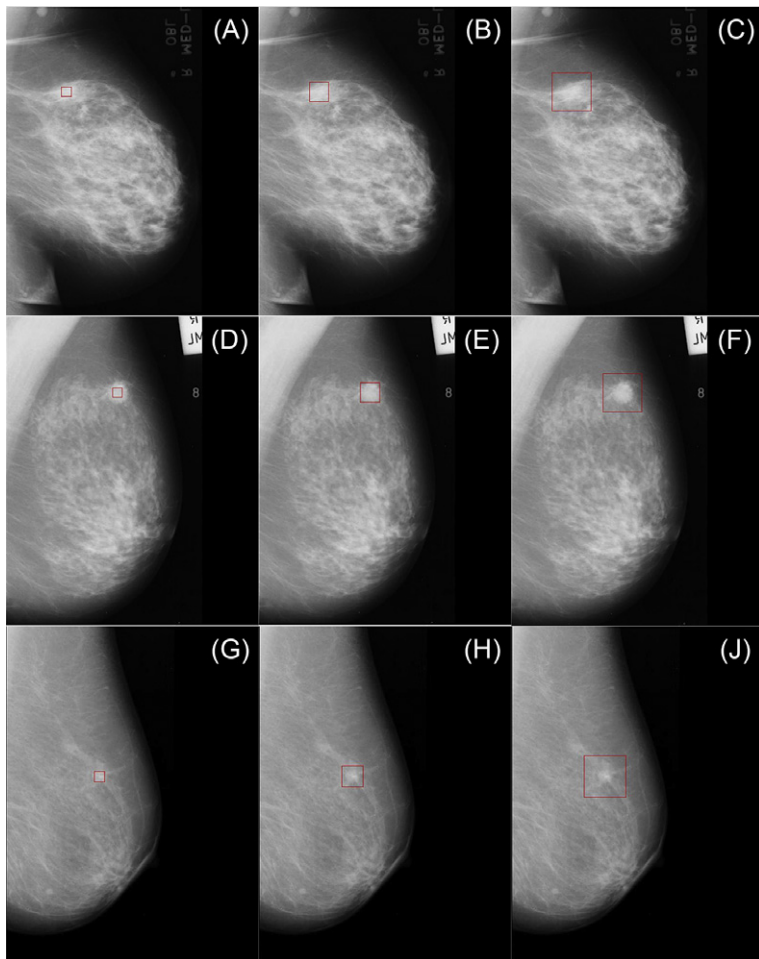
2.4 FEATURE EXTRACTION: GABOR WAVELET TRANSFORM FEATURES

Feature extraction is an imperative step for texture recognition. The texture information is represented as numeric values that are then further used by different machine learning algorithms for analyzing the texture [\[46,47\]](#). Feature extraction for texture representation can be done either on a single scale or multiple scales. The techniques for extraction of texture features on a single scale are: GLCM, gray level run length

Table 3 Brief Detail on Study of ROI Sizes Used for Classification on MIAS [2] Database

Related Study	Class of Abnormality	ROI Size (Pixels)
Beura et al. [7]	All	Size of abnormality
Eltoukhy et al. [11]	All	128 × 128
Shanthi et al. [12]	Microcalcifications, masses and AD	Size of abnormality
Leena Jasmine et al. [13]	Microcalcifications	800 × 800
Eltoukhy et al. [14]	All	128 × 128
Eltoukhy et al. [15]	All	128 × 128
Qayyum et al. [16]	All	201 × 201
Mousa et al. [18]	Mass and microcalcification	800 × 800
Buciu et al. [19]	Microcalcifications, circumscribed masses and spiculated masses	30 × 30 and 60 × 60
Jehlol et al. [21]	All	Size of abnormality
Lothe Savitha et al. [22]	Masses	Size of abnormality
Phadke et al. [23]	All	32 × 32 (local) and 128 × 128 (global)
Setiawan et al. [24]	All	128 × 128
Pratiwi et al. [25]	All	128 × 128
Qader et al. [26]	All	35 × 35 and 45 × 45
Patil et al. [64]	All, with fatty background tissue	16 × 16
Kamra et al. [65]	AD	Size of abnormality

matrix (GLRLM), gray level difference statistics (GLDS), statistical feature matrix (SFM), first-order statistics (FoS), etc. For feature extraction on multiple scales, transform domain techniques such as wavelets, ridgelets, curvelets, shearlets, and contourlets are used. The scale over which extraction of features is done is considered to be of importance because the human visual system is adapted to process images in a multiscale way [40,41]. Image analysis using Gabor wavelets is just like a human visual system, and thus these linear filters can be used for texture analysis, edge detection, and distinction. A two-dimensional (2D) Gabor filter is a Gaussian

**FIG. 29**

Sample images with marked ROIs: (A–C) “mdb032” with ROIs of size 32×32 pixels, 64×64 pixels and 128×128 pixels marked, respectively; (D–F) “mdb202” with ROIs of size 32×32 pixels, 64×64 pixels and 128×128 pixels marked, respectively; (G–I) “mdb158” with ROIs of size 32×32 pixels, 64×64 pixels and 128×128 pixels marked, respectively.

kernel function modulated by a sinusoidal plane wave. The application of 2D-GWT results in the formation of a set of filters that is frequency and orientation selective, that is, energy is captured by these filters at a particular frequency and orientation. A combination of Gabor wavelets with different orientations and scales provides a useful description of texture [65]. In the present work, three scales and seven different orientations are used to obtain maximum orientation selectivity, resulting in the

Table 4 Classification Performance for Different ROI Sizes

ROI Size	Confusion Matrix			Accuracy (%)
32 × 32	NOR	48	3	84.31
	ABNOR	13	38	
64 × 64	NOR	47	4	84.31
	ABNOR	12	39	
128 × 128	NOR	41	10	82.35
	ABNOR	8	43	

generation of 21 Gabor filters. Mean and standard deviation values are obtained from filtered ROI images, that is, Gabor outputs, resulting in 42 ($3 \times 7 \times 2$) texture features for each ROI. These features are used for the diagnosis of abnormal mammograms using the support vector machine (SVM) classifier.

2.5 SVM CLASSIFIER

The SVM classifiers are associated with learning algorithms and are used for two-group classification problems. These are based on the theory of decision planes or hyperplanes that define decision boundaries separating objects having different class memberships [70]. A set of training examples in which each data point is marked with the category to which it belongs is given. This data is represented as points in space. It is believed that the other, unknown data points follow the same distribution. The idea of SVM is to keep as much safety space, that is, margin, as possible. This margin implies how far apart the boundary decision line is from the data. If in original space the data points are not linearly separable, a kernel function is used, which is a dot product in higher dimensional space. The nonlinear data can thus be transformed in new space, where the data points can be separated by a linear function. This transformation is done using kernel functions. Different kernels available in the SVM algorithm are linear sigmoid, polynomial, and Gaussian radial basis function (GRBF). For the current problem under study, a GRBF kernel has been used. SVM is a sparse algorithm. Only those data points that are very close to the separating hyperplane are actually important to define the position of this hyperplane. It can be said that these points are supporting the location or position of the plane and hence they are called support vectors.

A set of 102 images comprising 51 normal and 51 abnormal mammograms is used for training the SVM classifier. The most favorable values of C (regularization parameter) and γ (kernel parameter) are derived by a comprehensive search [33]. Then, a set of testing data containing 102 mammograms (51 normal and 51 abnormal) is provided and the classification performance is evaluated.

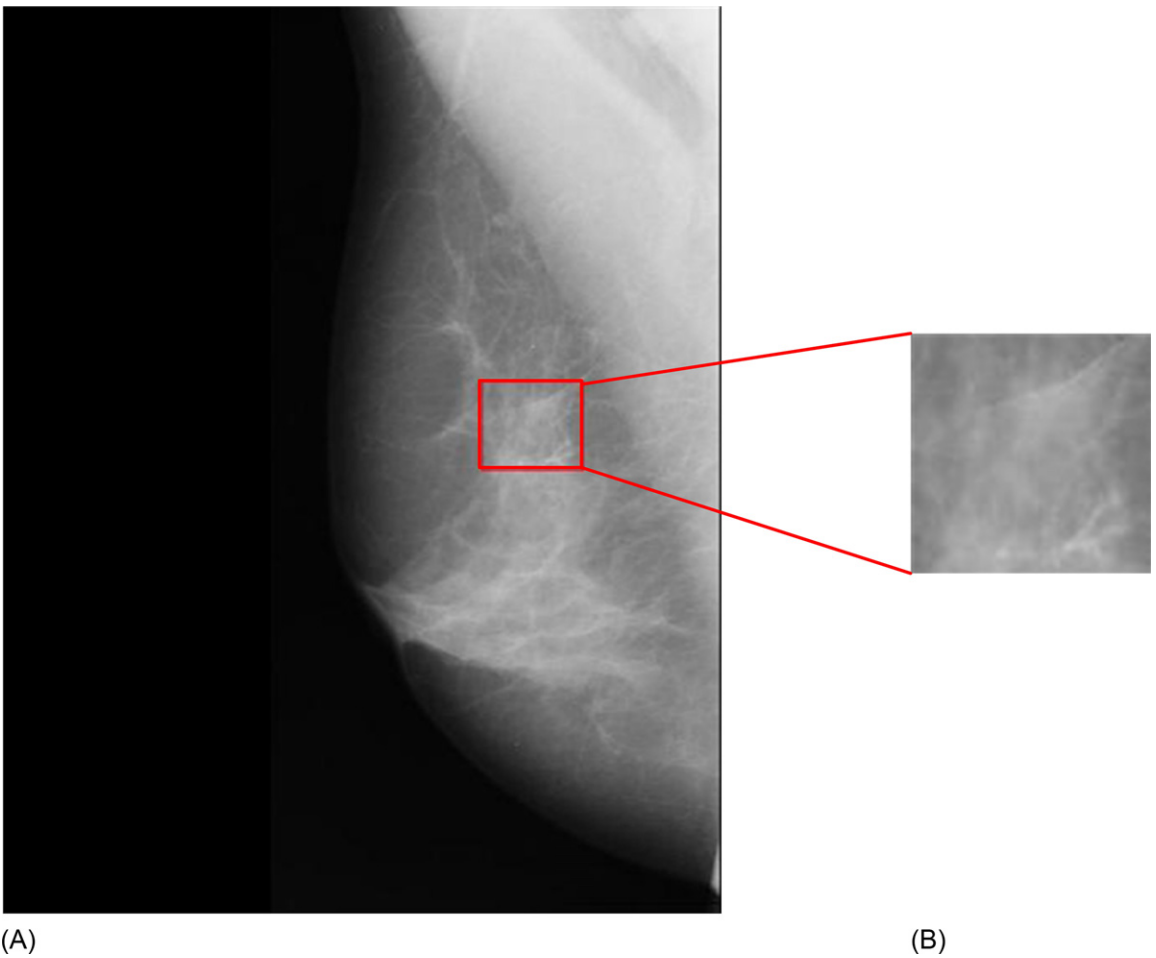


FIG. 30

Mammographic image “mdb149” from MIAS [2] with ROI marked: (A) original image (1024×1024); (B) extracted ROI (32×32).

3 EXPERIMENTAL RESULTS

To analyze the classification performance of the enhancement techniques applied on mammograms, exhaustive experiments were performed. The results of these experiments comprising the confusion matrix, the accuracy, and individual class accuracies for each enhancement method are discussed here.

3.1 OBTAINING THE ACCURACIES OF CLASSIFICATION OF ABNORMAL MAMMOGRAMS AFTER ENHANCEMENT WITH ALPHA TRIMMED MEAN FILTER

The classification performance of the extracted ROIs from alpha trimmed mean filter enhanced images is calculated. The resulting accuracies obtained by the SVM classifier are presented in [Table 5](#).

3.2 OBTAINING THE ACCURACIES OF CLASSIFICATION OF DIAGNOSIS OF ABNORMAL MAMMOGRAMS AFTER ENHANCEMENT WITH CONTRAST STRETCHING

The classification performance of the extracted ROIs from contrast stretched images is evaluated. The resulting accuracies obtained by the SVM classifier are presented in [Table 6](#).

Table 5 Results of Enhancement With Alpha Trimmed Mean Filter

Confusion Matrix			OCA (%)	ICA _A (%)	ICA _N (%)
NOR	NOR	ABNOR	79.4	70.6	88.2
	45	6			
ABNOR	15	36			

OCA, overall classification accuracy; ICA_A, individual abnormal class accuracy; ICA_N, individual normal class accuracy.

Table 6 Results of Enhancement With Contrast Stretching

Confusion Matrix			OCA (%)	ICA _A (%)	ICA _N (%)
NOR	NOR	ABNOR	88.2	86.3	90.2
	46	5			
ABNOR	7	44			

OCA, overall classification accuracy; ICA_A, individual abnormal class accuracy; ICA_N, individual normal class accuracy.

3.3 OBTAINING THE ACCURACIES OF CLASSIFICATION OF DIAGNOSIS OF ABNORMAL MAMMOGRAMS AFTER ENHANCEMENT WITH HISTOGRAM EQUALIZATION

The classification performance of the extracted ROIs from contrast stretched images is evaluated. The resulting accuracies obtained by the SVM classifier are presented in [Table 7](#).

3.4 OBTAINING THE ACCURACIES OF CLASSIFICATION OF DIAGNOSIS OF ABNORMAL MAMMOGRAMS AFTER ENHANCEMENT WITH CLAHE

The classification performance of the extracted ROIs from contrast stretched images is evaluated. The resulting accuracies obtained by the SVM classifier are presented in [Table 8](#).

3.5 OBTAINING THE ACCURACIES OF CLASSIFICATION OF DIAGNOSIS OF ABNORMAL MAMMOGRAMS AFTER ENHANCEMENT WITH RMSHE

The classification performance of the extracted ROIs from RMSHE enhanced images is evaluated. The resulting accuracies obtained by the SVM classifier are presented in [Table 9](#).

Table 7 Results of Enhancement With Histogram Equalization

Confusion Matrix			OCA (%)	ICA _A (%)	ICA _N (%)
NOR	NOR	ABNOR	74.5	74.5	74.5
	38	13			
ABNOR	13	38			

OCA, overall classification accuracy; ICA_A, individual abnormal class accuracy; ICA_N, individual normal class accuracy.

Table 8 Results of Enhancement With CLAHE

Confusion Matrix			OCA (%)	ICA _A (%)	ICA _N (%)
NOR	NOR	ABNOR	88.2	76.5	100
	51	0			
ABNOR	12	39			

OCA, overall classification accuracy; ICA_A, individual abnormal class accuracy; ICA_N, individual normal class accuracy.

Table 9 Results of Enhancement With RMSHE

Confusion Matrix			OCA (%)	ICA _A (%)	ICA _N (%)
NOR	NOR	ABNOR	84.3	72.5	96
	49	2			
ABNOR	14	37			

OCA, overall classification accuracy; ICA_A, individual abnormal class accuracy; ICA_N, individual normal class accuracy.

3.6 OBTAINING THE ACCURACIES OF CLASSIFICATION OF DIAGNOSIS OF ABNORMAL MAMMOGRAMS AFTER ENHANCEMENT WITH CONTRA-HARMONIC MEAN

The classification performance of the extracted ROIs from images enhanced with contra-harmonic mean is evaluated. The resulting accuracies obtained by the SVM classifier are presented in [Table 10](#).

3.7 OBTAINING THE ACCURACIES OF CLASSIFICATION OF DIAGNOSIS OF ABNORMAL MAMMOGRAMS AFTER ENHANCEMENT WITH MEAN FILTER

The classification performance of the extracted ROIs from images enhanced with a mean filter is evaluated. The resulting accuracies obtained by the SVM classifier are presented in [Table 11](#).

3.8 OBTAINING THE ACCURACIES OF CLASSIFICATION OF DIAGNOSIS OF ABNORMAL MAMMOGRAMS AFTER ENHANCEMENT WITH MEDIAN FILTER

The classification performance of the extracted ROIs from images enhanced with a median filter is evaluated. The resulting accuracies obtained by the SVM classifier are presented in [Table 12](#).

Table 10 Results of Enhancement With Contra Harmonic Mean

Confusion Matrix			OCA (%)	ICA _A (%)	ICA _N (%)
NOR	NOR	ABNOR	83.4	74.5	92.2
	47	4			
ABNOR	13	38			

OCA, overall classification accuracy; ICA_A, individual abnormal class accuracy; ICA_N, individual normal class accuracy.

Table 11 Results of Enhancement With Mean Filter

Confusion Matrix			OCA (%)	ICA _A (%)	ICA _N (%)
NOR	NOR	ABNOR	82.4	72.5	92.2
	47	4			
ABNOR	14	37			

OCA, overall classification accuracy; ICA_A, individual abnormal class accuracy; ICA_N, individual normal class accuracy.

Table 12 Results of Enhancement With Median Filter

Confusion Matrix			OCA (%)	ICA _A (%)	ICA _N (%)
NOR	NOR 47	ABNOR 4	80.4	68.7	92.2
	ABNOR 16	35			

OCA, overall classification accuracy; ICA_A, individual abnormal class accuracy; ICA_N, individual normal class accuracy.

3.9 OBTAINING THE ACCURACIES OF CLASSIFICATION OF DIAGNOSIS OF ABNORMAL MAMMOGRAMS AFTER ENHANCEMENT WITH HYBRID MEDIAN FILTER

The classification performance of the extracted ROIs from images enhanced with a hybrid median filter is evaluated. The resulting accuracies obtained by the SVM classifier are presented in [Table 13](#).

3.10 OBTAINING THE ACCURACIES OF CLASSIFICATION OF DIAGNOSIS OF ABNORMAL MAMMOGRAMS AFTER MORPHOLOGICAL ENHANCEMENT

The classification performance of the extracted ROIs from morphologically enhanced images is evaluated. The resulting accuracies obtained by the SVM classifier are presented in [Table 14](#).

Table 13 Results of Enhancement With Hybrid Median Filter

Confusion Matrix			OCA (%)	ICA _A (%)	ICA _N (%)
NOR	NOR 46	ABNOR 5	81.4	72.5	90.2
	ABNOR 14	37			

OCA, overall classification accuracy; ICA_A, individual abnormal class accuracy; ICA_N, individual normal class accuracy.

Table 14 Results of Enhancement With Morphological Enhancement

Confusion Matrix			OCA (%)	ICA _A (%)	ICA _N (%)
NOR	NOR 41	ABNOR 10	74.5	68.7	80.4
	ABNOR 16	35			

OCA, overall classification accuracy; ICA_A, individual abnormal class accuracy; ICA_N, individual normal class accuracy.

3.11 OBTAINING THE ACCURACIES OF CLASSIFICATION OF DIAGNOSIS OF ABNORMAL MAMMOGRAMS AFTER MORPHOLOGICAL ENHANCEMENT, FOLLOWED BY CONTRAST STRETCHING

The classification performance of the extracted ROIs from images enhanced by a combination of morphologically enhancement and contrast stretching is evaluated. The resulting accuracies obtained by the SVM classifier are presented in [Table 15](#).

3.12 OBTAINING THE ACCURACIES OF CLASSIFICATION OF DIAGNOSIS OF ABNORMAL MAMMOGRAMS AFTER UNSHARP MASKING

The classification performance of the extracted ROIs from images enhanced by unsharp masking is evaluated. The resulting accuracies obtained by the SVM classifier are presented in [Table 16](#).

3.13 OBTAINING THE ACCURACIES OF CLASSIFICATION OF DIAGNOSIS OF ABNORMAL MAMMOGRAMS AFTER UMCA

The classification performance of the extracted ROIs from images enhanced by unsharp masking followed by contrast stretching is evaluated. The resulting accuracies obtained by the SVM classifier are presented in [Table 17](#).

Table 15 Results of Enhancement With Morphological Enhancement and Contrast Stretching

Confusion Matrix			OCA (%)	ICA _A (%)	ICA _N (%)
NOR	NOR	ABNOR	92.2	90.2	94.1
	48	3			
ABNOR	5	46			

OCA, *overall classification accuracy*; ICA_A, *individual abnormal class accuracy*; ICA_N, *individual normal class accuracy*.

Table 16 Results of Enhancement With Unsharp Masking

Confusion Matrix			OCA (%)	ICA _A (%)	ICA _N (%)
NOR	NOR	ABNOR	84.3	72.5	96.1
	49	2			
ABNOR	14	37			

OCA, *overall classification accuracy*; ICA_A, *individual abnormal class accuracy*; ICA_N, *individual normal class accuracy*.

Table 17 Results of Enhancement With Unsharp Masking and Contrast Stretching

Confusion Matrix			OCA (%)	ICA _A (%)	ICA _N (%)
NOR	NOR	ABNOR	85.3	80.4	90.2
	46	5			
ABNOR	10	41			

OCA, overall classification accuracy; ICA_A, individual abnormal class accuracy; ICA_N, individual normal class accuracy.

Table 18 Results of Enhancement With Wavelet Based Subband Filtering

Confusion Matrix			OCA (%)	ICA _A (%)	ICA _N (%)
NOR	NOR	ABNOR	84.3	74.5	94.1
	48	3			
ABNOR	13	38			

OCA, overall classification accuracy; ICA_A, individual abnormal class accuracy; ICA_N, individual normal class accuracy.

3.14 OBTAINING THE ACCURACIES OF CLASSIFICATION OF DIAGNOSIS OF ABNORMAL MAMMOGRAMS AFTER WAVELET-BASED SUBBAND FILTERING

The classification performance of the extracted ROIs from images enhanced by wavelet-based subband filtering is evaluated. The resulting accuracies obtained by the SVM classifier are presented in [Table 18](#).

4 COMPARISON OF CLASSIFICATION PERFORMANCE OF THE ENHANCEMENT METHODS

A comparison on the basis of classification performance of all the enhancement methods used is shown in [Table 19](#). The table also provides the classification performance of raw mammograms, that is, without enhancements. It is observed from the table that enhancement with morphological enhancement and contrast stretching (MECA) results in the maximum overall classification accuracy of 92.2%. The individual class accuracy for the abnormal class shows significant results. It is obtained as 90.2%, which means that the ability to find the abnormal ROIs has largely improved as compared to that of the raw images, which is calculated as 74.5%.

Exhaustive experiments were carried out in the present work to investigate the effect of various enhancement methods on the classification performance of digital mammographic images. The mini-MIAS [2] mammographic database was used to obtain images for study. A total of 14 different enhancement methods were applied on mammograms and ROIs were cropped from these enhanced images. An ROI size

Table 19 Comparison of Classification Performance of the Enhancement Methods

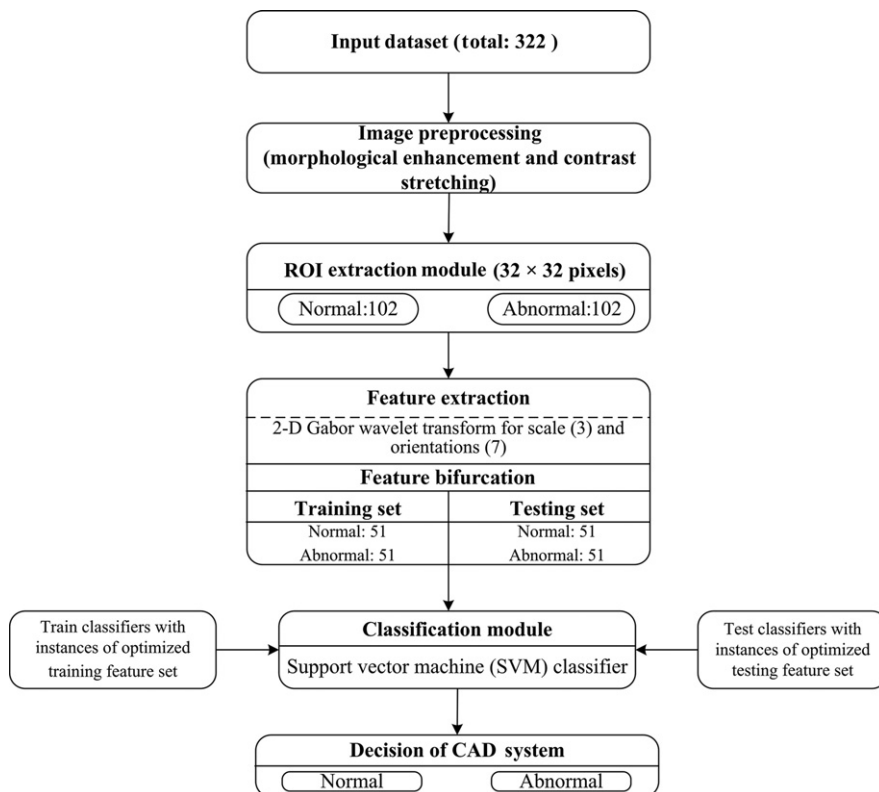
S. No.	Enhancement Method	OCA (%)	ICA _A (%)	ICA _N (%)
1	Raw images with no enhancement	84.3	74.5	94.1
2	Alpha trimmed mean	79.4	70.6	88.2
3	Contrast stretching	88.2	86.3	90.2
4	Histogram equalization	74.5	74.5	74.5
5	CLAHE	88.2	76.5	100
6	RMSHE	84.3	72.5	96
7	Contra harmonic mean	83.4	74.5	92.2
8	Mean filter	82.4	72.5	92.2
9	Median filter	80.4	68.7	92.2
10	Hybrid median filter	81.4	72.5	90.2
11	Morphological enhancement	74.5	68.7	80.4
12	MECA	92.2	90.2	94.1
13	Unsharp masking	84.3	72.5	96.1
14	UMCA	85.3	80.4	90.2
15	Wavelet-based subband filtering	84.3	74.5	94.1

OCA, overall classification accuracy; ICA_A, individual abnormal class accuracy; ICA_N, individual normal class accuracy.

of 32×32 pixels was used, after carefully examining the effects of different ROI sizes on the classification performance. The 42 Gabor features (resulting from 21 Gabor images) were extracted from these ROIs, which were bifurcated into training and testing sets, and the SVM classifier was used for classification into normal and abnormal mammograms. The classification performance of the enhancement methods used was evaluated and it was observed that enhancement with morphological enhancement followed by contrast stretching, that is, the MECA enhancement method, yielded the best results with an overall classification accuracy of 92.2%, an individual class accuracy (abnormal) of 90.2%, and an individual class accuracy (normal) of 94.1%. The proposed methodology for the design of the CAD system for the diagnosis of abnormal mammograms is depicted in Fig. 31. Thus, an ROI size of 32×32 pixels and mammogram enhancement with MECA is suggested for the diagnosis of abnormal mammograms.

5 GENETIC ALGORITHM-BASED METAHEURISTIC APPROACH TO CUSTOMIZE A COMPUTER-AIDED CLASSIFICATION SYSTEM FOR ENHANCED MAMMOGRAMS

Feature selection/optimization techniques have been used by various researchers in their studies carried out on different medical images for reducing the number of extracted features, that is, removing redundant features that give no information

**FIG. 31**

A CAD system for the diagnosis of enhanced abnormal mammograms without feature selection.

for tissue characterization [33–39]. This reduction in the feature set results in improved classification accuracy and reduced computation time.

Metaheuristic search procedures are used quite often for customizing the computer-aided classification systems, as these search procedures yield the set of most optimal features that yield larger class separation. In the present work, also the GA-SVM procedure, a well-known metaheuristic search procedure, has been applied to obtain optimal Gabor features for classification of mammographic images enhanced by the MECA method. The images enhanced by the MECA method have been subjected to GA-SVM because the images enhanced by the MECA method yield the maximum classification accuracy in comparison to images enhanced by other methods. Initially, the Gabor feature set of 42 features was subject to GA-SVM, which yielded the optimal set of 21 Gabor features {namely, Mean(0,5), Mean(0,6), Mean(0,7), Mean(1,2), Mean(1,3), Mean(1,7), Mean(2,3), Mean(2,4), Std(0,1), Std(0,2), Std(0,4), Std(0,5), Std(0,7), Std(1,5), Std(1,6), Std(1,7), Std(2,3), Std(2,4), Std(2,5), Std(2,6), Std(2,7)} out of a total of 42 Gabor features that

Table 20 Results of 21 Optimal Gabor Features Obtained From Images Enhanced With MECA Method

Confusion Matrix			OCA (%)	ICA _A (%)	ICA _N (%)
NOR	NOR	ABNOR	92.2	90.2	94.1
	48	3			
ABNOR	5	46			

OCA, overall classification accuracy; ICA_A, individual abnormal class accuracy; ICA_N, individual normal class accuracy.

are significant for differential diagnosis between normal and abnormal mammographic images. The classification results yielded from these 21 Gabor features obtained by applying the GA-SVM procedure are depicted in [Table 20](#).

By the comparison of results of images enhanced with the MECA method with (21 Gabor Features) and without feature selection (with 42 Gabor Features) i.e. by comparing the results of [Table 14](#) (Results obtained without Feature Selection) with [Table 19](#) (Results obtained by using GA-SVM feature selection) it can be observed that the same results are obtained by using the reduced feature set consisting of 21 Gabor features. Therefore, it is recommended that a reduced feature set of only 21 selected features should be used for designing the CAD system for classification of enhanced mammographic images.

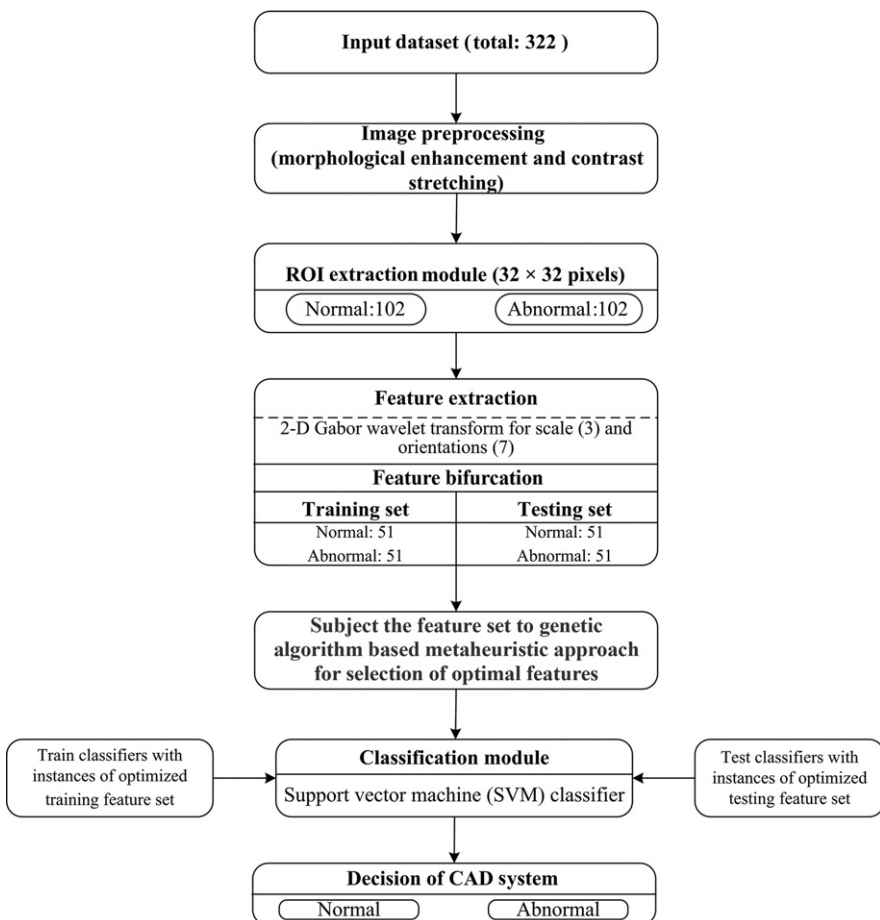
6 CONCLUSION

The design of a genetic algorithm-based metaheuristic approach to customize a computer-aided classification system for enhanced mammograms is shown in [Fig. 32](#).

The results of the exhaustive study carried out in the present work indicate that only 21 Gabor features selected by the GA-SVM procedure are significant for the classification of screen film mammograms enhanced by the MECA method. On the basis of the classification results as well as the clinical validation provided by the participating radiologist, it can also be concluded that the MECA method for enhancement is better suited for visual perception and classification purposes in characterizing the mammographic images to be normal or abnormal.

7 FUTURE SCOPE

The database used is MIAS [2], which only consists of screen film mammograms. Another database such as the INbreast database can be used as it contains full-field digital mammograms. Also, with the change in image resolution and the resolution of ROI, the noise levels and contrast changes. The MIAS [2] dataset includes all images of the same resolution. So, it can be analyzed whether the same multiresolution features applied on mammograms of different resolutions provide the same optimal results.

**FIG. 32**

A CAD system for the diagnosis of enhanced abnormal mammograms with feature selection.

REFERENCES

- [1] Breast cancer: prevention and control <http://www.who.int/cancer/detection/breastcancer/en/>.
- [2] J. Suckling, J. Parker, D.R. Dance, S. Astley, I. Hutt, et al., The Mammographic Image Analysis Society Digital Mammogram Database, in: A.G. Gale, S.M. Astley, D.R. Dance, A.Y. Cairns (Eds.), International Workshop on Digital Mammography, Elsevier, York, UK, 1994, pp. 375–378.
- [3] A.C. Phadke, P.P. Rege, Classification of architectural distortion from other abnormalities in mammograms, Int. J. Appl. Innov. Eng. Manage. 2 (2) (2013) 42–48.
- [4] A. Mencattini, M. Salmeri, P. Casti, in: Bilateral asymmetry identification for the early detection of breast cancer, Proceedings of IEEE International Workshop on Medical Measurements and Applications, Bari, Italy, 30–31 May 2011, 2011.

- [5] G.I. Andreea, R. Pegza, et al., The role of imaging techniques in diagnosis of breast cancer, *Curr. Health Sci. J.* 37 (2) (2011) 55–61.
- [6] Y.I. Anna Rejani, S.T. Selvi, Early detection of breast cancer using SVM classifier technique, *Int. J. Comput. Sci. Eng.* 1 (3) (2009) 127–130.
- [7] S. Beura, B. Majhi, R. Dash, Mammogram classification using two dimensional discrete wavelet transform and gray-level co-occurrence matrix for detection of breast cancer, *Neurocomputing* 154 (3) (2015) 1–14.
- [8] J.B. Jona, N. Nagaveni, A hybrid swarm optimization approach for feature set reduction in digital mammograms, *WSEAS Trans. Inf. Sci. Appl.* 9 (11) (2012) 340–349.
- [9] F. Ibrahim, in: A random feature selection method for classification of mammogram images, Proceedings of Third International Conference on Intelligent Systems Modeling and Simulation, 2012, pp. 330–333.
- [10] Amal AlQoud1, M. Arfan Jaffar, Hybrid Gabor based local binary patterns texture features for classification of breast mammograms, *Int. J. Comput. Sci. Netw. Secur.* 16 (2) (2016) 16–21.
- [11] M.M. Eltoukhy, S.J. Safdar Gardezi, I. Faye, in: A method to reduce curvelet coefficients for mammogram classification, IEEE Region 10 Symposium, 2014, pp. 663–666.
- [12] S. Shanthi, V. Murali Bhaskaran, A novel approach for classification of abnormalities in digitized mammograms, *Sadhana Indian Acad. Sci.* 39 (5) (2014) 1141–1150.
- [13] J.S. Leena Jasmine, S. Baskaran, A. Govardhan, A robust approach to classify microcalcification in digital mammograms using contourlet transform and support vector machine, *Am. J. Eng. Appl. Sci.* 6 (1) (2013) 57–68.
- [14] M.M. Eltoukhy, I. Faye, S. Brahim, A statistical based feature extraction method for breast cancer diagnosis in digital mammogram using multiresolution representation, *Comput. Biol. Med.* 42 (1) (2012) 123–128.
- [15] M.M. Eltoukhy, I. Faye, An optimized feature selection method for breast Cancer diagnosis in digital mammogram using multiresolution representation, *Appl. Math. Inform. Sci.* 8 (6) (2014) 2921–2928.
- [16] A. Qayyum, A. Basit, in: Automatic breast segmentation and cancer detection via SVM in mammograms, International Conference on Emerging Technologies, Islamabad, Pakistan, 2016.
- [17] H. Shah, Automatic classification of breast masses for diagnosis of breast cancer in digital mammograms using neural network, *Int. J. Sci. Technol. Eng.* 1 (11) (2015) 47–52.
- [18] R. Mousa, Q. Munib, A. Moussa, Breast cancer diagnosis system based on wavelet analysis and fuzzy-neural, *Expert Syst. Appl.* 28 (4) (2005) 713–723.
- [19] I. Buciu, A. Gacsadi, Directional features for automatic tumor classification of mammogram images, *Biomed. Signal Process. Control* 6 (4) (2011) 370–378.
- [20] K. Karmilasari, S. Widodo, E.T.P. Lussiana, M. Hermita, L. Mawadah, Classification of Mammogram Images Using Support Vector Machine, Available at https://saki.siit.tu.ac.th/acis2013/uploads_final/25_123822fb183b168b9e65fbae6300609f/ACIS%202013-0025.pdf.
- [21] H.B. Jehlol, Z.K. Abdalrdha, A.S. Abdulhussein Olewi, Classification of mammography image using machine learning classifiers and texture features, *Int. J. Innov. Res. Adv. Eng.* 2 (9) (2015) 56–63.
- [22] Lothe Savita A, Telgad Rupali L, Siddiqui Almas, Deshmukh Prapti D. Detection and classification of breast mass using support vector machine. *IOSR J. Comput. Eng.*, 01–06.

- [23] A.C. Phadke, P.P. Rege, Fusion of local and global features for classification of abnormality in mammograms, *Sadhana Indian Acad. Sci.* 41 (4) (2016) 385–395.
- [24] A.S. Setiawan, Elysia, J. Wesley, Y. Purnama, Mammogram classification using Law's texture energy measure and neural networks, *Procedia Comput. Sci.* 59 (2015) 92–97.
- [25] M. Pratiwi, Alexander, J. Harefa, S. Nanda, Mammograms classification using gray-level co-occurrence matrix and radial basis function neural network, *Procedia Comput. Sci.* 59 (2015) 83–91.
- [26] I.A. Qader, F.A. Amara, A computer-aided diagnosis system for breast cancer using independent component analysis and fuzzy classifier, *Model. Simul. Eng.* 2008 (1) (2008).
- [27] M. Talha, Classification of mammograms for breast cancer detection using fusion of discrete cosine transform and discrete wavelet transform features, *Biomed. Res.* 27 (2) (2016) 322–327.
- [28] I. Christoyianni, A. Koutras, E. Dermatas, G. Kokkinakis, Computer aided diagnosis of breast cancer in digitized mammograms, *Comput. Med. Imaging Graph.* 26 (2002) 309–319.
- [29] S. Sondele, I. Saini, Classification of mammograms using bi-dimensional empirical mode decomposition based features and artificial neural network, *Int. J. Bio-sci. Biotechnol.* 5 (6) (2013) 171–179.
- [30] Herwanto, A.M. Arymurthy, Association technique based on classification for classifying microcalcification and mass in mammogram, *Int. J. Comput. Sci. Issues* 10 (1) (2013) 252–259.
- [31] J. Anitha, J.D. Peter, in: A wavelet based morphological mass detection and classification in mammograms, *Machine Vision and Image Processing (MVIP)*, International Conference, 2012, pp. 25–28. ISBN 978-1-4673-2319-2.
- [32] V.D. Nguyen, T.V. Nguyen, T.D. Nguyen, D.T. Nguyen, H.V. Hoang, Detect abnormalities in mammograms by local contrast thresholding and rule-based classification. in: Proceedings of International Conference on Communications and Electronics, Nha Trang, Vietnam, 2010, <https://doi.org/10.1109/ICCE.2010.5670711>.
- [33] J. Virmani, V. Kumar, N. Kalra, N. Khandelwal, PCA-SVM based CAD system for focal liver lesions using B-mode ultrasound images, *Defence Sci. J.* 63 (5) (2013) 478–486.
- [34] R.K. Sivagaminathan, S. Ramakrishnan, A hybrid approach for feature subset selection using neural networks and ant colony optimization, *Expert Syst. Appl.* 33 (1) (2007) 49–60.
- [35] C.L. Huang, C.J. Wang, A GA-based feature selection and parameter optimization for support vector machines, *Expert Syst. Appl.* 31 (2) (2006) 231–240.
- [36] C.L. Huang, ACO-based hybrid classification system with feature subset selection and model parameters optimization, *Neurocomputing* 73 (1–3) (2009) 438–448.
- [37] M. Gletsos, S.G. Mougiakakou, G.K. Matopoulos, K.S. Nikita, A.S. Nikita, D. Kelekis, A computer-aided diagnostic system to characterize CT focal liver lesions: design and optimization of a neural network classifier, *IEEE Trans. Inform. Technol. Biomed.* 7 (3) (2003) 153–162.
- [38] H. Handels, T. Rob, J. Kreusch, H.H. Wolff, S.J. Poppl, Features election for optimized skin tumor recognition using genetic algorithms, *Artif. Intell. Med.* 16 (3) (1999) 283–297.
- [39] I. Babaoglu, O. findik, E. Ulker, A comparison of feature selection models utilizing binary particle swarm optimization and genetic algorithm in determining coronary artery disease using support vector machine, *Expert Syst. Appl.* 37 (4) (2010) 3177–3183.

- [40] J.G. Daugman, An information-theoretic view of analog representation in striate cortex, in: Computational Neuroscience, MIT Press, Cambridge, MA, 1993, pp. 403–423.
- [41] J. Virmani, V. Kumar, N. Kalra, N. Khandelwal, Prediction of liver cirrhosis based on multiresolution texture descriptors from B-mode ultrasound, *Int. J. Convergence Comput.* 1 (1) (2013) 19–37.
- [42] K. Sharma, J. Virmani, A decision support system for classification of normal and medical renal disease using ultrasound images: a decision support system for medical renal diseases, *Int. J. Ambient Comput. Intell.* 8 (2) (2017) 52–69.
- [43] N. Dey, A.S. Ashour, A.S. Althoupety, Thermal imaging in medical science, in: Recent Advances in Applied Thermal Imaging for Industrial Applications, IGI Global, USA, 2017, pp. 87–117.
- [44] L. Saba, N. Dey, A.S. Ashour, S. Samanta, S.S. Nath, S. Chakraborty, J.S. Suri, Automated stratification of liver disease in ultrasound: an online accurate feature classification paradigm, *Comput. Methods Prog. Biomed.* 130 (2016) 118–134.
- [45] S.S. Ahmed, N. Dey, A.S. Ashour, D. Sifaki-Pistolla, D. Bălas-Timar, V.E. Balas, J.M. R. Tavares, Effect of fuzzy partitioning in Crohn’s disease classification: a neuro-fuzzy-based approach, *Med. Biol. Eng. Comput.* 55 (1) (2017) 101–115.
- [46] Z. Li, K. Shi, N. Dey, A.S. Ashour, D. Wang, V.E. Balas, F. Shi, Rule-based back propagation neural networks for various precision rough set presented KANSEI knowledge prediction: a case study on shoe product form features extraction, *Neural Comput. & Applic.* 28 (3) (2017) 613–630.
- [47] N. Sambyal, P. Abrol, Feature based text extraction system using connected component method, *Int. J. Synth. Emot.* 7 (1) (2016) 41–57.
- [48] A.K. Jain, Fundamentals of Digital Image Processing, Prentice-Hall, Inc, Englewood Cliffs, New Jersey, 1989.
- [49] H.D. Cheng, X. Cai, X. Chen, L. Hu, X. Lou, Computer-aided detection and classification of microcalcifications in mammograms: a survey, *Pattern Recogn.* 36 (12) (2003) 2967–2991.
- [50] R.C. Gonzalez, R.E. Woods, Digital Image Processing, Pearson Education India, Delhi, 2009.
- [51] S.M. Pizer, E.O.P. Amburn, J.D. Austin, R. Cromartie, A. Geselowitz, T. Greer, et al., Adaptive histogram equalization and its variations, *Comput. Vis. Graph. Image Process.* 39 (3) (1987) 355–368.
- [52] E.D. Pisano, S. Zong, R.M. DeLuca, E. Johnston, K. Muller, M.P. Braeuning, et al., Contrast limited adaptive histogram equalization image processing to improve the detection of simulated spiculations in dense mammograms, *J. Digit. Imaging* 11 (4) (1998) 193–200.
- [53] S.-D. Chen, A.R. Ramli, Contrast enhancement using recursive mean-separate histogram equalization for scalable brightness preservation, *IEEE Trans. Consum. Electron.* 49 (4) (2003) 1301–1309.
- [54] M.R. Rakesh, B. Ajeya, A.R. Mohan, Hybrid median filter for impulse noise removal of an image in image restoration, *Int. J. Adv. Res. Electric. Electron. Instrum. Eng.* 2 (10) (2013) 5117–5124.
- [55] T.A. Mahmoud, S. Marshall, in: Medical image enhancement using threshold decomposition driven adaptive morphological filter, Proceedings of the 16th European Signal Processing Conference, Lausanne, Switzerland, 25–29 August 2008, 2008, pp. 1–5.
- [56] H.S. Jagannath, J. Virmani, V. Kumar, Morphological enhancement of microcalcifications in digital mammograms, *J. Inst. Eng. B (India)* 93 (3) (2012) 163–172.

- [57] B. Sridhar, K.V.V.S. Reddy, A.M. Prasad, Automatic detection of micro calcifications in a small field digital mammography using morphological adaptive bilateral filter and radon transform based methods, *Adv. Sci. Eng. Med.* 6 (12) (2015) 1290–1298.
- [58] H. Hassanpour, N. Samadiani, S.M. Mahdi Salehi, Using morphological transforms to enhance the contrast of medical images, *Egypt. J. Radiol. Nucl. Med.* 46 (2015) 481–489.
- [59] R. Firoz, et al., Medical image enhancement using morphological transformation, *J. Data Anal. Inform. Process.* 4 (2016) 1–12.
- [60] W.M. Morrow, R.B. Paranjape, R.M. Rangayyan, J.E.L. Desautels, Region based contrast enhancement of mammograms, *IEEE Trans. Med. Imaging* 11 (3) (1992) 392–406.
- [61] H. Moradmand, S. Setayeshi, A.R. Karimian, M. Sirous, M.E. Akbari, Comparing the performance of image enhancement methods to detect microcalcification clusters in digital mammography, *Iran. J. Cancer Prev.* 5 (2) (2012) 61–68.
- [62] J. Virmani, Wavelet Based Medical Image Analysis for Disease Diagnosis (Dissertation), IIT Roorkee, 2006.
- [63] B. Singh, M. Kaur, An approach for enhancement of microcalcifications in mammograms, *J. Med. Biol. Eng.* (2017) 1–13.
- [64] K.B. Patil, A.C. Phadke, Analysis and classification of abnormality in mammogram with fatty background tissue using Chebyshev moment, *Int. J. Eng. Res. Technol.* 4 (2) (2015) 155–158.
- [65] A. Kamra, V.K. Jain, S. Singh, Extraction of orientation field using Gabor filter and gradient based approach for the detection of subtle signs in mammograms, *J. Med. Imaging Health Inform.* 4 (3) (2014) 374–381.
- [66] Y.M. Kadah, A.A. Farag, J.M. Zurada, A.M. Badawi, A.M. Youssef, Classification algorithms for quantitative tissue characterization of diffuse liver disease from ultrasound images, *IEEE Trans. Med. Imaging* 15 (4) (1996) 466–478.
- [67] A.M. Badawi, A.S. Derbala, A.M. Youssef, Fuzzy logic algorithm for quantitative tissue characterization of diffuse liver diseases from ultrasound images, *Int. J. Med. Inform.* 55 (1999) 135–147.
- [68] K. Fukunaga, *Introduction to Statistical Pattern Recognition*, Academic Press, New York, 1990.
- [69] J. Virmani, V. Kumar, N. Kalra, N. Khandelwal, A comparative study of computer-aided classification systems for focal hepatic lesions from B-mode ultrasound, *J. Med. Eng. Technol.* 37 (4) (2013) 292–306.
- [70] C. Cortes, V.N. Vapnik, Support vector networks, *Mach. Learn.* 20 (1995) 273–297.

FURTHER READING

- [71] J. Dheeba, S. Tamil Selvi, in: *Classification of malignant and benign microcalcification using SVM classifier*, Proceedings of International Conference on Emerging Trends in Electrical and Computer Technology, Nagercoil, India, March, 2011, 2011.

This page intentionally left blank

Embedded healthcare system based on bioimpedance analysis for identification and classification of skin diseases in Indian context

11

Pradeep M. Patil*, Durgaprasad K. Kamat†

JSPM's JS COE, Pune, India* STES's SCOE, Pune, India†

CHAPTER OUTLINE

1 Introduction	262
2 Need of Bioimpedance Measurement for Identification and Classification of Skin Diseases	263
3 System Developed for the Measurement of Human Skin Impedance	266
3.1 Skin Electrode	267
3.2 Impedance Converter IC AD5933	267
3.3 Microcontroller IC CY7C68013A	268
3.4 Personal Computer	269
4 Generation of a Database of Indian Skin Diseases	269
5 Impedance Indices for Identification and Classification of Skin Diseases	270
6 Identification of Skin Diseases	272
6.1 Wilcoxon Signed Rank Test	277
7 Measures of Classification of Skin Diseases	278
7.1 Box and Whisker Plot of Impedance Indices	278
7.2 Mean and Standard Deviation of Impedance Indices	280
8 Classification of Skin Diseases Using Modular Fuzzy Hypersphere Neural Network	281
9 Conclusion	286
References	286

1 INTRODUCTION

Skin diseases are commonly observed in the primary healthcare centers of the regions of the world with infectious diseases. These diseases are looked at with a casual outlook and assumed to have a low mortality rate, which is fatal in many cases. The social standing of an individual and the quality of life is affected by skin diseases. Patients having skin diseases are larger in number in primary care settings than those with other diseases. There is significant impact of skin diseases on both personal and public health. The knowledge of the diverse range of skin diseases poses a challenge at the primary care level. The burden of illness of skin diseases can be reduced by systematic attempts through public health interventions [1].

In comparison with developed countries, skin diseases in India have different root causes. The huge population in India causes overcrowding and close contact of people in domestic and public places. In the rural areas of India, widespread poverty leads to a lack of running water, soap, and detergent that, in turn, leads to a low standard of hygiene. Poverty, illiteracy, and ignorance prevent people from visiting doctors, buying medicines for treatment, and gaining awareness of preventative measures. A lot of skin problems are also due to the equatorial climate with high levels of exposure to sunlight [2].

There are various skin diseases that prevail worldwide, including developed and developing countries such as India. One of the most common skin cancers that has a high mortality rate is melanoma. Melanoma develops because of a pigment-containing cell in the skin called melanocytes. The melanoma cases among the various skin cancers are <1%, but they are mostly fatal and result in death. The incidences of melanoma skin cancer have been observed to a large extent in Australia, New Zealand and the United States. The typical location of melanoma on the human body is on the skin and rarely in the inner body parts such as the intestine or mouth. Another class of skin cancer is nonmelanoma that starts in the skin cells and exhibits as a malignant tumor. Genetic disorders, although rare and affecting only one person in several thousands or millions, lead to sickle-cell anemia and genetic skin disorders. Fungal diseases are often not dangerous, but some types such as dermatophytosis can be harmful. Viral infections such as etiology, pathophysiology, rubella, and the human papillomavirus caused by microorganisms are widespread in developing countries. Sexually transmitted diseases such as trichomoniasis, genital herpes, candida, viral hepatitis, and scabies affect both men and women, although their severity in many cases is greater for women. The bacterial infections normally occurring in the surroundings include acne variants and autoimmune bullous diseases. There are some common skin diseases that prevail in developing countries such as psoriasis, pityriasis rubra pilaris, atopic dermatitis, and leprosy [3].

In the last few decades, the incidences of skin cancers has increased worldwide, and prominent among them is nonmelanoma skin cancer. The prevalence of skin cancer in India has been low due to the protective effects of melanin. The cases of nonmelanoma skin cancer may increase in India due to factors other than ultraviolet

radiation. These new outbreaks in the Indian scenario may pose challenges to dermatologists, indicating a need for the development of some novel techniques [4]. Historically, the treatment in the Indian scenario was with the help of plants, animals, or nonliving matter. The dermatology practices in India have evolved as a combination of allopathic, ayurvedic, acupuncture, and many more. The native tribal populations such as the Negrito and other aboriginal tribes that have lived for more than 50,000 years in the Andaman and Nicobar islands have their own indigenous medical system. These traditional practices form the base of the treatment of the primary health centers of local residents; therefore, the adoption of new practices is a challenging task for the local dermatologists. The role of the Indian Association of Dermatologists and Venereologists and Leprologists is important in this connection for framing therapeutic guidelines on various important dermatological disorders [5].

The common skin diseases observed in India are classified into infestations and infections. The diseases under the infestations category include scabies and pediculosis capitis. There are several infectious diseases such as warts, tinea corporis, and candidiasis. In India, almost 30% of skin problems are observed in children. The availability of a historic database is a challenge to dermatologists in India and hence the dermatologist requires an innovative methodology for the assessment of skin diseases [6]. The number of dermatologists in India has been increasing from a few in the 1960s, for a population of 449 million, to approximately 2000 in 1991, for a population of 843 million. The number of dermatologists today is close to 6000 for a population of 1.324 billion, meaning that there one dermatologist for every 220,000 people. Thus, getting expert advice is a challenging task for a dermatologist, making an objective methodology necessary for diagnosis [2].

The methods of classification of skin diseases based on image processing methods require costly cameras to accurately capture the images. A huge database of images is also required for training the classifier and hence such methods are subjective. So, there is a need for an objective method such as bioimpedance measurement for the identification and classification of skin diseases [7].

The skin cancer-affected population in United States amounts to 5.4 million every year. If skin cancer such as melanoma is detected in its early stages, the survival rate is approximately 97%. The detection of melanoma at later stages drops the survival rate to around 14%. Thus, early detection of skin cancer has a great impact on the survival rate. Hence, detecting skin cancer at the right stage is a challenge to a dermatologist, making an objective technique to detect skin cancer development necessary [8].

2 NEED OF BIOIMPEDANCE MEASUREMENT FOR IDENTIFICATION AND CLASSIFICATION OF SKIN DISEASES

The composition of the human body is analyzed using bioimpedance measurement. The measurements are noninvasive and have simple interfaces. The measured data is useful for disease analysis. Static characteristics are useful in volumetric

determination such as the measurement of body hydration and body fat. Another use of static characteristics is in bioimpedance tomography, which is an imaging application. The hemodynamic measurements record changes in the body over a specified time. This contributes to applications such as the estimation of blood flow or breathing patterns [9].

The bioelectrical impedance or simply bioimpedance of the body is the opposition offered by the biological matter of the body to the flow of alternating current through it. Passive electrical properties of cells and tissues are identified using bioimpedance measurement. Passive electrical properties such as conductivity and permittivity keep on changing based on the physiological and pathological states of the body and its organs. Bioelectrical impedance analysis (BIA) or simply bioimpedance analysis involves the measurement of bioimpedance for the identification of normal and diseased tissues. The safety and ease of use of bioimpedance analysis is appealing for its widespread use in the diagnosis of various diseases. BIA is normally employed in the analysis of the composition of the body. The methods used in body composition analysis divide the body into various compartments. The bioimpedance analysis assumes a two-compartment model consisting of fat mass and fat-free mass. The passage of alternating current through the body encounters two types of opposition: resistive and reactive. The resistive component of the impedance is due to electrolytic body fluids. The reactive component is due to cell membrane capacitance and tissue interface. The vector sum of resistance and capacitive reactance gives the impedance. BIA estimates the composition of the body and its segments, assuming them to be cylindrical structures. Hence, the BIA estimations are based on the length of the body part, the cross-section area, and the frequency of applied alternating current.

In BIA, the alternating current is applied to the body through electrodes. Normally, two and four electrode configurations are used. In the two-electrode configuration, the application of current and the measurement of response voltage are performed with the same electrode pair. The internal resistance of the electrodes affects the measured voltage. This drawback is overcome in the four-electrode configuration. In that configuration, two separate pairs of electrodes are employed. One pair applies current while the other pair measures voltage. So, the polarization effect due to electrodes is minimized in the four-electrode configuration. The location of electrodes is chosen depending on the application. In whole body measurements, electrodes are connected to the wrist and ankle while localized measurements require the most proximal connection of the electrode to the tissue under measurement.

BIA can be performed using single and multifrequency measurements. Single-frequency measurements are typically performed at 50 kHz. The frequency dependence of bioimpedance calls for multifrequency measurements. Measurement of human body impedance at different frequencies is especially useful in characterizing the reactive component of impedance. Hence, low-frequency measurements are useful in characterizing the extracellular fluid volumes while higher applied frequencies characterize the capacitive components of cell membranes and tissue interfaces.

The magnitude and phase angle are two different markers of measured bioimpedance. The magnitude is useful in the estimation of static parameters such as the estimation of body fat. The phase angle is useful in the identification of some disease states such as disorders in metabolism. The muscle mass and body proteins have a positive correlation with measured phase angle. Phase angle is a useful contributor in the diagnosis of hemodialysis patients [10,11].

The bioelectrical impedance measurements are useful in the assessment of skin cancers and other skin diseases. Aberg et al. [12] have used multifrequency bioimpedance measurements to identify the differences between cancerous and noncancerous skin lesions. The diagnosis results of skin cancer using bioimpedance measurements are equivalent or far better than the state-of-the-art visual tools used by dermatologists. The normal and diseased skin can be discriminated with the aid of bioimpedance. Also, the measurements are useful to separate malignant and benign tumors. Various melanoma and nonmelanoma skin cancers have been analyzed using bioimpedance measurements. The outwardly similar looking lesions such as basal cell carcinoma and benign nevi can be discriminated by using the bioimpedance technique. This avoids the necessity of excision of the unintended lesion for histopathological examination and avoids unnecessary pains to the patient. The dermatologists assess the skin diseases, typically by visual inspection, and apply subjective analysis for decision-making. The doubtful lesions are excised and the histopathological examination aids in decision-making. Dermoscopy is an additional tool that provides a microscopic view of skin lesions, but histopathological subjective bias of the expert still has to play a major role in decision-making. Bioelectrical measurement of the skin tissue proves to be a noninvasive, reliable, simple, safe, and objective technique. The noninvasive portable embedded healthcare system is described in histopathological next section for bioimpedance measurements of skin diseases, namely facial melanooses, acne vulgaris, folliculitis, and tinea corporis.

Facial melanooses cause cosmetic disfigurement in patients; it is a common skin disease in India. There are various causes of facial melanooses, prominent among them are Riehl's melanosis, erythema dyschromicum perstans, Lichen planus pigmentosus, melisma, poikiloderma of Civatte, and erythrosis. Chemical exposure in EDP is one of the factors responsible for facial melanooses. Riehl's melanosis is due to allergens exposure. Melisma is due to ultraviolet radiation. The clinical features are useful in the diagnosis of facial melanooses. Facial melanooses are treated by vigorous photoprotection, removing irritating factors, and reducing active pigments. Physical therapy for facial melanooses includes chemical peels. Laser treatment is also useful in some cases. Dermabrasion (skin refinishing) is useful in improving facial skin [13]. Acne vulgaris mainly affects the adolescent population. In acne vulgaris, the pilosebaceous units of skin inflate, making this a chronic disease condition. The severity of the disease is exhibited by pseudocysts and scarred nodules. Acne is associated with a greater psychological burden. Patients experience psychological burdens such as depression, anxiety, and low self-esteem because of acne.

Acne vulgaris remains one of the most common diseases affecting humanity and the measurement of its impact on a patient's quality of life is important [14].

Folliculitis involves inflammation of hair follicles normally caused by a bacterial or fungal infection. The initial symptoms of folliculitis include small whitehead pimples or red bumps around hair follicles. This further develops into nonhealing, crusty sores at later stages, though it is not life-threatening. Folliculitis can cause permanent hair loss and scarring. Folliculitis in the initial stages can be cured in a few days using domestic care measures while recurring folliculitis requires clinical treatment. Various types of folliculitis include razor bumps, barber's itch, and hot tub rash [15]. Tinea corporis is an infection by dermatophytes fungi; it is observed in nails, skin, and hair. Superficial mycotic is observed in 20%–25% of infections worldwide. Among these infections, the most common are dermatophytes. These infections can be treated by improving cell immunity. Delayed treatment can lead to chronic conditions. Developments in the areas of mass spectroscopy and polymerase chain reaction aid in the identification of strains of dermatophytes. The applications of anti-fungal gels and oral dosages are some of the treatments available for treating tinea corporis [16].

3 SYSTEM DEVELOPED FOR THE MEASUREMENT OF HUMAN SKIN IMPEDANCE

Skin diseases have been analyzed using the experimental setup shown in Fig. 1. It consists of a skin electrode, an impedance converter, a microcontroller, and a personal computer. The skin impedance is measured with the help of a skin electrode by attaching the electrode to the skin. The impedance converter IC AD5933 is useful in the measurement of the complex impedance of human skin in terms of its real and imaginary values. Cypress microcontroller CY7C68013A computes impedance with the help of real and imaginary values read from the impedance converter. The personal computer reads the impedance data from the microcontroller and stores it in the database for further analysis. The individual blocks are explained in detail in the following section.

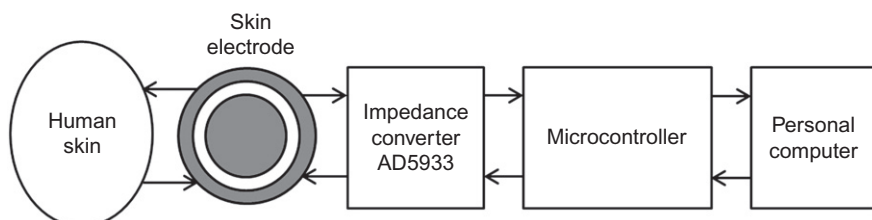


FIG. 1

Experimental setup for bioimpedance analysis of skin diseases.

**FIG. 2**

Developed skin electrode.

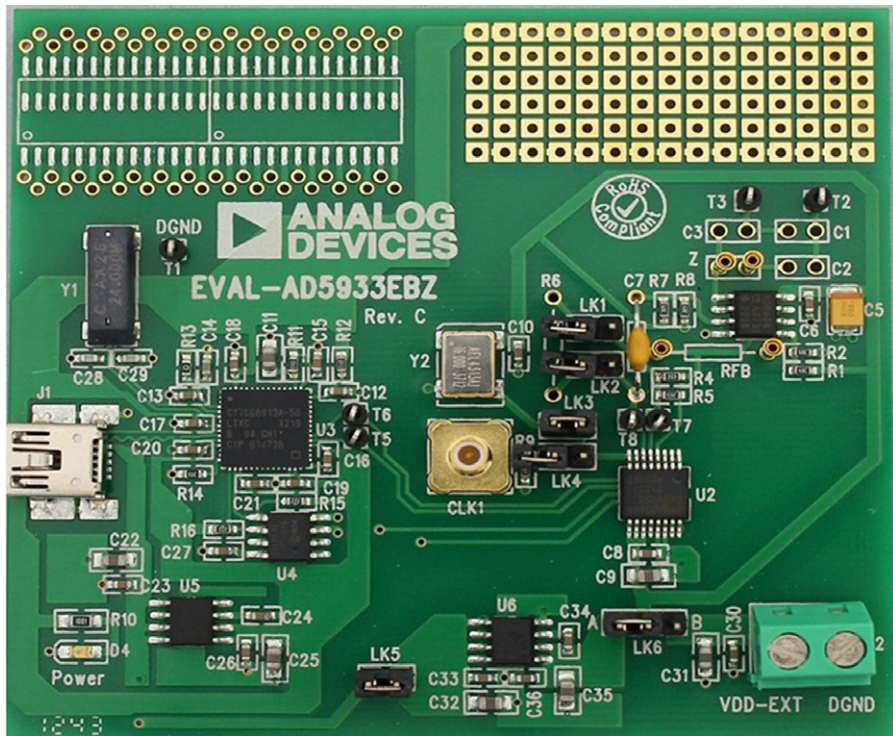
3.1 SKIN ELECTRODE

The impedance of human skin is measured with the help of a developed skin electrode, as shown in Fig. 2.

The skin electrode is fabricated using a glass epoxy material and coated with an Ag/AgCl material. The skin electrode consists of two concentric electrodes: the outer source and inner sink electrode. The size of the source and sink electrodes is chosen arbitrarily; so as to measure the impedance of diseased skin in an effective way. The outer source electrode is connected to the V_{out} pin while the inner sink electrode is connected to the V_{in} pin of AD5933. The insulating guard band between source and sink electrodes reduces the effects of surface currents. The inner circular sink electrode is approximately 10 mm in diameter. This diameter is chosen as the majority of skin lesions in our experimentation are larger than 10 mm in size. The outer source electrode applies an alternating current signal to the skin lesions while the inner sink electrode measures the response signal from the skin lesions [17]. The inner sensing area of the developed electrode needs to have a size matching that of the diseased skin. This is required to improve the accuracy of measurement. As the developed electrode is fabricated with the use of low-cost, flame-retardant materials, the fabrication of multiple electrodes is possible. This calls for the large-scale use of the system in U-healthcare applications.

3.2 IMPEDANCE CONVERTER IC AD5933

Fig. 3 shows the hardware board used in the analysis of skin diseases. The onboard AD5933 IC is used as an impedance converter. A frequency generator and analog-to-digital converter (ADC) are available onboard. The ADC resolution is 12 bits and the speed of conversion is 1 MSPS. A known frequency is applied by a frequency generator to the unknown external impedance to be measured. The signal received from

**FIG. 3**

Hardware board used in the analysis of skin diseases.

the unknown impedance is processed by the ADC. At each applied frequency, a discrete Fourier transform (DFT) is computed with the onboard digital signal processor (DSP). The temperature sensor available onboard is useful in the measurement of body temperature. The hardware board is powered by a USB interface connected to a PC. This USB interface is also useful in data transfer to the PC for database generation [18].

3.3 MICROCONTROLLER IC CY7C68013A

The microcontroller IC CY7C68013A is interfaced to AD5933 on the evaluation board AD5933EBZ. The microcontroller reads the impedance data from the impedance converter. It acts as a programmable interface between the impedance converter and the personal computer for database generation. The microcontroller IC CY7C68013A is based on enhanced 8051 microcontroller architecture. It is used in low-power, battery-operated applications. The code that runs in the internal RAM is compatible with the 8051 family code. The application code can be downloaded into program memory using a USB interface [19].

3.4 PERSONAL COMPUTER

The personal computer runs the front end visual basic program that is bundled with the evaluation board AD5933EBZ. The graphical user interface for setting the parameters of AD5933 has been developed in Visual Basic software. Fig. 4 depicts the graphical user interface that is run on the personal computer for impedance measurement.

4 GENERATION OF A DATABASE OF INDIAN SKIN DISEASES

The electrical impedance of affected skin and normal skin was measured in vivo at 20 and 500 kHz. Measurements were carried out with Analog Devices board AD5933EBZ (see Fig. 5) at Smt. Kashibai Navale Hospital located at Narhe (Bk), Pune, Maharashtra. The various skin diseases for which bioimpedance measurements were carried out were vitiligo, albinism, facial melanooses, intertrigo, acne vulgaris, urticaria, acne, folliculitis, melanocytic disease, eczema, melanosis solar, tinea corporis, keloid, impetigo, Hansen's disease, skin allergies, skin irritation, chronic mucocutaneous candidiasis (CMC), etc. Although readings were recorded for all the above-mentioned diseases, four diseases were chosen for analysis: facial melanooses, acne vulgaris, folliculitis, and tinea corporis. Our in-house generated dataset included 24 lesions for facial melanooses, 29 for acne vulgaris, 37 for folliculitis, and 18 for tinea corporis. The impedance of the normal skin adjacent to these lesions was measured for all 108 locations.

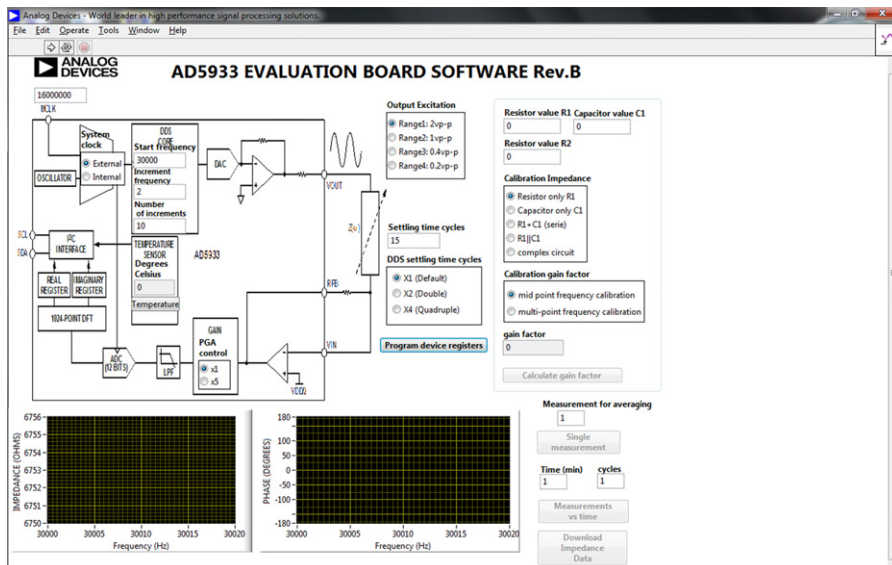
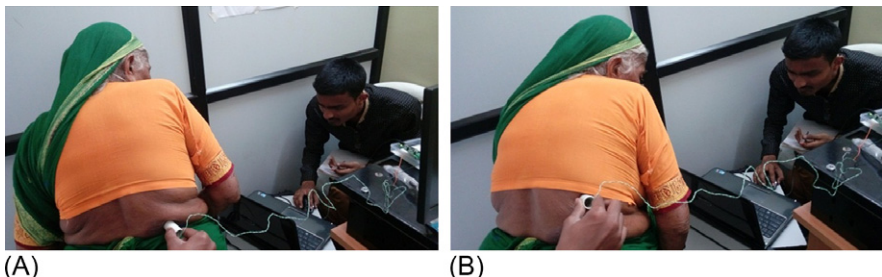


FIG. 4

Graphical user interface used for impedance measurement.

**FIG. 5**

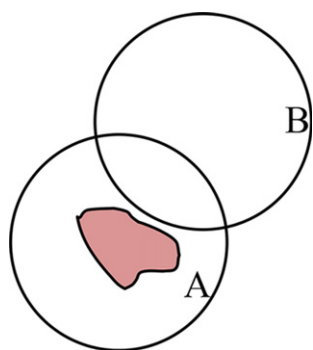
Measurement set up of Analog Devices board AD5933EBZ (A) diseased skin and (B) normal skin.

In a particular measurement, impedance is measured twice. Initially, impedance is measured on the diseased skin and then the impedance of the normal skin surrounding the diseased skin is also measured. Fig. 6 shows the measurement positions of the electrodes. The impedance of the diseased skin was measured by placing the electrode in such a way that the maximum size of the diseased skin is beneath the center of the electrode. The normal skin impedance adjacent to the diseased skin is also measured.

The lesions available in this work were of different sizes. Large lesions were completely covered beneath the inner circular electrode that measures the response signal. The bioimpedance measurement of small lesions is affected because of the inclusion of normal skin along with the lesion. The bioimpedance measurement in such a case includes normal skin impedance along with lesion impedance. In the case of measurements with small lesions, the proportion of normal skin impedance increases with a decrease in the size of the lesion. Lesions having a more protruding shape outside the skin have a greater proportion of normal skin impedance. The inclusion of normal skin impedance in the measured impedance of a lesion decreases measurement accuracy. In this work, the lesions best fitting the size of the measurement electrode were chosen for measurement so as to avoid inclusion of normal skin in impedance measurement of the lesion and get accurate measurement of the results. The experimental results are validated by medical professionals working at the SKN Hospital, Pune, Parashree Speciality Hospital, Amravati, Arunoday Hospital, Amravati, Gatelife Healthcare Hospital, Amravati, Rangari Surgical Home, Bhandara and Jankalyan Hospital, Pandharpur in Maharashtra State, India.

5 IMPEDANCE INDICES FOR IDENTIFICATION AND CLASSIFICATION OF SKIN DISEASES

The bioimpedance analysis of skin diseases involves the computation of four impedance indices using magnitude, phase, real-part, and imaginary part of measured bioimpedance.

**FIG. 6**

Electrode positions for skin impedance measurement (A) with diseased skin at the center of the measurement electrode and (B) for electrode placement on normal skin near the diseased skin.

Nicander et al. [20] performed an experiment for studying skin irritation due to the application of three different chemicals. The study was aimed at finding the relation between impedance and histopathological change. The impedance magnitude and phase were recorded after applying the irritants. The impedance indices have been formed for real, imaginary, magnitude, and phase of impedance. These indices created different patterns for various irritants. This helps in the classification of various skin diseases based on impedance indices. Emtestam et al. [21] used the electrical impedance method for nodular basal cell carcinoma (BCC). The results explain the utility of electrical impedance measurements as a simple, safe, fast, and inexpensive technique for BCC diagnosis. Beetner et al. [22] studied the electrical impedance measurements for BCC diagnosis. BCC and benign lesions can be differentiated using electrical impedance measurements.

The skin disease and normal tissues can be distinguished by using electrical impedance measurements. Electrical impedance characteristics of tissue are affected by its chemical composition and micro- as well as macrostructural characteristics. The electrical properties of the tissue vary depending on tissue state and tissue type. Diseased as well as normal tissues show different impedance levels. The *in vivo* studies use an impedance spectrometer to measure bioimpedance [23]. The upper layer of human skin is stratum corneum. It has less conductivity and high capacitance in comparison with the lower layers of skin. The bioimpedance spectra of low frequencies are characterized by dielectric dispersion parameters of stratum corneum. Skin diseases are characterized by changes in the dielectric properties of upper as well as lower layers of skin. Hence, the bioelectrical characterization of viable skin layers below the stratum corneum is also essential. One of the mechanisms is variation in applied frequency. The lower frequency is used to characterize the upper stratum corneum layer while the higher frequency characterizes the viable skin layers that are

beneath the stratum corneum. The spectrum of skin impedance exhibits a linear relationship between real and imaginary parts in the frequency range between 10 kHz and 1 MHz. Two significant points have been identified in this frequency range to represent almost all information of the entire frequency range. These two frequencies are 20 and 500 kHz [20,22].

Various skin diseases have been distinguished based on four computed indices: magnitude index (MIX), phase index (PIX), real-part index (RIX), and imaginary-part index (IMIX). These indices are defined as,

$$MIX = \frac{abs(Z_{20})}{abs(Z_{500})} \quad (1)$$

$$PIX = \arg(Z_{20}) - \arg(Z_{500}) \quad (2)$$

$$RIX = \frac{\operatorname{Re}(Z_{20})}{abs(Z_{500})} \quad (3)$$

$$IMIX = \frac{\operatorname{Im}(Z_{20})}{abs(Z_{500})} \quad (4)$$

where,

$abs(Z_i)$ is magnitude (in ohms),

$\arg(Z_i)$ is phase angle (in degrees),

$\operatorname{Re}(Z_i)$ is real part,

$\operatorname{Im}(Z_i)$ is imaginary part of impedance at frequency i .

The impedance indices can be used to classify skin diseases.

6 IDENTIFICATION OF SKIN DISEASES

The bioimpedance analysis of facial melanooses, acne vulgaris, folliculitis, and tinea corporis is performed for each measurement using the various impedance indices of skin (see Eqs. 1–4). It has been observed that the patient's age or the location of measurement does not affect the value of the indices. Also, the accuracy of measurement is subject to the size of the measurement electrode. This is because the diseased skin for which the measurements are to be carried out are of various shapes and sizes. If the size of the electrode is more than the size of the diseased skin, the inclusion of normal skin along with diseased skin affects measurement results. So, measurement accuracy can be improved with electrodes of different sizes.

Impedance measurements are performed at 20 and 500 kHz on the diseased skin and normal skin of the subjects having various skin diseases based on real part, imaginary part, magnitude, and phase of impedance, as shown in Table 1. Table 2 shows the values of indices for various skin diseases of affected and normal skin.

Table 1 Bioimpedance Measurement Readings for Various Skin Diseases

Type of Disease	Skin	Frequency	Impedance	Phase	Real	Imaginary	Magnitude
Vitiligo	Diseased	20,000	18,797	26	5046	5669	7589
		500,000	41,078	55	-12,843	7994	15,128
	Normal	20,000	190,965	14	6091	15,135	16,314
		500,000	194,989	21	-15,868	2803	16,114
Albinism	Diseased	20,000	199,615	2	7876	4099	8879
		500,000	205,929	1	-6235	2092	6577
	Normal	20,000	197,771	2	7804	4145	8836
		500,000	198,040	3	-6588	1963	6874
Facial melanooses	Diseased	20,000	200,054	6	1076	808	1346
		500,000	200,773	2	-5489	-9	5489
	Normal	20,000	160,116	4	-5846	16,902	17,884
		500,000	208,074	1	-2566	-14,367	14,595
Intertrigo	Diseased	20,000	160,116	4	-6209	16,044	17,204
		500,000	208,074	1	-2426	-15,027	15,222
	Normal	20,000	140,291	3	-9391	19,014	21,207
		500,000	170,011	2	-4117	-17,179	17,665
Acne vulgaris	Diseased	20,000	195,526	5	1331	3789	4016
		500,000	173,825	3	-8023	-4972	9439
	Normal	20,000	168,121	6	-5083	14,709	15,563
		500,000	147,289	2	-1434	-13,491	13,567
Urticaria	Diseased	20,000	14,962	5	2515	12,858	13,102
		500,000	12,071	2	-11,320	-9269	14,631
	Normal	20,000	209,272	3	-7099	14,911	16,515
		500,000	192,298	1	-10,027	-12,047	15,674

Continued

Table 1 Bioimpedance Measurement Readings for Various Skin Diseases—cont'd

Type of Disease	Skin	Frequency	Impedance	Phase	Real	Imaginary	Magnitude
Acne	Diseased	20,000	188,654	11	-15,591	6499	16,891
		500,000	191,288	6	-10,668	-11,819	15,922
	Normal	20,000	185,399	9	-7002	11,935	13,837
		500,000	195,180	5	-12,690	-6720	14,359
Folliculitis	Diseased	20,000	243,710	2	754	2405	2521
		500,000	197,179	1	160	2952	2957
	Normal	20,000	197,390	3	-14,618	7206	16,298
		500,000	196,083	2	-15,631	3059	15,928
Melanocytic disease	Diseased	20,000	218,364	8	-11,336	8443	14,135
		500,000	174,809	3	5131	-13,995	14,906
	Normal	20,000	187,049	2	-13,357	9438	16,355
		500,000	187,692	1	4922	-13,151	14,042
Eczema	Diseased	20,000	88,301	-20	3088	9291	9791
		500,000	297,320	7	61	-608	611
	Normal	20,000	180,763	-1	-12,329	11,582	16,916
		500,000	151,115	6	-106	-1086	1091
Melanosis solar	Diseased	20,000	186,678	5	-18,295	6709	19,487
		500,000	197,654	2	1847	4240	4625
	Normal	20,000	201,479	4	-17,083	6493	18,275
		500,000	226,115	2	1622	3445	3807
Tinea corporis	Diseased	20,000	191,563	9	4519	5703	7276
		500,000	181,857	11	-7236	-5726	9227
	Normal	20,000	194,364	1	-15,673	7012	17,170
		500,000	194,559	1	6155	-13,314	14,667

Keloid	Diseased	20,000	197,107	6	6520	7139	9668
		500,000	186,572	4	-6368	-3135	7098
	Normal	20,000	180,145	8	5641	6004	8239
		500,000	180,077	8	-5224	-2650	5858
Impetigo	Diseased	20,000	21,069	64	10,876	-2028	11,064
		500,000	217,041	1	-1013	357	1074
	Normal	20,000	28,915	22	12,099	1838	12,238
		500,000	312,285	-7	-991	549	1133
Hansen's disease	Diseased	20,000	213,386	-3	-4701	2967	5558
		500,000	179,890	-4	428	296	520
	Normal	20,000	195,159	2	-11,755	-10,461	15,736
		500,000	204,697	23	422	424	598
Skin allergy	Diseased	20,000	215,680	-2	946	2994	3140
		500,000	176,908	4	-5276	-3989	6614
	Normal	20,000	202,113	-9	3327	3790	5043
		500,000	201,989	-3	-8512	-6026	10,429
Skin irritation	Diseased	20,000	199,831	3	6231	-12,926	14,350
		500,000	198,947	1	11,300	-6329	12,952
	Normal	20,000	199,490	2	5812	-13,021	14,259
		500,000	201,031	-1	10,827	-6745	12,756
Chronic mucocutaneous candidiasis (CMC)	Diseased	20,000	197,181	3	4764	-13,053	13,895
		500,000	197,345	2	-551	9999	10,015
	Normal	20,000	196,930	3	4424	-13,047	13,777
		500,000	199,611	1	-424	9892	9901

Table 2 Values of Indices Computed Based on Bioimpedance Readings for Various Skin Diseases

Type of Disease	Skin	MIX	PIX	RIX	IMIX
Vitiligo	Diseased	0.50	-29.00	0.12	0.37
	Normal	1.01	-7.00	0.03	0.94
Albinism	Diseased	1.35	1.00	0.04	0.62
	Normal	1.29	-1.00	0.04	0.60
Facial melanooses	Diseased	0.25	4.00	0.01	0.15
	Normal	1.23	3.00	-0.03	1.16
Intertrigo	Diseased	1.13	3.00	-0.03	1.05
	Normal	1.20	1.00	-0.06	1.08
Acne vulgaris	Diseased	0.43	2.00	0.01	0.40
	Normal	1.15	4.00	-0.03	1.08
Urticaria	Diseased	0.90	3.00	0.21	0.88
	Normal	1.05	2.00	-0.04	0.95
Acne	Diseased	1.06	5.00	-0.08	0.41
	Normal	0.96	4.00	-0.04	0.83
Folliculitis	Diseased	0.85	1.00	0.00	0.81
	Normal	1.02	1.00	-0.07	0.45
Melanocytic	Diseased	0.95	5.00	-0.06	0.57
	Normal	1.16	1.00	-0.07	0.67
Eczema	Diseased	16.02	-27.00	0.01	15.20
	Normal	15.50	-7.00	-0.08	10.61
Melanosis solar	Diseased	4.21	3.00	-0.09	1.45
	Normal	4.80	2.00	-0.08	1.71
Tinea corporis	Diseased	0.79	-2.00	0.02	0.62
	Normal	1.17	1.00	-0.08	0.48
Keloid	Diseased	1.36	2.00	0.03	1.01
	Normal	1.41	0.00	0.03	1.02
Impetigo	Diseased	10.30	63.00	0.05	-1.89
	Normal	10.80	29.00	0.04	1.62
Hansen's disease	Diseased	10.68	1.00	-0.03	5.70
	Normal	26.30	-21.00	-0.06	-17.49
Skin allergy	Diseased	0.47	-6.00	0.01	0.45
	Normal	0.48	-6.00	0.02	0.36
Skin irritation	Diseased	1.11	2.00	0.03	-1.00
	Normal	1.12	3.00	0.03	-1.02
Chronic mucocutaneous candidiasis (CMC)	Diseased	1.39	1.00	0.02	-1.30
	Normal	1.39	2.00	0.02	-1.32

The impedance indices MIX, IMIX, and PIX have significantly different values over normal and diseased skin. The detailed analysis carried out for these diseases has been discussed in this section.

It is clearly observed from [Tables 1 and 2](#) that one cannot predict the type of disease and the difference between the normal and diseased skin with only the help of measured electrical bioimpedance, but one can reach a partial conclusion from the computed values of various indices.

The impedance measurements showed overlapping readings for different diseases so that indices computed based on impedance readings could be a mechanism for differentiation between the tissues of various diseases. The confirmation of the hypothesis to identify the difference between the diseased skin and the normal skin based on various indices can be carried out using the Wilcoxon signed rank test among the skin diseases having similar values of indices for normal skin. In our study, we found facial melanooses, acne vulgaris, folliculitis, and tinea corporis to have similar values of indices for normal skin.

In the work explained in this chapter, the depth of measurement was not considered as a parameter during the experimentation because it does not affect the results [\[23\]](#). Impedance indices change at various depths of measurement, but for a particular tissue, they maintain the same relationship.

6.1 WILCOXON SIGNED RANK TEST

Statistically significant differences between indices of diseased and normal skin were estimated using the Wilcoxon signed rank test. This test is useful in the statistical comparison of the average of two dependent samples and it is equivalent to the dependent *t*-test. The test is useful when one cannot use the dependent *t*-test. The null hypothesis tested in the Wilcoxon test assumes zero average signed ranks in two dependent samples. Two score sets that are recorded for the same participants are compared in the test. A continuous level should be used to measure the dependent variable. The categorically related groups should form an independent variable. The shape of the symmetrical distribution of the differences is required between two related groups. When the same subjects exist in both groups, it is a related group [\[24,25\]](#).

In this chapter, we have carried out the Wilcoxon signed-rank test with the help of SPSS, which is popularly used in health sciences. SPSS is useful in advanced statistical analysis. It comes bundled with a large library of machine learning algorithms. The latest updates are possible because of open source extensibility. Text analysis can be performed with the help of SPSS. SPSS can be easily integrated with various application platforms. SPSS helps the end user in finding new opportunities, improving efficiency, and minimizing risk. These features are provided because of a scalable, easy-to-use, and flexible platform that can be accessed even by a layman. SPSS can handle projects of different complexity levels and various sizes [\[26\]](#).

The comparison of similarity between the indices (MIX, PIX, RIX, and IMIX) of diseased and normal skin for facial melanooses, acne vulgaris, folliculitis, and tinea corporis has been carried out using SPSS. A person has a skin disease when the

probability of similarity between impedance indices of diseased and normal skin is <0.05 . [Table 3](#) depicts the probability of similarity between distributions of indices for diseased and normal skin.

As shown in [Table 3](#), significant differences have been observed between diseased and normal skin for MIX, PIX, and IMIX values of facial melanooses, acne vulgaris, folliculitis, and tinea corporis as the probability of similarity is far <0.05 . In the case of RIX, excepting the case of folliculitis, the distributions of all other diseases have shown significant differences. Hence, based on the significant differences, MIX, PIX, and IMIX contribute toward the differentiation between diseased and normal skin. Excepting the case of folliculitis, RIX also contributes to the differentiation between diseased and normal skin.

7 MEASURES OF CLASSIFICATION OF SKIN DISEASES

The possibility of classification of skin diseases has been identified by observing the box and whisker plots as well as the mean and standard deviation of impedance indices.

7.1 BOX AND WHISKER PLOT OF IMPEDANCE INDICES

The box and whisker plots for MIX, IMIX, PIX, and RIX of facial melanooses, acne vulgaris, folliculitis, tinea corporis, and normal skin are shown in [Fig. 7](#). The median of the dataset is represented by the middle value in each box. Boxes are drawn around

Table 3 Probability of Similarity Between Various Impedance Measures

Index	Similarity Between	Probability
MIX	Facial melanooses and normal skin	0.0000179835
	Acne vulgaris and normal skin	0.0000025288
	Folliculitis and normal skin	0.00000011
	Tinea corporis and normal skin	0.000189988
PIX	Facial melanooses and normal skin	0.0082524531
	Acne vulgaris and normal skin	0.0030399216
	Folliculitis and normal skin	0.0000001448
	Tinea corporis and normal skin	0.0075999592
RIX	Facial melanooses and normal skin	0.0000638237
	Acne vulgaris and normal skin	0.000004999
	Folliculitis and normal skin	0.1033675355(NS)
	Tinea corporis and normal skin	0.0001843516
IMIX	Facial melanooses and normal skin	0.0000175793
	Acne vulgaris and normal skin	0.0000025050
	Folliculitis and normal skin	0.0000001066
	Tinea corporis and normal skin	0.0001903234

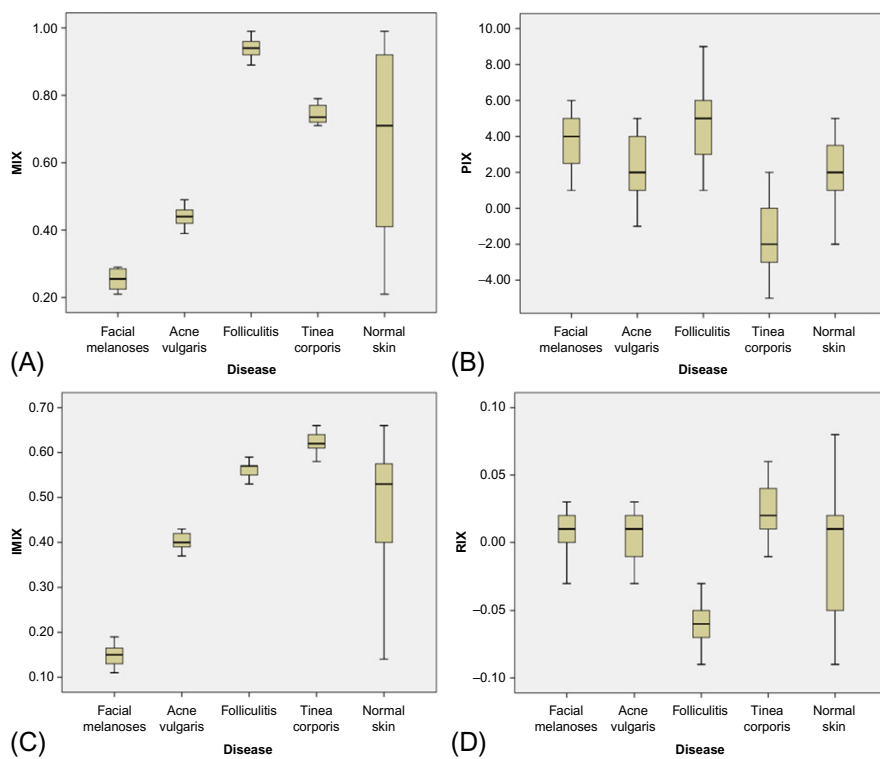


FIG. 7

Box and whisker plots for the four indices of facial melanoses, acne vulgaris, folliculitis, tinea corporis, and normal skin (A) MIX, (B) PIX, (C) IMIX, and (D) RIX.

the median so that 25% of the data points are included in both directions. Minimum and maximum values are represented by the end points of whiskers drawn around the median. Various skin diseases are shown along the X -axis and various indices are depicted on the Y -axis. Measurements at the surface position of diseased skin for each of the subjects along with the normal skin are included for the said diseases.

Box and whisker plots graphically display variations in a given dataset and are similar to a histogram. The shape of the distribution along with the central point and variability are exhibited by box and whisker plots. This is used to show the shape of the distribution, its central value (median), and its variability. The histogram in many statistical applications provides a sufficient display of the data. But the specificity of the box and whisker plot is that it provides more using descriptive statistics. Descriptive statistics use numbers to describe the similarity or difference in the datasets. Box and whisker plots offer the opportunity to researchers to display multiple sets of data in the same graph. Box and whisker plots display statistical data based on the summary of five numbers: minimum value, first quartile, median, third quartile,

and maximum value. The plots are easy to read and are used to summarize data from multiple independent sources, which are related in some way. Box and whisker plots facilitate easier and more effective decision-making by allowing data comparison from different categories.

In this chapter, we have plotted the box and whisker plots of MIX, PIX, IMIX, and RIX for facial melanoses, acne vulgaris, folliculitis, tinea corporis, and normal skin. The in-house generated database includes 24 subjects of facial melanoses, 29 subjects of acne vulgaris, 37 subjects of folliculitis, and 18 subjects of tinea corporis. The box and whisker plot of normal skin thus includes normal skin readings of all 108 subjects. In Fig. 7A, the MIX plot shows clearly distinguishable values of all the diseases between the ranges 0.2–1.0. Similarly, IMIX plots for the said diseases (see Fig. 7C) are also distinguishable in the range between 0.1 and 0.7. The PIX plot (see Fig. 7B) shows overlapping between values of the indices in the range –3 to 9. The RIX plot (see Fig. 7D) also shows overlapping values between the diseases of facial melanoses, acne vulgaris, and tinea corporis while the plot for folliculitis disease is seen in a different range between 0.1 and 0.075.

7.2 MEAN AND STANDARD DEVIATION OF IMPEDANCE INDICES

The statistical analysis is useful in understanding the probability of data distribution. For this purpose, the mean and standard deviation of MIX, PIX, IMIX, and RIX have been calculated for the said diseases. Many statistical applications use a 95% confidence interval. This is because, on a normal distribution, a 97.5 percentile point relates to 1.96 on normal distribution. The 1.96 of standard deviation indicates 95% of the normal curve area. Hence, the 95% confidence intervals are based on this number. In medical statistics, earth sciences, social sciences, and business research, it is a common convention to use A 95% confidence interval. The statistical significance of the results is based on either the significance level or confidence intervals. The distance between the sample mean and the null hypothesis decides the statistical significance. The confidence level defines the distance of confidence limits from the sample mean. A significance level (alpha) of 0.05 corresponds to a confidence level of 95%. Hypothesis testing involves checking the probability value and confidence interval. The probability value in a statistically significant hypothesis is less than significance level (alpha). The confidence interval in a statistically significant hypothesis does not include null hypothesis.

The possibility of classification of skin diseases is identified by computing the mean and standard deviation values of various indices for the said diseases, as summarized in Table 4.

The mean value of MIX was lowest for facial melanoses and highest for folliculitis while that for acne vulgaris and tinea corporis fall in between these two in increasing order. The mean value of MIX for normal skin was found to be the highest for all the diseases. Based on the observed mean values of MIX, two groups of diseases can be clearly identified: facial melanoses and acne vulgaris with lower values while folliculitis and tinea corporis have higher values of MIX. The mean value of

Table 4 Mean and Standard Deviation of Various Indices

Index	Measurement for	Mean \pm Standard Deviation
MIX	Facial melanooses (24)	0.2525 \pm 0.02923
	Acne vulgaris (29)	0.4393 \pm 0.02815
	Folliculitis (37)	0.9416 \pm 0.02598
	Tinea corporis (18)	0.7533 \pm 0.04911
	Normal skin (108)	1.1736 \pm 0.0507
PIX	Facial melanooses (24)	4.4583 \pm 0.97709
	Acne vulgaris (29)	2.5862 \pm 1.05279
	Folliculitis (37)	4.5946 \pm 1.01268
	Tinea corporis (18)	-0.8889 \pm 1.18266
	Normal skin (108)	2.1852 \pm 1.7938
RIX	Facial melanooses (24)	0.0075 \pm 0.018
	Acne vulgaris (29)	0.0069 \pm 0.01734
	Folliculitis (37)	0.0541 \pm 0.03320
	Tinea corporis (18)	0.0211 \pm 0.02026
	Normal skin (108)	-0.0513 \pm 0.02268
IMIX	Facial melanooses (24)	0.1479 \pm 0.0234
	Acne vulgaris (29)	0.4141 \pm 0.08555
	Folliculitis (37)	0.563 \pm 0.02039
	Tinea corporis (18)	0.6211 \pm 0.02564
	Normal skin (108)	0.8556 \pm 0.26789

PIX was found to be lowest for tinea corporis followed in increasing order by vulgaris, facial melanooses, and folliculitis. Significant differences were not observed between facial melanooses and folliculitis in terms of PIX. Significant differences generally were not found in terms of RIX for all the four diseases. Values of IMIX were significantly lower for facial melanooses in comparison with acne vulgaris, folliculitis, and tinea corporis. Among the later three, the values of IMIX were observed to follow an increasing trend.

8 CLASSIFICATION OF SKIN DISEASES USING MODULAR FUZZY HYPERSPHERE NEURAL NETWORK

In the field of biomedical engineering, a number of efforts have been made in terms of classification of various diseases and other associated activities. Support vector machines and probabilistic neural networks have been applied to mammographic images by Kriti et al. [27] for the classification of breast tissue density. Saba et al. [28] used the Levenberg-Marquardt back propagation network classifier for the detection of fatty liver disease. The diagnosis of Crohn's disease was presented

by Ahmed et al. [29] by combining a back propagation neural network fuzzy classifier and a neurofuzzy model. Using a small feature space made up of second order gray-level cooccurrence matrix statistical features, Sharma et al. [30] proposed a decision support system for neurofuzzy detection of renal disease. The raw renal ultrasound images have been used in computing statistical features. Dey et al. [31] reviewed various concepts of thermal imaging and application areas with special reference to neurofuzzy prediction of breast cancer. Li et al. [32] proposed an effective method for analyzing plantar pressure images in order to obtain the key areas of foot plantar pressure characteristics of diabetic patients. Dey et al. [33] explained the significance of biomedical imaging processing in the diagnosis of pathological conditions. The techniques of pattern recognition are divided into clustering and classification. Using operating time, Azzabi et al. [34] studied the diagnosis of failures with timed automata. A diagnoser that employs observable events for detection and location of faults has been constructed. Various techniques of feature extraction were analyzed in terms of classification by Khachane et al. [35]. MRI images of the brain and knee have been used for this purpose.

In this chapter, we have implemented the four-layer modular fuzzy hypersphere neural network (MFHSNN) for classifying four Indian skin diseases: facial melanoses, acne vulgaris, folliculitis, and tinea corporis [36]. The training phase involves four modules of MFHSNN as the database has four classes of skin diseases. As per application requirements, the first two layers of the feed forward neural network grow adaptively. The purpose of the first layer is to accept n -dimensional input patterns selected as the statistical information of the indices, along with individual values of the indices. During the training phase, hyperspheres (HSs) are created and they form the second layer. In this work, we have used minimum value, first quartile, median, third quartile, and maximum value of indices of a particular disease, along with MIX, PIX, IMIX, and RIX of diseased and normal skin for individual subjects as input features. Hence, the first layer has 13-dimensional input patterns along with the class label. An individual module in MFHSNN represents a skin disease and is trained with the patterns of that disease class. Thus, the features of individual skin diseases are learned by separate classes.

The weights between first and second layer, for any k^{th} module, represent center points and radii of hyperspheres that are created during the training phase. A matrix CP^k is used to store these weights. A row in the matrix CP^k has $(n + 1)$ elements. In every row of CP^k , the first n elements represent the center point while $(n + 1)^{th}$ element represents the HS radius. In this work, each row in CP^k is a 14-dimensional vector with the first 13 components relating to indices of diseased and normal skin of individual subjects and statistical parameters of indices of a particular disease. The 14th dimension represents the HS radius. Three parameters—center point, radius, and a fuzzy membership function—characterize the HS module. A value between 0 and 1 is returned by the fuzzy membership function. The computations are performed by j^{th} fuzzy HS node present in k^{th} module and represented by m_j^k . Every HS has a threshold input with a value set to 1 and is denoted by T . This value is weighted by the radius of HS m_j^k , and denoted by ζ_j^k . The training phase involves

updating the HS radius. The HS can grow to a certain limit, which is imposed by the user and denoted by λ . This λ is called growth parameter and its value lies between 0 and 1, that is, $0 \leq \lambda \leq 1$. Thus, the maximum limit of the HS radius is set by the growth parameter λ .

Assuming the training set defined as $R = \{R_h | h = 1, 2, \dots, P\}$, where $R_h = (r_{h1}, r_{h2}, \dots, r_{hn})$ is the h^{th} pattern, and representing the center point of HS m_j^k , as $C_j^k = (c_{j1}^k, c_{j2}^k, \dots, c_{jn}^k)$, the membership function of the HS node m_j^k is defined as:

$$m_j^k(R_h, C_j^k, \zeta_j^k) = 1 - f(l, \zeta_j^k, \gamma), \quad (5)$$

where $f(\cdot)$ is three-parameter ramp threshold function defined as,

$$f(l, \zeta_j^k, \gamma) = \begin{cases} 0 & \text{if } 0 \leq l \leq \zeta_j^k \\ l\gamma & \text{if } \zeta_j^k < l \leq 1 \\ 1 & \text{if } l > 1 \end{cases} \quad (6)$$

and the argument l is defined as,

$$l = \left(\sum_{i=1}^n (c_{ji}^k - r_{hi})^2 \right)^{1/2} \quad (7)$$

The return value of the fuzzy membership function is decided based on the inclusion or exclusion of input patterns in HS. Hence, if an HS includes a pattern R_h , then the fuzzy membership function m_j^k returns one, that is, $m_j^k = 1$. The rate of decrease of the fuzzy membership value implies an increase in the distance between R_h and C_j^k . This rate is controlled by a sensitivity parameter γ . The value of γ lies between zero and one, that is, $0 < \gamma \leq 1$.

The performance of MFHSNN is evaluated during the testing phase. Fig. 8 shows a four-layer feed-forward neural network architecture that has been used for testing the performance of MFHSNN. The first two layers shown in this architecture are constructed during the training phase. In the third layer, MAX Fuzzy Neurons (FNs) have been employed. Each class uses one FN. As there are four skin disease classes, four MAX Fuzzy Neurons have been used in this application.

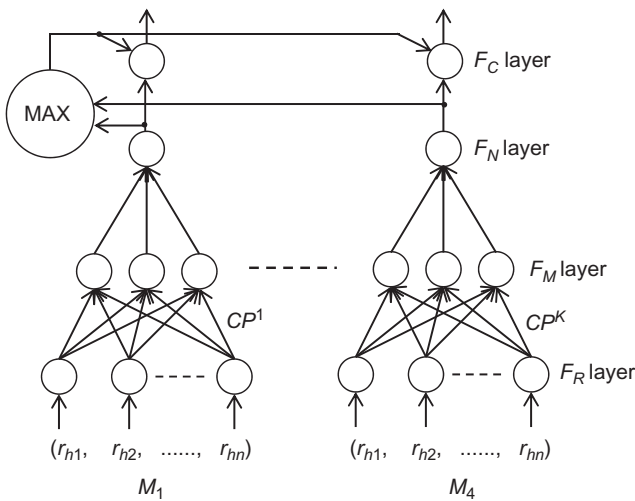
The output of k^{th} module, n^k , is calculated as,

$$n^k = \max_{j=1}^{q^k} m_j^k \quad \text{for } k = 1, 2, \dots, K, \quad (8)$$

where q^k represents number of HSs in k^{th} module created in training phase.

The third layer is a decision-making layer and hence it provides a fuzzy decision. The degree of membership of the input pattern to a particular class k is indicated by n^k . The fourth layer in the architecture is made of COMP-FNs. The purpose of the fourth layer is to provide nonfuzzy output. Hence, each node in F_C layer provides nonfuzzy output as,

$$C^k = \begin{cases} 0 & \text{if } n^k < T \\ 1 & \text{if } n^k = T \end{cases} \quad \text{for } k = 1 - 4, \quad (9)$$

**FIG. 8**

Testing phase architecture of MFHSNN [36].

where,

$$T = \max(n^k) \text{ for } k = 1 - 4$$

A. Learning Algorithm

In MFHSNN, the training set \$R\$ has a set of \$P\$ ordered pairs denoted by \$\{(R_h, d_h)\}\$, where \$R_h = (r_{h1}, r_{h2}, \dots, r_{hn}) \in I^n\$ is the \$h^{th}\$ input pattern and \$d_h \in \{1, 2, 3, 4\}\$ is class index. Two steps are involved in the learning algorithm of MFHSNN.

1. Initialization

The initialization of a module involves the creation of HS in it. Thus, initialization is performed for four modules by creating an HS in each module. While creating the HS, the first pattern belongs to that module class. At this stage, the network has four modules. Every module has one HS. Each HS has zero radius and the pattern of the corresponding class forming the center point.

2. Training

Initialization is followed by training. \$k^{th}\$ module is applied with class \$k\$ input pattern only. Calculation of the fuzzy membership function is then performed. The following two cases can happen.

Case I:

Accommodation by expansion of HS

The growth parameter \$\lambda\$ decides the maximum radius of every HS. As stated in Eq. (10), if after expansion of HS the radius is less than or equal to the growth parameter \$\lambda\$, then the pattern is included in the existing HS. If the

criterion stated in Eq. (10) is satisfied, then the HS radius is modified to include the input pattern by modifying its radius. The following two steps describe this.

Step 1:

Use Eq. (5) and determine whether the pattern R_h is contained within any one of the existing HSs. If R_h is included, then the remaining steps in the training process are skipped and training continues with the next training pair.

Step 2:

If the pattern R_h falls outside the HS, then the HS is expanded to include a pattern if the expansion criterion is met. For the HS m_j^k to include R_h ,

$$\left(\sum_{i=1}^n (c_{ji}^k - r_{hi})^2 \right)^{1/2} \leq \lambda \quad (10)$$

If the expansion criterion is satisfied then the pattern R_h is included as,

$$\zeta_j^{k_{new}} = \left(\sum_{i=1}^n (c_{ji}^k - r_{hi})^2 \right)^{1/2} \quad (11)$$

Case II:

Accommodation by creation of new HS

If case I fails, then to include the input pattern, a new HS is created as,

$$C_{new}^k = R_h \text{ and } \zeta_{new}^k = 0 \quad (12)$$

Table 5 shows the classification results in terms of the confusion matrix. It can be seen that MFHSNN is effective in the classification of the said skin diseases. Hence, the results can be generalized to other skin diseases also.

Table 6 shows the classification accuracy of the MFHSNN for the four skin diseases. MFHSNN provides good classification accuracy for the given database of skin diseases. The classification accuracy can be improved by increasing the training set.

MATLAB has been used for analyzing the timing performance of the developed system. The training time required to get a 100% recognition rate was 62.57 s. The recall time per pattern was 0.163 s.

Table 5 Confusion Matrix

	Facial Melanooses	Acne Vulgaris	Folliculitis	Tinea Corporis
Facial melanooses	13		1	
Acne vulgaris	1	17		1
Folliculitis	1	2	24	
Tinea corporis	1	1	1	5

Table 6 Classification Accuracy of the MFHSNN for the Four Skin Diseases

Skin Disease	Test Set Subjects	Correctly Classified	Mis-classified	Classification Accuracy (%)
Facial melanoses	14	13	1	92.86
Acne vulgaris	19	17	1	89.47
Folliculitis	27	24	3	88.89
Tinea corporis	8	5	3	62.5
Overall classification accuracy				83.43

9 CONCLUSION

The chapter described bioimpedance-based identification and classification of skin diseases in general and four Indian skin diseases in particular. The developed embedded healthcare system measures the bioimpedance of diseased and normal skin at 20 and 500 kHz, with the help of a developed skin electrode. Using the measured bioimpedance values, impedance indices—magnitude, phase, real-part, and imaginary part index—are computed for diseased as well as normal skin. The identification of skin diseases is performed by computing the probability of similarity between diseased and normal skin using the Wilcoxon signed rank test. It is observed that the probability of similarity between diseased and normal skin is <0.05 and hence the developed bioimpedance healthcare system can be successfully used in the identification of skin diseases. The box and whisker plot as well as the mean and standard deviation of impedance indices assist in identifying the possibility of classification of skin diseases. The skin diseases are classified by implementing the modular fuzzy hypersphere neural network. The performance of the system of classification, as observed by the confusion matrix and timing analysis, is found to be satisfactory. Hence, the developed embedded bioimpedance healthcare system can be used for the identification and classification of skin diseases.

REFERENCES

- [1] R. Hay, S. Beneck, S. Chen, R. Estrada, A. Haddix, T. McLeod, A. Mahe, Skin diseases, in: Disease Control Priorities in Developing Countries, The World Bank, Washington, DC, 2006, pp. 707–721. Chapter 37.
- [2] A. Rana, Scenario of Dermatology in India [Online], <http://skinmantra.over-blog.com/article-36831087.html>, 2009.
- [3] T. Krieg, D. Bickers, Y. Miyachi, Therapy of Skin Diseases, Springer-Verlag, Berlin, Heidelberg, 2010.

- [4] S. Panda, Nonmelanoma skin cancer in India: current scenario, *Indian J. Dermatol.* 55 (4) (2010) 373–378.
- [5] H. Rawlinson, Dermatology in India and Indian dermatology: a medico-historical perspective, *Indian Dermatol. Online J.* 7 (4) (2016) 235–243.
- [6] D. Thappa, Common skin problems, *Indian J. Pediatr.* 69 (8) (2002) 701–706.
- [7] A. Esteva, B. Kuprel, R. Novoa, J. Ko, S. Swetter, H. Blau, S. Thrun, Dermatologist-level classification of skin cancer with deep neural networks, *Nature* 542 (2017) 115–118.
- [8] Stanford University, ScienceDaily [Online], www.sciencedaily.com/releases/2017/01/170125145903.html, 2017.
- [9] A. Rawi, M. Moghavvimi, W. Ibrahim, Novel idea to monitor and measure blood hemoglobin noninvasively, *Afr. J. Biotechnol.* 9 (54) (2010) 9295–9306.
- [10] L. Pupim, C. Martin, T. Ikizler, Assessment of protein and energy nutritional status, in: J. Kopple (Ed.), *Nutritional Management of Renal Disease*, third ed., Academic Press, Elsevier, United Kingdom, 2013, pp. 137–158. Chapter 10.
- [11] D. Biswas, U. Kumar, D. Tibrewala, Development of low cost impedance analyzer for analyzing various biological samples, International conference of IEEE on communications, Devices, and Intelligent Systems (CODIS), Kolkata, 2012, pp. 508–511.
- [12] P. Aberg, I. Nicander, J. Hansson, P. Geladi, U. Holmgren, S. Ollmar, Skin Cancer identification using multifrequency electrical impedance—a potential screening tool, *IEEE Trans. Biomed. Eng.* 51 (12) (2004) 2097–2102.
- [13] N. Khanna, S. Rasool, Facial melanoses: Indian perspective, *Indian J. Dermatol. Venereol. Leprol.* 77 (5) (2011) 552–564.
- [14] P. Durai, D. Nair, Acne vulgaris and quality of life among young adults in South India, *Indian J. Dermatol.* 60 (1) (2015) 33–40.
- [15] N. Stollery, Skin infections, *Practitioner* 258 (1770) (2014) 32–33.
- [16] A. Sahoo, R. Mahajan, Management of tinea corporis, tinea cruris, and tinea pedis: a comprehensive review, *Indian Dermatol. Online J.* 7 (2) (2016) 77–86.
- [17] D. Kamat, P. Patil, Bio-impedance analysis for classification of various skin diseases in Indian context, *Res. J. Pharm. Biol. Chem. Sci.* 8 (3) (2017) 1217–1227.
- [18] Analog Devices, [www.analog.com](http://www.analog.com/media/en/technical-documentation/user-guides/UG-364.pdf), 2007. www.analog.com/media/en/technical-documentation/user-guides/UG-364.pdf.
- [19] Cypress Semiconductor Corporation, www.cypress.com, 2015. <http://www.cypress.com/search/all/CY7C68013A>.
- [20] I. Nicander, S. Ollmar, A. Eek, B. Lundh, R. Ozell, L. Emtestam, Correlation of impedance response patterns to histological findings in irritant skin reactions induced by various surfactants, *Br. J. Dermatol.* 134 (1996) 221–228.
- [21] L. Emtestam, I. Nicander, M. Stenstrom, S. Ollmar, Electrical impedance of nodular basal cell carcinoma: a pilot study, *Dermatology* 197 (1998) 313–316.
- [22] D. Beetner, S. Kapoor, S. Manjunath, X. Zhou, W. Stoecker, Differentiation among basal cell carcinoma, benign lesions, and normal skin using electric impedance, *IEEE Trans. Biomed. Eng.* 50 (8) (2003).
- [23] D. Smith, S. Potter, B. Lee, H. Ko, W. Drummond, J. Telford, A. Partin, In vivo measurement of tumor conductiveness with the magnetic bioimpedance method, *IEEE Trans. Biomed. Eng.* 47 (10) (2000) 1403–1405.
- [24] StatisticsSolutions. [Online]. <http://www.statisticssolutions.com/the-wilcoxon-sign-test-in-spss/>.
- [25] Laerd Statistics. [Online]. <https://statistics.laerd.com/spss-tutorials/wilcoxon-signed-rank-test-using-spss-statistics.php>.

- [26] IBM Analytics. [Online]. <https://www.ibm.com/analytics/data-science/predictive-analytics/spss-statistical-software>.
- [27] J.V. Kriti, N. Dey, V. Kumar, PCA-PNN and PCA-SVM based CAD systems for breast density classification, in: A. Hassanien, C. Grosan, M. Tolba (Eds.), Applications of Intelligent Optimization in Biology and Medicine, vol. 96, Springer International Publishing, Cham, 2015, pp. 159–180. Chapter 7.
- [28] L. Saba, N. Dey, A. Ashour, S. Samanta, S. Nath, S. Chakraborty, J. Sanches, D. Kumar, R. Marinho, J. Suri, Automated stratification of liver disease in ultrasound: an online accurate feature classification paradigm, *Comput. Methods Prog. Biomed.* 130 (2016) 118–134.
- [29] S. Ahmed, N. Dey, A. Ashour, D. Sifaki-Pistolla, D. Balas-Timar, V. Balas, J. Manuel, R. Tavares, Effect of fuzzy partitioning in Crohn's disease classification: a neuro-fuzzy-based approach, *Med. Biol. Eng. Comput.* 55 (1) (2017) 101–115.
- [30] K. Sharma, J. Virmani, A decision support system for classification of normal and medical renal disease using ultrasound images: a decision support system for medical renal diseases, *Int. J. Ambient Comput. Intell.* 8 (2) (2017) 52–69.
- [31] N. Dey, A. Ashour, A. Althoupety, Thermal imaging in medical science, in: Recent Advances in Applied Thermal Imaging for Industrial Applications, IGI Global, India, 2017, pp. 87–117. Chapter 4.
- [32] Z. Li, N. Dey, A. Ashour, L. Cao, Y. Wang, D. Wang, P. McCauley, V. Balas, K. Shi, S. Fuqian, Convolutional neural network based clustering and manifold learning method for diabetic plantar pressure imaging dataset, *J. Med. Imaging Health Inform.* 7 (3) (2017) 639–652.
- [33] N. Dey, A. Ashour (Eds.), Classification and Clustering in Biomedical Signal Processing, IGI Global, Hershey, 2016.
- [34] O. Azzabi, C. Njima, H. Messaoud, New approach of diagnosis by timed automata, *Int. J. Ambient Comput. Intell.* 8 (3) (2017) 76–93.
- [35] M. Khachane, Organ-based medical image classification using support vector machine, *Int. J. Synth. Emot.* 8 (1) (2017) 18–30.
- [36] P.M. Patil, U. Kulkarni, T. Sontakke, Modular fuzzy hypersphere neural network, IEEE International Conference on Fuzzy Systems (FUZZ), 2003, pp. 232–236.

A hybrid CAD system design for liver diseases using clinical and radiological data

12

Shrestha Bansal*, **Gaurav Chhabra†**, **B. Sarat Chandra†**, **Kriti‡**, **Jitendra Virmani§**

Indraprastha Institute of Information Technology, Delhi, India Jaypee University of Information Technology, Wakanaghhat, India† Thapar Institute of Engineering and Technology (deemed-to-be university), Patiala, India‡ CSIR-CSIO, Chandigarh, India§*

CHAPTER OUTLINE

1	Introduction	289
2	Methodology Adopted	291
2.1	CAD System Design A	293
2.2	CAD System Design B	301
2.3	CAD System Design C: Hybrid CAD System	307
3	Discussion	310
4	Conclusion and Future Scope	311
	References	311
	Further Reading	314

1 INTRODUCTION

The liver is the largest and the most vital organ of the human body. It performs many important functions, including the production and excretion of bile (a digestive fluid); cholesterol synthesis; the production of triglycerides (fats); the metabolism of proteins, fats, and carbohydrates; the storage of vitamins and minerals; the synthesis of plasma proteins; the breakdown of insulin and other hormones; blood pressure management; and blood detoxification. The liver is a metabolically active organ necessary for survival. The working cells of the liver (called *hepatocytes*) have the unique capability to reproduce whenever the liver is injured. Thus, liver regeneration can occur after surgical removal of a portion of the liver or after an injury that destroys a part of the liver. However, there is absolutely no way to compensate for long-term liver dysfunction because of the diversity of functions it handles.

Liver diseases are widely recognized to be an emerging health problem, particularly in South Asian countries. In clinical diagnosis, liver diseases are always taken seriously as it is a vital organ that performs very important functions required for the sound operation of the human body. Liver diseases are classified into two broad categories, that is, *diffuse liver diseases* and *focal liver diseases*.

Focal liver diseases, often referred to as focal liver lesions (FLLs), are the types of diseases in which the abnormality is concentrated in a small localized region of the liver parenchyma. Some of these commonly occurring diseases are liver cysts, hemangioma (HEM), hepatocellular carcinoma (HCC), and metastatic carcinoma (MET) [1–4].

In the case of diffuse liver diseases, the abnormality is distributed throughout the liver tissue. Different classes of diffuse liver diseases include hepatitis, fatty liver, and cirrhosis.

The field of medical imaging and image analysis has evolved due to the collective efforts from various disciplines such as medicine, engineering, and the basic sciences. In current medical practice, imaging procedures are one of the major bases for diagnosis apart from other procedures such as histological examinations and biopsies. The main aim of the medical imaging system is to obtain useful information about the physiological processes of the organs of the human body. The choice of the most appropriate imaging technique for any particular clinical application is based on several factors, including resolution, speed, convenience, acceptability, and safety. As an example, the ultrasound (US) imaging modality is ideally suited for imaging soft tissues over other techniques, accounting for all these factors. The other imaging modalities used for the diagnosis of liver diseases include magnetic resonance imaging (MRI) and computed tomography (CT). All these techniques are non-invasive imaging modalities. However, CT uses ionizing radiation that is otherwise harmful for the human body. On the other hand, US doesn't produce any known harmful effects on any of the tissues examined during clinical practice. The clinical relevance of the US imaging modality is high worldwide due to its versatility, widespread availability, portability, and ease of operation in comparison to CT and MRI.

The US is particularly useful for differentiating between *cystic* and *solid FLLs*, whereas CT and MRI are particularly sensitive for a differential diagnosis between solid FLLs. For a differential diagnosis between solid FLLs, the radiologists don't rely on US examinations alone because of varying overlapping sonographic appearances between them. Therefore, for confirming the diagnosis, radiologists resort to the administration of contrast agents, additional imaging procedures (CT and MRI) that are costlier and time consuming, or invasive procedures such as a biopsy. Furthermore, the diagnostic information extracted from the US examination is highly operator-dependent. However, this limitation can be overcome by proper training of the observer. In addition, obese patients can be difficult to scan with US, making it considerably difficult to obtain good quality diagnostic US images for these patients. Despite the disadvantages associated with US imaging modality, it is the most preferred option for liver screening. This is especially true in developing countries such as India where most of the patients generally come from a rural

environment and cannot afford the financial burden of radiological procedures, which are relatively costlier.

The appearance of a normal (NOR) liver on the US is homogeneous and has slightly more echogenicity as compared to the right kidney. The appearances of small HCC (SHCC) vary between hypoechoic and hyperechoic. Large HCC (LHCC) often has mixed echogenicity [3,5,6]. The sample images of NOR, SHCC, and LHCC cases are shown in Fig. 1.

Various algorithms for the classification of liver diseases have been intensively developed and proposed in recent years. A brief discussion of the algorithms tested on histological liver data as well liver US images are shown in Tables 1 and 2, respectively. The dataset considered for pathological liver data was a BUPA liver disorder dataset obtained from the UCI repository.

Most of the studies shown in Table 1 carried out on the BUPA liver dataset use an imbalanced training and testing dataset for classification purposes. Very few studies have been carried out in the literature as seen from Table 2 that consider the benign and malignant classes of liver disorders. As seen from Tables 1 and 2, different studies have been conducted over the past few years on both histological features and imaging features separately for the characterization of liver disorders. In any of the research work presented in the above tables, there has been no research on implementing a computer aided diagnostic (CAD) system that studies the effect of combining both histological and imaging features for the characterization of liver disorders. The current study has been carried out to propose a CAD system that explores the potential of both histological as well as imaging features for differentiating between benign and malignant liver tumors.

2 METHODOLOGY ADOPTED

The evolution of computer technology, image processing algorithms, and different artificial intelligence as well as data mining and machine learning techniques has provided ample opportunities to various researchers for investigating the potential of CAD systems for analysis and monitoring of different diseases using various imaging modalities such as X-ray, ultrasound, CT scan, PET scan, MRI, etc. [22–26]. The quantitative analysis of different FLLs using either histological or imaging data with the help of computer-based algorithms results in an accurate distinction between normal and abnormal liver tissues. Also, the transformation of normal or benign tissue to malignant tissue can be detected and monitored.

For the characterization of liver disorders, CAD systems prove to be useful in efficiently assisting the radiologists to validate their diagnosis [27–30]. There is a need of CAD systems for the differentiation of liver diseases because it has been noted that different FLLs have variable sonographic appearances, making it difficult for radiologists to clearly differentiate between the FLLs [3]. The CAD systems prove helpful in assisting the radiologists in interpreting the US of an FLL by providing a second opinion on the diagnosis.

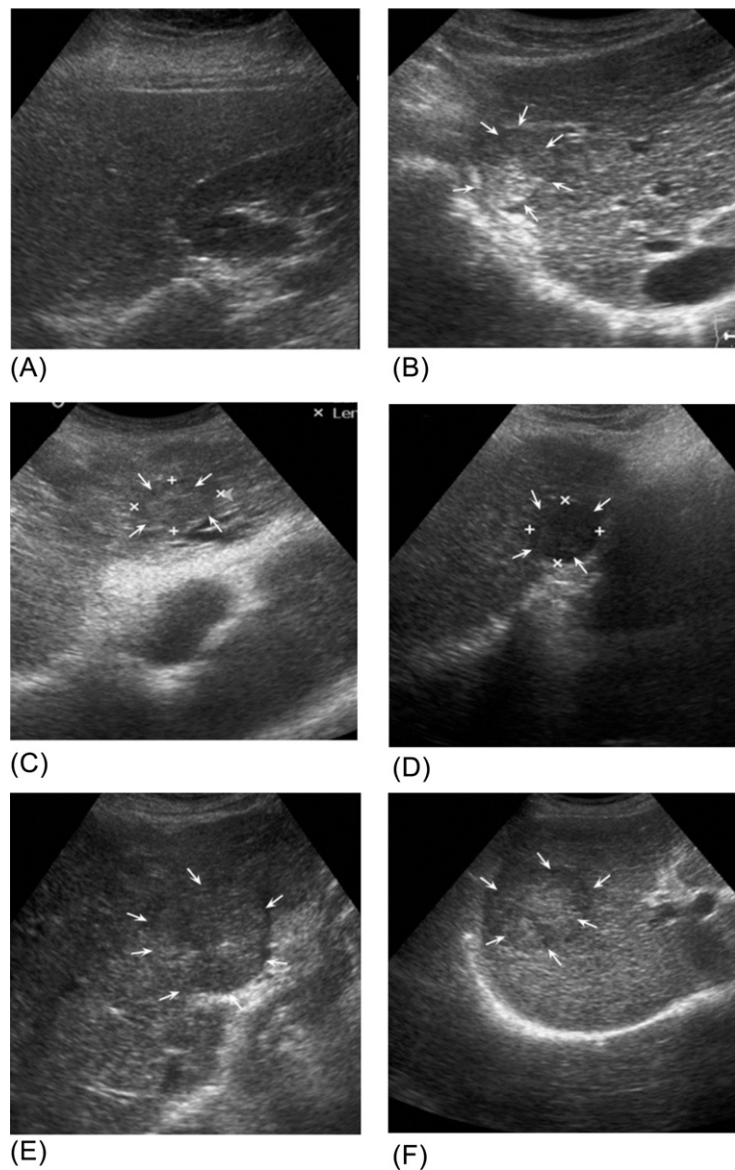


FIG. 1

Sample images depicting the sonographic appearance of liver (A) normal liver, (B) SHCC showing mixed echogenicity, (C) isoechoic SHCC, (D) hypoechoic SHCC, (E and F) heterogeneous echotexture exhibited by LHCC.

Table 1 Studies Carried Out on a BUPA Liver Disorder Dataset

Investigators	Description
Comak et al. [7]	Proposed a hybrid classification method using a combination of least squares support vector machine (LSSVM) classifier and a fuzzy-weighting preprocessing method. A classification accuracy of 94.29% was obtained
Polat et al. [8]	Proposed a fuzzy-artificial immune recognition system (AIRS) classification method and achieved an accuracy of 83.36%.
Chaudhari et al. [9]	Proposed a classifier using geometric programming and achieved an accuracy of 64.93%
Jeatrakul et al. [10]	Proposed different neural networks for binary classification of liver disorders. The highest accuracy of 70.29% came from using a complementary neural network (CMTNN)
Ramana et al. [11]	Used different classification algorithms such as Naïve Bayesian, C4.5, neural network (NN), and support vector machine (SVM). The highest accuracy of 66.66% was achieved using the NN classifier
Srimani et al. [12]	Compared the performance of different classifiers to classify the liver disorders and it was observed that the Random Forest classifier achieved the highest accuracy of 69.0%
Ubaidillah et al. [13]	Compared the performance of NN and SVM classifiers for liver disorder classification. The SVM classifier outperforms the NN classifier and obtains an accuracy of 63.11%
Gu et al. [14]	Proposed a fuzzy support vector machine (FSVM) for a class imbalance problem with linear and Gaussian kernels. The algorithm achieved an accuracy of 73.80 ± 0.054 and 79.92 ± 0.074 , respectively
Hashem et al. [15]	Classified the attributes present in the dataset using an SVM classifier and achieved an accuracy of 70.0%

In the current study, three CAD system designs have been proposed for classifying the liver masses into benign and malignant classes. The experimental workflow of these designs is shown in Fig. 2.

2.1 CAD SYSTEM DESIGN A

The CAD system design A is based on the histological data obtained from the BUPA liver disorder dataset. As shown in Fig. 2A, the attribute values taken from the dataset are subject to five different classifiers.

2.1.1 Dataset description

For implementing the CAD system design A, a BUPA liver disorders dataset was used. This dataset is a standard dataset used globally by researchers working on the classification of liver disorders. The dataset was created by BUPA Medical Research [31]. The description and bifurcation of the dataset are shown in Fig. 3.

Table 2 Studies Carried Out on Liver Ultrasound Images

Investigators	Description				
	No. of Images	Feature Extraction	Feature Selection	Classifier (No. of Classes)	Acc. (%)
Sujana et al. [16]	113	FoS, GLCM, GLRLM features	–	NN (2)	100
Yoshida et al. [17]	193	Multiresolution features: wavelet packet transform	–	NN (2)	–
Poonguzhalil et al. [18]	80	GLCM and Laws' features	PCA	<i>k</i> -means clustering (4)	70
Virmani et al. [1]	32	Laws' texture features	CFS	SVM (2)	92.56
Minhas et al. [19]	88	Wavelet packet transform based features	PCA	SVM (3)	95.4
Virmani et al. [2]	56	Multiresolution features: wavelet packet transform	GA-SVM	SVM (3)	88.8
Jeon et al. [20]	150	FoS, GLCM, AMI, AC, Laws', Gabor features	–	SVM (3)	80.0
Virmani et al. [3]	108	FoS, GLCM, GLRLM, FPS, Laws', Gabor features	PCA	NN (5)	87.7
Virmani et al. [5]	51	GLCM, GLRLM, FPS, Laws' features	GA-SVM	SVM (2)	91.6
Virmani et al. [6]	108	FoS, GLCM, GLRLM, FPS, Laws', Gabor features	PCA	SVM (5)	91.6
Virmani et al. [4]	108	FoS, GLCM, GLRLM, FPS, Laws', Gabor features	PCA	NN (5)	95.0
Manth et al. [21]	44	FoS, GLCM, GLRLM, FPS, Laws', Gabor features	–	SSVM (2)	94.3

FoS, first order statistics; GLCM, gray level cooccurrence matrix; AMI, algebraic moment-invariant; AC, autocorrelation; GLRLM, gray level run length matrix; FPS, Fourier power spectrum; CFS, correlation-based feature selection; PCA, principal component analysis; GA-SVM, genetic algorithm support vector machine; SVM, support vector machine; NN, neural network; SSVM, smooth support vector machine; Acc., accuracy.

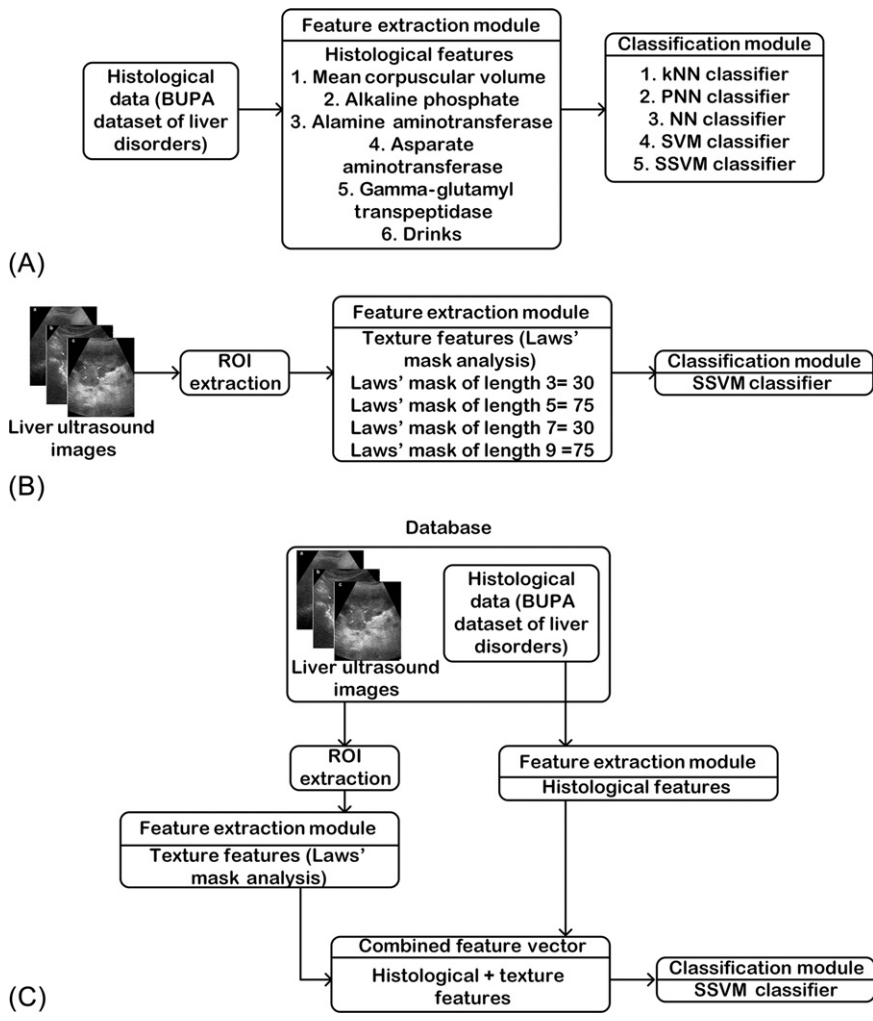
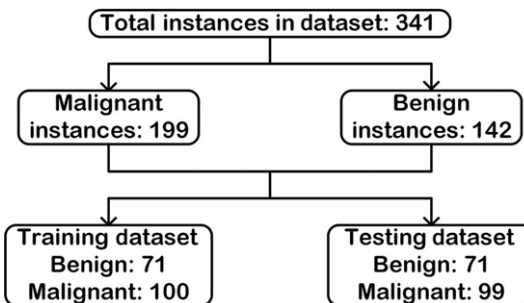


FIG. 2

Experimental workflow of different CAD system designs. (A) CAD system design A, (B) CAD system design B, and (C) CAD system design C.

2.1.2 Feature extraction

The BUPA dataset contains variables that represent the results of the blood tests that are considered to be indicative of liver disorders that might have developed due to excessive alcohol consumption. These variables are described in [Table 3](#). These attributes are used as features for the classification task.

**FIG. 3**

Description and bifurcation of BUPA liver disorders dataset.

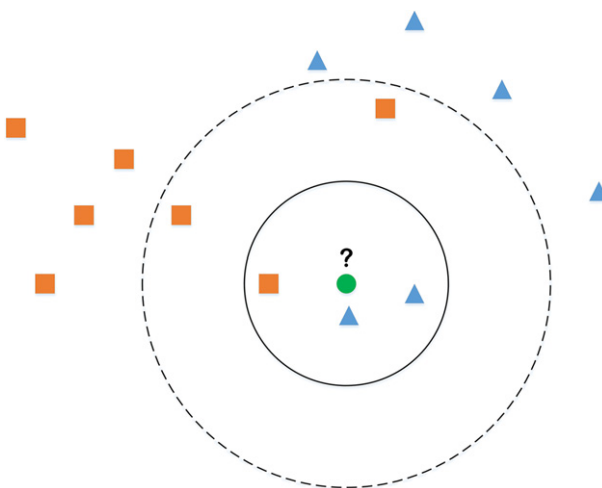
Table 3 Attributes Present in the BUPA Liver Disorders Dataset

Attribute Name	Information
Mean corpuscular volume	A measure of the average volume of red blood cells Normal values: MCV: 80–95 femtoliter
Alkaline phosphatase	An enzyme found in the bloodstream. ALP helps break down proteins in the body and exists in a different form Normal range: 20–140 IU/L
Alamine aminotransferase	The most commonly used indicators of liver damage enzymes normally found in liver cells Normal range: female \leq 34 IU/L, male \leq 45 IU/L
Aspartate aminotransferase	Found in red blood cells, liver, heart, muscle tissue, pancreas, and kidneys Normal range: female: 6–34 IU/L, male: 8–40 IU/L
Gamma-glutamyl transpeptidase	Primarily present in kidney, liver, and pancreatic cells. GGT activity is elevated all forms of liver disease Normal range: 7–35 U/L
Drinks	Number of half-pint equivalents of alcoholic beverages consumed per day
Selector field	Used to bifurcate the data into two sets

2.1.3 Feature classification

The classifiers are used to find the class to which an unknown instance belongs based on the information available from a set of instances whose class is already known [32]. The various classifiers used in the current study are:

- (a) *k*-nearest neighbor (*k*NN) classifier: This classifier works based on a distance metric that is computed between the unknown instance and each instance present in the training dataset. The number of nearest neighbors is then found on the basis of the value of parameter *k*. The class membership of the unknown instance is decided on the basis of majority voting among its *k* nearest neighbors [3,33–37]. Fig. 4 describes an example of the *k*NN classification.

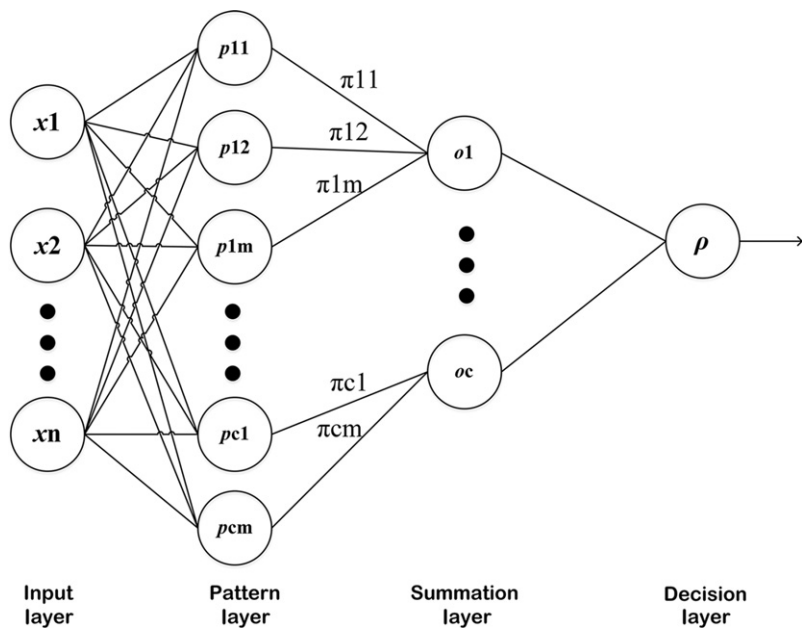
**FIG. 4**

Example depicting the working of a k NN classifier.

The figure describes the working of the k NN classifier using two different values of k ($k = 3$, $k = 5$). The green circle represents the unknown instance that should be classified into either of the two classes, a blue triangle or an orange square. When the value of k is 3 (represented as an inner circle with a solid line), the unknown instance is assigned to be a blue triangle as there are two triangles and one square as the nearest neighbors. If the value of k is 5 (represented as the outer circle with a dashed line), the unknown instance is assigned to be an orange square as there are two triangles and three squares as the nearest neighbors.

- (b)** Probabilistic neural network (PNN) classifier: In this classifier, the operations are organized in the form of a multilayered feed-forward network having four layers: input, pattern, summation, and output [38–42]. The schematic diagram of a PNN classifier is shown in Fig. 5. The steps followed in the classification algorithm are described in Fig. 6.
- (c)** Neural network (NN) classifier: The general framework of an NN classifier is shown in Fig. 7.

As seen from the figure, the nodes in the layers are interconnected using directed links showing the direction of information flow between each layer. The input values are modified in the hidden layer by using a set of unique weights and biases that are further used to find the prediction accuracy. During the training period, the predicted output of the classifier is continually compared to the actual output with an aim to reduce the difference between the two values and during each step, weights and biases are modified. The process works until a point is reached where there is a close match between the predicted output and the actual output [43–45].

**FIG. 5**

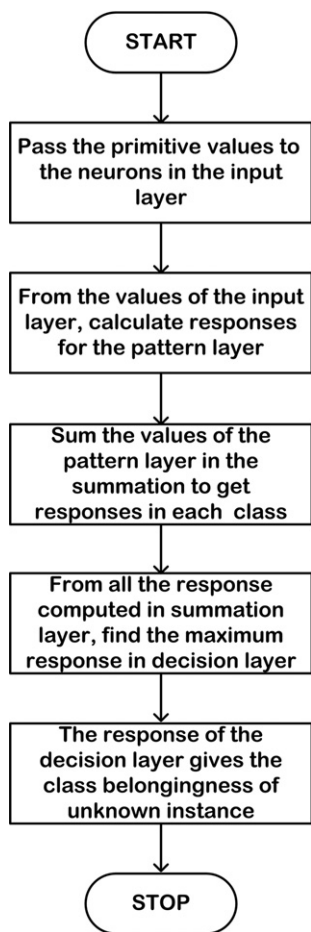
Layered architecture of PNN classifier.

- (d) Support vector machine (SVM) classifier: The basic concept behind the working of SVM classifiers is that of hyperplanes that are used to separate the two classes clearly. SVM classifiers work for both linearly separable and nonlinearly separable data. To convert the nonlinearly separable data to a linearly separable data, SVM uses different kernels to map the data points from a nonlinear space to a higher dimensionality space [2,3,6,24,38,46–48]. This mapping is shown in Fig. 8. In the current study, the LibSVM library has been used to implement the SVM classifier [49].
- (e) Smooth support vector machine (SSVM) classifier: It is an improvement of the support vector machine classifier, using the Newton-Amijo algorithm that converges quadratically and provides a unique solution [50,50a]. The SSVM toolbox has been used for implementation [50].

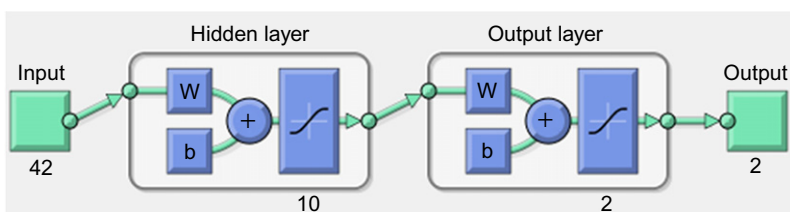
2.1.4 Classification results

The classification results of the conducted experiments for CAD system design A are graphically represented in Fig. 9 and explained in detail in Table 4.

As seen from the table, the SSVM classifier gives the highest accuracy of 81.76% in correctly differentiating between benign and malignant liver disorders. The sensitivity values obtained for each class are 71.83% and 88.89% respectively. That is,

**FIG. 6**

Steps followed in PNN classification.

**FIG. 7**

NN classifier framework.

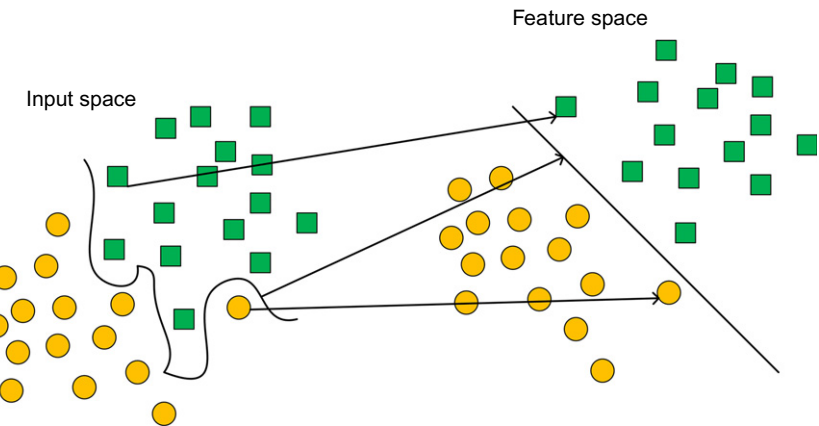


FIG. 8

Mapping of input space to higher dimensionality vector space for nonlinear SVM.

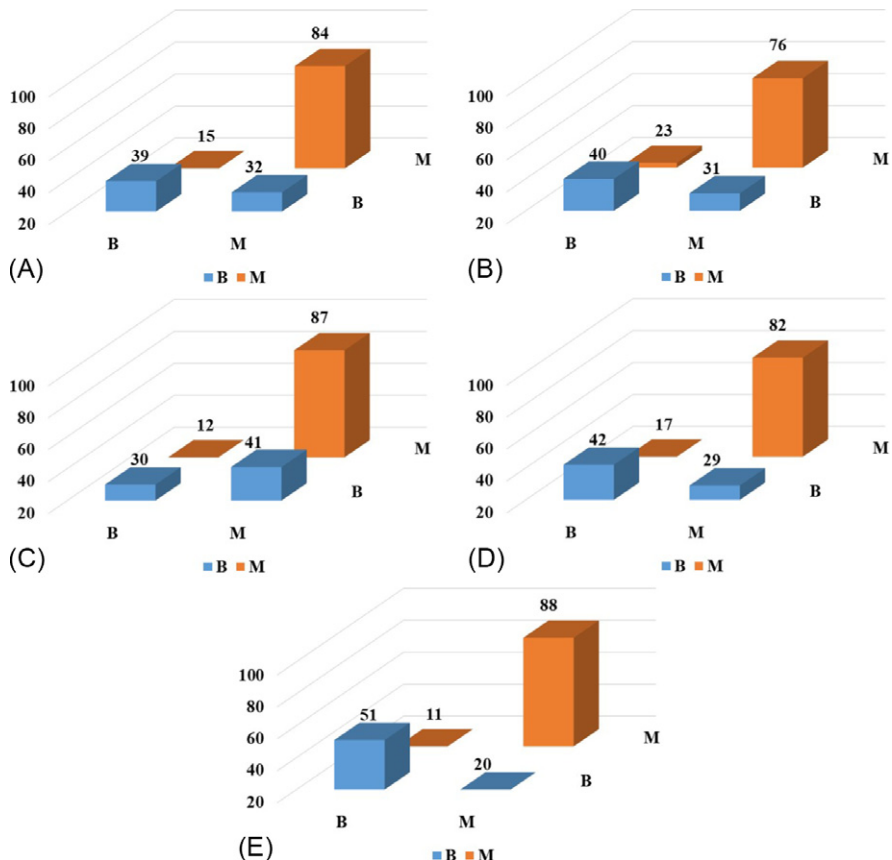


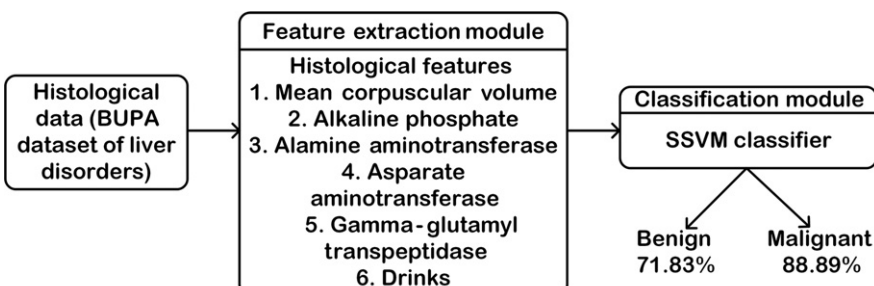
FIG. 9

Graphical representation of confusion matrices for CAD system design A using various classifiers (A) k NN classifier, (B) PNN classifier, (C) NN classifier, (D) SVM classifier, and (E) SSVM classifier.

Table 4 Performance Evaluation of TFV1 Using Different Classifiers

Classifier	CM		Acc. (%)	Sen. _B (%)	Sen. _M (%)
KNN	B	B	72.35	54.93	84.85
	M	M			
PNN	B	40	68.24	56.34	76.77
	M	23			
NN	B	30	68.862	42.25	87.88
	M	12			
SVM	B	42	72.94	59.15	82.83
	M	17			
SSVM	B	51	81.76	71.83	88.89
	M	11			

CM, confusion matrix; B, benign class; M, malignant class; Acc., accuracy; Sen._B, sensitivity of benign class; Sen._M, sensitivity of malignant class.

**FIG. 10**

Workflow of proposed CAD system design A.

out of 71 benign cases, 71.83% cases have been correctly identified to be benign and out of 99 malignant cases, 88.89% cases have been correctly identified. The total number of misclassified cases is 31/170.

Thus, from the results observed, the workflow of the proposed CAD system design A is presented in Fig. 10.

2.2 CAD SYSTEM DESIGN B

The CAD system design B is based on the imaging features obtained from the liver ultrasound images. As shown in Fig. 2B, the different texture feature vectors obtained after applying Laws' mask analysis are subjected to the SSVM classifier (the best classification result in CAD system design A).

2.2.1 Dataset description

The algorithms in this CAD design are implemented on liver US images obtained from the Post Graduate Institute of Medical Education and Research (PGIMER). The description and bifurcation of the dataset are shown in Fig. 11.

2.2.2 Feature extraction

In pattern recognition, the basic idea behind feature extraction is to find some mathematical descriptors that describe the visually extractable and nonextractable properties of the texture under examination [51].

For the liver US images, Laws' mask analysis has been used for extracting the textural information exhibited by different liver disorders, as represented on an ultrasound. The extracted regions of interest (ROIs) are subject to various filters that are useful in extracting the information related to Level (L), Edge (E), Spot (S), Wave (W), and Ripple (R). These filters can be used in different resolutions such as 3, 5, 7, and 9 [38,52–55]. The different filters and their corresponding two-dimensional masks are shown in Fig. 12.

The procedure followed in the features extraction using Laws' mask analysis can be described as below.

Step 1: Convolving an image $I_{i,j}$ with the filter masks resulting in a texture image (TI).

$$TI_{R5S5} = I_{i,j} \otimes R5S5 \quad (1)$$

Step 2: Normalizing the contrast of the resultant TI .

$$\text{Normalize}(TI_{R5R5}) = \frac{TI_{R5S5}}{TI_{L5L5}} \quad (2)$$

Step 3: Passing the normalized TIs through a 15×15 window to form a texture energy image (TEM).

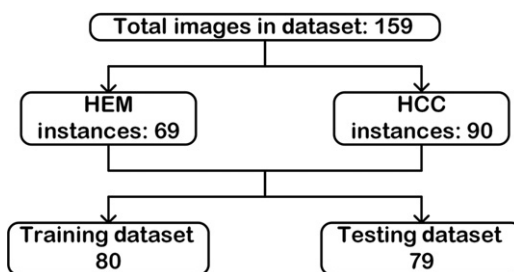


FIG. 11

Description and bifurcation of ultrasound liver images.

$L3 = [1, 2, 1]$	<table border="1"> <tr><td>L3L3</td><td>E3L3</td><td>S3L3</td></tr> <tr><td>L3E3</td><td>E3E3</td><td>S3E3</td></tr> <tr><td>L3S3</td><td>E3S3</td><td>S3S3</td></tr> </table>	L3L3	E3L3	S3L3	L3E3	E3E3	S3E3	L3S3	E3S3	S3S3																
L3L3	E3L3	S3L3																								
L3E3	E3E3	S3E3																								
L3S3	E3S3	S3S3																								
$E3 = [-1, 0, 1]$																										
$S3 = [-1, 2, -1]$																										
$L5 = [1, 4, 6, 4, 1]$	<table border="1"> <tr><td>L5L5</td><td>E5L5</td><td>S5L5</td><td>W5L5</td><td>R5L5</td></tr> <tr><td>L5E5</td><td>E5E5</td><td>S5E5</td><td>W5E5</td><td>R5E5</td></tr> <tr><td>L5S5</td><td>E5S5</td><td>S5S5</td><td>W5S5</td><td>R5S5</td></tr> <tr><td>L5W5</td><td>E5W5</td><td>S5W5</td><td>W5W5</td><td>R5W5</td></tr> <tr><td>L5R5</td><td>E5R5</td><td>S5R5</td><td>W5R5</td><td>R5R5</td></tr> </table>	L5L5	E5L5	S5L5	W5L5	R5L5	L5E5	E5E5	S5E5	W5E5	R5E5	L5S5	E5S5	S5S5	W5S5	R5S5	L5W5	E5W5	S5W5	W5W5	R5W5	L5R5	E5R5	S5R5	W5R5	R5R5
L5L5	E5L5	S5L5	W5L5	R5L5																						
L5E5	E5E5	S5E5	W5E5	R5E5																						
L5S5	E5S5	S5S5	W5S5	R5S5																						
L5W5	E5W5	S5W5	W5W5	R5W5																						
L5R5	E5R5	S5R5	W5R5	R5R5																						
$R5 = [1, -4, 6, -4, 1]$																										
$L7 = [1, 6, 15, 20, 15, 6, 1]$	<table border="1"> <tr><td>L7L7</td><td>E7L7</td><td>S7L7</td></tr> <tr><td>L7E7</td><td>E7E7</td><td>S7E7</td></tr> <tr><td>L7S7</td><td>E7S7</td><td>S7S7</td></tr> </table>	L7L7	E7L7	S7L7	L7E7	E7E7	S7E7	L7S7	E7S7	S7S7																
L7L7	E7L7	S7L7																								
L7E7	E7E7	S7E7																								
L7S7	E7S7	S7S7																								
$E7 = [-1, -4, -5, 0, 5, 4, 1]$																										
$S7 = [-1, -2, 1, 4, 1, -2, -1]$																										
$L9 = [1, 8, 28, 56, 70, 56, 28, 8, 1]$	<table border="1"> <tr><td>L9L9</td><td>E9L9</td><td>S9L9</td><td>W9L9</td><td>R9L9</td></tr> <tr><td>L9E9</td><td>E9E9</td><td>S9E9</td><td>W9E9</td><td>R9E9</td></tr> <tr><td>L9S9</td><td>E9S9</td><td>S9S9</td><td>W9S9</td><td>R9S9</td></tr> <tr><td>L9W9</td><td>E9W9</td><td>S9W9</td><td>W9W9</td><td>R9W9</td></tr> <tr><td>L9R9</td><td>E9R9</td><td>S9R9</td><td>W9R9</td><td>R9R9</td></tr> </table>	L9L9	E9L9	S9L9	W9L9	R9L9	L9E9	E9E9	S9E9	W9E9	R9E9	L9S9	E9S9	S9S9	W9S9	R9S9	L9W9	E9W9	S9W9	W9W9	R9W9	L9R9	E9R9	S9R9	W9R9	R9R9
L9L9	E9L9	S9L9	W9L9	R9L9																						
L9E9	E9E9	S9E9	W9E9	R9E9																						
L9S9	E9S9	S9S9	W9S9	R9S9																						
L9W9	E9W9	S9W9	W9W9	R9W9																						
L9R9	E9R9	S9R9	W9R9	R9R9																						
$E9 = [1, 4, 4, -4, -10, -4, 4, 4, 1]$																										
$S9 = [1, 0, -4, 0, 6, 0, -4, 0, 1]$																										
$W9 = [1, -4, 4, -4, -10, 4, 4, -4, 1]$																										
$R9 = [1, -8, 28, -56, 70, -56, 28, -8, 1]$																										

FIG. 12

Different Laws' one-dimensional filters and their corresponding masks.

$$TEM_{i,j} = \sum_{u=-7}^7 \sum_{v=-7}^7 |\text{Normalize}(TI_{i+u,j+v})| \quad (3)$$

Step 4: From the obtained 25 TEMs, obtain 15 rotationally invariant images (TR).

$$TR_{R5S5} = \frac{TEM_{R5S5} + TEM_{S5R5}}{2} \quad (4)$$

Step 5: From each TR image, statistical parameters such as mean, standard deviation (SD), entropy, skewness, and kurtosis have been computed as texture features. These features are represented as:

$$\text{Mean} = \frac{\sum_{i=0}^M \sum_{j=0}^N (TR_{i,j})}{M \times N} \quad (5)$$

$$SD = \sqrt{\frac{\sum_{i=0}^M \sum_{j=0}^N (TR_{i,j} - \text{Mean})^2}{M \times N}} \quad (6)$$

$$\text{Entropy} = \frac{\sum_{i=0}^M \sum_{j=0}^N (TR_{i,j})^2}{M \times N} \quad (7)$$

$$\text{Skewness} = \frac{\sum_{i=0}^M \sum_{j=0}^N (TR_{i,j} - \text{Mean})^3}{M \times N \times SD^3} \quad (8)$$

$$\text{Kurtosis} = \frac{\sum_{i=0}^M \sum_{j=0}^N (TR_{i,j} - \text{Mean})^4}{M \times N \times SD^4} - 3 \quad (9)$$

The representative images obtained after applying Laws mask of length 5 on standard test images are shown in [Figs. 13 and 14](#). These are standard test images and have been included in the text to highlight the working of each Laws' mask for understanding purposes as the benchmark images have all the types of texture information, that is, oriented texture, homogeneous texture, heterogeneous texture, and random texture etc. so the performance of various Laws' filters to capture the underlying textural properties of the region can be better understood using benchmark images. The corresponding application of Laws' mask to liver images is also shown in [Figs. 15 and 16](#).

The representative images showing the effect of the application of Laws' mask analysis on liver ultrasound images is shown in [Figs. 15 and 16](#).

The different feature vectors formed using the computed features can be described as in [Table 5](#).

2.2.3 Feature classification

From the results of the classification in the CAD system design A, it is seen that the SSVM classifier outperforms all other classifiers. Hence, in the CAD system, the design B SSVM classifier is used for the classification task.

2.2.4 Classification results

The classification results for CAD system design B are graphically represented in [Fig. 17](#) and detailed result analysis is shown in [Table 6](#).

As seen from the table, the texture feature vector obtained using Laws' mask of length 5 gives the highest accuracy of 81.01% in correctly differentiating between HEMs and HCCs. The sensitivity values obtained for each class are 95.56% and 61.76%, respectively. That is, out of 45 benign cases, 95.56% cases have been correctly identified to be benign and out of 34 malignant cases, 61.76% cases have been correctly identified. The total number of misclassified cases is 15/79.

Thus, from the results observed, the workflow of the proposed CAD system design B is presented in [Fig. 18](#).

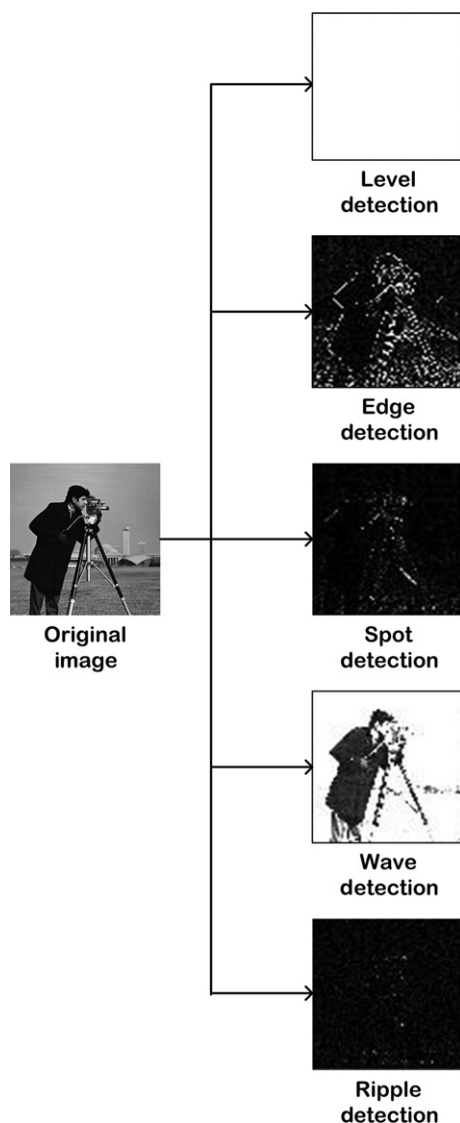


FIG. 13

Representative images demonstrating the effect of Laws' mask analysis on a Cameraman image.

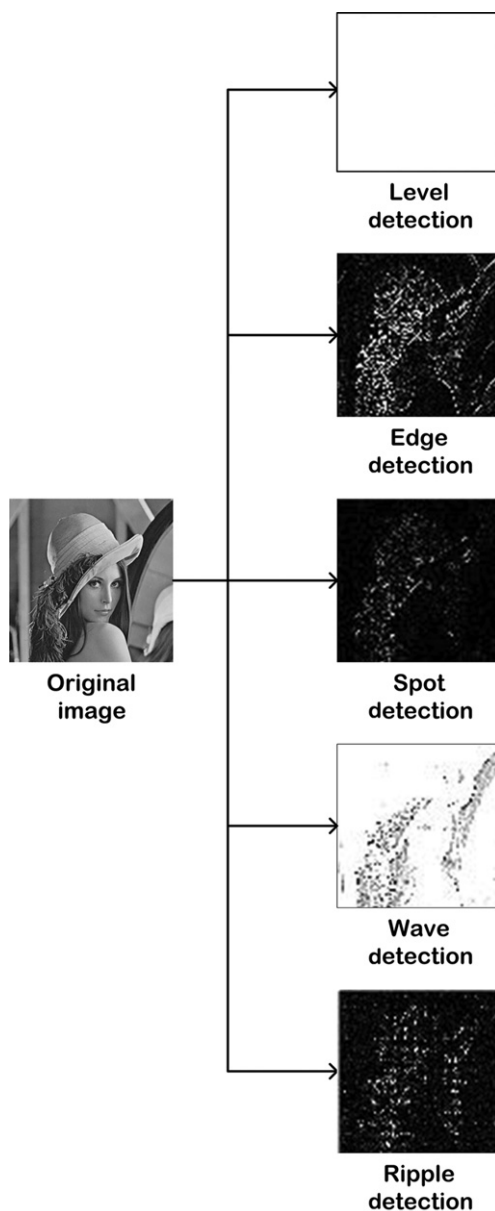


FIG. 14

Representative images demonstrating the effect of Laws' mask analysis on a Lena image.

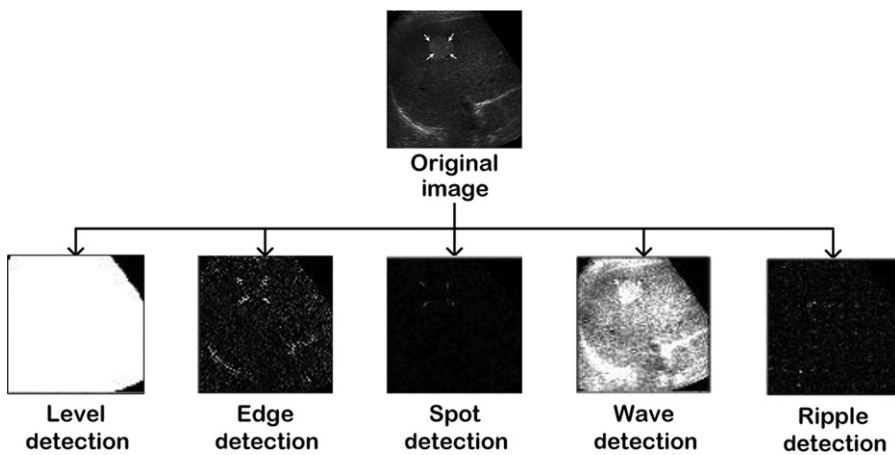


FIG. 15

Representative images demonstrating the effect of Laws' mask analysis on a benign liver ultrasound image.

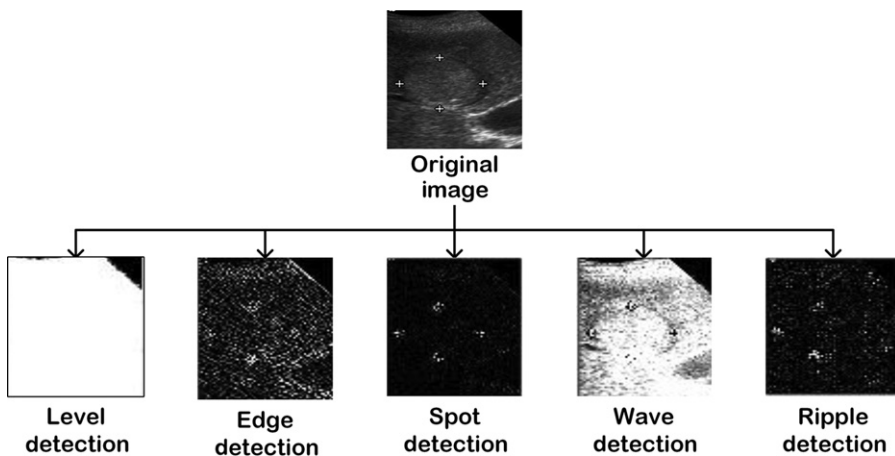


FIG. 16

Representative images demonstrating the effect of Laws' mask analysis on a malignant liver ultrasound image.

2.3 CAD SYSTEM DESIGN C: HYBRID CAD SYSTEM

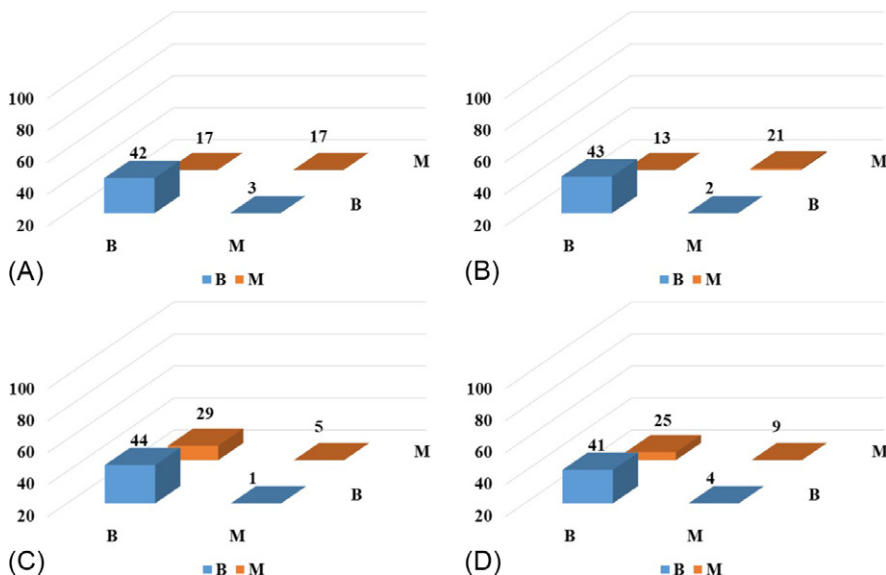
The CAD system design C represents a hybrid design based on both histological data as well as imaging features. As shown in Fig. 2C, the combined TFV is the combination of the features taken from CAD system design A and the best feature vector

Table 5 Description of Texture Feature Vectors

Texture Feature Vector (TFV)	Description
TFV 1	Contains 30 texture features (five features \times six TR images) from Laws' mask of length 3
TFV 2	Contains 75 texture features (five features \times 15 TR images) from Laws' mask of length 5
TFV 3	Contains 30 texture features (five features \times six TR images) from Laws' mask of length 7
TFV 4	Contains 75 texture features (five features \times 15 TR images) from Laws' mask of length 9

used in CAD system design B. The combined feature vector is then fed to the SSVM classifier. The obtained results are graphically represented in Fig. 19 and explained in detail in Table 7.

From the obtained results, it is observed that an accuracy of 86.07% has been achieved, which is greater than the accuracies obtained for the other two CAD system designs in differentiating between benign and malignant liver disorders. The sensitivity values obtained for each class are 95.55% and 73.52%, respectively. That is, 95.55% of benign cases are correctly identified out of 45 benign instances and

**FIG. 17**

Graphical representation of confusion matrices for CAD system design B (A) Laws' mask of resolution 3, (B) Laws' mask of resolution 5, (C) Laws' mask of resolution 7, and (D) Laws' mask of resolution 9.

Table 6 Performance Evaluation of TFVs Formed Using Laws' Masks of Various Resolutions

Mask Resolution	<i>l</i>	CM		Acc. (%)	Sen. _B (%)	Sen. _M (%)
3 × 3	30	B	42	76.48	93.33	50.00
		M	3			
5 × 5	75	B	43	81.01	95.56	61.76
		M	2			
7 × 7	30	B	44	62.02	97.78	14.7
		M	1			
9 × 9	75	B	41	63.29	91.11	26.47
		M	5			

l, length of feature vector; CM, confusion matrix; B, benign class; M, malignant class; Acc., accuracy; Sen._B, sensitivity of benign class, Sen._M, sensitivity of malignant class.

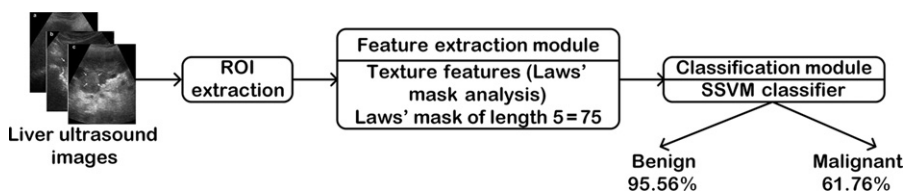


FIG. 18

Workflow of proposed CAD system design B.

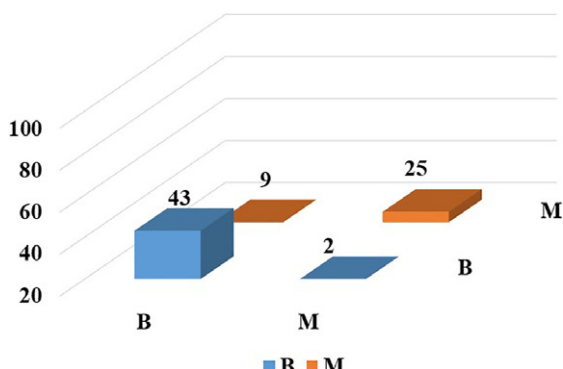


FIG. 19

Graphical representation of the obtained confusion matrix for CAD system design C.

Table 7 Performance Evaluation of Combined Feature Vector Formed Using Histological and Texture Features

Dataset	CM		Acc. (%)	Sen. _B (%)	Sen. _M (%)
Histological + texture features (Laws' 5 mask)	B	B	86.07	95.55	73.52
	M	M			
	43	2			
	9	25			

CM, confusion matrix; B, benign class; M, malignant class; Acc., accuracy; Sen._B, sensitivity of benign class; Sen._M, sensitivity of malignant class.

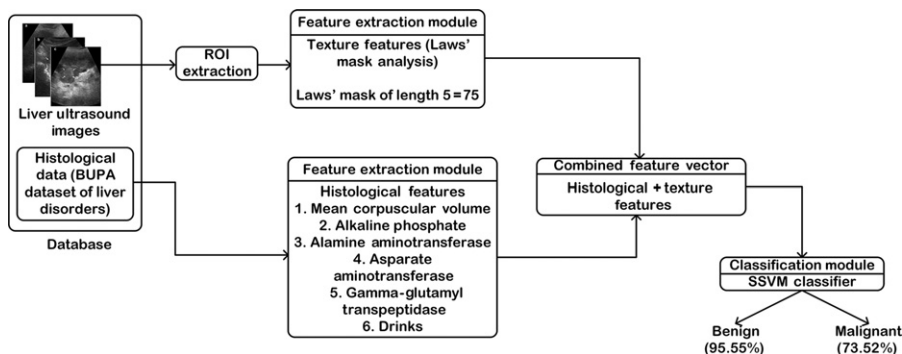


FIG. 20

Workflow of proposed CAD system design C: hybrid CAD system.

73.52% malignant cases are correctly identified out of 34 cases. The total number of misclassified instances is 9/79.

The proposed hybrid CAD system design is presented in Fig. 20.

3 DISCUSSION

The current study was carried out to investigate the potential of a CAD system design that incorporated both histological and imaging features for the characterization of liver disorders. In order to formulate a hybrid CAD system, different experiments were conducted in the present work.

First, a CAD system design A was proposed that worked based on the histological features for characterizing the BUPA liver disorder dataset. From the classification results obtained using this CAD system design, it was observed that out of all the used classifiers, the SSVM classifier was best suited for the classification purpose, achieving a highest classification accuracy of 81.76%.

Second, a CAD system design B was proposed that took into account the textural properties of benign and malignant liver disorders, as visible on an US image. Laws' masks of different resolutions were used to compute the texture features and the

extracted features were then fed to the SSVM classifier for classification purposes. From the results obtained, it was noted that the texture features computed using Laws' mask of resolution 7 were efficient for the characterization of liver tumors, achieving an accuracy of 81.01%.

As seen from the literature review, it was noted that all the studies considered either histological features or imaging features, but not both of them together for classification purposes. Thus, a hybrid CAD system design (CAD system design C) was proposed that used a combined feature set containing the histological features of the BUPA liver dataset and texture features (obtained from the US images of liver) computed using Laws' mask of length 7. It was noted that the classification accuracy of this CAD system was greater than the classification accuracies obtained for both CAD system designs A and B individually.

The main contribution of this work is the design of a hybrid CAD system that uses both histological as well as texture features. If we compare the performance of the proposed system with the existing ones, it is worth observing that a hybrid system with both types of features, that is, histological and texture, enhances the overall efficiency.

4 CONCLUSION AND FUTURE SCOPE

The current study incorporating the features of both histological and imaging data improved upon the classification accuracy, thus making the hybrid CAD system more efficient and accurate. This study can be extended by adding a feature selection module to reduce the length of the texture feature vector so that the accuracy and computational time of the classification algorithm can be improved, as most of the times some features are redundant and in no way help in the differentiation between the benign and malignant classes, thereby hampering the performance of the classifier.

REFERENCES

- [1] J. Virmani, V. Kumar, N. Kalra, N. Khandelwal, in: Prediction of cirrhosis from liver ultrasound B-mode images based on Laws' mask analysis, Proceedings of 2011 International Conference on Image Information Processing, 2011 Nov. 3–5, Shimla, India, 2011, pp. 1–5.
- [2] J. Virmani, V. Kumar, N. Kalra, N. Khandelwal, SVM based characterization of liver ultrasound images using wavelet packet texture descriptors, *J. Digit. Imaging* 26 (2012) 530–543.
- [3] J. Virmani, V. Kumar, N. Kalra, N. Khandelwal, A comparative study of computer-aided classification systems for focal hepatic lesions from B-mode ultrasound, *J. Med. Eng. Technol.* 37 (2013) 292–306.
- [4] J. Virmani, V. Kumar, N. Kalra, N. Khandelwal, Neural network ensemble based CAD system for focal liver lesions from B-mode ultrasound, *J. Digit. Imaging* 27 (2014) 520–537.

- [5] J. Virmani, V. Kumar, N. Kalra, N. Khandelwal, Characterization of primary and secondary malignant liver lesions from B-mode ultrasound, *J. Digit. Imaging* 26 (2013) 1058–1070.
- [6] J. Virmani, V. Kumar, N. Kalra, N. Khandelwal, PCA-SVM based CAD system for focal liver lesions using B-mode ultrasound images, *Defense Sci. J.* 63 (2013) 478–486.
- [7] E. Comak, K. Polat, S. Güneş, A. Arslan, A new medical decision making system: least square support vector machine (LLSVM) with fuzzy weighting pre-processing, *Expert Syst. Appl.* 32 (2007) 409–414.
- [8] K. Polat, S. Şahan, H. Kodaz, S. Güneş, Breast cancer and liver disorders classification using artificial immune recognition system (AIRS) with performance evaluation by fuzzy resource allocation mechanism, *Expert Syst. Appl.* 32 (2007) 172–183.
- [9] N.S. Chaudhari, A. Purohit, A. Tiwari, in: *A multiclass classifier using genetic programming*, Proceedings of 10th International Conference on Control, Automation, Robotics and Vision, 2008 Dec. 17–20, Hanoi, Vietnam, 2008, pp. 1884–1887.
- [10] Jeatrakul, P., & Wong, K. W. (2009). Comparing the performance of different neural networks for binary classification problems. Eighth International Symposium on Natural Language Processing, 2009 Oct. 20–22, Bangkok, Thailand; p. 111–5.
- [11] B.V. Ramana, M.S.P. Babu, N.B. Venkateswarlu, A critical study of selected classification algorithms for liver disease diagnosis, *Int. J. Database Manage. Syst.* 3 (2011) 101–114.
- [12] P.K. Srimani, S. Koti, Medical diagnosis using ensemble classifiers- a novel machine-learning approach, *J. Adv. Comput.* 1 (2013) 9–27.
- [13] S.F. Ubaidillah, R. Sallehuddin, N.A. Ali, Cancer detection using artificial neural network and support vector machine: a comparative study, *Jurnal Teknologi* 65 (2013) 73–81.
- [14] X. Gu, T. Ni, H. Wang, New fuzzy support vector machine for the class imbalance problem in medical datasets classification, *Sci. World J.* 2014 (2014) 1–12.
- [15] E.M. Hashem, M.S. Mabrouk, A study of support vector machine algorithm for liver disease diagnosis, *Am. J. Intell. Syst.* 4 (2014) 9–14.
- [16] H. Sujana, S. Swarnamani, S. Suresh, Application s artificial neural networks for the classification of liver lesions by image texture parameters, *Ultrasound Med. Biol.* 22 (1996) 1177–1181.
- [17] H. Yoshida, D.D. Casalino, B. Keserci, A. Coskun, O. Ozturk, A. Savranlar, Wavelet-packet based texture analysis for differentiation between benign and malignant liver tumors in ultrasound images, *Phys. Med. Biol.* 48 (2003) 3735–3753.
- [18] S. Poonguzhali, B. Deepalkshmi, G. Ravindram, Optimal feature selection and automatic classification of abnormal masses in ultrasound liver images, Proceedings of International Conference on Signal Processing, Communications and Networking, 2007 Feb. 22–24, Chennai, India, 2007, pp. 503–506.
- [19] F.A.A. Minhas, D. Sabih, M. Hussain, Automated classification of liver disorders using ultrasound images, *J. Med. Syst.* 36 (2012) 3163–3172.
- [20] J.H. Jeon, J.Y. Choi, S. Lee, Y.M. Ro, Multiple ROI selection based focal liver lesion classification in ultrasound images, *Expert Syst. Appl.* 40 (2013) 450–457.
- [21] N. Manth, J. Virmani, V. Kumar, N. Kalra, N. Khandelwal, Applications of texture features for classification of primary benign and primary malignant focal liver lesions, in: A. I. Awad, M. Hassaballah (Eds.), *Studies in Computational Intelligence*, Springer International Publishing, Switzerland, 2016, pp. 385–409.
- [22] S.S. Ahmed, N. Dey, A.S. Ashour, D. Sifaki-Pistolla, D. Bălas-Timar, V.E. Balas, J.M. R. Tavares, Effect of fuzzy partitioning in Crohn’s disease classification: a neuro-fuzzy-based approach, *Med. Biol. Eng. Comput.* 55 (2017) 101–115.

- [23] O. Azzabi, C.B. Njima, H. Messaoud, New approach of diagnosis by timed automata, *Int. J. Ambient Comput. Intell.* 8 (2017) 76–93.
- [24] M.Y. Khachane, Organ-based medical image classification using support vector machine, *Int. J. Synth. Emot.* 8 (2017) 18–30.
- [25] Z. Li, N. Dey, A.S. Ashour, L. Cao, Y. Wang, D. Wang, F. Shi, Convolutional neural network based clustering and manifold learning method for diabetic plantar pressure imaging dataset, *J. Med. Imaging Health Infor.* 7 (2017) 639–652.
- [26] K. Sharma, J. Virmani, A decision support system for classification of normal and medical renal disease using ultrasound images: a decision support system for medical renal diseases, *Int. J. Ambient Comput. Intell.* 8 (2017) 52–69.
- [27] B.B. Gosink, S.K. Lemon, W. Schieble, G.R. Leopold, Accuracy of ultrasonography in diagnosis of hepatocellular disease, *Am. J. Roentgenol.* 133 (1979) 19–23.
- [28] Rivas, E. C., Moreno, F., Benitez, A., Morocho, V., Vanegas, P., & Medina, R. Hepatic steatosis detection using the co-occurrence matrix in tomography and ultrasound images. Proceedings of 2015 20th Symposium on Signal Processing, Images and Computer Vision, 2015 Sep. 2–4, Bogota, Colombia; p. 1–7.
- [29] L. Saba, N. Dey, A.S. Ashour, S. Samanta, S.S. Nath, S. Chakraborty, et al., Automated stratification of liver disease in ultrasound: an online accurate feature classification paradigm, *Comput. Methods Programs Biomed.* 130 (2016) 118–134.
- [30] D. Schlaps, U. Räth, J.F. Volk, I. Zuna, A. Lorenz, K.J. Lehmann, D. Lorenz, J. Van Kaick, W.J. Lorenz, Ultrasonic tissue characterization using a diagnostic expert system, in: *Information Processing in Medical Imaging*, Springer, Dordrecht, 1996, pp. 343–363.
- [31] Forsyth, R. S., BUPA Medical Research Ltd. *Database*. Liver Disorders Dataset. <http://archive.ics.uci.edu/ml/datasets/Liver+Disorders>.
- [32] N. Dey, A.S. Ashour (Eds.), *Classification and Clustering in Biomedical Signal Processing*, IGI Global, Hershey, 2016.
- [33] R.U. Acharya, S.V. Sree, R. Ribeiro, G. Krishnamurthi, R.T. Marinho, J. Sanches, J. S. Suri, Data mining framework for fatty liver disease classification in ultrasound: a hybrid feature extraction paradigm, *Med. Phys.* 39 (2012) 4255–4264.
- [34] A. Andrade, J.S. Siva, J. Santos, P. Belo-Soares, Classifier approaches for liver steatosis using ultrasound images, *Procedia Technol.* 5 (2012) 763–770.
- [35] C. Li, S. Zhang, H. Zhang, L. Pang, K. Lam, C. Hui, S. Zhang, Using the k-nearest neighbor algorithm for the classification of lymph node metastasis in gastric cancer, *Comput. Math. Methods Med.* 12 (2012) 1–11.
- [36] O. Sertel, J. Kong, U.V. Catalyurek, G. Lozanski, J.H. Saltz, M.N. Gurcan, Histopathological image analysis using model based intermediate representations and color texture: follicular lymphoma grading, *J. Signal Process. Syst.* 55 (2009) 169–183.
- [37] G. Yang, Y. Zhang, J. Yang, G. Ji, Z. Dong, S. Wang, C. Feng, Q. Wang, Automated classification of brain images using wavelet-energy and biogeography-based optimization, *Multimed. Tools Appl.* 75 (2016) 15601–15617.
- [38] Kriti, J. Virmani, N. Dey, V. Kumar, PCA-PNN and PCA-SVM based CAD systems for breast density classification, in: A.E. Hassanien et al., (Ed.), *Applications of Intelligent Optimization in Biology and Medicine*, Springer International Publishing, Switzerland, 2016, pp. 159–180.
- [39] K.Z. Mao, K.C. Tan, W. Ser, Probabilistic neural-network structure determination for pattern classification, *IEEE Trans. Neural Netw.* 11 (2000) 109–1016.
- [40] M.F. Othman, M.A.M. Basri, Probabilistic neural network for brain tumor classification, *Proceedings of 2nd International Conference on Intelligent Systems, Modelling and Simulation*, 2011 Jan. 25–27, Kuala Lumpur, Thailand, 2011, pp. 136–138.

- [41] D.F. Specht, Probabilistic neural networks, *Neural Netw.* 3 (1990) 109–118.
- [42] G. Sun, X. Dong, G. Xu, Tumor tissue identification based on gene expression data using DWT feature extraction and PNN classifier, *Neurocomputing* 69 (2006) 387–402.
- [43] S.S. Cross, R.F. Harrison, R.L. Kennedy, Introduction to neural networks, *Lancet* 346 (1995) 1075–1079.
- [44] M. Glestsos, S.G. Mougiakakou, G.K. Matsopoulos, K.S. Nikita, A.S. Nikita, D. Kelekis, A computer-aided diagnostic system to characterize CT liver lesions: design and optimization of a neural network classifier, *IEEE Trans. Inform. Technol. Biomed.* 7 (2003) 153–162.
- [45] Z.H. Zhou, Y. Jiang, Y.B. Yang, S.F. Chen, Lung cancer cell identification based on artificial neural network ensembles, *Artif. Intell. Med.* 24 (2002) 25–36.
- [46] A. Alkan, M. Gunay, Identification of EMG signals using discriminant analysis and SVM classifier, *Expert Syst. Appl.* 39 (2012) 44–47.
- [47] A. Bazzani, A. Bevilacqua, D. Bollini, R. Brancaccio, R. Campanini, N. Lanconelli, A. Riccardi, D. Romani, An SVM classifier to separate false signals from microcalcifications in digital mammograms, *Phys. Med. Biol.* 46 (2001) 1651.
- [48] A.E. Hassanien, N.E. Bendary, M. Kudelka, V. Snasel, in: *Breast cancer detection and classification using support vector machines and pulse coupled neural network*, Proceedings of 3rd International Conference on Intelligent Human Computer Interaction, Prague, Czech Republic, 2011, 2011, pp. 269–279.
- [49] C.C. Chang, C.J. Lin, LIBSVM, a library of support vector machines, *ACM Trans. Intell. Syst. Technol.* 2 (2011) 1–27.
- [50] Y.J. Lee, O.L. Mangasarian, A smooth support vector machine, *Comput. Optim. Appl.* 20 (2001) 5–22.
- [50a] S.W. Purnami, A. Embong, J.M. Zain, S.P. Rahayu, A new smooth support vector machine and its applications in diabetes disease diagnosis, *J. Comput. Sci.* 5 (2009) 1003–1008.
- [51] N. Sambyal, P. Abrol, Feature based text extraction system using connected component method, *Int. J. Synth. Emot.* 7 (2016) 41–57.
- [52] H.A. Elnemer, Statistical analysis of Laws' mask texture features for cancer and water lung detection, *Int. J. Comput. Sci. Issues* 10 (2013) 196–201.
- [53] K.I. Laws, in: *Rapid texture identification*, Proceedings SPIE 0238, Image Processing for Missile Guidance, 1980. <https://doi.org/10.1117/12.959169>.
- [54] T. Ojala, M. Pietikainen, D. Harwood, A comparative study of texture measures with classification based on featured distributions, *Pattern Recogn.* 29 (1996) 51–59.
- [55] M. Rachidi, A. Marchadier, C. Gadois, E. Lespessailles, C. Chappard, C.L. Benhamou, Laws' mask descriptors applied to bone texture analysis: an innovative and discriminant tool in osteoporosis, *Skelet. Radiol.* 37 (2008) 541–548.

FURTHER READING

- [56] Y.M. Kadah, A.A. Faraq, J.M. Zurada, A.M. Badawi, A.M. Youssef, Classification algorithms for quantitative tissue characterization of diffuse liver disease from ultrasound images, *IEEE Trans. Med. Imaging* 15 (1996) 466–478.

Ontology-based electronic health record semantic interoperability: A survey

13

Ebtsam Adel*, **Shaker El-Sappagh[†]**, **Sherif Barakat***, **Mohammed Elmogy[‡]**

Information Systems Department, Faculty of Computers and Information, Mansoura University, Mansoura, Egypt Information Systems Department, Faculty of Computers and Informatics, Benha University, Benha, Egypt[†] Information Technology Department, Faculty of Computers and Information, Mansoura University, Mansoura, Egypt[‡]*

CHAPTER OUTLINE

1	Introduction	315
2	EHR and Its Interoperability	317
2.1	Introduction and Definitions	317
2.2	The Interoperability Benefits	319
2.3	The Different Interoperability Levels	320
2.4	EHR Semantic Interoperability Requirements	321
3	E-Health Standards and Interoperability	324
4	Ontologies and Their Role in EHR	332
5	Methods	336
5.1	Research Questions	336
5.2	Search Strategy	336
5.3	Search Results	337
5.4	Discussion	344
6	The Challenges of EHR Semantic Interoperability	346
7	Conclusion	347
	References	348

1 INTRODUCTION

With the increase in chronic diseases, society has become more health conscious and patients have become “health consumers” looking for better health management. The early detection of diseases requires a health-delivery system that can monitor health status. The early detection of physical and mental changes requires sensitive and frequent measurement of physiological and behavioral data. Physiological monitoring

of an individual's physical condition usually involves checking changes in heart rate, blood pressure, blood glucose levels, and day-to-day weight. However, gathering behavioral data requires intense monitoring, which is difficult and expensive to achieve in a clinical environment. The ubiquitous healthcare (u-Health) framework is a key to dealing with that problem. It adds to the medical history revolution by giving an instant overlook into the diseases and by providing patients an alert if there might be an occurrence of any chronic problem. In addition, it likewise empowers the administration providers/practitioners to remotely screen the patient's physiological information progressively. The healthcare domain produces large quantities of data from many different sources such as relational databases, standards, XML, ADL files, images, scans, and tabular records or any other source. These data have heterogeneous structures and semantics. In addition, they are vague and imprecise in most cases. U-Health objectives cannot be achieved without unifying these data using a standardized methodology. In this chapter, we intensely surveyed the current literature for aspects of semantic interoperability including its main definitions, standards, schemas, models, terminologies, barriers, and future challenges. In addition, we recommend fuzzy ontology to achieve the distributed electronic health records semantic interoperability because of its capabilities. As it resembles human reasoning, it can deal with both numeric and unstructured data, and it has the ability to reason and model with vague and uncertain data.

The electronic health record (HER) is the most widely used eHealth application. It can change the medicinal services framework from a paper-based industry to a digitized format. Its primary purpose is to provide a documented record of care that supports present and future care by the same or other clinicians [1]. The improvements of the healthcare domain using modern technology lead to the generation of a large amount of medical data from different heterogenous providers such as monitoring, diagnosis, clinical notes, billing services, and many other data. EHR integrates all those patient data from heterogeneous systems, which is necessary for knowledge discovery [2].

Interoperability in EHR systems is an urgent need and has many benefits [3]. These benefits include the ability of patients to access their medical history or any medical data at any time at any clinic or hospital; reductions in healthcare cost; workflow management; rapid medical decision-making; reducing clinical risks; and reducing duplication to save time. Semantic interoperability is defined as the capability of the receiving system to understand the meaning of the transmitted data. It plays an important role in the EHR environment. However, achieving this isn't an easy matter, as expected. The main problem is the heterogeneity, which is due to the difference of programs, based standards, and different database management systems between providers [4].

There are many different models used for storing EHRs, including the relational model, EAV [5], dynamic tables [6], and OCOM [7]. The relational model hasn't the ability to handle the mentioned challenges as relational databases have a static design. However, in the healthcare environment, there is continuous change in attributes and entities. Also, in the relational database, there are a limited maximum

number of predefined data type attributes. Batra and Sachdeva [8] did a comparative study of many models, including OEAV, dynamic tables, EAV, and OCOM, to tackle the issues of volatility and sparseness. The authors concluded that the dynamic table is the most successful one, but it lacks entity-centric queries. The essential contributions of this chapter are to deduce the EHR importance, realize the urgent need for interoperability in the EHR to improve healthcare quality, discuss some of the interoperability standards, study some of the leading interoperability problems, and finally suggest fuzzy ontologies as a good solution to the interoperability problems. Fuzzy ontology can deal with an imprecise and massive amount of information. It is useful in formally sharing this information across many different applications.

The chapter is organized as follows. Some of the basic concepts of EHR and its interoperability are debated in [Section 2](#), including definitions, levels, benefits, and requirements. The major *E*-health interoperability standards are discussed in [Section 3](#). [Section 4](#) manipulates ontologies and their role in EHRs. [Section 5](#) shows the bibliographic methodology used in the literature review in more detail, then explains the obtained results. EHR semantic interoperability challenges are shown in [Section 6](#). [Section 7](#) finishes the chapter.

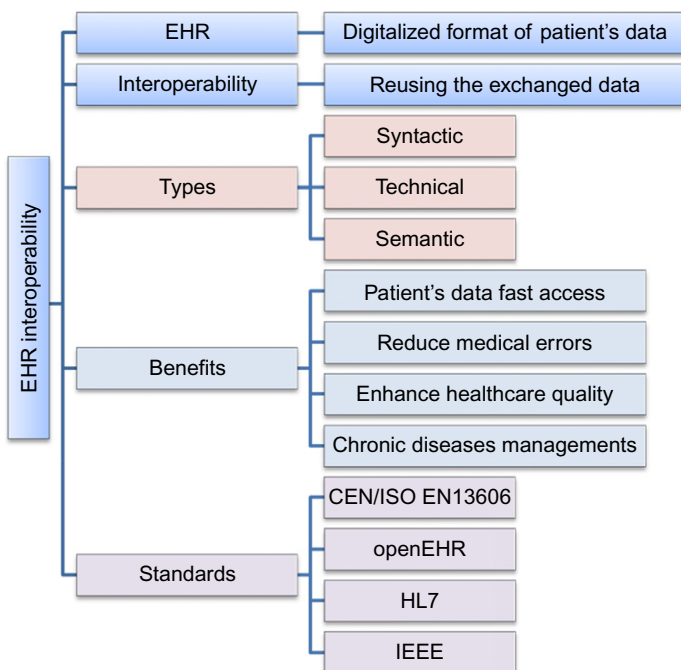
2 EHR AND ITS INTEROPERABILITY

2.1 INTRODUCTION AND DEFINITIONS

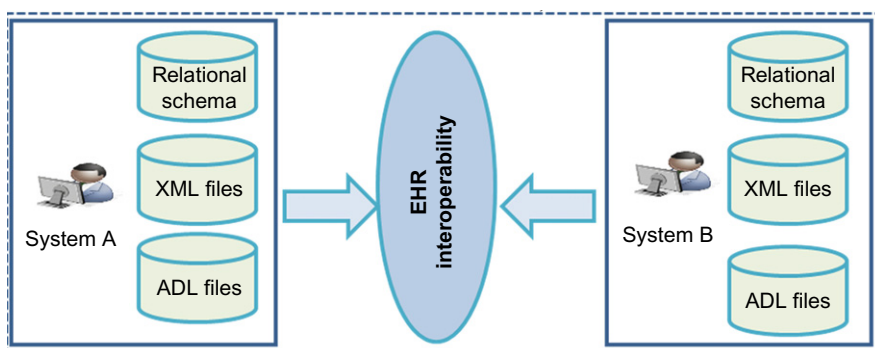
EHR is the storage of healthcare information in a digital format to easily support research, ensuring privacy for the patients and care continuity at all times. Interoperability enables the different software applications and technology systems to exchange data effectively and accurately. A comprehensive description of EHR interoperability will be shown in [Fig. 1](#).

Interoperability is defined as an “ability of two or more components to exchange information and to use the information that has been exchanged” [9]. Medical information could be stored in any file format. There are many heterogeneous data sources such as relational databases, standards, XML, ADL files, or any other source. The different sources of system data are illustrated in [Fig. 2](#). Achieving the interoperability between different organizations enables high-performance workflows, improves health outcomes, increases the quality of healthcare, reduces duplication, and reduces ambiguity.

EHRs may hold data from different medical sources such as labs, pharmacies, insurance agencies, and other providers. Data stocked in the EHR could be administrative or clinical. The administrative information may contain information about the identification of the patient, meetings, financials, lawful status, and insurance. The clinical information may include images, scans, and tabular records. [Fig. 3](#) depicts the various providers of EHRs. Interoperability in e-Health is defined as to which extent the devices and systems can exchange data and interpret those shared data [10]. This interpretation of the transmitted data can support clinical decision-making.

**FIG. 1**

A comprehensive description of EHR interoperability.

**FIG. 2**

The EHR interoperability concept.

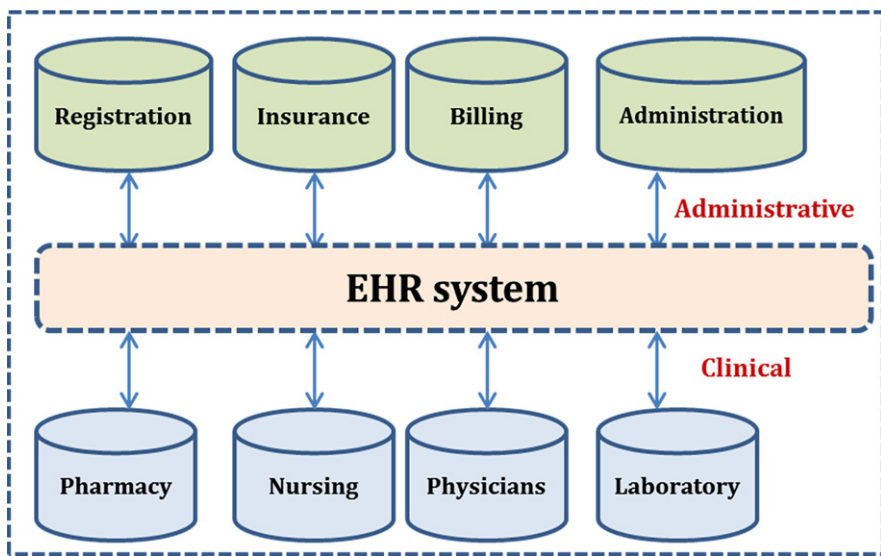


FIG. 3

The different providers of EHRs.

2.2 THE INTEROPERABILITY BENEFITS

According to [11], interoperability in a healthcare environment offers many benefits, such as:

- It can organize the patient's health records. EHR can update the patient's information effectively in a simple way.
- It can aggregate all patient clinical data from many different sources.
- EHR can both send data to and receive standardized data from other providers.
- It provides patients with fast access to their medical records in any location at any time.
- It enhances the care quality through improving the patient's healthcare experience.
- It reduces medical errors and prevents negative drug interactions.
- It reduces healthcare costs by eliminating duplicate tests, decreasing paperwork, and avoiding unnecessary tests and imaging procedures.
- It enables decision support systems by integrating patient information from multiple sources.

Table 1 shows some institutional studies that focus on the importance of EHR and EHR semantic interoperability in healthcare systems.

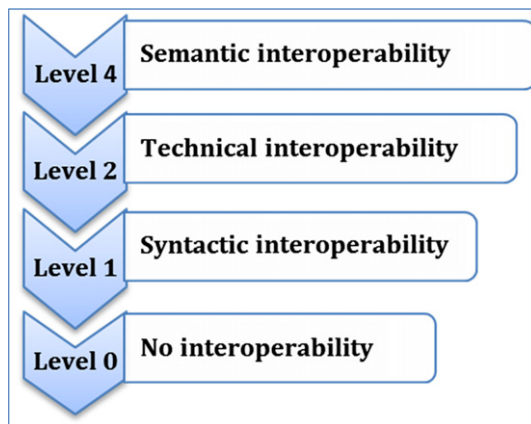
Table 1 Some Research Institutions That Assure the EHR and EHR Interoperability Importance

The Released Study	The Study Report
European Commission Semantic HEALTH Report (2009) [11]	Achieving interoperability in an EHR system is the most critical issue for perfecting the quality of patient care and supporting the patient's mobility
AHA survey (2009) [12]	This study found that around 1.5% of hospitals have a comprehensive EHR framework. Another 7.6% have an EHR being used in no less than one clinical unit. The leaders of the hospitals thought that the main adoption challenge was the cost maintenance and startup
California HealthCare Foundation (2010) [13]	EHR enables Americans to access their health reports easily while allowing them to have more knowledge about their health and take better care of themselves than others
NORC 2011 [14]	This study found that 78% of Americans prefer using electronic medical records, and 72% support sharing them
ITU-T (2011) [15]	This study found that, in the developing world, using the information and communication technologies improves global access to health information and healthcare services. This requires a universal interoperability standard to overcome the barriers of technical infrastructure and legal requirements
ITU-T Watch (2012) [16]	This report deduced that e-health frameworks could transfer healthcare data through mobile delivery and social applications of media e-health. This e-health advancement will be achieved only via the technology standards that facilitate interoperability between devices and systems
Software Advice survey [17]	46% of patients prefer their doctors to exchange health records directly, and 21% favor in-person delivery

2.3 THE DIFFERENT INTEROPERABILITY LEVELS

There are four different levels and categories of interoperability, as shown in Fig. 4. These levels are grouped regarding whether the data could be comprehended by machines or by the end user [11]. In the following subsections, we will introduce these categories in brief.

1. No interoperability: In this level of interoperability, information cannot be understood by humans or machines [11]. There is no IT information sharing such as mail, telephone, or fax.
2. Syntactic interoperability: The syntax “syntactic” interoperability concerns solving how to transfer data without regard to its meaning. According to ETSI, syntactic

**FIG. 4**

Levels of interoperability.

interoperability is usually related to the data formats. Therefore, the messages transferred by communication protocols need to have a well-defined syntax and encoding. However, many protocols can carry data, and this can be represented using high-level transfer syntaxes such as ASN.12, XML, or HTML [18].

3. Technical interoperability: According to ETSI, it is usually related to hardware/software components, systems, and platforms that enable machine-to-machine communication. This kind of interoperability is often centered on communication protocols and the infrastructure needed for those protocols to operate [18].
4. Semantic interoperability: Semantic interoperability creates coherence between the various systems and organizations that do not speak the same language. It enables better workflows and improves performance by making the correct information accessible at the ideal time. Semantic interoperability has many definitions. **Table 2** shows the different interpretations of EHR semantic interoperability by various organizations.

2.4 EHR SEMANTIC INTEROPERABILITY REQUIREMENTS

There are many requirements that have to be identified when establishing an EHR interoperability system, as shown in **Fig. 5**. We cannot discuss all of them in this paper. This section defines the most critical EHR features to be complete and communicable with the other heterogeneous systems. It will support shared patient care, retain integrity across systems, and make effective use of the resource. The required features are as follows:

(a) *Health domain data types*

Data put away in an EHR framework might be medical or nonmedical data. So, an EHR system must have the ability to comprise jointly structured and nonstructured

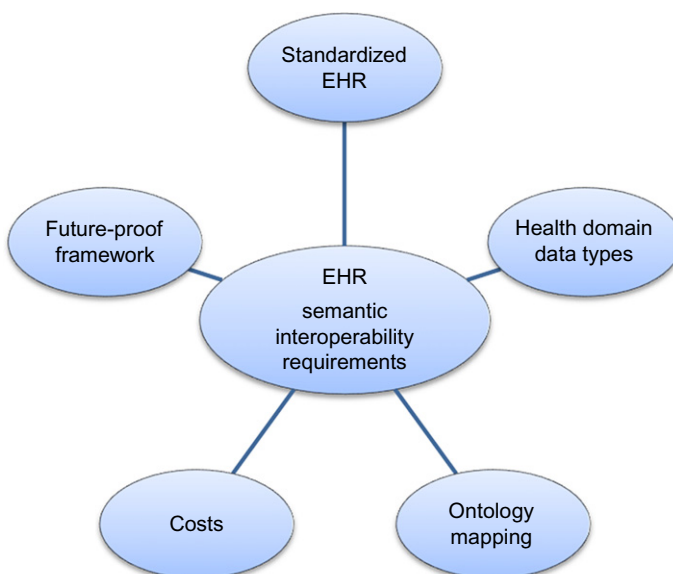
Table 2 The Different Semantic Interoperability Definitions

Organization	Semantic Interoperability Definition
Wikipedia [19]	The capacity of at least two frameworks to swap data and hold the importance of that data, consequently translated by the accepting framework precisely sufficient to make significant results
ISO [20]	The capacity of frameworks to share the information and comprehend it at the scale of characterized domain concepts
The IEEE standard glossary [21]	The capacity of the segments or the frameworks to exchange data and utilize that exchanged data
HL7 CDA [22]	The capacity of the frameworks and applications to share information, which will enable reliable support of decision-making
ONC (Office of the National Coordinator for Health Information Technology) [23]	All individuals have convenient access to their health information, which simplifies decision-making, supports coordinated management of health, allows patients to care more about their health, and enhances the overall healthcare
HIMSS [10]	Interoperability alludes to the health data framework's capacity to cooperate to improve the successful surrender of medicinal services for groups and people. There are three unique arrangements of health data interoperability: foundational, semantic, and structural
NHIN [24]	The capacity to translate and in this manner, to make compelling utilization of the data so exchanged
US Healthcare State of the Art [25]	"The capability of at least two computer system frameworks to exchange data and have the significance of that data consequently deciphered by the accepting framework precisely enough to create helpful outcomes to the end clients of the two frameworks"
The Joint Initiative for Global Standards Harmonization [26]	"The capability of systems to understand the shared data at the level in which the domain concepts are fully defined"

data. It should be possible to translate data into an intelligible and comprehensible dialect, reserving the dependability of the original data.

(b) *Ontology mapping*

The process of ontology mapping depends on showing the similarities between the concept definitions and articulating the semantics of those definitions [27].

**FIG. 5**

The EHR semantic interoperability requirements.

(c) Future-proof and flexible framework

ISO/TS 18308 realized that the architecture of EHR must be “future-proof,” meaning that it must have the capacity to speak to new data types, blend new record types, and be extensible [11].

(d) The EHR reference model standardization

The architecture of EHR information between the sender and the receiver must be standardized [10].

(e) Security in EHR systems

The data stored in an EHR is personal, particular, and secure in nature. Richard Rognehaug defined EHR privacy as “the privilege of people to shield data about themselves from being uncovered to others; the claim of people to be let alone, from observation or obstruction from different people, associations, or the legislature” [28]. Hospitals can improve their working by monitoring the health of the patients and performing automatic analysis of various health parameters inside the room. Security mechanisms can also be enhanced by only allowing authorized hospital staff and attendants in the ward. Jain et al. [29] implemented an algorithm in which they considered a specific room of a hospital as the environment with a patient monitored for health and security reasons. If nothing was allowed for the particular patient or there were some unwanted variations in the health parameters of the patient, the alarm rang and the patient’s assistants were notified.

(f) Costs

The cost has a strong influence on the development of EHRs. In first establishing an EHR system, there are numerous necessary technical requirements:

- Operating systems (e.g., Linux, UNIX, Windows, and OS X).
- Databases (e.g., SQL, Sybase, NoSQL, MySQL, and Oracle).
- Display and capture devices (e.g., laptops,).
- Networking (e.g., cabling, remote access capabilities, wireless, and web-based).
- Security costs.
- Maintenance costs. “The software has to be upgraded, and hardware must be replaced.”

To achieve EHR semantic interoperability, there are many techniques and methods of including traditional approaches, standards, ontologies, and terminologies. In the subsequent section, we will study some of the interoperability standards. In a later section, we will give a brief description of the ontologies and medical ontologies, explaining their advantages over traditional methods.

3 E-HEALTH STANDARDS AND INTEROPERABILITY

EHR interoperability is one of the primary interests and challenges of healthcare systems. Standards play a significant role in achieving that challenge. In the implementation area, standards act as the center ground that can coordinate the different applications and software systems. So, many researchers and institutions try to cooperate in finding practical solutions in this area, depending on various standards and technologies. The advantages of utilizing standards increment with the quantity of different frameworks needed to connect with each other.

To support full interoperability between systems, the standards have to cover both the semantics (meaning) and syntax (structure). The syntax is specified by the messaging standards of an electronic message, and terminological systems specify the semantics. To accomplish semantic interoperability, several standardizations and various efforts have been developed. There are about 22 different ICT standards in the healthcare domain. From those, there are seven main international organizations that are interested in eHealth standards, which are ISO, CEN, IHE, HL7, OpenEHR, IHTSDO, and DICOM. The abbreviation and other details of each organization will be indicated in [Table 3](#).

(a) CEN/ISO EN13606

ISO is a famous worldwide standard. The CEN/ISO EN13606 is a European norm and also is approved as an ISO standard. Its primary goal is to achieve interoperability in EHR systems by standardizing health information. That goal is achieved by defining a solid information architecture for communicating EHR systems or

Table 3 The Major International Organizations Involved in e-Health Standards

Organization	Membership	Type	Interesting Activities	Website
ISO	162 Members	Nongovernmental organization	Develop and publish international standards in many fields such as health and safety matters, security and resilience, healthcare administration, and information technology	www.iso.org
CEN	50 Countries	Standardization body	CEN supports standardization activities in many sectors and fields such as defense and security, food and feed, health and safety, healthcare, ICT, and air and space	www.cen.eu
IHTSDO	28 Countries	Nonprofit	IHTSDO can determine the global standards required for health terms, which improve healthcare	www.ihtsdo.org
HL7	ANSI-standard protocol	Nonprofit	HL7 is concerned with integration, exchanging, and retrieval of electronic health information	www.hl7.org
DICOM	Network communications protocol	Open standard	This is concerned with handling, printing, storing, and transmitting information in medical images	http://medical.nema.org
OpenEHR	Open standard	Nonprofit	It is focused on the storage, exchange, management, and retrieval of EHR health data	www.openehr.org
IHE	Sponsored by HIMSS	Nonprofit	IHE describes specific solutions to integration problems	www.ihe.net

between a centralized data repository and EHR systems [30]. Fig. 6 defines the main elements of the CEN/ISO EN13606 reference model.

The standard of CEN/ISO EN13606 structures its information into COMPOSITIONS that are incorporated into a hierarchy FOLDER. The COMPOSITIONS involves ENTRYs that are implicated in the hierarchy of the SECTION as depicted in Fig. 7.

To achieve semantic interoperability, CEN/ISO 13606 relied upon the structure of the dual model. The reference model (store data) contains the basic entities for representing the EHR information. Archetypes (describe data structures semantically) provide formal definitions of defined clinical concepts [30].

(b) HL7

HL7 is an ANSI that accredited standard protocol for exchanging electronic data in healthcare environments. It and its group members are considered the most

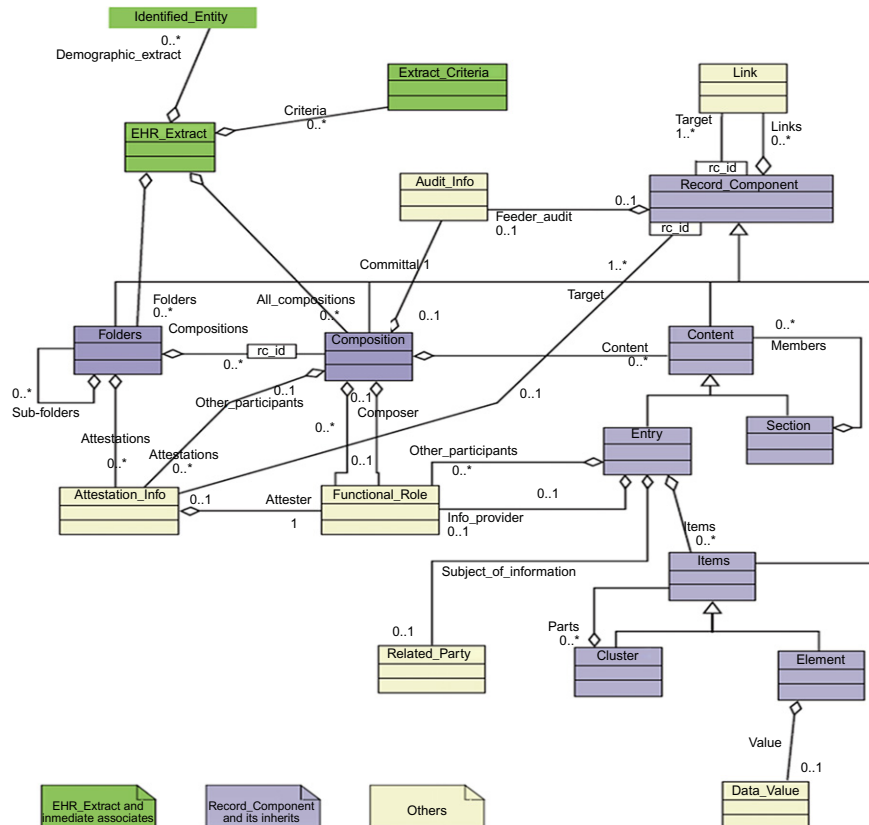
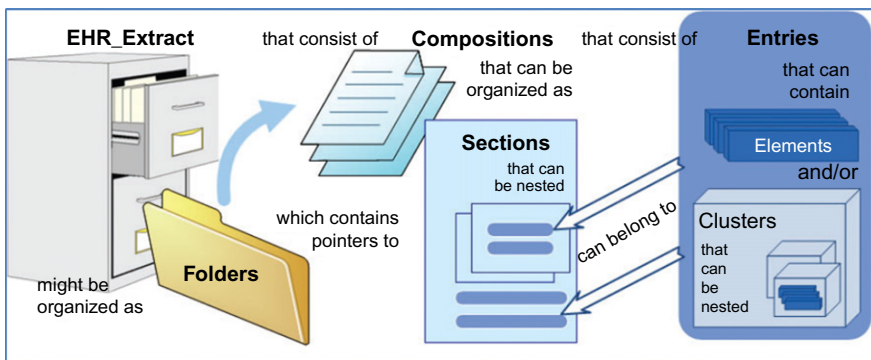


FIG. 6

The reference model of ISO/CEN 13606.

**FIG. 7**

The component relationships of the ISO/CEN13606 reference model.

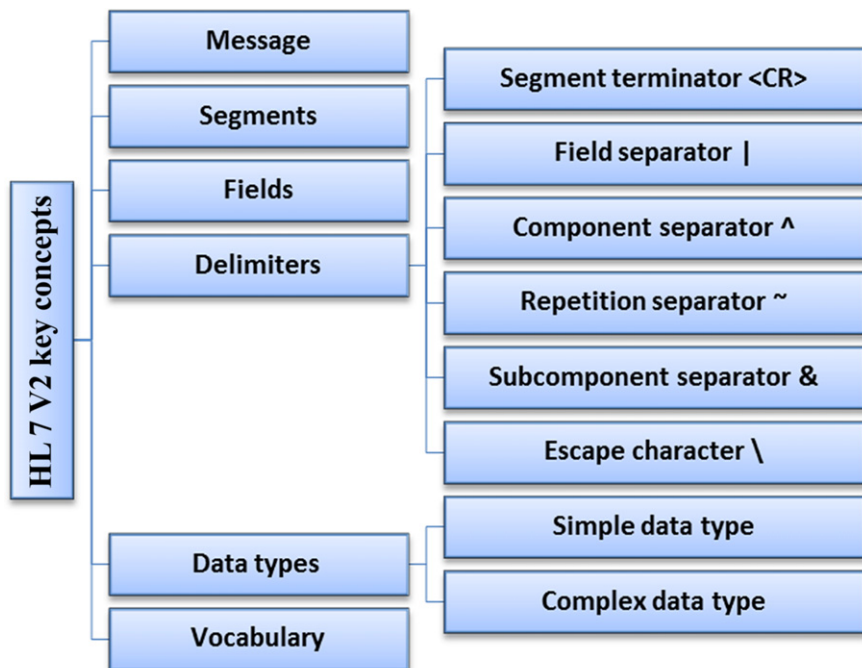
commonly utilized all over the world. These standards focus on the seventh level in the OSI model “application layer.” HL7 can improve care delivery, reduce ambiguity, optimize workflow, and perfect transferring knowledge between all stakeholders [31]. HL7 CDA is one of the HL7 members. It is used for transferring rich, detailed, and unambiguous clinical documents over the barriers of different software applications and islands. It can include text, sounds, images, and other multimedia content [22]. Fig. 8 shows the main key concepts of HL7. Fig. 9 shows the main basic components of segments and message sections of HL7 V2.

Fig. 10 shows HL7 and its derivations. To address the problem of interoperability, HL7 developed what it calls the SAIF that can provide the base for working on all aspects of standardization in HL7 [32].

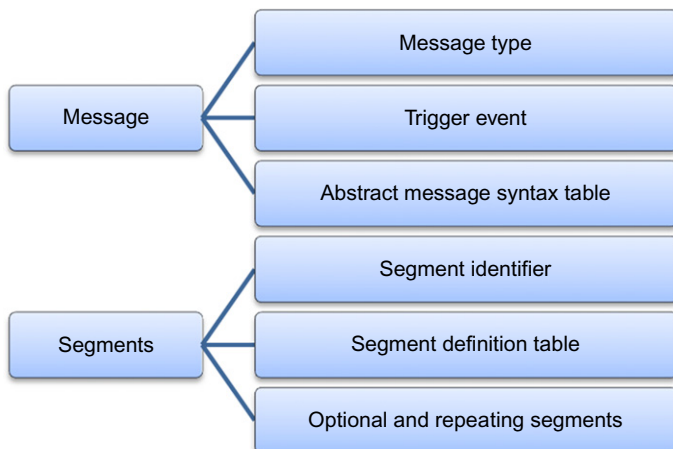
(c) DICOM

Utilizing ultrasound for disease detection is highly desirable due to its nonradiation nature, low cost, and ease of use. Saba et al. [33] selected 124 ultrasound sample images retrospectively from a database of 62 patients consisting of normal and cancerous fatty liver disease. The proposed training system generated offline parameters using a training liver image database. The classifier applied transformation parameters to an online system in order to facilitate real-time detection during the ultrasound scan.

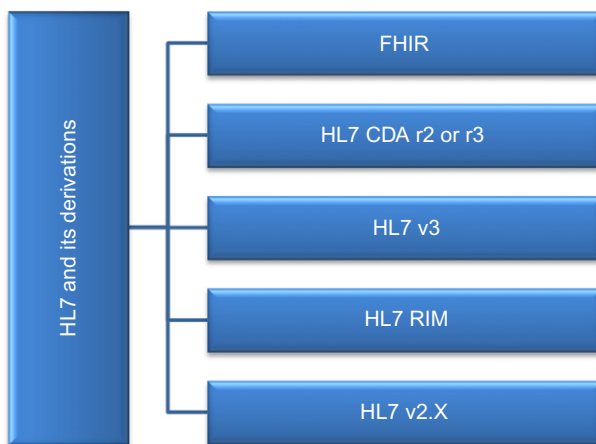
DICOM is a successful imaging standard that permits an image to be read on any machine. It enables storing, printing, handling, and transmitting medical information. It includes a protocol for network [communications](#) and a file format definition. DICOM enables integrating the medical images from multiple manufacturers’ devices [27]. The DICOM standard allows medical imaging interoperability by specifying protocols, transferring the syntaxes and semantics of commands, information conformance standards, security profiles, and management of the content. The fundamental base requirements for DICOM are issues relating to execution, security, sorted records for specific clinical ranges, and work process organization [34].

**FIG. 8**

The HL7 V2 main key concepts.

**FIG. 9**

The main components of HL7 V2 message and segments sections.

**FIG. 10**

HL7 and its derivations.

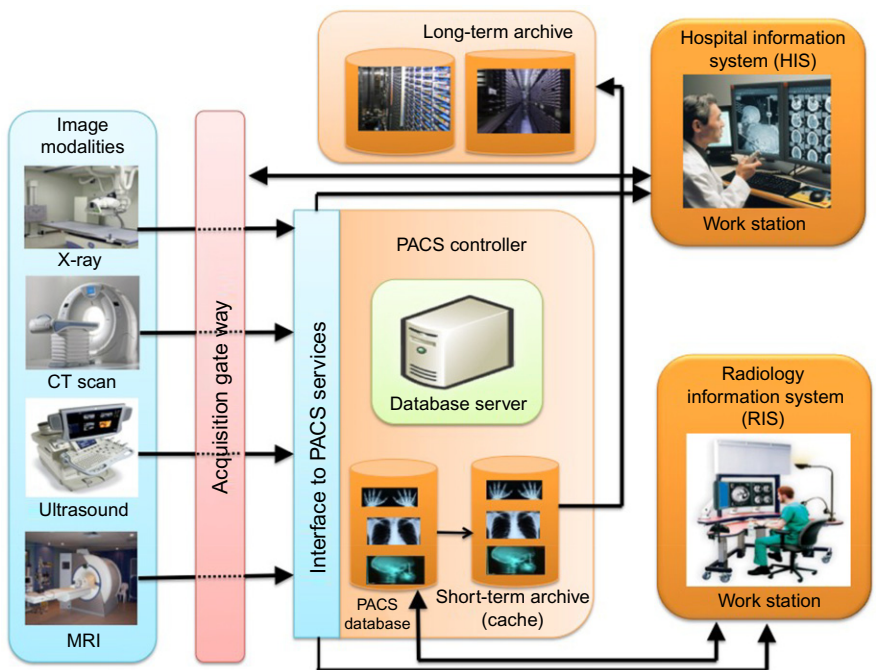
The settings of the semantic interoperability are DICOMs WG-08 on Structured Reporting and WG-20 on Mix of Imaging and Information Systems [25].

(d) PACS

PACS are modern systems used for storing and retrieving medical images [35]. A PACS is fit for securing putting away exchanging and recovering medical images in healthcare. It relies mostly on HL7 [31] and DICOM [34] standards for speaking with various picture modalities. It is used in an EHR environment to monitor the status of a patient going through treatment and recovery. As shown in Fig. 11, the main components of a PACS are image modalities, acquisition gateways, a PACS controller and associated database and server, long-term and short-term archives, and workstations [36].

PACS has an imaging system such as an MRI, CT, or an X-ray among other contrivances, workstations or mobile devices for viewing, analyzing, and deciphering images from medical procedures. DICOM is useful in operating the radiology department as well as for telemedicine and teleradiology. DICOM also provides space to include manufacturer-specific attributes for backward compatibility and smooth transition of products from old protocols to DICOM; however, it is complex [37]. Different medicinal imaging modalities, for example, X-ray, CT, ultrasound, and MRI are utilized to test human anatomy. Dey et al. [38] reviewed many usages and limitations of thermography in the biomedical field.

PACS has many advantages such as providing better tools and functionalities at the workstation and improving the job satisfaction of radiologists. As a result the fault diagnosis can be reduced. Despite those advantages, PACS has some limitations such as implementations is expensive. Also radiologists and physicians could be anxious about workflow changes when upgrading the old systems with PACS [35].

**FIG. 11**

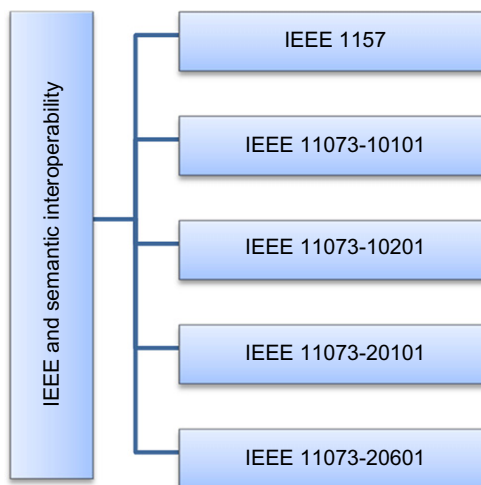
The global architecture of PACS [36].

(e) IEEE

IEEE [39] was established in 1963 from the convergence between the IRE and AIEE. It is interested in many different technologies, such as [electric power](#) and [energy](#), wire communications, biomedical and healthcare technology, vital searching digital library, and a significant publisher of [scientific journals](#). To the point of healthcare semantic interoperability, the standards are IEEE 11073 Standard for Medical Device Communications [40], and IEEE 1157, Standard for Health Data Interchange, as shown in Fig. 12.

(f) OpenEHR

The openEHR foundation is an international standard based on XML encoded data. It is a nonprofit organization that facilitates health record creation and sharing by clinicians and consumers via open-source. Its main aim is to administrate the EHR architecture validation via clinical evaluation and overall implementation [20]. It establishes architectural specifications. Then, it initiates the implementation projects via repeated refinement and testing to validate and enhance the requirements. This process is managed by a set of management tools and control processes [41]. OpenEHR organizes its data in compositions that are included in a folder hierarchy. It contains three main layers: a reference model (RM) utilized to describe the main

**FIG. 12**

IEEE and healthcare semantic interoperability.

components and health information characteristics; an archetype model (AM) that contains knowledge; and a service model (SM) that incorporates fundamental services and administrations in the health environment. Fig. 13 illustrates the relationships between these layers.

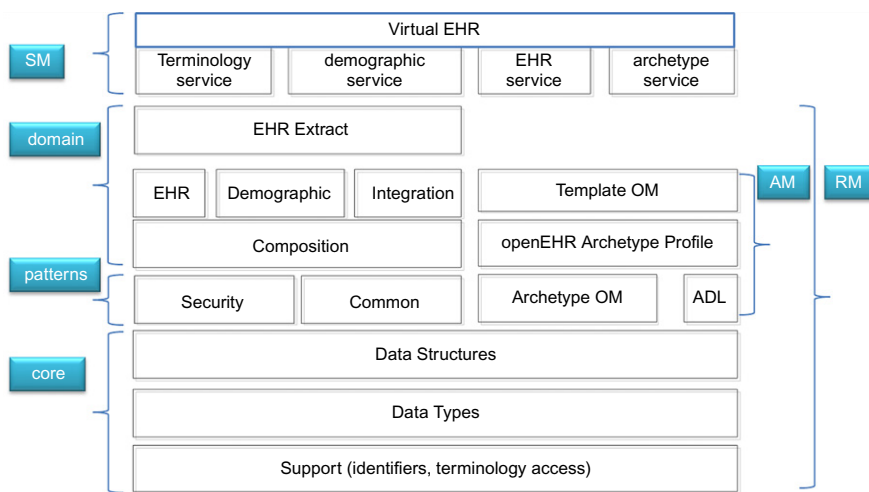
The ISO/CEN 13606 and OpenEHR are very homogeneous. However, OpenEHR is richer than ISO/CEN 13606 in data types and structures. Fig. 14 depicts the main data structures of a reference model of OpenEHR and ISO EN 13606.

(g) SNOMED CT

SNOMED CT is a nonprofit universal standard. It is viewed as the most multilingual, exact, and complete clinical wording everywhere throughout the world. It contains more than 370,000 concepts, 990,000 English portrayals and descriptions, and 1.5 million connections [31]. SNOMED CT consists of concepts, terms, and relationships. It is established to help in perfecting clinical data recordings, with the overall aim of enhancing the healthcare of patients. It manipulates many areas, such as operations, diseases, devices, symptoms, treatments, and drugs. SNOMED CT is helpful in decision-making and analysis, leading to higher quality and safety in healthcare delivery [42].

(h) OWL

The OWL is a universal markup language used to exchange and encode ontologies. It is designed for supporting the semantic web. OWL has more skills in expressing **semantics** and meaning than other markup languages, such as **RDF**, **XML**, and **RDF-S**. Thus, OWL has the same capabilities of these languages in addition to its ability for representing **web** machine interpretable contents. OWL facilitates interoperability while exchanging healthcare information. It gives a specialized structure

**FIG. 13**

The openEHR package structure.

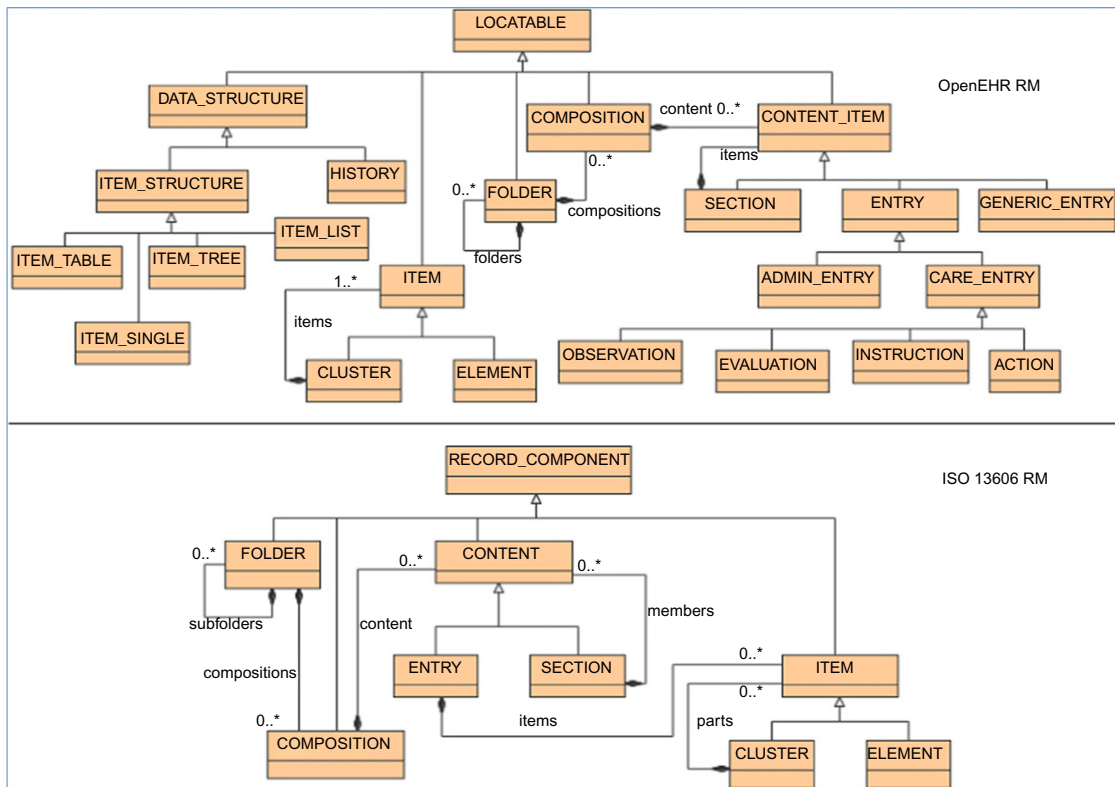
to reuse the current ontologies. Likewise, they offer formal systems for communicating sensible equivalences among properties and classes in various ontologies [43]. After studying some of the EHR standards, we found that these standards have some limitations during practical implementation. Some of these standards do not support semantic interoperability completely, some others have poor community support, and some do not provide the required level of security. Table 4 shows some of the advantages and disadvantages for each standard.

4 ONTOLOGIES AND THEIR ROLE IN EHR

Ontology is defined as a formal and explicit specification of a shared conceptualization [46]. Formal means the ontology is machine-readable. Explicit refers to the constraints of concepts. From the structure point of view, ontology is made by disjointed sets out of concepts, relations, attributes, and data types. Concepts are an organized collection of classes with normal features. Relations are a parallel relationship between concepts [47]. Ontologies play an important role in achieving EHR interoperability by supporting mappings between different EHR standards [48], and through defining clinical terminologies for precise and sharable expressions during data entry. Fig. 15 will show a comprehensive description of ontology.

The medical domain with its complexity is one of the most active domains that use ontologies for its many advantages such as:

1. The main focus of ontology is to give a clear definition and comprehension of the knowledge domain and its relations.

**FIG. 14**

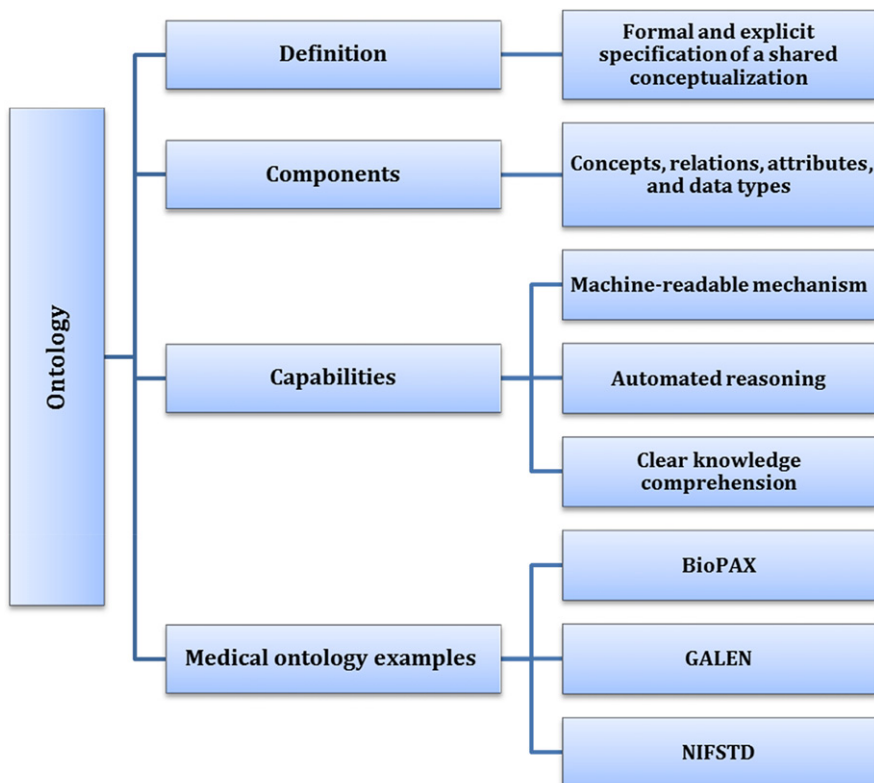
The main data structures of the ISO EN 13606 and OpenEHR reference model.

Table 4 The Advantages and Disadvantages of EHR Interoperability Standards

EHR Standard	Advantages	Disadvantages
HL7 [32]	<ul style="list-style-type: none"> ✓ Widely used ✓ Good tool support ✓ Mature ✓ Flexible ✓ Skills widely available ✓ European standards adoption ✓ Global ✓ Enables semantic interoperability ✓ Allows backward compatibility ✓ Open standard ✓ Provides semantic interoperability ✓ Provides service-oriented interfaces 	<ul style="list-style-type: none"> ✗ It does not support full semantic interoperability ✗ Exploiting the services-oriented architecture may be difficult ✗ Lack community support ✗ Lack of skills ✗ The absence of tool support ✗ Limited experience of implementation ✗ Complicated for simple messages ✗ Limited implementation experience
EN13606 [44]		
OpenEHR [45]		
SNOMED CT [42]	<ul style="list-style-type: none"> ✓ Data entry directly ✓ Reuse of data ✓ Legibility ✓ Coverage of the content and Development of the subset 	<ul style="list-style-type: none"> ✗ Ambiguity of terms ✗ Hierarchical relationships
DICOM [34]	<ul style="list-style-type: none"> ✓ DICOM also provides interconnectivity with diverse medical systems ✓ Comprehensive: supports all medical branches ✓ Less storage space 	<ul style="list-style-type: none"> ✗ Too many optional fields ✗ Large and complex ✗ Does not define hardware interfaces for equipment connection

2. Ontology is concerned with its reusability and the ability of automated reasoning. Ontologies aren't just used to present human information but also process and reason its contents.
3. Ontology has the ability to deal with imprecise and vague data.
4. Ontology is machine-readable. Ontology allows the machine interpretability by providing additional vocabulary along with a formal semantics.
5. Ontology defines a medical terminology with a nonconfusing and clear meaning that facilitates the exchange of information between different standards or systems [49].

Medical ontology contains all the relevant concepts associated with the medical domain such as treatment, diagnostics, patient data, and clinical procedures. There are various medical ontologies such as BioPAX, which is a standard language that aims to enable integration, exchange, visualization and analysis of biological pathway data [50]; and NIFSTD and BIRNLex are sets of ontologies for the neuroscience domain [51]. GALEN also is an important medical ontology example containing a huge number of concepts and procedures from all the fields of medical

**FIG. 15**

A comprehensive description of ontology.

specialization [52]. NCBO Bioportal, biological, and biomedical ontologies and associated tools allow us to search, browse and visualize [53].

Also, the fuzzy set theory has a fundamental role in managing uncertainty about patient administration and decision-making in healthcare. Ahmed et al. [54] proposed a framework concerning Crohn's disease classification using fuzzy partitioning in the neurofuzzy-based approach. The experimental results proved that the classification with level-8 partitioning provides a classification accuracy of 97.67%, with a sensitivity and specificity of 96.07% and 100%, respectively.

Over the traditional ontology, fuzzy ontology has many capabilities that enable it to solve the semantic interoperability in an EHR environment. In the following, we will study some of those:

1. Fuzzy ontology can be used in solving many real-world applications and complex problems.

2. Fuzzy ontology resembles human reasoning in its use of vague information, which can generate decisions correctly through its predicates [55].
3. Fuzzy ontology can deal with both numeric and unstructured data to facilitate the expression of rules and facts [55].
4. Fuzzy ontology can interact with the different interfaces used by various applications.
5. Fuzzy ontology permits reasoning and modeling the incomplete, ill-defined, vague, and uncertain knowledge [56].

5 METHODS

5.1 RESEARCH QUESTIONS

The main primary research questions of this review can be summarized as follows:

1. To what extent is semantic interoperability important and necessary in a EHR environment?
2. What is the role of EHR standards in achieving full semantic interoperability?
3. What is the degree of reliability and precision resulting from using these standards?
4. Is there a unified data model that can deal with all heterogeneous resources and uncertain medical data in a structured way?
5. What is the role of ontology in achieving EHR semantic interoperability?

5.2 SEARCH STRATEGY

A literature review was conducted of all English language studies from 2000 through December 2017. We selected a set of journal papers from several libraries and database search engines, such as IEEE [57], SpringerLink [58], PubMed [59], CiteSeerX [60], ScienceDirect [61], ELSEVIER [62], Science.gov [63], MEDLINE [64], Cochranelibrary [65], and Informatit [66]. Our search focused on the following criteria:

Language	English
Search key points	The main Keywords were: "electronic health record" OR "EHR," "semantic interoperability," OR "e-health" AND "ontology"
Search period	From the period of 2010 to December 2017
Content-Type	Journals and magazines, early access articles, and books only
Search Subjects	Computer science, medical informatics, biomedical and health informatics, e-health, and health science
Search in	We searched for the keywords in title, abstract, and keywords data fields or read the full article if necessary

5.3 SEARCH RESULTS

The results include the outcomes, and the final results from the literature review presented above. To be able to select an interesting paper from the several returned results, refinements in the search were processed in four filtration phases. In the first phase, the “electronic health record” OR “EHR” word was the main search key point. We screened for about 4043 articles. In the search second iteration, “semantic interoperability” AND “electronic health record” OR “EHR” were the main key points of the search. We found about 898 interesting articles. After that, in the third phase, we searched for “electronic health record” AND “semantic interoperability” AND “ontology” keywords. We found about 309 articles. [Fig. 16](#) shows the sequence of selecting the articles through an illustrative map.

[Table 5](#) and [Fig. 17](#) show the total number of citations obtained from the selected databases (IEEE Xplore, SpringerLink, PubMed, CiteSeerX, ScienceDirect, [Science.gov](#), ELSEVIER, MEDLINE, Cochanelibrary, and Informat).

After eliminating the duplicated and uninteresting papers, we chose 217 articles. We categorized the collected papers regarding the challenges, heterogeneous problem of interoperability, standardization approaches, and ontologies. In addition, we searched for the papers that introduce a framework for semantic interoperability in EHR environment. In the following section, we discuss the different considerations in grouping the most interesting collected papers.

- (a) Regarding papers concerned with barriers and the heterogeneous problem of EHR semantic interoperability

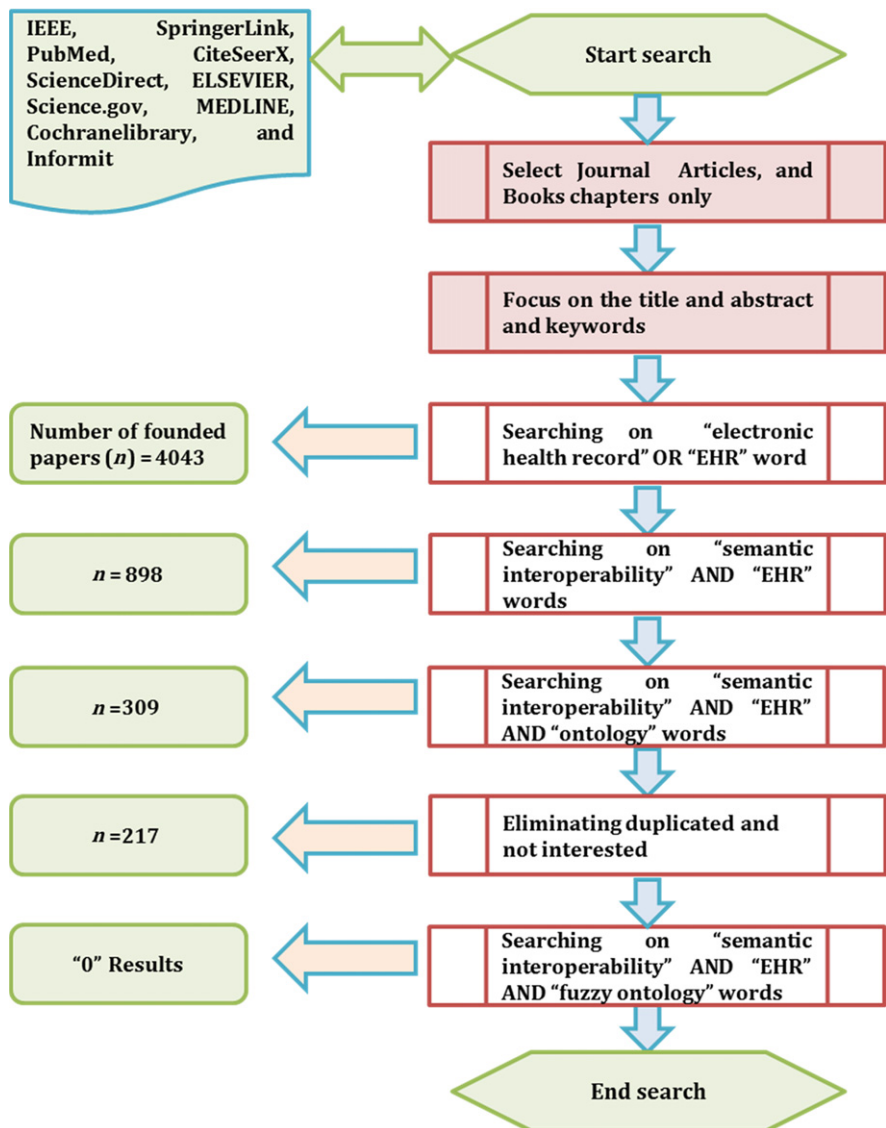
Based on the obtained results, about 40% of the collected papers manipulate challenges and barriers to semantic interoperability in an EHR environment. [Table 6](#) lists a selected set of articles focusing on that criterion. About 35% of the collected papers were concerned about standards in an interoperable EHR.

- (b) Regarding the standardization approaches in an interoperable EHR

From the obtained results, about 35% of the collected papers were concerned with standards in an interoperable EHR. [Table 7](#) lists a selected collection of articles focusing on that approach.

- (c) Regarding utilizing ontologies to solve the problems of interoperability

Ontology can be used to achieve semantic interoperability between heterogeneous healthcare systems. It has the ability to provide a homogeneous view of all different heterogeneous representations of input data resources. There are some emerging articles that rely on ontology to solve that problem in EHRs. [Table 8](#) presents a selected collection of articles concerned with using ontologies in solving the interoperability problems.

**FIG. 16**

An overview of the searching process.

- (d) Regarding papers introducing frameworks to solve semantic interoperability problems

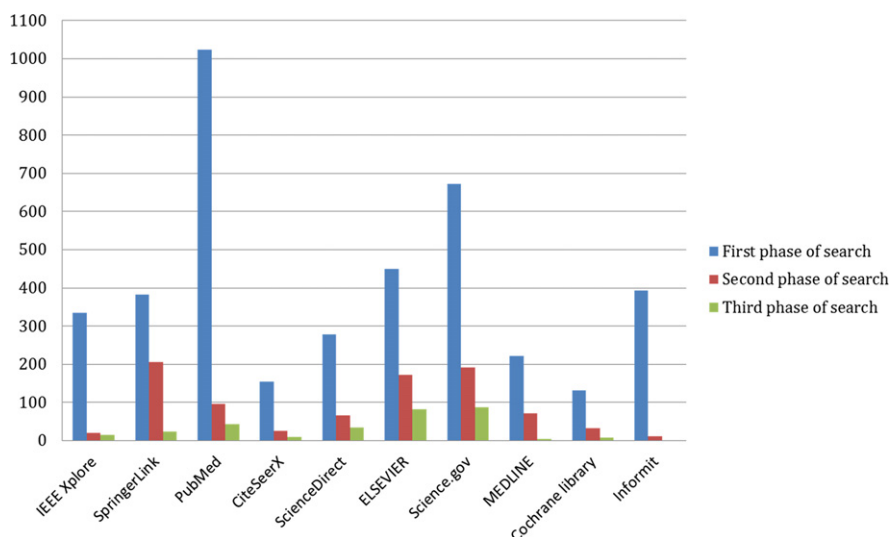
About 10% of the collected articles introduced frameworks that use different approaches to facilitate the information exchange of the EHR different systems

Table 5 The Number of Collected Papers for Each Database in the Three Searching Iterations

Database Engine	First Search Iteration	Second Search Iteration	Third Search Iteration
IEEE Xplore	335	21	15
SpringerLink	383	206	24
PubMed	1023	97	44
CiteSeerX	155	26	9
ScienceDirect	279	67	35
ELSEVIER	449	173	82
Science.gov	673	192	87
MEDLINE	222	72	4
Cochrane library	131	33	8
Informit	393	11	1
Total	4043	898	309

and solve semantic interoperability problems. **Table 9** shows a selected collection of those articles.

In the final fourth phase, we searched for “semantic interoperability,” and “EHR” and “fuzzy ontology” keywords in the determined searches. We obtained zero

**FIG. 17**

The number of initial papers obtained from the period of 2010–2017.

Table 6 Articles Concerned With Barriers and the Heterogeneous Problem of EHR Semantic Interoperability

Authors	Methods/Tools Used	Year
Li and Ling [67]	The authors aimed to provide a semiautomatic strategy for semantic interoperability data uniform. In the author's opinion, the semantic conflicts had to be resolved before achieving the interoperability and integration of the data. The authors showed how OWL could be used to detect these conflicts. The conflicts could be divided into three categories: scaling conflicts, naming conflicts, and confounding conflicts. They proposed an algorithm for identifying and resolving the semantic conflicts. However, they did not use an OWL for building ontologies	2004
Mecheri and Souici-Meslati [68]	The authors tried to create an interoperable information system and presented some technological tools achieving the semantic interoperability. After that, they tried to group the considered, studied work via a comparative table using a set of parameters	2010
Heidenreich and Angelidis [69]	The authors encouraged the integration of informal and technical specifications and introduced domain models to achieve semantic interoperability of the IT systems. The resulting domain models preserved the semantics of both messages and persistent records. However, in that approach domain models were static while complexity in healthcare requires dynamic ones	2010
Viangteeravat et al. [70]	The authors improved the incorporation efficiency of the heterogeneous health data by generating a model usage of the HL7 v3-RIM mapping capacity. The experimental results were perfect in enhancing the delivery of information and completing tasks. However, the authors did not actualize the results of the divergent framework subinquiries	2011
Sachdeva and Bhalla [71]	The authors focused on the role of semantics interoperability in the healthcare environment. They aimed to understand the current challenges in health informatics interoperability. They introduced the openEHR architecture as a framework for standardization and interoperability	2012
Lee et al. [72]	The authors evaluated three approaches of the database—NoSQL, native XML, and XML-enabled—to decide the most reasonable one for clinical information management. These approaches were evaluated to discover the advantages and disadvantages of each one for determining the best query performance. The results showed that the NoSQL database had the highest performance due to the highest querying speed, whereas XML databases were suitable for scalability, extensibility, and flexibility. Multiple databases with larger	2013

Table 6 Articles Concerned With Barriers and the Heterogeneous Problem of EHR Semantic Interoperability—cont'd

Authors	Methods/Tools Used	Year
Franz et al. [73]	datasets were not considered during the evaluation process. Also, new versions of the database software were not available	2013
COSTA et al. [74]	The authors tried to achieve the process and semantic interoperability by presenting a framework that used semistructured integration between metadata and underlying models. The approach was tested and presented high accuracy levels and better response times	2014
Bhartiya et al. [75]	To improve EHR semantic interoperability, the authors proposed a layered semantic-driven architecture fixed on a semantic mediator comprised of ontologies to formalize the clinical data meanings. This architecture was composed of five layers: structured heterogeneous data, semantic mapping, semantic mediator, virtual homogeneous data, and an application layer	2016

Table 7 Papers Concerned With Standards in an Interoperable EHR

Authors	Methods/Tools Used	Year
BGME et al. [76]	The authors tried to generate a semantically interoperable, highly specialized, and distributed healthcare system. They presented different approaches, such as OMG's CORBA 3 information system, GEHR /openEHR, and CEN EN 13606 EHR. These approaches were evaluated and compared using the generic component model, which depended on ISO principles and CORBA improvements, including their upgrade. They included HL7 Version 3, which was the most successful standard for achieving semantic interoperability	2006
Kilic and Dogac [48]	The authors described how R-MIM could be mapped to semantic tools by using archetypes. They demonstrated changing health level seven clinical instances to EHR clinical examples by utilizing the mapping definitions	2009

Continued

Table 7 Papers Concerned With Standards in an Interoperable EHR—cont'd

Authors	Methods/Tools Used	Year
Atalag et al. [77]	The authors aimed to give helpful insights to leaders for making the correct decisions by viewing from a more extensive edge to incorporate social and political drivers instead of adopting a specialized method. They made a snapshot of some existing standards to achieve e-Health systemic interoperability. The paper concluded by suggesting a combination of the current standards. However, the limitation of that paper is that some standards were not mentioned	2010
Kanagaraj et al. [78]	The authors mentioned that the computerized information systems helped in creating an accurate environment for storing the medical records of the patient electronically. A data warehouse might be used for achieving that. They tried to administrate the patient clinical data by suggesting the utilization of cloud computing implementing a PACS. PACS could deliver efficient access to images and at the same time save processing time	2011
Perakis et al. [79]	The authors explained that achieving semantic interoperability could provide improved patient outcomes, empower speedier access to powerful new medications, and give an essential foundation for personalized medicine. The authors aimed to describe the benefits of the Linked2Safety consortium for developing a high-performance interoperability framework	2013
Hammami et al. [80]	The authors tried to solve the challenges of exchanging information between different MIS (medical information system) healthcare. They did a comparative study of the new approaches, standards, and studies that tend to resolve heterogeneity problems in medical information systems. The authors proposed merging the concepts of the MIS technologies (such as merging SOA and ontology and merging cloud computing and ontology)	2014
Zhang et al. [81]	The authors proposed a semantic-based approach for clinical decision-making of patient data. A four-stage learning designing cycle was executed given in HL7 reference information model. However, big medical data were required to evaluate the proposed approach	2016

Table 8 Papers Concerned With Using Ontologies in Achieving the Interoperability Issues

Authors	Methods/Tools Used	Year
Lee et al. [82]	The authors suggested the mechanism of fuzzy inference to deduce similarity among the UMLS ontology and healthcare ontology, depending on the KL divergence value approach and the process of cosine measure. The results of the experiments proved that their approach could work efficiently to evaluate the similarity of the two ontologies	2006

Table 8 Papers Concerned With Using Ontologies in Achieving the Interoperability Issues—cont'd

Authors	Methods/Tools Used	Year
Ganguly et al. [83]	Ganguly et al. tried to solve some of the interoperability issues using various ontology-based mapping techniques. A dialogue framework was drawn. The authors made a comparison between many ontological negotiation protocols. They concluded that OWL Lite ontologies were the most appropriate for the semantic web environment. However, they had to resolve some of the challenges (such as reasoning) between the other versions of OWL-type ontologies	2008
Wang et al. [84]	Wang et al. suggested the fuzzy ontology property. They applied type-2 fuzzy dietary ontology and food ontology to the dietary estimation. The healthy dietary level was acquired to give users a reference for their eating. The results of experiments concluded that the suggested approach could evaluate the healthy dietary level for the gathered records	2010
Schulz et al. [85]	Schulz et al. tried to enhance the exchanging quality of the clinical data by providing the semantic standards. Their generalized methodology was based on OWL axioms. They suggested the use of formal ontologies using the description logic language OWL-DL that could mitigate the effort of semantic interoperability problems	2013
Piotr Szwed [55]	Piotr Szwed tried to solve two problems in e-health systems. The first one is interested in the medical guidelines implementation that can support chronic disease self-administration. The framework permitted the patients to enter the measured parameters, observed symptoms, then estimated the disease state and informed about required treatments. The second problem concerned reusing knowledge collected in ontologies and a semantic web application for performing fuzzy inference	2013

Table 9 Some of the Selected Papers Concerned With Introducing Frameworks to Solve Semantic Interoperability Problems

Authors	Methods/Tools Used	Year
Isela Macía [86]	The author proposed combining many various health standards (OpenEHR, HL7, and IHE). It described the software architecture that explained the role of different health standards in the environment of semantic interoperability. The framework architecture was composed of five main layers. It concluded that merging OpenEHR with interoperability standards was useful in increasing the consistency of the clinical document. However, the authors did not compare the obtained results of the proposed system with other existing ones	2014

Continued

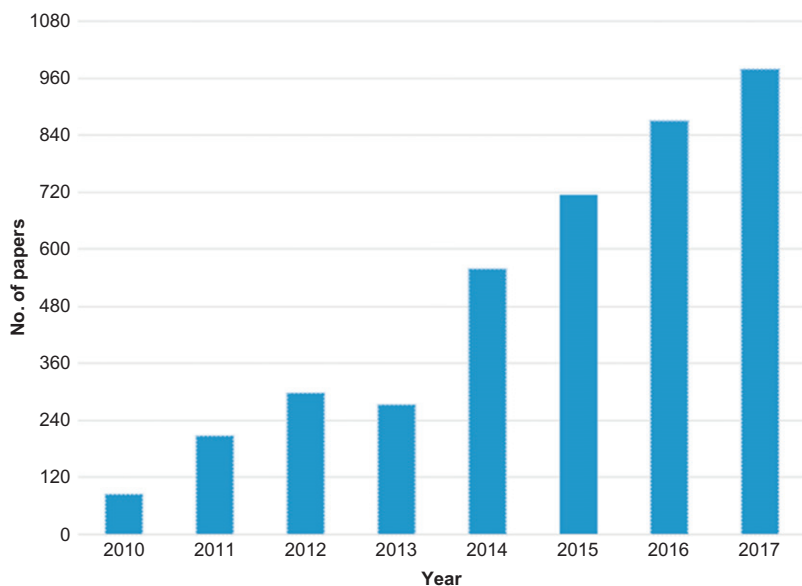
Table 9 Some of the Selected Papers Concerned With Introducing Frameworks to Solve Semantic Interoperability Problems—cont'd

Authors	Methods/Tools Used	Year
GONZÁLEZ et al. [87]	The authors presented an ontology-based approach to exchange knowledge and information with a PHR system and an EHR laboratory system. That approach included three systems: INDIVO, OpenMRS, and BikalIMS	2011
Iqbal et al. [88]	The authors proposed an ontology-based EMR centering on management of chronic disease. The EMR ontology could represent chronic disease knowledge. The clinical activities of the recommended ontology were converted into classes of HL7 RIM	2011
El Azami et al. [89]	The authors proposed a scalable and flexible architecture for healthcare institutions information systems integration. They took into consideration the three essential factors for entire system integration: data, workflow, and functions. The proposed architecture was mediation architecture of three levels: UI (user interface), middleware, and database levels. The intercession depended upon two fundamental segments: the adapter and the mediator	2012
Gaynor et al. [90]	The authors presented a framework to define and design a system that communicates information within a set of related medical applications. The proposed EHR graph system was composed of CD (clinical documentation) to register medical information, CPOE (electronic prescribing) to describe drugs, and CDS (clinical decision support) to check for adverse drug events	2014
Sun et al. [91]	That paper exhibited a way to deal with building semantic information virtualization layers over heterogeneous information sources. Information from various EHR structures as converted to RDF with its original meanings and afterward changed over into exemplifications with coincided domain meanings where both terminologies and ontologies are utilized to enhance reusability	2015

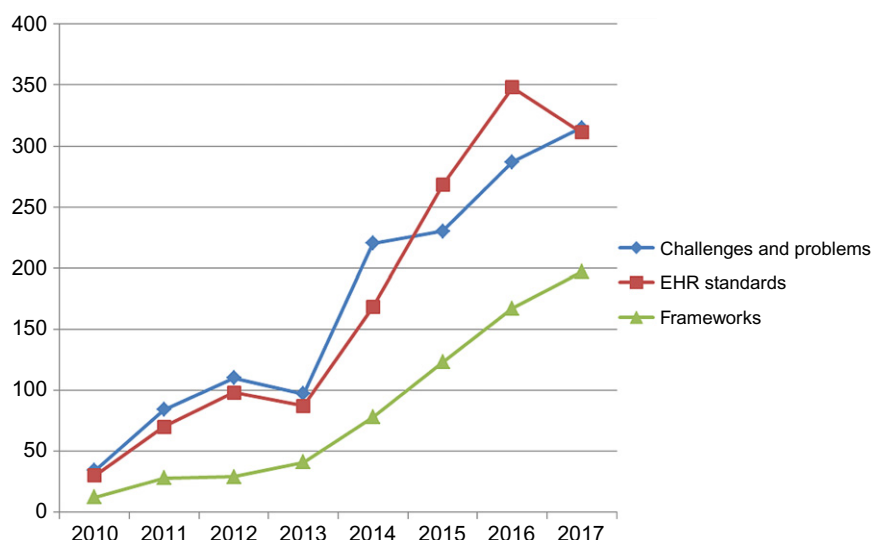
results. That means there is no paper or article that depends on fuzzy ontology to solve EHR semantic interoperability problems.

5.4 DISCUSSION

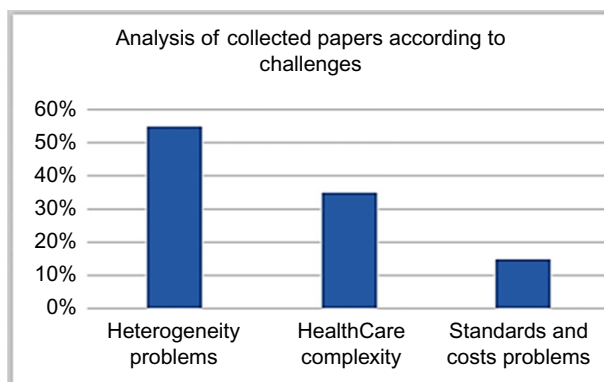
After all our literature reviews on EHR semantic interoperability, we noted that the number of published papers from the period of 2010 to December 2017 increased, as shown in Fig. 18. That increasing number of papers referring to semantic interoperability between different medical systems is becoming a top health IT topic, which means that researchers ought to adopt a more sensible strategy toward solving EHR semantic interoperability.

**FIG. 18**

The obtained results of the search process from the period of 2010–2017.

**FIG. 19**

The distribution of collected papers according to content.

**FIG. 20**

The number of collected papers discussing the barriers to EHR semantic interoperability.

Fig. 19 groups the collected papers according to papers manipulating challenges and problems of EHR (for about, 40% of the collected papers), papers manipulating EHR standards (35%), and papers manipulating interoperability frameworks (15%).

Fig. 20 lists the primary key terms of EHR semantic interoperability challenges and barriers identified during searching. Regarding papers manipulating challenges and problems of EHR, about 55% manipulate the heterogeneous problem, 35% focused on the health domain complexity as data types, 10% focused on standards problems, and a very small number took into account the cost factor. In the subsequent part of the chapter, we will debate the EHR semantic interoperability challenges.

6 THE CHALLENGES OF EHR SEMANTIC INTEROPERABILITY

Achieving interoperability in information systems has many problems and challenges. The primary one is that diverse frameworks in various healing centers and clinics have distinctive standards. The distinctive frameworks are furnished by different vendors with different standards and modules. Some of these problems are explained as follows [4]:

- (a) *Dynamics and complexities of healthcare systems:* The nature of medical data types is a structure that is more complex and has many parameters (each parameter has its contents). In addition, healthcare domains produce large quantities of data from many different sources. Also, the data in the medical domain may be missing.
- (b) *Heterogeneous framework condition,* which implies that the framework needs to consent to the particulars of various host languages, data models,

- architectures, communication protocols, operating systems, hardware, and programming languages.
- (c) *The problems of network communications* such as delaying, interruption, and missing data.
 - (d) *Security challenges* related to popular exchange of health information and also the servers of the database need protection from unauthorized access.
 - (e) *Costs associated with the exchange*. According to a 2015 survey conducted by KLAS and CHIME [92], 28% of healthcare executives cited cost as a top barrier to exchange in 2015. Stakeholders have characterized the fees associated with health information exchange interfaces as “prohibitive” while “set up of the required costs for the hardware equipment and web interfaces alongside subsequent maintenance of the system” has also been described as a problem.
 - (f) *The challenges of standards*: There are many standards that have been tried to achieve semantic interoperability in an EHR environment [15]. After studying some of these, we found that these standards have some limitations during practical implementation. The following are some examples of these limitations:
 - Many standards are difficult to understand and complex to implement, which increases the development costs [89].
 - Source information needs adaptation to the standard.
 - The standard has to expect all future uses.
 - A standard is one for its domain. It cannot be the best for all applications.
 - Adaptation of information to a standard may require interpretation (manual or automatic) [93].
 - Some other standards do not support SI completely, such as HL7.
 - Some standards do not put into consideration clinical, operational contexts, and workflows, which may differ among different points of system care and have a significant impact on how precisely clinicians translate information.
 - As there are so many developed EHR standards, different clinical information systems (CISs) might use different standards, which in the end do not contribute to seamless exchanging of clinical data.

7 CONCLUSION

We deeply surveyed the current literature for all aspects of semantic interoperability, including its main definitions, standards, schemas, models, terminologies, barriers, and future challenges. We depended on the existing database include ScienceDirect, IEEE Xplore, PubMed, and SpringerLink. We noted that the most intuitive EHR semantic interoperability approach is based on standards such HL7, DICOM, OpenEHR, DICOM, and EN13606, but they have some challenges. The medical domain is characterized by vagueness and uncertainty and all parties in it use imprecise

concepts to describe their ideas. Ontologies play an important role in achieving semantic interoperability in EHRs with their complexity. As a result, we recommend fuzzy ontology to achieve the target goal because of its capabilities, as we have shown. In the future, we want to exhibit the practicality of using fuzzy ontology in achieving EHR semantic interoperability in a large hospital information system.

REFERENCES

- [1] ISO/TC 215 Technical Report. “Electronic health record definition, scope, and context. Second Draft”, (2003).
- [2] Begoyan, An overview of interoperability standards for electronic health records, Integrated Design and Process Technology, IDPT, 2007.
- [3] S. Bhartiya, D. Mehrotra, Challenges and recommendations to healthcare data exchange in an interoperable environment, Electron. J. Health Inform. 8 (2) (2014) 1–24.
- [4] The Health Information Technology Policy Committee, Challenges and barriers to interoperability, Report to Congress, 2015.
- [5] V. Dinu, P. Nadkarni, Guidelines for the effective use of entity-attribute-value modeling for biomedical databases, Int. J. Med. Inform. 76 (11–12) (2007) 769–779.
- [6] J. Corwin, A. Silberschatz, P.L. Miller, L. Marenco, Dynamic tables: an architecture for managing evolving, heterogeneous biomedical data in relational database management systems, J. Am. Med. Inform. Assoc. (The Oxford University Press) 14 (1) (2007) 86–93.
- [7] R. Paul, A.S.M. Latiful Hoque, Optimized column-oriented model: a storage and search efficient representation of medical data, in: Information Technology in Bio-and Medical Informatics, ITBAM 2010, Springer, Heidelberg, 2010, pp. 118–127.
- [8] S. Batra, S. Sachdeva, Suitability of data models for electronic health records database, in: S. Srinivasa, S. Mehta (Eds.), Big Data Analytics: Third International Conference, BDA 2014, New Delhi, India, December 20–23, 2014. Proceedings, Springer International Publishing, Cham, 2014, pp. 14–32.
- [9] A. Geraci, et al., IEEE Standard Computer Dictionary: a compilation of IEEE standard computer glossaries, in: IEEE Std 610, 1991, pp. 1–217, <https://doi.org/10.1109/IEEESTD.1991.106963>.
- [10] HIMSS. “Definition of interoperability.” Approved by the HIMSS Board of Directors (April 5, 2013).
- [11] V. Stroetman, D. Kalra, P. Lewalle, A. Rector, J. Rodrigues, K. Stroetman, G. Surjan, B. Ustun, M. Virtanen, P. Zanstra, Semantic interoperability for better health and safer healthcare, The European Commission, 2009.
- [12] American Hospital Association, <http://www.aha.org/research/reports/tw/09nov-econimpsurvresults.pdf>. Tech. Rep. (November 11, 2009).
- [13] Portrait of promise: the California Statewide Plan to promote health and mental health equity, Tech. rep., California Health Care Foundation, 2015.
- [14] Social science research in action, N. O. R. C. tech. rep., NORC at the University of Chicago, 2011.
- [15] Audio-visual capabilities and applications supported by terrestrial IMT systems, Tech. rep., ITU-T Technology Watch, 2015.
- [16] IT U-T Technology Watch, E-health standards and interoperability, Tech. Rep. ITU-T Technology Watch Report, April(2012).

- [17] (CEO) Don Fornes, Available from: <http://www.softwareadvice.com>, 2005. Accessed 13 May 2017.
- [18] H. Kubicek, R. Cimander, H.J. Scholl, Layers of Interoperability, in: *Organizational Interoperability in E-Government*, Springer, Berlin, 2011, pp. 85–96.
- [19] Wikipedia's semantic interoperability definition 2017, Available from: https://en.wikipedia.org/wiki/Semantic_inter-operability, Accessed June 2017.
- [20] ISO/TR 20514 Technical Report, Health informatics—electronic health record—definition, scope and context, American National Standards Institute, 2005.
- [21] IEEE Standard Glossary, IEEE standard glossary of software engineering terminology, Technical report, IEEE, 1990.
- [22] R.H. Dolin, L. Alschuler, C. Beebe, P.V. Biron, S.L. Boyer, D. Essin, E. Kimber, T. Lincoln, J.E. Mattison, The HL7 Clinical Document Architecture, *J. Am. Med. Inform. Assoc.* 8 (6) (2011) 552–569.
- [23] A ten year vision to achieve an interoperable health IT infrastructure, Technical Report, (2014), Available from: <https://www.healthit.gov/sites/default/files/ONC10yearInteroperabilityConceptPaper.pdf>, Accessed June 2017.
- [24] IEEE-USA Medical Technology Policy Committee/Interoperability Working Group, in: NHIN: Interoperability for the National Health Information Network, IEEE USA Books & eBooks, 2006, 32pp.
- [25] W. Ceusters, B. Smith, *Semantic interoperability in healthcare state of the art in the US*, New York State Center of Excellence in Bioinformatics and Life Sciences Ontology Research Group, 2010, pp. 1–33.
- [26] The Joint Initiative for Global Standards Harmonization, Available from: <http://www.skmtglossary.org>, 2017. Accessed June 2017.
- [27] M. Mustra, K. Delac, M. Grgic, in: Overview of the DICOM standard, ELMAR, 2008, 50th International Symposium, 2008, pp. 39–44.
- [28] R. Rognehaugh, *The Health Information Technology Dictionary*, Aspen Pub., Gaithersburg, 1999.
- [29] A. Jain, V. Bhatnagar, Concoction of ambient intelligence and big data for better patient ministration services, *Int. J. Ambient Comput. Intell. (IGI Global)* 8 (4) (2017) 19–30.
- [30] ISO 13606 standard community, Available from: <http://www.en13606.org>. Accessed July 2016.
- [31] T. Benson, *Principles of Health Interoperability HL7 and SNOMED*, Springer, New York, 2012.
- [32] Health Level 7, Available from: <http://www.hl7.org>. Accessed June 2017.
- [33] L. Sabaa, N. Dey, et al., Automated stratification of liver disease in ultrasound: an online accurate feature classification paradigm, *Comput. Methods Programs Biomed.* (Elsevier) 130 (2016) 118–134.
- [34] D. Goldberg, Plato versus Aristotle: categorical and dimensional models for common mental disorders, *Compr. Psychiatry* (Elsevier) 41 (2) (2000) 8–13.
- [35] M. Hecht, *Pacs-Picture Archiving and Communication System*, Vienna University of Technology, University of Paderborn, 2008.
- [36] K. Sartipi, K.A. Kuriakose, W. Ma, in: An infrastructure for secure sharing of medical images between PACS and EHR systems, Proceedings of the 2013 Conference of the Center for Advanced Studies on Collaborative Research, 2013, pp. 245–259.
- [37] S. Cohen, F. Gilboa, U. Shani, *PACS and Electronic Health Records*, SPIE, San Diego, CA, 2002.

- [38] N. Dey, A.S. Ashour, A.S. Althoupety, Thermal imaging in medical science, in: Recent Advances in Applied Thermal Imaging for Industrial Applications, IGI Global, 2017, pp. 87–117, <https://doi.org/10.4018/978-1-5225-2423-6.ch004>.
- [39] Institute of Electrical and Electronics Engineers, Available from: <https://www.ieee.org>, Accessed June 2017.
- [40] J. Yao, S. Warren, Applying the ISO/IEEE 11073 standards to wearable home health monitoring systems, *J. Clin. Monit. Comput.* (Springer) 19 (6) (2005) 427–436.
- [41] OpenEHR, Available from: <http://www.openehr.org>. Accessed June 2016.
- [42] SNOMED CT the Global Language of Healthcare, Available from: <http://www.ihtsdo.org/snomed-ct>, 2017. Accessed July 2017.
- [43] World Wide Web Consortium (W3C), Available from: <https://www.w3.org>. Accessed July 2017.
- [44] D. Kalra, CEN prEN 13606 draft standard for Electronic Health Record Communication and its introduction to ISO TC/215, CEN/TC 251, Health Informatics, Brussels, Belgium, 2004.
- [45] T. Beale, S. Heard, The openEHR architecture: architecture overview, in: The openEHR Release 1.0.2, openEHR Foundation, 2007.
- [46] R. Studer, V.R. Benjamins, D. Fensel, Knowledge engineering: principles and methods, *Data Knowl. Eng.* (Elsevier) 25 (1–2) (1998) 161–197.
- [47] P. Buitelaar, P. Cimiano, B. Magnini, Ontology learning from text: an overview, in: *Ontology Learning From Text: Methods, Evaluation and Applications*, 123, IOS Press, Amsterdam, 2005, pp. 3–12.
- [48] O. Kilic, A. Dogac, Achieving clinical statement interoperability using R-MIM and archetype-based semantic transformations, *IEEE Trans. Inf. Technol. Biomed.* 13 (4) (July 2009) 467–477.
- [49] A. Valls, K. Gibert, D. Sánchez, M. Batet, Using ontologies for structuring organizational knowledge in Home Care assistance, *Int. J. Med. Inform.* (Elsevier) 79 (5) (2010) 370–387.
- [50] BioPAX: Biological Pathways Exchange, Available from: <http://www.biopax.org>. Accessed October 2017.
- [51] W. Bug, et al., The NIFSTD and BIRNLex vocabularies: building comprehensive ontologies for neuroscience, *Neuroinformatics* (Springer) 6 (3) (2008) 175–194.
- [52] A. Gangemi, D. Pisanello, G. Steve, Ontology integration: experiences with medical terminologies, in: *Formal Ontology in Information Systems*, IOS Press, 1998, pp. 46–98.
- [53] P. Whetzel, NCBO Team, NCBO technology: powering semantically aware applications, *J. Biomed. Semant.* (BioMed Central) 4 (1) (2013) S8.
- [54] S.S. Ahmed, N. Dey, A.S. Ashour, D. Sifaki-Pistolla, et al., effect of fuzzy partitioning in Crohn's disease classification: A neuro-fuzzy-based approach, *Med. Biol. Eng. Comput.* (Springer) 55 (1) (2017) 101–115.
- [55] P. Szwed, in: Application of fuzzy ontological reasoning in an implementation of medical guidelines, 2013 6th International Conference on Human System Interactions (HSI), 2013, pp. 342–349.
- [56] N. Rodríguez, M.P. Cuéllar, J. Lilius, M. Delgado Calvo-Flores, A fuzzy ontology for semantic modelling and recognition of human behaviour, *Knowl.-Based Syst.* (Elsevier) 66 (2014) 46–60.
- [57] IEEE Xplore Digital Library, Available from: <http://ieeexplore.ieee.org>, 2017. Accessed June 2017.

- [58] Springer Link, Available from: <https://link.springer.com>, 2017. Accessed June 2017.
- [59] U.S. National Library of Medicine National institutes of Health PubMed, Available from: <https://www.ncbi.nlm.nih.gov/pubmed>, 2017. Accessed 23 June 2017.
- [60] CiteSeerX, Available from: <http://citeseerx.ist.psu.edu>, 2017. Accessed 26 December 2017.
- [61] ScienceDirect, Available from: <http://www.sciencedirect.com>, 2017. Accessed 26 December 2017.
- [62] ELSEVIER, Available from: <https://www.elsevier.com>, 2017. Accessed 12 December 2017.
- [63] Science.gov, Available from: <https://www.science.gov>, 2017. Accessed December 2017.
- [64] MEDLINE, Available at: <https://www.nlm.nih.gov/pubs/factsheets/medline.html>, 2017. Accessed December 2017.
- [65] Cochrane library, Available from: <http://www.cochranelibrary.com/>, 2017. Accessed December 2017.
- [66] Informit, Available at: <https://search.informit.com.au>, 2017. Accessed December 2017.
- [67] C. Li, T.W. Ling, OWL-based semantic conflicts detection and resolution for data interoperability, in: Conceptual Modeling for Advanced Application Domains, Springer, Berlin, Heidelberg, 2004.
- [68] K. Mecheri, L. Souici-Meslati, in: Semantic interoperability of Web services: a survey, Machine and Web Intelligence (ICMWI), 2010 International Conference on, 2010, pp. 82–87.
- [69] G. Heidenreich, P. Angelidis, An approach towards semantic interoperability using domain models, Electron. J. Health Inform. 4 (1) (2010) 1–9.
- [70] T. Viangteeravat, M.N. Anyanwu, V.R. Nagisetty, E. Kuscu, M.E. Sakauye, D. Wu, Clinical data integration of distributed data sources using Health Level Seven (HL7) v3-RIM mapping, J. Clin. Bioinform. (BioMed Central) 1 (1) (2011).
- [71] Sachdeva S. and S. Bhalla. “Semantic interoperability in standardized electronic Health Record databases.” J. Data Inform. Qual. (ACM) 3, no. 1 (may 2012).1:1–1:37.
- [72] K.K. Lee, W.-C. Tang, K.-S. Choi, Alternatives to relational database: comparison of NoSQL and XML approaches for clinical data storage, Comput. Methods Programs Biomed. (Elsevier North-Holland, Inc.) 110 (1) (2013) 99–109.
- [73] B. Franz, A. Schuler, E. Helm, in: Analysis of clinical documents to enable semantic interoperability, Database and Expert Systems Applications, August 26–29, 2013.
- [74] C. Martínez-Costa, D. Kalra, S. Schulz, Improving EHR semantic interoperability: future vision and challenges. in: Studies in Health Technology and Informatics, vol. 205, 2014, pp. 589–593, <https://doi.org/10.3233/978-1-61499-432-9-589>.
- [75] S. Bhartiya, D. Mehrotra, A. Girdhar, Issues in achieving complete interoperability while sharing electronic health records, Procedia Comput. Sci. 78 (2016) 192–198.
- [76] B.G.M.E. Blobel, K. Engel, P. Pharow, HL7 version 3 compared to advanced architecture standards, Methods Inf. Med. 45 (2006) 343–353.
- [77] K. Atalag, D. Kingsford, C. Paton, J. Warren, Putting health record interoperability standards to work, Electron. J. Health Inform. 5 (1) (2010) 1–17.
- [78] G. Kanagaraj, A.C. Sumathi, Proposal of an open-source cloud computing system for exchanging medical images of a Hospital Information System, Trendz in Information Sciences Computing (TISC 2011), 2011, pp. 144–149.
- [79] K. Perakis, T. Bouras, D. Ntalaperas, P. Hasapis, in: Advancing patient record safety and EHR semantic interoperability, IEEE international conference on systems, Man, and Cybernetics, 2013, pp. 3251–3257.

- [80] R. Hammami, H. Bellaaj, A.H. Kacem, Interoperability for medical information systems: an overview, *Health Technol.* 4 (3) (2014) 261–272.
- [81] Y.-F. Zhang, T. Yu, T.-S. Zhou, K. Araki, J.-S. Li, Integrating HL7 RIM and ontology for unified knowledge and data representation in clinical decision support systems, *Comput. Methods Prog. Biomed.* 123 (2016) 94–108.
- [82] C.S. Lee, T.C. Hsieh, Y.S. Lai, M.H. Wang, C.N. Chen, in: *Apply fuzzy inference mechanism for supporting healthcare ontologies management*, 2006 IEEE International Conference on Systems, Man and Cybernetics, 2006, pp. 3458–3463.
- [83] P. Ganguly, S. Chattopadhyay, N. Paramesh, P. Ray, in: *An ontology-based framework for managing semantic interoperability issues in e-health, e-health Networking, Applications and Services*, HealthCom, 2008, pp. 73–78.
- [84] M.H. Wang, C.S. Lee, Z.W. Chen, C.F. Lo, S.E. Kuo, H.C. Kuo, H.H. Cheng, in: *Property and application of fuzzy ontology for dietary assessment*, Fuzzy Systems (FUZZ), 2010, pp. 1–8.
- [85] S. Schulz, C. Costa, in: *How ontologies can improve semantic interoperability in health care*, KR4HC/ProHealth, Springer, 2013, pp. 1–10.
- [86] I. Macía, Towards a semantic interoperability environment, *e-Health Networking, Applications and Services (Healthcom)*, 2014, pp. 543–548.
- [87] C. González, B.G.M.E. Blobel, D.M. López, Ontology-based framework for electronic health records interoperability. in: *Studies in Health Technology and Informatics*, vol. 169, 2011, pp. 694–698, <https://doi.org/10.3233/978-1-60750-806-9-694>.
- [88] A.M. Iqbal, M. Shepherd, S.S.R. Abidi, An ontology-based electronic medical record for chronic disease management, in: 2011 44th Hawaii International Conference on System Sciences, Kauai, HI, 2011, pp. 1–10, <https://doi.org/10.1109/HICSS.2011.61>.
- [89] I. El Azami, M. Malki, C. Tahon, Integrating hospital information systems in healthcare institutions: a mediation architecture, *J. Med. Syst.* (Springer) 36 (5) (2012) 3123–3134.
- [90] M. Gaynor, F. Yu, C.H. Andrus, S. Bradner, J. Rawn, A general framework for interoperability with applications to healthcare, *Health Policy Technol.* 3 (1) (2014) 3–12.
- [91] H. Sun, K. Depraetere, J. De Roo, G. Mels, B. De Vloed, M. Twagirumukiza, D. Colaert, Semantic processing of EHR data for clinical research, *J. Biomed. Inform.* 58 (Suppl. C) (2015) 247–259.
- [92] KLAS Technical Report, “KLAS: Medical Equipment Report”; (2015).
- [93] M. Patel, T. Koch, M. Doerr, C. Tsinaraki, *Semantic interoperability in digital library systems*, UKOLN, University of Bath, 2005.

A unified fuzzy ontology for distributed electronic health record semantic interoperability

14

Ebtsam Adel*, **Shaker El-Sappagh[†]**, **Sherif Barakat***, **Mohammed Elmogy[‡]**

Information Systems Department, Faculty of Computers and Information, Mansoura University, Mansoura, Egypt Information Systems Department, Faculty of Computers and Informatics, Benha University, Benha, Egypt[†] Information Technology Department, Faculty of Computers and Information, Mansoura University, Mansoura, Egypt[‡]*

CHAPTER OUTLINE

1	Introduction	354
1.1	EHR Clinical and Business Benefits and Outcomes	355
1.2	EHR Semantic Interoperability Barriers and Obstacles	357
2	Related Work	360
3	Preliminaries	362
3.1	Techniques and Approaches of EHR Semantic Interoperability	362
3.2	EHR Standards	363
3.3	Ontologies	363
3.4	Terminologies	367
3.5	Semantic Interoperability Frameworks	369
3.6	Privacy and Security in EHR Systems	372
4	Methodology	373
4.1	The Proposed Framework	374
4.2	A Prototype Problem Example	381
4.3	A Comparison Study	389
5	Conclusion	389
References	389	
Further Reading	395	

1 INTRODUCTION

With the increase of chronic diseases, an individual's acknowledgment is moving from the classic e-Health to ubiquitous healthcare (u-Health). It is normal that portable and pervasive telemedicine coordinated with a wireless body area network (WBAN), has incredible potential in encouraging the arrangement of cutting-edge u-Health. By utilizing WBAN, the patient will be provided with mobility. That mobility will enable a cheap and smart way of remote monitoring for patients suffering from chronic diseases such as blood pressure, heart disease, diabetes, etc. However, there are numerous angles and additional challenges related to the framework of u-Healthcare systems such as architectural design and execution issues, integration and interoperability of information and systems, and security and effective information transmission and administration. Semantic interoperability is required between different sensor data, between medical data and social media, between sensed data and electronic health record data, and between different systems such as mobile applications and hospital information systems. Without semantic interoperability, different medical data will work in isolation; healthcare organizations will not benefit from the massive data in analytics and decision-making. Moreover, the handling of medical data uncertainty is a critical issue when achieving semantic interoperability. In this chapter, a unified semantic interoperability framework for distributed EHR based on fuzzy ontology is proposed. The framework architecture consists of three main layers. The lowest layer (local ontologies construction) stores the EHR heterogeneous data with different database schemas, standards, terminologies, purposes, locations, and formats. The sources of this information may be different databases in heterogeneous schemas, EHR standards, XML files, spreadsheet files, or archetype definition language (ADL) files. These different inputs are transformed into crisp ontology using a mediator suitable for each type. In the middle layer (global ontology construction) the local ontologies are mapped to a crisp global one. The global reference ontology combines and integrates all local ontologies and therefore describes all data. Then this crisp ontology is converted to a unified fuzzy ontology.

EHR is defined by ISO [1] as “A repository of information regarding the health of a subject of care, in computer processable form.” In other words, it is a collection of patient’s related data to allow harmonic, effective, and general sharing of that data. It is considered a main component of the hospital management systems that manage all the aspects of hospital operations. EHRs can change the medicinal services framework from a paper-based industry to a digitized format that helps suppliers in conveying a higher nature of care to their patients. EHR interoperability is needed to improve healthcare quality, effectiveness, and productivity. That helps in delivering the right information in the right format whenever and wherever required, which eliminates unnecessary repetition, avoids errors, reduces delays, reduces the cost of healthcare, and, finally, supports sound real-time decisions.

Medical data are growing rapidly. These data are distributed and unstructured, and each data have their schema, structure, standard, format, coding system, level of abstraction, and semantic. The data of a single patient can be distributed over different EHRs with different ways of representation [2]. At the same time, physicians and healthcare providers often require access to these data in a unified way. In other words, medical personnel need to query the distributed EHR systems anonymously by using a single language. The problem of combination and integration of information is known as interoperability [3]. In the following, we will talk about a portion of the primary points identified with EHR and its semantic interoperability (SI).

1.1 EHR CLINICAL AND BUSINESS BENEFITS AND OUTCOMES

Achieving EHR and its SI in any clinical organization fulfills a great number of benefits and outcomes, as shown in Fig. 1. Many studies focus on EHR clinical and business outcomes [4].

1. EHR provides the patient with easy access to the computerized records and eliminates dangerous medical errors caused by the poor penmanship of physicians (many clinical items are in very poor handwriting and difficult to read) [5].
2. EHRs will play an important role in homecare, epidemiological situations, telemedicine, emergency situations, chronic disease management, and e-Health environments [6]. That e-environment will help to reduce duplication, prevent medication errors, and save time.
3. According to the CEN/ISSS e-Health Standardization Focus Group [7], EHR healthcare informatics have many goals and objectives, such as:

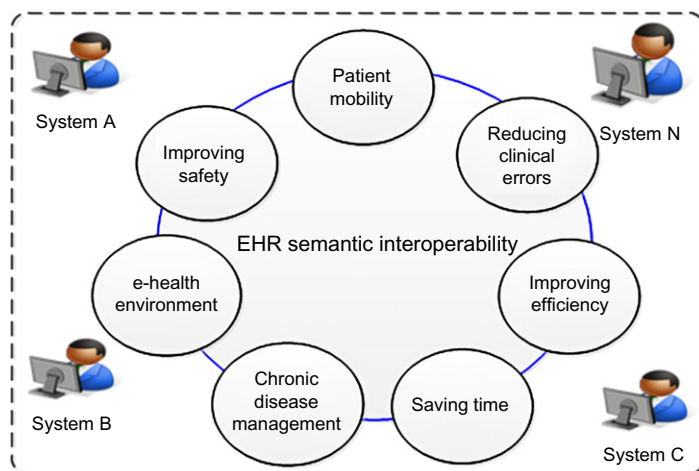


FIG. 1

Some EHR clinical and business outcomes.

- (a) Enabling quiet mobility to human healthcare.
- (b) Minimizing clinical blunders and enhancing safety.
- (c) Perfecting the access quality of health data for patients and experts.
- (d) Enhancing the effectiveness of the processes of human healthcare.

According to the Medicare and Medicaid Services Centers [8], “EHRs don’t accomplish their advantages only by exchanging data from paper shape into the advanced frame. EHRs can just convey their advantages when the data and the EHR are institutionalized, and ‘organized’ in uniform courses, similarly as automated teller machines (ATMs) rely upon the consistently organized information. Along these lines, the important utilized approach requires recognizable proof of norms for the EHR framework.” IEEE defined interoperability as “the capacity of various EHR structures and programming applications to bestow, swap data, and utilize that exchanged data” [9]. The standards of information exchanged and schema should permit data to be allowable via many needed systems such as clinicians, labs, pharmacies, and hospitals. Interoperability suggests the power of EHR systems to collaborate inside and across finished organizational boundaries, remembering the true objective to push the successful delivery of medicinal services for people and communities. [Fig. 2](#) shows that there are three unique sorts of interoperability including syntactic, semantic, and process. In the following; we will discuss these main types.

- *Technical “syntactic” interoperability:* Syntax is used to describe the sentence structure. Syntactic interoperability is defined as “the capability of two or more information and communication technology applications to accept data from each other and perform a given task in an appropriate and satisfactory manner without the need for extra operator intervention” [10]. It is when frameworks can

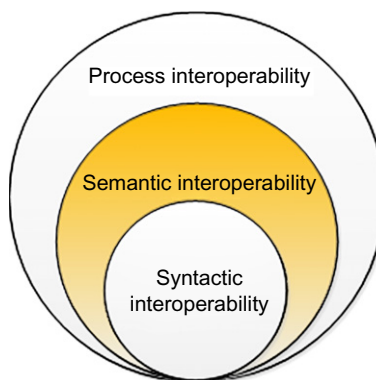


FIG. 2

The main types of interoperability.

send and get information effectively. According to [11], syntactic interoperability has many challenges:

1. Identifying and distinguishing all the elements in different systems.
 2. Constructing rules for structuring these elements.
 3. Creating crosswalks between equivalent elements.
- *Semantic interoperability (SI)*: Semantic interoperability is defined as “integrating resources that were developed using different vocabularies and different perspectives on the data. To achieve semantic interoperability, systems must be able to exchange data in such a way that the precise meaning of the data is readily accessible, and the data itself can be translated by any system into a form that it understands” [12]. It is where data is sent and received between frameworks without changes in its importance. SI is a huge problem in the healthcare industry [13]. It provides interoperability at the top level. It exploits the advantage of both *organizing* the exchange information and the *codification* of the information, including vocabulary, with the goal that the receiving EHR frameworks can translate the significance and meaning of information the same way as the sending systems. It expresses that the importance of data has to be saved from a user level to physical one via the logical level. Achieving interoperability requires a general framework that is made out of an arrangement of standards, strategies, details, principles, and methods [14], working in coordination to encourage building an arrangement of related applications that connects flawlessly.
 - *Process interoperability*: This is where the integrity of the work process of procedures can be kept up between frameworks. It guarantees consistent communication among various healthcare frameworks by creating shared comprehension of their process artifacts [15]. To accomplish process interoperability, there is a need to adjust the work process to standardized communication patterns. The ontologies play an important role in handling those alignments and patterns [15].

1.2 EHR SEMANTIC INTEROPERABILITY BARRIERS AND OBSTACLES

Achieving the collaboration and SI of information among systems and organizations has various challenges and barriers in the healthcare domain. Different healthcare organizations have their medicinal data frameworks to continue understanding a patient’s information with different data schemas, standards, and terminologies. Heterogeneous system environments have to comply with the specification of different encoding terminologies (e.g., SNOMED CT, ICD, DICOM, etc.), data models (relational object, object-oriented, EAV, OCOM, OEA, and dynamic tables), and architecture standards (HL7 RIM, OpenEHR, ISO/TS 18308:2004, ASTM E1238/1384, etc.). On the other hand, it isn’t practical to expect all the healthcare organizations to

adjust to a solo standard [16, 17], so there is an urgent need to handle the semantic interoperability to support the integration of different systems without affecting their internal structure. Achieving SI in an EHR environment has many challenges and problems [13]. Some of these challenges are discussed.

1.2.1 The heterogeneity problem

As shown in Fig. 3, the same health data can be presented in different ways. A heterogeneous environment implies that the framework needs to conform to the particulars of various data models, communication protocols, architectures, programming languages, and hardware. Distributed and heterogeneous data resources often lead to redundancy in existing data, which may lead to quality faults. Another problem of heterogeneity is the huge amount of different interfaces that are in use [18]. That difference comes from the fact that there are many high-level programming languages that could run on distinct operating systems (e.g., Linux, UNIX, Windows, and OS X), and the difference in process controls. For example, a Java or C++ software component might be run on a UNIX machine and it might also be run on a Windows machine.

1.2.2 Dynamics and complexities of healthcare systems

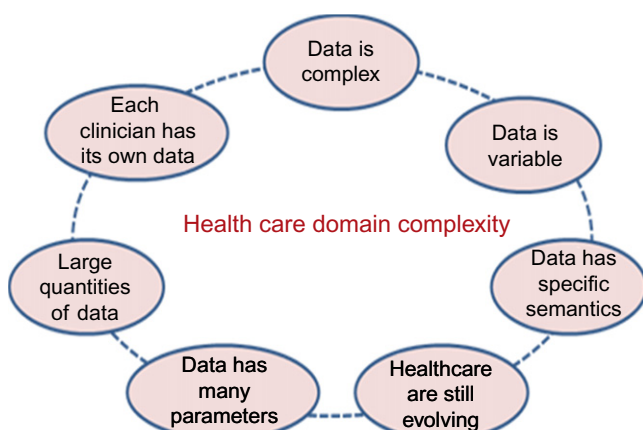
As shown in Fig. 4, healthcare in nature is very complex and fractal because of the following reasons:

- The healthcare domain produces large quantities of data from many different sources. Information comes from laboratory technicians, ECG traces, radiologists, pharmacists, nurses, physicians, and patients. All this is needed and used by the other sources. The medical domain big data is an upheaval for customized healthcare [19].
- The nature of medical data types is a structure that is more complex and has many parameters (each parameter has its contents). In addition, the data may be missing. For example, the temperature unit may be entered as Fahrenheit or

General Practice	Polyclinic	Restructured Hospital
Problem/Dx	Problem/Dx	Diagnosis
Prob/Dx: Cancer	Prob/Dx Name: Suspected cancer	Name: Suspected lung cancer
Body Site: Lung	Body Site: Lung	Body Site: Lung
Status: ● Suspected ● Confirmed ● Not found		
OK Cancel	OK Cancel	OK Cancel

FIG. 3

The different representations of the same clinical data.

**FIG. 4**

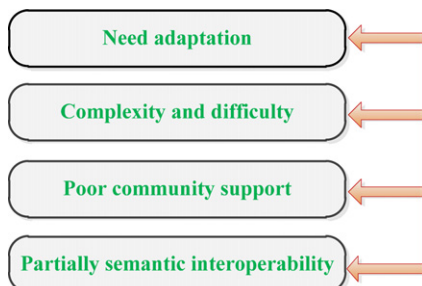
The healthcare domain complexity.

Celsius or may be outside the permissible range. In another example, one source may enter an attribute in inches while another had the same attribute in centimeters.

- The workflow of the medical domain is varied, depending upon the patient's issue and at what stage of the process [2].
- Each clinician has his own needs. Every specialty has its own particular training, administration, and quality affirmation necessities as well as its specific manners of working [2].

1.2.3 The challenges of standards

There are many standards to achieve the SI in the EHR environment [20]. In examining some of those standards, we found that they have a few constraints amid functional execution, as shown in Fig. 5. These are some examples of those limitations:

**FIG. 5**

The challenges of EHR SI standards.

- Many standards are difficult to understand and complex to implement, which increases the development costs [21].
- Source information needs adaptation to the standard.
- The standard has to expect all future uses.
- A standard is one for its domain. It cannot be the best for all applications.
- Adaptation of information to a standard may require interpretation (manual or automatic) [22].
- Some other standards do not support SI completely, such as HL7.
- The standards are either imperfect in functionality terms or without the detail of exact significance of the hidden information [23].
- Some standards don't take into account clinical, operational contexts, and workflows, which may differ among different points of system care. This has a significant effect on how clinicians understand and interpret information precisely [18].
- As there are so many developed EHR standards, different clinical information systems (CISs) might use different standards, which in the end do not contribute to a seamless exchange of clinical data [24].

The remainder of the chapter is sorted into four sections as follows. Some of the studies that tried to achieve EHR semantic interoperability depending on ontology framework will be outlined in [Section 2](#). [Section 3](#) discusses some of the main topics in EHR such as its approaches, standards, ontologies, terminologies, and some of the prior frameworks. [Section 4](#) will study the proposed framework of global architecture (design). [Section 5](#) reports the conclusion.

2 RELATED WORK

Using ontology to handle SI has been heavily studied. Berges et al. [25] tried to achieve the SI of a heterogeneous EHR. That study relied on medical diagnoses statements. First, it incorporates an acceptable ontology whose EHR-attached concepts concentrate on meanings and perspectives. Second, it oversees modules that permit acquiring rich ontological portrayals of EHR data controlled by restrictive models of medical data frameworks. The highlights of one particular module appear as a reference. Third, it considers the imperative mapping maxims among its concepts upgraded with the mappings. This element smoothed out the basic contrasts among heterogeneous EHR depictions and portrayals, and at the same time allowed appropriate alignment of information.

Ferrer et al. [26] represented and integrated a patient's data obtained from many different heterogeneous data resources and encouraged the conjunction of patient information with a rule-based CDSS. The authors attempted to close the hole between ISO/CEN 13606 and HL7 by utilizing the OpenEHR approach. They proposed to build up the PHR by consolidating the archetypes of OpenEHR and the HL7 vMR standard, bolstered by the service-oriented system for exchanging information.

They concluded that archetypes give a robust and adaptable technique while representing the clinical data. Despite that, the proposed framework had to be verified by more real data examples. Costa et al. [27] tended to the SI of two common standards of EHR including ISO EN 13606 and OpenEHR. The mentioned standards keep track of the approach of the dual model that classifies the knowledge and information using archetypes. That solution was considered an essential advance and a primary step toward the data instance transformations. That solution could generate OWL and ADL archetypes in the objective standard of EHR. The solution depended on mapping between the archetypes of ISO EN 13606 and OpenEHR and the other way around by consolidating model-driven and semantic web designing advancements. The architectures of that work consisted of two prime layers. The first one is the layer of ontology, which included a progression of ontologies that model the attached knowledge of various EHR standards. The second one is the layer of MDE that contained the metamodels compared to the semantic portrayals characterized in the first layer. Carolina Gonzalez et al. [23] aimed to propose an ontology-based interoperability framework to support SI among EHRs, regardless of the used standard. In view of the proposed structure, an interoperability scenario among an individual health record framework, an EHR, and a laboratory system was portrayed. The proposed interoperability scenario included three systems: INDIVO, OpenMRS, and BikaLIMS. In the implementation process, the use of formal application ontologies was necessary, thus improving the information representation of each system to interoperate.

However, the proposed framework had to be more heterogenetic to measure the degree of effectiveness and accuracy of the matching process. Carmen et al. [28] proposed an OWL web-based framework based on the archetype management system (ArchMS) for the investment of archetypes, ontologies, terminologies, and clinical data for SI environments. The main goals of this work were to reutilize substances from ontologies and existing archetypes for the investments and administration of EHR clinical models and data. Also, they wanted to reutilize the ArchMS in perspective of the utilization of semantic web depiction principles, although the authors had to integrate new standards in the transformation process. Sinaci et al. [29] discussed the fact that there are many organizations publishing regular information component dictionaries and normal models attempting to take care of the semantic interoperability issue. Those organizations include HITSP, CDISC, FHIR, ToC, and BRIDG. However, the interoperability crosswise over the application domain boundaries isn't consequently conceivable. The authors introduced a supporting framework and a unified methodology. They presented a unified semantic metadata registration structure by ISO/IEC 11179 standard extension, and empowered a mix of information component registries via the principles of LOD. Every common data element (CDE) could be interestingly indicated, questioned, and handled to enhance the SI and syntactic, although practical examples were needed to verify the framework. Santos et al. [16] explicated the importance of the EHR, which can make integration between different interface and software applications.

Also, they put the focus on some of the main requirements of interoperability identified with SES-MG members. Some of those requirements include (1) the EHR system should provide mechanisms for exchanging patient's demographic and clinical data with the central repository, (2) the central repository should permit structuring of its data elements through archetypes and standardized reference models, and (3) it should provide a terminology services repository, which would enable exchanging EHR information based on a common vocabulary. The authors presented an ISO 13606 EHR proposal architecture based on utilization of semantic technologies. From studying previous works in achieving SE, we detected that there isn't any data model that tries to integrate all heterogeneous input resources in a unified data structured model. Therefore the proposed framework complements and builds on all those previous works. Therefore, we suggest a unified fuzzy ontology semantic interoperability-based framework for EHR systems. This framework has a multilayer structure with multiple modules at every layer to properly and accurately preserve the medical data semantics between heterogeneous systems.

The proposed framework models EHR syntax based on a unified reference model such as openEHR or HL7 RIM; a data model based on archetypes, meaning relied upon standard terminologies such as SNOMED CT or UMLS; and fuzzy semantics based on fuzzy ontology. That framework has many benefits and advantages over previous frameworks, including:

1. It moves toward achieving full semantic interoperability of heterogeneous EHRs.
2. It supports the idea of plug and play where any system with any structure can be integrated anonymously with existing systems without affecting the current working environment.
3. It is more dynamic and helps in natural language querying.

3 PRELIMINARIES

To produce a self-contained chapter and collect all the required concepts and technologies, this section introduces the techniques and approaches of EHR semantic interoperability, including its standards, ontologies, and terminologies.

3.1 TECHNIQUES AND APPROACHES OF EHR SEMANTIC INTEROPERABILITY

Many techniques exist to solve all the previous challenges and barriers of SE. There are many database integration approaches, techniques, and approaches to use. One of those approaches is to integrate all source schemas into a global schema (*Schema Integration*) [30], but a global schema has many limitations such as its maintenance, which is a very difficult matter. The global schema does not have the ability to harmonize richer forms of general knowledge that might be reusable, and it does not provide enough semantics for the used concepts [31]. For a large-scale distributed

query engine that requires long running queries over heterogeneous data sources, the adaptive distributed query processing systems were presented [32]. In addition, it does not fulfill the SE. The most intuitive approach is based on standards. According to the SemanticHEALTH project [33], EHR standards, terminologies, and ontologies are the three primary factors required to accomplish SI in an EHR environment. In the next section, we will discuss with more insight those three keys.

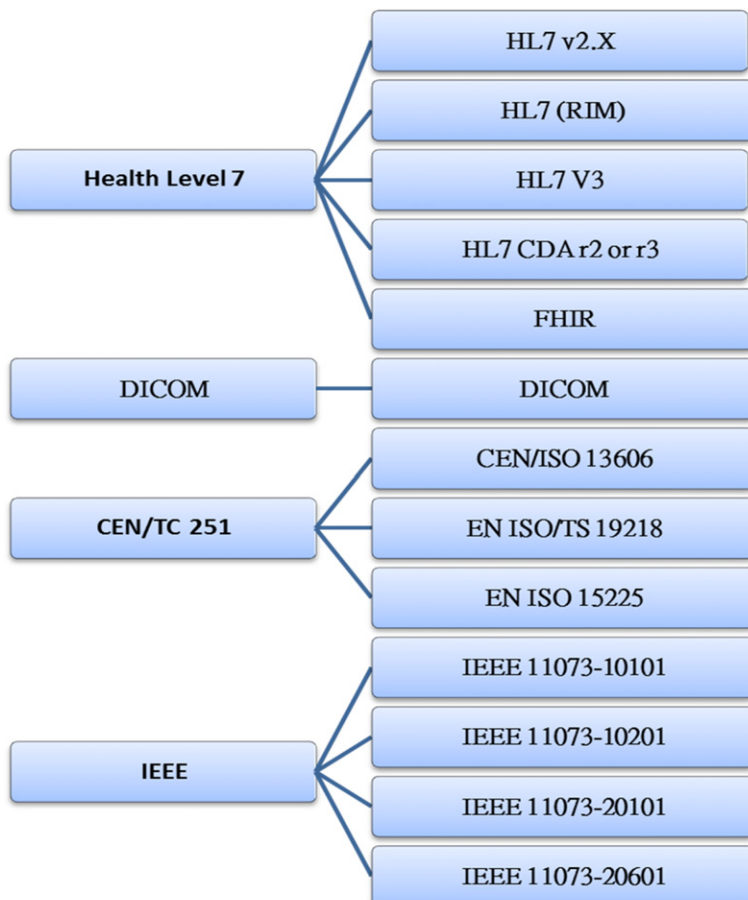
3.2 EHR STANDARDS

In the healthcare domain, the standards play a necessary function in presenting the required level of reliability and quality. The benefits of using standards increase exponentially in the case of increasing the number of involved parties. According to Benson [34], the quantity of required interfaces is expected to associate N frameworks utilizing the following function $(N^2 - N)/2$. Without utilizing a standard, connecting two hubs requires just a solitary interface. Connecting six hubs needs 15 interfaces while connecting 100 hubs requires about 4950 interfaces. As in Fig. 6, there are many proposed organizational standards to achieve the SE, including IHTSDO, DICOM [35], CDISC [36], IHE [37], MML [38], HL7 [39], CEN/ISO 13606 [40], and openEHR [41]. The last three are dual model architecture. The dual model architecture depends on recognizing two distinct scales: knowledge and information. The reference model gives the information level, and the level of the knowledge is given by the archetype model.

The archetype can be characterized as a specialization used to determine the scenarios of clinical recordings. It can be explained in the ADL [42], which is composed of four primary segments: header, description, definition, and ontology. The description and header sections are used to give universal data about the archetype, for example, author, name, purpose, and dialect. The definition area involves the imperatives and structures related to the clinical scenarios characterized by the archetype. The section of the ontology contains a depiction of every component in the definition segment and ties to different terminologies. There are several tools that are generated by the archetype community such as LinkEHR7 and the tools created by the openEHR, archetype editor [43] (AE), the clinical knowledge manager [44] (CKM), and the ADL workbench [45] (AW).

3.3 ONTOLOGIES

Ontology is considered an important science of philosophy in managing the idea of existence. It is defined in computer science by WordNet [46] as follows: *comprehensive and precise association of some knowledge domain that is typically various leveled and contains all the important substances and their relations*. From the mathematical point of view, concepts define an individual class. Instances are elements of classes, which are linked to classes through relations. Properties (relations) can be used to represent relationships between individuals. Ehrig and Staab [47, 48] defined ontology mathematically as follows:

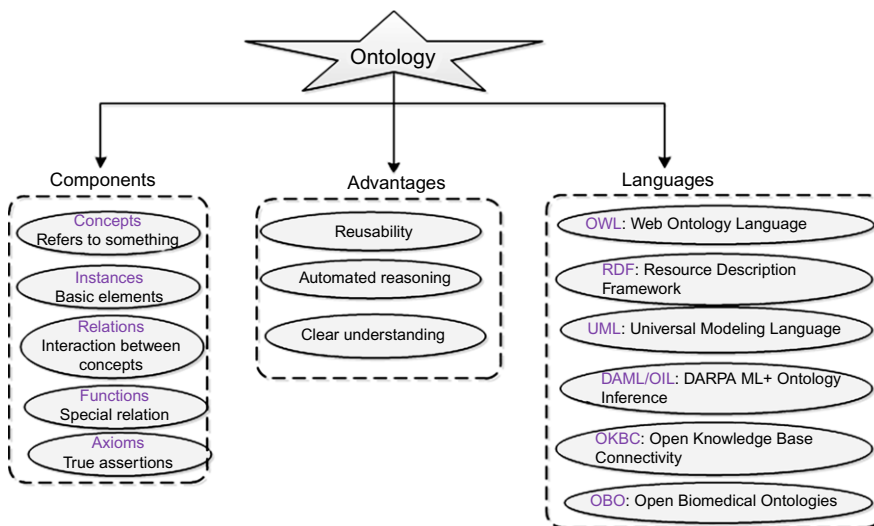
**FIG. 6**

The main EHR standards and their organizations.

$$O = (C, H_C, R_C, H_R, I, R_I, A)$$

- O is defined as an ontology for a specific domain.
- C is a group of concepts.
- H_C is hierarchy subsumption.
- R_C is an arrangement of relations among concepts.
- I is an arrangement of instances (individuals) of a specific concept in a domain.
- R_I is a group of relations among instances.
- A is a group of axioms holding between concepts, relations, or individuals.

Alalwan summarized the five basic components of ontology as [49] concepts, relations, functions, axioms, and instances, as shown in Fig. 7.

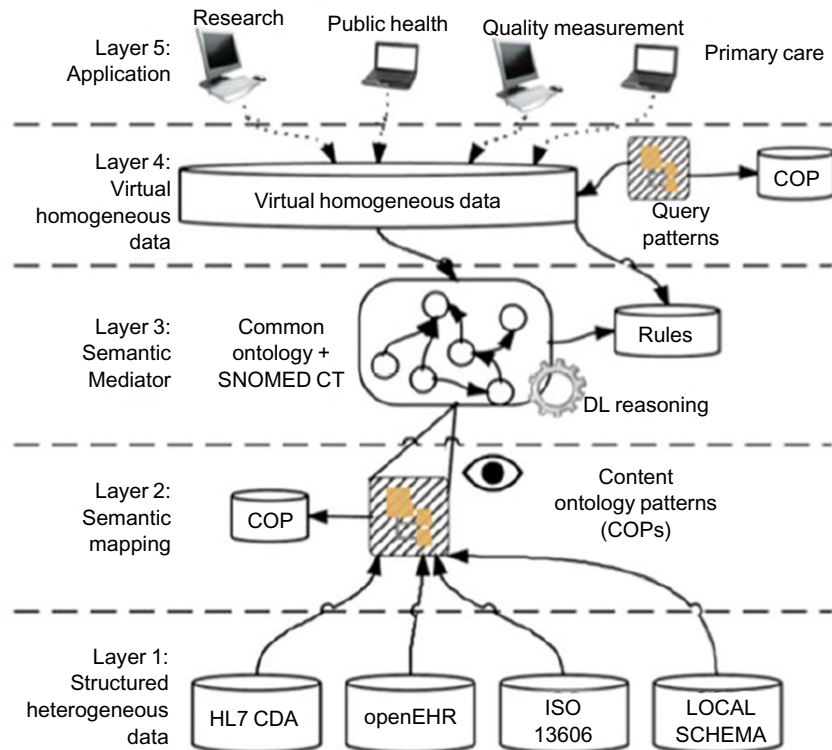
**FIG. 7**

A brief description of ontology and its modeling primitives.

The medical domain with its complexity is one of the most active domains that uses ontologies for its many advantages such as:

1. The main focus of ontology is to give a clear definition and comprehension of the knowledge domain and its relations.
2. Ontology is concerned with its reusability and the ability of automated reasoning. Ontologies aren't just used to present the human's information, but also process and reason its contents.
3. Ontology is machine-readable, which means that ontology allows the machine interpretability by providing additional vocabulary along with formal semantics.
4. An ontology defines a medical terminology with a nonconfusing and clear meaning that facilitates the exchange of information between different standards or systems [50].

As a result, it plays an important role in achieving SI. Ontology is based on open world assumption, where not existing information means not known. This is different from other modeling schemas such as databases, where not existing information means false information. In addition, ontology's formal representations are based on one of the families of formal description logics such as $\mathcal{SHOIN}(\mathcal{D})$, $\mathcal{SROIQ}(\mathcal{D})$, \mathcal{ALC} , etc. The OWL 2 language relies upon the description logic of SROIQ (D). In addition, ontologies are based on reasoner tools for checking ontology consistency and inferring hidden knowledge. Ontology has a big relation with clinical terminologies, and there are many publicly available standard biomedical ontologies on repositories such as BioPortal [51].

**FIG. 8**

The required SI level [33].

Based on the SemanticHealthNet report [33] as shown in Fig. 8, ontology can be used to achieve SI between heterogeneous healthcare systems. It has the ability to provide a homogeneous view of all different heterogeneous representations of input data resources.

Ontology mapping plays an important role in fulfilling SI between many different terminology structures, standards, and information models [52]. Ehrig et al. [47] defined the mapping between ontologies as follows “To map one ontology O1 onto another O2 implies that for every substance (class C, connection R, or occurrence I) in O1, we endeavor to find a comparing component that has the similar expected significance in O2.” Many types of research proposals seek to map between many different standards toward achieving complete SE. From these trials, Magni et al. [53] proposed a structure for the ortho-EPR. That structure includes integration of HL7 V3 and DICOM for sending and storing the orthodontic patient records via different software programs. That process had three main steps: planning, developing, and integration. Bicer et al. [54] developed an OWL mapping tool called OWLmt to underpin the semantic interoperability between many different standards such as HL7 CDA, CEN 13606, and openEHR.

Fuzzy ontology has many capabilities over traditional ontology. In the following, we will study some of the fuzzy ontology capabilities that make it able to solve the semantic interoperability in the EHR environment [55].

1. Fuzzy ontology can be used in solving many real-world applications and complex problems.
2. Fuzzy ontology resembles human reasoning in its use of vague information, which can generate decisions correctly through its predicates.
3. Fuzzy ontology can deal with both numeric and unstructured data to facilitate the expression of rules and facts.
4. Fuzzy ontology can interact with the different interfaces used by various applications.
5. Fuzzy ontology permits reasoning and modeling incomplete, ill-defined, vague, and uncertain knowledge [56].

3.4 TERMINOLOGIES

The medical terminology is characterized as “institutionalized concepts and their equivalent words that record understanding discoveries, conditions, occasions, and mediations with adequate detail to help clinical care, choice help, results in search, and change of the quality; and could be effectively converted into more extensive characterizations for administrative, authoritative, supervision and monetary necessities” [57]. There are many clinical terminologies such as ICD [58], UML [59, 60], LOINC [61], RxNorm [62], SNOMED CT [2] as shown in Fig. 9, and CPT [63]. A terminology is composed of a collection of words that give a controlled vocabulary and structured medically pertinent expressions, which can be utilized amid information passage. That empowers giving a more exact and sharable articulation when using free text. Table 1 shows some differences among ontology and terminology.

The UMLS tool is considered a storehouse of various biomedical words, as shown in Fig. 10.

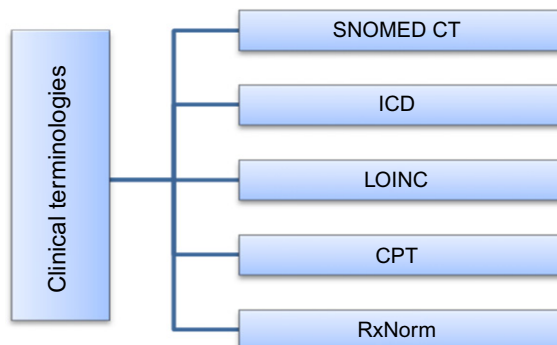
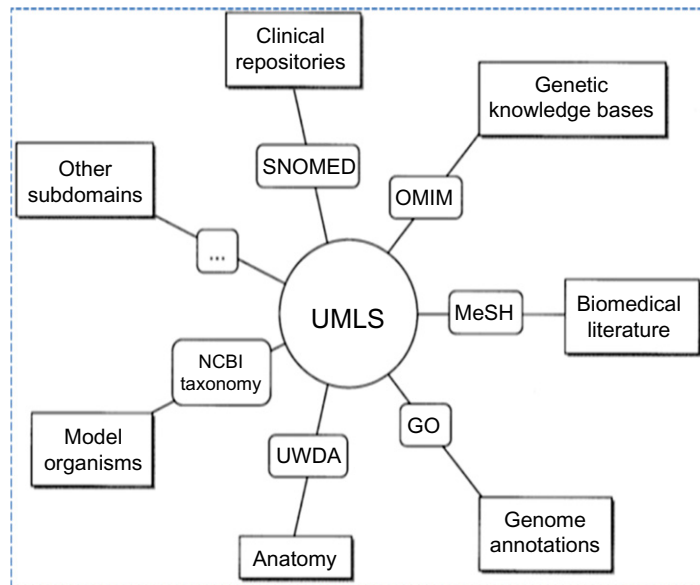


FIG. 9

The most familiar terminologies.

Table 1 The Difference Between Ontology and Terminology

Ontology	Terminology
<p><i>It is a specific theory about the idea of being or the sorts of existence [48]</i></p> <ul style="list-style-type: none"> • Communication among machines • Interpretation by machines • Enables machine inference to be able to add more knowledge to its database [65] 	<p>It is defined as the concepts or checking of terms and their usage. Terms may be words, composition words, or multiword verbalizations that in specific settings give inclusion and meaning. Terminology contrasts from what is called lexicography, as it includes the investigation of ideas, imaginary frameworks, and their names (terms) while lexicography ponders words and their implications [64]</p> <ul style="list-style-type: none"> • Communication between humans • Communication between human and machine • Concerned with the functions and the nature of language that enables the efficient transmission and representation of items exchanged between different systems [65]

**FIG. 10**

The different subdomains coordinated in the UMLS [66].

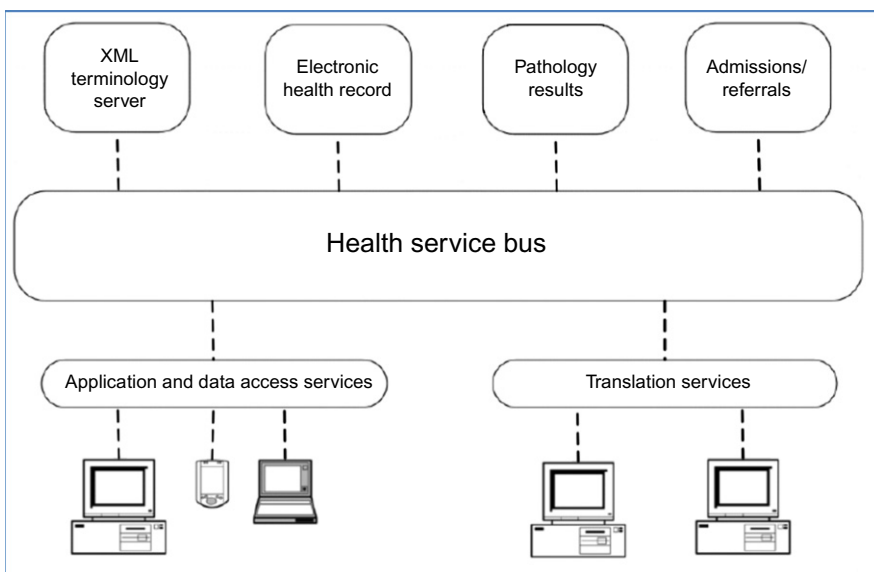


FIG. 11

The health service bus (HSB) architecture [67].

3.5 SEMANTIC INTEROPERABILITY FRAMEWORKS

This section describes and focuses on some frameworks that have been used to support semantic interoperability in a healthcare environment. For example, Shabo and Hughes [17] have focused on the semantic interoperability to comprehend the semantics of family history that is urgent for breast cancer patients. The proposed framework was able to automatically generate the XML schema from the different family history models. They utilized the HL7 methodology. They used services that transformed one arrangement to the next through the HL7 accepted representations. They added patient-particular BRCA groupings to outline the advantages of typifying crude genomic information with regards to BRCA risk evaluation.

Ryan and Eklund [67] presented an HSB framework that relied on the ESB, as shown below in Fig. 11. This framework was constructed based on the architecture of service-oriented, distributed, and scalable systems. ESB is an independent programming language and operating system that provides interoperability between the different input platforms [68]. It serves as a correspondence media among the medical heterogeneous resources and services. This framework was converted into the healthcare area utilizing an informing standard that bolsters the beliefs of the HL7 V3 Semantic Web united with the terminology of SNOMED CT.

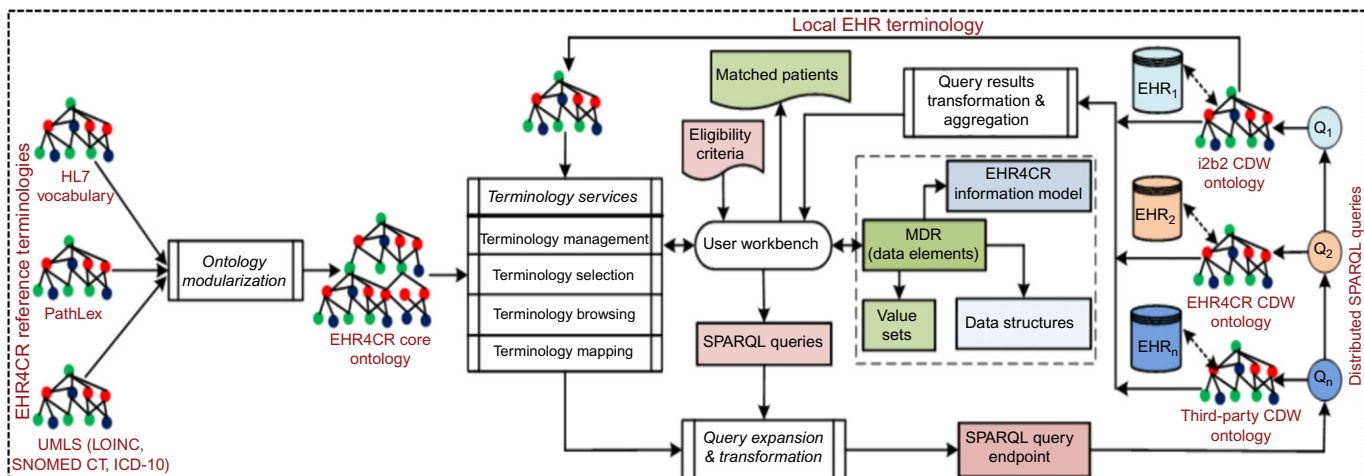
Hussain et al. [69] proposed an initial architecture of EHR for clinical research (EHR4CR) semantic interoperability framework utilizing semantic web advances.

The main aims of that project were to minimize the cost of conducting clinical trials and enhance the efficiency via better use of routinely gathered clinical information in the trial outline and life cycle of execution. The authors utilized the approach of model-driven engineering to deal with the semantic sources and built an HL7-based EHR4CR information model. The architecture's key elements are shown in Fig. 12.

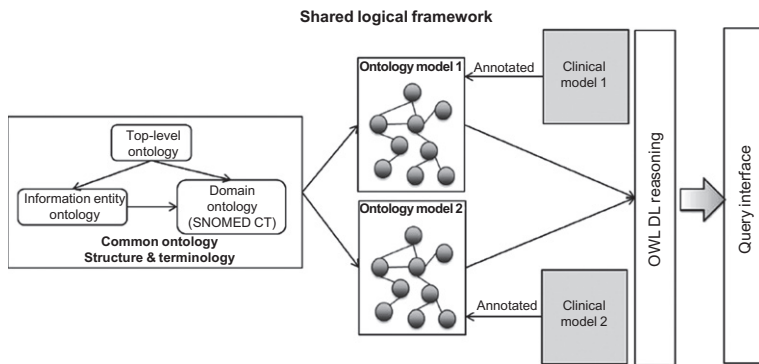
Costa et al. [70] proposed a semantic infrastructure with a main objective of managing heterogeneous portrayals of the same medical information data to permit their propelled exploitation by utilizing depiction logic thinking and reasoning. The proposed infrastructure consisted of an OWL DL ontological framework (*acts as an intermediate between heterogeneous portrayals*) and an arrangement of ontology content patterns (that permits *representing* the clinical data). According to Gangemi [71], there are two main characteristics of ontology content patterns. First, the ability to be sorted in orders of "hierarchies," which follows the concept of object-oriented design. Second, the arrangement allows covering bigger modeling use cases. In addition, the 7th European Programme Framework (SemanticHealthNet) [33] took into its consideration the different of input EHRs resources from several standards and proprietary implementations. It developed an ontology-based layered architecture consisting of five layers, as shown in Figs. 8 and 13. The first layer contained different inputs from HL7 CDA, openEHR, ISO 13606, and local schema. The second layer was semantic mapping containing content ontology patterns (COPs). The third layer contained a semantic mediator such as SNOMED CT. The fourth layer contained virtual homogenous data. The final layer represented the application interface. It highlighted three types of semantic concepts, as shown in Fig. 14: information models (e.g., EN ISO 13606, openEHR, etc.), ontology-based terminologies (e.g., SNOMED CT), and clinical practice guidelines.

Isela Macía [73] proposed an architecture that relied on the client-server style. It combined OpenEHR with interoperability standards (OpenEHR, IHE, and HL7), which helps to increase the consistency of the clinical documents. As shown in Fig. 15, the framework architecture is composed of five main layers, which are as follows:

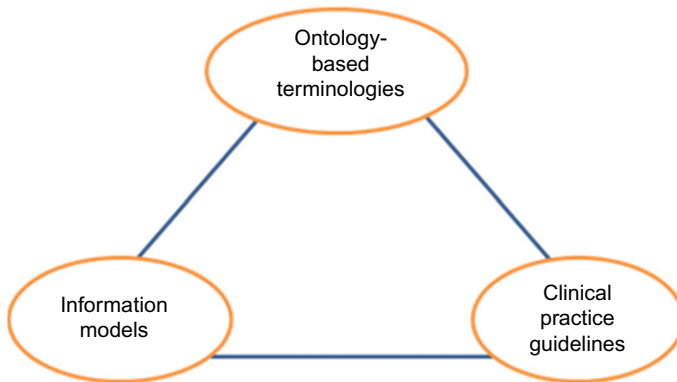
1. The first layer (*Application Layer*), which consists of health information systems that share and feed patient information.
2. The second layer (*Integration Layer*), which is comprised of the PIX Services, PDQ Services, and XDS Services components.
3. The third layer (*Cross-Reference Layer*), which is involved in the Master Patient Index (MPI) component that ensures patients have a unique identifier.
4. The fourth layer (*Validation Layer*), which is involved in the *Document Validation* component that ensures that clinical documents are corrected syntactically and semantically.
5. The fifth layer (*Persistence Layer*), which involved components that store and recover health information.

**FIG. 12**

The EHR4CR semantic interoperability framework [69].

**FIG. 13**

The logical SemanticHealthNet proposed framework [72].

**FIG. 14**

The main three artifacts in SemanticHealthNet (SHN).

3.6 PRIVACY AND SECURITY IN EHR SYSTEMS

The data stored in EHR is a personal, particular, and secure data in nature. Richard Rognehaugh defined EHR privacy as “the privilege of people to shield data about themselves from being uncovered to others; the claim of people to be let alone, from observation or obstruction from different people, associations, or the legislature” [74]. The shared data because of a clinical relationship is considered *confidential* and must be secured [75].

From our point of view, security is a very important issue in any developed system. However, the security is out of our scope. For EHR security, the EHR should support authentication, data integrity, confidentiality, and an audit of accessed information. It should restrict access to a group of users in part or whole of the EHR,

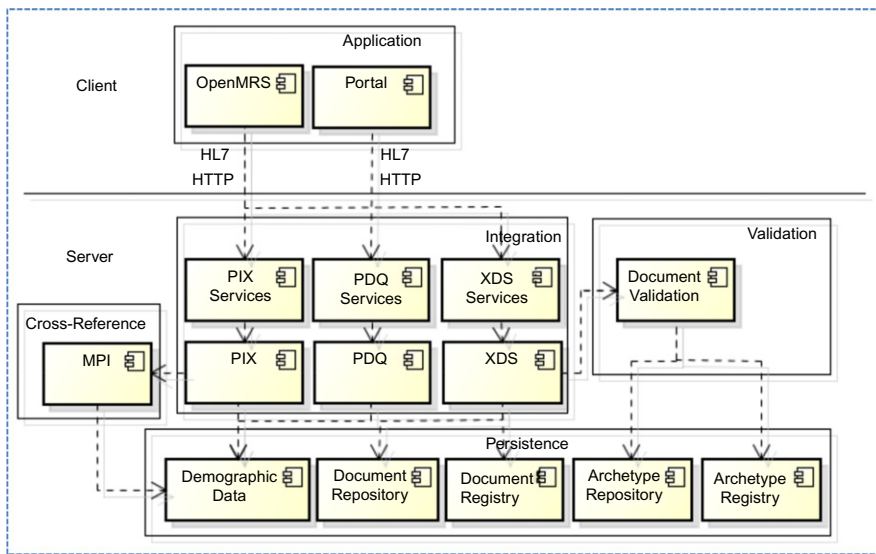


FIG. 15

The proposed architecture components diagram [73].

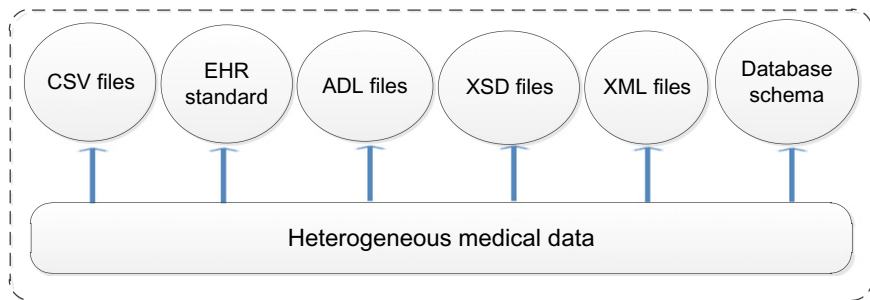
defining the level of what actions (read, write, update, verify, transmit) could be allowed. Data integrity is to be ensured at the time of storage and transfer of a part or whole of the EHR. Audit control mechanisms should keep track of who, when, and what type of access was made to EHR data [76].

According to Kluge [77], the EHR's security framework ought to contain protocols to ensure the assent privileges of the subjects of EHRs under typical conditions. Its architecture must likewise contain implies for reassigning the assent privileges of the subjects of EHRs.

4 METHODOLOGY

As we mentioned in [Section 1.2.2](#), the medical health data may contain data from many heterogeneous systems and documents (see [Fig. 16](#)). The input data differs semantically and syntactically. That data may be stored in different formats, different databases, different storage devices, and various data types. The vocabularies' differences and synonyms (distinctive illustrations and representations of similar information) between those sources lead to differences in semantics. The main research objective concerns how to solve that problem without any loss of input data and minimum human mediation.

In this chapter, a unified semantic interoperability framework for distributed EHR based on fuzzy ontology would be recommended. That framework has a multilayer structure with multiple modules at every layer to properly and accurately

**FIG. 16**

The difference between heterogeneous medical data resources.

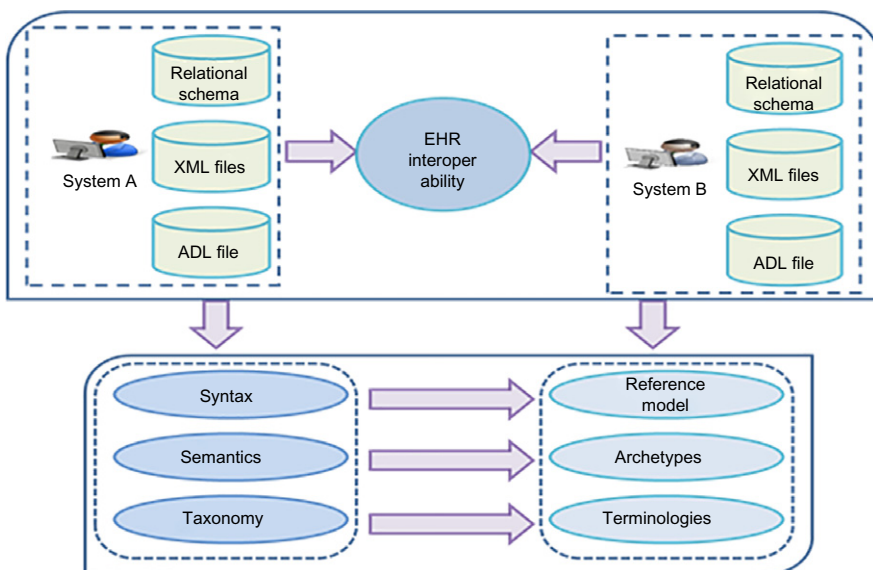
preserve the medical data semantics between heterogeneous systems. The proposed framework models EHR syntax based on a unified reference model such as openEHR or HL7 RIM; a data model based on archetypes, meaning relied upon standard terminologies such as UMLS or SNOMED CT; and fuzzy semantics based on fuzzy ontology. The research aims to establish a single unified view and efficient data model for handling the issues of data interoperability and integration between heterogeneous systems. Crisp ontology solves that problem to some extent. We expect, by extending crisp ontology to fuzzy ontology, that the proposed framework will provide a more realistic, applicable, accurate, medically acceptable, reliable, and global EHR interoperable environment. In the upcoming section, the proposed framework will be described in more detail.

4.1 THE PROPOSED FRAMEWORK

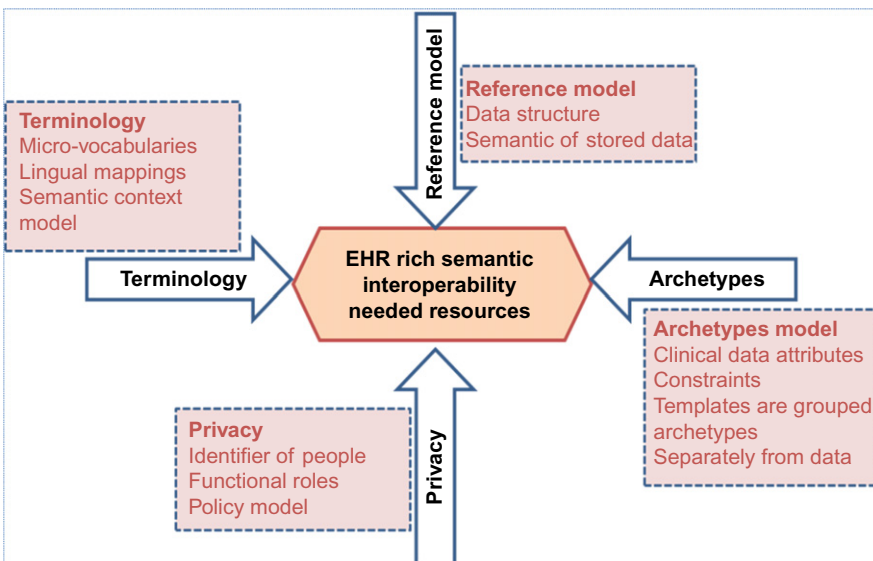
In the age of mobile Healthcare, distributed EHR systems with many components, as shown in Fig. 17. For wireless body area networks with IoT-based sensors, semantic heterogeneity is the most difficult issue of medical information unification. It requires comprehension of the connections between the information and this present reality objects. Achieving SI is relied basically on achieving syntactic interoperability firstly.

As shown in Fig. 18, the modeling of EHR data according to a syntax model is relied upon for unifying the reference model; according to the data, the model depends upon archetypes, and according to meaning, it depends on terminologies. Fig. 12 describes the differences between these technologies.

To accomplish the study goals, we have utilized some existing technologies, and our framework relied on ontology concepts. The main factor behind using ontology is that ontology allows independence for each input source so that integration will be a simple process [78]. Studer et al. [79] characterized ontology as “a clear particular expression of a common formulation.” Ontology guarantees maintenance of importance and exactness of the exchanged data because it formally characterizes the terms and their connections to expel any heterogeneity and take into account SI between

**FIG. 17**

EHR modeling matching.

**FIG. 18**

The needed support SI resources.

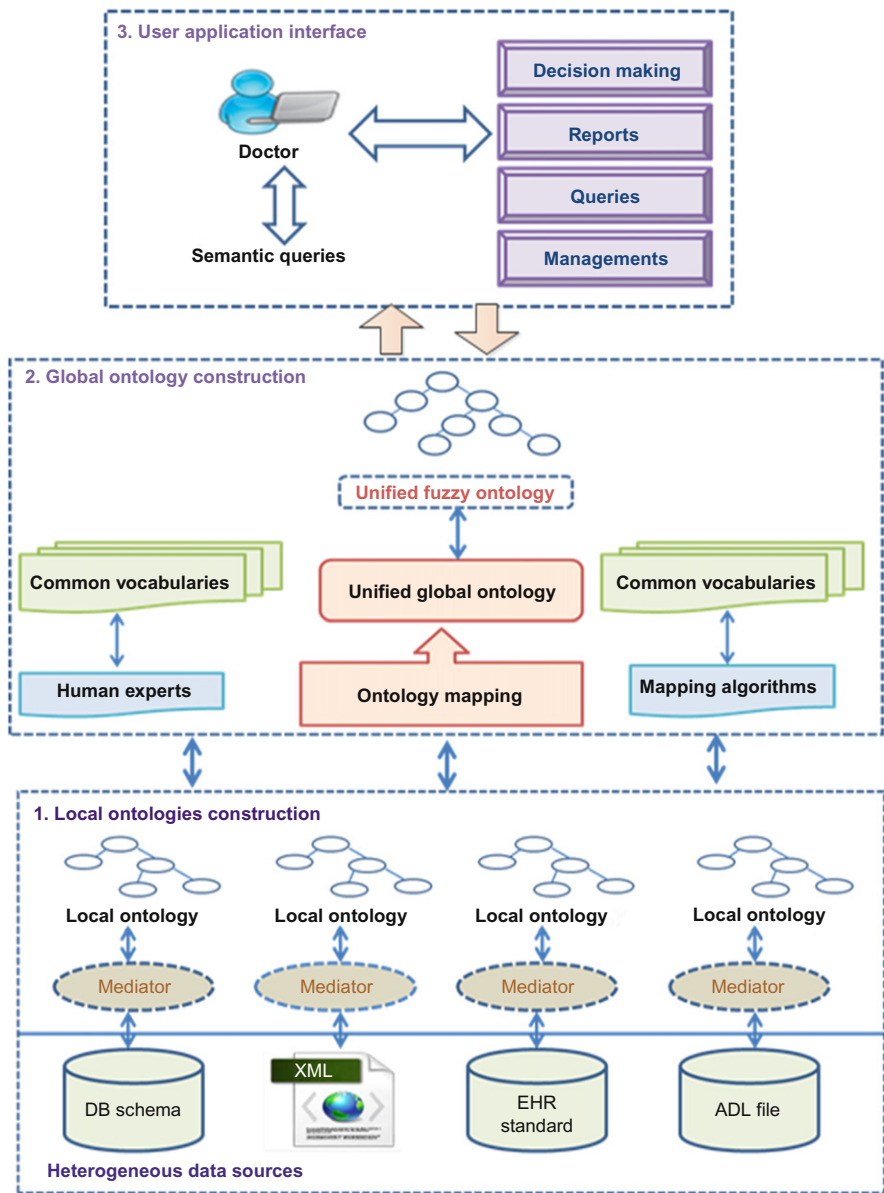


FIG. 19

The proposed fuzzy ontology SI framework.

various frameworks [80]. Ontologies allow domain knowledge reference, extensible hierarchy structure, reusability, and semantic reasoning [81]. Fig. 19 is the proposed framework architecture.

```

PROCEDURE: INTEGRATION and INTEROPERABLE UNIFIED DATA MODEL
INPUT: Structured heterogeneous data sources
OUTPUT: Unified fuzzy ontology data model
BEGIN
    Read input data source i, i= 1, 2... n, n is the number of data sources
    FOR (each input system i)
        IF the data source is a relational database
            Then use one of the databases-to-ontology tools to convert it into an ontology format
        ELSEIF data source is an XML file
            Then use one of the XML-to-ontology tools to convert it into an ontology format
        Else use one of the ADL-to-ontology tools to convert into an ontology format
        End if
    END FOR
    Use ontology mapping to create a global crisp ontology
    Construct a global fuzzy ontology
END

```

FIG. 20

The pseudocode of the proposed framework.

The proposed framework's global architecture consists of three main layers. The first lowest level layer (local ontologies construction layer) stores the EHR health-care information. The sources of this information are structurally heterogeneous. They can be a local database (e.g., MySQL, SQLServer, DB2, Access, and Oracle) with different schemas, EHR standards-based databases, XML files, spreadsheet files, or ADL files. These different inputs are transformed into ontologies using mediators (e.g., DB2OWL, ADL2OntoModule, or DB2OntoModule) suitable for each type. In the middle layer (global ontology construction), the local ontologies are mapped (using mapping algorithms and human experts based on common terminology vocabularies) to a global ontology. The resulting ontology is crisp, and it is capable of answering the physicians' semantic queries over structurally and semantically heterogeneous sources.

However, the impression of vagueness is the nature of medical data and domain expert queries. To handle these challenges, the resulting crisp ontology must be extended to handle the fuzzy semantics. We convert the crisp ontology to a unified fuzzy ontology. Finally, the higher layer is the user interface. When physicians or other specialists need to answer queries or want to make critical decisions, they will deal with the global reference fuzzy ontology. The framework pseudocode is analyzed in Fig. 20.

In the local ontologies construction layer, there are many heterogeneous data sources such as databases, standards, ADL files, or any other source. This step aims to build ontological components (concepts, properties, axioms, and individuals) from the different entry components. Ontology is differentiated from a database or any other source because of its utilization of more superior language and description logic to express the information itself in natural expressions [3].

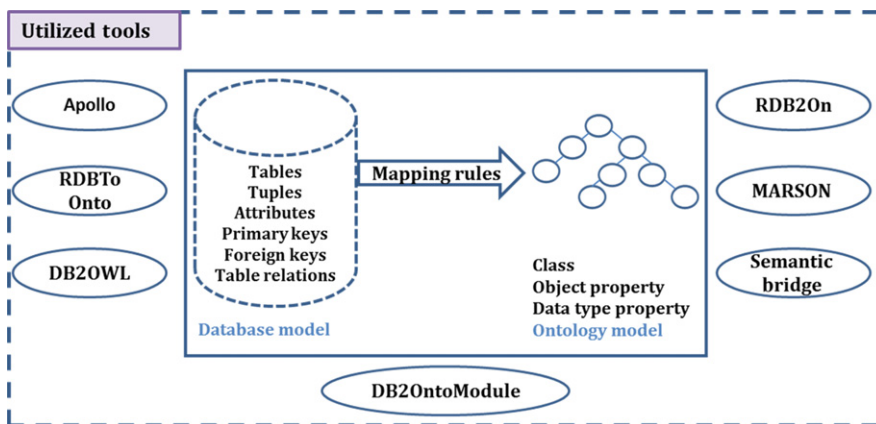


FIG. 21

The process of ontology construction from database sources.

The database provides the most efficient storage and retrieval data techniques that are secure and scalable with easy backup. However, it suffers from poor semantics. *For the process of changing over a relational database into ontology, it takes after certain mapping rules [82].* Those rules define how relational database components including tables, rows, columns, constraints, foreign keys, etc., can be changed over into ontology segments, for example, properties, classes, instances, and axioms. Many algorithms and software tools can convert a relational database into an ontology automatically. From those tools—Apollo [83], RDBToOnto [84], DB2OWL [78], R2O [85], OntoStudio [86], D2RQ [87], DB2OntoModule [25], DartGrid Semantic [88], Automapper [89], MARSON [90], and Ontology Generator (RDB2On) [91]—are some examples, as depicted in Fig. 21.

It is noted that there are some semantic similarities among relational models and ontologies. The previous tools depend on these similarities to achieve mapping. Table 2 shows some correspondence between them.

According to [92], the conversion of databases into the ontology format can be performed as in the following pseudocode (see Fig. 22). *For the process of converting an XML file into ontology, we want to explain some basic concepts.* XML (eXtensible Markup Language) is the most famous and powerful semistructured data source. It has a wide acceptance for storing and exchanging data between standards for many advantages [93]. These advantages are (1) its simplicity and flexibility of use, (2) it is readable by humans and is easy to understand, and (3) its compatibility with many OOP languages such as C++ and Java. But it neither supports semantics nor reasoning [94]. Ontology can support both semantics and reasoning of domain knowledge in an effective and powerful way. Therefore the solution of that problem is to translate XML into OWL or RDF.

Table 2 The Corresponding Between Relational Data and Ontology Concepts

Relational DB Item	Ontology Corresponding Item
Table	Concept
Tuple—Row	Instance
Field	Property
Constraint	Axioms
Inheritance relation	Object property

```

PROCEDURE: CONVRTING RELATIONAL DATABASE INTO OBTLOGIES
INPUT: input database source DB (tables, tuples, attributes)
OUTPUT: ontology format (Classes, Instances, Properties)
BEGIN
FOR (each tbl in DB)
  Map Table into Class
  FOR (each tup in tbl)
    Map tup to Instance
    FOR (each col in tup)
      Map column into instance property
      Map of non-referential integrity columns into data-type properties
      Map column constraints into property cardinalities
      Map referential Integrity relationships to Inheritance Hierarchy
      Map relationships represented by referential integrity columns into Object Properties
    END FOR
  END FOR
END FOR
END

```

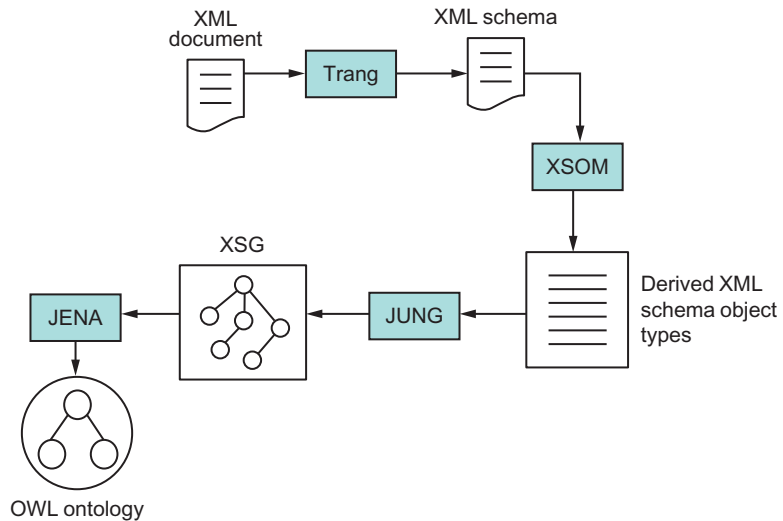
FIG. 22

A sample mapping of relational DB model to ontology.

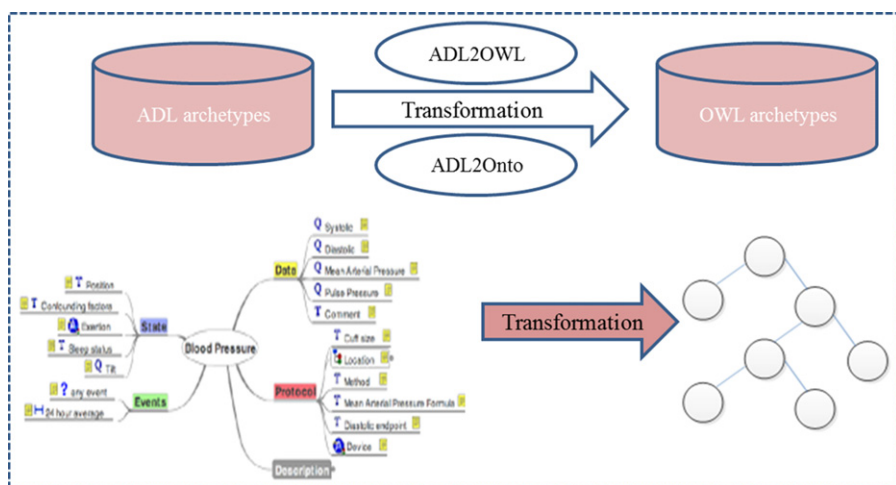
There are many strategies and tools related to the conversion of XML into OWL or RDF, such as XTR-RTO [95] and X2OWL [96]. For example, Bohring and Auer [97] have presented an efficient tool called xml2owl for generating an OWL ontology structure from existing XML schema through developing extensible style sheet language transformation (XSLT) instances. Nora et al. [94] presented a programmed strategy for generating OWL ontology from XML documents, as shown in Fig. 23.

According to that last mentioned method, the creation of the OWL ontology process from XML documents depends on XML schema. That process could be performed as follows: the XML archive is converted into XML-Schema utilizing the Trang API for java; at that point, XML-Schema is investigated utilizing XSOM; after that, the XSOM yield is utilized as a contribution to the JUNG to generate XSG, and then the output was used as input to produce OWL substances.

The translations between standards and any other sources and ontology would be performed using transformation modules, such as the ADL2Onto module [25] shown in Fig. 24. Based on the approach presented in [98], Costa et al. proposed an approach

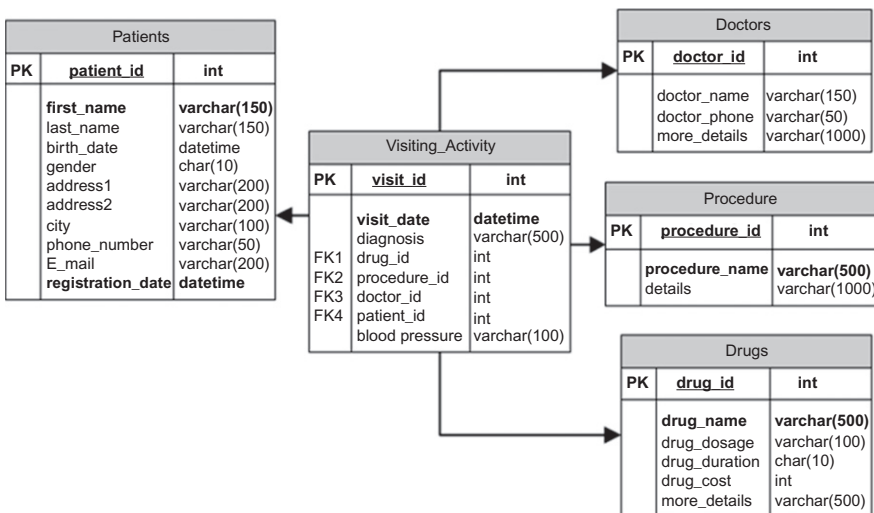
**FIG. 23**

The process of converting XML documents into OWL ontology [94].

**FIG. 24**

The transformation process of ADL archetypes into OWL ontologies.

to generate OWL archetypes from ADL ones in the standards that relied upon the dual model (which distinguishes between the archetype model and reference model). That approach transformed the archetypes of OpenEHR to ISO/EN 13606 and vice versa through combining model-driven engineering and semantic web technologies.

**FIG. 25**

A simple Microsoft SQL Server schema of a patient database.

```
<? Xml version="1.0" encoding="UTF-8"?>
<Patient data card1>
<first-name> Smith </first-name>
<last-name> Bill </last-name>
<Gender> M </Gender>
<address> 23 elsalam street. </address>
<Birthdate> 18/4/1976 </birthdate>
<Report_date> June, 27 2010 </Report_date>
<Blood group> A+ </Blood group>
<Blood Pressure> 150/80 </Blood Pressure>
<Passport> t123456 </Passport>
<E-mail> eng.drf@g.com </E-mail>
<diagnosis> acute Q wave infarction - anteroseptal </diagnosis>
</ Patient data>
```

FIG. 26

A small part of an XML patient document.

4.2 A PROTOTYPE PROBLEM EXAMPLE

To illustrate the medical benefits of the proposed framework and its technical applicability, let us consider a small real prototype situation in which a patient has data distributed in many different locations, and the data have many different formats. A specialist needs to ask a query regarding all these semantically and syntactically distributed different data. Fig. 25 shows a prototype example of Microsoft SQL Server patient local database schema. Fig. 26 shows another source of patient data

```

MSH|^~\&|^123457^LabS||200808141530||ORU^R01|123456789|P|2.4
PID||0001^^^SMH^P|| Smith ^ Bill ||19620114|
M||14 Disney Rd^Disneyland^^MM1 9DL
PV1||SN|||G123456^DR RICHARD
OBR||5432|666777^CULTURE^LN||20080802|||||SW^^FOOT^RT|C987654
OBX||CE|0^ORG|01|STAU|||||F
OBX |1 |NM |271649006 ^Systolic blood pressure ^SNOMED-CT ||132 |mm[Hg]|90-120 |H || |F || |20100511220525
OBX |2 |NM |271650006 ^Diastolic blood pressure ^SNOMED-CT ||86 |mm[Hg]|60-80 |H || |F || |20100511220525

```

FIG. 27

A small part of a HL7 V2.5 patient's blood pressure.

```

<-- OBSERVATION - blood pressure measurement
archetype_node_id = <[openEHR-EHR-OBSERVATION.blood_pressure]>
name = <value = <"BP measurement">>
data = <
  archetype_node_id = <[at0001]>
  origin = <2016-10-03T08:20:00>
  events = <
    [1] = <archetype_node_id = <[at0006]>
      name = <value = <"standing">>
      time = <2016-10-03T08:20:00>
      data = <
        archetype_node_id = <[at0003]>
        items = <
          [1] = <
            name = <value = <"systolic">>
            archetype_node_id = <[at0004]>
            value = <magnitude = <115.0> ...>
          >
          [2] = <
            name = <value = <"diastolic">>
            archetype_node_id = <[at0005]>
            value = <magnitude = <76.0> ...>
          >
        >
      >
    >
  >
>
```

FIG. 28

A small part of an openEHR patient's blood pressure example.

containing an XML file. HL7 V2.5 populated another source of patient data as depicted in Fig. 27. A small part of the openEHR patient's blood pressure example is shown in Fig. 28. Fig. 29 shows an ADL blood pressure example. Fig. 30 shows a small part of an HL7 CDA patient's blood pressure document (Tables 3 and 4).

In Fig. 31, we see a brief description of the blood pressure concept. Table 5 shows the different classifications of the blood pressure.

Fig. 32 shows the Blood Pressure Category SQL statements by CASE-WHEN.

```

=====
OBSERVATION[at1000.1] matches {-- complete blood picture
  name matches {
    CODED_TEXT matches {
      code matches {[ac0001]} -- complete blood count)}
  data matches {
    LIST_S[at1001] matches {-- battery
      items cardinality matches {0..*} \epsilon {
        ELEMENT[at1002.1] matches {-- haemoglobin
          name matches {
            CODED_TEXT matches {
              code matches {[ac0003]} -- haemoglobin}}
          value matches {
            QUANTITY matches {
              value matches {0..1000}
              units matches {"g/l|g/dl|.+^}}}
        ELEMENT[at1002.2] occurrences matches {0..1} matches
        {-- haematocrit
          name matches {
            CODED_TEXT matches {
              code matches {[ac0004]}-- haematocrit}}
          value matches {
            QUANTITY matches {
              value matches {0..100}
              units matches {"%"}})}
      ELEMENT[at1002.3] occurrences matches {0..1} matches
      {-- platelet count
        name matches {
          CODED_TEXT matches {
            code matches {[ac0005]} -- platelet count}}
        value matches {
          QUANTITY matches {
            value matches {0..100000}
            units matches {"/cm^3"}}
        }}}}}}}}
=====
```

FIG. 29

The complete blood count archetype ADL definition [99].

Consider, for example, the given queries in Fig. 33 when a physician needs to know some information about the history of a patient's blood pressure for a specific period.

The heterogeneous and distributed data resources have different representations from the same data, which may lead to incorrect results. Those systems don't seem to have a unified structure. It is noticed that different systems are not able to communicate with each other as they used different modules with different specifications. Also, physicians can send fuzzy questions to EHR systems and need answers from these distributed systems.

```

| <entry>
|   <Observation>
|     <code code="251076008" codeSystem="2.16.840.1.113883.6.96" codeSystemName="SNOMED CT" display
|       Name="Cuff blood pressure"/>
|     <effective Time value="200004071430"/>
|     <target Site Code code="368208006" codeSystem="2.16.840.1.113883.6.96" code System
|       Name="SNOMED CT" display Name="Left arm"/>
|     <entry Relationship type Code="COMP">
|       <Observation>
|         <code code="271649006" codeSystem="2.16.840.1.113883.6.96" codeSystemName="SNOMED CT" display
|           Name="Systolic BP"/>
|         <effective Time value="200004071530"/>
|         <value xsi:type="PQ" value="132" unit="mm[Hg]"/>
|       </Observation>
|     </entry Relationship>
|     <entry Relationship type Code="COMP">
|       <Observation>
|         <code code="271650006" codeSystem="2.16.840.1.113883.6.96" codeSystemName="SNOMED CT" display
|           Name="Diastolic BP"/>
|         <effective Time value="200004071530"/>
|         <value xsi:type="PQ" value="86" unit="mm[Hg]"/>
|       </Observation>
|     </entry Relationship>
|   </Observation>
| </entry>
| 
```

FIG. 30

Small part of an HL7 CDA document blood pressure example [100].

In this chapter, a unified semantic interoperability framework for distributed EHR based on fuzzy ontology would be suggested. This framework translates each input data source into the local ontology. Then, all local ontologies are grouped into a global one using ontology mapping techniques. After that, the global crisp ontology is translated into global fuzzy ontology. That global ontology preserves the medical data semantics between all heterogeneous systems. If physicians need any semantic query, they deal with fuzzy ontology, as shown in Fig. 34. According to Table 4 and Fig. 26, if the physician poses the following query “find the patient that has the heart attack disease”? This is because heart attack = myocardial infarction and “acute Q wave infarction—anteroseptal” is a subclass of myocardial infarction. The proposed system with support of UMLS tools can query that semantic statement easily. In our next study, we will implement this framework. We expect that it will have a great impact in improving the (fuzzy) semantic interoperability between EHR subsystem components.

The proposed system provides the physicians the ability to do all the following tasks:

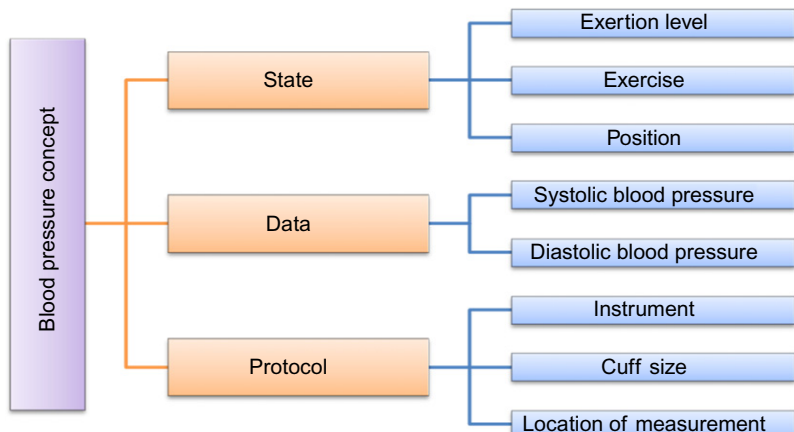
1. They can ask uncertain and imprecise queries by using the fuzzy ontology semantic inference mechanism according to fuzzy ontology reasoners such as FuzzyDL [101].

Table 3 A Sample of Patients

Patient_id	First_name	Last_name	Birth_date	Gender	Address1	Address2	City	Phone_number	E_mail	Registration_date
0001	Smith	Bill	April 18, 1976	M	23 elsalam street	–	Cairo	010888888	dfr@rdf. com	23-4-2010
0002	Cindy	Frog	March 12, 1974	F	g.tahrir street	–	Cairo	020345666	cindy@rdf. com	20-1-2011

Table 4 A Sample of Visiting_Activity

Visit_id	Patient_id	Visit_date	Blood_pressure	Diagnosis	Drug_id	Procedure_id	Doctor_id
1	0001	May 17, 2010	160/100	Myocardial infarct	0001	0001	0001
2	0002	Feb 23, 2011	120/90	Diabetes mellitus	-	0023	0054

**FIG. 31**

A brief description of the blood pressure concept.

Table 5 The Major Classification of Blood Pressure

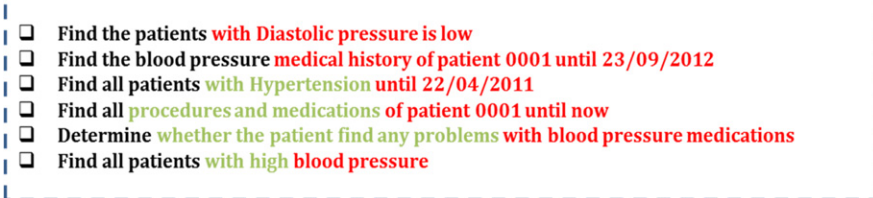
Blood Pressure Category	Systolic Pressure	Diastolic Pressure
Normal	120	80 mmHg
Prehypertension	120–139	80–89
Stage 1 hypertension	140–159	90–99 mmHg
Stage 2 hypertension	160 or greater	100 or greater

```

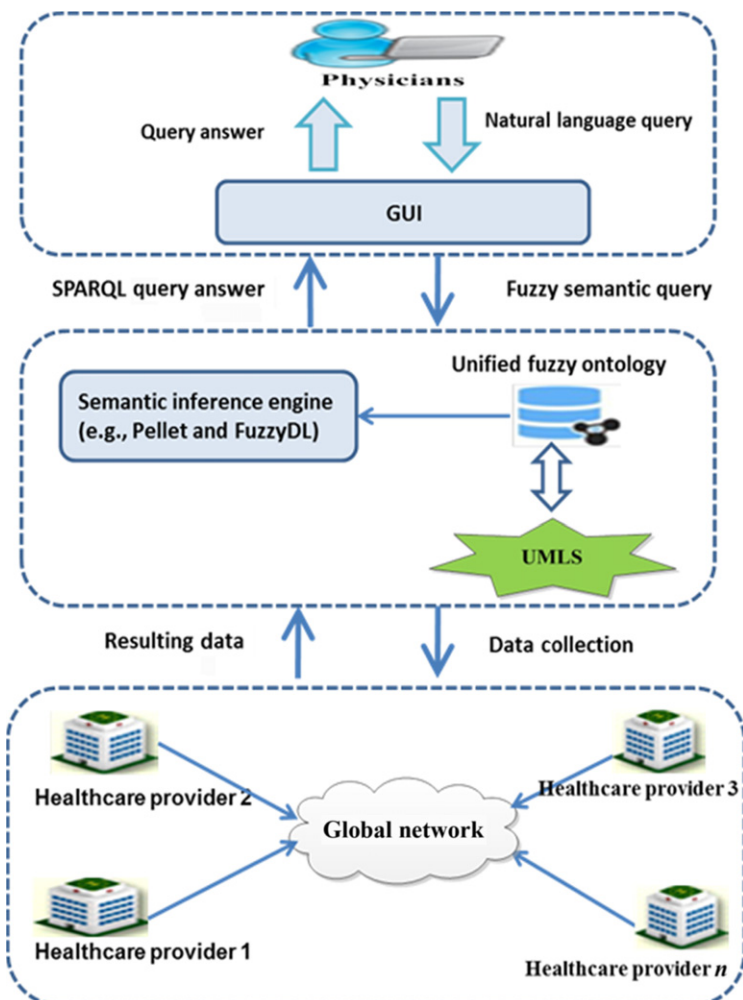
CASE
WHEN BP_Systolic < '120' AND BP_Diastolic < '80' THEN 'Normal'
WHEN BP_Systolic BETWEEN '120' AND '139' OR BP_Diastolic BETWEEN '80' AND '89' THEN      'Prehypertension'
WHEN BP_Systolic BETWEEN '140' AND '159' OR BP_Diastolic BETWEEN '90' AND '99' THEN 'Stage 1 Hypertension'
WHEN BP_Systolic >= '160' OR BP_Diastolic >= '100' THEN 'Stage 2 Hypertension'
END AS BP_Category
  
```

FIG. 32

Blood Pressure Category SQL statements.

**FIG. 33**

Samples of physician's queries.

**FIG. 34**

The physician's query architecture.

Table 6 A Comparison Study of the Proposed Framework and Other Previous Ones

Frameworks/ Criteria	Isela Macía [73]	Gaynor et a. [21]	Gonzalez et al. [23]	Proposed Framework
Manipulating different standards	Yes	Yes	Yes	Yes
Manipulating custom database	No	No	Yes	Yes
Handling vague and imprecise problems	No	No	No	Yes
Framework main idea	The proposed architecture relied on the client-server style	Interoperability matrix and a related interoperability flow graph were defined. That representation enabled a multidimensional, visual view of the main attributes of interoperability	Ontology-based approach regardless of EHR used standard	Fuzzy ontology as shown in Fig. 19
Limitations	There is a need to perform more implementation studies, and the framework wasn't compared with any other existing ones	There is an urgent need to apply that framework practically with measuring validation parameters	The effectiveness of the matching process and the accuracy of the exchanged information weren't determined	The framework is still under development

2. They can aggregate data with heterogeneous structures but that have the same meaning, thanks to the syntax interoperability. The normal case is when data with different structures have different meanings.
3. It can infer the clinical similarity between apparently different semantic medical concepts, thanks to the semantic interoperability.

Protégé and the OWL2 language are a widely used ontology editing platform that offers fantastic scalability and extensibility. Its extensibility is due to plug-ins developed by semantic web experts [102]. It can build local ontology representations with

the help of medical experts and existing services tools. Then we use the resulting ontologies to build your OWL 2 ontology for the crisp global ontology, and finally, the resulting crisp ontology will be extended into fuzzy ontology utilizing the Fuzzy OWL2 plug-in in protégé 4.1 [103].

There are numerous fuzzy ontology development methodologies such as UFOC [104], IKARUS-Onto [105], OntoMethodology [106] and UPFON [107]. In addition, many fuzzy ontology representation dialects were suggested in [101]. The reasoners of fuzzy ontology incorporate DeLorean, Fire, and FuzzyDL. Fuzzy reasoners utilize the description logics of fuzzy such as fuzzy SHIN, Fuzzy ALC, Fuzzy SROIQ (D), and fuzzy SHOID (D).

4.3 A COMPARISON STUDY

We have done a comparison between the proposed framework and other previous frameworks. Table 6 summarizes that comparison. The key requirements of the comparison were handling different used standards, a custom database, and handling imprecise and vague data.

5 CONCLUSION

In this chapter, a framework is recommended for a trial to solve the issue of SI in a structured heterogeneous EHR environment. There are many factors that lead to challenges and problems in achieving EHR information system SI. Many organizations use various databases to store their information (e.g., MySQL, SQLServer, DB2, Access, and Oracle) or any other independent file systems. Different clinics and hospitals may use different standards or any other sources of the input data. The framework aims to create an integrated single unified fuzzy ontology model, which can be used for querying, analyzing, or making decisions. The proposed framework tries to construct a local ontology from each heterogeneous input and then creates a global reference fuzzy one in an integration model. In the future, we want to measure the degree of feasibility of our algorithm in achieving the SI in an EHR environment practically in a large EHR system. In addition, we may use one of the modern technologies such as big data beyond fuzzy ontology as a part of our future works.

REFERENCES

- [1] Technical Committee ISO/TC 215, Health informatics, Electronic health record definition, scope, and context. Second Draft, August, (2003).
- [2] T. Benson, Principles of Health Interoperability HL7 and SNOMED, Health Informatics, Springer, London, 2012.
- [3] A. Begoyan, An overview of interoperability standards for electronic health records, Integrated Design and Process Technology, IDPT, 2007.

- [4] S. Bhartiya, D. Mehrotra, Challenges and recommendations to healthcare data exchange in an interoperable environment, *Electron. J. Health Informatics* 8 (2) (2014).
- [5] F.J. Rodríguez-Vera, Y. Marín, A. Sánchez, C. Borrachero, E. Pujol, Illegible handwriting in medical records, *J. Royal Soc. Med. (JRS)* (SAGE Publications) 95 (11) (2002) 545.
- [6] S. Sachdeva, S. Bhalla, Semantic Interoperability in Standardized Electronic Health Record Databases, ACM, New York, 2012. ISSN: 1936-1955, <https://doi.org/10.1145/2166788.2166789>.
- [7] CEN/ISSS. eHealth Standardization Focus Group.“Current and future standardization issues in the eHealth domain: Achieving interoperability.” Tech. rep. 01.03.2005.
- [8] Centers for Medicare and Medicaid Services, <https://www.cms.gov>. (Accessed 23 September 2017).
- [9] IEEE Standard Glossary, *IEEE standard glossary of software engineering terminology*, Tech. rep.IEEE, 1990
- [10] eHealth Governance Initiative. “Discussion paper on semantic and technical interoperability. Proposed by the eHealth Governance Initiative eHGI, 22 October 2012 n.d.
- [11] K.H. Veltman, Syntactic and semantic interoperability: new approaches to knowledge and the semantic web, *New Rev. Inform. Netw.* (Taylor & Francis) 7 (1) (2001) 159–183.
- [12] J. Heflin, J. Hendler, Semantic interoperability on the web, Tech. rep., Maryland Univ College Park Dept of Computer Science(2000).
- [13] The Health Information Technology Policy Committee, Challenges and barriers to interoperability, Tech. Rep., Report to Congress(2015).
- [14] M. Botterman, C. van Oranje-Nassau, J. Rothenberg, Towards a Dutch interoperability framework, RAND Corporation Tech. rep.(2008)
- [15] W. Khan, M. Hussain, K. Latif, M. Afzal, F. Ahmad, S. Lee, Process interoperability in healthcare systems with dynamic semantic web services, *Computing* 95 (9) (2013) 837–862.
- [16] M.R. Santos, M.P. Bax, D. Kalra, Building a logical EHR architecture based on ISO 13606 standard and semantic web technologies, *Stud. Health Technol. Inform.* 160 (Part 1) (2010) 161–165.
- [17] A. Shabo, K. Hughes, Family history information exchange services using HL7 clinical genomics standard specifications, in: *Semantic Web-Based Information Systems: State-of-the-Art Applications*, vol. 1, IGI Global, IBM Research Lab, Haifa, 2007, pp. 44–67 (4).
- [18] G.A. Lewis, E. Morris, S. Simanta, L. Wrage, in: Why standards are not enough to guarantee end-to-end interoperability, *Seventh International Conference on Composition-Based Software Systems (ICCBSS)* 2008, 2008, pp. 164–173.
- [19] P. Groves, B. Kayyali, D. Knott, S.V. Kuiken, The big data revolution in healthcare: accelerating value and innovation, Center for US Health System Reform Business Technology Office, (2016).
- [20] ITU-T Technology Watch Report, E-health standards and interoperability, Tech. Rep (2012).
- [21] M. Gaynor, Y. F., C.H. Andrus, S. Bradner, J. Rawn, A general framework for interoperability with applications to healthcare, *Health Policy Technol.* 3 (1) (2014) 3–12.
- [22] M. Patel, T. Koch, T. Doerr, C. Tsinaraki, Semantic interoperability in digital library systems, UKOLN, University of Bath, 2005.
- [23] C. Gonzalez, B. Blobel, D.M. Lopez, Ontology-based framework for electronic health records interoperability, *Stud. Health Technol. Inform.* (2010) 694–698.

- [24] H. Sun, K. Depraetere, B. De Vloed, G. Mels, and D. Colaert, "Semantic integration and analysis of clinical data," CoRR abs/1210.4405 (2012).
- [25] I. Berges, J. Bermudez, A. Illarramendi, Toward semantic interoperability of electronic health records, *IEEE Trans. Inform. Technol. Biomed.* (IEEE) 16 (3) (2012) 424–431.
- [26] A. Gonzalez-Ferrer, B. Verhees, C. Marcos, Data integration for clinical decision support based on open EHR archetypes and HL7 virtual medical record, in: *Process Support and Knowledge Representation in Health Care*, Springer, 2013. 84–71.
- [27] C. Martinez-Costa, M. Tortosa, J. Breis, An approach for the semantic interoperability of ISO EN 13606 and OpenEHR archetypes, *J. Biomed. Inform.*(Elsevier) (2010) 736–746.
- [28] C. Martinez-Costa, M. Tortosa, J.T. Fernandez-Breis, A semantic web-based framework for the interoperability and exploitation of clinical models and EHR data, *Knowl.-Based Syst.* (Elsevier) (2016) 175–189.
- [29] A. Sinaci, G.B. Laleci Erturkmen, A federated semantic metadata registry framework for enabling interoperability across clinical research and care domains, *J. Biomed. Inform.* (Elsevier) (2013) 784–794.
- [30] C. Batini, M. Lenzerini, S.B. Navathe, A comparative analysis of methodologies for database schema integration, *ACM Comput. Surveys (CSUR)* (ACM) 18 (4) (1986) 323–364.
- [31] A. Sheth, J. Larson, Federated database systems for managing distributed, heterogeneous, and autonomous databases, *ACM Comput. Surveys (CSUR)* (ACM) 22 (3) (1990) 183–236.
- [32] Y. Zhou, Adaptive Distributed Query Processing (VLDB PhD Work), (2003).
- [33] SemanticHealthNet, Semantic interoperability for health network, Tech. rep., July 31, (2015).
- [34] T. Benson, *Principles of Health Interoperability SNOMED CT, HL7 and FHIR*, Springer, Boston, 2017.
- [35] Digital Imaging and Communications in Medicine (DICOM), <http://dicom.nema.org>. (Accessed June 2017).
- [36] Clinical Data Interchange Standards Consortium (CDISC), <https://www.cdisc.org>. (Accessed June 2017).
- [37] E. Siegel, D. Channin, Integrating the healthcare enterprise: A primer: Part radiological Society of North America, *Radiographics* 21 (5) (2001) 1339–1341.
- [38] K. Araki, K. Ohashi, S. Yamazaki, et al., Medical markup language (MML) for XML-based hospital information interchange, *J. Med. Syst.* (Springer) 24 (2000) 195–211.
- [39] Health Level 7, Available from: https://en.wikipedia.org/wiki/Health_Level_7. (Accessed May 2017).
- [40] EN 13606 Association, Available from: <http://www.en13606.org>. (Accessed May 2017).
- [41] OpenEHR, Available from: <http://www.openehr.org>. (Accessed May 2017).
- [42] T. Beale, Archetypes: constraint-based domain models for future-proof information systems, in: OOPSLA 2002 Work. Behav. Semant., No. 21, pp. 1–69, 2001.
- [43] Available from: <http://www.openehr.org/downloads/archetypeeditor/home>. (Accessed May 2017).
- [44] Clinical Knowledge Manager, Available from: <http://www.openehr.org/ckm>. (Accessed May 2017).
- [45] ADLworkbench, Available from: <http://www.openehr.org/downloads/ADLworkbench/home>. (Accessed May 2017).
- [46] WordNet: A Lexical Database for English, ontology.Wordnet 3.0. 2008, Available at <http://wordnetweb.princeton.edu/perl/webwn>, Last accessed May, 2017.

- [47] M. Ehrig, S. Staab, QOM—quick ontology mapping, *The Semantic Web—ISWC*, November 2004: Third International Semantic Web Conference, Hiroshima, Japan, 2004, pp. 7–11.
- [48] M. Ehrig, Y. Sure, in: *Ontology mapping—an integrated approach*, *The Semantic Web: Research and Applications: First European Semantic Web Symposium, ESWs 2004* Heraklion, Crete, Greece, Springer, Berlin, Heidelberg, May, 2004.
- [49] N. Alalwan, H. Zedan, F. Siewe, in: *Generating OWL ontology for database integration, Advances in Semantic Processing, 2009. SEMAPRO'09*. Third International Conference on, 2009, pp. 22–31.
- [50] A. Valls, K. Gibert, D. Sánchez, M. Batet, Using ontologies for structuring organizational knowledge in Home Care assistance, *Int. J. Med. Inform.* (Elsevier) 79 (5) (2010) 370–387.
- [51] Bioportal, Available from: <https://bioportal.bioontology.org>. (Accessed June 2017).
- [52] A. Ducrou, *Complete Interoperability in Healthcare: Technical, Semantic and Process Interoperability Through Ontology Mapping and Distributed Enterprise Integration Techniques*, (Ph.D. dissertation), Faculty of Informatics, University of Wollongong (2009).
- [53] A. Magni, R. Albuquerque, R.I. Timóteo, Solving incompatibilities between electronic records for orthodontic patients, *Am. J. Orthod. Dentofac. Orthop.* 132 (1) (2007) 116–121.
- [54] V. Bicer, O. Kilic, A. Dogac, G.B. Laleci, Archetype-based semantic interoperability of web service messages in the health care domain, *Int. J. Semant. Web Inf. Syst.* 1 (4) (2005) 1–23.
- [55] Szwed."Application of fuzzy ontological reasoning in an implementation of medical guidelines." 2013 6th International Conference on Human System Interactions (HSI). 2013. 342–349.
- [56] N. Rodriguez, M.P. Cuéllar, J. Lilius, M.D. Calvo-Flores, A fuzzy ontology for semantic modelling and recognition of human behaviour, *Knowl.-Based Syst.* (Elsevier) 66 (2014) 46–60.
- [57] C. Chute, Clinical classification and terminology, *J. Am. Med. Inform. Assoc.* (The Oxford University Press) 7 (2000) 298–303.
- [58] International Classification of Diseases, Available from: <http://www.who.int/classifications/icd/en>. (Accessed March 2017).
- [59] The Unified Medical Language System, UMLS terminology services. Available from: <http://umlsks.nlm.nih.gov> Accessed March 2017 2017.
- [60] D. Lindberg, B. Humphreys, A. McCray, The unified medical language system, *Methods Inform. Med.* (1993) 281–291.
- [61] Logical Observation Identifiers Names and Codes, Available from: <https://loinc.org>. (Accessed March 2017).
- [62] RxNorm: National Library of Medicine, Available from: <https://www.nlm.nih.gov/research/umls/rxnorm>. (Accessed March 2017).
- [63] H. Hameed, Current procedural terminology, in: J.E. Pope, T.R. Deer (Eds.), *Treatment of Chronic Pain Conditions: A Comprehensive Handbook*, Springer New York, New York, NY, 2017, pp. 333–334.
- [64] Terminology in Wikipedia, Available from: <https://en.wikipedia.org/wiki/Terminology>. (Accessed June 2017).
- [65] Ceusters W. "Terminology and ontology in semantic interoperability of electronic health records." Tech. rep., European Centre for Ontological Research Saarland University.

- [66] O. Bodenreider, The unified medical language system (UMLS): integrating biomedical terminology, *Nucleic Acids Res.* (Oxford University Press) 32 (Suppl. 1) (2004) D267–D270.
- [67] A. Ryan, P. Eklund, A framework for semantic interoperability in healthcare: a service-oriented architecture based on health informatics standards, *Stud. Health Technol. Inform.* (IOS Press) 1999 (136) (2008) 759.
- [68] D. Chappell, Enterprise service bus, *JavaSPEKTRUM* 2005 (04) (2004) 16–18.
- [69] S. Hussain, D. Ouagne, E. Sadou, T. Dart, M.-C. Jaulet, B. De Vloed, D. Colaert, C. Daniel, EHR4CR: a semantic web-based interoperability approach for reusing electronic healthcare records in protocol feasibility studies, *SWAT4LS*, 2012.
- [70] C. Martínez-Costa, M.C. Legaz-García, S. Schulz, J.T. Fernández-Breis, in: Ontology-based infrastructure for a meaningful EHR representation and use, *IEEE-EMBS International Conference on Biomedical and Health Informatics (BHI)*, 2014, pp. 535–538.
- [71] A. Gangemi, in: *Ontology design patterns for semantic web content*, *International Semantic Web Conference*, 2005, pp. 262–276.
- [72] Schulz, S., and C. Costa. "How ontologies can improve semantic interoperability in health care." *KR4HC/ProHealth*. 2013. 1–10.
- [73] I. Macía, in: *Towards a semantic interoperability environment, e-Health Networking, Applications and Services (Healthcom)*, 2014 IEEE 16th International Conference on, 2014, pp. 543–548.
- [74] L.B. Harman, *Ethical Challenges in the Management of Health Information*, in: Jones & Bartlett Learning, Burlington, 2001.
- [75] R. Rognehaugh, *The Health Information Technology Dictionary*, Aspen Publishers, USA, 1999, 286.
- [76] HIMSS. "Definition of interoperability." Approved by the HIMSS Board of Directors, April 5, 2013.
- [77] E.H. Kluge, Informed consent and the security of the electronic health record (EHR): some policy considerations, *Int. J. Med. Inform.* 73 (3) (2004) 229–234.
- [78] N. Cullot, R. Ghawi, and K. Yétongnon. "DB2OWL: a tool for automatic database-to-ontology mapping." *SEBD* 2007. 491–494.
- [79] R. Studer, V.R. Benjamins, D. Fensel, *Knowledge engineering: principles and methods*, *Data Knowl. Eng.* 25 (1998) 161–197.
- [80] I.F. Cruz, H. Xiao, Ontology-driven data integration in heterogeneous networks, in: *Complex Systems in Knowledge-Based Environments: Theory, Models, and Applications*, Springer, Berlin, 2009, pp. 75–98.
- [81] N.F. Noy, D.L. McGuinness, *Ontology development 101: a guide to creating your first ontology*, Knowledge Systems Laboratory Stanford University (2001).
- [82] Z. Telnarova, Relational database as a source of ontology creation, *Proc. International Multiconference on Computer Science and Information Technology*, Wisla, Poland, 2010, pp. 135–139.
- [83] Apollo Mapping, Available from: <https://apolломapping.com>. (Accessed June 2017).
- [84] RDBToOnto, Available from: <https://sourceforge.net/projects/rdbtoonto>. (Accessed June 2017).
- [85] J. Barrasa, Ó. Corcho, A. Gómez-Pérez, in: *R2O, an extensible and semantically based database-to-ontology mapping language*, *Proceedings of the 2nd Workshop on Semantic Web and Databases (SWDB2004)*, Springer, 2004, pp. 1069–1070.

- [86] M. Weiten, OntoSTUDIO® as a ontology engineering environment, in: J. Davies, M. Grobelnik, D. Mladeni (Eds.), Semantic Knowledge Management: Integrating Ontology Management, Knowledge Discovery, and Human Language Technologies, Springer Berlin Heidelberg, Berlin, Heidelberg, 2009, pp. 51–60.
- [87] D2RQ: Accessing Relational Databases as Virtual RDF Graphs, Available from: <http://d2rq.org/d2rq-language>. (Accessed June 2017).
- [88] Z. Wu, H. Chen, C. Changhuang, G. Zheng, X. Jiefeng, DartGrid: semantic-based database grid, in: M. Bubak, G.D. van Albada, P.M.A. Sloot, J. Dongarra (Eds.), Computational Science—ICCS 2004: 4th International Conference, Kraków, Poland, June 6–9, 2004, Proceedings, Part I, Springer Berlin Heidelberg, Berlin, Heidelberg, 2004, pp. 59–66.
- [89] M. Fisher, M. Dean, Automapper: relational database semantic translation using OWL and SWRL, 01 (2007).
- [90] W. Hu, Y. Qu, Discovering simple mappings between relational database schemas and ontologies, Proc. 6th International Semantic Web Conference, Busan, Korea, 2007, pp. 225–238.
- [91] S. Zhou, H. Ling, M. Han, H. Zhang, Ontology generator from relational database based on Jena, Comput. Inf. Sci. 3 (2) (2010) 263–267.
- [92] K. Mogotlane, J. Dombeu. 2016 "Automatic conversion of relational databases into ontologies: a comparative analysis of Protégé plug-ins performances." CoRR abs/1611.02816.
- [93] P.T.T. Thuy, Y.-K. Lee, S. Lee, in: DTD2OWL: automatic transforming XML documents into OWL ontology, International Conference on Interaction Sciences, 2009.
- [94] N. Yahia, S. Mokhtar, A.W. Ahmed, Automatic generation of OWL ontology from XML data source, Int. J. Comput. Sci. Issues 9 (2) (2012).
- [95] J. Xu, W. Li, in: Using relational database to build OWL ontology from XML data sources, 2007 International Conference on Computational Intelligence and Security Workshops (CISW 2007), 2007, pp. 124–127.
- [96] R. Ghawi, N. Cullot, in: Building ontologies from XML data sources, 20th International Workshop on Database and Expert Systems Application, 2009, pp. 480–484.
- [97] H. Bohring, S. Auer, Mapping XML to OWL ontologies, in: Leipziger Informatik-Tage, 2005.
- [98] C. Martinez-Costa, Semantic interoperability of dual-model EHR clinical standards, (2010) Departamento de Informática y Sistemas, Facultad de Informática Universidad de Murcia, Murcia.
- [99] A. Dogac, G. Laleci, S. Heard, C. Mattocks, Exploiting ebXML registry semantic constructs for handling archetype metadata in healthcare informatics, Int. J. Metadata Semant. Ontol. (InderScience Publishers) 1 (1) (2006) 21–36.
- [100] HL7 CDA Sample, Available from: <https://www.w3.org/TR/grddl-primer/hl7-sample.xml>, 2017. (Accessed June 2017).
- [101] F. Bobillo, U. Straccia, The fuzzy ontology reasoner fuzzy DL, Knowl.-Based Syst. (Elsevier) 95 (2016) 12–34.
- [102] C. Li, T.W. Ling, in: Owl-based semantic conflicts detection and resolution for data interoperability, International Conference on Conceptual Modeling, 2004, pp. 266–277.
- [103] F. Bobillo, U. Straccia, Fuzzy ontology representation using OWL 2, Int. J. Approx. Reason. (Elsevier) 52 (7) (2011) 1073–1094.

- [104] G. H.-M., X. Wang, Y. Ling, J.-Q. Shi, in: Building a fuzzy ontology of edutainment using OWL, International Conference on Computational Science, 2007, pp. 591–594.
- [105] P. Alexopoulos, M. Wallace, K. Kafentzis, D. Askounis, IKARUS-Onto: a methodology to develop fuzzy ontologies from crisp ones, *Knowl. Inform. Syst.* (Springer) 32 (3) (2012) 667–695.
- [106] H. Ghorbel, A. Bahri, R. Bouaziz, in: Fuzzy ontologies building method: fuzzy onto methodology, 2010 Annual Meeting of the North American Fuzzy Information Processing Society, 2010, pp. 1–8.
- [107] A.U. Baldárrago, M.T.P. Santos, A.F. do Prado, in: UPFON: Unified Process for building fuzzy ontology, 2012 9th International Conference on Fuzzy Systems and Knowledge Discovery, 2012, pp. 617–622.

FURTHER READING

- [108] D. Kalra, P. Lewalle, A. Rector, J.M. Rodrigues, K.A. Stroetmann, G. Surjan, B. Ustun, M. Virtanen, P.E. Zanstra, Semantic Interoperability for Better Health and Safer Healthcare, in: V.N. Stroetmann (Ed.), Tech. rep. The European Commission, 2009.

This page intentionally left blank

Index

Note: Page numbers followed by *f* indicate figures, *t* indicate tables, and *b* indicate boxes.

A

Abnormal mammograms, CAD systems
enhancement methods, 229–237
feature extraction, 241–244
image data set, 228
normal and abnormal breast tissues, 226–227
ROIs, selection of, 237–241
SVM classifiers, 244–245
textural patterns, 226–227
Adaptive boosting (AdaBoost), 184
ADL2Onto module, 379–380
ADL workbench (AW), 363
AFE4300 body composition analyzer, 98, 115
AFE4300 EVM-PDK demonstration
board, 100–101, 100f
digital-to-analog converter, 99–100
FWR mode, 101–103, 101–102f
I/Q demodulation mode, 101, 101f, 103–105, 104f
on-chip analog-to-digital converter, 99–100
operating temperature, 100
Analog Devices board AD5933EBZ, 269, 270f
Analog-to-digital converter (ADC), 6, 267–268
Apollo, 378
Archetype definition language (ADL), 354
Archetype editor (AE), 363
Archetype management system (ArchMS), 361
Archetype model (AM), 330–331
Arduino kit, 6, 9f
Area under the receiver operating characteristic
(AU-ROC) curve, 191
Artificial bee colony (ABC), 198–199
Artificial neural network (ANN)
architecture, 40, 207t
challenges, 198
component of, 198
genetic algorithm, 198–199
gradient decent, 198
PSO, 198–199
Auto-Encoder, 45, 46f
Automapper, 378
Automated teller machines (ATMs), 356–357

B

Back propagation (BP), 198–199
Back-propagation neural network fuzzy classifier,
94–95

Backtracking search algorithm on a neural network
architecture (BSA-NN), 26
Bagging algorithms, 184
Bandpass filtering, 20
Basal cell carcinoma (BCC), 271
Basic Formal Ontology (BFO 2), 151–152
Bayesnet algorithm, 198
Bayes theorem, 188–189
Bee algorithms, 199
Bee colony optimization (BSO), 199
Bee system (BS), 199
Benign liver disorder, CAD system design.
See Computer-aided diagnostic (CAD)
systems
Big data analytical tools, 2
Bioelectrical impedance analysis (BIA)
body composition measurement, 91–93
AFE4300 (*see* AFE4300 body composition
analyzer)
capacitive reactance, 91–92
cell membranes, 92
chronic kidney disease (*see* Chronic kidney
disease (CKD))
congestive heart failure (*see* Congestive heart
failure (CHF))
cylindrical conductor, uniform resistivity,
96–97, 96f
developed model, validation of, 105
fat-free mass, 97–98
frequency-dependent behavior, 92–93
intracellular and extracellular fluids, 92
magnitude-phase representation, 91–92
malnourished patients, 94
measurement electrodes, 99
predictive regression models (*see* Predictive
regression model)
reactance-resistance relationship, 91–92
segmental body composition analysis, 96–97
total body water, 93–94, 97–98
uniform cylinder, 97
skin diseases (*see* Skin diseases)
Bioelectrical impedance spectroscopy, 92
Bioinformatics, 38–39, 39f
Biomedical imaging processing, 94–95
BioPAX, 334–335
BioPortal, 365

- BIRNLex, 334–335
- Body composition
- anthropometric data, 91
 - bioelectrical impedance analysis, 91–93
 - AFE4300 (*see AFE4300 body composition analyzer*)
 - capacitive reactance, 91–92
 - cell membranes, 92
 - chronic kidney disease (*see Chronic kidney disease (CKD)*)
 - congestive heart failure (*see Congestive heart failure (CHF)*)
 - cylindrical conductor, uniform resistivity, 96–97, 96*f*
 - day-to-day fitness, 95
 - developed model, validation of, 105
 - fat-free mass, 97–98
 - frequency-dependent behavior, 92–93
 - intracellular and extracellular fluids, 92
 - magnitude-phase representation, 91–92
 - malnourished patients, 94
 - measurement electrodes, 99
 - predictive regression models (*see Predictive regression model*)
 - reactance-resistance relationship, 91–92
 - segmental body composition analysis, 96–97
 - total body water, 93–94, 97–98
 - uniform cylinder, 97
 - chemical analysis, 91
 - chemical compounds, 90–91
 - fat percentages, 90–91
 - four-compartment model, 91
 - hydrostatic weighing, 91
 - skinfolds, 91
 - three-compartment model, 91
 - two-compartment model, 91
- Bootstrap aggregating. *See Bagging algorithms*
- Brain computer interfaces (BCI), 15–16
- C**
- CAD systems. *See Computer-aided diagnostic (CAD) systems*
- Cardiovascular diseases (CVD), 179–180
- Case-based reasoning (CBR)
- advantage and disadvantages, 61–62, 63*f*
 - problem-solving, general description of, 65, 66*f*
 - selected papers concerned with cancer, 75–82, 76–81*t*
- CDSS. *See Clinical decision support system (CDSS)*
- CEN/ISO EN13606, 324, 333*f*
- CHF. *See Congestive heart failure (CHF)*
- Chi Squared Automated Interaction Detector (CHAID) method, 185
- Chronic kidney disease (CKD)
- bioimpedance analysis, 94
 - nutritional status, determination of, 95
 - overhydration state, assessment of, 95
 - predictive regression model, 112–113, 112–113*t*, 115
 - cardiac disease, 111–112
 - ECF volume, disorders in, 111–112
 - type II diabetes and hypertension, 111–112
- Classification error percentage (CEP), 204–208, 209*t*, 211*t*
- Clinical decision support system (CDSS)
- advantage and disadvantages, 61–62, 63*f*
 - case-based reasoning (*see Case-based reasoning (CBR)*)
 - challenges and future trends, 82–83
 - component, 61–62, 62*f*
 - description, 63*f*
 - for diabetes diagnosis
 - antidiabetes drug recommendation, 150
 - coronary artery disease, fuzzy CDSS for, 150
 - EHR data, 148–150
 - fuzzy and ontology reasoning, 155
 - fuzzy logic, 149–150, 154
 - fuzzy ontologies, 155
 - fuzzy rule-based systems, 155
 - impact factors, 148, 149*f*
 - knowledge-based systems, 154
 - OBFDSS hybrid model (*see Ontology-based fuzzy decision support system (OBFDSS)*)
 - OntoDiabetic, 154–155
 - single input rule modules, 154
 - standard medical ontologies, 150
 - fuzzy ontology system
 - T1FO vs. T2FO, 62, 64*t*
 - vagueness-handling and modeling capabilities, 62
 - model-based reasoning, 61–62, 63*f*
 - OBFDSS, 75
 - ontology reasoning, 74–75
 - ontology system, 62, 64*f*
 - paper screening, 69–70
 - relevant papers, selection of, 71
 - rule-based reasoning (*see Rule-based reasoning (RBR)*)
 - search methodology
 - research questions, 67
 - search strategy, 68, 68*f*
 - selection criteria, 67
 - Clinical information systems (CISs), 347, 360

- Clinical knowledge manager (CKM), 363
 Common data element (CDE), 361
 Computed tomography (CT), 290–291
 Computer aided characterization (CAC) system, for FHTs. *See* Hierarchical CAC system, for benign and malignant FHTs
 Computer-aided diagnostic (CAD) systems, 220, 291
 abnormal mammograms
 enhancement methods, 229–237
 feature extraction, 241–244
 image data set, 228
 normal and abnormal breast tissues, 226–227
 ROIs, selection of, 237–241
 SVM classifiers, 244–245
 textural patterns, 226–227
 enhanced mammographic images,
 classification of
 feature selection/optimization techniques, 252–253
 21 Gabor features, 253–254, 254*t*
 GA-SVM procedure, 253–254
 MECA method, 253–254
 metaheuristic search procedures, 253–254
 FLLs, 291
 histological data, liver disorders, 310
 BUPA liver disorders dataset, 293–295, 296*f*, 296*t*
 classification results, 298–301, 301*t*
 experimental workflow, 293, 295*f*
 kNN classifier, 296, 297*f*, 300*f*
 NN classifier, 297, 299*f*
 PNN classifier, 297, 298–300*f*
 SSVM classifiers, 298, 300*f*
 SVM classifiers, 298, 300*f*
 hybrid CAD system, liver disorders, 295*f*, 307–311, 309–310*f*, 310*t*
 liver ultrasound images, 310–311
 classification results, 304–306, 308*f*, 309*t*
 dataset description and bifurcation, 302, 302*f*
 experimental workflow, 295*f*, 301, 304, 309*f*
 Laws' mask analysis, features extraction, 302–304, 303*f*, 305–307*f*, 308*t*
 SSVM classifier, 304
 Computerized tomography (CT), 220
 Congestive heart failure (CHF)
 bioimpedance analysis, 94
 body hydration status, monitoring of, 95–96
 electrocardiogram and thoracic electrical bioimpedance, 95–96
 predictive regression model, 113–114, 114*t*
 cardiovascular conditions, 113
 causal factors, 113
 physical symptoms of, 113
 Content ontology patterns (COPs), 370
 Converse wavelet transform (CWT), 21, 22*f*
 Convolutional Auto-Encoder (CAE), 57
 Convolution neural network (CNN), 45–49, 52
 Coronary artery disease (CAD), 150
 Correlation-based feature selection (CFS), 182
 Crohn's disease, 335
 Cuckoo algorithm, 201
 Custom epoch extractor, 21
- D**
- DartGrid Semantic, 378
 Data-mining techniques, 197–198
 DBC algorith. *See* Directed bee colony (DBC) algorithm
 DB2OntoModule, 378
 DB2OWL, 378
 DDO. *See* Diabetes diagnosis ontology (DDO)
 Decision tree (DT), 181–182
 Deep belief networks (DBNs)
 basic flow of, 43, 44*f*
 learning features, 43
 RBM, 43–45
 Deep learning (DL), 39
 accurate analysis and diagnosis results, 37–38
 Auto-Encoder, 45, 46*f*
 automated feature selection, 37–38
 bioinformatic data modalities, 38–39, 39*f*
 challenges, 59
 convolution neural network, 45–49, 52
 deep belief networks
 basic flow of, 43, 44*f*
 learning features, 43
 RBM, 43–45
 deep neural network, 38–42
 feature learning, 40
 Google's DeepMind, 38
 hidden layers, 42
 IBM's WATSONS, 38
 input layer, 42
 library ranking, 53–55, 55–56*t*
 vs. machine learning, 40, 41*t*
 medical image processing, application in challenges, 58
 current research applications, 56–57
 hybrid architectures, 57, 57*f*
 multilayer perceptron, 42, 43*f*
 output layer, 42
 recurrent neural network
 advantages, 51
 architecture, 50
 deep learning structure, 50, 50*f*
 feed-forward neural network, 51

- Deep learning (DL) (*Continued*)
 GRU, 51
 LSTM, 51–52, 52*f*
 sequential data, 50
 toolkit selection/evaluation criteria, 53, 53–54*t*
 tools and technology, 53, 54–55*t*
- DeepMind, 38
- Deep neural network (DNN), 38–42
- Deep Spatiotemporal Neural Networks (DST-NNs), 57
- Denoising Auto-Encoder, 45
- Dermabrasion (skin refinishing), 265
- Dermatophytes, 265–266
- Dermoscopy, 265
- Description logic (DL), 154–155
- Diabetes diagnosis ontology (DDO), 74, 151–152, 163–164
- Diabetes mellitus (DM)
 CDSS system
 antidiabetes drug recommendation, 150
 coronary artery disease, fuzzy CDSS for, 150
 EHR data, 148–150
 fuzzy and ontology reasoning, 155
 fuzzy logic, 149–150, 154
 fuzzy ontologies, 155
 fuzzy rule-based systems, 155
 impact factors, 148, 149*f*
 knowledge-based systems, 154
 OBFDSS hybrid model (*see* Ontology-based fuzzy decision support system (OBFDSS))
 OntoDiabetic, 154–155
 single input rule modules, 154
 standard medical ontologies, 150
 morbidity and mortality, 147–148
 problem description, 152–153
 risk score calculators, 153
- Diabetes rule based classification model, 154
- DICOM, 327
- Diffuse liver diseases, 290
- Digital image analysis, 37–38
- Digital signal processor (DSP), 267–268
- Directed bee colony (DBC) algorithm, 199, 205*b*
 vs. bioinspired algorithms
 average CEP and ranking, 204–208, 209*t*
 average standard deviation and ranking, 204–208, 210*t*, 212*t*
 classification accuracy, 204–208
 computational time, 209, 213*t*
 classification accuracy, 213–214
 classification error percentage, 204, 211*t*
 consensus and quorum, 201–204
 flowchart of, 204, 207*f*
 food quality index, 202–204
- FSR, 202
- NM algorithm, 202, 206*b*
- search methodology and analogy, 202, 203*f*
- statistical analysis, 209–213, 213*t*
- Discrete Fourier transform (DFT), 267–268
- DNN. *See* Deep neural network (DNN)
- D2RQ, 378
- Dual-energy X-ray absorptiometry, 91

E

- EAPSONN, 199
- Electrocardiogram, 95–96
- Electroencephalogram (EEG), 16. *See also* P300 signals, EEG
- Electronic health records (EHR). *See also* Semantic interoperability (SI), EHR
 ontology based
 administrative information, 317
 advantages and disadvantages, 334*t*
 barriers and heterogeneous problem of, 340–341*t*
 CEN/ISO EN13606, 324, 333*f*
 clinical decision making, 317
 clinical information, 317
 DICOM, 327
 different providers of, 317, 319*f*
 heterogeneous data sources, 317
 HL7, 326, 328–329*f*
 IEEE, 330, 331*f*
 ontology, 332–336
 openEHR foundation, 330, 332–333*f*
 OWL, 331
 PACS, 329, 330*f*
 research questions, 336
 search results, 337–344
 search strategy, 336
 SNOMED CT, 331
 u-Health framework, 315–316
- unified fuzzy ontology
 BikaLIMS, 360–361
 challenges of standards, 359–360
 clinical and business benefits and outcomes, 355–357
 data model, archetypes, 373–374
 dynamics and complexities, healthcare systems, 358–359
 healthcare organizations, 357–358
 heterogeneity, 357–358
 heterogeneous medical data resources, 373–374, 374*f*
- HL7vMR standard, 360–361
- INDIVO, 360–361

- medical data, 355
ontology, 363–367, 368*t*
OpenEHR approach, 360–361
OpenMRS, 360–361
OWL web-based framework, 361
privacy and security in, 372–373
proposed framework, 374–380
prototype problem, 381–389
SNOMED CT/UMLS, 362
standards, 363
techniques and approaches of, 362–363
terminology, 367–368, 368*t*
unified reference model, 373–374
WBAN, 354
- Enhanced Feedback for Effective Cardiac Treatment (EFFECT), 182
- Ensemble learning systems
classification model, prediction accuracy of, 183
combining ensemble members, 184–185
diversity, 184
schematic diagram of, 183, 183*f*
training ensemble members, 184
- Erythema dyschromicum perstans (EDP), 265
- Event-related desynchronization (ERD), 16
- Evolutionary search (ES), 199
- Extracellular fluid (ECF), 111–112
- Extreme learning machine (EML), 182
- F**
- Facial melanoses, 265
False discovery rate (FDR), 190
False negatives (FNs), 190
False positive (FP), 190
Fandom forest technique, 182
Fat-free mass (FFM), 97–98
Feed-forward neural networks, 188
First differential of time series, 25
First-order statistical (FOS), 127–128, 128*f*
Focal hepatic tumor (FHTs)
B-mode US, 120
CAC systems (*see* Hierarchical CAC system, for benign and malignant FHTs)
Focal liver lesions (FLLs), 290–291
Food quality index (FQI), 202–204
Food value (FV), 202–204
Four-compartment model, 91
Fourier power spectrum (FPS), 127–128, 128*f*
Fourier transform, 22
FRBSs. *See* Fuzzy rule-based systems (FRBSs)
Full-wave rectifier (FWR), 101–103, 101–102*f*
Fuzzy decision trees (FDTs), 170–171
Fuzzy diabetes ontology (FDO), 155
- Fuzzy inference system (FIS), 63–64, 65*f*
Fuzzy model
features definition and fuzzification, 165–168, 166*f*, 167–168*t*
features selection and DT induction, 169, 169*t*
knowledge, 164–165
raw EHR data preprocessing, 165
Fuzzy ontology, 335–336, 389
T1FO vs. T2FO, 62, 66*t*, 74–75
vagueness-handling and modeling capabilities, 62
- FuzzyOWL2Ontology, 155
- Fuzzy rule-based systems (FRBSs), 73–74
fuzzy inference system, 63–64, 65*f*
general review of, 63–64, 65*f*
Mamdani vs. TSK approach, 64–65, 66*t*
- Fuzzy set theory, 335
- FWR. *See* Full-wave rectifier (FWR)
- G**
- Gabor wavelet transform (GWT), 127–129, 128–131*f*, 241–244
GALEN, 334–335
Gaussian function, 128
Genetic algorithm (GA), 198–199
Genetic algorithm-based metaheuristic approach, enhanced mammograms
feature selection/optimization techniques, 252–253
21 Gabor features, 253–254, 254*t*
GA-SVM procedure, 253–254
MECA method, 253–254
metaheuristic search procedures, 253–254
Gradient-based approaches, 199
Gradient tree boosting, 184
Graphical user interface (GUI), 269*f*
Gravitational search algorithm (GSA), 182
Gray-level cooccurrence matrix (GLCM), 94–95
Gray level run length matrix (GLRLM), 127–128, 128*f*
GWT. *See* Gabor wavelet transform (GWT)
- H**
- Health service bus (HSB) architecture, 369, 369*f*
Heart disease prediction
ANN, 185, 188
base classifier, 182
CHAID method, 185, 187*f*
confusion matrix, 191–192, 191*t*
controlling factors, 179–180
CVDs, 179–180
EML, 182

- Heart disease prediction (*Continued*)
- ensemble learning systems
 - classification model, prediction accuracy of, 183
 - combining ensemble members, 184–185
 - diversity, 184
 - schematic diagram of, 183, 183*f*
 - training ensemble members, 184
 - false negatives, 190
 - false positive, 190
 - fandom forest technique, 182
 - hybrid genetic-fuzzy model, 182
 - logistic regression, 185–188
 - machine learning algorithms, 180–182
 - majority vote rule, combining classifiers using, 189
 - MLP, 188
 - naïve Bayes, 185, 188–189
 - OLPP technique, 182
 - performance metrics, 190–191
 - accuracy, 190
 - AU-ROC, 191
 - false negatives, 190
 - false positive, 190
 - FDR, 190
 - F* score, 191
 - MCC, 190
 - NPV, 190
 - PPV, 190
 - sensitivity, 190
 - specificity, 190
 - true negative, 190
 - true positives, 190
 - rotation forest ensemble classifier, 182
 - sensitivity, 190
 - SPSS software tool, 185
 - StatLog heart disease dataset, 185, 186*t*, 191–192, 192–193*f*
 - stored patients' data, 180
 - tree-based method, 182
 - UCI-ML datasets, 182
 - U-Healthcare system, 180–181
 - Heart rate variability (HRV), 181
 - Hemangioma (HEM), hierarchical CAC system.
 - See* Hierarchical CAC system, for benign and malignant FHTs
 - Hepatocellular carcinoma (HCC), hierarchical CAC system. *See* Hierarchical CAC system, for benign and malignant FHTs
 - Hierarchical CAC system, for benign and malignant FHTs
 - challenging factors, 120–122
 - data collection protocol, 123
 - dataset collection, 123, 124*f*
 - dataset description, 123, 124*t*
 - experimental workflow for, 137, 138*f*
 - IROIs, 122, 124, 126*f*
 - liver ultrasound images, 120, 121*f*
 - related studies, 122, 122*t*
 - ROI size selection, 122, 125–127
 - SROIs, 122, 124, 126*f*
 - SSVM classifiers, 141–143
 - advantages, 137
 - SSVM-based hierarchical classifier, 132–137, 137*f*, 138*t*, 139–140, 140*t*
 - three-class classifier vs. hierarchical classifier, 138*t*, 140–141, 141–142*t*
 - three-class SSVM classifier, 132–137, 137*f*, 138–139*t*, 139
 - texture feature extraction methods, 127–132
 - first-order and higher-order statistical features, 127–128, 128–129*f*
 - FPS and GWT-based features, 127–129, 128–131*f*
 - signal processing-based Laws' features, 127–128, 128–129*f*, 131–132, 132–136*f*
 - training and testing dataset description, 123, 125*t*
 - workflow, 143, 143*f*
 - High performance computing (HPC), 37–38
 - Hjorth parameters, 24
 - HL7, 326, 328–329*f*
 - Human skin impedance
 - Cypress microcontroller CY7C68013A, 266
 - impedance converter IC AD5933, 266–268
 - microcontroller IC CY7C68013A, 268
 - personal computer, 269
 - skin electrode, 267, 267*f*
 - Hydrostatic weighing, 91
 - HyFOM reasoner, 157, 158*f*
 - Hyperspheres (HSs), 282
- |
- IEEE, 330, 331*f*
 - IKARUS-Onto fuzzy ontology development methodology, 389
 - Imaginary part index (IMIX), 272, 277–278
 - Impedance quotient, 97–98
 - Indian skin diseases, 269–270
 - Information and communication technology (ICT), 180–181
 - Inside regions of interest (IROIs), 122, 124, 126*f*
 - Internet of things (IoT), 1–2, 180–181
 - ISO/CEN13606 reference model, 327*f*
 - Isotopic dilution method, 91

K

- Kernel-based learning methods, 17
k-nearest neighbor (*k*NN) classifier, 181–182, 296, 297f, 300f
 Knowledge acquisition (KA), 160–162, 162t
 Knowledge-based (KB) systems, 154
 Knowledge reasoning
 defuzzification methods, 171
 framework evaluation, 171–172, 173t
 initial fuzzy knowledge base construction, 170
 knowledge base enhancement, 170–171, 170f
 Mamdani fuzzy inference engine, 171, 172f
 Kurtosis, 24

L

- Large hepatocellular carcinomas (LHCCs), 120, 121f, 126f, 291, 292f
 Least squares support vector machine (LS-SVM), 17
 Levenberg-Marquardt back propagation network (BPN) classifier, 94–95
 Levenberg Marquardt training networks, 199
 Light-emitting diode (LED), 6, 8–9
 Linear discriminant analysis (LDA), 25–26, 28t, 30–31, 30–31f
 Liver disease
 BUPA liver disorder dataset, 291, 293t
 diffuse liver diseases, 290
 focal liver diseases, 290–291
 histological data, CAD system, 310
 BUPA liver disorders dataset, 293–295, 296f, 296t
 classification results, 298–301, 301t
 experimental workflow, 293, 295f
 *k*NN classifier, 296, 297f, 300f
 NN classifier, 297, 299f
 PNN classifier, 297, 298–300f
 SSVM classifiers, 298, 300f
 SVM classifiers, 298, 300f
 hybrid CAD system, 295f, 307–311, 309–310f, 310t
 liver ultrasound images, CAD system, 310–311
 classification results, 304–306, 308f, 309t
 dataset description and bifurcation, 302, 302f
 experimental workflow, 295f, 301, 304, 309f
 Laws' mask analysis, features extraction, 302–304, 303f, 305–307f, 308t
 SSVM classifier, 304
 NOR, SHCC, and LHCC, US images of, 291, 292f
 Liver ultrasound images. *See* Ultrasound (US) imaging, liver disorders
 “Locked-in” syndrome, 15–16

M

- Machine learning (ML)
 algorithms, 38, 40, 180–182
 ANN architecture, 40
 DL techniques (*see* Deep learning (DL))
 and HPC collaborations, 37–38
 Magnetic resonance imaging (MRI), 220, 290–291
 Magnitude index (MIX), 272, 277–278
 Majority vote rule, 189, 192
 Malignant liver disorder, CAD system design.
 See Computer-aided diagnostic (CAD) systems
 Mamdani fuzzy inference technique, 64–65, 66t, 171, 172f
 Mammographic Image Analysis Society (MIAS) database, 218–220
 abnormal mammograms, CAD systems
 enhancement methods, 229–237
 feature extraction, 241–244
 image data set, 228
 normal and abnormal breast tissues, 226–227
 ROIs, selection of, 237–241
 SVM classifiers, 244–245
 textural patterns, 226–227
 architectural distortion, 223f
 classification performance of enhancement, comparison of, 251–252, 252t
 digital mammograms, 254
 experimental results
 alpha trimmed mean filter, 246
 CLAHE, 247, 247t
 contra-harmonic mean, 248, 248t
 contrast stretched images, 246, 250, 250–251t
 histogram equalization, 247
 hybrid median filter, 249, 249t
 mean filter, 248, 248t
 median filter, 248, 249t
 morphological enhancement, 249–250, 249–250t
 RMSHE enhanced images, 247, 247t
 UMCA, 250, 251t
 unsharp masking, 250
 wavelet-based subband filtering, 251, 251t
 feature extraction techniques, 222–226
 feature selection algorithms, 222–226
 INbreast database, 254
 mammograms classification, 220, 222–226, 224–226t
 normal mammogram, 218, 219f

- Mammographic Image Analysis Society (MIAS)
database (Continued)
 sample mammogram, 220–222*f*
 architectural distortion, 223*f*
 circumscribed mass, 221*f*
 ill-defined mass, 222*f*
 spiculated mass, 221*f*
 screen film mammograms, 254
- Mammography, 220
- MARSON, 378
- Matthews correlation coefficient (MCC), 190
- Maximally stable extremal regions (MSERs), 94–95
- Mean square error (MSE), 200
- Medical image processing
 digital image analysis, 37–38
 DL techniques (*see* Deep learning (DL))
 malicious application detection and
 classification, 39
 ML algorithms, 38
- Melisma, 265
- Metafeature extractor, 25
- Metastatic carcinoma (MET), hierarchical CAC system. *See* Hierarchical CAC system, for benign and malignant FHTs
- MITHrill, 2–3
- MLP. *See* Multilayer perceptron (MLP)
- Model-based reasoning (MBR), 61–62, 63*f*
- Modular fuzzy hypersphere neural network (MFHSNN)
 biomedical imaging processing, 281–282
 breast tissue density, 281–282
 classification accuracy of, 286*t*
 COMP-FNs, 283
 Crohn’s disease, 281–282
 decision-making layer, 283
 feature extraction, 281–282
 hyperspheres, 282–283
 learning algorithm, 284
 Levenberg-Marquardt back propagation network
 classifier, 281–282
 MAX Fuzzy Neurons, 283
 pattern recognition technique, 281–282
 plantar pressure images, 281–282
 testing phase, 283, 284*f*
- Morphological enhancement and contrast stretching (MECA), 251
- Multidimensional Recurrent Neural Network (MD-RNNs), 57
- Multilayer perceptron (MLP), 42, 43*f*, 188
- Multiple regression analysis, 106–109
- MYCIN, 154
- N**
- Naïve Bayes classification algorithm, 185, 188–189
- NCBO Bioportal, 334–335
- Negative predictive value (NPV), 190
- Nelder-Mead (NM) algorithm, 202, 206*b*
- Neural network (NN)
 architecture, 200, 201*f*
 classifier, 297, 299–300*f*
 cost function, 200
 DBC optimization algorithm (*see* Directed bee colony (DBC) algorithm)
 DNN, 38–39
 fitness function, 200
 input-hidden-output layer, 200
 MSE function, 200
 sigmoid function, 200
- Neurofuzzy model, 94–95
- Neutron activation analysis, 91
- NIFSTD, 334–335
- O**
- OntoDiabetic, 154–155
- Ontology-based fuzzy decision support system (OBFDSS), 75, 156–157
- fuzzy intelligent system architecture, 157–160, 159*f*
- fuzzy model
 features definition and fuzzification, 165–168,
 166*f*, 167–168*t*
 features selection and DT induction, 169, 169*t*
 knowledge, 164–165
 raw EHR data preprocessing, 165
 fuzzy rule and ontology reasoning, 160
- HyFOM reasoner architecture, 157, 158*f*
- knowledge acquisition, 160–162, 162*t*
- knowledge reasoning
 defuzzification methods, 171
 framework evaluation, 171–172, 173*t*
 initial fuzzy knowledge base construction, 170
 knowledge base enhancement, 170–171, 170*f*
 Mamdani fuzzy inference engine, 171, 172*f*
- knowledge reasoning block diagram, 157, 158*f*
- semantic modeling, 163–164, 163–164*f*
 structure, 160, 161*f*
- Ontology Generator (RDB2On), 378
- Ontology mapping, 322, 366
- Ontology reasoning, 74–75, 160
- Ontology system, 62, 64*f*
- OntoMethodology, 389
- OntoStudio, 378
- OpenEHR foundation, 330, 332–333*f*

Optimization algorithms, 201. *See also* Directed bee colony (DBC) algorithm
 Orthogonal local preserving projection (OLPP) technique, 182
 OWL 2 language, 365, 388–389

P

PACS, 329, 330f
 Particle swarm optimization (PSO), 198–199
 Peaks of Fourier transform, 24
 Phase angle, 265
 Phase index (PIX), 272, 277–278
 PNN classifier. *See* Probabilistic neural network (PNN) classifier
 Positive predicted value (PPV), 190
 Predictive regression model
 AFE4300 development board (*see* AFE4300 body composition analyzer)
 chronic kidney disease
 ANOVA table for, 112, 112t
 coefficients table for, 112–113, 113t
 hemodialysis patients, 115
 model summary table, 112, 112t
 congestive heart failure, 115
 ANOVA table for, 113, 114t
 coefficients table for, 113–114, 114t
 model summary table, 113, 114t
 database generation, 105–106
 for day-to-day fitness, 95, 115
 ANOVA table for, 109, 110t
 anthropometric parameters, 106
 coefficients table for, 110–111, 110t
 healthy female subjects, database for, 106, 107t
 healthy male subjects, database for, 106, 108t
 model summary table, 109, 109t
 multiple regression analysis, 106–109
 TBW, 106
 SPSS, 97–98, 105–106
 system development, block diagram of, 98, 98f
 Principle component analysis (PCA), 23
 Probabilistic neural network (PNN) classifier, 297, 298–300f
 Process interoperability, 357
 Protégé, 388–389
 P300 signals, EEG, 26f
 BSA-NN, 26
 comprehensive testing, 19
 custom epoch extractor, 21
 data acquisition process, 27f
 dataset, 27
 framework block diagram, 18f
 initialization, 19–20

LDA-based classifier, 25–26, 28t, 30–31, 30–31f
 linear support vector machines, 25–26
 modularity, 19
 open source implementation, 32
 performance comparison, 31–32, 32t
 postprocessors, 29–30
 CWT, 21, 22f
 experiment information, 22
 first differential of time series, 25
 Fourier transform, 22
 Hjorth parameters, 24
 peaks of Fourier transform, 24
 statistical features, 24
 time series EEG, 22
 wavelet transform, 23
 xDAWN filtering, 23
 preprocessors, 20–21, 29
 P300 waveform at Cz channel, 16, 16f
 Random forest ensembles, 26
 RBM-SVM, 26
 speed and parallelism, 19
 SVMs, 17, 19t
 Pulse sensor, 6

R

Radial bias function (RBF), 198
 Random subspace methods (RSM), 184
 RapidMinerStudio 7.0 software tool, 191–192
 RBR. *See* Rule-based reasoning (RBR)
 RDBToOnto, 378
 Real-part index (RIX), 272, 277–278
 Recurrent neural network (RNN), 188
 advantages, 51
 architecture, 50
 deep learning structure, 50, 50f
 feed-forward neural network, 51
 GRU, 51
 LSTM, 51–52, 52f
 sequential data, 50
 Reference model (RM), 323, 330–331
 Region of interest (ROI), 122, 125–127, 218–220
 Remote monitoring systems, 3–5, 3f
 Representation learning. *See* Deep learning (DL)
 Riehl's melanosis, 265
 R2O, 378
 Rule-based reasoning (RBR), 73–74
 advantage and disadvantages, 61–62, 63f
 FRBS systems
 fuzzy inference system, 63–64, 65f
 general review of, 63–64, 65f
 Mamdani vs. TSK approach, 64–65, 66t
 Rule-level fuzzy value (RLFV), 171

S

- Segmental body composition analysis, 96–97
 Self-training LSSVM (ST-LSSVM), 17
 SemanticHealthNet (SHN), 372*f*
 Semantic interoperability (SI), EHR, 355, 357
 barriers and obstacles
 challenges of standards, 359–360
 dynamics and complexities, healthcare systems, 358–359
 healthcare organizations, 357–358
 heterogeneity, 357–358
 benefits, 319
 challenges of, 346–347
 concept, 317, 318*f*
 costs, 324
 definition, 317, 322*t*
 description of, 317, 318*f*
 frameworks, 369–371, 371*f*
 future-proof and flexible framework, 323
 health domain data types, 321
 no interoperability, 320
 ontology mapping, 322
 reference model standardization, 323
 Research Institutions, 320*t*
 security in, 323
 syntactic interoperability, 320
 technical interoperability, 321
 Seminaive Bayes, 181–182
 Sequential updating self-training-LSSVM (SUST-LSSVM), 17
 Service model (SM), 330–331
 SHCCs. *See* Small hepatocellular carcinomas (SHCCs)
 Singular value decomposition (SVD), 23
 Skewness, 24
 Skin diseases
 bioimpedance measurement, 263–266
 noninvasive measurement, 263–264
 readings, 273–275*t*
 values of indices, 272, 276*t*
 classification of
 box and whisker plots, impedance indices, 278–280
 mean and standard deviation, impedance indices, 280–281
 equatorial climate, 262
 genetic disorders, 262
 hardware board, 268*f*
 human skin impedance
 Cypress microcontroller CY7C68013A, 266
 impedance converter IC AD5933, 266–268
 microcontroller IC CY7C68013A, 268
 personal computer, 269
 skin electrode, 267, 267*f*
 identification of, 272–278
 image processing methods, 263
 impedance indices, 270–272
 Indian skin diseases, 269–270
 infestations and infections, 263
 melanoma skin cancer, 262
 modular fuzzy hypersphere neural network
 biomedical imaging processing, 281–282
 breast tissue density, 281–282
 classification accuracy of, 286*t*
 COMP-FNs, 283
 Crohn's disease, 281–282
 decision-making layer, 283
 feature extraction, 281–282
 hyperspheres, 282–283
 learning algorithm, 284
 Levenberg-Marquardt back propagation
 network classifier, 281–282
 MAX Fuzzy Neurons, 283
 pattern recognition technique, 281–282
 plantar pressure images, 281–282
 testing phase, 283, 284*f*
 nonmelanoma skin cancer, 262–263
 public health interventions, 262
 Slow cortical potential (SCP), 16
 Small hepatocellular carcinomas (SHCCs), 120, 121*f*, 126*f*, 291, 292*f*
 Smooth support vector machine (SSVM) classifier
 CAD systems, liver disorders, 298, 300*f*, 304
 hierarchical CAC system, for FHTs, 141–143
 advantages, 137
 SSVM-based hierarchical classifier, 132–137, 137*f*, 138*r*, 139–140, 140*t*
 three-class classifier vs. hierarchical classifier, 138*t*, 140–141, 141–142*t*
 three-class SSVM classifier, 132–137, 137*f*, 138–139*t*, 139
 SNOMED CT (SCT), 150, 331
 Sobel edge detector, 94–95
 SPARQL, 154–155
 Sparse Auto-Encoder, 45
 Spatial filtering technique, 23
 SQWRL, 154–155
 Stacked Auto-Encoder (SAE), 45
 Statistical analysis
 DBC algorithm, 209–213, 213*t*
 SPSS, 105
 Statistical Package for the Social Sciences (SPSS), 97–98, 105

Steady-state visually evoked potential (SSVEP), 16
 Superficial mycotic, 265–266
 Supervised learning algorithms, 198
 Support vector machine (SVM) classifier, 180–182, 244–245, 298, 300^f
 Surrounding regions of interest (SROIs), 122, 124, 126^f
 Swarm-inspired algorithms, 201
 SWRL, 154–155
 Syntactic interoperability, 320
 System-level fuzzy value (SLFV), 171

T

Takagi-Sugeno-Kang (TSK) model, 64–65, 66^t
 Technical interoperability, 321
 Technical syntactic interoperability, 356
 Telemedicine, 4–5
 Temperature sensor, 6
 Thoracic electrical bioimpedance, 95–96
 Three-compartment model, 91
 Time Series EEG, 22
 Tinea corporis, 265–266
 Toeplitz matrix, 23
 Total body water (TBW), 93–94, 97–98
 True negative (TN), 190
 True negative rate (TNR), 190
 True positive rate (TPR), 190
 True positives (TPs), 190
 T-statistics criteria, 17
 Two-compartment model, 91, 98
 Type-1 fuzzy ontology (T1FO), 62, 64^t, 74–75
 Type-2 fuzzy ontology (T2FO), 62, 64^t, 74–75

U

Ubiquitous healthcare (u-Health), 180–181
 Ubiquitous healthcare monitoring (U-HRM)
 system, 2
 Android device, application on, 10^f, 11
 Big data analytical tools, 2
 fingertip reading for measurement, 7–8, 9^f
 function diagram of, 7, 8^f
 heart rate and body temperature, measurement
 of, 8–11
 in India, 4
 insight block diagram of, 7, 8^f
 MIThrill, 2–3
 modules, 7–8, 9^f
 requirements, 6–7

security and user's privacy concerns, 5–6
 sports, application in, 5
 telemedicine, 4–5
 wearable suits, 5
 working principal, flow chart of, 10^f, 11
 UFOC fuzzy ontology development methodology, 389

U-Health framework, 315–316

Ultrasound (US) imaging, liver disorders, 290

CAD system, 310–311
 classification results, 304–306, 308^f, 309^t
 dataset description and bifurcation, 302, 302^f
 experimental workflow, 295^f, 301, 304, 309^f
 Laws' mask analysis, features extraction,
 302–304, 303^f, 305–307^f, 308^t
 SSVM classifier, 304
 cystic and solid FLLs, 290–291
 HEM, HCC, MET FHTs, 120, 121^f, 124–125,
 126^f
 limitation, 290–291
 NOR, SHCC, and LHCC, sample images of, 291,
 292^f
 studies carried out on, 291, 294^t
 UMLS, 367, 368^f, 373–374

University of California at Irvine Machine Learning
 (UCI-ML), 181, 185
 UPFON fuzzy ontology development methodology,
 389

V

Visual Basic software, 269

W

Wavelet transform, 23
 Wearable devices
 applications, 2–3
 integrated wearable sensors, objectives of, 1–2
 requirement of, 7
 ubiquitous healthcare devices (*see* Ubiquitous
 healthcare monitoring (U-HRM) system)
 Wearable tech, 1–2
 Weka 3.8 software tool, 191–192
 Wilcoxon signed rank test, 277–278
 Wireless body area network (WBAN), 354

X

xDAWN filtering, 23
 XGBoost, 184
 XML (eXtensible Markup Language) 378

This page intentionally left blank

U-HEALTHCARE MONITORING SYSTEMS DESIGN AND APPLICATIONS

U-Healthcare Monitoring Systems: Design and Applications focuses on the design of efficient U-healthcare systems which require the integration and development of information technology facilities, wireless sensors technology, wireless communication tools, and localization techniques along with health management monitoring. U-healthcare systems allow users to remotely check and manage the health conditions of their patients, and this volume will provide readers with a solid basis in understanding their design and application.

Bringing together contributions from some of the leading experts in the field, initial chapters discuss wearable U-HRM devices for rural application, medical image diagnosis for disease detection, reasoning methodologies in clinical decision support systems, and ontology-enhanced fuzzy clinical decision support systems. Later topics address the areas of improving prediction accuracy in heart disease with ensemble learning and majority voting rule, machine learning for medical diagnosis, a hybrid CAD system for liver diseases using clinical and radiological data, and a unified fuzzy ontology for distributed electronic health record semantic interoperability.

U-Healthcare Monitoring Systems: Design and Applications will be an invaluable resource to help researchers and engineers design sensors, wireless systems, and embedded networks in the development of integrated U-healthcare monitoring systems.

KEY FEATURES

- Covers design and applications of U-healthcare monitoring systems
- Focuses on biomedical sensor devices
- Provides the concept of U-healthcare monitoring systems and its requirements with focus on medical sensors and wireless sensors communication

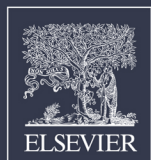
VOLUME EDITORS

Nilanjan Dey is an assistant professor in the Department of Information Technology, Techno India College of Technology, Kolkata, India. **Amira S. Ashour** is a professor in the Department of Electronics and Electrical Communications Engineering, Faculty of Engineering, Tanta University, Egypt. **Simon James Fong** is an associate professor in the Department of Computer and Information Science Data Analytics and Collaborative Computing Laboratory, University of Macau, China. **Surekha Borra** is a professor in the Department of Electronics and Communication Engineering, K.S. Institute of Technology, Bangalore, India.

ABOUT THE SERIES

Series Editors: Dr. Nilanjan Dey, Dr. Amira S. Ashour, Dr. Simon James Fong

Advances in Ubiquitous Sensing Applications for Healthcare is a multi-volume, interdisciplinary series exploring the groundbreaking field of ubiquitous sensing for healthcare (USH), with a focus on real-world healthcare applications. It is an essential reference for researchers in engineering, software design, communication systems, and physicians and academicians working directly on the development of U-healthcare systems.



ACADEMIC PRESS

An imprint of Elsevier
elsevier.com/books-and-journals

ISBN 978-0-12-815370-3

